

Aboul Ella Hassanien  
Ahmad Taher Azar *Editors*

# Brain-Computer Interfaces

Current Trends and Applications

# **Intelligent Systems Reference Library**

## **Volume 74**

### **Series editors**

Janusz Kacprzyk, Polish Academy of Sciences, Warsaw, Poland  
e-mail: kacprzyk@ibspan.waw.pl

Lakhmi C. Jain, University of Canberra, Canberra, Australia  
e-mail: Lakhmi.Jain@unisa.edu.au

### *About this Series*

The aim of this series is to publish a Reference Library, including novel advances and developments in all aspects of Intelligent Systems in an easily accessible and well structured form. The series includes reference works, handbooks, compendia, textbooks, well-structured monographs, dictionaries, and encyclopedias. It contains well integrated knowledge and current information in the field of Intelligent Systems. The series covers the theory, applications, and design methods of Intelligent Systems. Virtually all disciplines such as engineering, computer science, avionics, business, e-commerce, environment, healthcare, physics and life science are included.

More information about this series at <http://www.springer.com/series/8578>

Aboul Ella Hassanien · Ahmad Taher Azar  
Editors

# Brain-Computer Interfaces

## Current Trends and Applications



Springer

*Editors*

Aboul Ella Hassanien  
Department of Information Technology  
Cairo University  
Giza  
Egypt

Ahmad Taher Azar  
Faculty of Computers and Information  
Benha University  
Benha  
Egypt

ISSN 1868-4394  
ISBN 978-3-319-10977-0  
DOI 10.1007/978-3-319-10978-7

ISSN 1868-4408 (electronic)  
ISBN 978-3-319-10978-7 (eBook)

Library of Congress Control Number: 2014952782

Springer Cham Heidelberg New York Dordrecht London

© Springer International Publishing Switzerland 2015

This work is subject to copyright. All rights are reserved by the Publisher, whether the whole or part of the material is concerned, specifically the rights of translation, reprinting, reuse of illustrations, recitation, broadcasting, reproduction on microfilms or in any other physical way, and transmission or information storage and retrieval, electronic adaptation, computer software, or by similar or dissimilar methodology now known or hereafter developed. Exempted from this legal reservation are brief excerpts in connection with reviews or scholarly analysis or material supplied specifically for the purpose of being entered and executed on a computer system, for exclusive use by the purchaser of the work. Duplication of this publication or parts thereof is permitted only under the provisions of the Copyright Law of the Publisher's location, in its current version, and permission for use must always be obtained from Springer. Permissions for use may be obtained through RightsLink at the Copyright Clearance Center. Violations are liable to prosecution under the respective Copyright Law.

The use of general descriptive names, registered names, trademarks, service marks, etc. in this publication does not imply, even in the absence of a specific statement, that such names are exempt from the relevant protective laws and regulations and therefore free for general use.

While the advice and information in this book are believed to be true and accurate at the date of publication, neither the authors nor the editors nor the publisher can accept any legal responsibility for any errors or omissions that may be made. The publisher makes no warranty, express or implied, with respect to the material contained herein.

Printed on acid-free paper

Springer is part of Springer Science+Business Media ([www.springer.com](http://www.springer.com))

# **Foreword**

Interest in Brain-Computer Interfacing (BCI) is growing. This can be concluded from the number of BCI papers appearing in neuro-engineering and neuroscience journals and that are being presented at BCI conferences and workshops. More importantly, it can also be concluded from the growing number of BCI publications that appear in journals and in conference and workshop proceedings that consider brain activity as one of the many modalities that provide a system or a device with knowledge of its human interaction partners, including the situation where a human interaction partner directly addresses the system or device, using BCI. That is, currently, we are seeing brain computer interaction becoming integrated with other interaction possibilities and other interaction devices. This is an extremely important development. Integration means that information coming from other modalities such as speech, eye gaze, gestures, facial expressions, body postures, and various physiological modalities (heart rate, blood pressure, and skin conductivity) can be fused with detected brain signals to make it more easily possible to give a context-aware and context-dependent interpretation of these signals. It means that BCI technology needs to be integrated with, for example, wearable sensors, speech processing and computer vision technology. However, it also means new challenges for (computational) neuroscience researchers and that brain signals need to be processed in non-clinical situations.

Presently we see a lot of application-oriented research that aims at providing users, not only disabled users, with the capability to control devices or sensors and actuators in their environment, where these environments and devices can range from wheelchairs and artificially controlled hands for grasping, to entertainment applications including artful visualization and musification, digital painting, game control, interaction with social robots or virtual humans, and domestic applications. With these applications for the general audience we cannot be surprised to see the appearance of companies focusing on commercial BCI devices and applications. A possible mass market for BCI technology will help to forward BCI research in general and it will certainly help to increase awareness of BCI technology and its possibilities. No wonder that in recent years science policy makers and funding agencies have decided that it is time to have new and original views on possible

short-term and long-term developments in this research field and possible ways to steer these developments. Hence, there has been a veritable avalanche of state-of-the-art reports of BCI research, assessments of BCI research and roadmaps for BCI research. Apart from many scientific challenges, one of the (European Union) roadmaps mentioned the following four challenges: (1) the growing need for standards is still unmet, (2) there is inadequate interaction within the BCI community, (3) there is inadequate dissemination outside of the BCI community, and (4) there is little agreement on the most promising future directions.

Of course, such issues have become prominent now that different research groups, user groups, companies, and decision makers without the traditional clinical BCI background have entered the field. It has also led to discussions about the ‘definition’ of a BCI, maybe comparable with a less than fruitful discussion about a definition of ‘artificial intelligence’ in the 1950s of the previous century. In the traditional definitions intentional control of a device by modulating brain signals and explicit feedback to the user was emphasized. Now we see descriptions that include multiple users, multiple BCI paradigms used in parallel or sequentially, fusion of features or decisions that involve both BCI information and information obtained from other modalities and, exploiting brain signals in interaction situations where they are not necessarily intentionally modulated by the user and where no immediate explicit feedback is given. BCI research is supposed to lead to technology in which brain signals are used to support people in their interaction activities.

It has been a long road from the early BCI investigations to the current day’s investigations and applications. There can be applications that do not require or aim at using perfect detection or perfect interpretation of brain signals in order to be successful. But, of course, possible improvements that can be obtained from fundamental research in BCI and underlying research areas are necessary to improve and to extend the current limited range of real-world BCI applications. In this book Prof. Aboul Ella Hassanien and Dr. Ahmad Taher Azar have collected and edited contributions of well-known researchers in the BCI field in order to provide a representative view, also from the observations presented above, of current trends and applications in BCI research. Their efforts have been successful. Therefore, it has been a pleasure to write a Foreword for this book.

Anton Nijholt  
Professor, Human-Computer Interaction  
Human Media Research group  
University of Twente, Enschede  
The Netherlands

# Preface

Brain Computer Interface (BCI) is a challenging application of signal processing and neuroscience. A BCI system uses mental activity, voluntarily produced by the patient, to control a computer or an embedded system via electroencephalogram (EEG) signals which allow communication or interaction with the surrounding environment. Like any communication or control system, a BCI has input (e.g., electrophysiological activity from the user), output (i.e., device commands), components that translate input into output, and a protocol that determines the onset, offset, and timing of operation. The success of a BCI system depends as much on the system itself as on the user's ability to produce distinctive EEG activity. BCI systems can be divided into two groups according to the placement of the electrodes used to detect and measure neurons firing in the brain. These groups are: invasive systems, electrodes are inserted directly into the cortex are used for single cell or multi unit recording, and electrocorticography (EcoG), electrodes are placed on the surface of the cortex (or dura); noninvasive systems, they are placed on the scalp and use electroencephalography (EEG) or magnetoencephalography (MEG) to detect neuron activity.

The book is divided into three parts. Part I of the book from Chaps. 1–4 covers overviews of Brain Computer Interface. Part II of the book from Chaps. 5–9 describes new theoretical developments of BCI systems. Part III of the book from Chaps. 10–14 covers views on real applications of BCI systems.

It is hoped that the book will be a very good compendium for almost all readers—from students of undergraduate to postgraduate levels and also for researchers, professionals, etc.—who wish to enrich their knowledge on BCI systems' principles and applications with a single book in the best manner. As the editors, we hope that the chapters in this book will stimulate further research in BCI systems and utilize them in real-world applications. We hope that this book, covering so many different

aspects, will be of value to all readers. We would like to thank also the reviewers for their diligence in reviewing the chapters. Special thanks go to our publisher, Springer, especially for the tireless work of the series editor of *Intelligent Systems Reference Library*, Dr. Thomas Ditzinger.

Aboul Ella Hassanien  
Ahmad Taher Azar

# Contents

## Part I General Views on Brain-Computer Interfacing

<b>1</b>	<b>Brain Computer Interface: A Review . . . . .</b>	<b>3</b>
	Mohamed Mostafa Fouad, Khalid Mohamed Amin, Nashwa El-Bendary and Aboul Ella Hassanieh	
1.1	Introduction . . . . .	4
1.2	Neuroimaging-Based Approaches in the BCI . . . . .	5
1.2.1	The Neuroimaging Modalities . . . . .	5
1.3	Control Signals in BCI Systems . . . . .	12
1.3.1	EEG Signal Processing for BCI . . . . .	12
1.3.2	Preprocessing Techniques that Deal with EOG/EMG Artifacts. . . . .	16
1.3.3	Feature Extraction for BCI Designs. . . . .	17
1.3.4	Classification Methods and Post-processing . . . . .	19
1.3.5	Classification Performance Metrics . . . . .	24
1.4	Conclusion. . . . .	25
	References. . . . .	25
<b>2</b>	<b>Basics of Brain Computer Interface . . . . .</b>	<b>31</b>
	Rabie A. Ramadan, S. Refat, Marwa A. Elshahed and Rasha A. Ali	
2.1	Introduction . . . . .	32
2.2	Brain Anatomy. . . . .	33
2.3	Brain Computer Interface Types . . . . .	35
2.3.1	Invasive BCI Acquisition Techniques . . . . .	35
2.3.2	Partially Invasive BCI Acquisition Techniques . . . . .	36
2.3.3	Non Invasive BCI Acquisition Techniques. . . . .	36
2.4	Types of BCI Signals . . . . .	37
2.5	Components of Interest . . . . .	38
2.5.1	Oscillatory EEG Activity . . . . .	39
2.5.2	Event-Related Potentials . . . . .	39
2.6	Monitoring Brain Activity Using EEG. . . . .	40

2.7	BCI System . . . . .	42
2.8	BCI Monitoring Hardware and Software . . . . .	43
2.9	Brain Computer Interface Applications . . . . .	45
2.10	BCI Trends . . . . .	47
2.11	Conclusion . . . . .	48
	References . . . . .	49
<b>3</b>	<b>Noninvasive Electromagnetic Methods for Brain Monitoring: A Technical Review . . . . .</b>	<b>51</b>
	Tushar Kanti Bera	
3.1	Introduction . . . . .	52
3.2	Human Brain Anatomy . . . . .	54
3.3	Brain Diseases . . . . .	55
3.4	Noninvasive Brain Monitoring . . . . .	56
3.4.1	Advantages of PET . . . . .	58
3.4.2	Disadvantages of PET . . . . .	58
3.5	Electromagnetic Brain Monitoring Methods . . . . .	58
3.5.1	Brain Metabolism and Brain Imaging . . . . .	59
3.5.2	Electroencephalography (EEG) . . . . .	59
3.5.3	Magnetoencephalography (MEG) . . . . .	69
3.5.4	Electrocorticography (ECoG) . . . . .	71
3.5.5	Electroneurogram (ENG) . . . . .	72
3.5.6	MRI . . . . .	72
3.5.7	Electrical Impedance Tomography (EIT) . . . . .	76
3.5.8	Present Scenario and the Future Trends . . . . .	82
3.5.9	Conclusions . . . . .	83
	References . . . . .	84
<b>4</b>	<b>Translational Algorithms: The Heart of a Brain Computer Interface . . . . .</b>	<b>97</b>
	Harsimrat Singh and Ian Daly	
4.1	Introduction . . . . .	97
4.2	Sources of Information for a BCI . . . . .	99
4.2.1	Electroencephalogram . . . . .	99
4.2.2	Functional Magnetic Resonance Imaging and Magneto Encephalography . . . . .	102
4.2.3	Intracranial Recordings ECoG (Electrocorticogram) . . . . .	104
4.2.4	Functional Near Infra-red Spectroscopy . . . . .	104
4.3	BCI Development Process . . . . .	105
4.4	Types of BCI . . . . .	106
4.4.1	Invasive and Non-invasive BCIs . . . . .	106
4.4.2	Synchronous and Asynchronous BCIs . . . . .	107

4.5	Computational Techniques . . . . .	107
4.5.1	Dimensionality Reduction . . . . .	108
4.5.2	Feature Extraction . . . . .	110
4.5.3	Feature Selection . . . . .	111
4.5.4	Classification Techniques . . . . .	113
4.6	BCI Evaluation . . . . .	114
4.7	Conclusion . . . . .	115
	References . . . . .	117

## Part II New Theoretical Developments

<b>5</b>	<b>Source Localization for Brain-Computer Interfaces . . . . .</b>	<b>125</b>
	Aleksandr Zaitcev, Greg Cook, Wei Liu, Martyn Paley and Elizabeth Milne	
5.1	Introduction to the Source Localization Problem . . . . .	126
5.2	Head and Source Models . . . . .	128
5.2.1	Physics of EEG . . . . .	128
5.2.2	Source Models . . . . .	129
5.2.3	Head Models . . . . .	133
5.2.4	The Forward Problem . . . . .	135
5.3	Source Localization . . . . .	137
5.3.1	The Inverse Problem . . . . .	137
5.3.2	Anatomical Constraints for Source Localization . . . . .	138
5.3.3	Source Localization for BCI . . . . .	141
5.4	Sparse Brain Imaging . . . . .	144
5.4.1	Introduction to Sparse Brain Imaging . . . . .	144
5.4.2	Approaches to Sparse Source Localization . . . . .	145
5.4.3	Examples of Sparse Source Localization . . . . .	147
5.5	Chapter Summary . . . . .	150
	References . . . . .	152
<b>6</b>	<b>Hippocampal Theta-Based Brain Computer Interface . . . . .</b>	<b>155</b>
	L.C. Hoffmann, J.J. Cicchese and S.D. Berry	
6.1	Introduction . . . . .	156
6.2	Related Work . . . . .	158
6.2.1	Model System: Rabbit Eyeblink Conditioning . . . . .	158
6.2.2	Theta-Triggering Interface Development and Initial Applications . . . . .	161
6.2.3	Extra-Hippocampal Modulation Using Our BCI . . . . .	166
6.2.4	Amelioration of Age-Related Learning Deficits . . . . .	169
6.2.5	Current Directions . . . . .	171

6.3	Discussion . . . . .	172
6.3.1	Models of Learning: Theta and Plasticity . . . . .	173
6.3.2	Theta-Modulated Interactions in the Eyeblink Circuitry . . . . .	174
6.3.3	Future Directions and Applications . . . . .	176
6.4	Conclusion . . . . .	177
	References . . . . .	178
<b>7</b>	<b>Advanced fMRI and the Brain Computer Interface . . . . .</b>	<b>185</b>
	Martyn Paley, Shwan Kaka, Heather Hilliard, Aleksandr Zaytsev, Adriana Bucur, Steven Reynolds, Wei Liu, Elizabeth Milne and Greg Cook	
7.1	Introduction . . . . .	186
7.2	BOLD Versus Direct Electromagnetic Detection fMRI . . . . .	188
7.2.1	Spatial Resolution of BOLD Versus dfMRI . . . . .	189
7.2.2	Temporal Resolution of BOLD Versus dfMRI . . . . .	190
7.2.3	Fast EPI fMRI Acquisition Method for dfMRI . . . . .	190
7.2.4	GRACE Method for High Spatial and Temporal Resolution dfMRI . . . . .	192
7.2.5	TENS Stimulation of the Median Nerve for dfMRI . . . . .	195
7.3	Novel Low Field MRI Technology for dfMRI . . . . .	198
7.3.1	Compact Low Field MRI Systems for dfMRI Research . . . . .	198
7.3.2	Cryogenic Coils for Improved Sensitivity of Low Field MRI . . . . .	199
7.3.3	Overhauser Enhanced MRI . . . . .	202
7.3.4	An Ultra-low Field Overhauser Enhanced dfMRI System . . . . .	203
7.3.5	Dissolution Dynamic Nuclear Polarization Enhanced dfMRI . . . . .	205
7.4	A dfMRI Brain Computer Interface Proposal . . . . .	208
7.4.1	Advanced Open dfMRI System Design . . . . .	208
7.4.2	The dfMRI BCI . . . . .	209
7.5	Discussion and Conclusions . . . . .	210
	References . . . . .	211
<b>8</b>	<b>Detection of Human Emotions Using Features Based on the Multiwavelet Transform of EEG Signals . . . . .</b>	<b>215</b>
	Varun Bajaj and Ram Bilas Pachori	
8.1	Introduction . . . . .	216
8.2	Methodology . . . . .	222
8.2.1	Experimental Setup . . . . .	222
8.2.2	Pre-processing . . . . .	223
8.2.3	Multiwavelet Transform . . . . .	224

8.2.4	Features Extraction . . . . .	227
8.2.5	Multiclass Least-Squares Support Vector Machine . . . . .	229
8.3	Results and Discussion . . . . .	231
8.4	Conclusion . . . . .	233
	References . . . . .	234
<b>9</b>	<b>A Configurable, Inexpensive, Portable, Multi-channel, Multi-frequency, Multi-chromatic RGB LED System for SSVEP Stimulation . . . . .</b>	<b>241</b>
	Surej Mouli, Ramaswamy Palaniappan and Ian P. Sillitoe	
9.1	Introduction . . . . .	242
9.2	Related Work . . . . .	245
9.3	Materials and Methods . . . . .	249
9.3.1	Design of Visual Stimulator . . . . .	249
9.4	Results . . . . .	260
9.4.1	Frequency Test . . . . .	260
9.4.2	Single Frequency . . . . .	261
9.4.3	Multiple Frequency . . . . .	263
9.5	Discussion . . . . .	264
9.6	Conclusion . . . . .	265
	References . . . . .	266

### **Part III Views on Applications**

<b>10</b>	<b>EEG Based Brain Computer Interface for Speech Communication: Principles and Applications . . . . .</b>	<b>273</b>
	Kusuma Mohanchandra, Snehanshu Saha and G.M. Lingaraju	
10.1	Introduction . . . . .	274
10.2	Evidences of Speech Communication in Locked-in Patients . . . . .	276
10.3	Supplementary Target BCI Applications for Speech Communication . . . . .	278
10.4	BCI Design Principles . . . . .	279
10.4.1	Types of BCI . . . . .	280
10.4.2	EEG Based BCI . . . . .	282
10.4.3	Control Signals Used in BCI for Speech Communication . . . . .	283
10.5	Challenges and Future Research Directions for Speech Communication BCI . . . . .	287
10.6	Conclusion . . . . .	288
	References . . . . .	289

<b>11 Web-Based Intelligent EEG Signal Authentication and Tamper Detection System for Secure Telemonitoring . . . . .</b>	295
Aniruddha Mukherjee, Goutami Dey, Monalisa Dey and Nilanjan Dey	
11.1 Introduction . . . . .	296
11.2 Related Work . . . . .	298
11.3 Electroencephalographic Signal (EEG) . . . . .	300
11.4 Proposed Method . . . . .	301
11.5 Explanation of the Proposed Method . . . . .	304
11.6 Results and Discussion . . . . .	306
11.7 Conclusion . . . . .	310
References . . . . .	311
<b>12 Competing and Collaborating Brains: Multi-brain Computer Interfacing . . . . .</b>	313
Anton Nijholt	
12.1 Introduction . . . . .	314
12.1.1 Organization of this Chapter . . . . .	316
12.2 Brain Activity Measurements from Multiple Brains . . . . .	316
12.2.1 Early Multi-brain BCI Applications . . . . .	316
12.2.2 Current Multi-brain BCI Research and Applications . . . . .	318
12.3 Competition and Collaboration Using BCI . . . . .	321
12.4 More About Multi-brain Games . . . . .	326
12.5 Distinguishing Multi-brain Games . . . . .	330
12.6 Discussion . . . . .	331
12.7 Conclusions . . . . .	332
References . . . . .	333
<b>13 Mood Recognition System Using EEG Signal of Song Induced Activities . . . . .</b>	337
Rakesh Deore and Suresh Mehrotra	
13.1 Introduction . . . . .	338
13.2 Literature Survey . . . . .	339
13.3 Experimental Setup . . . . .	341
13.3.1 EEG Equipments . . . . .	341
13.3.2 Artifacts . . . . .	344
13.3.3 Rhythmic Brain Activity . . . . .	345
13.3.4 Application of EEG . . . . .	346
13.3.5 Human Brain . . . . .	346
13.3.6 BCI Framework . . . . .	348
13.3.7 Categorization . . . . .	350

13.4	Materials and Methodology . . . . .	352
13.4.1	Subject Selection . . . . .	353
13.4.2	Procedure . . . . .	354
13.4.3	Apparatus and Recording Procedure . . . . .	354
13.5	Data Analysis. . . . .	356
13.5.1	Region Wise Data Analysis . . . . .	357
13.5.2	Linear Discriminate Analysis on Alpha Power Rhythm . . . . .	369
13.6	Conclusion. . . . .	372
	References. . . . .	372
<b>14</b>	<b>Digit Recognition System Using EEG Signal . . . . .</b>	<b>375</b>
	Rakesh Deore, Bharati Gawali and Suresh Mehrotra	
14.1	Introduction . . . . .	376
14.2	Literature Survey . . . . .	378
14.3	Experimental Data Acquisition . . . . .	379
14.3.1	Methodology . . . . .	379
14.3.2	Apparatus and Recording Procedure . . . . .	379
14.4	Experimental Analysis. . . . .	381
14.4.1	Linear Discriminate Analysis . . . . .	381
14.4.2	Principle Component Analysis . . . . .	383
14.4.3	Comparative Study of LDA and PCA . . . . .	385
14.4.4	Region Wise Data Analysis . . . . .	391
14.5	Feature Extraction. . . . .	400
14.6	Conclusion. . . . .	414
	References. . . . .	415

**Part I**

**General Views on Brain-Computer  
Interfacing**

# Chapter 1

## Brain Computer Interface: A Review

**Mohamed Mostafa Fouad, Khalid Mohamed Amin,  
Nashwa El-Bendary and Aboul Ella Hassanien**

*Quiet people have the loudest minds.*  
Stephen Hawking

**Abstract** A brain-computer interface (BCI) systems permit encephalic activity to solely control computers or external devices. Accordingly, people suffering from neuromuscular diseases can highly benefit from these technologies, since a computer could allow them to perform multiple tasks, such as accessing computer-based entertainment (videos, games, books, music, movies, etc.), communication (Internet, VoIP, e-mails, text processors, speech synthesis, etc.) and means of research (computational capacity, programming languages, simulation applications, etc.). Moreover, nowadays a computer can control various electronic devices, from TVs, DVD and CD players to electric wheel chairs, elevators, doors and lights. The purpose of this chapter is to discuss the concept of brain computer interface (BCI) along with presenting its definition, description, and classification of BCI systems. Also, provides insights on the Neuroimaging modalities for BCI systems such as Electroencephalography (EEG), Electrocorticography (ECOG), and Magnetoencephalography (MEG) approaches. Moreover, this chapter addresses EEG signal processing for BCI from the different perspectives of preprocessing techniques that deal with EOG/EMG artifacts, feature extraction approaches for BCI designs, classification methods and Post-processing. Furthermore, the chapter gives a brief survey of classifiers used in BCI research along with classification performance

---

M.M. Fouad (✉) · N. El-Bendary

Arab Academy for Science, Technology, and Maritime Transport, Cairo, Egypt  
e-mail: mohamed\_mostafa@aast.edu

N. El-Bendary

e-mail: nashwa.elbendary@ieee.org

K.M. Amin

Faculty of Computers and Information, Menofia University, Menofia, Egypt  
e-mail: kh.amin.0.0@gmail.com

A.E. Hassanien

Faculty of Computers and Information, Cairo University, Cairo, Egypt  
e-mail: aboitcairo@gmail.com  
URL: <http://www.egyptscience.net>

M.M. Fouad · K.M. Amin · N. El-Bendary · A.E. Hassanien  
Scientific Research Group in Egypt (SRGE), Cairo, Egypt

metrics utilized for BCI systems. Finally, the chapter concludes with outlining ongoing research directions for Brain–computer interface (BCI) systems.

**Keywords** Brain computer interface (BCI) · Neuroimaging · Electroencephalography (EEG) · Electrocorticography (ECoG) · Magnetoencephalography (MEG) · Near infrared spectroscopy (NIRS) · Intracortical neuron recording · Functional magnetic resonance imaging (fMRI) · Feature extraction

## 1.1 Introduction

The interaction way between humans and computers has greatly evolved since the appearance of when the first commercial computer, the UNIVAC, in the year of 1951. The only way to control that complicated piece of machinery was a modified IBM electric typewriter, and feedback to the user was given through a Tektronix oscilloscope. Modern computers are completely mobile and even though they are mainly controlled by a mouse and a keyboard, several alternative human-computer interfaces have been developed during the last two decades using haptics, voice and gaze [1].

Brain computer interface (BCI), also known as brain machine interface (BMI), is a system that enables humans to interact with their surroundings via employing control signals generated from electroencephalographic (EEG) activity, without the intervention of peripheral nerves and muscles. BCI presents a muscular-free channel for conveying individuals' purposes of certain actions to external devices such as computers, speech synthesizers, assistive appliances, and neural prostheses. BCI systems are of particular attraction for individuals with severe motor disabilities as such systems would improve their quality of life and would, at the same time, reduce the cost of intensive care.

A brain computer interface (BCI) systems permit encephalic activity to solely control computers or external devices. Hence, the basic goal of BCI systems is to provide communications capabilities to severely disabled people who are totally paralyzed or ‘locked in’ by neurological neuromuscular disorders, such as amyotrophic lateral sclerosis, brain stem stroke, or spinal cord injury [2].

Typically, a BCI is an artificial intelligence based system that can recognize a certain set of patterns in brain EEG signals via a number of consecutive phases; namely, signal acquisition for brain signals capturing, preprocessing or signal enhancement for preparing the signals in a suitable form for further processing, feature extraction for identifying discriminative information in the brain signals that have been recorded, classification for classifying the signals based on the extracted feature vectors, and finally the control interface phases for translating the classified signals into meaningful commands for any connected device, such as a wheelchair or a computer [3].

This chapter discusses the concept of Brain computer interface (BCI) along with presenting its structure and classification. Also, it provides insights on the Neuro-imaging modalities for BCI systems such as Electroencephalography (EEG), Electrocorticography (ECOG), Magnetoencephalography (MEG), Intracortical Neuron Recording, and Functional magnetic resonance imaging, (fMRI) approaches.

Moreover, this chapter addresses EEG signal processing for BCI from the different perspectives of preprocessing techniques that deal with EOG/EMG artifacts, feature extraction approaches for BCI designs, classification methods and Post-processing. Furthermore, the chapter gives a brief survey of classifiers used in BCI research along with classification performance metrics utilized for BCI systems. Finally, the chapter concludes with outlining ongoing research directions for Brain computer interface (BCI) systems.

## 1.2 Neuroimaging-Based Approaches in the BCI

Neuroimaging is a new paradigm in medicine that studies the physiological response in the brain. In other words it could be considered as a window to brain. However neuroimaging of a brain is useful to detect damages in brain tissue, the skull fractures, injuries, today it used to diagnose behavioral problems, metabolic diseases and lesions on a finer scale.

The neuroimaging are categorized into two main categories:

**Structural neuroimaging:** It applied to capture the brain structure including skull bone structure, tissues, blood vessel, or the existence of a tumor.

**Functional neuroimaging:** It used to detect the electrical impulses, flowing rate of blood within vessel, and changes of metabolic activity happened as a response for specific task.

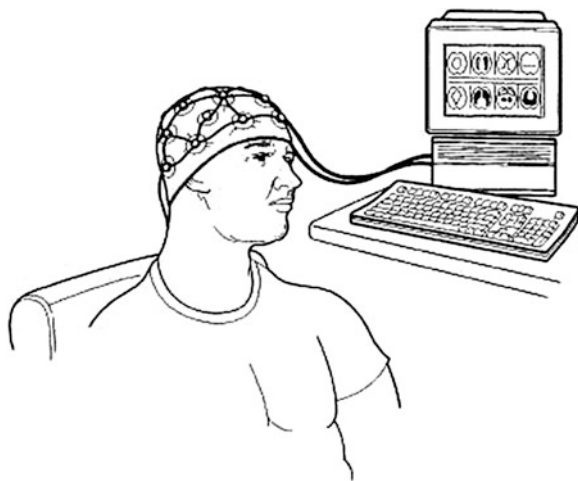
### 1.2.1 *The Neuroimaging Modalities*

The following subsections will review the state of art in neuroimaging based approaches

#### 1.2.1.1 **Electroencephalography**

Brain neurons communicate with each other by producing tiny electrical signals, called impulses. These impulses can be measured using the EEG test. Electrodes, or sensors, are placed on the patient's scalp to capture brain electrical signals in a form of polygraph.

**Fig. 1.1** A wearable EEG a cap equipped with electrodes [5]



Although EEG signals are used to diagnose brain diseases, such as Alzheimer's disease, epilepsy disease, they also suitable tests for evaluating sleeping, learning, and attentional disorders, moreover monitor the brain responses during brain surgery. Quantitative Electroencephalography (qEEG) processing technique uses mathematical techniques such as Fourier and wavelet analysis to analysis recordings captured from multi- EEG electrodes [4]. This analysis views the dynamic changes taking place throughout the brain during cognitive processing tasks, as illustrated in Fig. 1.1.

Currently, EEG technologies are used to study cognitive development of infants [6] to record interactive trials in which infants activated a novel object using their own hands or feet in a form of somatotopic patterns. Reference [7] hypothesized that these somatotopic patterns index an inter-corporeal mapping of corresponding body parts between self and other.

Emotion recognition has emerged as a promising research topic since it provides a window on the user's internal mental state. Researchers are looking forward to surpass the existing emotions recognition based on facial expressions, and body language to EEG technology [8]. The work of [9] presented a study and evaluation criteria to discriminate between positive and negative affective states based on EEG-derived profiles. The classification model was built on collecting EEG data from 167 healthy participants (not including people with sleep disorders, eating disorder, diabetes, or pregnant women). Participants were watching two conflicting types of videos; a video that reflect a negative affective state, and the other to encourage positive affect state. The accuracy of their model as a discriminator between the negative and positive affective states was promising that it reached over 90 %.

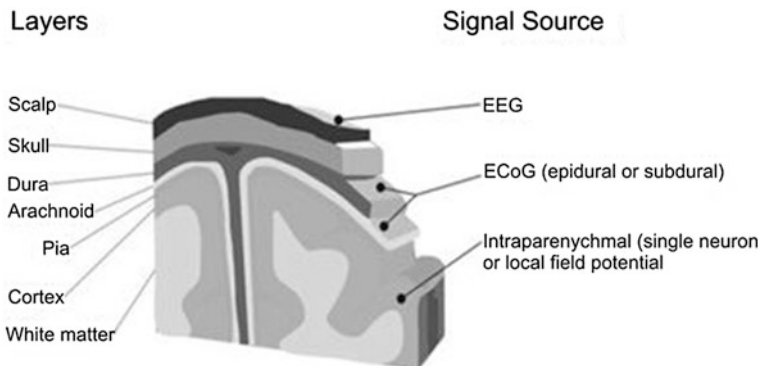


**Fig. 1.2** Signals for BCI and their locations relative to the brain layers [12]

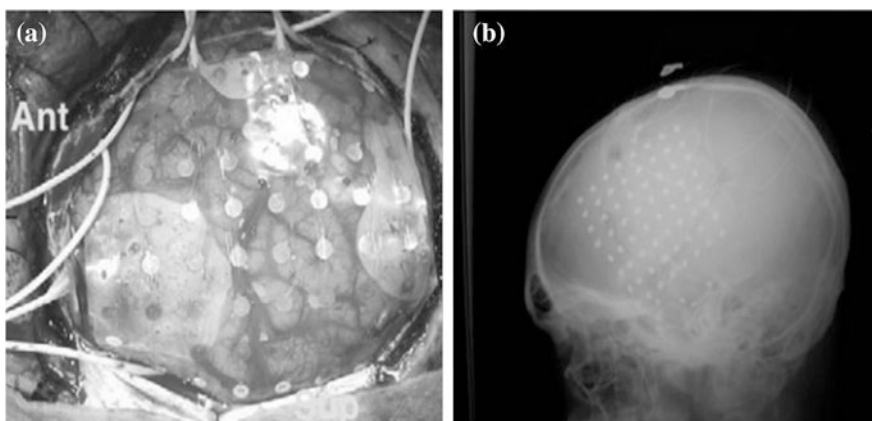


**Fig. 1.3** Examples of electrode placement and ECoG signals. **a** Intra-operative placement of a 64-electrode subdural array. Inter-electrode spacing was 1 cm and electrode diameter was 2 mm. **b** Post-operative lateral skull radiograph showing grid placement [13]

### 1.2.1.2 Electrocorticography

Although, the EEG readings are recorded from the scalp and signal neuron captured from the cortex, they may not be sufficient to explore all brain activities and reactions. Therefore there are a number of neuroscience researches still focuses on using Electrocorticography (ECoG) to record directly from the surface of the brain. Compared with the EEG, the ECoG has higher spatial resolution, broader bandwidth, higher amplitude, and less sensitivity to artifacts such as electromyographic (EMG) signals [10, 11]. ECoG signals are captured through placing a number of electrodes under the skull (either above the epidural or below subdural) as illustrated within Figs. 1.2, and 1.3.

Leuthardt et al. [13] identified ECoG signals that associated with different types of motor and speech imagery in order to master closed-loop control system. They achieved success rates of 74–100 % in controlling the move of one-dimensional computer cursor rapidly and accurately. Other movement primitives can be decoded offline from ECoG signals, such as 7 degrees of freedom of arm movements [14], individual finger movements [15] and natural grasps [16].

### 1.2.1.3 Magnetoencephalography

Magnetoencephalography (MEG) is a technique used to investigate human brain activities through measuring the magnetic fields generated by charged ions excited within neuron cells [2]. The use of MEG has a number of advantages. First, MEG is high temporal resolution technique; that it can resolve small time scaled events (milliseconds) [17]. Therefore MEG signals are more reliable and they speed up BCI communication than EEG signals [18]. Moreover it does not require the injection of isotopes or exposure to X-rays or magnetic fields (non-invasive technique). It is known as a patient-friendly diagnosis system as it is suitable for studding children and infants as it is shown in Fig. 1.4.

Superconducting Quantum Interference Device (SQUID) is the device that used to scan the magnetic waves produced by neural cells [20]. Zimmerman invented the base for Superconducting Quantum Interference Device [21]. David Cohen, at the MIT, significantly improved his MEG device and published the first modern MEG recordings in 1972 [20]. This quantum device should be used in a magnetically shielded room in order to reduce the magnetic field of the earth (noise) [22].

Today, the focus goes toward the use of Magnetoencephalography (MEG) for diagnosis modern neuronal diseases. For example it is now used as a tool in Alzheimer's Disease (AD) and pre-AD research [23]. The future role of MEG as a biomarker not only as a clinical diagnosis but also as a new mode for AD stage discovery [24]. There is a mounting consensus that such disease modifying

**Fig. 1.4** The MEG system [19]



compounds and/or interventions are more likely to be effectively administered as early as possible.

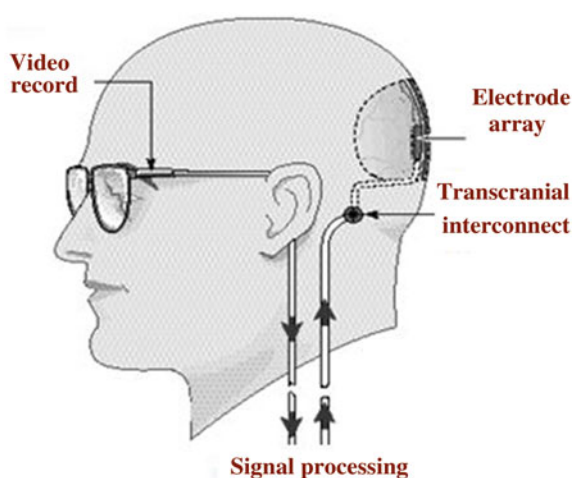
#### 1.2.1.4 Intracortical Neuron Recording

Gray matter or grey matter is a type of neural tissue which is found in the brain and spinal cord. It composed primarily of cell bodies, along with their dendrites. Since most of researches associate gray matter with intelligence and intellect, it is important to measure electrical activity inside them. Intracortical neuron recording is used neuroimaging technique to this type of measurement. The technique records gray matter signals through a microelectrode arrays implemented inside the brain cortex as it is illustrated in Fig. 1.5.

The various components of this electrode system have been developed over years; all developed components are varying in shape (cylindrical, planar), size (15, 50 and 75 mm), and tethering (electrode connections to connector with (tethered) and without tethering cable (untethered)) using histological, transcriptomic, and electrophysiological analyses over acute (3 day) and chronic (12 week) timepoints [26]. Although the focus is going to implant small electrode size [27] and neuro integrative and anti-inflammatory bioactive coatings [28, 29], there are ongoing studies to address the effects of electrode design on tissue response such as the study in [26] that concluded that the extent of brain tissue inflammatory response is significantly influenced by electrode design factors. Moreover it shows that there is a direct correlation between the chronic upregulation of neuro toxic cytokine encoding transcripts and chronic intracortical electrode recording failure.

Although, the intracortical neuron recordings were firstly tested on animals [30], there are ongoing researches focused to use the intracortical neuron recordings for people with limb loss (or experience some form of paralysis) to build technological

**Fig. 1.5** Intracortical neuron recording [25]



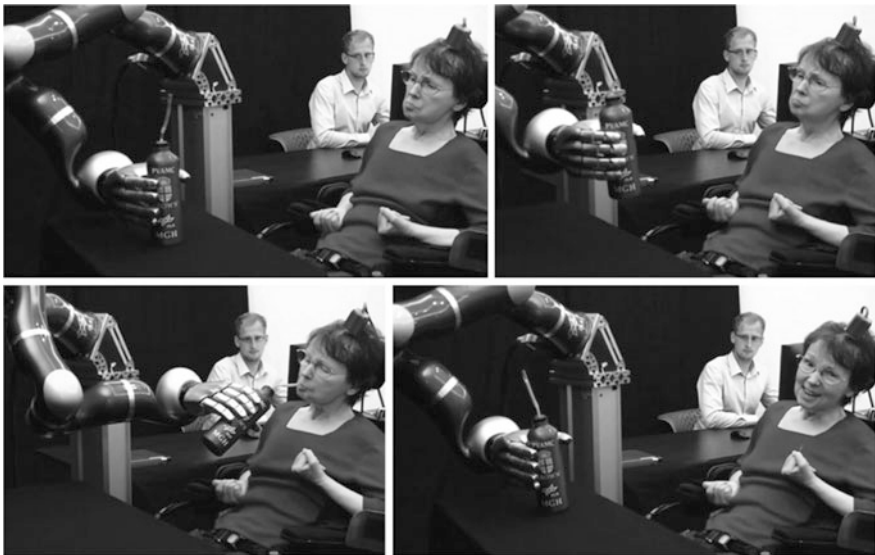


**Fig. 1.6** A successful experiment neuronal control of robotic arm to reach and grasp a thermos of coffee by a person with tetraplegia [32]

bridges between the motor cortex and external devices in order to restore motor function [31]. Figure 1.6 shows a successful experiment neuronal control of robotic arm to reach and grasp a thermos of coffee by a person with tetraplegia.

#### 1.2.1.5 Functional Magnetic Resonance Imaging

Functional magnetic resonance imaging, or fMRI, is a relatively new procedure that uses magnetic resonance imaging (MRI) to establishing an activation map as indication for brain activity. It measures the changes in blood oxygenation and flow that occur in response to neural activity. The idea is simple that when parts of the brain were involved in a particular mental process they consume more oxygen and to meet this increased demand blood flow increases to these parts. Figure 1.7 shows the result of a fMRI scan.

As it appears in Fig. 1.8 there is a change in specific brain areas. This change happens according to the increasing demand for oxygen to regions of increased neural activity. Therefore, the MRI signal depends on the degree of oxygenation (blood oxygenation level dependent (BOLD) imaging). That blood oxygenation varies according to the levels of neural activity these differences can be used to detect brain activity as shown in Fig. 1.7 [33].

Not only fMRI is used to record brain activities when doing different mental tasks, but also there is a trend to use this technology to diagnosis psychological diseases, such as dyslexia, which is a learning disability, makes it difficult for children to break words down into phonemes [34]. fMRI is used to study autism in

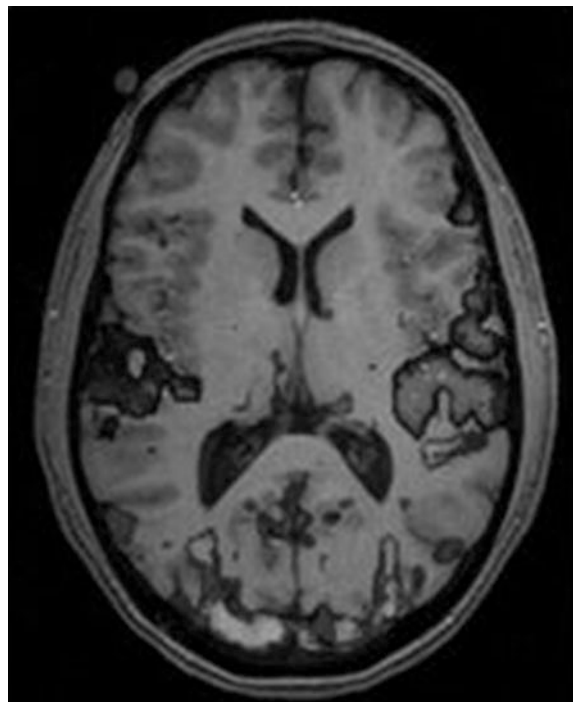


**Fig. 1.7** Results of a kind of fMRI experiment [33]

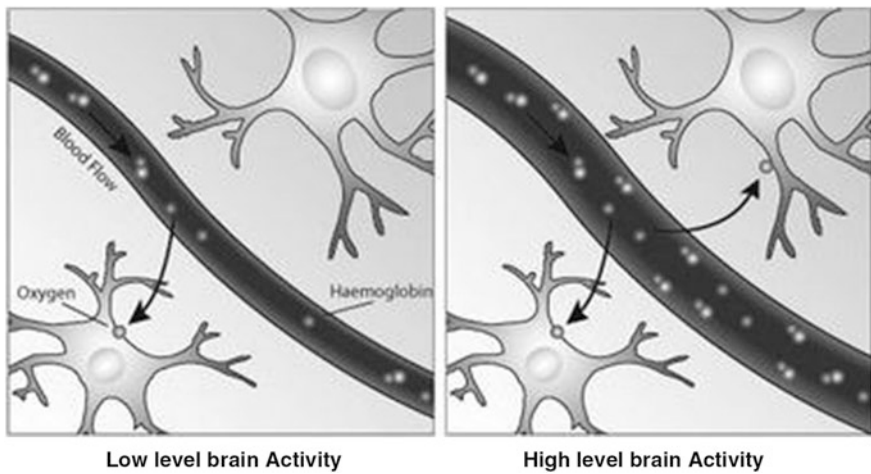


**Fig. 1.8** Blood flow degree changes according to brain activities

order to found various regions related to reactions of people with autism [35]; for example, the study done by Koshino et al. [36] to define reaction of them towards memory for faces, also the work of Welchew et al. [37] that used to define responses of autism people towards different emotions.

### 1.2.1.6 Near Infrared Spectroscopy

William Herschel had discovered the radiation beyond the visible red light in 1,800 [38]. However, Near Infrared (NIR) region was not considered useful for spectroscopy. Recently NIRS turned into a measurement tool that used in a wide range of applications including chemistry, agriculture, environmental analysis, etc.

Infrared is used through penetrating the skull either in the frontal cortex or occipital cortex in order to assess the hemodynamic alterations accompanying brain activation (oxygenated hemoglobin and deoxygenated hemoglobin levels) [39]. It may appear similar to fMRI but it had a number of advantages over the fMRI that it is cheap, high portable, and it has an acceptable temporal resolution. The key limitation of the NIRS is its attachment to the nature of the hemodynamic response, since the vascular changes occur a certain number of seconds after its associated neural activity [2, 40].

## 1.3 Control Signals in BCI Systems

### 1.3.1 EEG Signal Processing for BCI

Electroencephalography (EEG) is one of the key tools for observing brain activity. With respect to other data acquisition techniques (see Fig. 1.9 for comparison), its main advantages are low costs, relative ease of use and excellent time resolution (millisecond scale temporal resolution) [41]. However, it has poor spatial resolution [42]. EEG is considered the only practical non-invasive brain imaging modality for repeated real-time brain behavioral analysis [43]. For this reason, we will focus on EEG as the input brain imaging modality for BCI design.

EEG signal changes according to the brain activity states. Depending on these states, we can distinguish several rhythms (waves) [44]: “Delta” waves lie within the range of 0.5–4 Hz, “Theta” waves lie within the range of 4–7 Hz, with an amplitude usually greater than 20  $\mu$ V. “Alpha” with a rate of change lies between 8 and 13 Hz, with 30–50  $\mu$ V amplitude, “Beta”, the rate of change lies between 13 and 30 Hz, and usually has a low voltage between 5 and 30  $\mu$ V. Beta is the brain wave usually associated with active thinking, active attention, and focus on the outside world or solving concrete problems. Finally, the “Gamma” waves which lie within the range of 35 Hz and up. It is thought that this band reflects the mechanism of consciousness.

Figure 1.10 illustrates a typical block diagram that illustrates different stages of EEG signal processing for BCI. Subjects will generate brain activity through an

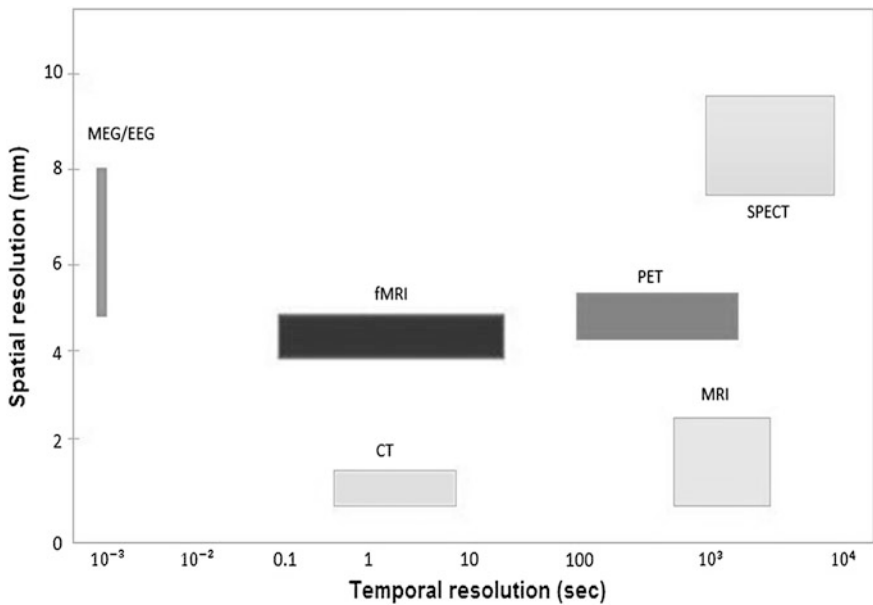


**Fig. 1.9** Scale of spatio-temporal resolution of various brain imaging techniques

experimental paradigm that would depend on the particular BCI approach. The protocol to be followed by the subjects could be thinking about making imaginary movements, focusing on flashing characters on a screen, and so forth [45].

In the following subsections, different EEG signal processing stages will be studied with highlights of recent advances.

### 1.3.1.1 Data Collection Through Electrodes

Brain activity is picked by one of different types of electrodes. In their most simple method, they are placed on the scalp using gel as a conducting material. The placement of electrodes commonly follows the 10–20 system (as illustrated in Fig. 1.11) or extensions of this system (32, 64, 128, or 256 electrodes) [45]. During the last 3 years, many research works had been done on such electrodes to maximize their performance. In a recent work of [46], they demonstrated that dry and water-based electrodes can replace gel ones in BCI applications where lower communication speed is acceptable. In [47], they presented a wireless EEG monitoring system. The system is capable of processing brain signals on-board recorded from non-contact sensors. It provides an excellent option for developing a compact BCI with a direct connection to the external device e.g. robot or prosthesis without employing a personal computer. The problem of interference pick-up by electrodes was addressed by the recent work of [48]. They hypothesized that interference pick-up could be effectively reduced by an optimized silver or graphite shielded construction.

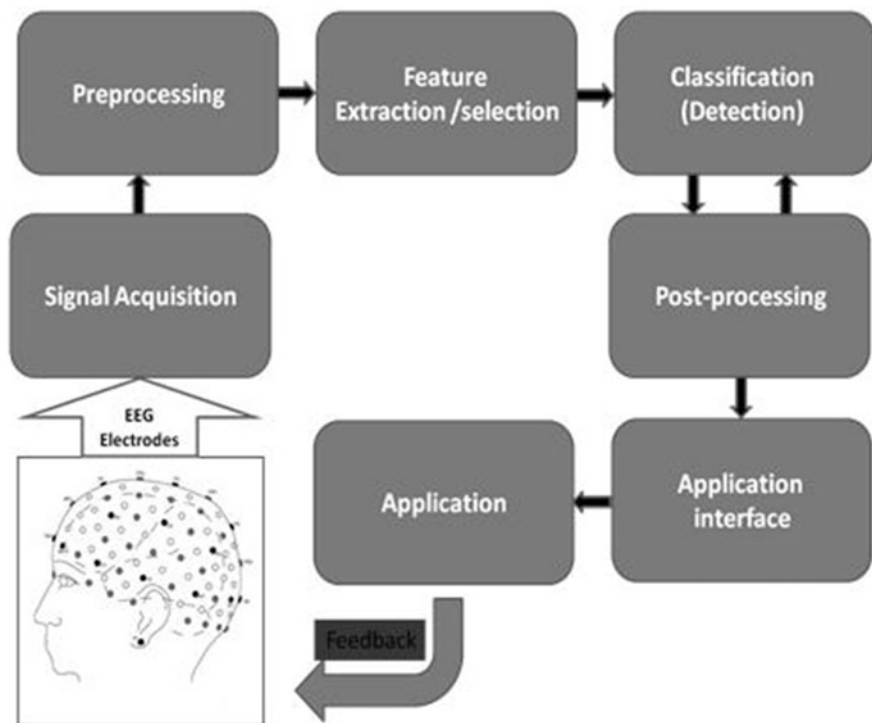


**Fig. 1.10** Typical block diagram to illustrate different stages of EEG signal processing for BCI applications

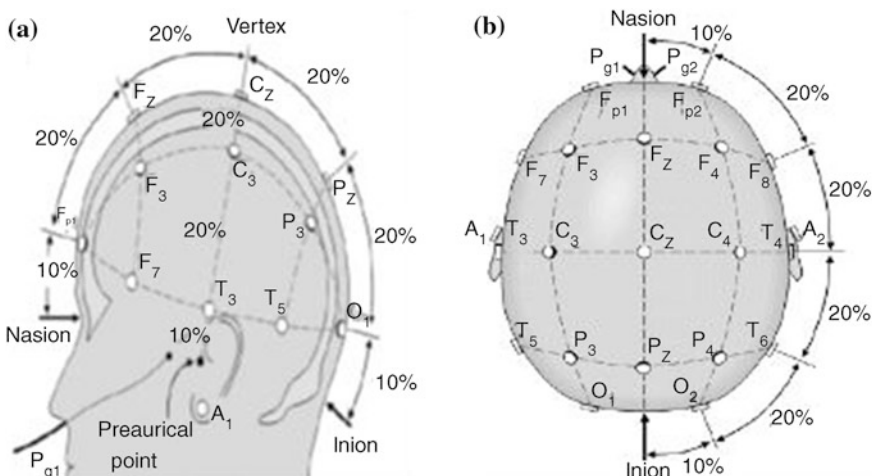


**Fig. 1.11** Electrode placement over scalp according to the international 10/20 system. **a** As seen from left side. **b** As seen from top

### 1.3.1.2 Pre-processing Methods in BCI Designs

Preprocessing is carried out to remove any unwanted components embedded within the EEG signal. Good preprocessing leads to increase in signal quality which in turn resulting in better feature separability and classification performance.

### 1.3.1.3 Sources of Noise in EEG Signal

One of the biggest challenges in using EEG is the very small signal-to-noise ratio (SNR) of the brain signals that we are trying to observe, coupled by the wide variety of noise sources as illustrated in Fig. 1.12. Any signal other than that of interest could be termed as an interference, artifact, or simply noise. EEG signal suffers mainly from two types of noise. The first type, which is considered the easiest source of noise to deal with, includes external, environmental sources of noise, such as AC power lines, lighting and a large array of electronic equipments (from computers, displays and TVs to wireless routers, notebooks and mobile phones). The most basic steps in dealing with environmental noise are removing any unnecessary sources of electro-magnetic (EM) noise from the recording room and its immediate vicinity, and, where possible, replacing equipment using alternate current with equipment using direct current (such as direct current lighting). A more

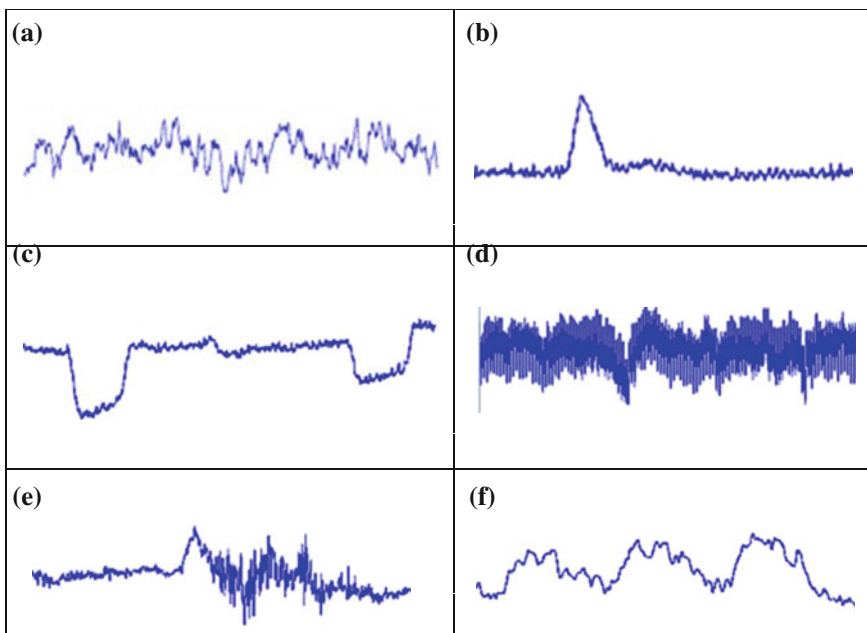


**Fig. 1.12** Several types of artifacts in EEG signal. **a** Clean EEG. **b** Eye blink. **c** Eye movement. **d** 50 Hz. **e** Muscle activity. **f** Pulse

advanced and costly measure is to insulate the recording room from EM noise by use of a Faraday cage [41, 44]. The second type of noise sources is the physiological artifacts which arise from a variety of body activities that are either due to movements, other bioelectrical potentials or skin resistance fluctuations. The predominant physiological artifacts include electrooculographic activity (EOG, eye), scalp recorded electromyographic activity (EMG, muscle), electrocardiographic activity (ECG, heart), ballistocardiographic activity (heart-related pulsatile motion) and respiration. These artifacts are always present to some extent and are typically much more prominent on the scalp than the macroscopic cerebral potentials. This results in an undesirable negative signal-to-noise ratio in the EEG. Physiological artifacts are often involuntary and hence cannot be controlled or ‘turned off’ during acquisition. Traditionally non-cerebral recordings such as EOG, ECG or EMG are also performed to aid in the discrimination and potentially the removal of the relevant artifacts from the EEG signals as will be discussed later [43].

In addition to the previous noise sources, anatomical factors such as the intervening tissue and the skull act as a signal attenuators further muddying the spatial resolution of the oscillations. The techniques used in the signal preprocessing stage are also dependent on the eventual type of feature classification one wishes to do, as certain classification algorithms work better with data preprocessed in specific ways.

### **1.3.2 Preprocessing Techniques that Deal with EOG/EMG Artifacts**

Electrooculography (EOG) and electromyography (EMG) artifacts are considered among the most important sources of physiological artifacts in BCI systems. In this section, we briefly address methods of handling such artifacts. The first step in handling artifacts is to avoid their occurrence by issuing proper instructions to users. For example, users are instructed to avoid blinking or moving their body during the experiments [49, 50].

Artifact rejection is the second choice, where it refers to the process of rejecting the trials affected by artifacts. The rejection process can be done manually or automatically. An advantage of the automatic rejection approach over that of manual rejection is that it is less labor intensive. However, automatic rejection still suffers from sampling bias and loss of valuable data [51]; Moreover, in the case of EOG artifacts, the automatic rejection approach does not allow the rejection of contaminated trials when EOG amplitude is small [52].

Artifact removal is the last choice and the most challenge one. Artifact removal is the process of identifying and removing artifacts from brain signals. An artifact-removal method should be able to remove the artifacts as well as keeping the related neurological phenomenon intact [50].

Common methods for removing artifacts in EEG signals are a very topical research area and may be divided into two different approaches: Filtering and Higher-Order statistical separation [43].

Filtering involves the development of a filter model to emulate the artifact activity and use it to remove the artifact from the EEG recorded signals. The filter coefficients can be established from empirical processing of the non-cerebral bio-electrical artifact recordings such as EMG and EOG. This may result in a conventional low-pass, high-pass, band-pass and notch filter or a more complex filter model. Typically continuous adaptive regressive filtering is used in this approach [53]. Regressive filtering methods in the time or frequency domain can, despite their computational efficiency, overcompensate for the artifact contribution resulting in the loss of EEG information or the introduction of new artifacts [43].

Due to the large number of unknown sources of neuronal and non-neuronal origins contributing to the recorded signal, it becomes a blind source separation (BSS) challenge to identify and remove artifacts on a single trial basis. The BSS method exploits the higher-order statistical differences between the contributory signals to discriminate possible artifact and cerebral components. This is a very difficult problem if one is uncertain of the properties of the artifacts one wishes to separate from the EEG. Artifacts such as EOG and EMG activity can be monitored and used as inputs in such algorithms to identify the isolated components and subsequently filter out their contributions to the EEG recordings without smearing the underlying EEG activity. The work of [54] successfully employ Independent Component Analysis (ICA), a BSS method, to remove blink (EOG), EMG and also line interference artifacts and highlight its superiority over PCA and regressive methods. Although this approach is computationally intensive, many recent research works are directed to such direction [55–57].

### 1.3.3 Feature Extraction for BCI Designs

Different thinking activities result in different patterns of brain signals. BCI is seen as a pattern recognition system that classifies each pattern into a class according to its features. The performance of a pattern recognition system depends on both the features and the classification algorithm employed. Features constitute a new form of expressing the data, and can be binary, categorical or continuous. They represent attributes or direct measurements of the signal.

#### 1.3.3.1 EEG Features

A great variety of features have been used in the literature such as; amplitude values of EEG signals, Band Powers (BP), Power Spectral Density (PSD) values, Auto-Regressive (AR) and Adaptive AutoRegressive (AAR) parameters, Time-frequency features and inverse model-based features [58].

Concerning the design of a BCI system, some critical properties of these features must be taken into consideration [58]. The first property of BCI features that they are noisy or contain outliers because EEG signals have a poor signal-to-noise ratio.

Second, always in BCI systems, feature vectors are often of high dimensionality. Indeed, several features are generally extracted from several channels and from several time segments before being concatenated into a single feature vector. The third property; BCI features should contain time information as brain activity patterns are generally related to specific time variations of EEG. Finally, BCI features are non-stationary since EEG signals may rapidly vary over time and more especially over sessions.

### 1.3.3.2 Feature Dimension Reduction Techniques

As stated above, dimension of the feature space that contains features extracted from raw EEG signals is often very large (102–103 features) [59]. High dimensionality increases the time and space requirements for processing the data. Moreover, in the presence of many irrelevant and/or redundant features, learning methods tend to over-fit and become less interpretable. A common way to resolve this problem is dimensionality reduction, which has attracted much attention in machine learning community in the past decades. Generally speaking, dimensionality reduction can be achieved by either feature selection or subspace learning (a.k.a. feature transformation). The philosophy behind feature selection is that not all the features are useful for learning. Hence it aims to select a subset of most informative or discriminative features from the original feature set. Given a feature set of size M, the feature selection problem is to find a feature subset of size n ( $n \ll M$ ) that maximizes the system's ability to classify object instances. The basic idea of subspace learning is that the combination of the original features may be more helpful for learning. As a result, it aims at transforming the original features to a new feature space with lower dimensionality [60, 61]. In the following paragraphs, some well-known feature selection methods are briefly discussed.

Fisher criterion [60] plays an important role in dimensionality reduction. It aims at finding a feature representation by which the within-class distance is minimized and the between-class distance is maximized. Based on Fisher criterion, two representative methods have been proposed. One is Fisher Score [62], which is a feature selection method. The other is linear discriminant analysis (LDA) [60], which is a subspace learning method. In a very recent work of [63], a modified version of fisher score was used and gave advanced classification accuracy. In [61], LDA method was used for features reduction. Their experiments illustrated that it is possible to classify successfully the “mental tasks” with the use of only 8 electrodes. They proved that linear discriminant analysis is a good tool for feature reduction. Only two components of LDA were used.

Principal components analysis (PCA) and independent component analysis (ICA) are also well-known feature selection methods [64]. Principal Component Analysis (PCA) is a classical technique in statistical data analysis, feature extraction and data reduction. Given a set of multivariate measurements, the purpose is to find a smaller set of variables with less redundancy, which would give as good representation as possible. The redundancy is measured by correlations between data

elements. Since PCA utilizes the first and second moments of the measured data, it relies heavily on Gaussian features. Independent Component Analysis (ICA) is a technique of data analysis accounting for higher order statistics. ICA is a generalization of PCA. Moreover, PCA can be used as preprocessing step in some ICA algorithm. In [65] both ICA and PCA were used for comparison. They illustrated that when using ICA method, only eight independent sources are probably sufficient to recover most of the EEG signals instead of the correlated signals from 28 electrodes. Moreover, they found that only two of these eight sources are required to analyze the P300 curve. These two components summarize the information in the parietal and frontal areas and enable the analysis of two phenomena (P3a and P3b) mixed in the original signals. With PCA, they found only one independent component needed to analyse the P300 peak. They conclude finally that ICA is very promising to analyse multidimensional biomedical signals and much more efficient than PCA in the EEG analysis context [66].

Finally, The genetic algorithm (GA) is a frequently used approach in BCI applications [59, 67, 68]. Its main advantage is that during the exploration of the space of possible solutions, it does not evaluate solutions one by one, but evaluates a set of solutions simultaneously. Moreover, it is not prone to get stuck at local minima and it does not require assumptions about the interactions between features [59]. In [67], GA was used and gave results that indicate its effectiveness for many BCI problems.

### **1.3.4 Classification Methods and Post-processing**

In order to control a BCI, the user must produce different brain activity patterns that will be identified by the system and translated into commands. In most existing BCI, this identification relies on a classification algorithm, i.e., an algorithm that aims at automatically estimating the class of data as represented by a feature vector. Due to the rapidly growing interest for EEG-based BCI, a considerable number of published results is related to the investigation and evaluation of classification algorithms. In order to choose the most appropriate classifier for a given set of features, the properties of the available classifiers must be known.

#### **1.3.4.1 Properties of Classifiers**

Some definitions, commonly used to describe the different kinds of available Classifiers, are reviewed briefly here [58]:

- **Generative/discriminative:** generative (also known as informative) classifiers, e.g., Bayes quadratic, learn the class models. To classify a feature vector, generative classifiers compute the likelihood of each class and choose the most likely. Discriminative ones, e.g., Support Vector Machines, only learn the way

of discriminating the classes or the class membership in order to classify a feature vector directly.

- **Static/dynamic:** static classifiers, e.g., multilayer perceptrons, cannot take into account temporal information during classification as they classify a single feature vector. On the contrary, dynamic classifiers, e.g., hidden Markov model, can classify a sequence of feature vectors and thus, catch temporal dynamics.
- **Stable/unstable:** stable classifiers, e.g., Linear discriminant analysis, have a low complexity (or capacity). They are said stable as small variations in the training set does not affect considerably their performance. On the contrary, unstable classifiers, e.g., multilayer perceptron, have a high complexity. As for them, small variations of the training set may lead to important changes in performances.
- **Regularized:** Regularization consists in carefully controlling the complexity of a classifier in order to prevent overtraining. A regularized classifier has good generalization performances and is more robust with respect to outliers.

A summary of several classifiers used previously in BCI research and their properties is shown in Table 1.1 [58].

#### 1.3.4.2 Brief Survey of Classifiers Used in BCI Research

The classification algorithms used to design BCI systems are divided into five different categories: linear classifiers, neural networks, nonlinear bayesian classifiers, nearest neighbor classifiers and combinations of classifiers. The most popular are briefly described and their most important properties for BCI applications are highlighted [58].

#### 1.3.4.3 Linear Classifiers

Linear classifiers are discriminant algorithms that use linear functions to distinguish classes. They are probably the most popular algorithms for BCI applications. Two main kinds of linear classifier have been used for BCI design, namely, Linear Discriminant Analysis (LDA) and Support Vector Machine (SVM).

The aim of LDA (also known as Fisher's LDA as discussed above) is to use hyperplanes to separate the data representing the different classes. This technique has a very low computational requirement which makes it suitable for online BCI system. Moreover this classifier is simple to use and generally provides good results. Consequently, LDA has been used with success in a great number of BCI systems such as motor imagery based BCI [69], P300 speller [62], multiclass [70] or asynchronous [71] BCI. The main drawback of LDA is its linearity that can provide poor results on complex nonlinear EEG data [72].

The SVM also uses a discriminant hyperplane to identify classes. However, concerning SVM, the selected hyperplane is the one that maximizes the margins,

**Table 1.1** Summary of properties of a great variety of classifiers used in BCI [58]

Classifier	Properties					
	Linear “L”/ Non-linear “NL”	Generative “G”/ Discriminant “D”	Dynamic “DY”/ Static “St”	Regularized	Stable “B”/ unstable “U”	High dimension robust
FLDA	L	D	St		B	
RFLDA	L	D	St	✓	B	
Linear - SVM	L	D	St	✓	B	✓
RBF- SVM	NL	D	St	✓	B	✓
MLP	NL	D	St		U	
BLR- NN	NL	D	St		U	
ALN- NN	NL	D	St		U	
FIR- NN	NL	D	Dy		U	
GDNN	NL	D	Dy		U	
Gaussian NN	NL	D	St		U	
LVQ- NN	NL	D	St		U	
Perceptron	L	D	St		U	
RBF NN	NL	D	St		U	
PeGNC	NL	D	St	✓	U	
Fuzzy Artmap NN	NL	D	St	✓	U	
HMM	NL	G	Dy		U	
IO- HMM	NL	D	DY		U	
Bayes quadratic	NL	G	St		U	
Bayes graphical network	NL	G	St		U	
K- NN	NL	D	St		U	
Mahalanobis distance	NL	D	St		U	

i.e., the distance from the nearest training points. Maximizing the margins is known to increase the generalization capabilities. SVM classifier uses a regularization parameter C that enables accommodation to outliers and allows errors on the training set. This classifier has been applied, always with success, to a relatively large number of synchronous BCI problems [70, 73]. However, it is possible to create nonlinear decision boundaries, with only a low increase of the classifier's complexity, by using the “kernel trick”. It consists in implicitly mapping the data to another space, generally of much higher dimensionality, using a kernel function K ( $x; y$ ).

The kernel generally used in BCI research is the Gaussian or Radial Basis Function (RBF) kernel. The corresponding SVM is known as Gaussian SVM or RBF SVM [74]. RBF SVM has also given very good results for BCI applications [70]. As LDA, SVM has been applied to multiclass BCI problems using the OVR strategy [75]. SVM have several advantages. Actually, thanks to the margin maximization and the regularization term, SVM are known to have good generalization properties [76], to be insensitive to overtraining [77] and to the curse-of-dimensionality [74, 76].

Finally, SVM have a few hyper-parameters that need to be defined by hand, namely, the regularization parameter C and the RBF width—if using kernel. These advantages are gained at the expense of a low speed of execution.

#### 1.3.4.4 Neural Networks

Neural Networks (NN) are, together with linear classifiers, the category of classifiers mostly used in BCI research (see, e.g., [78]). The most widely used NN for BCI, is the Multi-Layer Perceptron (MLP) which have been applied to almost all BCI problems [58, 79, 80]. However, the fact that MLP are universal approximators makes these classifiers sensitive to overtraining, especially with such noisy and non-stationary data as EEG, e.g., [81]. Therefore, careful architecture selection and regularization is required [77]. The Gaussian classifier [82, 83] is another type of NN classifiers. Each unit of this NN is a Gaussian discriminant function representing a class prototype. This NN outperforms MLP on BCI data and can perform efficient rejection of uncertain samples [82]. As a consequence, this classifier has been applied with success to motor imagery [84] and mental task classification, particularly during asynchronous experiments [82].

#### 1.3.4.5 Nonlinear Bayesian Classifiers

This section introduces two Bayesian classifiers used for BCI: Bayes quadratic and Hidden Markov Model (HMM). These classifiers produce nonlinear decision boundaries. Furthermore, they are generative, which enables them to perform more efficient rejection of uncertain samples than discriminative classifiers. However,

these classifiers are not as widespread as linear classifiers or Neural Networks in BCI applications.

Bayesian classification aims at assigning to a feature vector the class it belongs to with the highest probability. The Bayes rule is used to compute the so-called a posteriori probability that a feature vector has of belonging to a given class. Using the Maximum-A Posteriori (MAP) rule and these probabilities, the class of this feature vector can be estimated. Even though this classifier is not widely used for BCI, it has been applied with success to motor imagery and mental task classification [80, 84].

Hidden Markov Models (HMM) are popular dynamic classifiers in the field of speech recognition. An HMM is a kind of probabilistic automaton that can provide the probability of observing a given sequence of feature vectors. Each state of the automaton can modelize the probability of observing a given feature vector. For BCI, these probabilities usually are Gaussian Mixture Models (GMM), e.g., [85]. HMM are perfectly suitable algorithms for the classification of time series [86]. As EEG components used to drive BCI have specific time courses, HMM have been applied to the classification of temporal sequences of BCI features [85] and even to the classification of raw EEG [87]. HMM are not much widespread within the BCI community but these studies revealed that they were promising classifiers for BCI systems. Another type of HMM which has been used to design BCI is the Input-Output HMM (IOHMM) [79]. IOHMM is not a generative classifier but a discriminative one. The main advantage of this classifier is that one IOHMM can discriminate several classes, whereas one HMM per class is needed to achieve the same operation.

#### 1.3.4.6 Nearest Neighbor Classifiers

The classifiers presented in this section are relatively simple. They consist in assigning a feature vector to a class according to its nearest neighbor(s). This neighbor can be a feature vector from the training set as in the case of k-Nearest Neighbors (kNN), or a class prototype as in Mahalanobis distance. They are discriminative nonlinear classifiers. In the case of k- Nearest Neighbors, the aim of this technique is to assign to an unseen point the dominant class among its k nearest neighbors within the training set [88]. For BCI, these nearest neighbors are usually obtained using a metric distance, e.g., [89]. With a sufficiently high value of k and enough training samples, KNN can approximate any function which enables it to produce nonlinear decision boundaries. KNN algorithms are not very popular in the BCI community, probably because they are known to be very sensitive to the curse-of-dimensionality [90], which made them fail in several BCI experiments [89]. However, when used in BCI systems with low-dimensional feature vectors, KNN may prove to be efficient [91].

The Mahalanobis distance based classifiers is a simple yet robust classifier, which even proved to be suitable for multiclass [89] or asynchronous BCI systems [92]. Despite its good performances, it is still scarcely used in the BCI literature.

### 1.3.4.7 Combinations of Classifiers

In most papers related to BCI, the classification is achieved using a single classifier. A recent trend, however, is to use several classifiers, aggregated in different ways. The classifier combination strategies used in BCI applications are the following:

- Boosting:

Boosting consists in using several classifiers in cascade, each classifier focusing on the errors committed by the previous ones. It can build up a powerful classifier out of several weak ones, and it is unlikely to over-train. Unfortunately, it is sensible to mislabels. Boosting had been experimented with MLP and Ordinary Least Square [93, 94].

- Voting:

While using Voting, several classifiers are being used, each of them assigning the input feature vector to a class. The final class will be that of the majority. Voting is the most popular way of combining classifiers in BCI research, probably because it is simple and efficient. For instance, Voting with LVQ NN [95], MLP [96] or SVM [97] have been attempted.

- Stacking:

Stacking consists in using several classifiers, each of them classifying the input feature vector. These classifier are called level-0 classifiers. The output of each of these classifiers is then given as input to a so-called meta-classifier (or level-1 classifier) which makes the final decision. Stacking has been used in BCI research using HMM as level-0 classifiers, and an SVM as meta-classifier [98]. The main advantage of such techniques is that a combination of similar classifiers is very likely to outperform one of the classifiers on its own. Actually, combining classifiers is known to reduce the variance and thus the classification error.

### 1.3.5 Classification Performance Metrics

In the literature, Classifiers performance is usually evaluated using the classifiers' accuracy [58]. Comparison of classifiers from different aspects can be done using different metrics such as sensitivity, specificity, Youden's Index, discriminant power and computation time [99]. Classifiers performance can be improved using a post-processing stage. Some parameters of the classifier can be optimized, according to some measurements in the post-processing block, to reduce the number of false detections [100].

## 1.4 Conclusion

Recent advances in the field of neural prosthetics have led to a renewed interest in the use of brain-computer interfaces (BCIs). One of the most exciting areas of BCI research is the development of devices that can be controlled only through brain signals. These researches aim to use this technological breakthrough to help severely disabled people to function independently. Ranges of non-invasive method were defined in these researches such as electroencephalogram (EEG) and electrocorticographic (ECoG) electrode arrays. Sometimes scientists implanted electrodes directly into the gray matter of the brain itself or on the surface of the brain, beneath the skull in order to have high-resolution signals such as Intracortical neuron recording technique. The chapter provides information about the state of art in neuroimaging based approaches and their related applications. Also the chapter evaluates different classification methodology applied to the brain's captured signals. The BCI related researches will continue to use its modalities to diagnose and suggest treatments for mental diseases. Moreover BCI is directed to robotics industry as the best solution to come up with a robot that senses and acts like human. Also currently scientists study the ways a human user can get a feedback on what the robot hand is experiencing; for example catching a ball or touching hot objects.

## References

1. Cabrera, A.: Feature extraction and classification for brain-computer interfaces. Ph.D. thesis, Brain-Computer Interface Laboratory, Center for Sensory-Motor Interaction (SMI), Department of Health Science and Technology, Aalborg University, Denmark (2009)
2. Nicolas-Alonso, L.F., Gomez-Gil, J.: Brain computer interfaces, a review. *Sensors* **12**(2), 1211–1279 (2012)
3. Khalid, M.B., Rao, N.I., Rizwan-i-Haque, I., Munir, S., Tahir, F.: Towards a brain computer interface using wavelet transform with averaged and time segmented adapted wavelets. In: Proceedings of the 2nd International Conference on Computer, Control and Communication (IC4'09), Karachi, Sindh, Pakistan, 17–18 Feb 2009, pp. 1–4
4. Coburn, K., Lauterbach, E., Boutros, N., Black, K., Arciniegas, D., Coffey, C.: The value of quantitative electroencephalography in clinical psychiatry: a report by the Committee on Research of the American Neuropsychiatric Association. *J. Neuropsychiatry Clin. Neurosci.* **18**(4), 460–500 (2006)
5. Romanowski, P.: How products are made, EEG machine article vol. 7. <http://www.madehow.com/Volume-7/EEG-Machine.html> (2014). Accessed 1 July 2014
6. Marshall, P.J., Saby, J.N., Meltzoff, A.N.: Infant brain responses to object weight: exploring goal-directed actions and self-experience. *Infancy* **18**, 942–960 (2013)
7. Marshall, P.J., Saby, J.N., Meltzoff, A.N.: Imitation and the developing social brain: infants' somatotopic EEG patterns for acts of self and other. *Int. J. Psychol. Res.* **6**, 22–29 (2013)
8. Bos, D.O.: EEG-based emotion recognition—the Influence of visual and auditory stimuli. *Emotion* **57**(7), 1798–1806 (2006)
9. Stikic, M., Johnson, R., Tan, V., Berka, C.: EEG-based classification of positive and negative affective states. *Brain Comput. Interfaces* **1**(2), 99–112 (2014)

10. Freeman, W.J., Holmes, M.D., Burke, B.C., Vanhatalo, S.: Spatial spectra of scalp EEG and EMG from awake humans. *Clin. Neurophysiol.* **114**(6), 1053–1068 (2003)
11. Schwartz, A.B., Cui, X.T., Weber, D.J., Moran, D.W.: Brain-controlled interfaces: movement restoration with neural prosthetics. *Neuron* **52**(1), 205–220 (2006)
12. Leuthardt, E.C., Schalk, G., Roland, J., Rouse, A., Moran, D.W.: Evolution of brain-computer interfaces: going beyond classic motor physiology. *Neurosurg. Focus* **27**(1), E4 (2009)
13. Leuthardt, E.C., Schalk, G., Wolpaw, J.R., Ojemann, J.G., Moran, D.W.: A brain-computer interface using electrocorticographic signals in humans. *J. Neural Eng.* **1**(2), 63–71 (2004)
14. Chao, Z.C., Nagasaka, Y., Fujii, N.: Long-term asynchronous decoding of arm motion using electrocorticographic signals in monkeys. *Frontiers Neuroeng.* **3**(3), 1–10 (2010)
15. Kubanek, J.O.J.W.G.S.J., Miller, K.J., Ojemann, J.G., Wolpaw, J.R., Schalk, G.: Decoding flexion of individual fingers using electrocorticographic signals in humans. *J. Neural Eng.* **6**(6), 066001 (2009)
16. Pistoohl, T., Schulze-Bonhage, A., Aertsen, A., Mehring, C., Ball, T.: Decoding natural grasp types from human ECoG. *Neuroimage* **59**(1), 248–260 (2012)
17. Baillet, S., Mosher, J.C., Leahy, R.M.: Electromagnetic brain mapping. *Sig. Process. Mag. IEEE* **18**(6), 14–30 (2001)
18. Mellinger, J., Schalk, G., Braun, C., Preissl, H., Rosenstiel, W., Birbaumer, N., Kübler, A.: An MEG-based brain-computer interface (BCI). *Neuroimage* **36**(3), 581–593 (2007)
19. The National Research Council (NRC): Canada, Laboratory for Clinical Magnetoencephalography, ARCHIVED—magnetoencephalography system. <http://archive.nrc-cnrc.gc.ca/eng/facilities/ibd/imaging-research/halifax/meg-research.html>. Accessed 1 July 2014
20. Cohen, D.: Magnetoencephalography: detection of the brain's electrical activity with a superconducting magnetometer. *Science* **175**(4022), 664–666 (1972)
21. Zimmerman, J.E., Thiene, P., Harding, J.T.: Design and operation of stable rf-Biased superconducting point-contact quantum devices, and a note on the properties of perfectly clean metal contacts. *J. Appl. Phys.* **41**(4), 1572–1580 (1970)
22. Manoach, D.S., Halpern, E.F., Kramer, T.S., Chang, Y., Goff, D.C., Rauch, S.L., Kennedy, D.N., Gollub, R.L.: Test-retest reliability of a functional MRI working memory paradigm in normal and schizophrenic subjects. *Am. J. Psychiatry* **158**(6), 955–958 (2001)
23. Zamrini, E., Maestu, F., Pekkonen, E., Funke, M., Makela, J., Riley, M., Bajo, R., Sudre, G., Fernandez, A., Castellanos, N., Pozo, F.D., Stam, C. J., Dijk, B.W.V., Bagic, A., Becker, J. T.: Magnetoencephalography as a putative biomarker for Alzheimer's disease. *Int. J. Alzheimer's Dis.*, vol. 2011, Article 280289, pp. 1-10, 2011
24. Hampel, H., Listá, S., Teipel, S.J., Garaci, F., Nisticò, R., Blennow, K., Zetterberg, H., Bertram, L., Duyckaerts, C., Bakardjian, H., Drzezga, A., Colliot, O., Epelbaum, S., Broich, K., Lehéricy, S., Brice, A., Khachaturian, Z.S., Aisen, P.S., Dubois, B.: Perspective on future role of biological markers in clinical therapy trials of Alzheimer's disease: a long-range point of view beyond 2020. *Biochem. Pharmacol.* **88**(4), 426–449 (2014)
25. Rousche, P.J.: Bio-MEMS: designs and applications of cortical interfaces for neuroscience and neuroprosthetics. Lecture notes, Department of Bioengineering, University of Illinois, Chicago, USA. <http://tigger.uic.edu/classes/bioe/bioe200/Rouschelecture.ppt> (2014). Accessed 1 July 2014
26. Karumbaiah, L., Saxena, T., Carlson, D., Patil, K., Patkar, R., Gaupp, E.A., Betancur, M., Stanley, G.B., Carin, L., Bellamkonda, R.V.: Relationship between intracortical electrode design and chronic recording function. *Biomaterials* **34**(33), 8061–8074 (2013)
27. Kozai, T.D., Langhals, N.B., Patel, P.R., Deng, X., Zhang, H., Smith, K.L., Lahann, J., Kotov, N.A., Kipke, D.R.: Ultrasmall implantable composite microelectrodes with bioactive surfaces for chronic neural interfaces. *Nat. Mater.* **11**, 1065–1073 (2012)
28. He, W., McConnell, G.C., Bellamkonda, R.V.: Nanoscale laminin coating modulates cortical scarring response around implanted silicon microelectrode arrays. *J. Neural Eng.* **3**(4), 316–326 (2006)

29. Azemi, E., Stauffer, W.R., Gostock, M.S., Lagenaur, C.F., Cui, X.T.: Surface immobilization of neural adhesion molecule L1 for improving the biocompatibility of chronic neural probes: in vitro characterization. *Acta Biomater.* **4**(5), 1208–1217 (2008)
30. Schwartz, A.B.: Motor cortical activity during drawing movements: population representation during sinusoid tracing. *J. Neurophysiol.* **70**(1), 28–36 (1993)
31. Homer, M.L., Nurmi, A.V., Donoghue, J.P., Hochberg, L.R.: Implants and decoding for intracortical brain computer interfaces. *Annu. Rev. Biomed. Eng.* **15**, 383–405 (2013)
32. Hochberg, L.R., Bacher, D., Jarosiewicz, B., Masse, N.Y., Simeral, J.D., Vogel, J., Haddadin, S., Liu, J., Cash, S.S., Smagt, P., Donoghue, J.: Reach and grasp by people with tetraplegia using a neurally controlled robotic arm. *Nature* **485**, 372–375 (2012)
33. Devlin, H.: What is functional magnetic resonance imaging (fMRI)? <http://psychcentral.com/lib/what-is-functional-magnetic-resonance-imaging-fmri/0001056> (2014). Accessed 1 July 2014
34. Richards, T.L., Berninger, V.W.: Abnormal fMRI connectivity in children with dyslexia during a phoneme task: Before but not after treatment. *J. Neurolinguistics* **21**(4), 294–304 (2008)
35. Wass, S.: Distortions and disconnections: disrupted brain connectivity in autism. *Brain Cogn.* **75**(1), 18–28 (2011)
36. Koshino, H., Kana, R.K., Keller, T.A., Cherkassky, V.L., Minshew, N.J., Just, M.A.: fMRI investigation of working memory for faces in autism: visual coding and underconnectivity with frontal areas. *Cereb. Cortex* **18**(2), 289–300 (2008)
37. Welchew, D.E., Ashwin, C., Berkouk, K., Salvador, R., Suckling, J., Baron-Cohen, S., Bullmore, E.: Functional disconnectivity of the medial temporal lobe in Asperger's syndrome. *Biol. Psychiatry* **57**(9), 991–998 (2005)
38. Norris, K.H.: History of NIR. *J. Near Infrared Spectrosc.* **4**, 31–37 (1996)
39. Villringer, A., Planck, J., Hock, C., Schleinkofer, L., Dirnagl, U.: Near infrared spectroscopy (NIRS): a new tool to study hemodynamic changes during activation of brain function in human adults. *Neurosci. Lett.* **154**(1), 101–104 (1993)
40. Taga, G., Homae, F., Watanabe, H.: Effects of source-detector distance of near infrared spectroscopy on the measurement of the cortical hemodynamic response in infants. *Neuroimage* **38**(3), 452–460 (2007)
41. Repovas, G.: Dealing with noise in EEG recording and data analysis. *Informatica Medica Slovenica J.* **15**(1), 18–25 (2010)
42. Tan, D., Nijholt A.: Brain-Computer Interaction: Applying Our Minds to Human-Computer Interaction. Springer, London (2010)
43. Smith, R.C.: Electroencephalograph based brain computer interfaces. M. Sc. thesis, University College Dublin, Duplin, Ireland (2004)
44. Semmlow, J.: Biosignal and Medical Image Processing, vol. 1. CRC press, Boca Raton (2011)
45. Palaniappan, R., Syan, C.S., Paramesran, R.: Current Practices in Electroencephalogram-Based Brain-Computer interfaces. Encyclopedia of Information Science and Technology, vol. II, 2nd edn. IGI Global, Hershey, pp. 888–901 (2009)
46. Mihajlović, V., Garcia-Molina, G., Peuscher, J.: Dry and water-based EEG electrodes in SSVEP-based BCI applications. In: Biomedical Engineering Systems and Technologies. Springer, Berlin, pp. 23–40 (2013)
47. Hazrati, M.K., Husin, H.M., Hofmann, U.G.: Wireless brain signal recordings based on capacitive electrodes. In: IEEE 8th International Symposium on Intelligent Signal Processing, pp. 8–13 (2013)
48. Lepola P., Myllymaa, S., Toyras, J., Mervaala, E., Lappalainen, R., Myllymaa, K.: Shielded design of screen-printed EEG electrode set reduces interference pick-up. *Sensors J. IEEE*, 1–1 (2014)
49. Sabarigiri, B., Suganyadevi, D.: A hybrid pre-processing techniques for artifacts removal to improve the performance of electroencephalogram (EEG) features extraction. In:

- International Conference on Artificial Intelligence and Evolutionary Algorithms in Engineering Systems, Kumara coil (2014)
- 50. Fatourechi, M., Bashashati, A., Ward, R. K., Birch, G.E.: EMG and EOG artifacts in brain computer interface systems: a survey. *Clin. Neurophysiol.* **118**(3), 480–494 (2007)
  - 51. Millán, J.R., Mourão, J.: Asynchronous BCI and local neural classifiers: an overview of the adaptive brain interface project. *IEEE Trans. Neural Syst. Rehabil. Eng.* **11**(2), 159–161 (2003)
  - 52. Croft, R.J.: Barry RJ (2000) Removal of ocular artifact from the EEG: a review. *Neurophysiologie Clinique/Clin. Neurophysiol* **30**(1), 5–19 (2000)
  - 53. Makeig, S., Kothe, C., Mullen, T., Bigdely-Shamlo, N., Zhang, Z., Kreutz-Delgado, K.: Evolving signal processing for brain-computer interfaces. *Proc. IEEE*, **100** (Special Centennial Issue), 1567–1584 (2012)
  - 54. Jung, T.P., Makeig, S., Humphries, C., Lee, T.W., McKeown, M.J., Iragui, V., Sejnowski, T. J.: Removing electroencephalographic artifacts by blind source separation. *Psychophysiology* **37**(2), 163–178 (2000)
  - 55. Lio, G., Boulinguez, P.: Greater robustness of second order statistics than higher order statistics algorithms to distortions of the mixing matrix in blind source separation of human EEG: implications for single-subject and group analyses. *NeuroImage* **67**, 137–152 (2013)
  - 56. Zhang, Y., Tang, A.C., Zhou, X.: Synchronized network activity as the origin of a P300 component in a facial attractiveness judgment task. *Psychophysiology* **51**(3), 285–289 (2014)
  - 57. Bono, V., Jamal, W., Das, S., Maharatna, K.: Artifact reduction in multichannel pervasive EEG using hybrid WPT-ICA and WPT-EMD signal decomposition technique. In: *IEEE International Conference on Acoustic, Speech and Signal Processing (ICASSP)*, Florence, IT, pp. 1–5 (2014)
  - 58. Lotte, F., Congedo, M., Lécuyer, A., Lamarche, F., Arnaldi, B.: A review of classification algorithms for EEG-based brain-computer interfaces. *J. Neural Eng.* **4**, R1–R13 (2007)
  - 59. Kołodziej, M., Majkowski, A., Rak, R.J.: A new method of EEG classification for BCI with feature extraction based on higher order statistics of wavelet components and selection with genetic algorithms. In: *Adaptive and Natural Computing Algorithms*. Springer, Berlin, pp. 280–289 (2011)
  - 60. García-Laencina, P., Rodríguez-Bermudez G., Roca-Dorda, J.: Exploring dimensionality reduction of EEG features in motor imagery task classification. *J. Expert Syst. Appl.* **41**(11), 5285–5295 (2014)
  - 61. Kołodziej, M., Majkowski, A., Rak, R.J.: Linear discriminant analysis as EEG features reduction technique for brain-computer interfaces. *PRZEGŁĄD ELEKTROTECHNICZNY (Electr. Rev.) R.* **88** NR 3a, 28–30 (2012)
  - 62. Bostanov, V.: BCI competition 2003{data sets ib and iib: feature extraction from event-related brain potentials with the continuous wavelet transform and the t-value scalogram. *IEEE Trans. Biomed. Eng.* **51**(6), 1057–1061 (2004)
  - 63. Şen, B., Peker, M., Çavuşoğlu, A., Çelebi, F.V.: A comparative study on classification of sleep stage based on EEG signals using feature selection and classification algorithms. *J. Med. Syst.* **38**(3), 1–21 (2014)
  - 64. Peterson, D.A., Knight, J.N., Kirby, M.J., Anderson, C.W., Thaut, M.H.: Feature selection and blind source separation in an EEG-based brain-computer interface. *EURASIP J. Appl. Sig. Process.* **19**, 3128–3140 (2005)
  - 65. Gu, Q., Li, Z., Han, J.: Linear discriminant dimensionality reduction. In: *Machine Learning and Knowledge Discovery in Databases*. Springer, Berlin, pp. 549–564 (2011)
  - 66. Bugli, C., Lambert, P.: Comparison between principal component analysis and independent component analysis in electroencephalograms modelling. *Biometr. J.* **49**, 312–327 (2007)
  - 67. Dal Seno, B., Matteucci, M., Mainardi, L.: A genetic algorithm for automatic feature extraction in P300 detection. In: *Neural Networks, IJCNN 2008.(IEEE World Congress on Computational Intelligence)*, pp. 3145–3152 (2008)
  - 68. Yom-Tov, E., Inbar, G.F.: Feature selection for the classification of movements from single movement-related potentials. *IEEE Trans. Neural Syst. Rehabil. Eng.* **10**(3), 170–177 (2002)

69. Pfurtscheller, G., Lopes da Silva, F.H.: Event-related EEG/MEG synchronization and desynchronization: basic principles. *Clin. Neurophysiol.* **110**(11), 1842–1857 (1999)
70. Garrett, D., Peterson, D.A., Anderson, C.W., Thaut, M.H.: Comparison of linear, nonlinear, and feature selection methods for EEG signal classification. *IEEE Trans. Neural Syst. Rehabil. Eng.* **11**, 141–144 (2003)
71. Scherer, R., Muller, G.R., Neuper, C., Graimann, B., Pfurtscheller, G.: An asynchronously controlled EEG-based virtual keyboard: Improvement of the spelling rate. *IEEE Trans. Biomed. Eng.* **51**(6), 979–984 (2004)
72. Garcia, G.N., Ebrahimi, T., Vesin, J.-M.: Support vector EEG classification in the fourier and time-frequency correlation domains. In: Proceedings of the IEEE EMBS 1st International Conference on Neural Engineering, pp. 591–594 (2003)
73. Guerrero-Mosquera, C., Verleysen, M., Navia-Vazquez, A.: Dimensionality reduction for EEG classification using Mutual Information and SVM. In: Machine Learning Signal Processing Conference, pp. 18–21 (2011)
74. Burges, C.J.: A tutorial on support vector machines for pattern recognition. *Data Min. Knowl. Disc.* **2**(2), 121–167 (1998)
75. Schlögl, A., Lee, F., Bischof, H., Pfurtscheller, G.: Characterization of four-class motor imagery EEG data for the BCI-competition 2005. *J. Neural Eng.* **2**(4), L14 (2005)
76. Bennett, K.P., Campbell, C.: Support vector machines: hype or hallelujah? *ACM SIGKDD Explor. Newsl.* **2**(2), 1–13 (2000)
77. Jain, A.K., Duin, R.P.W., Mao, J.: Statistical pattern recognition : a review. *IEEE Trans. Pattern Anal. Mach. Intell.* **22**(1), 4–37 (2000)
78. Gandhi, V., Prasad, G., Coyle, D., Behera, L., McGinnity, T.M.: Quantum neural network-based EEG filtering for a brain-computer interface. *IEEE Trans. Neural Netw. Learn. Syst.* **25**(2), 278–288 (2014)
79. Chiappa, S., Donckers, N., Bengio, S., Vrins, F.: HMM and IOHMM modeling of EEG rhythms for asynchronous BCI systems. In: ESANN, pp. 193–204 (2004)
80. Barreto, G.A., Frota, R.A., de Medeiros, F. N.S.: On the classification of mental tasks: a performance comparison of neural and statistical approaches. In: Proceedings of the IEEE Workshop on Machine Learning for Signal Processing, pp. 529–538 (2004)
81. Balakrishnan, D., Puthusserypady, S.: Multilayer perceptrons for the classification of brain computer interface data. In: Proceedings of the IEEE 31st Annual Northeast Bioengineering Conference, pp. 118–119 (2005)
82. Millan, J.D.R., Mourino, J., Babiloni, F., Cincotti, F., Varsta, M., Heikkonen, J.: Local neural classifier for EEG-based recognition of mental tasks. *Int. J. Conf. Neural Netw. IEEE-INNS-ENNS* **3**, 3632–3632 (2000)
83. Millan, J.R., Renkens, F., Mourino, J., Gerstner, W.: Noninvasive brain-actuated control of a mobile robot by human EEG. *IEEE Trans. Biomed. Eng.* **51**(6), 1026–1033 (2004)
84. Solhjoo, S., Moradi, M.H.: Mental task recognition: a comparison between some of classification methods. In: BIOSIGNAL 2004 International EURASIP Conference, pp. 24–26 (2004)
85. Obermeier, B., Guger, C., Neuper, C., Pfurtscheller G.: Hidden markov models for online classification of single trial EEG. *Pattern Recognit. Lett.* **22**, 1299–1309 (2001)
86. Rabiner, L.R.: A tutorial on hidden markov models and selected applications in speech recognition. *Proc. IEEE* **77**, 257–286 (1989)
87. Solhjoo, S., Nasrabadi, A.M., Golpayegani, M.R.H.: Classification of chaotic signals using HMM classifiers: EEG-based mental task classification. In: Proceedings of the European Signal Processing Conference (2005)
88. Duda, R.O., Hart, P.E., Stork, D.G.: *Pattern Classification*, 2nd edn. Wiley Interscience, New York, (2000)
89. Blankertz, B., Curio, G., Muller, K.R.: Classifying single trial EEG: towards brain computer interfacing. *Adv. Neural Inf. Process. Syst. (NIPS 01)*, **14**, 157–164 (2002)
90. Friedman, J.H.K.: On bias, variance, 0/1-loss, and the curse-of-dimensionality. *Data Min. Knowl. Disc.* **1**(1), 55–77 (1997)

91. Borisoff, J.F., Mason, S.G., Bashashati, A., Birch, G.E.: Brain-computer interface design for asynchronous control applications: improvements to the LF-ASD asynchronous brain switch. *IEEE Trans. Biomed. Eng.* **51**(6), 985–992 (2004)
92. Cincotti, F., Scipione, A., Timperi, A., Mattia, D., Marciani, M.G., Millan, J., Bablioni, F.: Comparison of different feature classifiers for brain computer interfaces. In: First International IEEE EMBS Conference on Neural Engineering, pp. 645–647 (2003)
93. Boostani, R., Moradi, M.H.: A new approach in the BCI research based on fractal dimension as feature and adaboost as classifier. *J. Neural Eng.* **1**(4), 212–217 (2004)
94. Hoffmann, U., Garcia, G., Vesin, J., Diserens, K., Ebrahimi, T.: A boosting approach to P300 detection with application to brain-computer interfaces. In: Proceedings of the 2nd International IEEE EMBS Conference on Neural Engineering. IEEE, pp. 97–100 (2005)
95. Pfurtscheller, G., Flotzinger, D., Kalcher, J.: Brain-computer interface—a new communication device for handicapped persons. *J. Microcomput. Appl.* **16**, 293–299 (1993)
96. Qin, J., Li, Y., Cichocki, A.: ICA and committee machine-based algorithm for cursor control in a BCI system. In: Advances in Neural Networks. Springer, Berlin, pp. 973–978 (2005)
97. Rakotomamonjy, A., Guique, V., Mallet, G., Alvarado, V.: Ensemble of SVMs for improving brain computer interface P300 speller performances. In: Artificial Neural Networks: Biological Inspirations. Springer, Berlin, pp. 45–50 (2005)
98. Wolpert, D.H.: Stacked generalization. *J. Neural Netw.* **5**, 241–259 (1992)
99. Aydemir, O., Kayikcioglu, T.: Comparative performance assessment of classifiers in low-dimensional feature space which are commonly used in BCI applications. *Elektrorevue J.* **2**(4), 58–63 (2011)
100. Mohammadi, R., Mahloojifar A., Coyle, D.: A combination of pre- and postprocessing techniques to enhance self-paced BCIs. *Adv. Human-Comput. Interact.* **2012**(3), (2012)

# **Chapter 2**

## **Basics of Brain Computer Interface**

**Rabie A. Ramadan, S. Refat, Marwa A. Elshahed and Rasha A. Ali**

**Abstract** Brain-Computer Interface (BCI) is a fast-growing emergent technology in which researchers aim to build a direct channel between the human brain and the computer. It is a collaboration in which a brain accepts and controls a mechanical device as a natural part of its representation of the body. The BCI can lead to many applications especially for disabled persons. Most of these applications are related to disable persons in which they can help them in living as normal people. Wheelchair control is one of the famous applications in this field. In addition, the BCI research aims to emulate the human brain. This would be beneficial in many fields including the Artificial Intelligence and Computational Intelligence. Throughout this chapter, an introduction to the main concepts behind the BCI is given, the concepts of the brain anatomy is explained, and the BCI different signals are stated. In addition, the used hardware and software for the BCI are elaborated.

**Keywords** Brain computer interface · Systems of BCI · BCI monitoring hard ware and software · BCI trends

---

R.A. Ramadan (✉)

Computer Engineering Department, Cairo University, Cairo, Egypt  
e-mail: rabie@rabieramadan.org

S. Refat · M.A. Elshahed · R.A. Ali

Physics Department, Faculty of Women for Arts, Sciences and Education,  
Ain Shams University, Cairo, Egypt  
e-mail: Samah\_refat2006@hotmail.com

M.A. Elshahed

e-mail: m\_3li4@yahoo.com

R.A. Ali

e-mail: rasha\_abd\_elnaby@yahoo.com

## 2.1 Introduction

Brain Computer Interface (BCI) is a direct connection between computer(s) and human brain. It is the most recent development of Human Computer Interface (HCI). Unlike the traditional input devices (keyboard, mouse, pen... etc.), the BCI reads the waves produced from the brain at different locations in the human head, translates these signals into actions, and commands that can control the computer (s). The BCI can lead to many applications especially for disabled persons such as [1]: (1) new ways for gamers to play games using their heads, (2) social interactions; enabling social applications to capture feelings and emotions, (3) helping—partially or fully-disabled people to interact with different computational devices, and (4) helping understanding more about brain activities and human neural networks. These applications depend on the basic understanding of how the brain works. BCI applications utilize the brain and its nervous system functions where the human's central nervous system consists of the spinal cord and the brain. One of its tasks is to process and integrate incoming sensory stimuli received via peripheral nerves and to give impulses back to actuators, e.g. to muscles or glands which cause automatic or voluntary action. Furthermore the central nervous system, particularly the brain, is responsible for higher integrative abilities such as thinking, learning, production, and understanding of speech, memory, emotion etc. Finally vegetative functions such as respiration and the cardio-vascular system are controlled by the central nervous system.

The brain computer interface was not studied only for human but also for animals. A Monkey in 2008 [2] was able to move a screen cursor as well as controlling a robot arm. The benefit of such study is to know how animals can think and discover their brains as well. In addition, BCI is used with different human patients capturing their brain signals. The BCI science goes beyond a communication tool for people who are not able to communicate. It is gaining more attention from healthy people for other purposes such as rehabilitation or hands-free gaming. However, BCI tools still limited and need expert to deal with them which is one of the BCI research challenges.

However, there are many challenges that faces the BCI when used in real world tasks as follows:

- (1) **Low BCI signal strength**: it has been noticed that extracting signals from the brain is not an easy task since the signal strength in most of the cases are low. In most of the cases, signal amplification is required. Many of the used toolkits include such amplifiers while some others do not include good amplifiers.
- (2) **Data transfer rate (bandwidth)**: the best data transfer rate from a subject was 3 characters. Certainly, this is very low data transfer that makes the BCI applications suffer from fast response as well as accurate control.
- (3) **High error rate**: it is obvious that due to the low data transfer rate and the low signal strength, the error percentage became high. In addition, the brain signal is very high variability. Therefore, the expected error rate is high.

- (4) **Inaccurate signal classification:** brain have some centers that signals can be captured from them using electrodes. Classifying the captured signals suffer from high interference and inaccurate classification. There are many signal classification techniques are utilized including the computational intelligence techniques that are recently proposed by authors in [3].

The goal of this chapter is to provide the reader with basic concepts of the BCI as a science and from it came from. The anatomy of the brain is elaborated for better understanding to the brain signals. The chapter goes on by providing the different signals that were able to be captured recently. These signals are classified and their characteristics are explained. Finally, the chapter explains the current hardware and software components of the BCI including the commercial devices and their properties.

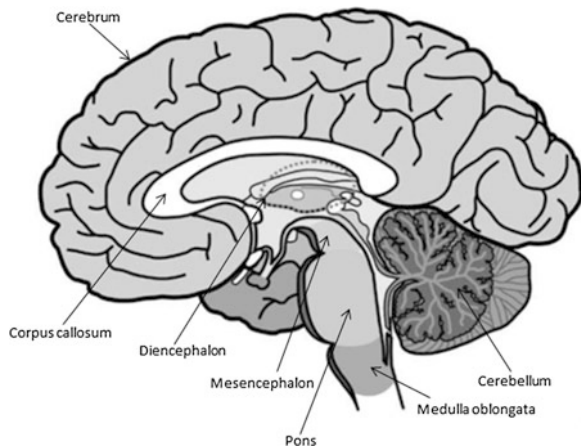
## 2.2 Brain Anatomy

Amazingly, nothing in the world can be compared with the human brain. The three-pound organ controls all body functions including receiving and interpreting information from the outside world, and expressing the essence of the mind and soul. Intelligence, creativity, emotion, and memories are a few of the many things governed by the brain. The brain receives information through different sensors such as sight, smell, touch, taste, and hearing. The brain constructs the received data from the different sensors and form a meaningful message. The brain controls our body movement of the arms and legs, thoughts, memory and speech. It also determines how a human respond to different situations such as stress by regulating our heart and breathing rate.

As it is known, the nervous system is another essential system in the human body. The nervous system divided into central and peripheral systems. The central nervous system is composed of two main parts which are the brain and spinal cord. The peripheral nervous system is composed of spinal nerves that branch from the spinal cord and cranial nerves that branch from the brain. The peripheral nervous system includes the autonomic nervous system, which controls vital functions such as breathing, digestion, heart rate, and secretion of hormones.

The brain skull represents the shield of the brain from injury. It is formed from 8 bones. These bones include the frontal, two parietal, two temporal, sphenoid, occipital and ethmoid. The face is formed from 14 paired bones including the maxilla, zygoma, nasal, palatine, lacrimal, inferior nasal conchae, mandible, and vomer [4].

Anatomically five basic parts of the brain can be distinguished including Cerebrum, Diencephalon, Cerebellum, Mesencephalon, and Medulla oblongata as shown in Fig. 2.1. The cerebrum, located directly under the skull surface, is the largest part of the brain. Its main functions are: (1) the initiation of complex movement, (2) speech and language understanding and production, (3) memory, and (4) reasoning. Brain monitoring techniques which make use of sensors placed

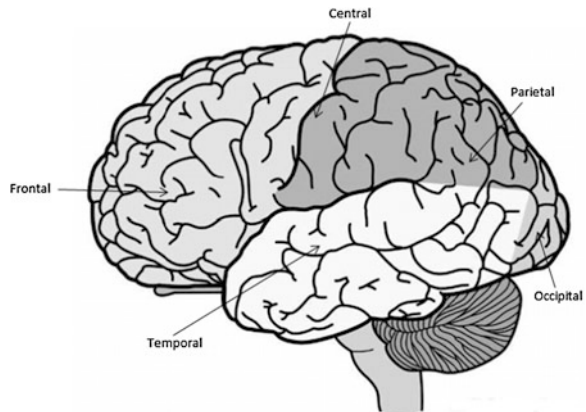
**Fig. 2.1** Brain anatomy [8]

on the scalp mainly record activities from the outermost part of the cerebrum; the cortex. More inside the cerebrum the basal ganglia can be found which consists of a number of nuclei controlling the direction of slow movements [5]. Also the thalamus is located here which directs sensory information to appropriate parts of the cortex. The second part of the brain is the Diencephalon. One important function of the diencephalon is the forwarding of sensory information to other brain areas. Besides that, it contains the hypothalamus which controls the body temperature, the water balance and the ingestion to assure the state of homeostasis for the body, i.e. “good working conditions” for all body cells. The coordination of all kinds of movements is done in the third part which is the cerebellum. Therefore, it cooperates closely with structures from the cerebrum (e.g. the basal ganglia). Cerebellum and Cerebrum are connected via the Pons. However, the largest part of the reticular system is located in the Mesencephalon where it controls vigilance and the sleep-wake rhythm.

The Medulla Oblongata connects the brain with the spinal cord. Respiration and the cardiovascular system are controlled by that part of the central nervous system. Furthermore, a huge number of peripheral nerves pass through the medulla oblongata. Compared to the brains of other mammals, the human brain has the largest and best developed cortex. Neural processes related to abilities like complex reasoning, speech and language etc. which distinguish humans from other mammals take place in that part of the brain [6, 7].

Moreover, the cortex consists of two hemispheres which are connected via a beam called corpus callosum. Each hemisphere is dominant for specific abilities. For right handed persons, the right hemisphere is activated more during the recognition of geometric patterns, spatial orientation, the use nonverbal memory and the recognition of non-verbal noises [8]. More activity in the left hemisphere can be observed during the recognition of letters and words, the use verbal memory and auditory perception of words and language. Each hemisphere is partitioned into five anatomically well-defined regions, the so called lobes as given in Fig. 2.2.

**Fig. 2.2** Hemisphere partitions [8]



## 2.3 Brain Computer Interface Types

Brain computer interface can be classified into three main groups as shown in Fig. 2.3. Classification depends on the way that the electrical signal is obtained from neuron cells in the human brain.

### 2.3.1 Invasive BCI Acquisition Techniques

In invasive BCI techniques, special devices have to be used to capture the brain signals. Such devices are called Invasive BCI devices; devices that are based on detecting from single area of brain cells is called single unit while the detection from multiple areas is called multi-units [9]. Invasive BCI devices are inserted directly into the human brain by a critical surgery as can be seen in Fig. 2.4. The electro-corticogram (ECoG) are the obtained signals from these inserted electrodes [10]. These devices have the highest quality of human brain signals but have the risk of forming scar tissue.

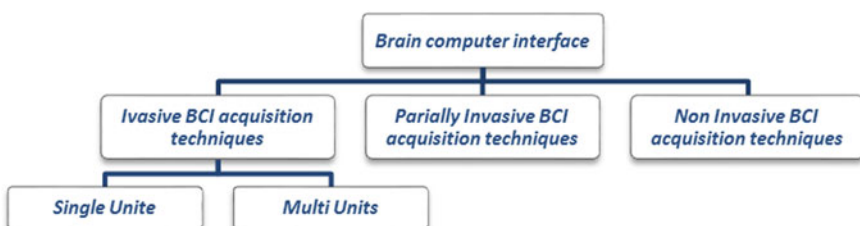


**Fig. 2.3** Brain computer interface types

**Fig. 2.4** Invasive BCI electrodes [10]

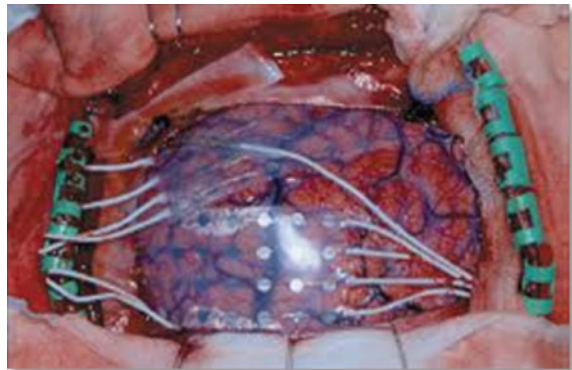
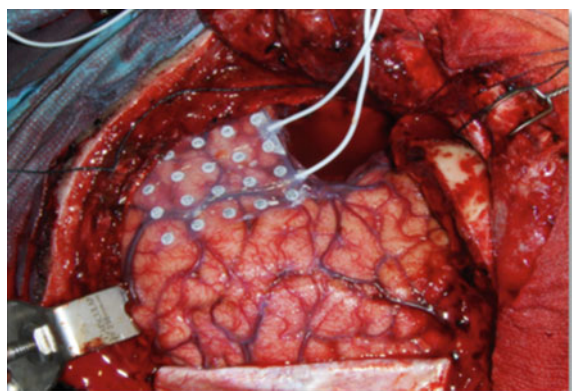


**Fig. 2.5** Partially invasive BCI electrodes



### 2.3.2 *Partially Invasive BCI Acquisition Techniques*

Other devices that can capture the signal from the brain are the partially invasive BCI devices. Devices are inserted in the skull on the top of human brain as depicted in Fig. 2.5. These devices have bit weaker quality of human brain signals than invasive BCIs and have less risk of forming scar tissue [11, 12].

### 2.3.3 *Non Invasive BCI Acquisition Techniques*

Non Invasive BCI devices are considered the safest type and low cost type of devices. However, these devices have weaker human brain signals than other BCI devices due to the skull. The detection of signals is done by some electrodes placed on the scalp as given in Fig. 2.6. At the same time, placing such electrodes is easy as well as portable. Most noninvasive techniques are constructed by recording ElectroEncephaloGraphs (EEG) from the scalp. Recent EEG Non Invasive BCI

**Fig. 2.6** A wireless non-invasive signal capturing device



devices have better temporal resolution due to use up to 256 electrodes on the whole area of the human scalp. While others, Non Invasive BCI devices, use functional Magneto-Resonance Imaging (fMRI), Positron Electron Tomography (PET), MagnetoEncephaloGraphy (MEG) and Single Photon Emission Computed Tomography (SPECT) [13, 14].

## 2.4 Types of BCI Signals

The brain generates an amount of neural activity. There are a plethora of signals, which can be used for BCI. These signals are divided into two classes: spikes and field potentials [11]. Spikes reflect the action potentials of individual neurons and acquired through microelectrodes implanted by invasive techniques. Field potentials are measures of combined synaptic, neuronal, and axonal activity of groups of neurons and can be measured by EEG or implanted electrodes. The following is the classification of EEG signals based on their frequencies/bands [15, 10].

- **Delta Signal.** It is captured within the frequency range of 0.5–3.5 Hz. It tends to be the highest in amplitude and the slowest waves. It is seen normally in adults in slow wave sleep as well as in babies. A sample from the Delta signals is shown in Fig. 2.7.
- **Theta.** The frequency of this signal ranges from 3.5 to 7.5 Hz. Theta is linked to inefficiency and daydreaming. In fact, the very lowest waves of theta represent the fine line between being awake or in a sleep. However, as shown in Fig. 2.8, high levels of theta are considered abnormal in adults.



**Fig. 2.7** Delta wave sample



**Fig. 2.8** Theta wave sample



**Fig. 2.9** Alpha wave sample



**Fig. 2.10** Beta wave



**Fig. 2.11** Gamma wave

- **Alpha.** As shown in Fig. 2.9, this signal frequency ranges from 7.5 to 12 Hz. Hans Berger [12] named the first rhythmic EEG activity he saw, the “alpha wave”. Range seen in the posterior regions of the head on both sides, being higher in amplitude on the dominant side. It is brought out by closing the eyes and by relaxation. Several studies have found a rise in alpha power after smoking marijuana.
- **Beta.** Beta is another brain signal in which its frequency ranges from 12 Hz to about 30 Hz. It is seen usually on both sides in a symmetrical distribution and it is most evident frontally. Beta waves are often divided into  $\beta_1$  and  $\beta_2$  to get more specific range. The waves are small and fast when resisting or suppressing movement, or solving a math task. It has been noticed in these cases that there is an increase of beta activity. The shape of such signal is shown in Fig. 2.10.
- **Gamma.** It is a signal with frequency range of 31 Hz and up. It reflects the mechanism of consciousness. Figure 2.11 shows the shape of the Gamma signal.

## 2.5 Components of Interest

Components of particular interest to BCI can be divided into four categories which are oscillatory EEG activity, event-related potentials (ERP), slow cortical potentials (SCP), and neuronal potentials.

### 2.5.1 Oscillatory EEG Activity

Oscillatory EEG activity is caused by complex network of neurons that create feedback loops. The synchronized firing of the neurons in these feedback loops generates observable oscillations. There are two distinct oscillations of interest which are: (1) the Rolandic mu-rhythm, in the range 10–12 Hz, and (2) the central beta rhythm, in the range 14–18 Hz. This activity represents “idling” or rest state [10].

### 2.5.2 Event-Related Potentials

Event-Related Potentials (ERPs) are time-locked responses by the brain that occur at a fixed time after a particular external or internal event. These potentials occur when subjected to sensory, mental event, or the omission of a constantly occurring stimulus. Exogenous ERP components occur due to processing of the external event but independent of the role of the stimuli in the processing of information. On the other hand, Endogenous ERP components occur when an internal event is processed. It depends on the role of the stimulus in the task and the relationship between the stimulus and the context in which it occurred [10]. The ERP events can be classified as follows:

- *Event-Related Synchronization/(De) synchronization*

A particular type of ERP is characterized by the occurrence of an event-related desynchronization (ERD) and an event-related synchronization (ERS). A decrease in the synchronization of neurons causes decrease of power in specific frequency bands. This phenomenon is defined as an ERD and can be identified by a decrease in signal amplitude. ERS is characterized by an increase of power in specific frequency bands that is generated by an increase in the synchronization of neurons and/or in signal amplitude.

- *Visual-Evoked Potentials*

Another type of ERF commonly used in BCI is the visual-evoked potential (VEP), an EEG component that occurs in response to a visual stimulus. VEPs are dependent on the user’s control of their gaze and thus require coherent muscular control [16]. P300 is ERP component elicited in the process of decision making. The P300 is thought to reflect processes involved in stimulus evaluation or categorization. It is usually elicited using the oddball paradigm, in which low-probability target items are mixed with high-probability non-target item [17]. The user is presented with a task that cannot be accomplished without categorization into both categories. When an event from the rare category is displayed, it elicits a P300 component, which is a large positive wave that occurs approximately 300 ms after event onset [10].

- *Slow Cortical Potential*

It is the slow cortical potential, which is caused by shifts in the depolarization levels of certain dendrites. Negative SCP indicates the sum of synchronized potentials, but positive SCP indicates the reduction of synchronized potentials from the dendrites.

- *Neuronal Potential*

Neuronal potential is a voltage spike from individual neurons. This potential can be measured for a particular neuron or a group of neurons. The signal is a measure of the average rate, correlation, and temporal pattern of the neuronal firing. Learning can be measured through changes in the average firing rate of neurons located in the cortical areas associated with the task [8].

## 2.6 Monitoring Brain Activity Using EEG

Several techniques have been used to monitor brain activities such as (1) Electroencephalography (EEG), (2) Magnetoencephalography (MEG), (3) Functional Magnetic Resonance Imaging (fMRI), (4) Functional Near-Infrared Spectroscopy (fNIRS), (5) Single Photon Emission Tomography (SPECT), and (6) Proton Emission Tomography (PET). Each method has its own characteristics as well as pros and cons. However, for several reasons the potential differences which can be measured between two points of the scalp are very different from those could be measured when electrodes were implanted directly in the brain. For instance, the activity of the potential generators could be measured directly by:

1. A superposition of potentials generated in different areas of the cortex is measured using scalp electrodes since brain tissue and the liquor are conductive.
2. The amplitude of the originally generated potential differences is attenuated because of the resistive properties of the tissue between the potential generators and the electrode (e.g. liquor, skin, bone of the skull).
3. Capacities caused by cell membranes and other inhomogeneities (e.g. liquor-skull, skull-skin) between potential generators and electrodes influence the amplitude of the EEG signals as a function of their frequency.

Therefore, the positions for EEG electrodes should be chosen in a way, which all cortex regions are covered. For most applications, this is usually the whole cortex. An internationally accepted standard for electrode placements is the 10–20 system (electrodes are placed at distances of 10 or 20 % of the length of several connections between some reference points) introduced in 1957 by the International EEG Federation [18]. Electrodes were placed according to the 10–20 system. Three anatomical reference points must be determined before the 10–20 system electrode positions which are:

1. Nasion: the onset of the nose on the skull, below the forehead.
2. Inion: the bony protuberance which marks the transition between skull and neck.
3. Pre-auricular reference point: located before the cartilaginous protrusion of the acoustic meatus (the auditory canal).

Figure 2.12 shows the electrode positions of the 10–20 system in their projection on the cortex. The name for a particular electrode position reflects the anatomical region of the cortex above which it is located. Fp stands for frontopolar, F stands for frontal, T stands for temporal, C stands for central, P stands for parietal, O stands for occipital and A stands for auricular while G denotes the ground electrode. Even numbers denote the right part of the head, odd numbers refer the left part.

Generally, there are two categories of artifacts can be distinguished in EEG measurements which are biological and technical. The biological artifacts are caused by the recorded subject and technical artifacts are caused by the EEG recording device. The sources of many biological artifacts are dipoles originating for example from muscular activities which are much stronger than the EEG related

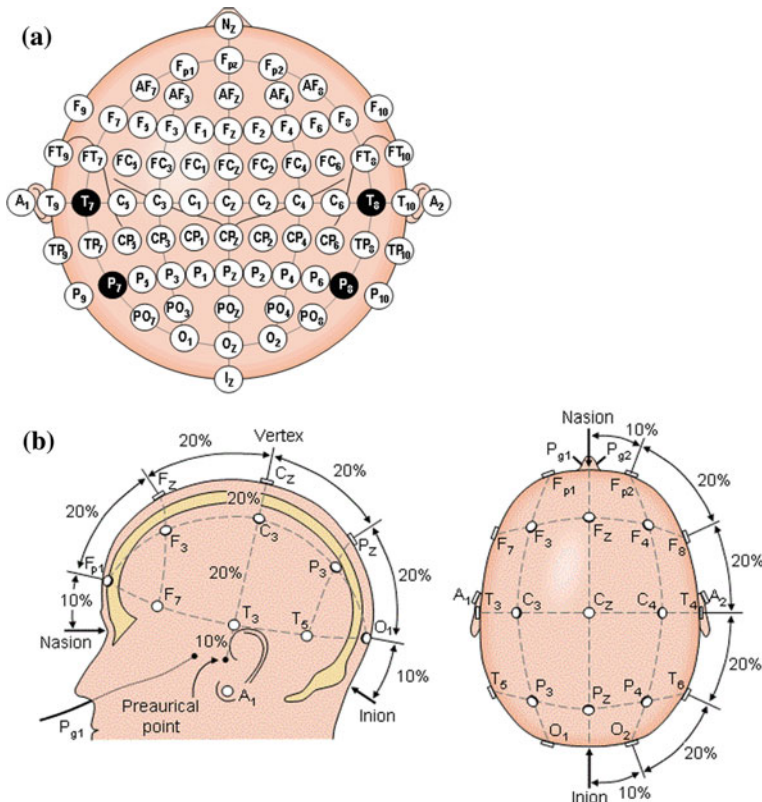


**Fig. 2.12** Electrode position. **a** Brain electrodes. **b** top view of the brain and electrodes positions [12]

dipoles. A superposition of both types of dipoles causes artifacts in the signal which are often characterized by large peaks or fluctuations of a particular morphology. Sometimes, however, they can hardly be distinguished from the actual EEG. Other biological artifacts influence the contact between skin and electrode or the electrical properties of the medium between potential generators and electrodes.

## 2.7 BCI System

Forming a BCI system requires following three main steps as shown in Fig. 2.13:

**Step 1** is the signal acquisition, **Step 2** is the signal processing, and **Step 3** is the data manipulation.

**Step 3:** Using these obtained signals to control in external devices or computer depending on the application.

### **Step 1: Signal Acquisition**

Signal acquisition process is required to capture the brain electric signals. The electric signals could be recorded from the scalp, the surface of the brain, or from the neural activity. Since the capture signals strength are usually low, they need to be amplified. Then, to be used by computer applications, they need to be digitized.

### **Step 2: Signal Processing**

In this step, obtained signals in step 1 are analyze to get the control signals. Signal processing could be done through some other sub operations as follows:

- *Preprocessing*

The first part of signal processing is preparing the recording electric signal for processing like enhancement to make the features clear for detection. Some filtering techniques could be used in the preprocessing operation.

- *Feature extraction*

Simply, feature extraction means extracting specific signal features. EEG recordings not only contain electrical signals from the brain, but also several

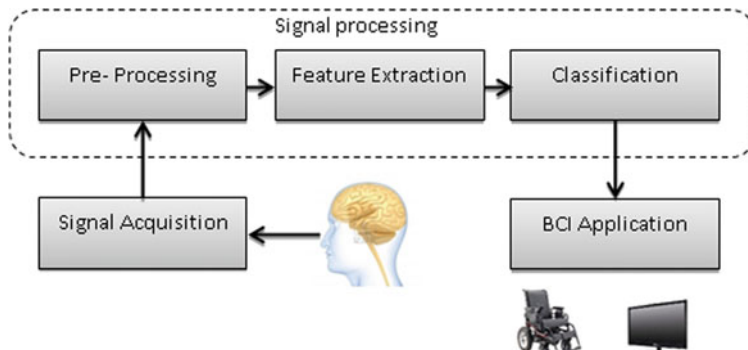


**Fig. 2.13** BCI signal processing

unwanted signals. Those unwanted signals may bias the analysis of the EEG and may lead to wrong conclusions. Therefore, the digitized signals are subjected to feature extraction procedures.

- **Signal Classification: translation algorithm**

The next stage, the translation algorithm, in which it translates the extracted signal features into device commands orders that carry out the user's intent. The signals are classified on both frequency and on their shape; the classification algorithm might use linear methods or nonlinear methods.

**Step 3: Data Manipulation**

Once the signals are classified, the output is manipulated to suite the output devices (e.g. computer screen).

## 2.8 BCI Monitoring Hardware and Software

BCI signals are very week signals that need special treatments to be handled correctly. The strength of the measured signals is usually between 1  $\mu$ V and 100 mV along with the scalp impedance and other noises. In order to receive such signals and display them on digital formats, suitable amplifiers should be used. Therefore, the BCI hardware can be divided into three classes; the first class is the electrodes while the second class is the signal amplifiers. The third class is the real time signal handling. Throughout this section, a brief description to each class is provided.

The EEG measurement electors are usually made of gold or Ag/AgCl. The gold electrodes are effective in measuring EEG, EMG or ECG signals as well. However, the Ag/AgCl electrodes proved to be more effective when the EEG frequencies below 0.1 Hz. In addition, there are two types of electrodes which are active and passive electrodes. The active electrodes contain an amplifier with gain 1–10 inside it in which it reduces the noise and cable interferences. On the other hand, passive electrodes do not include any amplifiers in electrodes service. Such electrodes are usually distributed on the scalp from 10 to 20 electrodes in most of the cases (Fig. 2.14).

**Fig. 2.14** Gold electrodes  
[13]



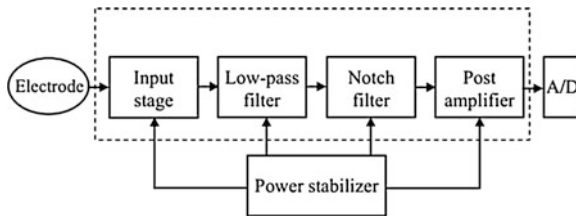
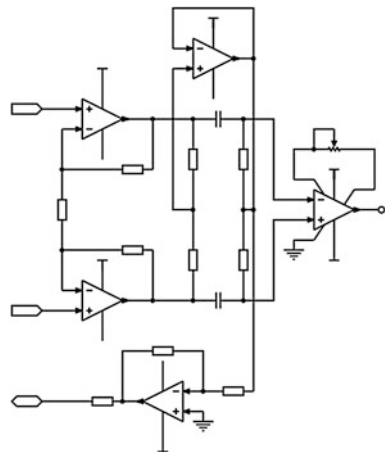


**Fig. 2.15** Electrode's signal filters

**Fig. 2.16** Electrode's amplifier



The other part of the BCI hardware is the biological signal amplifier. It is one of the important parts of physiological recording and analysis in which the brain signals are very weak and it is used to amplify them. Figure 2.15 [19] is a sample of BCI amplifier. As can be seen in the Figure, signals captured by electrodes are amplified through handling by the input stage component to remove the possible noise produced from electrode-skin interfaces. In fact, it is a pre-amplified circuit that could be simply based on simple op-amp OPA2277 devices as shown in Fig. 2.16. The signal is also passed through two filters which are Low-pass filter and Notch filter. After all, the signal is post amplified.

Real time signal recording and analysis is managed on different Operating Systems including windows and Linux as well as Mac OS. C++ is one of the most used language for analysis over C++ LabVIEW (National Instruments Corp., Austin, TX, USA) and MATLAB (The MathWorks Inc., Natick, USA) are mostly used as programming languages. Different signals are utilized to control many applications. There is some commercial software and hardware kits are already used in some of the BCI applications. One of the software kits is the neurobci [8] in which it allows users to develop their own Brain Computer Interface (BCI), bio- or neurofeedback application, as created in Html/Jscript, C++, or Matlab. FieldTrip

**Fig. 2.17** Emotive headset

[20] is a MATLAB toolbox that is used for analysis. It utilizes TCP connections for multiple clients as at the same time.

*DataSuite* [21] is another software tool for data acquisition. The DataSuite consists of two parts including the DataRiver and MatRiver. DataRiver is a data management and synchronization real time engine while MatRiver is a MATLAB client toolbox for DataRiver. The following Figure shows the data flow of DataSuite. For more details about other BCI tools, the reader is encouraged to read the survey by Arnaud et al. [22] Fig. 2.17: DataSuite data flow. Two computers each running an instance of DataRiver are represented. One acquires data (left); the other (right) uses MatRiver to perform data classification and feedback visualization. Dashed lines indicate control signals.

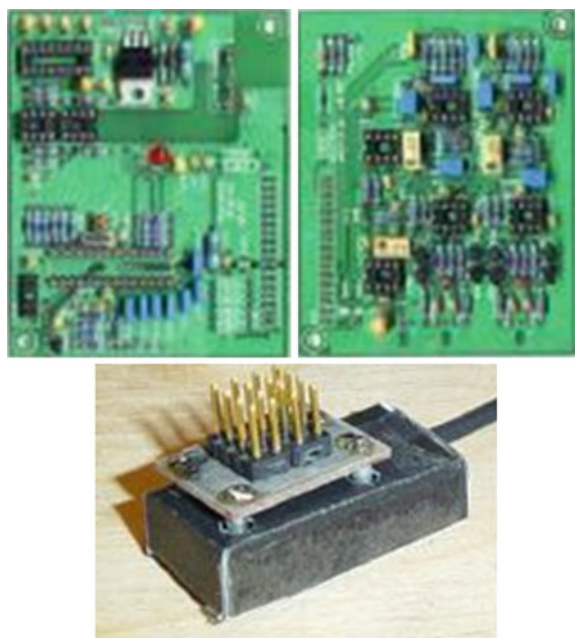
*Emotiv* EEG neuroheadset [23] is a wireless BCI set; this set is a neuro-signal acquisition and processing wireless neuroheadset. The set can be wirelessly connected to a computer. One advantage of the set is it has 14 saline sensors offer optimal positioning for accurate spatial resolution.

ModularEEG [24] is another EEG hardware created by the OpenEEG hardware developers. The modularEEG has two or more EEG amplifiers, and a 6-channel signal capture board that connects to a PC via a standard serial cable. The modularEEG has two types of electrodes which are active and passive electrodes. Some skin preparation is required while there is no preparation is required when active electrodes are used. Figure 2.18 shows the modularEEG board and the active electrodes.

## 2.9 Brain Computer Interface Applications

BCI is interesting area to researchers because it can solve many problems which seem to be impossible. The essential target of BCI applications is to convert the user's intent or thoughts to an action in external device or computer and control to

**Fig. 2.18** ModularEEG device



these devices. Many applications of BCI concerned on patients suffer from disorders of consciousness (DOC). These patients unable to make communication with their around world [25].

By using BCI, these patients can control some devices to perform basic and important jobs they need without helping like moving with wheelchair, getting something for eating or drinking by using robotic legs or arms controlled by brain. BCI technologies are used to restore the vision to blinds by connecting an external camera with brain [26]. Applications on device control not include patients only, but also healthy users like whose needs to perform many jobs at the same time like divers, astronauts and drivers where they keep their hands on swimming, operate equipment and the steering wheel [27].

Rabie et al. [28] developed a BCI based system that can help disabled persons to use the web through their brains only. The authors developed a technique that captures the eye signals through the brain to select the appropriate letters as well as words to be written on the web browser. Another application that has been developed is the wheelchair simulator that is controlled also by the BCI signals.

BCI used also on User-state monitoring which make alert to sleepy drivers or students. Also, it extended physically to measure the heart beats for users. Many applications focused in entertainment and playing games especially after using 3D monitors, certain glasses and an EEG headset where the control on the game by thoughts. EEG combined sometimes with eye movement on some applications for security and safety where the system can monitor suspicious objects, deviant behavior or arousal state. A common BCI application is neurofeedback training to

improve working, attention, executive functions and memory. Neuroergonomics is an evaluation application used to estimate how well human abilities match a technology. BCI used also in education and training techniques [25]. By sing BCI based on EEG, patient can control or move the cursor by mental thoughts where the patient can select words or letters [26].

## 2.10 BCI Trends

The BCI technology has achieved many goals in different working areas of medical and nonmedical during the last ten decades. Researchers in this filed are looking in the future for more development in trends and applications. Since the current trends are focused on utilizing of motor system which is related to: (1) the electroencephalogram (EEG) signals for neurorehabilitation, (2) controlling of robot and exoskeleton based on EEG signal, (3) implementation of BCI component on field programmable and reconfigurable computing system, and (4) solving the interoperability and standardization issues of BCI software platforms. Researchers looking for developing a common file format for BCI data exchange and introducing an accurate and robust pre-processing and feature extraction techniques of BCI signals.

One of the most future trends is introducing a new kind of sensory modality that is more accurate and safe [29]. The revolution in nanotechnology will contribute in the progress of BCI by producing a smaller and far superior chips that can implant safely in the brain to yield high quality signals. The target is to increase the BCI reliability and accuracy to be clinically useful. Moreover, a wireless brain implant is an important technology today that lets people with mobility problems control a computer or wheelchair with their thoughts. The wireless brain sensor can record the activity of dozens of neurons in freely moving subjects [30]. Even though wireless BCI systems may provide a number of advantages. There are still many issues that need to be resolved including improving signal quality, more compact and stylish system designs, and implementation of useful applications [31].

BCIs driven by auditory stimuli are a relatively new phenomenon. With some key publications over the last 5 years, the auditory BCI approach has gained and continues to gain momentum. It is underpinned by the BCI community's efforts to find alternatives to the traditional BCI paradigms to meet the needs of end users who require a non-visual communication system. The trends now are seeking to study the effect of BCI auditory not only in communication field but also in attention monitoring and neurofeedback training to improve performance. In addition, how BCI auditory can contribute in diagnosis and treatment of disorders that have an auditory component is another issue to be handled.

Another trend now is Tactile and Bone-Conduction based BCI Paradigms. It has been proposed to offer alternative ways to deliver sensory stimulation inputs which could be crucial for patients suffering from weak or lost eye-sight or hearing. Already several preliminary techniques have been developed to connect the BCI to a traditional haptic interface or to utilize those interfaces as stimulation sources.

Vibrotactile stimulation brings also a possibility to create bone-conduction sensory effect in case of the head area excitors application. This point is still very preliminary yet relative to the existing applications. It brings a very interesting possibility to deliver multimodal stimuli (somatosensory and auditory combined) to TLS/ALS subjects with a very fast information transfer rate.

Currently, the field of BCI requires deeper insights on how to capture the right signals and then process them suitably. Efforts are being made to recognize the objects as they are seen by the brain. These efforts will bring in newer dimensions in the understanding of brain functioning, damage and repair. It is possible to recognize the thoughts of the human brain by capturing the right signals from the brain in future [8].

The P300 is an event related potential, a measurable electrical charge that is directly related with impulse. Therefore, by capturing the P300, a BCI can directly translate a person's intent into electrical commands that control artificial devices. A P300 speller is based on this principle, where the detection of P300 waves allows the user to write characters [26]. The trend now is solving the P300 speller classification problems such as, the detection of the presence of a P300 in the electroencephalogram (EEG) and the combination of different P300 responses for determining the right character to spell.

Over the past 20 years, Brain-Computer Interfaces (BCI) have been shown to be very promising for numerous applications, such as rehabilitation or entertainment, among many others. Despite this potential, most BCI applications remain prototypes that are not used in practice, outside laboratories. The main reason is the widely acknowledged low reliability of current BCI systems that are based on the translation of the spontaneous non-invasive electroencephalogram (EEG); mental tasks performed by the user are being too often incorrectly recognized by the BCI. Poor recognition performances are due in part to "imperfect" signal processing algorithms used to analyze EEG signals. However, another component in the BCI loop may also be deficient such as the signal generator, i.e., the user him/herself who may not be able to reliably produce EEG patterns. Indeed, it is widely acknowledged that BCI use is a skill, which means the user must be properly trained to achieve successful BCI control. So the main trend now is improving reliability of BCI by teaching and training the users to the BCI skills.

## 2.11 Conclusion

The BCI reads the waves produced from the brain at different locations in the human head, translates these signals into actions, and commands that can control the computer(s). Brain computer interface can be classified into three main groups which depend on the way that the electrical signal is obtained from neuron cells in the human brain. The brain generates an amount of neural activity. There are a plethora of signals, which can be used for BCI. These signals divide into two classes: spikes and field potentials, Components of particular interest to BCI can be

divided into four categories which are oscillatory EEG activity, event-related potentials (ERP), slow cortical potentials (SCP), and neuronal potentials. Several techniques have been used to monitor brain activities; each technique has its own characteristics as well as pros and cons. BCI is interesting area to researchers because it can solve many problems which seem to be impossible. Many applications focused in entertainment and playing games especially after using 3D monitors, certain glasses and an EEG headset where the control on the game by thoughts. Researchers in this field are looking in the future for more development in trends and applications. Since the current trends are focused on utilizing of motor system.

## References

1. Melody, M.: Real-world applications for brain-computer interface technology. *IEEE Trans. Neural Syst. Rehabil. Eng.* **11**(2), 162–165 (2003)
2. Pei, X., Barbour, D., Leuthardt, E., Schalk, G.: Decoding vowels and consonants in spoken and imagined words using electrocorticographic signals in humans. *J. Neural. Eng.* **8**(4), 1–11 (2011)
3. Azar, A.T., Balas, V.E., Olariu, T.: Classification of EEG-based brain-computer interfaces. advanced intelligent computational technologies and decision support systems. *Stud. Comput. Intell.* **486**, 97–106 (2014)
4. Buckner, R., Andrews-Hanna, J., Schacter, D.: The brain's default network: anatomy, function, and relevance to disease. *Ann. N. Y. Acad. Sci.* **1124**, 1–38 (2008)
5. Minshew, N., Keller, T.: The nature of brain dysfunction in autism: functional brain imaging studies. *Curr. Opin. Neurol.* **23**, 124–130 (2010)
6. Gilbert, S., Dumontheil, I., Simons, J., Frith, C., Burgess, P.: Wandering minds: the default network and stimulus-independent thought. *Sci. Mag.* **315**(5810), 393–395 (2007)
7. Looney, D., Kidmose, P., Mandic, P.: Ear-EEG: user-centered and wearable BCI. *Brain-Comput. Interface Res. Biosyst. Biorobot.* **6**, 41–50 (2014)
8. Kameswara, T., Rajyalakshmi, M., Prasad, T.: An exploration on brain computer interface and its recent trends. *Int. J. Adv. Res. Artif. Intell. (IJARI)* **1**(8), 17–22 (2013)
9. Wolpaw, J., Birbaumer, N., McFarland, D., Pfurtscheller, G., Vaughan, T.: Brain–computer interfaces for communication and control. *Clin. Neurophysiol.* **113**, 767–791 (2002)
10. He, B.: Neural engineering. Springer publisher, New York, ISBN:978-1-4614-5226-3 (2013)
11. Wolpaw, J.: Brain-Computer interfaces: signals, methods, and goals. Proceeding of 1st international IEEE EMBS conference on neural engineering, vol. 1, pp. 584–585 (2003)
12. Lebedev, M., Nicolelis, M.: Brain–machine interfaces: past, present and future. *Trends Neurosci.* **29**(9), 536–546 (2006)
13. Pfurtscheller G. Neuper. C.: Motor imagery and direct brain computer communication. *Proc. IEEE* **89**(7), 1123,113 (2001)
14. Schalk, G., Mellinger, J.: A practical guide to brain-computer interfacing with BCI. Springer, ISBN:978-1849960915 (2010)
15. Yang, Z., Wang, Y., Ouyang, G.: Adaptive neuro-fuzzy inference system for classification of background EEG signals from ESES patients and controls. *Sci. World J.* **2014**, 140863 (2014)
16. Middendorf, M., Mcmillan, G., Calhoun, G., Jones, K.S.: Brain computer interfaces based on steady state visual evoked response. *IEEE Trans. Rehabil. Eng.* **8**(2), 211–214 (2000)
17. Tamara, B., Howard, J.: Privacy by design in brain-computer interfaces. University of Washington, UWEE, technical report number UWEETR-2013-0001 (2013)

18. Ebner, A., Sciarretta, G., Epstein, C., Nuwer, M.: EEG instrumentation. The international federation of clinical neurophysiology. *Electroencephalogr. Clin. Neurophysiol. Suppl.* **52**, 7–10 (1999)
19. Xian-Jie, P., Tie-Jun, L., De-Zhong, Y.: Design of an EEG preamplifier for brain-computer interface. *J. Electr. Sci Technol China* **7**(1), 56–60 (2009)
20. Robert, O., Pascal, F., Eric, M., Jan-Mathijs, S.: FieldTrip: open source software for advanced analysis of MEG, EEG, and invasive electrophysiological data. *J. Comput. Intell. Neurosci.* **2011**, 156869 (2011)
21. Lingaratnam, S., Murray, D., Carle, A., Kirsa, S., Paterson, R., Rischin, D.: Developing a performance data suite to facilitate lean improvement in a chemotherapy day unit. *J. Oncol. Pract.* **9**(4), 115–121 (2013)
22. Arnaud, D., Christian K., Andrey V., Nima B., Robert O., Thorsten Z., Scott M.: MATLAB-based tools for BCI research. In: Desney, S.T., Anton, N. (eds.) (B + H)CI: the human in brain-computer interfaces and the brain in human-computer interaction book. ISBN 978-1-84996-271-1, Springer, Chap. 14, pp. 241–259 (2010)
23. Arindam, D., Robins, K., Suruchi, M., Sanjay, C., Alakananda, B., Anirban, D.: A low-cost point-of-care testing system for psychomotor symptoms of depression affecting standing balance: a preliminary study in india. *Depression Res. Treat.* **2013**, 640861 (2013)
24. Setijadi, A., Novanda, O., Mengko, T.: Development of an experimental portable electroencephalograph (case study: alpha wave detector). International conference on electrical engineering and informatics (ICEEI), vol. 1, no. 6, pp. 17–19 (2011)
25. Chatelle, C., Chennu, S., Noirhomme, Q., Cruse, D., Owen, A.M., Laureys, S.: Brain-computer interfacing in disorders of consciousness. *Brain Inj.* **26**(12), 1510–1522 (2012)
26. Anupama, H., Cauvery, N., Lingaraju, G.: Brain computer interface and its types-a study. *Int. J. Adv. Eng. Technol. (IJAET)* **3**(2), 739–745 (2012)
27. Jan, B., Van, E., Fabien, L., Michael, T.: Brain computer interfaces: beyond medical applications. *IEEE Comput. Soc.* **45**(4), 26–34 (2012)
28. Rabie, A., Ahmed, E., Mohamed, A.: JustThink: smart BCI applications. Proceedings of seventh international conference on bio-inspired computing: theories and applications. advances in intelligent systems and computing, vol. 201, pp. 461–472 (2012)
29. Alwasiti, H., Aris, I., Jantan, A.A.: Brain computer interface design and applications: challenges and future. *World Appl. Sci. J.* **11**(7), 819–825 (2010)
30. Wang, U., Wang, Y., Jung, T.: A cell-phone based brain-computer interface for communication in daily life. Proceedings of the 2010 international conference on artificial intelligence and computational intelligence (AICI'10), pp. 233–240 (2010)
31. Reza Fazel-Rezai (ed.): *Brain-Computer Interface Systems - Recent Progress and Future Prospects*, ISBN: 978-953-51-1134-4, InTech, Chap. 11, pp. 37–39, (2013)

## **Chapter 3**

# **Noninvasive Electromagnetic Methods for Brain Monitoring: A Technical Review**

**Tushar Kanti Bera**

**Abstract** Human brain is a large, complex and most important organ in its nervous system. The brain works as a central processing unit (CPU) of the human body and performs, coordinate, control and regulate an incredible number of tasks to keep the human body healthy and alive. Though the brain is highly protected inside the rigid skull, meninges and cerebral spinal fluid (CSF), the human brain is still sometimes gets injured, damaged and gets several number of diseases. Therefore the study of brain is important and very essential for diagnose and treatment of the diseases like stroke, brain tumors, traumatic brain injury, encephalitis, meningitis, Parkinson's disease, intracerebral hemorrhage, brain aneurysm, multiple sclerosis, hydrocephalus etc. As the electromagnetic brain imaging methods have drawn a lot of attentions of the medical doctors, clinicians and biomedical researchers for their unique advantages. This chapter will present the review of the studies on the noninvasive electromagnetic methods for brain monitoring, diagnosis and treatment. The chapter will try to present the detail technical aspects of different electromagnetic brain monitoring modalities (EBMM), their applications and challenges. The chapter will start by introducing to the human brain and its diseases followed by a discussion on the history and the developments of the brain monitoring techniques. It will discuss about the present scenario of the conventional brain monitoring methods with their merits and demerits. The chapter will explain the electromagnetic brain monitoring techniques in detail such as Electroencephalography (EEG), Magnetoencephalography (MEG), Electrocorticography (ECoG), electroneurogram (ENG), electrical impedance tomography (EIT), Quantitative susceptibility mapping (QSM) and other advanced brain monitoring modalities. The chapter will discuss about their working principles, applications, advantages, disadvantages, present scenario. The chapter will summarize the studies on the electromagnetic methods for brain monitoring and it will conclude with a discussion on the present challenges and future trends.

---

T.K. Bera (✉)

Department of Computational Science and Engineering, Yonsei University, Seoul 120749,  
South Korea

e-mail: tkbera77@gmail.com

**Keywords** Human brain · Brain function and brain diseases · Brain monitoring · Electromagnetic brain monitoring modalities

### 3.1 Introduction

Human brain [41, 52, 79, 161] is one of the most important organs of the human anatomy [65] which controls all other organ performing a number of tasks to keep the human body healthy and alive. Brain is developed with more than 100 billion nerves [52], that communicate in trillions of connections called synapses. It is not only the main organ in the nervous system [12, 152], but also it is one of the largest and most complex organs in the human body. The human brain is suspended in cerebrospinal fluid (CSF) [41, 52, 79, 161] covered by the brain membrane called meninges which is surrounded, supported and protected by skull [41, 52, 79, 161].

Brain is developed with a large number of nerve cells called neurons. *Neurons*, or nerve cells, which generate the brain potentials and act as the communication units to perform all of the communication and processing within the brain to keep the human body healthy and well functioning. The human brain can be segmented by three main components: the cerebrum, the cerebellum, and the brainstem each of which has its own important and distinct functions [96]. The cerebrum which is the largest and most developmentally advanced part of the human brain [96] which is responsible for several higher functions, including higher intellectual function, speech, emotion, integration of sensory stimuli of all types, initiation of the final common pathways for movement, and fine control of movement. Being the second largest area of the brain, the cerebellum maintains the body balance and further control of movement and coordination [96]. The brain stem which acts as the final pathway between cerebral structures and the spinal cord controls a variety of automatic functions, respiratory control, heart rate control, and blood pressure control, wakefulness, arousal and attention [96].

The human is a living central processing unit in our body which receives input from the sensory organs and sends output to the muscles and other organs or body parts. Being the CPU of the human body the brain receives the information from the rest of the body, process and interpreting that information, respond to send the signal to the organs or the body parts to act accordingly. It gives us awareness by processing a constant stream data received by the sensing parts of the body and controls the movements of the body parts by contracting or relaxing the muscles, functioning of the organs including the control of the vital operations like breathing, maintaining body temperature and blood pressure, and releasing hormones. Brain also controls heart rhythms, body movement and balancing, hearing, eyesight, swallowing, speech, emotion and sleep. Though there are different ways of dividing the brain anatomically into regions, but generally, based on embryonic development, the brain is divided into three main regions: the forebrain, midbrain and hindbrain. The forebrain or prosencephalon is made up the cerebrum, thalamus,

hypothalamus and pineal gland among other features where as the midbrain or mesencephalon is developed with the portion of the brainstem. The hindbrain or rhombencephalon is developed with the remaining brainstem and the cerebellum and pons.

The brain is protected from damage by several layers of solid or liquid envelopes. The human brain is suspended in a fluid called cerebrospinal fluid (CSF) which is covered by a thin membrane called meninges. The meninges is covered by the outermost solid and rigid bones which developed a solid and protective envelop called skull. Though the brain is highly protected inside the rigid skull, meninges, CSF and isolated from the bloodstream by the blood-brain barrier (BBB), the human brain is still prone to injury, damage and several number of disease [65] such as stroke, brain tumors, traumatic brain injury, encephalitis, meningitis, Parkinson's disease, intracerebral hemorrhage, brain aneurysm, multiple sclerosis, hydrocephalus etc. Therefore the study of brain is important and very essential for diagnose and treatment of the diseases.

Noninvasive diagnoses have always been found with number of advantages in most of the medical diagnoses and clinical investigations. Though X-Ray computed tomography [4, 56, 75, 85] and magnetic resonance imaging (MRI) [75, 121, 184, 207] provides a lot of information about the human brain anatomy and physiology, still, the electromagnetic methods have their own advantages and potentials in brain monitoring. Being the fast, radiation free and noninvasive techniques, the electromagnetic brain monitoring and investigations [8, 10, 23, 24, 97, 98, 153, 157, 181] are being researched by a number of research groups over the world.

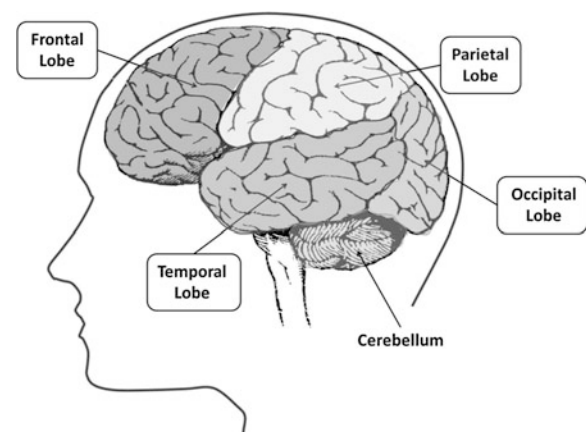
In this direction the present chapter will present a detail discussion and review on the noninvasive electromagnetic methods for brain monitoring, diagnosis and treatment. The chapter will try to present the detail technical aspects of different electromagnetic brain monitoring modalities (EBMM), their applications and challenges. The chapter will start with an introduction to the human brain and its diseases along with a discussion on the history, developments of the brain monitoring techniques. It will then present the present scenario of the conventional brain monitoring methods with their merits and demerits. The chapter will next present the introduction to the electromagnetic brain monitoring techniques such as Electroencephalography (EEG) [7, 10, 98, 137], Magnetoencephalography (MEG) [10, 98, 157], Electrocorticography (ECoG) [153], electroneurogram (ENG) [181], electrical impedance tomography (EIT) [23, 24], Quantitative susceptibility mapping (QSM) [135, 136] and other advanced brain monitoring modalities. The chapter will discuss about their working principles and other technical aspects along with their advantages, disadvantages and challenges. The chapter will also discuss the historical development of the electromagnetic technologies for brain monitoring along with their present scenario. After that a detail discussion will be presented on the different applications of the electromagnetic methods for brain monitoring, mapping and imaging. It will summarize the chapter presented on the electromagnetic methods for brain imaging and it will conclude with a discussion on present challenges and future trends.

### 3.2 Human Brain Anatomy

Human brain, which is developed with more than 100 billion nerves, is one of the most important organs of the human body which controls all other organ performing a number of essentials tasks to keep the human body healthy and alive. It is not only the main organ in the nervous system, but also it is one of the largest and most complex organs in the human body. In the human body, the brain is suspended in cerebrospinal fluid (CSF) covered by the brain membrane, called meninges, which is surrounded, supported and protected by skull. Being the main controlling unit of the body, the brain controls the entire nervous system [12, 152] and all the other systems in human body including cardiovascular system [1], respiratory system [208], gastrointestinal system [124], renal system [163], endocrine system [80] etc. It continuously observe, supervise and controls the performance of all the other organs by sending physiological signals through the nervous system [12, 152] connecting the brain to the other parts of the body [65, 161].

Thus the brain works as a central processing unit (CPU) of the human body and performs, coordinate, control and regulate an incredible number of tasks [161] including the controlling the heart function, breathing activity, blood pressure, body temperature, activities of body receptors and sensors and so on. The human brain gives us the power to move, walk, speak, listen, understand, memorize, think, imagine, dream, reason, and solve a number of problems and experiences emotions. As per the positions and functions, the brain can be divided in different parts such as cerebrum, cerebellum, and brainstem [161] which have their own particular functions. The cerebrum, which is divided into four lobes (Fig. 3.1): frontal, parietal, temporal, and occipital, is the largest part of the brain and it performs the most sophisticated functions such as interpreting touch, vision and hearing, speaking, reasoning, emotions, learning, and fine control of movements. On the other hand, the cerebellum, located under the cerebrum, controls the muscle movements and maintains posture, balance and main movements. The brainstem is developed with

**Fig. 3.1** Anatomy of the human brain



the midbrain, pons, and medulla; and performs as a relay center connecting the cerebrum and cerebellum to the spinal cord of the human body and conducts and controls a number of automatic functions such as breathing, heart rate, body temperature, wake and sleep cycles, digestion, sneezing, coughing, vomiting, and swallowing.

Thus the brain is made up of the following specialized regions:

- *The cortex* it is the outermost layer of brain cells which controls the thinking and voluntary movements.
- *The brain stem* it is between the spinal cord and the rest of the brain which controls the basic functions like breathing and sleep.
- *The basal ganglia* they are a cluster of structures in the center of the brain which coordinate messages between other brain areas.
- *The cerebellum* it is at the base and the back of the brain which controls the coordination and balance.

The brain is also divided into several lobes:

- *The frontal lobes* they are responsible for problem solving and judgment and motor function.
- *The parietal lobes* they manage sensation, handwriting, and body position.
- *The temporal lobes* they are involved with memory and hearing.
- *The occipital lobes* they contain the brain's visual processing system.

### 3.3 Brain Diseases

The brain controls the functioning of all the organs inside the human body. It controls thoughts, memory, speech, movement, emotions etc. When the brain is healthy and functioning properly all the organs are in control and perform their own work in a regular and routine manner but as soon as the brain gets any disease it starts malfunctioning. The malfunctioning of the brain affect the functioning of the other organs in the body sometimes creates some life threatening situations.

The physiological change such as inflammation, loss of brain cells, tumors etc. in the brain create a number of problems. As for example, the inflammation in the brain can produce vision loss, weakness and paralysis where as the thinking capability is affected by the loss of brain cells produced by stroke. Brain tumors can lead to a lot of problem including the abnormal pressure on nerve cells which severely affect the normal brain function. Brain disease may occur due to the physiological changes in the brain, accidents or sometime it may be genetic even the sources of some brain diseases are still required to be explored such as Alzheimer's disease [99]. In the brain diseases the physiological changes or the damage in the brain is permanent whereas in some other cases, proper diagnosis, analysis and treatments such as surgery, medicines, or physical therapy can correct the source of the problem or improve symptoms [99].

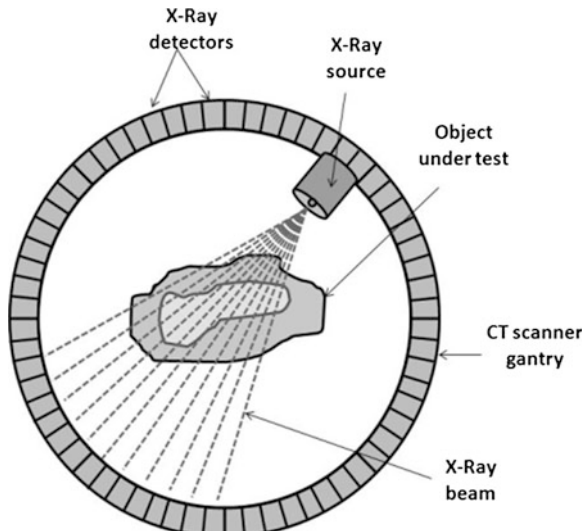
The malfunctioning of normal brain due to the anatomical and/or physiological changes in the brain itself or in the other body parts is called the brain disorder or brain disease. There are a number of diseases which can be diagnosed, studied and analyzed by EEG such as: Headache [81], Brain aneurysm [166], Parkinson's disease [129], Meningitis [170], Epilepsy [31], Encephalitis [134], Brain tumor [71], Stroke (brain infarction) [147], Subdural hematoma [182], Epidural hematoma [77], Autism [216], Cerebral edema [158], Schizophrenia [123, 192], Traumatic brain injury [179, 201], Intracerebral hemorrhage [201], Alzheimer's Disease [54], Dyslexia [180], Attention Deficit Hyperactivity Disorder (ADHD) [142, 143], Brain abscess [202], etc.

### 3.4 Noninvasive Brain Monitoring

The study of brain is essential for diagnose, study and analyze and treatment of the diseases. Noninvasive disease diagnosing procedures have always been found with number of advantages in medical science and as the brain is very important and complex part of the life controlling all the other body parts, the noninvasive brain disease diagnoses are always preferred.

X-Ray Computed Tomography (CT) [65], or Computed Axial Tomography (CAT) is a computer based tomographic imaging procedure which produces the cross sectional view (image) of the spatial distribution of a X-Ray attenuation coefficient of an object under test from the attenuated X-Ray data generated by a rotating X-Ray beam passing through the object (Fig. 3.2). In X-Ray CT scanner, the object is placed inside an aperture or hole in the scanner called gantry containing

**Fig. 3.2** Positron emission tomography schematic



the rotating X-Ray source and an array of X-Ray detectors placed at the periphery of the gantry. The X-Ray beam is passed through the object and the attenuated X-Ray data are collected on the X-Ray receivers and the spatial distribution of the X-Ray attenuation co-efficient of the object is reconstructed and displayed as an tomographic image using one mathematical algorithm called the image reconstruction algorithm [42, 204].

Single Photon Emission Computed Tomography (SPECT or SPET) [35, 44, 59, 95, 150, 169] is also a computed tomographic technique which is used reconstruct the image of the distribution of the radiopharmaceuticals applied to the patient body by collecting and processing the gamma-rays (produced by the radioisotope) at different projection angles around the patient using a gamma camera rotating around the patient. During the SPECT procedure, a radiopharmaceuticals, which is a radioactive pharmaceutical called radioisotope and is used in the field of nuclear medicine as the tracers in the diagnosis and treatment of many diseases, is injected or inhaled, or ingested inside the patient body and the gamma rays produced by the radioisotope is collected at different angle by rotating the a gamma ray receiving instrument called gamma camera and the cross sectional anatomy of the object.

Positron emission tomography (PET) [64, 69, 100, 169] works with the similar principle of the transverse SPECT [150] except the type of the radiation detected at the receiving points. In PET, the tracer applied to the patient's body emits positrons that annihilate with electrons up to a few millimeters away, causing two gamma photons to be emitted in opposite directions (Fig. 3.3), on the contrary, the tracer used in SPECT, emits gamma radiation that is measured directly. Actually, in PET procedure, the directionality of the annihilation photons (two 511-keV annihilation photons emitted in opposite directions), which are produced by the radiation caused by the annihilation of positrons with electrons, provides a mechanism for localizing the origin of the photons [100]. Thus, when two diametrically opposite detectors in the detector array (surrounding the patient) of a PET system register annihilation photons simultaneously, the positron decay process that created the photons is assumed to have occurred along a line between the detectors [100].

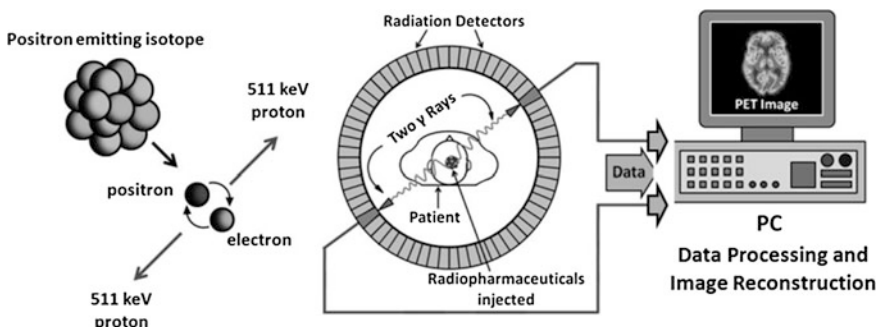


**Fig. 3.3** Positron emission tomography schematic

### ***3.4.1 Advantages of PET***

PET method has the following advantages [70]:

1. PET can provide the absolute measures of regional cerebral blood flow (rCBF), which are very difficult to obtain with other modalities.
2. PET provides the possibility of mapping the particular receptor in the brain by using appropriate radioisotope.

### ***3.4.2 Disadvantages of PET***

PET method has the following disadvantages [70]:

1. PET is invasive,
2. Radioactive materials are injected to the body during the PET procedures.
3. PET is very expensive (partly because the radioactive tracers need to be manufactured on the spot).
4. PET has relatively poor temporal resolution (it requires at least 40s to obtain an image).

## **3.5 Electromagnetic Brain Monitoring Methods**

The CT uses the X-Rays which is an ionizing radiation and PET and SPECT both procedures inject an radioactive materials inside the patient's body. Though the brain monitoring techniques with X-Ray computed tomography [92], PET, SPECT [61, 190] provides a lot of information about the human brain anatomy and physiology, still, the electromagnetic methods have their own advantages and potentials in brain monitoring. Electromagnetic brain monitoring methods are safe, radiation free, noninvasive, and hence, the electromagnetic brain monitoring methods are being studied by a number of research groups for studying the brain function and diagnosing, analyzing and evaluation a number of brain diseases. The electromagnetic brain monitoring methods can be broadly classified as signal acquisition or signal processing methods and imaging methods. Among the signal acquisition method the major electromagnetic methods are electroencephalography (EEG), Magnetoencephalography (MEG), Electrocorticography (ECoG), electro-neurogram (ENG). On the other hand, the magnetic resonance imaging (MRI) [40, 73, 101, 133, 168, 205], Functional MR Imaging (fMRI) [37, 39, 68, 132, 146, 172] and electrical impedance tomography (EIT) [23, 24] are the brain imaging modalities.

The CT, SPECT and PET, are relatively older methods of brain imaging. CT images the brain anatomy in terms of the X-Ray attenuation coefficient of the brain tissue by applying X-Rays whereas the SPECT and PET reconstructs the local changes in blood flow by injecting the radioactive tracers into the bloodstream. The MRI and fMRI are comparatively newer methods and are found as provide considerably better spatial resolution and involves no radioactivity [37].

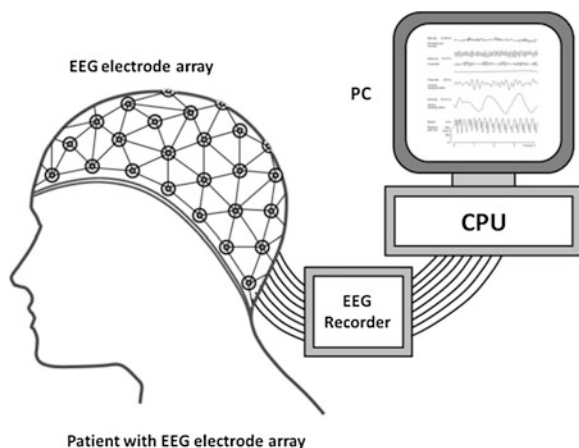
### 3.5.1 Brain Metabolism and Brain Imaging

Although the human brain represents only 2 % of the body weight, the brain consumes up to twenty percent of the energy used by the human body, more than any other organ [38]. Brain consume mainly the bloodglucose as an energy source by receiving 15 % of the cardiac output, 20 % of total body oxygen consumption, and 25 % of total body glucose utilization [46]. Due to the lack of glucose, which is happened in case of hypoglycemia [53], the brain activity is affected and it can result in loss of consciousness [102]. Though the energy consumed by the brain does not vary greatly over time, but active regions of the cortex consume comparatively more energy than the inactive regions: this fact forms the basis for the functional brain imaging methods such as PET and fMRI [102, 173].

### 3.5.2 Electroencephalography (EEG)

Electroencephalography (EEG) is the neurophysiologic measurement technique (Fig. 3.4) which measures and record the electrical activity of the brain of the

**Fig. 3.4** Schematic of the electroencephalography (EEG)



electrical activity of the brain using surface electrodes placed on the scalp. The method is known as the electroencephalography where as the recorded signal which is the recorded oscillations of brain electric potentials is called electroencephalogram. Measuring and studying the EEG doctors and clinicians can get the information about the brain activities which help them not only to study the normal brain activity but also to diagnose a number of brain diseases and neurological disorders. In 1924, the German psychiatrist Hans Berger first recorded the human EEG.

### 3.5.2.1 History

The history and evolution of Electroencephalography (EEG) [49] can be related to the works conducted on Electrophysiology by Luigi Galvani, in the 18th century what discovered the electrical potential of living tissue [50] when he observed that the muscles of dead frog legs contracted when struck by a spark in 1771 [112]. After that, with the theories developed and experimentations conducted by Ohm and Faraday on the electric potential, electric conductors and electric insulators and the magnetic fields, when Johan Poggendorff developed the mirror galvanometer in 1826, the era of the EEG was just about to come [112]. After that, Richard Caton first recorded electrical activity from exposed brains of rabbits and monkeys as the first electroencephalography by using high-quality electrodes to reduce the effects of artifacts and noise [112] and he studied the EEG variation due to the sleep, wakefulness, anesthesia, death and responses to food on 40 animals. In 1924, Hans Berger first recorded the human EEG signals of a 17-year-old boy during his head surgery for tumor using non-polarizable clay cylinder electrodes and Edelmann's small string galvanometer [113].

### 3.5.2.2 EEG Potentials

EEG signal can be classified as two types depending on the generation of the brain signals such as Event related potentials (ERPs) [144] and Spontaneous or free-running EEG [118].

1. **Event related potentials (ERPs) or Evoked Potentials:** It is the measured brain potential signal which is directly generated as a stereotyped electrophysiological response to a stimulus such as a specific sensory, cognitive, or motor event. The evoked potentials are generated and recorded by the patient's brain by applying a stimulus, such as a flash light or loud click to the sensory system of the patient.
2. **Spontaneous or free-running EEG:** It is the found naturally produced and rhythmic brainwaves which are generated by outside activity.

### 3.5.2.3 Source of Brain Potentials

The neurophysics of EEG is governed by the electric fields of the brain [162]. The potentials are generated by the brain's electrical charges which are maintained by billions of brain cells called neurons inside the brain. The membrane transport proteins pump the ions across their membranes of the brain cell and hence the brain cells or neurons are electrically charged or "polarized". To maintain some physiological state or phenomena essential for normal brain functioning such as resting potential and to propagate action potentials, the neurons are constantly exchanging ions with the extracellular milieu inside the brain. The ions pushed by some neurons when comes to the other ions with similar polarity generated or pushed by the other neurons repel each other. When many ions are pushed out of many neurons at the same time, these ions push their neighbouring ions that again push their neighbouring ions and so on and a wave of ions is generated which is actually an ionic conduction inside the brain. The ionic conduction inside the brain is converted to the electron conduction inside the EEG recording cables (outside the brain) by the surface electrodes attached to the scalp. Using amplifier and measuring devices the electric voltage signals are measured and recorded as EEG. Thus the EEG measures voltage fluctuations resulting from ionic current flows within the neurons of the brain [159]. The brain voltage signals are collected by the surface electrodes from the pairs of electrodes and hence the EEG signals represent the voltage difference between two scalp electrodes. As the individual brain potentials appearing on each electrode is fluctuating over time, the EEG signals measured across two electrodes are also found as the fluctuating voltage signal over time [198]. EEG activity is always reflects the summation of the synchronous activity of a huge number of neurons that have similar spatial orientation inside the brain because the electric potential generated by an individual neuron is very small to be recorded by an EEG instrument [103]. If the cells do not have similar spatial orientation, their ions do not line up and create waves to be detected. Pyramidal neurons of the cortex are thought to produce the most EEG signal because they are well-aligned and fire together. Because voltage fields fall off with the square of distance, activity from deep sources is more difficult to detect than currents near the skull [130].

### 3.5.2.4 The EEG Interpretation

The EEG waves obtained from the scalp electrodes shows oscillations at a variety of frequencies and each wave having characteristic frequency ranges, spatial distributions and are associated with different states of brain functioning such as waking and the various sleep stages etc. [103]. Among the different EEG oscillations representing the synchronized activities over different network of neurons called neuronal networks, some oscillations are well understood, while many others are not [103].

### 3.5.2.5 Brain Waves and EEG Diagnosis

The level of consciousness and brain activity and functions can be evaluated from the EEG signal (Fig. 3.5) because the brain potentials are closely related to the person's brain activities [130]. As for example, when the eyes are closed, the alpha waves begin to dominate the EEG. It is observed that, as the brain activity increases, the EEG signals shift to higher dominating frequency and the signal amplitude decreases whereas, the dominant EEG frequency decreases when the activity reduces or during the sleep [130]. The EEG waves also help us to detect the different phase of sleeps (Fig. 3.5) such as rapid eye movement (REM sleep) and non-rapid eye movement (NREM or non-REM sleep) [130]. In REM sleep the person dreams and has active movements of the eyes which is reflected in the characteristic EEG signal. The EEG signal of a person in deep sleep has the brain waves with large and slow deflections [130]. No brain signal is generated for a patient with complete cerebral death and hence, no cerebral activity can be detected from the EEG signal measured.

The human brain is made up of billions of brain cells called neurons, which all generates some electricity to communicate with each other and hence the electric potential signal generated by a large number of neurons produces an enormous amount of electrical activity in the brain, called brain wave, which can be detected by EEG. The different types of brain waves are explained below (Fig. 3.6):

The delta wave [76] which is the slowest band of brain waves, is a high amplitude brain wave with a frequency of oscillation between 0–4 Hz. Delta waves,

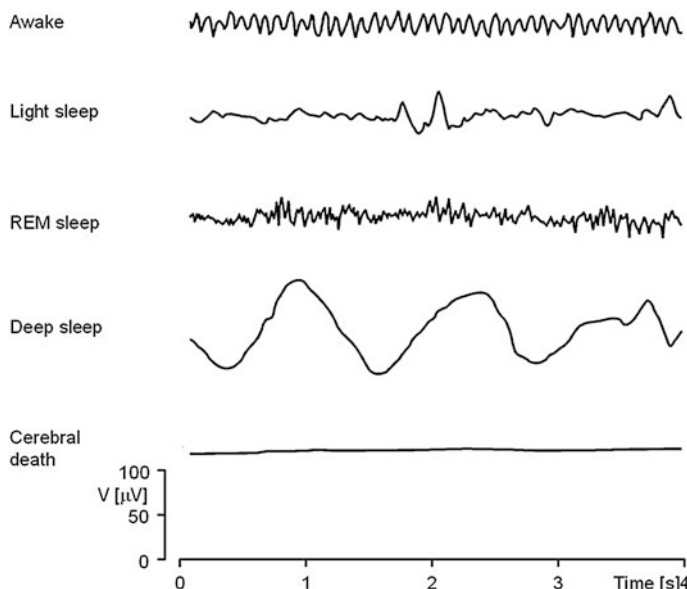


**Fig. 3.5** Brain waves in different sleeping conditions (Photo courtesy: Ref. [148] <http://www.bem.fi/book/13/13.htm>)

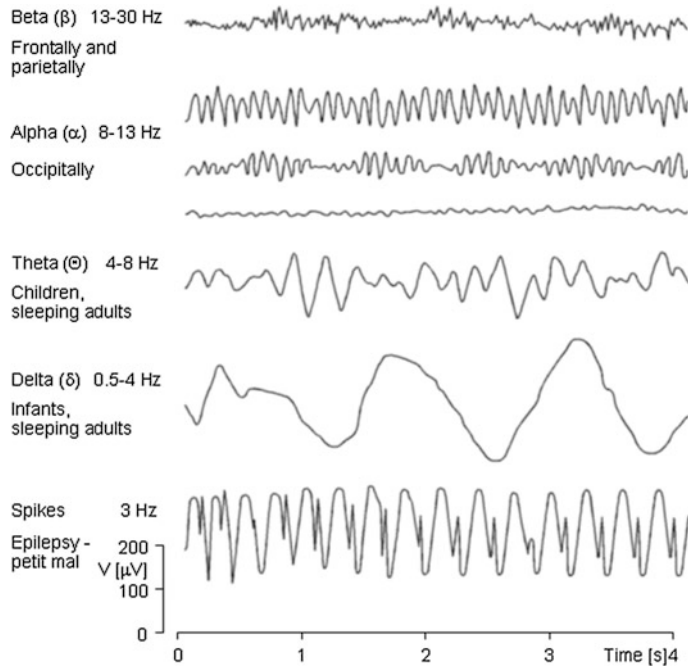


**Fig. 3.6** Some examples of EEG waves (Photo courtesy: Ref. [148] <http://www.bem.fi/book/13/13.htm>)

are usually associated with the deep sleep, dreamless sleep, deep stage 3 of NREM sleep, also known as slow-wave sleep (SWS). Delta waves, are used to characterize the depth of sleep. Thus, the dominant brainwave of a person is delta, the body is assumed to be healing itself and “resetting” its internal clocks with no dreams almost with unconsciousness [34].

The theta wave [82], which is associated with the Light sleep or extreme relaxation, is an oscillatory pattern in electroencephalography (EEG) signals which is found to be recorded with a frequency range of the 4–7 Hz range.

Alpha waves [114], found with the frequency range of 7.5–12.5 Hz, associated with the awake state but relaxed with the brain not processing much information such as the state after getting up in the morning as well as just before going to sleep. Actually, when a person closes his eyes his brain automatically starts producing more alpha waves [104].

Mu waves [66], found with the frequency range of 7.5–12.5 Hz, are found as the synchronized patterns of electrical activity involved in the large numbers of neurons, probably of the pyramidal type, in the part of the brain that controls voluntary movement [66].

The sensorimotor rhythm (SMR) [6], which is an oscillatory idle rhythm of synchronized electromagnetic brain activity, appears in spindles in recordings of EEG, MEG, and ECoG with the frequency range of 13–15 Hz [6, 103].

Beta wave [174], or beta rhythm is associated with wide awake condition or normal waking consciousness and found between 12.5 and 30 Hz frequency range. The people with insufficient beta activity may suffer from mental or emotional disorders such as depression and ADD [62, 84] and insomnia [104].

A gamma wave is associated with the formation of ideas, language and memory processing, and various types of learning [36, 51, 104, 154] a frequency between 25 and 100 Hz, [93] though 40 Hz is typical [94]. Gamma waves have been shown to disappear during deep sleep induced by anesthesia, but return with the transition back to a wakeful state [1, 104, 119, 156].

### 3.5.2.6 Why EEG

The brain electrical activity reflects the brain function as well as the health status of the brain. The EEG of a normal and healthy brain will differ from a brain with disease or functioning abnormally or in different health status. Thus, as the EEG provides the brain electrical activity, the EEG can be used to study and analyze the people who have problems associated with brain functions such as coma, memory disorder, tumors, brain death or even malfunctioning of certain body parts. A number of the brain diseases are possible to diagnose, study and analyze by the EEG. The diseases which can be evaluated by EEG procedures are Headache, Brain aneurysm, Parkinson's disease, Meningitis, Epilepsy, Encephalitis, Brain tumor, Stroke (brain infarction), Subdural hematoma, Epidural hematoma, Autism, Cerebral edema, Schizophrenia, Traumatic brain injury, Alzheimer's Disease, Dyslexia, Attention Deficit Hyperactivity Disorder (ADHD), Intracerebral hemorrhage, Brain abscess, etc.

### 3.5.2.7 How It Works

The EEG system is generally composed of amplifiers, filters, and paper chart or computer monitor. The cells in the brain communicate themselves by producing tiny electrical potentials in the form of impulses. In an EEG, the surface electrodes are placed on the scalp of the head and the patterns of brain electrical activities are detected and recorded. The recorded signals are transmitted to the EEG instrumentation (Fig. 3.7) where it is amplified filtered and displayed or printed as per the requirements or instrument facilities.

### 3.5.2.8 EEG Instrumentation

1. An EEG system will have the following components:
2. EEG electrodes,
3. Electrode connecting wires or lead wires
4. EEG electrode cap

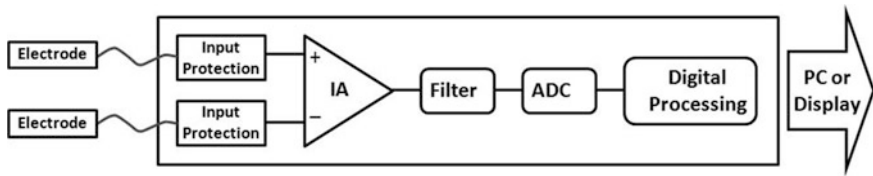


**Fig. 3.7** Schematic of an EEG scanner instrumentation

5. EEG electronic instrumentation or EEG measuring circuit (contains instrumentation amplifiers (IA), filters and signal processors)
6. EEG output or display such as PC monitor or printer

EEG electrode may be attached individually on the scalp or they may be housed on a electrode caps or electrode helmets. EEG system should have 21 electrodes for a standard 10–20 measurement system though there are several electrode caps containing different numbers of electrodes (19, 32, 64, up to 256 electrodes) which are available in several sizes for the patients of different age groups like adults and children. EEG electrodes are placed on the scalp of the head and the brain signals are collected by the electrodes. The EEG waves as the voltage signals available on the scalp electrodes are sent to the EEG electronic instrumentation through the lead wires and the instrumentation amplifies filters and processes the signal and sends to the display unit.

In wireless EEG system [60] there are, no wire connection between the recording instrumentation and the display unit. In wireless EEG system, the portable measuring instrument is fixed on the patient's body either on head [60] or on any other part of the body as per the comfort of the patient.

### 3.5.2.9 Preparation for an EEG Test

1. Patient should wash and clean his/her hair to make the hair free from any oily or greasy products or dusts.
2. Hair of the patient must be dry
3. Patient should eat regular meals without any foods or drinks that contain caffeine, alcohol or any other stimulant for at least 4 h before the test.
4. Patient should sleep in the day before the test as per the doctor's prescription
5. Patient should continue to take his/her regular medications, unless the doctor prescribes to do so.
6. Patient should lie on a table or sit in a chair.
7. 20–256 electrodes are attached to the human scalp with some washable glue or conducting gels.
8. The technician will remove the electrodes and you should wash the glue out of your hair.

9. Most of the time during the test, the patient is asked to lie still with the eyes closed but, sometimes, the technician or clinician may ask you to perform few small physical activities such as to open and close your eyes or look at a flashing light, to take deep breath and/or rapidly breath.

The EEG may be of different types depending upon the procedure of performing the test such as Regular or Standard EEG, Sleep-deprived EEG, Long Term EEG, Ambulatory EEG or sometimes Video EEG.

#### **3.5.2.10 Regular or Standard EEG**

Regular or Standard EEG procedure is performed for about 60–90 min. The Regular EEG is normally performed in normal clinical circumstances and normal patient conditions. Though sometimes the procedure can be completed within 30 min when very short measurements are performed.

#### **3.5.2.11 Sleep-Deprived EEG**

Sleep-deprived EEG procedure is performed for 2–3 h on a patient who have been asked to sleep only 4 h in the night before the test to record the abnormal brain waves which may appear when the body is stressed or fatigued.

#### **3.5.2.12 Long Term EEG**

When a short term or routine EEG is found insufficient to provide the required information to the doctors and clinicians the long term EEG is performed. In the cases of Long term EEG, the patient is asked to stay in the clinic or hospital for several days and the EEG is constantly being recorded for long time span.

#### **3.5.2.13 Ambulatory EEG**

Ambulatory EEG is one kind of long term EEG but it is not performed on the patient admitted to the clinic or hospital rather it is performed on the patient involved in his/her daily activities in his/her house. Ambulatory EEG is the performed on a patient with a portable EEG recorder attached to his/her waist just to record the long term EEG just like the ambulatory ECG procedure. The EEG electrodes are attached to the patient's head and the cables are connected to the portable EEG recorder fixed with a belt wore by the patient for several days. Similar to the ambulatory ECG procedure, the patient under Ambulatory EEG recording is given a diary you note his/her daily activities and drug dosages over time to provide the information to the doctors and clinicians to help them to relate the brain activities and functions with the EEG signals recorded at the same time.

### 3.5.2.14 Advantages of EEG

EEG method has the following advantages [70]:

1. Provides a lot of information about the brain activity
2. EEG is very suitable and efficient for diagnosing some brain diseases like epilepsy
3. It is very effective and efficient to detect sleep disorders, coma, encephalopathies, and brain death.
4. Most inexpensive methods of neuroimaging [70]
5. EEG high temporal resolution (millisecond range)
6. No harmful side effect of this process on human health is reported.
7. EEG procedure indeed measure electrical voltages which is generated naturally in the brain dose not inject any electrical signal.
8. No voltage goes out from the measuring device

### 3.5.2.15 Disadvantages

EEG method has the following disadvantages [70]:

1. EEG is less helpful than imaging techniques in determining the location of tumor, injuries and the precise nature for some diseases like stroke etc.
2. EEG is a signal measurement technique and hence does not provide the image of the brain cross sections.
3. EEG cannot indicate the location of the brain activity on the surface of the brain very well.

### 3.5.2.16 Electrode Placement in EEG: 10–20 System (EEG)

The 10–20 system [105, 106, 115, 122, 131, 148] or International 10–20 system of EEG measurement procedure which is developed by the International Federation of Clinical Neurophysiology (IFCN) recognized as the internationally standardized 10–20 system is used to determine and fix the location of scalp electrodes in the context during an EEG test or experiment. In the 10–20 system is generally used to record the spontaneous EEG by attaching 21 electrodes located on the surface of the scalp, as shown in Fig. 3.8a.

This 10–20 system is developed with the relationship between the location of a scalp electrodes and the underlying area of cerebral cortex of the patient which refer to the fact that the actual distances between adjacent electrodes are either 10 % or 20 % of the total front–back or right–left distance of the skull [106].

According to the 10–20 electrodes placement scheme (Fig. 3.8a), three distances are measured [107]:

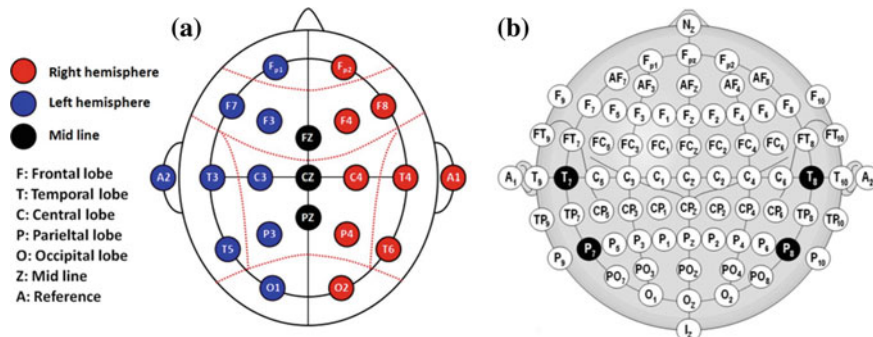


**Fig. 3.8** Electrode placement in EEG **a** Location and nomenclature of the scalp electrodes in the international 10–20 system as standardized by the International Federation of Clinical Neurophysiology (IFCN), **b** Location and nomenclature of the scalp electrodes in the international 10–20 system with the intermediate 10 % electrodes as standardized by the American Electroencephalographic Society (Photo courtesy: Ref. [148] <http://www.bem.fi/book/13/13.htm>)

1. Distance between two preauricular points,
2. Distance between the nasion (nose bridge) and inion (the occipital bone mount),
3. Distance both across vertex, and the circumference between the last two point of the skull.

These distances are divided in proportion of 10 %-20 %-20 %-20 %-20 %-10 % along both the orthogonal axes and the circumference of the scalp area and a net of imaging quadrates is built [107].

The EEG signal is measured across two electrodes among which one is the reference electrode. Reference electrode recording is an electrode, relative to which the electric brain potentials in all other electrodes are measured and hence it should be placed on a presumed “inactive” zone on the scalp region. In common practice the reference electrode is placed on the left or right earlobe or both of them. For an EEG system with a single reference electrode placed on a particular earlobe, though the topography of EEG rhythms is rather close to true [107], but EEG amplitude is decreased on the electrodes closer to the reference earlobe electrode. On the other hand, if two reference electrodes are used on both the earlobes and used as the linked reference earlobes electrodes, then though the asymmetry obtained in the single reference electrode system is avoided but the link wire between two reference electrodes affects the intracranial currents which produce the EEG potentials and hence distort the EEG picture [107]. Alternatively, the EEG signals are recorded on all the scalp electrodes making all the scalp electrode as a reference and the EEG signals are estimated by computing the average reference as a mean of all electrodes measurements [107].

For measuring the distances on the scalp region the *nasion* (the delve at the top of the nose, level with the eyes) and *inion* (the bony lump at the base of the skull on the midline at the back of the head) are taken as the references and the distances are

measured in the transverse and median planes by dividing these perimeters into 10 and 20 % intervals and the scalp electrodes placed.

In addition to the 21 scalp electrodes of the international 10–20 system, addition intermediate 10 % electrode positions are also used (Fig. 3.8b) as per the standard provided by the American Electroencephalographic Society [189] and hence the four electrodes are found with different names compared to the 10–20 system; viz T<sub>7</sub>, T<sub>8</sub>, P<sub>7</sub>, and P<sub>8</sub>. These electrodes are drawn black with white text in the figure. Besides the international 10–20 system, a number of other electrode systems have been proposed for recording EEG signals on the scalp.

### 3.5.3 Magnetoencephalography (MEG)

Magnetoencephalography (MEG) [108, 171, 194] is a functional neuroimaging technique that measures the magnetic fields generated by brain activity from the outside of the head and it is used for identifying and analyzing brain activity. MEG is now in routine clinical practice throughout the world [194] and it is used in the following two primary clinical applications:

1. localizing the area or areas from which the seizures arise in epilepsy patients
2. identifying regions of normal brain function in patients undergoing surgery for treating either epilepsy or tumor or other mass lesion.

MEG has become a recognized and vital part of the presurgical evaluation of patients with epilepsy and patients with brain tumors. As the physical properties of magnetic waves differ from the electrical waves, MEG provides different, complementary information than the EEG. MEG also has very good temporal resolution like EEG but with much better spatial resolution compared to EEG. The major disadvantage of the MEG is that it can detect the neural activity relatively close to the surface of the brain to detect its magnetic field because the magnetic fields generated by neural activity are very small.

#### 3.5.3.1 History

Prof. David Cohen first recorded the MEG signals in the University of Illinois in 1968 [47, 108] using a copper induction coil as the detector. Though the measurements were made inside a magnetically shielded room, to reduce the background noise, but the less sensitive coil detector provide a poor and noisy MEG measurements [108]. Using high sensitive superconducting quantum interference devices (SQUID) [185] developed by James E. Zimmerman, a researcher at Ford Motor Company [225], Cohen recorded significantly improved MEG signal [48] in a better shielded room at MIT.

### 3.5.3.2 Why Is an MEG Performed?

MEG is used to localize the source of epileptiform brain activity of a epilepsy patient, which considered as the source of seizures by, generally, performed with EEG simultaneously.

### 3.5.3.3 How MEG Work

The MEG procedure measures the magnetic field produced by the net effect of ionic currents flowing in the dendrites of neurons during synaptic transmission. But the magnetic field produced by the brain's electrical activity is considerably smaller than the ambient magnetic noise in an urban environment [108] and hence, approximately 50,000 active neurons are needed to generate a detectable signal. Therefore the weakness of the biomagnetism and MEG signal relative to the sensitivity of the detectors and the environmental noise is a major challenge in MEG technology.

As the neuromagnetic signals generated by the brain are extremely small almost (a billionth of the strength of the earth's magnetic field) MEG scanners require superconducting sensors, called superconducting quantum interference device (SQUID) sensors bathed in a cooling medium of large liquid helium of temperature approximately  $-269^{\circ}\text{C}$  [213]. The SQUID at this extreme low temperature becomes superconducting and show very small impedance and hence the MEG device can detect and amplify the brain magnetic fields generated by the neurons a few centimeters away from the SQUID.

### 3.5.3.4 Advantages of MEG

MEG method has the following advantages [70]:

1. MEG has an excellent temporal resolution (milliseconds).
2. MEG has better spatial resolution than EEG, because unlike electric fields, magnetic fields are not distorted as they pass through the brain and scalp [70].
3. EEG is not good in are at indicating the brain activity in the neural structures located deep beneath the surface [70].
4. In MEG the magnetic fields are less influenced than electrical currents in EEG by conduction through brain tissues, cerebral spinal fluid, the skull and scalp.
5. MEG provides both the timing and spatial information of brain activity [105].
6. MEG helps in identifying the seizure focus in patients with epilepsy.
7. MEG also helps the surgeon in facilitating the planning of surgery.
8. MEG signals provide the information about the neural activity because MEG obtain signal directly from neuronal electrical activity but the fMRI signals show the brain activity indirectly in terms of oxygenation of blood flowing near active neurons [105].

### 3.5.3.5 Disadvantages of MEG

MEG method has the following disadvantages [70]:

1. MEG also presents disadvantages, such as the fact that it only detects magnetic fields oriented in parallel to the surface of the skull (neurons in cerebral sulcus).
2. MEG equipment is very expensive (MEG equipment costs at least 10 times more than the cost of EEG [70]).
3. MEG cannot indicate the location of the brain activity on the surface of the brain very well [70].
4. EEG is not good in are at indicating the brain activity in the neural structures located deep beneath the surface [70].
5. MEG is extremely sensitive to external noise as the brain magnetic field activity is very weak

### 3.5.4 Electrocorticography (ECoG)

Electrocorticography (ECoG) [109] or intracranial EEG (iEEG) is a invasive procedure of measuring brain potentials by the electrodes placed directly on the surface of the brain (usually on the patients with his or her skull removed during the surgery). Thus the ECoG acquires the brain signal directly from the exposed surface of the brain with the electrodes placed on it to record the brain electrical activity and hence it offers better spatial resolution than electroencephalography.

In the early in 1950s, Wilder Penfield and Herbert Jasper, neurosurgeons at the Montreal Neurological Institute ECoG performed ECoG to treat patients with severe epilepsy [165]. From the ECoG, they used the cortical potentials to identify and remove the epileptogenic zones (regions of the cortex that generate epileptic seizures surgically) [109]. To explore the functional anatomy of the brain, mapping speech areas and identifying the somatosensory and somatomotor cortex areas to be excluded from surgical removal, Penfield and Jasper used electrical stimulation during ECoG recordings [67].

#### 3.5.4.1 Clinical Applications

ECoG has been used

1. to localize epileptogenic zones
2. to remove the epileptogenic zones during surgery planning,
3. to map out cortical functions
4. to explore the functional anatomy of the brain
5. to mapping speech areas
6. to identifying the somatosensory and somatomotor cortex areas
7. to predict the success of epileptic surgery.

### 3.5.4.2 Advantages of ECoG

1. Direct measurement of brain signal is possible.
2. Signal quality is high.
3. In ECoG flexible placement of recording and stimulating electrodes are possible.
4. ECoG helps us to localize epileptogenic zones and to remove the epileptogenic zones during surgery planning,
5. ECoG can be performed at any stage before, during, and after a surgery
6. Using direct electrical stimulation of the brain, ECoG helps us to identify the critical regions of the cortex to be excluded from surgical removal.
7. Greater precision and sensitivity than an EEG scalp recording—spatial resolution is higher and signal-to-noise ratio is superior due to greater proximity to neural activity.

### 3.5.4.3 Disadvantages of ECoG

1. electrode placement is limited by the exposed cortex area and time available during surgery.
2. Recording is subject to the influence of anesthetics, narcotic analgesics, and the surgery itself [67].
3. In ECoG recording the limited sampling time—seizures (ictal events) may not be recorded.

## 3.5.5 *Electroneurogram (ENG)*

An electroneurogram (ENG) [110, 160, 210] record the electrical activity generated by the neurons in the central nervous system (brain, spinal cord) or the peripheral nervous system (nerves, ganglia) by the electrodes electrode in the neural tissue [110]. The neuron electrical activity recorded by the electrodes in ENG system is transmitted to a signal acquisition system and then processed and displayed as the activity of the neuron [160]. An electroneurogram [210] can contain the activity of a single neuron to thousands of neurons depending upon the precision of the electrodes used in an ENG system [110] and hence electrode precision is set as per the requirement of the test either the activity of a single neuron or a group of neurons are to be recorded [110].

## 3.5.6 *MRI*

Magnetic resonance imaging (MRI), sometimes called nuclear magnetic resonance imaging (NMRI) or magnetic resonance tomography (MRT), is a medical imaging technique which produces the tomographic images (cross-sectional images) of the

subject under test as a function of proton spin density and relaxation times (or spectra of  $^{31}\text{P}$  and  $^1\text{H}$  in NMR spectroscopy) of the subject (patient's body) tissue using nuclear magnetic resonance (NMR) technology [45].

The MRI scanners use a superconductive electromagnet developed with a conducting coil in liquid Helium (He) at  $-269^\circ\text{C}$ . The conducting coils at such a low temperature become superconductor by losing their resistance to the flow of electrons and a stable and a very strong superconductive electromagnet is developed. 1.5 Tesla (1 Tesla = 10,000 Gauss) magnets are generally used in MRI scanners which is very strong compared to the earth's magnetic field (earth's magnetic field is 0.00005 Tesla or 0.5 Gauss).

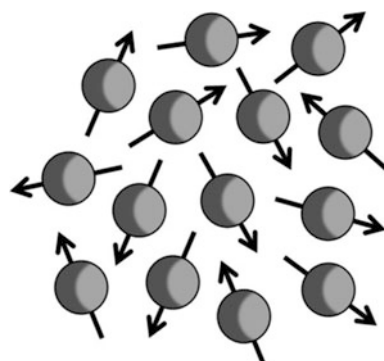
### 3.5.6.1 Physics of MRI Imaging

The protons of the hydrogen atoms of the human body tissue are all rotating at random fashion (Fig. 3.9) and there is no net magnetization. An even number of them will cancel each other's spin and hence, a net resultant spin would be resulted in the nucleus only when it contains an odd number of protons, an odd number of neutron or both. In presence of an external magnetic field the protons either may align parallel (known as spin-up position with lower energy state) or anti-parallel (known as spin-down position with higher energy state) to the applied field. When the MRI scanner applies its magnetic field ( $B_0$ ) the axes of the protons will mostly align parallel (called parallel alignment) with the main magnetic field, though some will align opposite the magnetic field (called anti-parallel alignment). In both the cases, this creates a net magnetization in the direction of the magnetic field ( $B_0$ ) created by the MRI machine. The protons rotating around their own axis revolve (precess) around the direction of the magnetic field ( $B_0$ ) by making an angle ( $\theta$ ) with  $B_0$  and hence the protons are only 'partially polarize'.

Now, by the Larmor relationship, the frequency of precession (the frequency of rotation) is given by:

$$f = \frac{\omega}{2 * \pi} = \frac{yB_0}{2 * \pi}$$

**Fig. 3.9** Magnetic dipoles created by the spinning of the Hydrogen atoms



Where,

w = angular freq. in radians per second;  $2\pi$  radians =  $360^\circ$

y = the magnetogyric (gyromagnetic) ratio, nuclear constant characteristic of every isotope (for proton ( $^1\text{H}$ ) it is 42.5 MHz/T);

$B_0$  = static magnetic field

In MRI, a radio frequency (RF) pulse at the Larmor frequency [72] (perpendicular to the magnetic field) is applied to the protons to disturb their natural alignments (i.e. to disturb the net magnetization of the protons) and hence the magnetic component ( $B_1$ ) of this electromagnetic wave temporarily knocks the protons out of alignment (see picture). In the presence of the RF pulse the protons are pushed out of alignment temporarily and as the pulse disappears, they ‘relax’ back to their natural ‘equilibrium’ positions emitting a rotating magnetic field parallel with the applied magnetic field. The magnetic field emitted relaxed protons during the absence of the RF magnetic field is recorded to construct an image of the scanned area of the body. Due to the huge number of protons a lot of signals of different frequencies are present in the acquired signal and hence all the signals are plotted in ‘frequency domain’ and processed with Discrete Fourier Transform (DFT). Depending on the material properties the nature of relaxation changes, and that is how we get the different contrast for different materials in the MRI images. Magnetic field gradients cause the proton nuclei to rotate at different locations with different speeds and hence by using gradients in different directions 2D images or 3D images can be obtained. Therefore, the gradient of the magnetic field is varied with the gradient coils in the MRI scanner to get the positional information of the protons in space.

### 3.5.6.2 MRI Scanner

An MRI scanner (Fig. 3.10), generally, consists of superconducting magnet, gradient coils, R.F. transmitter and receiver and the computer [45]. MRI systems generates high-quality diagnostic images through the use of an effective, yet safe, magnetic field generated by the main magnet. Hydrogen protons of the water molecules within the body align with the main magnetic field. RF coil applies the short radio frequency (RF) pulses to a specific anatomical slice of interest. The protons in the slice absorb energy at this resonant frequency, causing them to spin perpendicular to the main magnetic field. As the RF field is ceased, all the protons rotating perpendicularly to the main magnetic field relax back and get aligned with the main magnetic field exerting a signal which is received by the RF coil. The signal absorbed by the RF coil is processed by a computer to produce the tomographic images of the slice of interest by using a computer program called image reconstruction algorithm.

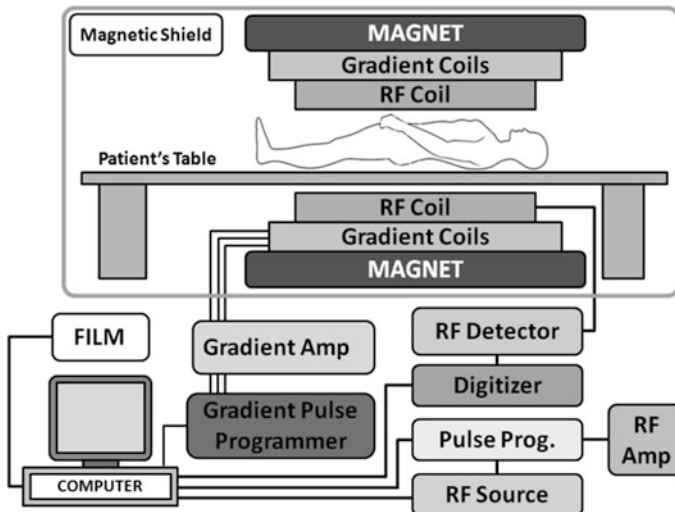


**Fig. 3.10** Schematic of an MRI scanner instrumentation

### 3.5.6.3 Advantages of fMRI

fMRI method has the following advantages [70]:

1. MRI has relatively good spatial and temporal resolution, it is also widely available (most hospitals have an MRI machine)
2. MRI is relatively inexpensive compared to PET
3. MRI procedure is very noisy;
4. the shifting of the magnetic fields cause physical movements of the magnets
5. MRI technique is very sensitive to motion.
6. fMRI is a very useful tool for learning which brain regions are involved in a given behavior,
7. non-invasive

### 3.5.6.4 Disadvantages of fMRI

MRI method has the following disadvantages [70]:

1. MRI is relatively inexpensive compared to EEG
2. The hole in the MRI scanner gantry is relatively narrow but very deep which provides some discomfort to some patients
3. temporal resolution is poor
4. gives little information about the temporal dynamics of their responses.

### 3.5.7 Electrical Impedance Tomography (EIT)

The Electrical Impedance Tomography (EIT) [11, 19, 22, 33, 43, 58, 78, 88, 186, 209] is computed tomographic technique which provides the 2d or 3D images of the spatial distribution of the electrical properties of a domain under test ( $\Omega$ ) such as electrical conductivity or resistivity from the set of voltage-current data (Fig. 3.11) measured at the domain boundary ( $\partial\Omega$ ) surrounded by an array of surface electrodes [29, 140, 206]. EIT is a low cost portable, non-invasive, non-ionizing imaging modality EIT provides few unique advantages over the conventional medical imaging methods like planer X-Ray radiography, X-Ray CT, PET, SPECT, MRI, ultrasound etc. Hence it is being used in clinical diagnosis, industrial process tomography, civil engineering, geotechnology, material engineering, biotechnology, and other fields of engineering and technologies.

An EIT system (Fig. 3.1) injects a constant amplitude, low frequency sinusoidal current through the driving electrodes and the boundary voltages are measured on the sensing electrodes with four electrode method [28, 209] using an electronic instrumentation [13, 14, 20, 25, 32, 125, 164, 176]. For a current injection through a particular current electrode pair, the boundary voltage current data are collected from all voltage electrode pairs excluding the pairs containing one or two current electrodes. Current injection through a particular current electrode pair and the voltage data collection from all the voltage electrode pairs is called a projection [19, 23, 29, 30]. The fashion in which the current injection electrodes and voltage collections electrodes are switched is called the current pattern [19, 23, 29, 30]. The boundary data are processed in PC and the spatial distribution of the electrical conductivity of the domain under test (DUT) is reconstructed from the boundary voltage data sets using image reconstruction algorithm [15–18, 21, 27, 139, 193, 220, 221] which is developed with two main computer programs called forward solver (FS) [16, 17, 22, 27, 220] and inverse solver (IS). FS solves the

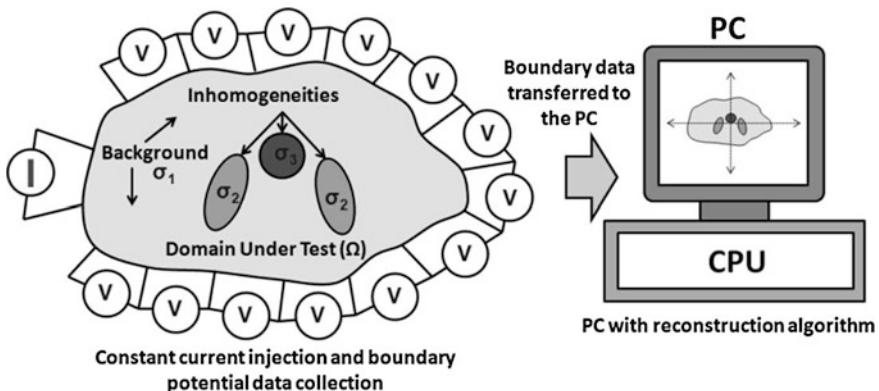


**Fig. 3.11** Schematic of EIT scanning with constant current injection and voltage measurement through surface electrodes

forward problem (FP) [16, 17, 22, 26, 27, 220] and calculates boundary potentials for a constant current simulation in a computer simulated domain resembling the real domain under test and the IS solves and inverse problem (IP) [16, 17, 22, 26, 27, 220] and tries to reconstruct the conductivity distribution by comparing the computed boundary data with the boundary data measured in a real domain with real current injection.

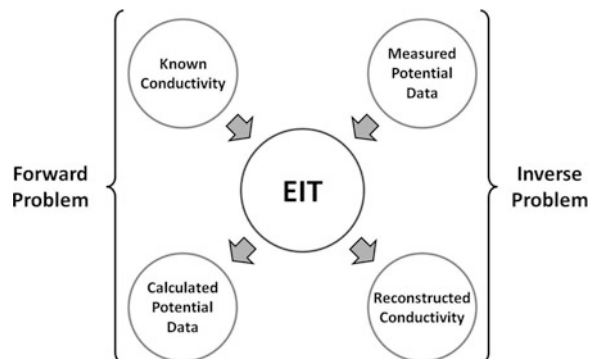
In EIT, a constant amplitude electrical current is injected through the driving electrodes and the boundary voltages are measured on the sensing electrodes using an instrumentation and the impedance images are reconstructed from the boundary data using the reconstruction algorithm. Boundary data quality depends on the number, geometry and the material of the surface electrodes used in the EIT system. Electrode material is a very important parameter which influences the quality of the boundary data collected for impedance image reconstruction. In this paper, different electrode materials used for EIT electrodes proposed by different research groups are studied and a technical review on the EIT electrode materials is presented.

### 3.5.7.1 Forward Modeling

The EIT problem has two parts: forward problem (FP) and inverse problem (IP). The FP computes the boundary potential from a known conductivity distribution and a known current simulation whereas the inverse problem (IP) reconstructs the conductivity distribution from the measured boundary potential data and same current injection in real system (Fig. 3.12).

The EIT image reconstruction algorithm is developed with two parts: forward solver (FS) which solve the forward problem and the inverse solver (IS) which solves the inverse problem. In forward solver the forward model is developed by finite element method (FEM) [2, 138, 175, 177, 188, 217] formulation applied on the governing equation, Eq. 3.1, of the domain under test (DUT). Developing the forward model, the forward solver solves the governing equation and calculates the boundary potential data by simulating a constant current within the modeled

**Fig. 3.12** The image reconstruction process in EIT image reconstruction algorithm developed with forward solver (FS) and inverse solver (IS)



domain of interest in PC. The inverse solver compares the calculated potential data ( $V_c$ ) data with the measured potential data ( $V_m$ ) obtained by practical current injection in the real EIT domain and tries to reconstruct the conductivity distribution of DUT by minimizing the difference between  $V_m$  and  $V_c$  called the voltage mismatch vector ( $\Delta V = V_m - V_c$ ).

The FS derives the forward model of a DUT from its governing equation (Eq. 3.1) by applying the FEM formulation and imposing the boundary conditions [16, 17, 22, 27, 220] for the system under test. Assuming an initial guessed conductivity distribution, say  $[\sigma_0]$ , and nodal coordinates  $(x, y)$ , the FS develops the forward model which is a system of equations represented in the form of a matrix equation (Eq. 3.2).

Thus the forward model (Eq. 3.2), represents the relationship between the current injection matrix  $[C]$  (matrix of the applied current signal), and the nodal potential matrix  $[\Phi]$  (matrix of the developed voltage signal) through the transformation matrix  $[K(\sigma_e)]$  as given below [16, 17, 22, 27, 220]:

$$\nabla \cdot \sigma \nabla \phi = 0 \quad (3.1)$$

$$[\Phi] = [K(\sigma_e)]^{-1} [C] \quad (3.2)$$

where  $\sigma_e$  is the elemental conductivity distributions within the domain under test.

### 3.5.7.2 Conductivity Reconstruction

In EIT, the computed boundary potential data obtained by FS by solving the FM is compared with the measured boundary potential data in IS and the desired elemental conductivity distribution  $[\sigma]$  is obtained by a mathematical algorithm (MA) developed with Gauss-Newton based minimization algorithm (GNM-MA) and Newton Raphson Iteration Technique (NRIT). In EIT reconstruction algorithm the FS calculates the boundary data using a known conductivity distribution and known current injection whereas the IS calculates the conductivity distribution using the boundary data developed for the same current injection at the boundary. Thus in the EIT image reconstruction algorithm IS logically works just in opposite to the process executed in FS and hence it is known as the inverse solver. In IS, the GNM-MA first defines an objective function ( $s$ ) from computationally predicted data  $[V_c]$  and the data collected from the experimental measurements  $[V_m]$  and runs iteratively to minimize the function ( $s$ ) to obtain an optimized elemental conductivity values  $[\sigma]$ . The minimization algorithm [16, 17, 22, 27, 220] defines an objective function ( $s$ ) from with the difference between computationally predicted data  $[V_c]$  and the experimental measurement data  $[V_m]$  called the voltage mismatch vector  $[\Delta V = V_m - V_c]$  and then tries to minimize it in an iterative way.

If the forward solver discretizes the DUT with an FEM mesh with  $e$  number of finite elements and  $n$  number of nodes and calculates the boundary data matrix  $[V_c]$  for a known conductivity distribution and known current injection  $[C]$ , the Gauss-Newton

method based minimization algorithm [1, 80, 99, 124, 135, 136, 163, 208] defines an object function using the experimental measurement data  $[V_m]$  as [16, 17, 22, 27, 220]:

$$s = \frac{1}{2} \|V_m - f\|^2 = \frac{1}{2} (V_m - f)^T (V_m - f) \quad (3.3)$$

Where  $f$  is a function mapping an e-dimensional impedance distribution into a set of M (M is the number of the available experimental boundary measurement data ( $[V_m]$ )) boundary potential data.

The EIT minimization algorithm [16, 17, 22, 27, 220] tries to obtain a least square solution of the minimized object function (s) using by a Gauss-Newton method and NRIT based iterative approximation techniques.

Now, differentiating the object function (s') in Eq. 3.3 w.r.t. the conductivity  $\sigma$ , we have:

$$s' = -[f']^T [V_m - f] = -J^T \Delta V \quad (3.4)$$

Where the matrix  $J = f'$  is known as Jacobin matrix [16, 17, 22, 27, 220] and  $J^T$  represents the transpose of the matrix  $J$ . The Jacobian matrix  $J$  may be computed by using a method as described in or by the adjoint method represented by the Eq. 3.6 [16, 17, 22, 27, 220]:

$$J = \oint_{\Omega} \nabla \Phi_s \cdot \nabla \Phi_d d\Omega \quad (3.5)$$

Where,  $\Phi_s$  is the forward solution for a particular location say “source location” and  $\Phi_d$  is the forward solution for the adjoint position of the “source location” i.e. the “adjoint location” (source at the detector location and detector at the source location).

Now, differentiating  $s'$  in Eq. 3.4 w.r.t.  $\sigma$  again, it reduces to:

$$s'' = [f']^T [f'] - [f'']^T [V_m - f] \quad (3.6)$$

By Gauss-Newton method, if  $f(x)$  is a twice-differentiable function well approximated by its second order Taylor expansion and the initial guess  $x_0$  is chosen close enough to  $x^*$ , the sequence  $(x_n)$  defined by:

$$\Delta x = x - x_n = -\frac{f'(x_n)}{f''(x_n)}, \quad (3.7)$$

$$x_{n+1} = x_n - \frac{f'(x_n)}{f''(x_n)}, \quad n = 0, 1, 2 \dots \quad (3.8)$$

will converge towards the root of  $f'$  i.e.  $x^*$  for which  $f'(x^*) = 0$ .

Thus, in EIT using the Gauss-Newton method, the conductivity update vector  $[\Delta\sigma]$  is given by,

$$\Delta\sigma = -\frac{s'}{s''} = \frac{\mathbf{J}^T \Delta V}{[f']^T [f'] - [f'']^T \Delta V} \quad (3.9)$$

Therefore, the conductivity update vector  $[\Delta\sigma]$  can be simplified as:

$$\Delta\sigma = \left[ [f']^T [f'] - [H]^T \Delta V \right]^{-1} \mathbf{J}^T \Delta V \quad (3.10)$$

Where, the higher order term  $H = [f'']$  is known as the *Hessian matrix* [16, 17, 22, 27, 220] which is generally neglected. Thus, in Eq. 3.10 neglecting  $H$ , the  $\Delta\sigma$  vector reduces to:

$$\Delta\sigma = \left[ [f']^T [f'] \right]^{-1} \mathbf{J}^T [\Delta V] \quad (3.11)$$

In general, using NRIT method, for  $k$ th iteration (where,  $k$  is a positive integer), the conductivity update vector obtained in Eq. 3.11 can be represented as:

$$\Delta\sigma_k = \left[ [J_k]^T [J_k] \right]^{-1} [J_k]^T [\Delta V_k] \quad (3.12)$$

Where  $[\Delta V_k]$  and  $[J_k]$  are the voltage mismatch vector and Jacobian matrix respectively both calculated at the  $k$ th iteration.

In Eq. 3.11, the matrix  $[f']^T$  is always ill-conditioned, and hence a small error in measured data will produce a large error in the solution of Eq. 3.12. In order to make the EIT problem wellposed, generally, the regularization techniques [16, 17, 22, 27, 117, 195, 220] are incorporated into the EIT reconstruction algorithm by including a regularizing term in the object function. The object function, therefore, is redefined with regularization parameters as [16, 17, 22, 27, 220]:

$$s_r = \frac{1}{2} \|V_m - f\|^2 + \frac{1}{2} \lambda \|G\sigma\|^2 \quad (3.13)$$

Where,  $G$  is the regularization operator and  $\lambda$  (positive scalar) is called the regularization coefficient.

The object function ( $s_r$ ) thus represents the constrained least-square error of the regularized reconstructions which is developed by the boundary voltage mismatch vector and controlled by the regularizing term as:

$$s_r = \frac{1}{2} (V_m - f)^T (V_m - f) + \frac{1}{2} \lambda (G\sigma)^T (G\sigma) \quad (3.14)$$

Now, by differentiating the object function in Eq. 3.14 with respect to the elemental conductivity ( $\sigma$ ) the Eq. 3.14 yields [16, 17, 22, 27, 220]:

$$s'_r = - (f')^T (V_m - f) + \lambda (G)^T (G\sigma) \quad (3.15)$$

Again differentiating the Eq. 3.15 with respect to the elemental conductivity ( $\sigma$ ) the Eq. 3.15 yields:

$$s''_r = (f')^T (f') - (f'')^T (V_m - f) + \lambda G^T G \quad (3.16)$$

Now, from Eq. 3.15 and Eq. 3.16, the conductivity update vector  $[\Delta\sigma]$  is calculated using the Gauss Newton (GN) method based minimization technique as [16, 17, 22, 27, 220]:

$$\Delta\sigma = \frac{s'_r}{s''_r} = \frac{(f')^T (V_m - f) - \lambda (G)^T (G\sigma)}{(f')^T (f') - (f'')^T (V_m - f) + \lambda G^T G} \quad (3.17)$$

Neglecting the higher order matrix  $[f'']^T$  called the *Hessian matrix* [163] in Eq. 3.17, the conductivity update vector  $[\Delta\sigma]$  reduces to:

$$\Delta\sigma = \frac{s'_r}{s''_r} = \frac{(f')^T (V_m - f) - \lambda (G)^T (G\sigma)}{(f')^T (f') + \lambda G^T G} \quad (3.18)$$

The matrix  $[f']$  is called the Jacobian matrix of the system and hence it is replaced by the symbol  $[J]$  and hence Eq. 3.18 reduces to:

$$\Delta\sigma = \frac{J^T (V_m - f) - \lambda I\sigma}{J^T J + \lambda I} \quad (3.19)$$

Where the matrix  $J = f'$  is the Jacobin and  $I$  represents the identity matrix  $G^T G$ .

Thus the update in the conductivity distribution of the domain under test in EIT image reconstruction process which is called the conductivity update vector ( $[\Delta\sigma]$ ) is found as:

$$\Delta\sigma = (J^T J + \lambda I)^{-1} (J^T (V_m - f) - \lambda I\sigma) \quad (3.20)$$

In some cases, the reconstruction process is also conducted by neglecting the last term ( $\lambda I\sigma$ ) and the conductivity update vector  $[\Delta\sigma]$  is calculated as [16, 17, 22, 27, 220]:

$$\Delta\sigma = (J^T J + \lambda I)^{-1} J^T (V_m - f) \quad (3.21)$$

Therefore, in general, the EIT image reconstruction algorithm calculates the updated solution of the conductivity distribution of the DUT at the kth iteration of the algorithm as [16, 17, 22, 27, 220]:

$$\sigma_{k+1} = \sigma_k + \left( (J^T J + \lambda I)^{-1} (J^T (V_m - f) - \lambda I \sigma) \right)_k \quad (3.22)$$

### 3.5.7.3 EIT for Brain Imaging

EIT has been studied for imaging of brain [5, 9, 55, 63, 74, 86, 87, 89, 90, 111, 149, 178, 191, 197, 199, 200, 203, 218, 219, Holder et al. 2006] for past few years in two dimension or three dimension. In brain EIT, a constant is injected to the head by scalp electrodes and the surface potential data are collected. Boundary voltage data are processed and used for reconstructing the spatial distribution of the brain impedance. The brain EIT has been applied for a number of application such as: imaging brain function [86, 87, 111], imaging brain tumours [178], imaging arteriovenous malformations [178], imaging stroke [149, 178], detection of cerebral ischaemia [86, 87], physiological brain activity [199], fast neural activity [74], imaging of physiologically evoked responses [90], identifying and studying the regional conductivity changes in human brain during epileptic seizures [63], imaging brain function in ambulant human subjects (Holder et al. 2006) and so on.

### 3.5.8 Present Scenario and the Future Trends

Though the EEG and other brain signal monitoring procedures providing the information in through the neural potential waveforms are very powerful and essential in diagnosis, analysis and treatment of several brain diseases an studying the brain functions, but visualizing the brain anatomy and physiology in 2D or 3D tomographic images have a number of advantages in medical analysis and clinical studies. Therefore, a lot of studies have been conducted and is being conducted in tomographic imaging techniques human brain monitoring. X-Ray CT, MRI, fMRI, PET, SPECT all have been well established methods in brain imaging filed. X-Ray CT applies radiation; PET and SPECT are invasive and inject the radioactive chemical inside the body. Hence CT, PET, SPECT procedures have some disadvantages. Recently, EIT, magnetic resonance electrical impedance tomography (MREIT) [116, 126, 127, 151, 167, 183, 214], magnetic resonance electrical property tomography (MREPT) [222, 223, 224], Quantitative Susceptibility Mapping (QSM) [141, 145, 211, 212] have been studied for brain imaging.

MREIT is a new tomographic imaging modality which provides the image the electrical properties of human body tissue using MRI phase information along with an external current injection [151]. MREIT is based on the Magnetic Resonance Current Density Imaging (MRCDI) [120] technique which requires current injection into the body within an MRI scanner [223]. Recent in vivo MREIT studies

conducted on animal and human have demonstrated that the different physiological and pathological conditions of tissues or organs can be visualized with some unique conductivity contrasts [151].

MREPT is a new imaging modality which produces the cross-sectional images of the distribution of admittance ( $\gamma = \sigma + i\omega\epsilon$ , where  $\sigma$  and  $\epsilon$  denote electrical conductivity and permittivity, respectively) inside the human body at the Larmor frequency in an MRI scanner [187] using B1 mapping technique which was developed to measure the rotating RF field components [3, 187, 223].

MREIT and MREP are conducted in different frequency ranges to visualize the electrical permittivity and conductivity distributions of the body tissue [128]. MREIT provides images of the tissue conductivity at the low frequency range below 10 kHz by post-processing phase images subject to externally injected currents [128]. MREPT works in the frequency range of 10–200 MHz and provides the images of the admittance (complex permittivity) of the body tissue by post-processing B1 maps obtained by using a standard RF coil of an MR system [128].

QSM [1, 196, 211, 212, 215] a novel procedure which enables us to investigate of tissue magnetic susceptibility in a quantitative and specific manner [155] using magnetic resonance imaging (MRI). QSM is different from the traditional Susceptibility Weighted Imaging [57, 83] which helps in identifying and quantifying the specific biomarkers including iron, calcium, gadolinium, and super paramagnetic iron oxide (SPIO) nano-particles. Due to its specificity, QSM is more sensitive to nuance differences in susceptibility that may be otherwise overriden by relaxation effect. The quantitative nature facilitates longitudinal investigations or multi-center comparison studies.

Though these recent imaging modalities have some advantages over the conventional imaging procedures, but all of these methods have a number of challenges to be overcome and hence a lot of scopes are there in these research fields. A number of researchers are continuously working on these methods to solve the problems and overcome the challenges. A lot of studies are still required to make these modalities more efficient and effective and to explore more in the field of brain signal analysis, brain imaging and other electromagnetic brain monitoring techniques.

### 3.5.9 Conclusions

Human brain, which is developed with billions of nerve cells, is very complex and one of the most important organs in the human body which controls all other organ performing a number of tasks to keep the human body healthy and alive. The brain monitoring is not only essential to study the brain anatomy and physiology of a normal and healthy subject but also it is essential for diagnosing, analyzing and treating a number of brain disease and brain malfunction. Before going to the operation theatre, all the surgeons always prefer to plan the surgery by visualizing the brain anatomy, physiology or the brain function profiles so that the affected regions and the non affected regions are clearly identified. With the necessity of

visualizing the brain function, the EEG, and other brain signal monitoring techniques are invented. The urge and necessary of visualizing the brain and its functioning in cross section images, inspired the researchers and scientist to invent a number of brain imaging modalities such as X-Ray CT, PET and SPECT. With the limitations of the imaging methods and the urge of getting more information about the brain anatomy, physiology and pathology, the electromagnetic brain imaging methods such as MRI, fMRI, EIT, MREIT, MREPT are introduced and studied. The chapters reviewed the electromagnetic brain monitoring modalities discussing their working principle, advantages, limitations and applications. The chapter discusses about the present scenario, challenges of the field of electromagnetic brain monitoring along with the future scopes. After reviewing the several electromagnetic brain monitoring technologies, the chapter summarize all the modalities along with focuses on the recent advances and future trends. The recent advances and future trends in the electromagnetic brain monitoring field show that, though these recent brain imaging modalities are found with some advantages over the conventional imaging procedures, but all of these methods still have a number of challenges to be overcome and hence a lot of scopes are found in these research fields. As a result, to solve the problems and overcome the challenges, a number of researchers are dedicatedly working on these methodologies. A lot of studies are still required to make these modalities more efficient and effective. The field of the electromagnetic brain monitoring is thus found as a emerging field which is required to be explored more to make the existing technologies more efficient and effective as well as to develop a number of new electromagnetic brain monitoring techniques.

## References

1. Aaronson, P.I., Ward, J.P.T.: The Cardiovascular System at a Glance, 3rd edn. Wiley-Blackwell, Oxford (2007)
2. Aizat, R.M., Kadir, M.R.A., Rahman, S.A., Shihabudin, T.M.T.M., Robson, N., Kamarul, T.: Biomechanical comparative analyses between the anterolateral and medial distal tibia locking plates in treating, complex distal tibial fracture: a finite element study. *J. Med. Imaging Health Inf.* **3**, 532–537 (2013)
3. Akoka, S., Franconi, F., Seguin, F., Lepape, A.: Radiofrequency map of an NMR coil by imaging. *Magn. Reson. Imaging* **11**(3), 437–441 (1993)
4. Andria, G., Attivissimo, F., Lanzolla, A.M.L.: A statistical approach for MR and CT images comparison. *Measurement* **46**(2013), 57–65 (2013)
5. Aristovich, K.Y., Santos, G.S., Packham, B.C., Holder, D.S.: A method for reconstructing tomographic images of evoked neural activity with electrical impedance tomography using intracranial planar arrays. *Physiol. Meas.* **35**(6), 1095–1109 (2014)
6. Arroyo, S., Lesser, R.P., Gordon, B., Uematsu, S., Jackson, D., Webber, R.: Functional significance of the mu rhythm of human cortex: an electrophysiologic study with subdural electrodes. *Electroencephalogr. Clin. Neurophysiol.* **87**(3), 76–87 (1993). doi:[10.1016/0013-4694\(93\)90114-B](https://doi.org/10.1016/0013-4694(93)90114-B)

7. Azar, A.T., Balas, V.E., Olariu, T.: Classification of EEG-Based Brain-Computer Interfaces. *Adv. Intell. Comput. Technol. Decis Support Systems, Stud Comput Intell* **486**, 97–106 (2014)
8. Baillet, S., Mosher, J.C., Leahy, R.M.: Electromagnetic brain mapping. *IEEE Sign. Process. Mag.* **18**(6), 14–30 (2001)
9. Bagshaw, A.P., Liston, A.D., Bayford, R.H., Tizzard, A., Gibson, A.P., Tidswell A.T., Sparkes, M.K., Dehghani, H., Binnie, C.D., Holder, D.S.: Electrical impedance tomography of human brain function using reconstruction algorithms based on the finite element method. *NeuroImage* **20**, 752–764 (2003)
10. Baillet, S., Friston, K., Oostenveld, R.: Academic software applications for electromagnetic brain mapping using MEG and EEG. *Comput. Intell. Neurosci.* **2011** (Article ID 972050), 4 (2011)
11. Bayford, R.H.: Bioimpedance tomography (electrical impedance tomography). *Ann. Rev. Biomed. Eng.* **8**, 63–91 (2006)
12. Bear, M.F., Connors, B.W., Paradiso, M.A.: *Neuroscience: Exploring the Brain*, 3rd Revised edn. Lippincott Williams and Wilkins, Philadelphia (2006)
13. Bera, T.K., Nagaraju, J.: A Multifrequency constant current source for medical electrical impedance tomography. In: Proceedings of the IEEE International Conference on Systems in Medicine and Biology (ICSMB), Kharagpur, India, pp. 278–283. 16th–18th Dec 2010
14. Bera, T.K., Nagaraju, J.: Switching of a sixteen electrode array for wireless EIT system using A RF-based 8-Bit digital data transmission technique. *Commun. Comput. Inform. Sci. Springer, Part I, CCIS 269, ObCom 2011* **2012**(20), 202–211 (2011)
15. Bera, T.K., Biswas, S.K., Rajan, K., Nagaraju, J.: Improving conductivity image quality using block matrix-based multiple regularization (BMMR) technique in EIT: a simulation study. *J. Electr. Bioimpedance* **2**, 33–47 (2011)
16. Bera, T.K., Biswas, S.K., Rajan, K., Nagaraju, J.: Improving the image reconstruction in electrical impedance tomography (EIT) with block matrix-based multiple regularization (BMMR): a practical phantom study. *IEEE World Congr. Inform. Commun. Technol. (WICT-2011) India* **2011**, 1346–1351 (2011b)
17. Bera, T.K., Biswas, S.K., Rajan, K., Nagaraju, J.: Improving image quality in electrical impedance tomography (eit) using projection error propagation-based regularization (pepr) technique: a simulation study. *J. Electr. Bioimpedance* **2**, 2–12 (2011). doi:[10.5617/jeb.158](https://doi.org/10.5617/jeb.158)
18. Bera, T.K., Biswas, S.K., Rajan, K., Nagaraju, J.: A model based iterative image reconstruction (MoBIIR) algorithm for conductivity imaging in EIT using simulated boundary data. In: AIP Conference Proceedings, Optics: Phenomena, Materials, Devices, and Characterization: Optics 2011: International Conference on Light, Kerala, (India), pp. 489–491. 23–25 May (2011d)
19. Bera, T.K., Nagaraju, J.: Studying the resistivity imaging of chicken tissue phantoms with different current patterns in electrical impedance tomography (EIT). *Measurement* **45**(2012), 663–682 (2012)
20. Bera, T.K., Nagaraju, J.: Surface electrode switching of A 16-electrode wireless EIT system using RF-based digital data transmission scheme with 8 channel encoder/decoder ICs. *Measurement* **45**, 541–555 (2012)
21. Bera, T.K., Biswas, S.K., Rajan, K., Nagaraju, J.: Image reconstruction in electrical impedance tomography (EIT) with projection error propagation-based regularization (PEPR): a practical phantom study. In: *Lect. Notes Comput Sci Springer 2012* **7135/2012**, 95–105, ADCONS 2011 (2012)
22. Bera, T.K.: Studies on multifrequency multifunction electrical impedance tomography (MfMf $\square$ EIT) to improve bio $\square$ impedance imaging. PhD Thesis, IISc, Bangalore, India, Department of Instrumentation and Applied Physics, Indian Institute of Science, Bangalore, India (2013)
23. Bera, T.K., Nagaraju, J.: A MATLAB-based boundary data simulator for studying the resistivity reconstruction using neighbouring current pattern. *J. Med. Eng.* **2013**(Article ID 193578), 15 (2013a)

24. Bera, T.K., Nagaraju, J.: Electrical impedance tomography (EIT): A Harmless Medical Imaging Modality, Research Developments in Computer Vision and Image Processing: Methodologies and Applications, IGI Global, Chap 13, pp. 235–273 (2013b)
25. Bera, T.K., Nagaraju, J.: A LabVIEW based multifunction multifrequency electrical impedance tomography (MfMf-EIT) instrumentation for flexible and versatile impedance imaging. In: 15th international conference on electrical bio-impedance (ICEBI) and 14th conference on electrical impedance tomography (EIT), April 22–25, 2013, Germany, p. 216 (2013c)
26. Bera, T.K., Maity, P., Halder, S., Nagaraju, J.: A MatLAB based virtual phantom for 2D electrical impedance tomography (MatVP2DEIT): studying the medical EIT reconstruction in computer. *J. Med. Imaging Health Inform.* **4**, 147–167 (2014)
27. Bera, T.K., Biswas, S.K., Rajan, K., Nagaraju, J.: Projection Error Propagation-based regularization (PEPR) method for resistivity reconstruction in electrical impedance tomography (EIT). *Measurement* **49**, 329–350 (2014)
28. Bera, T.K., Mohamadou, Y., Lee, K.H., Wi, H., Oh, T.I., Woo, E.J., Soleimani, M., Seo, J. K.: Electrical impedance spectroscopy for electro-mechanical characterization of conductive fabrics. *Sensors* **14**, 9738–9754 (2014)
29. Bera, T.K., Nagaraju, J.: Sensors for electrical impedance tomography, 2nd edn. In: Webster, J.G. (ed.) The measurement, instrumentation, and sensors handbook, Chap. 61, pp 61.1–61.30. CRC Press (2014)
30. Bera, T.K., Nagaraju, J.: Studies and evaluation of EIT image reconstruction in EIDORS with simulated boundary data. In: Proceedings of the second international conference on soft computing for problem solving (SocProS 2012) December 28–30. Advances in intelligent systems and computing, vol. 236, pp. 1573–1581 (2014b)
31. Blume, W.T.: EEG and the diagnosis of epilepsy. In: Kaplan, P.W., Fisher, R.S. (eds.) Imitators of epilepsy. 2nd edn. Demos Medical Publishing, New York. <http://www.ncbi.nlm.nih.gov/books/NBK7442/>
32. Boone, K.G., Holder, D.S.: Current approaches to analogue instrumentation design in electrical impedance tomography. *Physiol. Meas.* **17**, 229 (1996)
33. Borcea, L.: Electrical impedance tomography. *Topical Rev. Inverse Probl.* **18**, R99–R136 (2002)
34. Botella-Soler, V., Valderrama, M., Crépon, B., Navarro, V., Le Van Quyen, M.: Large-scale cortical dynamics of sleep slow waves. *PLoS one* **7**(2), e30757, 1–10 (2012)
35. Brandon, D., Alazraki, A., Halkar, R.K., Alazraki, N.P.: The role of single-photon emission computed tomography and SPECT/computed tomography in oncologic imaging. *Semin. Oncol.* **38**(1), 87–108 (2011)
36. Burle, B., Bonnet, M.: High-speed memory scanning: a behavioral argument for a serial oscillatory model. *Cogn. Brain. Res.* **9**(3), 327–337 (2000)
37. Buxton, R.B.: Introduction to functional magnetic resonance imaging: principles and techniques, 2 edn. Cambridge University Press, Cambridge (2009)
38. Caplan, D., Waters, G., DeDe, G., Michaud, J., Reddy, A.: A study of syntactic processing in aphasia I: behavioral (psycholinguistic) aspects. *Brain Lang.* **101**(2), 103–150 (2007)
39. Cascino, G.: Functional MRI for language localization. *Epilepsy Curr.* **2**(6), 178–179 (2002)
40. Castellanos, F.X., Giedd, J.N., Marsh, W.L., Hamburger, S.D., Vaituzis, A.C., Dickstein, D. P., Sarfatti, S.E., Vauss, Y.C., Snell, J.W., Lange, N., Kayser, D., Krain, A.L., Ritchie, G.F., Rajapakse, J.C., Rapoport, J.L.: Quantitative brain magnetic resonance imaging in attention-deficit hyperactivity disorder. *Arch. Gen. Psychiatry* **53**(7), 607–616 (1996)
41. Carter, R.: The Human Brain Book. Dorling Kindersley Ltd, Har/Dvd edition (2009)
42. Szi-Wen, C., Chang-Yuan, C.: A comparison of 3D cone-beam Computed Tomography (CT) image reconstruction performance on homogeneous multi-core processor and on other processors. *Measurement* **44**(10), 2035–2042 (2011)
43. Cheney, M., Isaacson, D., Newell, J.C.: Electrical impedance tomography. *SIAM Rev.* **41**(1), 85–101 (1999)

44. Cho, M.J., Lyoo, I.K., Lee, D.W., Kwon, J.S., Lee, J.S., Lee, D.S., Jung, J.K., Lee, M.C.: Brain single photon emission computed tomography findings in depressive pseudodementia patients. *J. Affect. Disord.* **69**(1–3), 159–166 (2002)
45. Clare, S.: Functional MRI: methods and applications. PhD Thesis, University of Nottingham, UK (1997)
46. Clark, D.D., Sokoloff, L.: In: Siegel, G.J., Agranoff, B.W., Albers, R.W., Fisher, S.K., Uhler, M.D. (ed.) Basic neurochemistry: molecular, cellular and medical aspects. Lippincott, Philadelphia, pp. 637–670. ISBN 978-0-397-51820-3
47. Cohen, D.: Magnetoencephalography: evidence of magnetic fields produced by alpha rhythm currents. *Science* **161**, 784–786 (1968)
48. Cohen, D.: Magnetoencephalography: detection of the brain's electrical activity with a superconducting magnetometer. *Science* **175**, 664–666 (1972)
49. Collura, T.F.: History and evolution of electroencephalographic instruments and techniques. *J. Clin. Neurophysiol.* **10**(4), 476–504 (1993)
50. Collura, T.F.: History and evolution of computerized electroencephalography. *J. Clin. Neurophysiol.* **12**(1995), 214–229 (1995)
51. Crone, N.E., Hao, L., Hart, J., Boatman, D., Lesser, R.P., Irizarry, R., Gordon, B.: Electrocorticographic gamma activity during word production in spoken and sign language. *Neurology* **57**(11), 2045–2053 (2001)
52. Crossman, A.R., Neary, D.: Neuroanatomy: an illustrated colour text, 4e, 4 edn. Churchill Livingstone (2010)
53. Cryer, P.E.: Hypoglycemia, functional brain failure, and brain death, *J Clin Invest. Apr 2* **117** (4), 868–870 (2007)
54. Dauwels, J., Vialatte, F., Cichocki, A.: Diagnosis of Alzheimer's disease from EEG signals: where are we standing? *Curr. Alzheimer Res.* **7**(6), 487–505 (2010)
55. Davidson, J.L., Wright, P., Ahsan, S.T., Robinson, R.L., Pomfrett, C.J.D., McCann, H.: fEITER – a new EIT instrument for functional brain imaging. *J. Phys: Conf. Ser.* **224**, 012025 (2010)
56. Davis, J., Wells, P.: Computed tomography measurements on wood. *Ind. Metrol.* **2**(3–4), 195–218 (1992)
57. Deistung, A., Rauscher, A., Sedlacik, J., Stadler, J., Witoszynskyj, S., Reichenbach, J.R.: Susceptibility weighted imaging at ultra high magnetic field strengths: theoretical considerations and experimental results. *Magn. Reson. Med.* **60**(5), 1155–1168 (2008). doi:[10.1002/mrm.21754](https://doi.org/10.1002/mrm.21754)
58. Denyer, C.W.L.: Electronics for real-time and three-dimensional electrical impedance tomographs, PhD Thesis, Oxford Brookes University (1996)
59. Devous, M.D.: Single-photon emission computed tomography in neurotherapeutics. *NeuroRx.* **2**(2), 237–249 PMCID: PMC1064989 (2005)
60. Dias, N.S., Carmo, J.P., Mendes, P.M., Correia, J.H.: Wireless instrumentation system based on dry electrodes for acquiring EEG signals. *Med. Eng. Phys.* **34**(7), 972–981 (2012)
61. Donta, S.T., Noto, R.B., Vento, J.A.: SPECT brain imaging in chronic Lyme disease. *Clin. Nucl. Med.* **37**(9), e219–e222 (2012)
62. Eigner, T., Gruzelier, J.H.: EEG biofeedback of low beta band components: frequency-specific effects on variables of attention and event-related brain potentials. *Clin. Neurophysiol.* **115**(1), 131–139 (2004)
63. Fabrizi, L., Sparkes, M., Horesh, L., Perez-Juste, Abascal J.F., McEwan, A., Bayford, R.H., Elwes, R., Binnie, C.D., Holder, D.S.: Factors limiting the application of electrical impedance tomography for identification of regional conductivity changes using scalp electrodes during epileptic seizures in humans. *Physiol. Meas.* **27**, S163–S174 (2006)
64. Facey, K., Bradbury, I., Laking, G., Payne, E.: Overview of the clinical effectiveness of positron emission tomography imaging in selected cancers. *Health Technol. Assess.* **11**(44), iii–iv, xi–267 (2007)
65. Faiz, O., Blackburn, S., Moffat, D.: Anatomy at a Glance, 3rd edn. Wiley-Blackwell, Chichester (2011)

66. Florin, A., da Silva, F.L.: Cellular substrates of brain rhythms. In: Schomer, D.L., da Silva Fernando L. Niedermeyer's electroencephalography: basic principles, clinical applications, and related fields 6th edn., pp. 33–63. Lippincott Williams & Wilkins, Philadelphia (2010)
67. Flink, K.R.: Intraoperative electrocorticography in epilepsy surgery: useful or not? *Seizure* **12**(8), 577–584 (2003). doi:[10.1016/S1059-1311\(03\)00095-5](https://doi.org/10.1016/S1059-1311(03)00095-5)
68. Fox, M.D., Raichle, M.E.: Spontaneous fluctuations in brain activity observed with functional magnetic resonance imaging. *Nat. Rev. Neurosci.* **8**(9), 700–711 (2007)
69. Frey, K.A.: Positron emission tomography. In: Siegel, G.J., Agranoff, B.W., Albers, R.W. et al., (eds.) Basic neurochemistry: molecular, cellular and medical aspects, Chap. 54, 6th edn. Lippincott-Raven, Philadelphia
70. Ganis, G., Kosslyn, S.M.: ‘Neuroimaging’. In: Ramachandran V.S. (ed.) Encyclopedia of the human brain, pp. 493–505 (2002)
71. Gastaut, J.L., Michel, B., Hassan, S.S., Cerdá, M., Bianchi, L., Gastaut, H.: Electroencephalography in brain edema (127 cases of brain tumor investigated by cranial computerized tomography). *Electroencephalogr. Clin. Neurophysiol.* **46**(3), 239–255 (1979)
72. Gerrard, P., Malcolm, R.: Mechanisms of modafinil: a review of current research. *Neuropsychiatr. Dis. Treat.* **3**(3), 349–364 (2007)
73. Giedd, J.N.: Structural magnetic resonance imaging of the adolescent brain. *Ann. N. Y. Acad. Sci.* **1021**, 77–85 (2004)
74. Gilad, O., Holder, D.S.: Impedance changes recorded with scalp electrodes during visual evoked responses: implications for electrical impedance tomography of fast neural activity. *Neuroimage* **15**, 47(2), 514–522 (2009)
75. Gillespie, J.E., Jackson, A.: MRI and CT of the Brain, 1 edn. CRC Press (2000)
76. Gloor, P., Ball, G., Schaul, N.: Brain lesions that produce delta waves in the EEG. *Neurology* **27**(4), 326–333 (1977)
77. Götzte, W., Schulze, A., Kubicki, S.: Concerning the diagnosis of epidural hematoma in the EEG. *Electroencephalogr. Clin. Neurophysiol.* **13**(1) 111–113 (1961)
78. Graham, B.M.: Enhancements in electrical impedance tomography (EIT) image reconstruction for 3D Lung Imaging, PhD thesis, University of Ottawa (2007)
79. Greenfield, S.: The human brain: a guided tour (SCIENCE MASTERS). Phoenix, Reissued 2001 edn (1997)
80. Greenstein, B., Wood, D.: The endocrine system at a glance, 3 edn. Wiley-Blackwell (2011)
81. Gronseth, G.S., Greenberg, M.K.: The utility of the electroencephalogram in the evaluation of patients presenting with headache: a review of the literature. *Neurology* **45**(7), 1263–1267 (1995)
82. Grunwald, M., Weiss, T., Krause, W., Beyer, L., Rost, R., Gutberlet, I., Gertz, H.J.: Power of theta waves in the EEG of human subjects increases during recall of haptic information. *Neurosci. Lett.* **260**(3), 189–192
83. Haacke, E.M., Mittal, S., Wu, Z., Neelavalli, J., Cheng, Y.C.: Susceptibility-weighted imaging: technical aspects and clinical applications, part 1. *AJNR Am. J. Neuroradiol.* **30**(1), 19–30 (2009). doi:[10.3174/ajnr.A1400](https://doi.org/10.3174/ajnr.A1400)
84. Hauri, P.: Treating psychophysiological insomnia with biofeedback. *Arch. Gen. Psychiatry* **38** (7), 752 (1981)
85. Hiller, J., Reindl, L.M.: A computer simulation platform for the estimation of measurement uncertainties in dimensional X-ray computed tomography. *Measurement* **45**(8), 2166–2182 (2012)
86. Holder, D.S.: Electrical impedance tomography of brain function. *Brain Topogr.* **5**(2), 87–93 (1992)
87. Holder, D.S.: Detection of cerebral ischaemia in the anaesthetised rat by impedance measurement with scalp electrodes: implications for non-invasive imaging of stroke by electrical impedance tomography. *Clin. Phys. Physiol. Meas.* **13**(1), 63–75 (1992)
88. Holder, D.S., Hanquan, Y., Rao, A.: Some practical biological phantoms for calibrating multifrequency electrical impedance tomography. *Physiol. Meas.* **17**, A167–A177 (1996)

89. Holder, D.S., Rao, A., Hanquan, Y.: Imaging of physiologically evoked responses by electrical impedance tomography with cortical electrodes in the anaesthetized rabbit. *Physiol. Meas.* Nov **17**(Suppl 4A), A179–A186 (1996b)
90. Holder, D.S., Rao, A., Hanquan, Y.: Imaging of physiologically evoked responses by electrical impedance tomography with cortical electrodes in the anaesthetized rabbit. *Physiol. Meas.* **17**, A179–A186 (1996)
91. Holder, D.S., González-Correa, C.A., Tidswell, T., Gibson, A., Cusick, G., Bayford, R.H.: Assessment and calibration of a low-frequency system for electrical impedance tomography (EIT) optimized for use in imaging brain function in ambulant human subjects. *Ann New York Acad. Sci.* **873**(1), 512–519 (1999)
92. Huang, W.-Y., Muo, C.-H., Lin, C.-Y., Jen, Y.-M., Yang, M.-H., Lin, J.-C., Sung, F.-C., Kao, C.-H.: Paediatric head CT scan and subsequent risk of malignancy and benign brain tumour: a nation-wide population-based cohort study. *British J. Cancer Adv.* [10.1038/bjc.2014.103](https://doi.org/10.1038/bjc.2014.103) (2014)
93. Hughes, J.R.: Gamma, fast, and ultrafast waves of the brain: their relationships with epilepsy and behavior. *Epilepsy Behav.* **13**(1), 25–31 (2008)
94. Gold, Ian: Does 40-Hz oscillation play a role in visual consciousness? *Conscious. Cogn.* **8** (2), 186–195 (1999). doi:[10.1006/ccog.1999.0399](https://doi.org/10.1006/ccog.1999.0399)
95. Imperiale, C., Imperiale, A.: Some fast calculations simulating measurements from single-photon emission computed tomography (SPECT) imaging. *Measurement* **37**(3), 218–240 (2005)
96. Internet Article 1: Anatomy of the Brain <http://www.strokecenter.org/professionals/brain-anatomy/anatomy-of-the-brain/>. Accessed 16th May 2014
97. Internet Article 2: Non-Invasive electromagnetic technique for monitoring physiological changes in the brain. <http://www.jhuapl.edu/ott/technologies/technology/articles/P00197.asp>. Accessed 26th August 2013
98. Internet Article 3 Ashrafulla S.: EEG and MEG: functional brain imaging with high temporal resolution. [http://www.usc.edu/programs/neuroscience/private/mona\\_journal\\_club/Syed\\_EEG\\_MEG.pdf](http://www.usc.edu/programs/neuroscience/private/mona_journal_club/Syed_EEG_MEG.pdf) (2013). Accessed 26th August 2013
99. Internet Article 4: Brain diseases. <http://www.nlm.nih.gov/medlineplus/braindiseases.html> 2013. Accessed 26th August 2013
100. Internet Article 5: Technology—positron emission tomography (Pet) imaging. <http://www.cellsighttech.com/technology/pet.html> 2014. Accessed 20th April 2014
101. Internet Article 6: Head MRI. <http://www.ncbi.nlm.nih.gov/pubmedhealth/PMH0004250/> 2014. Accessed 20th April 2014
102. Internet Article 7: Human brain. [http://en.wikipedia.org/wiki/Human\\_brain#refBuxton](http://en.wikipedia.org/wiki/Human_brain#refBuxton) 2014. Accessed 16th April 2014
103. Internet Article 10: Electroencephalography. <http://en.wikipedia.org/wiki/Electroencephalography> 2014. Accessed 16th April 2014
104. Internet Article 11: Brainwaves overview. <http://www.transparentcorp.com/products/np/brainwaves.php> 2014. Accessed 16th April 2014
105. Internet Article 12: What is Magnetoencephalography (MEG)? <http://ilabs.washington.edu/what-magnetoencephalography-meg> 2014. Accessed 20th April 2014
106. Internet Article 13: 10–20 system (EEG). [http://en.wikipedia.org/wiki/10-20\\_system\\_\(EEG\)](http://en.wikipedia.org/wiki/10-20_system_(EEG)) 2014. Accessed 20th April 2014
107. Internet Article 14: EEG recording. <http://www.aha.ru/~geivanit/EEGmanual/Recording.htm> 2014. Accessed 20th April 2014
108. Internet Article 15: Magnetoencephalography. [http://en.wikipedia.org/wiki/Human\\_brain](http://en.wikipedia.org/wiki/Human_brain) 2014. Accessed 20th April 2014
109. Internet Article 16: Electrocorticography. <http://en.wikipedia.org/wiki/Electrocorticography> 2014. Accessed 22nd April 2014
110. Internet Article 17: Electroneurogram. <http://en.wikipedia.org/wiki/Electroneurogram> 2014. Accessed 23th April 2014

111. Internet Article 18: Electrical impedance tomography of brain function. [http://www.ucl.ac.uk/medphys/research/eit/pubs/brain\\_EIT\\_overview.pdf](http://www.ucl.ac.uk/medphys/research/eit/pubs/brain_EIT_overview.pdf) 2014. Accessed 24th April 2014
112. Internet Article 8: History of electroencephalography. <https://wiki.engr.illinois.edu/display/BIOE414/History+of+Electroencephalography> 2014. Accessed 20th April 2014
113. Internet Article 9: Millet, D.: The origins of EEG. <http://www.bri.ucla.edu/nha/ishn/ab24-2002.htm> 2002. Accessed 20th April 2014
114. Iwata, K., Nakao, M., Yamamoto, M., Kimura, M.: Quantitative characteristics of alpha and theta EEG activities during sensory deprivation. *Psychiatry Clin. Neurosci.* **55**(3), 191–192 (2001)
115. Jasper, H.H.: The ten-twenty electrode system of the International Federation. *Electroencephalogr. Clin. Neurophysiol.* **10**, 371–375 (1958)
116. Jeon, K., Chang-Ock, L.: CoReHA 2.0: a software package for in vivo MREIT experiments. *Comput. Math. Methods Med.* **2013**(Article ID 941745) 8 (2013)
117. Jing, L., Liu, S., Zhihong, L., Meng, S.: An image reconstruction algorithm based on the extended Tikhonov regularization method for electrical capacitance tomography. *Measurement* **42**(3), 368–376 (2009)
118. Jo, H.G., Hinterberger, T., Wittmann, M., Borghardt, T.L., Schmidt, S.: Spontaneous EEG fluctuations determine the readiness potential: is preconscious brain activation a preparation process to move? *Exp. Brain Res.* **231**(4), 495–500 (2013)
119. John, E.R., Prichep, L.S., Kox, W., Valdes-Sosa, P., Bosch-Bayard, J., Aubert, E., Gugino, L.D.: Invariant reversible QEEG effects of anesthetics. *Conscious. Cogn.* **10**(2), 165–183 (2001)
120. Joy, M., Scott, G., Henkelman, M.: In vivo detection of applied electric currents by magnetic resonance imaging. *Magn. Reson. Imaging* **7**(1), 89–94 (1989)
121. Li-Hong, J., Ming-Ni, W.: MRI brain lesion image detection based on color-converted K-means clustering segmentation. *Measurement* **43**(7), 941–949 (2010)
122. Jurcak, V., Tsuzuki, D., Dan, I.: 10/20, 10/10, and 10/5 systems revisited: their validity as relative head-surface-based positioning systems. *Neuroimage*. **15**, **34**(4), 1600–1611. Epub 2007 Jan 4
123. Karson, C.N., Coppola, R., Daniel, D.G., Weinberger, D.R.: Computerized EEG in schizophrenia. *Schizophr. Bull.* **14**(2), 193–197 (1988)
124. Keshav, S., Bailey, A.: The Gastrointestinal System at a Glance, 2 edn. Wiley-Blackwell
125. Khalighi, M., Vosoughi Vahdat, B., Mortazavi, M., Soleimani, M.: Practical design of low-cost instrumentation For industrial Electrical Impedance Tomography (EIT). In: IEEE international instrumentation and measurement technology conference, 2012-05-01, Graz (2012)
126. Khang, H.S., Lee, B.I., Oh, S.H., Woo, E.J., Lee, S.Y., Cho, M.Y., Kwon, O., Yoon, J.R., Seo, J.K.: J-substitution algorithm in magnetic resonance electrical impedance tomography (MREIT): phantom experiments for static resistivity images. *IEEE Trans. Med. Imaging* **21**(6), 695–702 (2002)
127. Kim, H.J., Oh, T.I., Kim, Y.T., Lee, B.I., Woo, E.J., Seo, J.K., Lee, S.Y., Kwon, O., Park, C., Kang, B.T., Park, H.M.: In vivo electrical conductivity imaging of a canine brain using a 3T MREIT system. *Physiol. Meas.* **29**, 1145–1155 (2008)
128. Kim, D.-H., Ghim, M.-O., Kwon, O., Kim, H., Seo, J., Woo, E.: MREIT and EPT: a comparison of two conductivity imaging modalities. *Proc. Int. Soc. Mag. Reson. Med.* **19**, 4468 (2011)
129. Klassen, B.T., Hentz, J.G., Shill, H.A., Driver-Dunckley, E., Evidente, V.G., Sabbagh, M.N., Adler, C.H., Caviness, J.N.: Quantitative EEG as a predictive biomarker for Parkinson disease dementia. *Neurol.* **12**, **77**(2), 118–124 (2011)
130. Klein, S., Thorne, B.M.: Biological Psychology, 1 edn. Wiley, New York (2006)
131. Klem, G.H., Lüders, H.O., Jasper, H.H., Elger, C.: The ten-twenty electrode system of the international federation. *Electroencephalogr. Clin. Neurophysiol.* **52**, 3–6 (1999)
132. Kong, J., Ma, L., Gollub, R.L., Wei, J., Yang, X., Li, D., Weng, X., Jia, F., Wang, C., Li, F., Li, R., Zhuang, D.: A pilot study of functional magnetic resonance imaging of the brain

- during manual and electroacupuncture stimulation of acupuncture point (LI-4 Hegu) in normal subjects reveals differential brain activation between methods. *J. Altern. Complement. Med.* **8**(4), 411–419 (2002)
133. Kwong, K.K., Belliveau, J.W., Chesler, D.A., Goldberg, I.E., Weisskoff, R.M., Poncelet, B. P., Kennedy, D.N., Hoppel, B.E., Cohen, M.S., Turner, R., et al.: Dynamic magnetic resonance imaging of human brain activity during primary sensory stimulation. *Proc. Natl. Acad. Sci. USA* **89**(12), 5675–5679 (1992)
134. Lai, C.W., Gragasin, M.E.: Electroencephalography in herpes simplex encephalitis. *J. Clin. Neurophysiol.* Jan **5**(1), 87–103 (1988)
135. Langkammer, C., Liu, T., Khalil, M., Enzinger, C., Jehna, M., Fuchs, S., Fazekas, F., Wang, Y., Ropele, S.: Quantitative susceptibility mapping in multiple sclerosis. *Radiology* **267**, 551–559 (2013)
136. Langkammer, C., Schweser, F., Krebs, N., Deistung, A., Goessler, W., Scheurer, E., Sommer, K., Reishofer, G., Yen, K., Fazekas, F., Ropele, S., Reichenbach, J.R.: Quantitative susceptibility mapping (QSM) as a means to measure brain iron? A post mortem validation study. *Neuroimage* **62**(2–3), 1593–1599 (2012)
137. Lay-Ekuakille, A., Vergallo, P., Trabacca, A., De Rinaldis, M., Angelillo, F., Conversano, F., Casciaro, S.: Low-frequency detection in ECG signals and joint EEG-Ergospirometric measurements for precautionary diagnosis. *Measurement* **46**(1), 97–107 (2013)
138. Letosa, J., Artal, J.S., Sampón, M., Usón, A., Arcega, F.J.: Modelization of current sensors by finite elements method. *Measurement* **35**(3), 233–241 (2004)
139. Lionheart, W.R.B.: EIT reconstruction algorithms: pitfalls, challenges and recent developments, REVIEW ARTICLE. *Physiol. Meas.* **25**(2004), 125–142 (2004)
140. Liu, H., Tao, X., Xua, P., Zhang, H., Bai, Z.: A dynamic measurement system for evaluating dry bio-potential surface electrodes. *Measurement* **46**, 1904–1913 (2013)
141. Liu, J., Liu, T., de Rochefort, L., Khalidov, I., Prince, M., Wang, Y.: Quantitative susceptibility mapping by regulating the field to source inverse problem with a sparse prior derived from the Maxwell equation: validation and application to brain. *Proc. Intl. Soc. Mag. Reson. Med.* **18**(2010), 4996 (2010)
142. Loo, S.K., Makeig, S.: Clinical utility of EEG in attention-deficit/hyperactivity disorder: a research update. *Neurotherapeutics* **9**(3), 569–587 (2012)
143. Loo, S.K., Barkley, R.A.: Clinical utility of EEG in attention deficit hyperactivity disorder. *Appl. Neuropsychol.* **12**(2), 64–76 (2005)
144. Luck, S.J.: An Introduction to the Event-Related Potential Technique. The MIT Press, Cambridge (2005). ISBN 0-262-12277-4
145. Ludovic, D.R., Tian, L., Bryan, K., Jing, L., Pascal, S., Vincent, L., Jianlin, W., Yi, W.: Quantitative susceptibility map reconstruction from MR phase data using bayesian regularization: validation and application to brain imaging. *Magn. Reson. Med.* **63**(1), 194–206 (2009). doi:[10.1002/mrm.22187](https://doi.org/10.1002/mrm.22187)
146. Maas, L.C., Lukas, S.E., Kaufman, M.J., Weiss, R.D., Daniels, S.L., Rogers, V.W., Kukkes, T.J., Renshaw, P.F.: Functional magnetic resonance imaging of human brain activation during cue-induced cocaine craving. *Am. J. Psychiatry* **155**(1), 124–126 (1998)
147. Macdonell, R.A., Donnan, G.A., Bladin, P.F., Berkovic, S.F., Wriedt, C.H.: The electroencephalogram and acute ischemic stroke. Distinguishing cortical from lacunar infarction. *Arch. Neurol.* **45**(5), 520–524 (1988)
148. Malmivuo, J., Plonsey, R.: Bioelectromagnetism: Principles and Applications of Bioelectric And Biomagnetic Fields, Chap. 13. Oxford University Press, Oxford (1995)
149. McEwan, A., Romsauerova, A., Yerworth, R., Horesh, L., Bayford, R., Holder, D.: Design and calibration of a compact multi-frequency EIT system for acute stroke imaging. *Physiol. Meas.* **27**, S199–S210 (2006)
150. Meeus, I., Galdermans, D., Roland, J., Slabbynck, H., van Schaardenburg, C., Coolen, D.: Spectacular bone scintigraphy and transverse SPECT images in primary osteosarcoma of the pleura. *Clin. Nucl. Med.* **19**(8), 738–740 (1994)

151. Meng, Z.J., Sajib, S.Z.K., Chauhan, M., Sadleir, R.J., Kim, H.J., Kwon, O.I., Woo, E.J.: Numerical simulations of MREIT conductivity imaging for brain tumor detection. *Comput. Math. Methods Med.* **2013**(Article ID 704829), 10 (2013)
152. Michael-Titus, A.T., Revest, P., Shortland, P.: The Nervous System: Systems of the Body Series, 2 edn. Churchill Livingstone, Edinburgh (2010)
153. Miller, K.J., denNijs, M., Shenoy, P., Miller, J.W., Rao, R.P.N., Ojemann, J.G.: Real-time functional brain mapping using electrocorticography. *Techn. Note NeuroImage* **37**, 504–507 (2007)
154. Miltner, W.H., Braun, C., Arnold, M., Witte, H., Taub, E.: Coherence of gamma-band EEG activity as a basis for associative learning. *Nature* **397**(6718), 434–436 (1999)
155. Mittal, S., Wu, Z., Neelavalli, J., Haacke, E.M.: Susceptibility-weighted imaging: technical aspects and clinical applications, part 2. *AJNR Am. J. Neuroradiol.* **30**(2), 232–252 (2009). doi:[10.3174/ajnr.A1461](https://doi.org/10.3174/ajnr.A1461)
156. Munk, M.H., Roelfsema, P.R., König, P., Engel, A.K., Singer, W.: Role of reticular activation in the modulation of intracortical synchronization. *Science* **272**(5259), 271–274 (1996)
157. Murakami, S., Okada, Y.: Contributions of principal neocortical neurons to magnetoencephalography and electroencephalography signals. *J Physiol* **575**(Pt 3), 925–936 (2006). doi:[10.1113/jphysiol.2006.105379](https://doi.org/10.1113/jphysiol.2006.105379)
158. Newey, C.R., Sarwal, A., Hantus, S.: Continuous electroencephalography (cEEG) changes precede clinical changes in a case of progressive cerebral edema. *Neurocrit. Care* **18**(2), 261–265 (2013). doi:[10.1007/s12028-011-9650-4](https://doi.org/10.1007/s12028-011-9650-4)
159. Niedermeyer, E., da Silva F.L.: *Electroencephalography: Basic Principles, Clinical Applications, and Related Fields*. Lippincott Williams & Wilkins, New York (2004)
160. Nikolić, Z.M., Popović, D.B., Stein, R.B., Kenwell, Z.: Instrumentation for ENG and EMG recordings in FES systems. *IEEE Trans. Biomed. Eng.* **41**(7), 703–706 (1994)
161. Nolte, J.: *The Human Brain: An Introduction to its Functional Anatomy*, 6th edn. Mosby, Philadelphia (2008)
162. Nunez, P.L., Srinivasan, R.: *Electric Fields of the Brain: The Neurophysics of EEG*. Oxford University Press, New York (1981)
163. O'Callaghan, C.: *The Renal System at a Glance*, 3 edn. Wiley-Blackwell, Oxford (2009)
164. Oh, T.I., Koo, H., Lee, K.H., Kim, S.M., Lee, J., Kim, S.W., Seo, J.K., Woo, E.J.: Validation of a multi-frequency electrical impedance tomography (mfEIT) system KHU Mark1: impedance spectroscopy and time-difference imaging. *Physiol. Meas.* **29**(3), 295–307 (2008)
165. Palmini, A.: The concept of the epileptogenic zone: a modern look at Penfield and Jasper's views on the role of interictal spikes. *Epileptic Disorders* **8**(Suppl 2), S10–S15 (2006)
166. Parenti, G., Marconi, F., Fiori, L.: Electrophysiological (EEG-SSEP) monitoring during middle cerebral aneurysm surgery. *J. Neurosurg. Sci.* **40**(3–4), 195–205 (1996)
167. Park, C., Kwon, O.I.: Current density imaging using directly measured harmonic data in MREIT. *Comput. Math. Methods Med.* **2013**(Article ID 381507), 9 (2013)
168. Petry, K.G., Boiziau, C., Dousset, V., Brochet, B.: Magnetic resonance imaging of human brain macrophage infiltration. *Neurotherapeutics* **4**(3), 434–442 (2007)
169. Piwnica-Worms, D.: Clinical molecular imaging today: PET and SPECT. In: Kufe, D.W., Pollock, R.E., Weichselbaum, R.R., et al. (eds.) *Holland-Frei Cancer Medicine*, 6th edn. BC Decker, Hamilton (ON) (2003)
170. Pollak, L., Klein, C., Schifferer, J., Flechter, S., Rabey, J.: Electroencephalographic abnormalities in aseptic meningitis and noninfectious headache. A comparative study. *Headache* **41**(1), 79–83 (2001)
171. Preissl, H.: *Magnetoencephalography*, 1 edn. Academic Press, New York (2005)
172. Purnell, J.Q., Klopstein, B.A., Stevens, A.A., Havel, P.J., Adams, S.H., Dunn, T.N., Krisky, C., Rooney, W.D.: Brain functional magnetic resonance imaging response to glucose and fructose infusions in humans. *Diab. Obes. Metab.* **13**(3), 229–234 (2011). doi:[10.1111/j.1463-1326.2010.01340.x](https://doi.org/10.1111/j.1463-1326.2010.01340.x)

173. Raichle, M., Gusnard, D.A.: Appraising the brain's energy budget. *Proc. Natl. Acad. Sci. USA* **99**(16), 10237–10239 (2002)
174. Rangaswamy, M., Porjesz, B., Chorlian, D.B., Wang, K., Jones, K.A., Bauer, L.O., Rohrbaugh, J., O'Connor, S.J., Kuperman, S., Reich, T., Begleiter, H.: Beta power in the EEG of alcoholics. *Biol. Psychol.* **52**(8), 831–842 (2002)
175. Reddy, J.N.: An Introduction to the Finite Element Method, 3rd edn. McGraw-Hill Science/Engineering/Math (2005)
176. Riu, P.J., Rosell, J., Lozano, A., Pallás-Areny, R.: Multi-frequency static imaging in electrical impedance tomography: Part 1. Instrum. Requirements Med. Biol. Eng. Comput. **33**(6), 784–792 (1995)
177. Roesler, C.R.M., Horn, F.J., Moré, A.D.O., Fancello, E.A.: A biomechanical analysis of titanium miniplates used for treatment of mandible condylar fracture with the finite element method. *J. Med. Imaging Health Inf.* **4**, 106–112 (2014)
178. Romsauerova, A., McEwan, A., Horesh, L., Yerworth, R., Bayford, R.H., Holder, D.S.: Multi-frequency electrical impedance tomography (EIT) of the adult human head: initial findings in brain tumours, arteriovenous malformations and chronic stroke, development of an analysis method and calibration. *Physiol. Meas.* **27**, S147–S161 (2006)
179. Ronne-Engstrom, E., Winkler, T.: Continuous EEG monitoring in patients with traumatic brain injury reveals a high incidence of epileptiform activity. *Acta Neurol. Scand. Jul* **114**(1), 47–53 (2006)
180. Rothenberger, A., Moll, G.H.: Standard EEG and dyslexia in children—new evidence for specific correlates? *Acta Paedopsychiatr.* **56**(3), 209–218 (1994)
181. Rozman, J., Zorko, B., Bunc, M.: Recording of electroneurograms from the nerves innervating the pancreas of a dog. *J. Neurosci. Methods.* **15**, **112**(2), 155–162 (2001)
182. Rudzinski, L.A., Rabinstein, A.A., Chung, S.Y., Wong-Kisiel, L.C., Burrus, T.M., Lanzino, G., Westmoreland, B.F.: Electroencephalographic findings in acute subdural hematoma. *J. Clin. Neurophysiol.* **28**(6), 633–641 (2011)
183. Sadleir, R.J., Grant, S.C., Woo, E.J.: Can high-field MREIT be used to directly detect neural activity? *Theor. Considerations NeuroImage* **52**(1), 205–216 (2010)
184. Sathy, P.D., Kayalvizhi, R.: Amended bacterial foraging algorithm for multilevel thresholding of magnetic resonance brain images. *Measurement* **44**(10), 1828–1848 (2011)
185. Schneiderman, J.F.: Information content with low- versus high-T(c) SQUID arrays in MEG recordings: the case for high-T(c) SQUID-based MEG. *J. Neurosci. Methods.* **30**, **222**, 42–46. doi: [10.1016/j.jneumeth.2013.10.007](https://doi.org/10.1016/j.jneumeth.2013.10.007). Epub 2013 Nov 1
186. Seo, J.K., Woo, E.J.: Nonlinear Inverse Problems in Imaging, 1 edn. Wiley, New York (2012)
187. Seo, J.K., Min-Oh, Kim, Lee, J., Choi, N., Woo, E.J., Kim, H.J., Kwon, O.I., Dong-Hyun, Kim: Error analysis of nonconstant admittivity for mr-based electric property imaging. *IEEE Trans. Med. Imaging* **31**(2), 430–437 (2012)
188. Shafi, A.A., Kadir, M.R.A., Sulaiman, E., Kasim, N.H.A., Kassim, N.L.A.: The effect of dental implant materials and thread profiles—a finite element and statistical study. *J. Med. Imaging Health Inf.* **3**, 509–513 (2013)
189. Sharbrough, F., Chatrian, G.-E., Lesser, R.P., Lüders, H., Nuwer, M., Picton, T.W.: American electroencephalographic society guidelines for standard electrode position nomenclature. *J. Clin. Neurophysiol.* **8**, 200–202 (1991)
190. Sieg, K.G., Gaffney, G.R., Preston, D.F., Hellings, J.A.: SPECT brain imaging abnormalities in attention deficit hyperactivity disorder. *Clin. Nucl. Med.* **20**(1), 55–60 (1995)
191. Soleimani, M., Mitchell, C.N.: Electrical impedance tomography guided cryosurgery for the brain using a temporally correlated image reconstruction. In: XXIX General Assembly of the International Union of Radio/Union Radio Scientifique Internationale, 2008, USA
192. Sritharan, A., Line, P., Sergejew, A., Silberstein, R., Egan, G., Copolov, D.: EEG coherence measures during auditory hallucinations in schizophrenia. *Psychiatry Res.* **15**, **136**(2–3), 189–200 (2005)

193. Stephenson, D.R., Davidson, J.L., Lionheart, W.R.B., Grieve, B.D., York, T.A.: Comparison of 3D image reconstruction techniques using real electrical impedance measurement data. In: 4th World Congress on Industrial Proceedings Tomography, 2005, Japan, pp. 1–8
194. Stufflebeam, S.M., Tanaka, N., Ahlfors, S.P.: Clinical applications of Magnetoencephalography. *Hum. Brain Mapp.* **30**(6), 1813–1823 (2009)
195. Szczecinski, L., Morawski, R.Z., Barwicz, A.: Original-domain Tikhonov regularization and non-negativity constraint improve resolution of spectrophotometric analyses. *Measurement* **18**(3), 151–157 (1996)
196. Tan, H., Liu, T., Wu, Y., Thacker, J., Shenkar, R., Mikati, A.G., Shi, C., Dykstra, C., Wang, Y., Prasad, P.V., Edelman, R.R., Awad, I.A.: Evaluation of iron content in human cerebral cavernous malformation using quantitative susceptibility mapping. *Invest. Radiol.* **49**(7), 498–504 (2014). doi:[10.1097/RIN.0000000000000043](https://doi.org/10.1097/RIN.0000000000000043)
197. Tang, T.: Detection of intraventricular hemorrhage in neonates using electrical impedance tomography, Ph.D. Thesis, University of Florida, USA (2010)
198. Tatum, W.O., Husain, A.M., Benbadis, S.R.: Handbook of EEG Interpretation. Demos Medical Publishing, New York (2008)
199. Tidswell, T., Gibson, A., Bayford, R.H., Holder, D.S.: Three-dimensional electrical impedance tomography of human brain activity. *NeuroImage* **13**(2), 283–294 (2001)
200. Turovets, S., Poolman, P., Salman, A., Li, K., Malony, A., Tucker, D.: Bounded electrical impedance tomography for noninvasive conductivity estimation of the human head tissues, EIT 2009. Manchester, UK (2009)
201. Vespa, P.: Continuous EEG monitoring for the detection of seizures in traumatic brain injury, infarction, and intracerebral hemorrhage: “to detect and protect”. *J. Clin. Neurophysiol.* **22** (2), 99–106 (2005)
202. Vignadndra, V., Ghee, L.T., Chawla, J.: EEG in brain abscess: its value in localization compared to other diagnostic tests. *Electroencephalogr. Clin. Neurophysiol.* **38**(6), 611–622 (1975)
203. Vonach, M., Marson, B., Yun, M., Cardoso, J., Modat, M., Ourselin, S., Holder, D.: A method for rapid production of subject specific finite element meshes for electrical impedance tomography of the human head. *Physiol. Meas.* **33**, 801–816 (2012)
204. Li-ming, Wang, Ying-liang, Zhao, Fang-lin, Chen, Han, Y.: The 3D CT reconstruction algorithm to directly reconstruct multi-characteristic based on EMD. *Measurement* **44**(10), 2043–2048 (2011)
205. Wang, C., Zheng, D., Xu, J., Lam, W., Yew, D.T.: Brain damages in ketamine addicts as revealed by magnetic resonance imaging. *Front. Neuroanat.* **7**, 23 (2013)
206. Wang, P., Guo, B., Li, N.: Multi-index optimization design for electrical resistance tomography sensor. *Measurement* **46**(8), 2845–2853 (2013)
207. Yun-Heng, Wang, Qiao, J., Jun-Bao, Li, Fu, P., Shu-Chuan, Chu, Roddick, J.F.: Sparse representation-based MRI super-resolution reconstruction. *Measurement* **47**, 946–953 (2014)
208. Ward, J.P.T., Ward, J., Leach, R.M.: The Respiratory System at a Glance, 3rd edn. Wiley-Blackwell, Oxford (2010)
209. Webster, J.G.: Electrical impedance tomography. Adam Hilger Series of Biomedical Engineering, Adam Hilger, New York (1990)
210. Weese-Mayer, D.E., Brouillette, R.T., Klemka, L., Hunt, C.E.: Effects of almitrine on hypoglossal and phrenic electroneurograms. *J. Appl. Physiol.* **59**(1), 105–112 (1985)
211. Wei, L., Bing, W., Chunlei, L.: Quantitative susceptibility mapping of human brain reflects spatial variation in tissue composition. *NeuroImage* **55**(4), 1645–1656 (2011)
212. Wei, L., Bing, W., Chunlei, L.: Quantitative susceptibility mapping of human brain reflects spatial variation in tissue composition. *NeuroImage* **55**(4), 1645–1656 (2011). doi:[10.1016/j.neuroimage.2010.11.088](https://doi.org/10.1016/j.neuroimage.2010.11.088)
213. Wilson, A.J., Felton, E.A., Garell, C.P., Schalk, G., Williams, J.C.: ECoG factors underlying multimodal control of a brain-computer interface. *IEEE Trans. Neural Syst. Rehabil. Eng.* **14** (2), 246–250 (2006)

214. Woo, E.J.: Functional Brain Imaging using MREIT and EIT: Requirements and Feasibility. NFSI & ICBEM, Banff, Canada, May 13–15 (2011)
215. Xu, B., Spincemaille, P., Liu, T., Prince, M.R., Dutruel, S., Gupta, A., Thimmappa, N.D., Wang, Y.: Quantification of cerebral perfusion using dynamic quantitative susceptibility mapping. *Magn. Reson. Med.* Apr 14 doi: [10.1002/mrm.25257](https://doi.org/10.1002/mrm.25257) (2014)
216. Yasuhara, A.: Correlation between EEG abnormalities and symptoms of autism spectrum disorder (ASD). *Brain Dev.* 2010 Nov **32**(10), 791–798 (2010)
217. Ye, L., Yang, M., Xu, L., Guo, C., Li, L., Wang, D.: Optimization of inductive angle sensor using response surface methodology and finite element method. *Measurement* **48**, 252–262 (2014)
218. Yerworth, R.J., Bayford, R.H., Cusick, G., Conway, M., Holder, D.S.: Design and performance of the UCLH Mark 1b 64 channel electrical impedance tomography (EIT) system, optimized for imaging brain function. *Physiol. Meas.* **23**, 149–158 (2002)
219. Yerworth, R.J., Bayford, R.H., Brown, B., Milnes, P., Conway, M., Holder, D.S.: Electrical impedance tomography spectroscopy (EITS) for human head imaging. *Physiol. Meas.* **24**, 477–489 (2003)
220. Yorkey, T.J.: Comparing reconstruction methods for electrical impedance tomography, PhD thesis, University of Wisconsin at Madison, Madison (1986)
221. Yorkey, T.J., Webster, J.G., Tompkins, W.J.: Comparing reconstruction algorithms for electrical impedance tomography. *IEEE Trans. Biomed. Eng.* **BME-34**(11), 843–852 (1987)
222. Zhang, X., Zhu, S., He, B.: Imaging electric properties of biological tissues by RF field mapping in MRI. *IEEE Trans. Med. Imaging* **29**(2), 474–481 (2010)
223. Zhang, X., He, B.: Imaging electric properties of human brain tissues by b1 mapping: a simulation study. *J. Phys: Conf. Ser.* **224**, 012077 (2010)
224. Zhang, X., Van de Moortele, P.F., Schmitter, S., He, B.: Complex B1 mapping and electrical properties imaging of the human brain using a 16-channel transceiver coil at 7T. *Magn. Reson. Med.* **69**(5), 1285–1296 (2013)
225. Zimmerman, J.E., Theine, P., Harding, J.T.: Design and operation of stable rf-biased superconducting point-contact quantum devices, etc. *J. Appl. Phys.* **41**, 1572–1580 (1970)

# **Chapter 4**

# **Translational Algorithms: The Heart of a Brain Computer Interface**

**Harsimrat Singh and Ian Daly**

**Abstract** Brain computer Interface (BCI) development encapsulates three basic processes: data acquisition, data processing, and device control. Since the start of the millennium the BCI development cycle has undergone a metamorphosis. This is mainly due to the increased popularity of BCI applications in both commercial and research circles. One of the focuses of BCI research is to bridge the gap between laboratory research and commercial applications using this technology. A vast variety of new approaches are being employed for BCI development ranging from novel paradigms, such as simultaneous acquisitions, through to asynchronous BCI control. The strategic usage of computational techniques, comprising the heart of the BCI system, underwrites this vast range of approaches. This chapter discusses these computational strategies and translational techniques including dimensionality reduction, feature extraction, feature selection, and classification techniques.

**Keywords** Event related (de)synchronisation • Principal component analysis • Feature extraction • Feature selection • BCI classification

## **4.1 Introduction**

Brain-computer interfacing (BCI) is a highly challenging multidisciplinary area of research. Since the start of the millennium, research groups exploring this area have made increasingly impressive progress. The core BCI research has opened up hundreds of avenues for its applications. There have been interesting revelations in

---

H. Singh (✉)

Department of Medical Physics and Bioengineering, University College London,  
London, UK

e-mail: singhharsimrat@gmail.com

I. Daly

Brain Embodiment Lab, University of Reading, Berkshire, UK  
e-mail: i.daly@reading.ac.uk

the field of rehabilitation [1, 5], gaming [51], composing music [44], and other biophysics applications based on BCI. However, there are still a lot of unanswered questions facing the BCI community, which impedes the launch of mainstream commercial BCI applications. The first five international meetings of BCI community [27, 78, 79, 77, 81] have evolved sufficient consensus on the BCI terminology, signals used and the computational techniques used but questions relating to user variability, session variability and optimal training remain a major research issues. The inherent complexity and enormity of the neural data from measurement techniques such as electroencephalogram (EEG), Electrocorticogram (ECoG), functional near infra-red spectroscopy (fNIRS), and functional Magnetic resonance Imaging (fMRI) warrants sophistication in computational strategies for meaningful interpretation.

Research areas of BCI evolved from the work of Hans Berger, a German Psychiatrist who first recorded EEG in 1929. Since then EEG has served as a standard Clinical diagnostic tool for a range of neurological complexities [76]. Among several definitions, an EEG is expressed as sustained fluctuations of electric potential, recorded from the human scalp which can be used to decipher corresponding variations in the cortex of the brain. Our ability to feel, think and act can be attributed to these variations of electrical activity. Farwell and Donchin [15] first demonstrated that the ability of EEG response to change to an externally accentuated event can be developed as a non-muscular communication channel for sending messages and commands to the outside world for control purposes; this is popularly known as the brain-computer interface. Subsequently, clinical BCI applications such as a speller have underlined the popularity of the event related potential (ERP) as one of the basis of EEG based BCIs [65].

The principles underlying this opening up of a communication channel between the brain and the computer are based on the classification of the changes in the EEG which relate to, for example, the imagination of movements [55]. The heart of the BCI is the translational algorithm which converts the electrophysiological measurements from the user into output that controls external devices [82]. We use the term EEG here to typify the signal which is used as the vehicle for development of the BCI; EEG being the most popular and easy to record—other brain-related signals include electrocorticogram (ECoG), magnetoencephalogram (MEG), and functional magnetic resonance (fMRI) images. These will be discussed in the section—‘Sources of Information for a BCI’. Ideally an interface may suggest a two way communication channel but the present state of the art in BCI purposes a one way communication i.e. from the brain to the computer. Information from the brain in the form of signals or images has been sufficient to realise a plethora of applications [5, 22, 53] for medical rehabilitation and for gaming by companies like Emotiv (Emotiv, Australia) and Neurosky (Neurosky, USA).

This chapter proceeds as follows. Section 4.2 gives an overview of sources of information for BCI. Section 4.3 considers the BCI development process. Section 4.4 is concerned with the types of BCI. Section 4.5 discusses nomenclature for feature extraction and classification. Sections 4.6 and 4.7 cater to evaluation criteria, conclusions and future work.

## 4.2 Sources of Information for a BCI

A brain computer interface is developed on the basis of the knowledge that can be extracted from various sources of information from the brain, mapped to our abilities to feel, think, and act. These sources are in the form of signals or images. Scalp EEG has been one of the most popular signals used in BCI research [28]. Over the years, the efforts of neuroscientists to investigate EEG [13, 25] has proved to be a real benefit to the BCI development process as it has provided more avenues to implement the mapping of our cognitive processes to the characteristics of the EEG Signal.

### 4.2.1 *Electroencephalogram*

EEG is clinically defined as the mean electrical activity of the brain recorded as the summed action potentials of thousands of neurons firing together [50]. It is composed of electrical rhythms and transient discharges which are distinguished by location, frequency, amplitude, form, periodicity, and functional properties [64]. EEG activity has been classified on the basis of these attributes. The most widely accepted basis of classification of EEG activity is done using frequency segregation into prototypical bands, referred to as delta, theta, alpha, beta, gamma, and mu rhythms. Table 4.1 lists the various EEG rhythms, their frequency and amplitude range, the brain regions in which they are most prominent, and the events most often related to each of them.

#### 4.2.1.1 Slow Cortical Potentials

Slow cortical potentials (SCPs) are related to the emergence of a BCI application known as a thought translational device (TTD) [4]. SCPs are understood to be the result of shifts in the depolarization level of the upper cortical dendrites, caused by the intracortical and thalamocortical afferent inflow to neocortical layers I and II. The TTD has been designed for completely paralyzed patients and has been tested on patients with ALS (Amyotrophic Lateral Sclerosis) [5]. However, the use of SCPs has recently declined in EEG based BCI research in favour of other features such as ERPs or sensorimotor rhythm activations [28].

#### 4.2.1.2 Event Related Potentials

The event-related potential (ERP) is a common title for the potential changes in the EEG that occur in response to a particular “event” or a stimulus [39]. These changes occur at very small amplitudes. Therefore, in order to reveal them, EEG samples have to be averaged over many repetitions. This removes the “random” fluctuations

**Table 4.1** Classification of frequency components in rhythmic brain activity

Frequency band	$\delta$ (Delta)	$\theta$ (Theta)	$\alpha$ (Alpha)	$\mu$ (Mu)	$\beta$ (Beta)	$\gamma$ (Gamma)
Freq range (Hz)	0.5–4	4–8	8–13 dev > 0.5	Approx 10	13–22	22–30
Amp range ( $\mu$ V)	50–100	<100	<10	<50	<20	<2
Prominent related brain region	Central region	Central region	Posterior brain	Somato-sensory cortex	Central region	
Examples of corresponding events	Infants (Age: 2 months), adults in sleep	Children, adults: drowsiness, sleep	Opening the eyes and focussing attention	Movement	High state of wakefulness	Sensory stimulation and attention

of the EEG, which are not stimulus-locked. ERPs can be divided into exogenous and endogenous. Exogenous ERPs occur up to about 100 ms after the stimulus onset. They depend on the properties of the physical stimulus (intensity, loudness etc.). The potentials from 100 ms post-stimulus onward are called endogenous [14]. They depend largely on psychological and behavioural processes related to the event. The most commonly studied ERP is the P300.

A popular example of a BCI based upon ERPs is the P300 speller, which is underwritten by the neuroscientific concept that a slow, large neural response is elicited after 300 ms of a rarely occurring stimulus in a train of consecutive, continuously occurring stimuli [52]. A P300 BCI speller operates by presenting users with a matrix of alphanumeric letters. Each row and column of the matrix flashes and a higher amplitude peak in the EEG (a P300 ERP) may be observed to occur 300 ms after the target letter flash is presented. Interestingly it has been found that the greater the number of letters the higher number of flashes in the matrix and, subsequently, the better is the P300 response [47].

#### 4.2.1.3 Sensorimotor Rhythm Activations

Sensorimotor rhythm activations are changes in activation levels that may be observed over the sensorimotor cortex during a range of cognitive events [55]. Sensorimotor rhythm changes are referred to as event related desynchronisation (ERD) in the event of a decrease in cortical activity and event-related synchronisation (ERS) in the event of an increase in motor cortical activity. They are most often associated with movement planning and execution [55], but may also be observed during tasks such as mental arithmetic [17], and mental rotation [6].

Unlike the ERP, the ERD/S is not phase locked to a stimulus presentation and, therefore, may not be identified via averaging of EEG amplitudes. Instead band-power is measured in frequency bands of interest (typically the alpha and beta bands) relative to a pre-stimulus baseline period. Significant decreases or increases in band power indicate the presence of an ERD/S and the cortical region at which it is observed identifies the corresponding cognitive process. For example, ERD over the left primary motor cortex hand representation area may indicate movement or planning of movement in the right hand.

Finally, ERD/S may also be observed during motor imagery. Thus, BCI users may attempt to control a BCI by imagining the feeling of moving their body (kinesthetic motor imagery) to control a BCI without actually performing overt movement [48].

#### 4.2.1.4 Case Study: ERD/S Detection

An example of the ERD/S phenomena is described using a classical 8 s BCI paradigm for left and right hand motor imagery [56]. The paradigm consisted of a random repetition of cue-based trials. The subject was seated in a relaxing chair

with armrests and was instructed to perform imagery movements prompted by a visual cue. Each trial started with an empty black screen; at time point  $t = 2$  s a short beep was presented and a cross ‘+’ appeared on the screen to arouse the subject’s attention. Then at second 3 ( $t = 3$  s) an arrow appears pointing either to the left or right. Each position indicated by this arrow prompts the subject to imagine either a left hand or a right hand movement. The respective movement imagination should be performed until the cross disappears at  $t = 8$  s. The next trial started after a very short resting period, during which the EEG was continuously recorded.

The time frequency approach was used to display the significant power increase or decrease in a predefined frequency band, thereby representing clear and easy visualisation of the movement-related behaviour of the induced activity averaged over several trials. In a pedagogical sense, increases or decreases of the power of the EEG related to a particular event is represented by the increase or decrease in the synchrony of the neuronal populations. Averaging over trials has been employed to deal with evoked potentials in order to improve the signal to noise ratio. This deals with any on-going base EEG activity, which may be considered to be noise as opposed to the actual potential instigated by the event or the task. The ratio of power calculated after averaging over all the trials to the power within a reference interval expressed in terms of percentage is the ERD/S strength.

ERD/S is not phase locked but time locked and specific to a frequency range. It is therefore conceivable that nearly identical ERD/S activity can be observed at different spatial locations. This will be indicative from some of the Fig. 4.1a, b.

The timeline for each trial is shown in Fig. 4.1. The vertical black line shows the presentation of the cue at time = 3 s. It is clearly observed that the activity in all the channels before the presentation of the cue is statistically significantly (bootstrap test) [21] less when compared to the activity after the cue ( $p < 0.05$ ). So the activity before the cue acts as a kind of reference to ascertain the fact that there is a clear increase or decrease in the ‘indicative power levels’ for a particular frequency band after the presentation of the cue. This is also seen in Fig. 4.1b for right hand motor imagery. Visual inspection of Fig. 4.1a, b provides clear demarcation in the level of power activity in particular frequency bands: 8–13 Hz (alpha) and 20–30 Hz (upper beta), for the two respective tasks. This information is used for the manual selection of the frequency bands to be used for feature extraction. These bands can be employed for computing band power features.

#### **4.2.2 Functional Magnetic Resonance Imaging and Magneto Encephalography**

The relative suitability of each of the brain sources for BCI purposes may depend on the specific application(s) being considered i.e. the relative suitability of each source is relative to the anticipated outcome of the interfacing process. The metabolic consequences of neural activity is observed as the changes in blood flow and

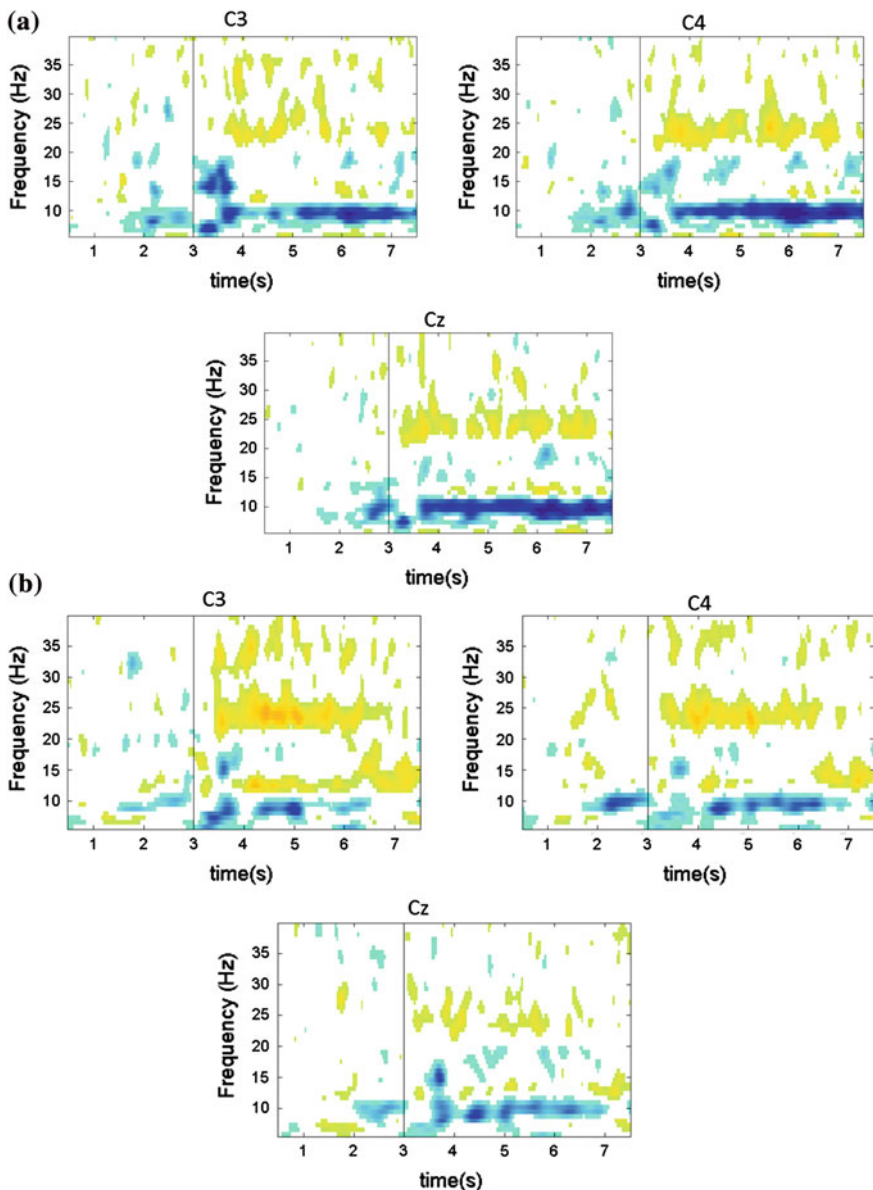


**Fig. 4.1** ERD/S maps for **a** *Left hand motor imagery* and **b** *Right hand motor imagery*. Three maps are presented for three channels  $C3$ ,  $C4$ , and  $Cz$ . The *vertical black line* indicates the start of the motor imagery period at  $t = 3$  s and the maps were computed with a baseline period of  $0.5\text{--}1.5$  s

metabolism. Imaging techniques like functional magnetic resonance imaging (fMRI) and positron emission tomography (PET) help us to visualise these changes in the form of images and may be used in BCI applications, for example [71].

Associated magnetic fields produced by the neuronal activity can be detected as the magnetoencephalogram (MEG). MEG is more susceptible to noise and is not portable compared to EEG but has a far better spatial resolution ( $<1$  cm) and depth sensitivity ( $\sim 4$  cm), while also having a similar time resolution. MEG has been used for BCI control. For example, in [36, 42] a MEG based BCI is proposed and discussed.

#### ***4.2.3 Intracranial Recordings ECoG (Electrocorticogram)***

The Electrocorticogram (ECoG) is recorded by placing invasive electrodes under the skull on the surface of the cortex. A surgical procedure is required to place these intra cranial electrodes. Experience suggests that the quality of the signal is better for ECoG than the scalp EEG and is less contaminated with artifacts, but that the ease of recording of the scalp EEG is superior to ECoG for BCI purposes [60]. It has also been observed in some studies that the performance of the classifier is dependent on the user population [26].

#### ***4.2.4 Functional Near Infra-red Spectroscopy***

Diffuse Optical imaging (DOI) is another method to measure distributions and concentrations of Oxy(HbO) and deoxy (HbR) haemoglobin in the brain. This technique is based on near-infrared (NIR) light and provides continuous measures of changes in oxygenated haemoglobin (HbO), deoxygenated haemoglobin (HbR) and total haemoglobin (HbT) concentrations [19, 29, 80].

A recent review of current state of the art in the brain computer interface technology at the fourth international meeting of the BCI community has stressed the need to develop robust and wearable brain acquisition methods for domesticating BCIs [79, 49]. Near infrared spectroscopy (NIRS) has been identified to provide a better, easier asynchronous control of BCI applications for people unable to control EEG based BCIs [46, 58, 73]. But there are limitations of transfer rates for a BCI developed using only NIRS [8, 70]. Interestingly, a BCI developed using simultaneous NIRS and EEG acquisitions has been reported to enhance the BCI performance by at least 5 % [16]. It is envisaged that, if combined, EEG and NIRS can provide robust BCI control by providing an accessible, portable, wearable solution not only on the bedside but also for home-use. There are several advantages of combining a NIRS-EEG for BCI development. Specifically, NIRS is relatively robust to movement, has better spatial sensitivity, and allows non-invasive

measurement of localized cognitive activity, thereby, empowering the BCI with minimal training while EEG provides optimized, precise sensor placement and quick transfer rates.

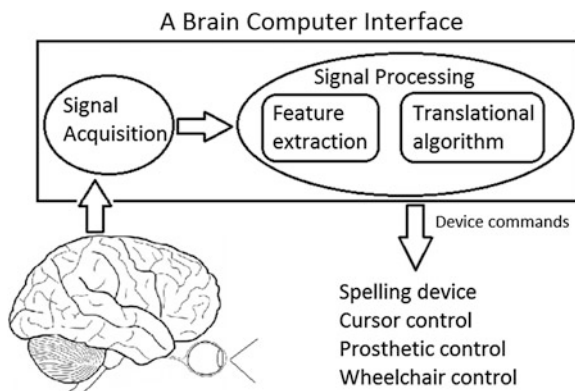
### 4.3 BCI Development Process

The building blocks of a BCI are depicted in Fig. 4.2. The signals from the brain are acquired by scalp electrodes, or intracranial electrodes and are processed to extract features such as the amplitudes of evoked potentials, sensorimotor cortex rhythms, or firing rates of cortical neurons that reflect the user's intent. These features are then translated into commands that operate devices such as a simple word processing program [35], a wheelchair [37], or a neuroprosthesis [61].

A more standardized model of a BCI was presented by Mason and Birch [41], who presented a taxonomy of the terms more often used in development of the BCI [41]. This model lists the main components which would define the basic BCI arrangement, namely the user (the person/the subject), electrodes (sensors to convert the user's brain state to electrical signals), amplifier, feature extractor (transforms the amplified electrical signals that correspond to related neurological states into feature values), feature translator (converts the feature values into logical and 'feedable' control signals), the control interface (maps the control signals to the specific device to be controlled), the device controller (translates semantic control signals from the control interface into physical signals that can be used within a device) and the device itself. This was regarded as a standard model and streamlined the BCI terminology but still required some clarifications. For example, the feature translator may be renamed the feature classifier or simply the classifier for discrete control signals.

This model, shown in Fig. 4.3, was designed using EEG signals as the 'source of information'; a similar analogy can be inferred for imaging sources such as fMRI

**Fig. 4.2** The basic framework of a BCI (adopted from [61])



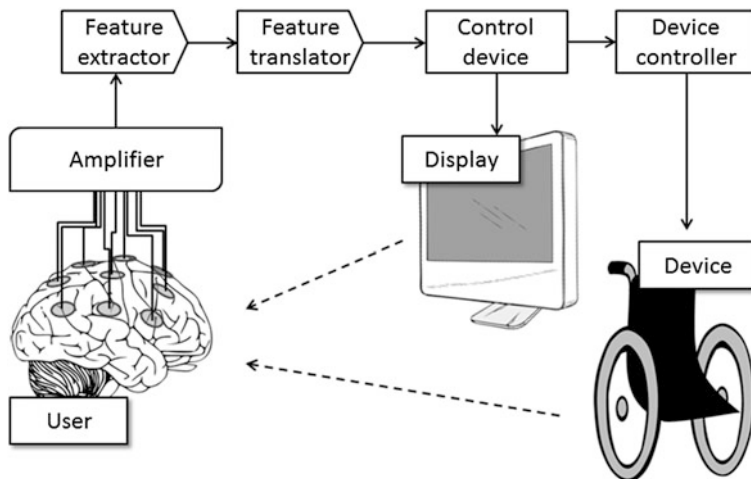


**Fig. 4.3** The BCI block diagram (adopted from [41])

and positron emission tomography (PET). To explain the analogy, the subject would remain the same, while the counterpart of the electrodes, would be replaced by the imaging equipment. The other terminology for the model in terms of its applicability to the imaging techniques explicitly remain identical but have significant implicit changes for feature extraction and translational algorithms. It is pertinent to state here that for BCI development, the imaging techniques works in tandem with signals as sources to extract relevant information from the brain and its underlying processes while the task is being performed by the subject. The imaging techniques, so far, have not been justified as sources of information which could sustain BCI development on their own.

## 4.4 Types of BCI

BCIs are categorised on the basis of their method of working and their functionality. Some of the key classifications and terminology associated with present day BCIs are considered as follows.

### 4.4.1 Invasive and Non-invasive BCIs

Non-invasive BCIs are based on signals recorded without the need for surgery, for example, EEG measured with the scalp electrodes. In invasive BCIs, the signals are recorded from inside the head (e.g. from the cerebral cortex) via, for example,

intracranial electrodes or microelectrodes. These BCIs can be based on, for example, ECoG recordings [60, 62]. Microelectrodes can also be used to record activity of a single neuron which gives rise to ‘spikes’ as sources of brain information from which BCIs can be developed [31].

#### ***4.4.2 Synchronous and Asynchronous BCIs***

Many BCIs work in a synchronous mode, i.e. in an externally paced mode. This requires the user to produce specific mental states in a predefined time window. For synchronous BCI, the control is system-initiated. In an asynchronous mode, the brain activity is analyzed continuously and the user can freely initiate the specific mental task(s) used as the control signal(s); the control is not system-initiated but user-initiated. This requires the BCI to detect when the EEG correlates of intended control occur. For example, Mason and Birch have tried to implement an asynchronous BCI with a switch [41].

### **4.5 Computational Techniques**

The heart of the BCI development process concerns the techniques employed for feature extraction and classification of the data. Apart from the application, the construction and detailed implementation aspects of the central translational algorithm i.e. the methods used for feature extraction and classification also determine the selection of the different brain signals, the recording technique and the equipment. All these are interrelated and the selection of these regulates the aspects of the efficiency and reliability of the BCI module developed. In this section we try to establish benchmark criteria for selection of the various techniques being used by BCI researchers. The international meetings on brain computer interface technology [27, 77–79, 81] have been instrumental in providing a forum for research and clinical experts. The discussions at such meetings have been documented and have helped in identifying the desirable characteristics of these techniques. Some of the key characteristics are precision, responsiveness (speed), interpretability and ease of setting up.

To get more information from the brain, medical instrumentation companies have come up with computer based monitoring systems which can record a large number of channels from the brain giving rise to multichannel data (for example, 128 channel recordings). The challenge lies in the processing of this data and for example cleaning it of artefacts and then modifying it in order to extract relevant information/knowledge about the underlying neurological processes going on in the brain at the time it is recorded. In the case of online BCIs, where the data is processed in real time, it is necessary to use appropriate techniques for processing. These might be different from the techniques used for offline processing of the BCI data or to investigate novel paradigms.

### 4.5.1 Dimensionality Reduction

BCIs base their control upon the characterisation and classification of biophysiological datasets such as EEG [50] or ECoG [43]. However, biophysiological datasets may often be multi-dimensional. For example, EEG data may be recorded from a large number of electrodes positioned across the scalp. The data is often broad frequency and spread across a range of time periods, resulting in potentially very high dimensional data for use in BCI control.

However, for many cognitive tasks, changes in neurological activity may only be observed in a subset of the data, for example within specific time periods, particular frequency bands, and/or over certain channels. Additionally, effects such as volume conduction (the spread of electrophysiological activity across the scalp resulting in similar activity being recorded at several EEG electrodes) and high levels of redundancy in the data may mean similar information is available across multiple dimensions in the data.

Dimensionality reduction techniques aim to identify an optimal sub-set of dimensions from a highly dimensional dataset. For example, they may be used to extract a subset of EEG channels that contain the most relevant information pertaining to a particular cognitive process [67, 69, 84].

A number of computational techniques are available for dimensionality reduction. These include principal component analysis (PCA), singular value decomposition (SVD), and canonical correlation analysis (CCA) etc. These three examples of dimensionality reduction methods are each discussed below.

#### 4.5.1.1 Principal Component Analysis

Principal component analysis (PCA) attempts to identify an orthogonal transformation that translates a set of potentially correlated variables into a set of linearly uncorrelated variables. These new variables are referred to as the principal components (PCs) [72].

PCA operates by first subtracting the mean from the data to centre it. Thus, for a feature set  $X$  a new, zero mean, feature set  $\bar{X}$  is derived by subtracting the mean from  $X$ . The covariance matrix of the zero mean feature set  $\bar{X}$  is then used to measure the strength of the relationships between all rows of  $\bar{X}$ . This is defined as the matrix  $C$  where each element  $C_{i,j}$  denotes the covariance between rows  $i$  and  $j$  in the feature set  $\bar{X}$ .

$$C_{i,j} = \frac{\sum_{k=1}^n (X_{i,k} - \bar{X}_{i,:})(X_{j,k} - \bar{X}_{j,:})}{(n - 1)} \quad (5.1)$$

where  $X_{i,k}$  and  $X_{j,k}$  denote the  $k$ th features from different examples of the data  $i$  and  $j$ , of the data and  $\bar{X}_{i,:}$  denotes the mean over a feature vector for an individual example of the data  $i$ .

The covariance matrix is then decomposed into a matrix of eigenvectors and a vector of eigenvalues. This may be defined as

$$Cu = \lambda u,$$

where  $u$  denotes an eigenvector of the covariance matrix  $C$ , and  $\lambda$  denotes the corresponding eigenvalue.

The eigenvalues identified for  $C$  may be ranked in decreasing value. The corresponding eigenvectors then contain projections of the feature set onto the principal components and are ordered by decreasing variance. Thus, the eigenvector corresponding to the largest eigenvalue contains a projection of the feature set  $X$  which has the greatest variance.

PCA is used in a large number of BCIs where dimensionality reduction is required. For example, in [34]. PCA is used to identify a subset of electrodes for classifying 5 different mental tasks (resting, letter association, math, visual counting, and geometric figure rotation) via an artificial neural network (ANN). Accuracies of up to 100 % are achieved when PCA is used, which is reported to be significantly higher than accuracies achieved without PCA. PCA is also very helpful in initial data exploration and to estimate the interrelationships between BCI classes/tasks in the data [69]. It can also indicate the minimum number of channels that can be used for classification of novel BCI tasks [2, 68].

#### 4.5.1.2 Singular Value Decomposition

Singular value decomposition (SVD) attempts to identify a factorization of a matrix of dimensions  $m \times n$ . SVD is closely related to eigen decomposition, but may be applied to matrices of any values of  $m$  and  $n$ , whereas eigen decomposition may only be applied to square matrices.

For a matrix  $A$  of dimensions  $m \times n$  the SVD is given by

$$A = USV^T,$$

where  $U$  and  $V$  denote orthogonal matrices of dimensions  $m \times n$  and  $n \times m$  respectively, and  $S$  denotes an  $m \times n$  rectangular diagonal matrix. The columns of  $U$  are denoted  $u_i$  and contain the left singular vectors, while the columns of  $V$  are denoted  $v_i$  and contain the right singular vectors. The diagonal elements of  $S$  are denoted  $\sigma_i$  and contain the singular values. Singular values are sorted in descending order and used to identify the first  $n$  left or right singular vectors. These singular vectors may then be taken to represent a reduced subset of the data.

Singular value decomposition may be used directly with EEG data to reduce dimensionality. For example, in [12] three approaches to artefact removal are compared, including an approach, originally proposed in [75], for using singular value decomposition as a dimensionality reduction step in an artefact removal method.

The SVD-based artefact removal method is observed to remove significant proportions of ocular artefacts and is comparable in performance to a number of other state-of-the-art artefact removal methods.

#### 4.5.1.3 Canonical Correlation Analysis

Canonical correlation analysis (CCA) is a method for identifying pairs of vectors from two matrices with maximum correlations. For example, for two matrices  $X$  and  $Y$  of dimensions  $x \times n$  and  $y \times n$  respectively CCA will attempt to find a subset of elements of  $X$  and  $Y$  which are maximally correlated.

CCA may be defined as a maximisation problem, which can be solved by maximising the following term

$$\max_{w_x, w_y} \rho(u, v) = \frac{w_x^T C_{xy} w_y}{\sqrt{(w_x^T C_{xx} w_x)(w_y^T C_{yy} w_y)}}$$

where  $C_{xx}$  and  $C_{yy}$  denote the autocovariance matrices of  $X$  and  $Y$  respectively and  $C_{xy}$  denotes the cross covariance matrix of  $X$  and  $Y$ .

CCA may be used to identify a subset of dimensions of an EEG dataset which maximally correlate with some interesting properties of the data. For example, in [7] CCA is used to identify muscle artefacts in the EEG via their relatively low auto-correlation with one another when compared to the EEG.

CCA is also commonly used as the basis for classifying steady state visual evoked potentials (SSVEPs). For example, in [9] CCA is used in an online brain-computer interface (BCI) to identify frequency bands in the EEG which maximally correlate with SSVEP stimulation frequencies, and hence identify which stimuli a user is attending to and, therefore, their intended control action.

#### 4.5.2 Feature Extraction

Biophysiological data may be described via a number of different feature types. When considering neurological data measured by, for example, the EEG or ECoG there are three broad groups of features that may be extracted. These are features based upon the amplitude of the data, features based upon the frequency content of the data, and features based upon the phase content of the data [38, 28]. It's also possible to consider feature types in which two or more types of feature are combined. For example, time-frequency features may be used to describe changes in amplitude of the data across different frequency bands.

Features based upon the amplitude of the data include measures of the peaks in the data. For example, the event-related potential (ERP) is a change in amplitude of the EEG in response to certain stimuli or cognitive processes and may be identified

via the size and/or latency of the peak amplitude. Amplitude based features may also include measures of distributions of the data, measures of relationships between different amplitudes (e.g. correlation), and statistical measures of amplitude differences in the data.

Frequency based features may be used to describe how the frequency content of the signals change over time or in relation to certain events or stimuli. For example, BCI control may be based upon SSVEPs, an increase in frequency content in a narrow frequency band, in response to entrainment by an external stimuli, of particular neural oscillators in the visual cortex [45]. Relationships between different measures of frequency content (e.g. coherence) may also be used to measure how frequency content changes across particular regions of the brain.

Phase based features are traditionally used much less in BCI control than other feature types [28]. However, they have been shown, in some cases, to exhibit significant improvements in performance compared to some traditional features such as the event-related (de)synchronisation (a combined amplitude-frequency feature) [11].

Features based upon a combination of different feature types are becoming increasingly popular in BCI research [28]. It's likely that the recent development and exploration of hybrid BCIs (BCIs that combine two or more control mechanisms or physiological measures [57]) are driving an increased interest in combined feature types [28].

#### 4.5.3 Feature Selection

Feature selection refers to techniques which search a set of possible features and identify a subset of those features which are optimal for some purpose. For example, consider EEG recorded during an ERP oddball task from 19 channels positioned over the scalp. The oddball task is designed to produce a P300 ERP by presenting a selection of stimuli with a small probability of an out of sequence stimuli (i.e. different in some property from the majority of the other stimuli). The resulting P300 ERP is usually most apparent over the occipital and parietal cortices. Hence, EEG channels positioned over these regions are more likely to see increased EEG amplitude. A feature selection approach may be used to identify which channels exhibit this increase in amplitude in response to the unexpected (target) stimuli.

Feature selection may be described as manual, automated, or semi-automated. Manual feature selection refers to the process of selecting feature sets based upon prior knowledge of the dataset and expected features of interest. Automated feature selection refers to computer driven selection of features and may often be performed via a machine learning (ML) technique. Semi-automated techniques attempt to combine these two methods to take advantage of the benefits of both. For example, a region of interest may be manually selected and an automated method then used to select the best feature set from within this region.

Automated feature selection may be performed by either supervised or unsupervised methods. Supervised methods include meta data about the training data in the selection processes, while unsupervised methods do not. Typically, unsupervised methods amount to dimensionality reduction methods as discussed in Sect. 4.5.4.

Supervised methods may be described as filter based methods; wrapper based methods, or embedded methods.

Filter based methods attempt to select features independently of the classification step [74]. Relationships between different features may be used to identify the most relevant features i.e. those which give the most information about the cognitive phenomena of interest. As such filter methods may be either supervised or unsupervised.

The main advantage of filter methods often lies in their computational efficiency. There is no need to optimize an objective function by repeated re-evaluations with a filter method as one would when applying a wrapper [32]. As such they can be considered independent of the classification method chosen. This makes filter methods very scalable and potentially able to offer similar levels of performance on both large and small data-sets.

Typical examples of filter techniques include clustering techniques for dimensionality reduction [18] and measures of feature similarity such as correlation [24]. When applying a similarity measure features that are very similar to another can be thought to be redundant and hence removed. When a supervised filter is applied the amount of information each feature gives about the class labels, for example the correlation between features and the class labels, can give an indication of how suitable a particular feature is for classifying the dataset correctly [24].

A wrapper method attempts to optimize an objective function by repeated re-evaluation with different candidate feature sets [32]. The objective function is the chosen classifier for the BCI hence the choice of classifier becomes an integral part of the feature selection process. Subsequently the classifier cannot be evaluated without the class labels and all wrapper methods are, therefore, supervised.

Many wrapper methods are based upon the idea of meta-heuristics. A meta-heuristic search attempts to traverse a search space in such a way as to avoid getting stuck in local optima solutions [23]. They do this by either using multiple population members with randomization, by allowing backtracking of some variety, or a combination of the two. They are often based upon biologically inspired search metaphors [32].

Examples of meta-heuristic wrapper techniques that are popular in BCI research include Genetic Algorithms (GAs), which are inspired by natural evolution [32, 85]. A population of candidate feature sets is created. Each member of this population is then evaluated against some objective function (the classifier) and the members that give the highest classification accuracies are taken to be the ‘fittest’. These members are ‘bred’ with other fit members to create new ‘fitter’ child members [85]. Over enough generations the overall fitness of the population increases and in ideal circumstances arrives at an optimal feature set which allows highly accurate classification of the data. Random mutation is applied to each

generation to attempt to avoid the solution getting stuck in local maxima in the way a simple gradient ascent algorithm would [20].

An example of a type of genetic algorithm being used in feature selection for BCIs is provided in [10]. In this example differential evolution (a variant of a genetic algorithm) is used to identify optimal channels and frequency bands for ERD detection during a motor imagery task.

An embedded method attempts to combine feature selection and classification into one step [23]. An example of this is an Artificial Neural Network (ANN). In the training routine for ANNs the weights of the network are adjusted such that optimal classification accuracy may be achieved with the best feature set. Therefore the neural network incorporates both a feature selection step and a classification step [61]. Embedded techniques are often quicker than wrapper techniques as there is often less need for multiple re-evaluations of candidate feature sets against an objective function in the training process [23].

Several BCI systems incorporate embedded methods for feature selection. However, it is not always clear that this is what is happening as the feature sets may be selected based, in part, upon a priori knowledge of the paradigm. Thus, systems such as [59] select a set of features that are known a priori to be effective at differentiating classes related to the paradigm. This feature set is then passed to a classifier with a further embedded feature selection step which sub-selects optimal features from this candidate feature set.

#### 4.5.4 Classification Techniques

Classification techniques attempt to identify which class a previously unseen dataset belongs to by applying a classification rule to the data. The classification rule is typically trained on previously seen examples of the data from each of the available classes before being applied to new data.

Formally, for a two class problem a function is estimated as  $f : R^N \rightarrow \{-1, +1\}$ , where a new, previously unseen, dataset is labelled either as  $-1$  or  $+1$  depending upon which side of a decision boundary it falls. The process of identifying an optimal function  $f$  from training data effectively amounts to learning the class membership and learning the inter-class decision boundary.

Classifier training may often be split into several stages to attempt to minimise the bias-variance trade-off problem. This typically involves using a training set to first estimate the classifier's decision boundary, followed by a validation set, which may be used to test and further refine the boundary. The final data the classifier is to be applied to is referred to as the testing set.

Classifier techniques are used in the majority of BCI applications [28]. For example, in [30] a Bayesian linear discriminant analysis (BLDA) classifier is used to identify trials which contain P300 event-related potentials (ERPs) for the control of an ERP based online BCI. BLDA operates by attempting to identify a linear

combination of features which optimally separate them into the correct classes via a decision boundary. Mean online classification accuracies of  $94.5 \pm 5.1\%$  are obtained.

Other types of classification technique that are popular for use in BCIs include support vector machines (SVMs), hidden markov models (HMMs), artificial neural networks (ANNs) etc. [28]. To discuss an example of one more of these classifier types hidden markov models (HMMs) are considered.

HMMs attempt to characterise the temporal dynamics of a time series of bio-signals as a markov process. Specifically, the observed datasets are assumed to be generated by an underlying markov process, with each state in that markov process generating the observed features according to some probability distribution. Estimation of these distributions and state transition probabilities for a markov process may be performed as part of the classifier training process. A HMM is typically trained for each class and then used to classify new data by identifying which HMM has the greatest probability of having generated the new data.

HMMs have been successfully applied to classify EEG data in a BCI context in [11]. In this example EEG data recorded during a motor imagery task is first characterised via phase based features before HMMs are trained to differentiate left versus right index finger motor imagery. Highly significant classification accuracies are achieved using this approach.

Another algorithm used for classification purposes is the Linear Discriminant Analysis (LDA) classifier. LDA is a simple technique widely used in BCI applications because it is computationally efficient and robust. This method maximizes the ratio of ‘between-class’ variance to the ‘within-class’ variance in any particular dataset thereby guaranteeing maximal separability [54]. It can also handle the cases in which the ‘within-class’ frequencies are unequal. Evolving from the same principles as of PCA, it holds the advantage over PCA in that the shape and location of the original datasets changes when transformed to a different space whereas LDA does not change the location but only tries to provide more class separability and identifies a decision boundary between the given classes.

The future of the BCI techniques lies in the standardisation of the computational methods. This will not only help to launch a BCI based product in the market but will also broaden the spectrum of BCI applications.

## 4.6 BCI Evaluation

BCI research has reached a level where there are large varieties of combinations of feature extraction and classification techniques being used by research groups all over the world [28]. It is important to have benchmark criteria which not only provides a quick and easy means of identifying the relative success of the technique but also acts as a standard to compare the relative performance of all the techniques. Possible criteria are discussed in [3] and include classification accuracy, Cohen’s Kappa coefficient, mutual information of discrete, and continuous output.

Two measures of classification accuracy may be considered, overall accuracy and individual accuracy. Overall accuracy is calculated as the ratio of the sum of the diagonal elements of the classifier generated confusion matrix and the total number of samples. The specific accuracy for each class is the ratio of the diagonal element (hits) for that particular class and the total number of sample points for that class (sum of the row elements of the confusion matrix for that particular class).

The output of the validation procedure is devised in the form of specific parameters using BCI terminology. Transfer rates may be calculated to measure the speed with which users may operate a BCI. Cohen's kappa coefficient, which is reported to be a better representation of the accuracy as it takes into account the occurrence of a chance [63], may also be used. Kappa coefficient is 1 in case of a perfect classification and is 0 if the predicted class has no correlation with the actual class. Specific accuracy for each of the two classes gives an idea of the performance of the classification algorithm for each of the classes. Correlation and signal to noise ratio may also be used.

## 4.7 Conclusion

Brain computer interfaces (BCIs) are a rapidly growing field [28], with a large and growing number of researchers attempting to tackle the multiple challenges presented by this highly interdisciplinary area of research.

BCIs may be described by multiple component stages. These have been outlined and described in this chapter and include components for data acquisition, pre-processing, dimensionality reduction, feature extraction/selection, classification, and application. Each of these component parts is researched with the aim of developing novel and improved components and applications to allow BCIs to meet the needs of new user groups and improve the performance of BCI systems provided to existing user groups.

One such example is the hybrid BCI, in which two or more different data acquisition methods or BCI paradigms may be combined [57]. For example, simultaneous electroencephalogram (EEG) and near infrared spectroscopy (NIRS) may be combined with the aim of using the combination of electrophysiological and haemodynamic responses to provide more accurate control to BCI user groups [16].

Another example is the use of BCIs in neuro-rehabilitation for stroke [1]. This represents a novel application of BCI technology, in which closed loop BCI control of an application is utilised to induce changes in levels of neuroplasticity in the user. The aim is to promote beneficial neuroplastic changes which allow compensatory neural areas to “take over” from lesioned cortical regions [66].

In each of these new developments in BCI technology the heart of the BCI remains the translational algorithms. Indeed, translational algorithms retain an essential role in all types of BCI, that of converting raw, noisy, non-stationary neural data into stable and realisable control commands for a computer, robotic device, or other application.

We categorise translational algorithms into four different types: dimensionality reduction, feature extraction, feature selection, and classification. Not every BCI type requires every one of these types of translational algorithm, but all BCI types require some combination of some of these translational algorithms.

Dimensionality reduction algorithms are typically used as a pre-processing step in the processing pipeline at the heart of a BCI. They aim to take a high dimensional dataset (for example, one composed of multiple channels, sample points, frequency bands, etc.) and reduce it to just the most relevant dimensions of interest. Typical examples of dimensionality reduction methods were discussed in this chapter and include methods such as principal component analysis and singular value decomposition.

Feature extraction refers to the method(s) by which raw brain signals are translated into features describing some relevant property of the brain state. Raw signals are the signals recorded from the brain at the data acquisition stage and can include EEG amplitudes, electrocorticogram (ECoG) amplitudes, blood oxygenation levels (fNIRS, fMRI) etc. The process of converting these raw signals to features of interest may vary considerably depending on the type of raw data, the cognitive task(s) the user is attempting in order to control the BCI, and the processing limitations of the available computers. Examples can include measures of signal magnitude (e.g. EEG amplitude), measures of frequency content of the data, and more complex measures such as connectivity measures between different regions of interest within the brain.

Feature selection refers to the automated or semi-automated selection of a relevant subset of the features extracted from the raw brain signals. Automated feature selection may be used in cases where there is not a clear set of well known “good features” for the particular cognitive paradigm. It may also be used to provide some compensation for the problem of inter-subject variability in neural data [50]. The neurological data recorded from two individuals is not completely alike and automated feature selection may be used to find the best set of features for a particular individual during a particular BCI control task. Feature selection is most commonly performed using methods from machine learning and may include methods such as genetic algorithms, random forest searches etc.

Finally, classification refers to the identification of corresponding discrete class labels for a selected feature set. This may also be performed using tools taken from the machine learning toolbox, for example, support vector machines (SVMs) or linear discriminant analysis (LDA) classifiers, and may be combined with the feature selection method or performed independently.

New algorithms and methods are in a constant state of development by the BCI community and are opening up increasing possibilities for applications, data acquisition types, and target user groups. Many of these new possibilities require advancements in translational algorithms. Thus, research and development of translational algorithms, both by the BCI community and others, may be seen as the engine of BCI research and development and forms a vital part of the field of multidisciplinary BCI research.

Regarding the future directions of BCI research it is possible to make a few statements about the role of translational algorithms. First, every existing method of data acquisition from the central nervous system produces data which is non-stationary and noisy. Thus, there is likely to be a need for a number of the translational algorithms described in this chapter for the foreseeable future in BCI for tasks such as de-noising the data, extracting and selecting features of interest, and identifying the relevant class labels corresponding to the data. Second, while there will be a need for these algorithms they will not all be required in every application. For example, features may be mapped directly to a control action, removing the need for a classifier to identify corresponding class labels, or the need for feature selection may be mitigated if *a priori* knowledge of suitable features is available.

Finally, advances in computational technology and machine learning research mean that new and more advanced translational algorithms are constantly being developed. This development is not just confined to the BCI research community and often machine learning algorithms developed for other purposes are co-opted into the community (for example LDA classifiers [83]), while algorithms developed within the community may also find other uses elsewhere (for example common spatial patterns [33]). This process is likely to continue and accelerate over the coming years as advancements in computing technology allow the deployment of ever increasingly advanced algorithms. An example of this may be seen in the use of machine learning algorithms for feature selection. More advanced machine learning algorithms may be employed as computing technology allows them to be run in sufficiently short times to allow their use during online BCI applications.

**Acknowledgments** The authors are thankful to Mathew Dyson, Ph.D. student, Computer Science Department, University of Essex for his support in recording the dataset used in the case study described in this work. The authors are thankful to the BCI research community for their support and guidance through their publications and resources on the web.

## References

1. Ang, K.K., Guan, C., Chua, K.S.G., et al.: Clinical study of neurorehabilitation in stroke using EEG-based motor imagery brain-computer interface with robotic feedback. In: Conference of the IEEE Engineering in Medicine and Biology Society (2010)
2. Azar, A., Balas, V., Olariu, T.: Classification of EEG-based brain-computer interfaces. In: Iantovics, B., Kountchev, R. (eds.) Advanced Intelligent Computational Technologies and Decision Support Systems SE—9, Studies in Computational Intelligence, pp. 97–106. Springer, New York (2014)
3. Billinger, M., Daly, I., Kaiser, V., et al.: Is it significant? Guidelines for reporting BCI performance. In: Toward Practical BCIs: Bridging the Gap from Research to Real-World Applications (2012)
4. Birbaumer, N.: The thought-translation device (TTD): neurobehavioral mechanisms and clinical outcome. Rehabilitation **11**(2), 120–123 (2003)
5. Birbaumer, N.: Breaking the silence: brain-computer interfaces (BCI) for communication and motor control. Psychophysiology **43**(6), 517–532 (2006)

6. Chen, X., Bin, G., Daly, I., et al.: Event-related desynchronization (ERD) in the alpha band during a hand mental rotation task. *Neurosci. Lett.* **541**, 238–242 (2013)
7. De Clercq, W., Vergult, A., Vanrumste, B., et al.: Canonical correlation analysis applied to remove muscle artifacts from the electroencephalogram. *IEEE Trans. Bio-med. Eng.* **53**(12 Pt 1), 2583–2587 (2006)
8. Coyle, S.M., Ward, T.E., Markham, C.M.: Brain-computer interface using a simplified functional near-infrared spectroscopy system. *J. Neural. Eng.* **4**, 219–226 (2007). doi: [10.1088/1741-2560/4/3/007](https://doi.org/10.1088/1741-2560/4/3/007)
9. Daly, I., Billinger, M., Laparra-Hernández, J., et al.: On the control of brain-computer interfaces by users with cerebral palsy. *Clin. Neurophysiol.: Off. J. Int. Fed. Clin. Neurophysiol.* **124**(9), 1787–1797 (2013)
10. Daly, I., Nasuto, S.J., Warwick, K.: Single tap identification for fast BCI control. *Cogn. Neurodyn.* **5**(1), 21–30 (2011)
11. Daly, I., Nasuto, S.J., Warwick, K.: Brain computer interface control via functional connectivity dynamics. *Pattern Recogn.* **45**(6), 2123–2136 (2012)
12. Daly, I., Nicolaou, N., Nasuto, S.J., et al.: Automated artifact removal from the electroencephalogram: a comparative study. *Clin. EEG Neurosci.* **44**(4), 291–306 (2013)
13. Donchin, E., Heffley, E., Hillyard, S.A., et al.: Cognition and event-related potentials II. The orienting reflex and P300. *Ann. NY Acad. Sci.* **425**(1 Brain and Inf), 39–57 (1984)
14. Ebersole, J.S., Pedley, T.A.: Current practice of clinical electroencephalography, 3rd edn. *Eur. J. Neurol.* **10**(5), 604–605 (2003)
15. Farwell, La, Donchin, E.: Talking off the top of your head: toward a mental prosthesis utilizing event-related brain potentials. *Electroencephalogr. Clin. Neurophysiol.* **70**(6), 510–523 (1988)
16. Fazli, S., Mehnert, J., Steinbrink, J., et al.: Enhanced performance by a hybrid NIRS-EEG brain computer interface. *NeuroImage* **59**(1), 519–529 (2012)
17. Friedrich, E.V.C., Scherer, R., Neuper, C.: The effect of distinct mental strategies on classification performance for brain-computer interfaces. *Int. J. Psychophysiol.* **84**, 86–94 (2012)
18. Gan, G.: Data Clustering: Theory, Algorithms and Applications. SIAM, Philadelphia (2007)
19. Gibson, A., Dehghani, H.: Diffuse optical imaging. *Philos. Trans. Ser. A Math. Phys. Eng. Sci.* **367**(1900), 3055–3072 (2009)
20. Goldberg, D.E., Holland, J.H.: Genetic algorithms and machine learning. *Mach. Learn.* **3**(2), 95–99 (1988)
21. Graimann, B., Huggins, J., Levine, S., et al.: Visualization of significant ERD/ERS patterns in multichannel EEG and ECoG data. *Clin. Neurophysiol.* **113**(1), 43–47 (2002)
22. Guger, C., Harkam, W., Hertnaes, C., et al.: Prosthetic control by an EEG-based brain-computer interface (BCI). In: Proceedings of the AAATE Conference (1999)
23. Guyon, I.: An introduction to variable and feature selection. *J. Mach. Learn. Res.* **3**(7–8), 1157–1182 (2003)
24. Hall, M.A.: Correlation-based feature selection for machine learning. Ph.D. thesis (1999)
25. Handy, T.C.: Event-related Potentials: A Methods Handbook. MIT Press, Cambridge (2005)
26. Hill, N.J., Lal, T.N., Schröder, M., et al.: Classifying EEG and ECoG signals without subject training for fast BCI implementation: comparison of nonparalyzed and completely paralyzed subjects. *IEEE Trans. Neural Syst. Rehabil. Eng.* **14**(2), 183–186 (2006)
27. Huggins, J.E., Guger, C., Allison, B., et al.: Workshops of the fifth international brain-computer interface meeting: defining the future. *Brain-Comput. Interfaces* **1**(1), 27–49 (2014)
28. Hwang, H.-J., Kim, S., Choi, S., et al.: EEG-based brain-computer interfaces (BCIs): a thorough literature survey. *Int. J. Human-Comput. Int.* **29**(12), 130429122442009 (2013)
29. Izzetoglu, M., Izzetoglu, K., Bunce, S., et al.: Functional near-infrared neuroimaging. *IEEE Trans. Neural Syst. Rehabil. Eng.: Publ. IEEE Eng. Med. Biol. Soc.* **13**(2), 153–159 (2005)
30. Jin, J., Sellers, E.W., Zhang, Y., et al.: Whether generic model works for rapid ERP-based BCI calibration. *J. Neurosci. Methods* **212**(1), 94–99 (2013)
31. Kennedy, P., Andreassen, D., Ehirim, P., et al.: Using human extra-cortical local field potentials to control a switch. *J. Neural Eng.* **1**(2), 72–77 (2004)

32. Kohavi, R.: Wrappers for feature subset selection. *Artif. Intell.* **97**(1–2), 273–324 (1997)
33. Koles, Z.J., Lazar, M.S., Zhou, S.Z.: Spatial patterns underlying population differences in the background EEG. *Brain Topogr.* **2**(4), 275–284 (1990)
34. Kottaimalai, R., Rajasekaran, M.P., Selvam, V., et al.: EEG signal classification using principal component analysis with neural network in brain computer interface applications. In: 2013 IEEE International Conference on Emerging Trends in Computing, Communication and Nanotechnology (ICECCN), pp. 227–231 (2013)
35. Krusienski, D.J., Sellers, E.W., McFarland, D.J., et al.: Toward enhanced P300 speller performance. *J. Neurosci. Methods* **167**(1), 15–21 (2008)
36. Lal, T.N., Schr, M., Hill, N.J., et al.: A brain computer interface with online feedback based on magnetoencephalography. In: Proceedings of 22nd International Conference on Machine Learning (2005)
37. Leeb, R., Friedman, D., Müller-Putz, G.R., et al.: Self-paced (asynchronous) BCI control of a wheelchair in virtual environments: a case study with a tetraplegic. *Comput. Intell. Neurosci.* 79642 (2007)
38. Lotte, F., Congedo, M., Lécuyer, A., et al.: A review of classification algorithms for EEG-based brain-computer interfaces. *J. Neural. Eng.* **4**, R1–R13 (2007). doi: [10.1088/1741-2560/4/2/R01](https://doi.org/10.1088/1741-2560/4/2/R01)
39. Luck, S.J.: Ten simple rules for designing ERP experiments. In: Handy, T.C. (ed.) *Event-Related Potentials—A Methods Handbook*, pp. 17–32. MIT Press, Cambridge (2005)
40. Mappus IV, R.L., Venkatesh, G.R., Shastry, C., et al.: An fNIR based BMI for letter construction using continuous control. *CHI '09 Extended Abstracts on Human Factors in Computing Systems*. ACM, New York, pp. 3571–3576 (2009)
41. Mason, S.G., Birch, G.E.: A general framework for brain-computer interface design. *IEEE Trans. Neural Syst. Rehabil. Eng.: Publ. IEEE Eng. Med. Biol. Soc.* **11**(1), 70–85 (2003)
42. Mellinger, J., Schalk, G., Braun, C., et al.: An MEG-based brain-computer interface (BCI). *NeuroImage* **36**(3), 581–593 (2007)
43. Menon, V., Freeman, W.J., Cutillo, B.A., et al.: Spatio-temporal correlations in human gamma band electrocorticograms. *Electroencephalogr. Clin. Neurophysiol.* **98**(2), 89–102 (1996)
44. Miranda, E.R., Magee, W.L., Wilson, J.J., et al.: Brain-computer music interfacing (BCMI): from basic research to the real world of special needs. *Music Med.* **3**(3), 134–140 (2011)
45. Müller-Putz, G.R., Scherer, R., Brauneis, C., et al.: Steady-state visual evoked potential (SSVEP)-based communication: impact of harmonic frequency components. *J. Neural Eng.* **2**(4), 123–130 (2005)
46. Naito, M., Michioka, Y., Ozawa, K., et al.: A Communication Means for Totally Locked-in ALS Patients Based on Changes in Cerebral Blood Volume Measured with Near-Infrared Light. *IEICE Trans Inf Syst.* E90-D:1028–1037 (2007)
47. Nam, C.S., Li, Y., Johnson, S.: Evaluation of P300-based brain-computer interface in real-world contexts. *Int. J. Human-Comput. Interact.* **26**(6), 621–637 (2010)
48. Neuper, C., Scherer, R., Reiner, M., et al.: Imagery of motor actions: differential effects of kinesthetic and visual-motor mode of imagery in single-trial EEG. *Brain Res. Cogn. Brain Res.* **25**(3), 668–677 (2005)
49. Nicolas-Alonso, L.F., Gomez-Gil, J.: Brain computer interfaces, a review. *Sensors (Basel)* **12**, 1211–79 (2012). doi: [10.3390/s12020121](https://doi.org/10.3390/s12020121)
50. Niedermeyer, E., Da Silva, F.H.L.: *Electroencephalography: Basic Principles, Clinical Applications, and Related Fields*. Lippincott Williams & Wilkins, Philadelphia (2005)
51. Nijholt, A., Desney, T.: BCI for Games: a State of the Art Survey. *Lecture Notes in Computer Science*. Springer, Berlin (2009)
52. O'Brien, J.H.: P300 wave elicited by a stimulus-change paradigm in acutely prepared rats. *Physiol. Behav.* **28**(4), 711–713 (1982)
53. Perelmouter, J., Birbaumer, N.: A binary spelling interface with random errors. *IEEE Trans. Rehabil. Eng.* **8**(2), 227–232 (2000)
54. Perez, J.L.M., Cruz, A.B.: Linear discriminant analysis on brain computer interface. In: 2007 IEEE International Symposium on Intelligent Signal Processing, pp. 1–6 (2007)

55. Pfurtscheller, G., Lopes da Silva, F.H.: Event-related EEG/MEG synchronization and desynchronization: basic principles. *Clin. Neurophysiol.* **110**(11), 1842–1857 (1999)
56. Pfurtscheller, G., Müller-Putz, G.R., Schlogl, A., et al.: 15 years of BCI research at Graz University of Technology: current projects. *IEEE Trans. Neural Syst. Rehabil. Eng.* **14**(2), 205–210 (2006)
57. Pfurtscheller, G., Allison, B.Z., Brunner, C., et al.: The hybrid BCI. *Front. Neuroprosthetics* **4**(30) (2010)
58. Power, S.D., Falk, T.H., Chau, T.: Classification of prefrontal activity due to mental arithmetic and music imagery using hidden Markov models and frequency domain near-infrared spectroscopy. *J. Neural. Eng.* **7**, 26002 (2010). doi: [10.1088/1741-2560/7/2/026002](https://doi.org/10.1088/1741-2560/7/2/026002)
59. Pregenzer, M., Pfurtscheller, G.: Frequency component selection for an EEG-based brain to computer interface. *IEEE Trans. Rehabil. Eng.* **7**(4), 413–419 (1999)
60. Schalk, G., Leuthardt, E.C.: Brain-computer interfaces using electrocorticographic signals. *IEEE Rev. Biomed. Eng.* **4**, 140–154 (2011)
61. Schalk, G., McFarland, D.J., Hinterberger, T., et al.: BCI2000: a general-purpose brain-computer interface (BCI) system. *IEEE Trans. Bio-med. Eng.* **51**(6), 1034–1043 (2004)
62. Scherer, R., Graimann, B., Huggins, J.E., et al.: Frequency component selection for an ECoG-based brain-computer interface. *Biomed. Tech. Biomed. Eng.* **48**(1–2), 31–36 (2003)
63. Schlogl, A., Kronegg, J., Huggins, J.E., et al.: Evaluation Criteria in BCI Research. MIT Press, Cambridge (2007)
64. Schomer, L., Lopes de Silva, F., (eds.): Niedermeyer's Electroencephalography: Basic Principles, Clinical Applications, and Related Fields, 6th edn. Lippincott Williams & Wilkins, Philadelphia (2011)
65. Sellers, E.W., Donchin, E.: A P300-based brain-computer interface: initial tests by ALS patients. *Clin. Neurophysiol.: Off. J. Int. Fed. Clin. Neurophysiol.* **117**(3), 538–548 (2006)
66. Silvoni, S., Ramos-Murguialday, A., Cavinato, M., et al.: Brain-computer interface in stroke: a review of progress. *Clin. EEG Neurosci.* **42**(4), 245–252 (2011)
67. Singh, H., Qin, X., Hines, E., et al.: Classification and feature extraction strategies for multi channel multi trial BCI data. *Int. J. Bioelectromagn.* **9**(4), 233–236 (2007)
68. Singh, H.: Development of EEG Based BCI Approaches for Detection of Awareness in Human Disorders of Consciousness (2009)
69. Singh, H., Yang, J., Singh, S., et al.: Channel selection for multi channel multi trial invasive BCI data. In: Shama, K., Nayak, K.P., Bhat, S. (eds.) Electronic Design and Signal Processing, pp. 92–96 (2012)
70. Sitaram, R., Caria, A., Birbaumer, N.: Hemodynamic brain-computer interfaces for communication and rehabilitation. *Neural. Netw.* **22**, 1320–1328 (2009). doi: [10.1016/j.neunet.2009.05.009](https://doi.org/10.1016/j.neunet.2009.05.009)
71. Sitaram, R., Caria, A., Veit, R., et al.: fMRI brain-computer interface: a tool for neuroscientific research and treatment. *Comput. Intell. Neurosci.* 25487 (2007)
72. Smith, L.I.: A Tutorial on Principal Components Analysis. Cornell University, USA (2002)
73. Sorger, B., Reithler, J., Dahmen, B., Goebel, R.: A real-time fMRI-based spelling device immediately enabling robust motor-independent communication. *Curr. Biol.* **22**, 1333–1338 (2012). doi: [10.1016/j.cub.2012.05.022](https://doi.org/10.1016/j.cub.2012.05.022)
74. Tangermann, M.W.: Feature selection for brain-computer interfaces. *Naturwissenschaften* (2007)
75. Teixeira, A.R., Tome, A.M., Lang, E.W., et al.: On the use of clustering and local singular spectrum analysis to remove ocular artifacts from electroencephalograms. In: Proceedings of International Joint Conference on Neural Networks, pp. 2514–2519 (2005)
76. Tudor, M., Tudor, L., Tudor, K.I.: [Hans Berger (1873–1941)—the history of electroencephalography]. *Acta Med. Croat.: Cas. Hrvatske Akademije Medicinskih Znanosti* **59**(4), 307–313 (2005)
77. Vaughan, T.M., Heetderks, W.J., Trejo, L.J., et al.: Brain-computer interface technology: a review of the Second International Meeting. *IEEE Trans. Neural Syst. Rehabil. Eng.: Publ. IEEE Eng. Med. Biol. Soc.* **11**(2), 94–109 (2003)

78. Vaughan, T.M., Wolpaw, J.R.: The third international meeting on brain-computer interface technology: making a difference. *IEEE Trans. Neural Syst. Rehabil. Eng.: Publ. IEEE Eng. Med. Biol. Soc.* **14**(2), 126–127 (2006)
79. Vaughan, T.M., Wolpaw, J.R.: Special issue containing contributions from the fourth international brain-computer interface meeting. *J. Neural Eng.* **8**(2), 020201 (2011)
80. Wolf, M., Ferrari, M., Quaresima, V.: Progress of near-infrared spectroscopy and topography for brain and muscle clinical applications. *J. Biomed. Opt.* **12**(6), 062104 (2007)
81. Wolpaw, J.R., Birbaumer, N., Heetderks, W.J., et al.: Brain-computer interface technology: a review of the first international meeting. *IEEE Trans. Neural Syst. Rehabil. Eng.: Publ. IEEE Eng. Med. Biol. Soc.* **8**(2), 164–173 (2000)
82. Wolpaw, J.R., McFarland, D.J., Vaughan, T.M., et al.: The Wadsworth Center brain-computer interface (BCI) research and development program. *IEEE Trans. Neural Syst. Rehabil. Eng.: Publ. IEEE Eng. Med. Biol. Soc.* **11**(2), 204–207 (2003)
83. Xu, P., Yang, P., Lei, X., et al.: An enhanced probabilistic LDA for multi-class brain computer interface. *PLoS ONE* **6**(1), e14634 (2011)
84. Yang, J., Singh, H., Hines, E.L., et al.: Channel selection and classification of electroencephalogram signals: an artificial neural network and genetic algorithm-based approach. *Artif. Intell. Med.* **55**(2), 117–126 (2012)
85. Yorn-Tov, E., Inbar, G.F.: Selection of relevant features for classification of movements from single movement-related potentials using a genetic algorithm. In: 2001 Conference Proceedings of the 23rd Annual International Conference of the IEEE Engineering in Medicine and Biology Society, pp. 1364–1366 (2001)

## **Part II**

# **New Theoretical Developments**

# **Chapter 5**

## **Source Localization for Brain-Computer Interfaces**

**Aleksandr Zaitcev, Greg Cook, Wei Liu, Martyn Paley  
and Elizabeth Milne**

**Abstract** Brain-computer interfaces provide a way to operate software without the requirement for physical movement. Electroencephalography (EEG) can be utilized to detect electrical activity in the brain during the execution of certain mental tasks, which can be used as a control signal for an interface. Automatic interpretation of BCI control signals from multichannel EEG data is generally done by application of a classification algorithm from a particular machine learning paradigm. Classification accuracy and overall BCI performance depends on a feature extraction method, which is used to represent the EEG data according to the characteristic features of a chosen BCI control signal. Certain types of control signals used in BCI can be characterized by their spatial properties. Source localization methods can be used to localize electrically active areas of the user's brain and, hence, represent the EEG signal by its spatial features. This chapter is dedicated to the essential theory related to electromagnetic source localization problem with a particular focus on the family of sparse localization approaches. First we discuss general electromagnetic head modelling methods used to solve the EEG forward problem. Approaches to inverse problem solving, anatomical regularization and application of source localization to BCI are described later in the chapter. Finally we will discuss sparse source localization methods and present relevant simulation results.

---

A. Zaitcev · G. Cook · W. Liu (✉)

Department of Electronic and Electrical Engineering, The University of Sheffield, Sheffield S1 3JD, UK

e-mail: w.liu@sheffield.ac.uk

A. Zaitcev

e-mail: adzaytsev1@sheffield.ac.uk

G. Cook

e-mail: g.cook@sheffield.ac.uk

M. Paley

Department of Cardiovascular Science, The University of Sheffield, Sheffield S10 2RX, UK  
e-mail: m.n.paley@sheffield.ac.uk

E. Milne

Department of Psychology, The University of Sheffield, Sheffield S10 2TP, UK  
e-mail: E.Milne@sheffield.ac.uk

**Keywords** Electromagnetic head modelling · Brain computer interface · Source localisation · EEG signal analysis · Sparsity

## 5.1 Introduction to the Source Localization Problem

Electromagnetic brain imaging has been used extensively in the area of neurophysiological and psychology-related research for the past two decades. While originally being a useful tool for biomedical data analysis and visualization, brain imaging techniques have recently gained additional attention, due to their applications in the area of brain-computer interfacing.

There are various ways to detect neural activity. Electroencephalography (EEG) is a non-invasive way to record electrical potentials on the head surface. Although the EEG signal is prone to artifacts and suffers from low signal-to-noise ratio (SNR), it has become a common technology for BCI signal acquisition, due to its mobility, low price and excellent temporal resolution [24]. The current chapter is particularly focused on EEG source reconstruction due to its significance for BCI research. However, many of the imaging methods and approaches described here are also applicable to MEG data.

Generally, BCI can be described as a machine learning system, which recognizes a certain set of patterns in control signal acquired directly from the user's brain. Although there are many feasible approaches to BCI design, there is a common resemblance, which allows us to sort out a general architecture, as shown in Fig. 5.1. Prior to classification the preprocessed EEG data has to be represented as a feature vector in such a way that the most characteristic features of the corresponding data class are emphasized. Ideally feature extraction maximizes the difference between feature vectors for different classes, which leads to maximization of classification accuracy and as a result the overall system performance. Hence, the desire for more reliable BCIs creates motivation for development of efficient feature extraction methods.

EEG-based BCIs are generally operated by non-muscular control signals evoked by the user in voluntary manner (motor imagery, slow cortical potentials) or

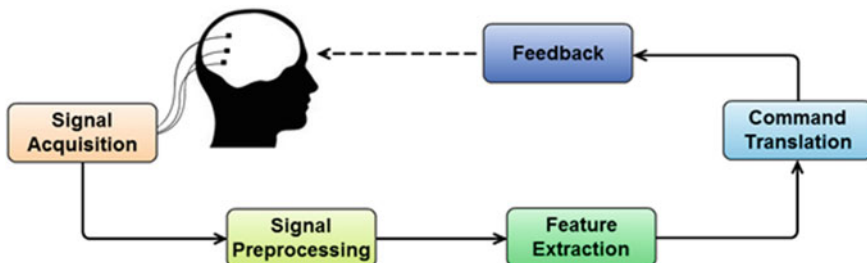


**Fig. 5.1** Functional architecture of a typical BCI

semi-voluntarily triggered by a particular stimulation paradigm (P300, steady state visually evoked potentials). Motor imagery (MI), or imagination of movement, was repeatedly proven to be a suitable neurophysiological basis for BCIs [21]. It is characterized by mu-band event-related desynchronization/synchronization (ERD/ERS) localized in the motor cortex area corresponding to the muscles involved in the motor imagery task being performed [28]. Therefore, various source localization methods can be used to estimate the cortical power distribution topography and form feature vectors to be interpreted by a particular choice of a classifier. Since feature extraction based on source reconstruction was proven to be particularly effective for MI classification, the current chapter will contain examples primarily for this type of EEG data.

The fundamental idea of EEG source localization is mapping of multichannel EEG recording onto the source space of higher dimensionality. The source space is comprised by a large number of sources, which are individually modelled as current dipoles or multipoles. Given that the number of EEG electrodes is normally on the order of 10 and number of sources is on the order of 1,000, the problem is severely underdetermined. This means that in order to obtain a realistic source localization solution, which fits into the nature of EEG, it is required to utilize the prior knowledge about the EEG physics, human anatomy and neurophysiology.

The majority of brain imaging approaches relies on the model described by the following equation:

$$M = LD + \varepsilon, \quad (5.1)$$

where  $M$  is the measurement matrix of size  $m$ -by- $k$ , with  $m$  being the number of EEG channels, and  $k$  is the number of time samples in the recording. It holds multichannel values of recorded potentials over time.  $L$  is commonly referred to as lead field matrix (or gain matrix) of size  $m$ -by- $n$ , where  $n$  is the number of elements in source model. It relates each source activation to the voltage on EEG sensors. Matrix  $D$  of size  $n$ -by- $k$  holds the solution to the problem, magnitudes of source activations over time. Finally  $\varepsilon$  is the noise perturbation matrix.

Lead field matrix  $L$  is comprised by the individual forward problem solutions for each dipole in the chosen source model. In the area of brain imaging the forward problem stands for linking of the source unit activations to the EEG electrode potentials. The information about how each individual dipole influences the EEG recording allows us to obtain the inverse problem solution, which is source localization itself. This chapter is dedicated to the essential theory related to electromagnetic source localization problem with a particular focus on the family of sparse localization approaches. Besides the forward problem solution, which incorporates the anatomical priors and EEG physics properties, sparse brain imaging methods also rely on the fundamental assumption that within a given short time interval there are very few electrically active regions in the whole brain volume. This assumption can also be interpreted as the main constraint to the solution, which substantially alleviates the ill-posed nature of the problem [5].

The following section “Head and source models” is dedicated to the various aspects of forward problem solving, such as numerical approaches to brain electrical field modelling, realistic head and source models. Section 5.3 “Source localization” defines the inverse problem and discusses common methods of solving it. Besides that, in Sect. 5.3 we explain anatomically validated considerations for source localization, as well as applications of brain imaging methods in BCIs. In the Sect. 5.4 “Sparse brain imaging” we describe and contrast various sparse source localization methods, and also present and discuss relevant simulation results. The summary of this chapter is given in the Sect. 5.5 “Conclusions”.

## 5.2 Head and Source Models

EEG brain imaging methods rely on a mathematical model comprising of many aspects of EEG physics, human neurophysiology and anatomy. This model is used to solve both the forward and inverse problems. The following section is dedicated to the forward problem solution. We will discuss the origins of EEG signal, approaches to head and source modelling required to solve the forward problem.

### 5.2.1 Physics of EEG

Before introducing the mathematical model utilized in the source localization process, it is important to give a brief overview of the neurophysiological basis of the EEG signal.

Neurons generate electrical current by pumping charged ions across neuron membranes through axons in the direction defined by the potential on the cell membrane, as shown in Fig. 5.2. Under certain circumstances neural cells are

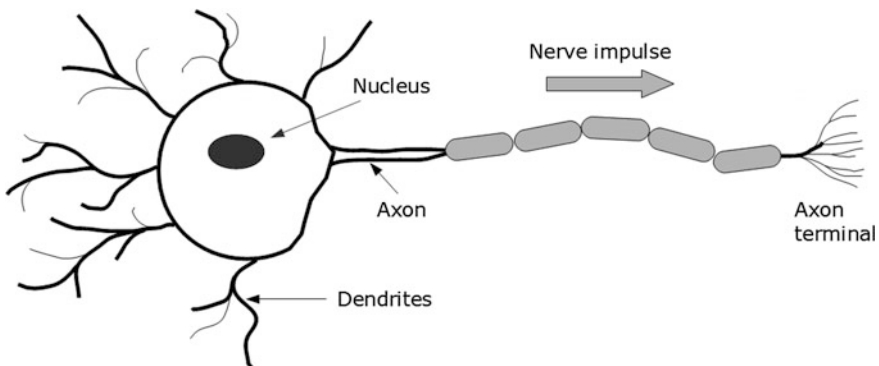


**Fig. 5.2** Structure of a nerve cell

capable of firing the so called Action Potentials (AP), which are considered to be the main carriers for different types of information transmitted through the CNS [31].

The EEG sensors, which detect surface potentials are large and remote, when compared to individual neurons. Electrical activity of a single neuron cannot be picked up by the surface sensors, since it is so overwhelmed by the activity of adjacent cells [25]. Relatively low electrode sensitivity substantially limits the EEG to detection of summarized electrical activity of many simultaneously active cells. The APs may have large amplitude (up to 110 mV), but they have very short duration (about 0.3 ms). Hence, superposition of such electrical events is highly unlikely. On the other hand, postsynaptic potentials, which can trigger the AP generation, have smaller amplitude (0.1–10 mV), but significantly longer time course (10–20 ms). Postsynaptic potentials are more likely to create a field superposition, noticeable by the EEG, and therefore, they are considered to be the primary EEG generators [2, 12].

Besides the requirement for synchronization, neurons must have a certain spatial alignment in order to create an observable surface potential. Neighboring neurons have to be arranged in a way to amplify the reciprocal electrical fields. Populations of pyramidal cells located in gray matter of the human brain usually have such spatial properties. Their apical dendrites are arranged parallel to each other and orthogonal to the cortical surface. Therefore, these neurons are considered to be the main contributors to EEG signal generation [12].

However, not all types of neurons have such alignment properties. Cells with arbitrarily aligned dendrites may have their extracellular potential fields cancelled by adjacent electrical activity. In this case the contribution to EEG signal is highly unpredictable. Hence, it can be stated that EEG predominantly reflects postsynaptic electrical activity of a certain subgroup of neurons with specific spatial properties.

### 5.2.2 *Source Models*

As was discussed in the previous section, the EEG signal is mainly composed of synchronous electrical activities of a certain subgroup of pyramidal cells. The following section introduces a mathematical approach to EEG source modelling.

#### 5.2.2.1 Modelling the Sources of EEG Signal

Since EEG signal frequency generally lies within the 0.1–100 Hz band, the mathematical analysis of electrical fields can be performed under quasi-static conditions. This means that despite the fact that neural activity changes over time, these changes occur substantially slower than the propagation effects of electromagnetic fields [2].

As was stated previously, electrical activity of a single neuron does not produce sufficient potential field observable on the surface of the scalp. Due to the identical

alignment of pyramidal cells in the gray matter, the superposition of individual electrical activities leads to the amplification of the resulting potential fields. Hence, a large group of synchronously active neurons located on a small area of the cortex is commonly represented as a single current dipole in the EEG source model.

A current dipole model can also be used to represent a single neuron on the microscopic level. Within a dipole model the current sink at position  $r_1$  represents the removal of positively charged ions from the apical dendrite of a neuron. Consequently, the current source at location  $r_2$  stands for the injection of positive ions into the cell. For such a dipole it is possible to estimate the current density  $J$  at position  $r$ :

$$\nabla \cdot J = I\delta(r - r_2) - I\delta(r - r_1), \quad (5.2)$$

where  $\delta$  represents the delta function and  $I$  is the current density within the dipole. It is possible then to relate the current density  $J$  to the electric field  $E$  through the Ohm's law:

$$J = \sigma E, \quad (5.3)$$

where  $\sigma$  is the location dependent tissue conductivity. Generally for the source localization problem it is assumed that tissue conductivity is isotropic for a given tissue type. Although this assumption substantially reduces the calculation complexity, it might also result in localization errors, since some tissues can have direction dependent conductivity. For example, skull consists of two hard layers with a spongiform layer between them. As a result, the tissue conductivity in a direction tangential to the skull surface is about 10 times larger than the conductivity in the direction normal to the surface. When the tissue conductivity is direction dependent, it is called anisotropic conductivity [12].

Taking into account the quasi-static conditions, it is possible to link the potential field  $V$  with electric field  $E$  through the Poisson's equation:

$$E = -\nabla V. \quad (5.4)$$

The orientation of vector  $\nabla V$  points to the direction, where the magnitude of scalar  $V$  increases most rapidly. The combination of Eqs. (5.2), (5.3) and (5.4) yields the following relationship between the dipole current density and potential field at  $r$ :

$$\nabla \cdot (\sigma \nabla (V)) = -I\delta(r - r_2) + I\delta(r - r_1). \quad (5.5)$$

When explicitly extended onto Cartesian coordinate system, this relationship takes the following form:

$$\begin{aligned} \frac{\partial}{\partial x} \left( \sigma \frac{\partial V}{\partial x} \right) + \frac{\partial}{\partial y} \left( \sigma \frac{\partial V}{\partial y} \right) + \frac{\partial}{\partial z} \left( \sigma \frac{\partial V}{\partial z} \right) = -I\delta(x - x_2)\delta(y - y_2)\delta(z - z_2) \\ + I\delta(x - x_1)\delta(y - y_1)\delta(z - z_1). \end{aligned} \quad (5.6)$$

As mentioned previously, there are tissues with direction dependent conductivity. However, Eq. (5.6) describes the relationship between potential field  $V$  and dipole current density  $I$  for homogenous isotropic conductivity, meaning that the tissue conductivity is assumed to be coordinate and direction independent.

### 5.2.2.2 Boundary Conditions

Since the potential field generated by neural electrical activity propagates through different types of tissue, it is necessary to consider the boundary conditions, when the field passes from volume with conductivity  $\sigma_1$  to volume with conductivity  $\sigma_2$ , as shown in Fig. 5.3.

It is assumed that no charge can be accumulated at the boundary between different compartments, which means that all current leaving the volume with conductivity  $\sigma_1$  will enter the volume with conductivity  $\sigma_2$ :

$$\begin{aligned} J_1 e_{n1} &= J_2 e_{n2} \\ (\sigma_1 \nabla V_1) e_{n1} &= (\sigma_2 \nabla V_2) e_{n2} \end{aligned} \quad (5.7)$$

At the boundary between the head surface and air it is assumed that no current can be injected outside the human body, due to the low air conductivity:

$$\begin{aligned} J_1 e_{n1} &= 0 \\ (\sigma_1 \nabla V_1) e_{n1} &= 0. \end{aligned} \quad (5.8)$$

Another condition applies only to boundaries not connected to air. This condition yields that potential cannot be accumulated at the compartment interface, hence:

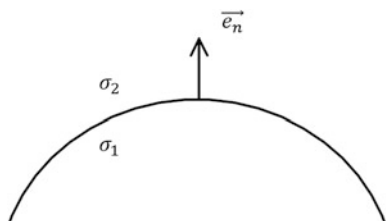


**Fig. 5.3** Boundary between two types of tissue with conductivity parameters  $\sigma_1$  and  $\sigma_2$  with  $\mathbf{e}_n$  representing the surface normal vector

$$V_1 = V_2. \quad (5.9)$$

Conditions (5.7) and (5.9) are often referred to as Neumann boundary condition and Dirichlet boundary conditions respectively.

### 5.2.2.3 Dipole Moment

As was explained earlier in this section, the current dipole can be used to represent an active pyramidal cell on a microscopic level or a large group of active cells on a macroscopic level. Within such a dipole the current source and sink input and remove equal amount of current density  $I$ , respectively. The magnitude of source activation is generally modelled by the dipole moment  $\mathbf{d}$ :

$$\mathbf{d} = I p \mathbf{e}_d, \quad (5.10)$$

where  $p$  is the distance between the current source and the current sink,  $\mathbf{e}_d$  is the unit vector holding the dipole orientation (direction from the sink to source). Hence, the scalar magnitude of the dipole can be defined as:

$$d = \|\mathbf{d}\| = I p. \quad (5.11)$$

It is a common practice to decompose such a current dipole into its components in a Cartesian coordinate system. Therefore, an arbitrarily oriented dipole is represented by three dipoles directed along the Cartesian axes:

$$\mathbf{d} = d_x \mathbf{e}_x + d_y \mathbf{e}_y + d_z \mathbf{e}_z. \quad (5.12)$$

The location parameter of a dipole  $r_{dip}$  is generally chosen to be in the middle between two monopoles. Hence, a single active EEG source can be represented by 6 parameters: three coordinates defining the source location and three Cartesian dipole components  $d_x$ ,  $d_y$  and  $d_z$ .

In much the same way the surface potential  $V$  at location  $r$  can be decomposed into its Cartesian components:

$$\mathbf{V}(r, r_{dip}, \mathbf{d}) = d_x V(r, r_{dip}, \mathbf{e}_x) + d_y V(r, r_{dip}, \mathbf{e}_y) + d_z V(r, r_{dip}, \mathbf{e}_z). \quad (5.13)$$

### 5.2.2.4 General Forward Problem Formulation

Previously we have introduced the mathematical approach to EEG source modelling. Hence, it is possible to formulate the forward problem set for a single current dipole  $\mathbf{d}$  at position  $r_{dip}$  and a single surface electrode at position  $r$ . In such settings, the forward problem solution is the surface potential  $l(r, r_{dip}, \mathbf{d})$ , which can be estimated by solving Poisson's Eq. (5.6). In case of multiple dipoles constituting the

chosen source model, the surface electrode potential is obtained as a linear superposition of potentials induced by multiple sources:

$$V(r) = \sum_i l(r, r_{dip}, \mathbf{d}_i) = \sum_i l(r, r_{dip}, \mathbf{e}_i) d_i. \quad (5.14)$$

In practice, multiple EEG electrodes are used for signal recording. For  $m$  EEG electrodes and  $n$  dipoles in the source model, the forward problem can be reformulated as follows:

$$V = \begin{bmatrix} V(r_1) \\ \vdots \\ V(r_m) \end{bmatrix} = \begin{bmatrix} l(r_1, r_{dip_1}, \mathbf{e}_1) & \cdots & l(r_1, r_{dip_n}, \mathbf{e}_n) \\ \vdots & \ddots & \vdots \\ l(r_m, r_{dip_1}, \mathbf{e}_1) & \cdots & l(r_m, r_{dip_n}, \mathbf{e}_n) \end{bmatrix} \begin{bmatrix} d_1 \\ \vdots \\ d_n \end{bmatrix} = L \begin{bmatrix} d_1 \\ \vdots \\ d_n \end{bmatrix}. \quad (5.15)$$

Matrix  $L$  is often called the lead field matrix, gain matrix or signal dictionary. It holds the forward problem solution for all the dipoles in the source model. When the EEG signal is analyzed over a given time course of  $k$  discrete sample points, Eq. (5.15) takes the following form:

$$V = \begin{bmatrix} V(r_1, 1) & \cdots & V(r_1, k) \\ \vdots & \ddots & \vdots \\ V(r_m, 1) & \cdots & V(r_m, k) \end{bmatrix} = L \begin{bmatrix} d_{1,1} & \cdots & d_{1,k} \\ \vdots & \ddots & \vdots \\ d_{n,1} & \cdots & d_{n,k} \end{bmatrix} = LD. \quad (5.16)$$

Equation (5.16) relate the source activations to surface potentials at multiple positions for a given experimental configuration. One can notice that it is very similar to the general inverse problem formulation (5.1). The difference is that in practice the EEG recording  $M$  reflects the voltage between the given electrode and the reference electrode, while  $V$  holds the surface potentials at the same electrode positions. Hence, prior to source localization it is required to re-reference the multichannel EEG signal and obtain surface potential approximations instead of voltages.

### 5.2.3 Head Models

In the previous section we have introduced the mathematical formulation of the forward problem and discussed how currents within the brain tissue can be related to the surface potentials. However, in order to solve the forward problem for all dipoles in the source model, it is necessary to take into account the anatomical properties of a subject. These properties are commonly embedded into a chosen head model, which largely defines the forward problem solution.

There are various known approaches to head model generation. In its simplest form the head model can be represented by a single shell sphere with isotropic homogenous conductivity within its volume. In this case the variation of conductivity in different tissues is not taken into account, which substantially reduces the calculation complexity, but obviously results in localization errors.

The consistent extension of a single sphere model is a multishell spherical head model, generally comprised of three or four concentric spheres, which represent different types of tissue, as shown in Fig. 5.4. The four-shell spherical model includes brain volume, a layer of cerebro-spinal fluid (CSF), skull and scalp.

There were many attempts to empirically estimate the conductivity of different tissue types by means of electrical impedance tomography (EIT), which is carried out by injecting a relatively small current of 1–10  $\mu\text{A}$  between pairs of EEG electrodes. However, the results obtained vary vastly: 0.22–0.749 S/m at the scalp, 0.0081–0.015 S/m at the skull, and 0.22–0.33 S/m in brain tissue. The CSF conductivity was quite accurately estimated to be 1.79 S/m. These conductivity values were obtained *in vitro* from postmortem tissue, where the conductivity properties can be significantly different compared to *in vivo* measurements [2].

Since the CSF conductivity is relatively large, the CSF layer is often omitted from the anatomy, which results in a simplified three-shell model. The typical radii

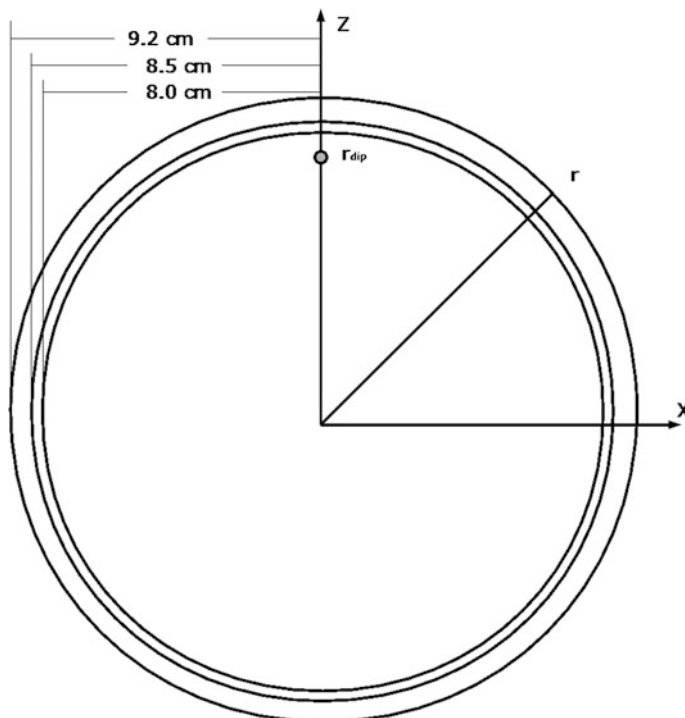


**Fig. 5.4** Visualization of a three-shell concentric sphere model

of surface boundaries used in such model are 8.0, 8.5 and 9.2 cm for brain tissue, skull and scalp respectively.

While spherical head models are widely used in research and clinical applications, it is obvious that such models do not reflect realistic geometry properties of the human head. In reality, the human head is inhomogeneous, anisotropic and has a more complex shape.

A more accurate approach to head model generation is extraction of spatial anatomical properties from high-resolution volumetric MRI images. Realistic head geometry is obtained as a set of complex shaped surfaces with certain conductivity properties, representing the interfaces between different tissue types. These tissue boundaries can be extracted from MR scans by many automated or semiautomated methods.

The approaches to head model generation are tightly interconnected with the chosen forward problem solution method. The relevant assumptions and conditions utilized in the solving process often must be embedded in the head model. Amongst the variety of approaches to forward problem solution for realistic model geometry, the most common techniques are boundary element method (BEM), finite element method (FEM) and finite difference method (FDM). The following section briefly contrasts these methods and the corresponding head models.

### 5.2.4 The Forward Problem

As pointed out already, the source localization processes rely on prior knowledge about the nature of the EEG signal and human anatomy, which is partially embedded in the forward problem solution  $L$  in (5.16).

The general approach to lead field matrix estimation is individually solving the forward problem for all sources in the chosen source model. The potential field at point  $r$  created by a single current dipole  $\mathbf{d}$  at position  $r_{dip}$  in infinite homogenous isotropic space with conductivity  $\sigma$  is given by:

$$V(r, r_{dip}, \mathbf{d}) = \frac{d(r - r_{dip})}{4\pi\sigma\|r - r_{dip}\|^3}. \quad (5.17)$$

If the current dipole is set to be in the origin of the Cartesian coordinate system and aligned along the  $z$ -axis, then (5.17) can be reformulated as:

$$V(r, 0, d) = \frac{d \cos \theta}{4\pi\sigma r^2}, \quad (5.18)$$

where  $\theta$  is the angle between  $r$  and the  $z$ -axis. In order to obtain a similar solution for dipoles oriented along the  $x$ -axis and the  $y$ -axis, the coordinate system can be rotated accordingly.

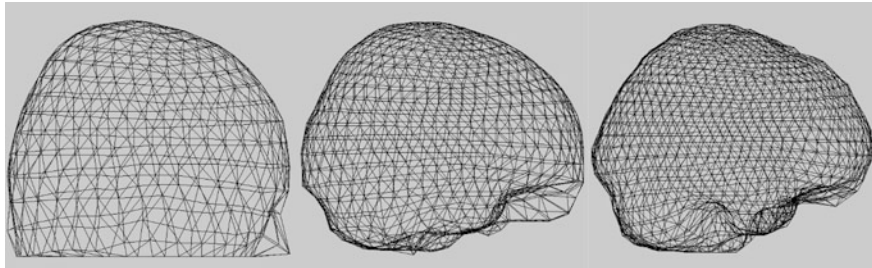


**Fig. 5.5** Visualization of a realistic BEM head geometry

The multishell concentric sphere model assumes homogeneity and isotropy of compartments encapsulated by the spheres. A semi-analytical method of solving the forward problem for this geometry is described in [30]. The computational simplicity of this method allows it to be used in practical real-time applications, such as BCIs. Besides that, this technique can be extended to anisotropic conductors, where the conductivity in the tangential direction can be set to be different from the conductivity in the orthogonal direction [6, 36].

The boundary element method (BEM), which originates from the field of electrocardiography, is a further step to realistic electromagnetic head modelling. It still assumes volume homogeneity and isotropy, but can use a more complex head geometry to deal with the varying thickness and curvature of the skull. As the method's name implies, it provides a solution to the forward problem by estimating the values of potentials at the boundaries between head volumes. The BEM head model is generally comprised by three surfaces, each tessellated by multiple flat triangular elements, as shown in Fig. 5.5. Assuming the general convexity of the human head, in such a model there will be only three triangular elements on the line between the current dipole and any point at the scalp surface. A numerical approach to the BEM forward problem solution was first presented in [15].

More recently, the finite element method (FEM) and the finite difference method (FDM) were applied to the forward problem, providing means to deal with conductor anisotropy and tissue inhomogeneity. In both FEM and FDM, the whole 3D volume of the brain is segmented into small volumetric elements. Thus each individual volumetric component borders several adjacent ones. It is possible to define the conductivity values at every interface between these elements and within their volume, and hence, deal with conductor anisotropy and inhomogeneity. The head model for FDM and FEM is defined by the sparse system matrix, containing relative directional conductivity properties of every volumetric constituent. Unlike BEM, FDM and FEM approaches rely on iterative minimization of a predefined cost function. This process is computationally highly intensive. However, in practical applications, it is required to be performed only once for every subject. Detailed description of the forward problem solution with FEM can be found in [16, 35]. Numerical approaches related to FDM can be found in [17].

## 5.3 Source Localization

In the previous section we have discussed the general mathematical model, which allows the estimation of surface potentials for a defined current dipole located within the brain volume. After the forward problem is solved for a given anatomical model, EEG equipment configuration and source model, it is possible then to perform the source localization by solving the inverse problem for a given segment of EEG recording. The following section addresses the general aspects of source localization, characterizes the main anatomical constraints to inverse problem solution and describes how source localization can be utilized in a BCI system.

### 5.3.1 The Inverse Problem

Equation (5.1) presents the general model for the inverse problem. The aim of the inverse problem is estimation of  $n \times k$  dipole moments, located within a certain head geometry over  $n$  positions, for a given  $m$ -channel EEG recording of length  $k$ , forward solution  $L$  and noise perturbation matrix  $\varepsilon$ :

$$\begin{aligned} M &= LD + \varepsilon \\ \begin{bmatrix} M(r_1, 1) & \cdots & M(r_1, k) \\ \vdots & \ddots & \vdots \\ M(r_m, 1) & \cdots & M(r_m, k) \end{bmatrix} &= \begin{bmatrix} l(r_1, r_{dip_1}, \mathbf{e}_1) & \cdots & l(r_1, r_{dip_n}, \mathbf{e}_n) \\ \vdots & \ddots & \vdots \\ l(r_m, r_{dip_1}, \mathbf{e}_1) & \cdots & l(r_m, r_{dip_n}, \mathbf{e}_n) \end{bmatrix} \begin{bmatrix} d_{1,1} & \cdots & d_{1,k} \\ \vdots & \ddots & \vdots \\ d_{n,1} & \cdots & d_{n,k} \end{bmatrix} + \varepsilon \end{aligned} \quad (5.19)$$

EEG-based tomography aims to estimate the electrical brain activity over a large number of cortical points to provide a higher localization resolution. Due to the fact that  $n \gg m$  in most of the imaging applications, the EEG inverse problem can be characterized as an ill-posed one. Besides that, EEG inverse solutions are unstable, which means that a small deviation of a noisy EEG signal can substantially alter the localization results.

As was explained in the previous section, dipoles within the chosen source model represent large populations of electrically active pyramidal cells. Each source is defined by 6 parameters: three values to set the source location  $r_{dip}$  in Cartesian coordinates and three values for dipole moment projections onto the  $x$ -,  $y$ - and  $z$ -axes. Alternatively, dipoles can be represented by three values for  $r_{dip}$ , two values for dipole orientation (angles  $\theta$  and  $\phi$ ) and source magnitude  $d$ .

According to which parameters in (5.19) are set to be fixed and which are being estimated, it is possible to separate the inverse problem approaches into two categories: non-parametric and parametric methods. Non-parametric techniques are also often called distributed inverse solutions (DIS) or imaging methods. This class of methods relies on a distributed source model covering the whole brain volume or

its particular compartments. Each source in this model has a constant pre-defined position  $r_{dip}$  and possibly fixed orientation. Since the source parameters are calculated beforehand and  $n \gg m$ , the non-parametric EEG inverse problem is an example of a linear underdetermined problem. The latter means that the solution is non-unique and multiple mathematically feasible solutions exist for this problem. Amongst a great variety of non-parametric inverse problem solvers, it is possible to list the most commonly used and influential approaches: Low Resolution Electromagnetic Tomography (LORETA) [27] and its derivations LORETA-FOCUSS (Focal underdetermined system solution) [11], Standartized Shrinking LORETA-FOCUSS (SSLOFO) [19], Linearly Constrained Minimum Variance (LCMV) beamformer [33], Minimum Norm Estimates (MNE), and Weighted Minimum Norm Estimates (WMNE) [11].

Parametric source localization approaches do not assume fixed positions and orientations of dipoles within the brain. These methods are also referred to as Concentrated Source Models, Equivalent Current Dipole methods or Dipole Fit methods. In contrast to non-parametric techniques, the source model is not calculated beforehand for this class of localization methods. Parametric approaches aim to represent the given segment of EEG recording by fitting multiple dipoles with flexible parameters into the chosen electromagnetic brain model. Hence, it is required to estimate parameters  $d, \mathbf{e}, r_{dip}$  for every dipole for a given  $M$  and forward solution  $L$ . If the number of dipoles is not set in advance, the problem is non-linear. Most common examples of parametric methods are the non-linear least squares solver [8, 34], Multiple Signal Classification [23, 32], and parametric adaptations of beam forming techniques [2]. Due to the computational intensity and undetermined source model, parametric methods are more applicable to the area of neurophysiological research rather than brain-computer interfacing. In the following sections we will discuss various general aspects of imaging localization techniques. More information about non-parametric inverse problem solvers can be found in [2, 11].

### 5.3.2 Anatomical Constraints for Source Localization

Solving the EEG inverse problem with non-parametric approaches generally puts high requirements for method regularization. Due to the model formulation (5.19), the inverse problem can be interpreted as solving a system of  $m$  linear equations with  $n$  unknowns. Due to  $n \gg m$ , the problem is underdetermined with multiple mathematically feasible solutions. While fitting perfectly into (5.19), these solutions do not necessarily fit into the nature of EEG and human neurophysiology. Hence, it is required to limit the subspace of allowable solutions by putting additional constraints, which utilize more information about the human anatomy and EEG physics.

Multiple anatomically justified assumptions are already embedded into the forward problem solution. As it was shown earlier, information about the tissue conductivity, head geometry, properties and locations of EEG sources and recording

equipment is used to solve the forward problem. Nevertheless, in order to produce feasible results and/or improve localization accuracy, it is often required to consider more aspects of EEG data.

### 5.3.2.1 Locations of Sources

Dipoles within the source model represent currents originating from synchronous electrical activity of multiple neurons. Currents, generated by a single cell do not produce sufficient potential field to be detected on the head surface. However, if multiple cells have similar alignment, postsynaptic potentials are mutually amplified to create a potential field of the magnitude detectable by modern EEG equipment. Pyramidal cells, located within a cortical layer of gray matter possess such orientation properties. Hence, the EEG recording mainly reflects electrical activity of this particular subgroup of cells. Therefore, it is a common practice to represent the given segment of data  $M$  only by current dipoles within a 1–2 cm thin cortical area of gray matter. It can be done at the forward problem solving stage by restricting the fixed locations of sources to that cortical area. In this case the computational intensity of the localization process can be substantially reduced, since the number of dipoles  $n$  is smaller.

Alternatively it is possible to apply a pre-defined spatial filter to the estimated inverse problem solution. Let  $S$  be the spatial filter, which limits the solution.  $S$  is a diagonal matrix of size  $n$ -by- $n$  with spatial weight values on the main diagonal. The localization solution  $D$  can then be represented as:

$$\hat{D} = SD, \quad (5.20)$$

where  $\hat{D}$  is the spatially filtered localization result. The problem formulation then becomes:

$$M = L\hat{D} + \varepsilon. \quad (5.21)$$

The weight values on the main diagonal of  $S$  can be defined in various ways. One of the most powerful approaches is based on statistical analysis of individual subject's MR images. Spatial weights can be given values in range from 0 to 1, corresponding to the probability of a dipole being located in the gray matter layer or otherwise. In contrast to manual and semi-automated weight assignment methods, utilization of anatomical priors from MR scans allows for more flexible control of localization spatial properties. However, it is more computationally complex, since the number of sources  $n$  is not reduced.

As can be seen from (5.21), the EEG recording  $M$  is being explained through the activations of sources, located within a pre-defined cortical area. However, besides the signal of interest,  $M$  is comprised of random neural activity from areas other than a thin layer of gray matter. Since the source model is restricted to a certain area, the background noise and muscular artifacts will also be introduced into the

inverse problem solution for that area, which can severely impair the localization accuracy and limit the resolution. However, it is possible to alleviate these effects at the signal preprocessing stage by applying algorithms like Independent Component Analysis (ICA) to extract the relevant signal components and improve SNR [1].

### 5.3.2.2 Orientations of Sources

Distributed imaging methods assume multiple fixed dipole locations within the chosen source model. As described earlier, sources are oriented normally to the cortical surface, due to the alignment properties of neurons which they represent. The orientation of sources is generally defined in a forward problem solving process, since it is required to relate the dipole currents to the surface potentials. However, such assumptions about neuron alignment are often overly generalized, which can impair the localization accuracy of a method. In a real human head there is a certain level of cell organization irregularity, which is very difficult to predict. In order to deal with this effect, it is possible to give a certain degree of freedom for source orientation parameters at the inverse problem solving stage.

In general, because the orientation  $\mathbf{e}$  is set beforehand for every dipole  $\mathbf{d}$ , imaging methods are used to find only dipole moments  $d$ , which are positive values, and hence  $D \in \mathbb{R}_+^{n \times 1}$ . If dipole orientation values are not set to be constant, it is required then to estimate  $D \in \mathbb{R}^{n \times 3}$ , where columns of  $D$  hold  $d_x$ ,  $d_y$  and  $d_z$  components of sources. In order to control the deviation of estimated dipole orientation  $\mathbf{e}'$  from the original orientation  $\mathbf{e}$ , it is required to set a new boundary. The angle  $\varphi$  between  $\mathbf{e}$  and  $\mathbf{e}'$  is given by:

$$\varphi = \arccos \frac{(\mathbf{e} \cdot \mathbf{e}')}{|\mathbf{e}| |\mathbf{e}'|}, \quad (5.22)$$

where  $\mathbf{e} \cdot \mathbf{e}'$  denotes the dot product of two vectors. By keeping the value  $\varphi$  within small pre-defined boundaries, it is possible to get more realistic localization results. However, such regularization makes the problem much more computationally complex.

### 5.3.2.3 Spatio-Temporal Smoothness

A straight-forward approach to localization accuracy improvement is utilization of a larger number of densely located dipoles in a source model. Many EEG imaging methods tend to produce spiky solutions, when a large portion of solution energy is concentrated over a few dipoles, while adjacent sources are electrically idle. These solutions do not fit into expectations about the nature of EEG. When the inter-node distance between sources is small, it is required to take into account the local current propagation effects. Hence, it is necessary to apply additional constraints to the spatial smoothness of the inverse problem solution.

Similar principle applies to the temporal smoothness. If the measurement matrix  $M$  contains EEG recording over multiple sampling points and when the source magnitudes vary slowly with respect to the sampling frequency, it is required to set a certain penalty for large changes between the sampling points.

A general formulation of how these constraints can be applied in practice was proposed by [4]. This method involves application of spatial and temporal bases in order to limit the solution subspace. Within this approach the problem formulation (5.1) is extended to the following form:

$$M = LS\Theta T + \varepsilon, \quad (5.23)$$

where  $S$  and  $T$  are the pre-defined spatial and temporal bases respectively, and matrix  $\Theta$  holds the new optimization variables to be estimated.

Matrix  $S$  is composed of concatenated column vectors, each corresponding to a spatial filter for a certain cortical patch. These filters set particular weights for dipoles within the patch and set zero values to weights of dipoles which lay outside it. In this manner the spatial smoothness property can be implemented. Examples of approaches to spatial bases generation can be found in [4, 18]. The choice of spatial bases significantly influences the method's performance and accuracy. It is possible to implement other various spatial constraints to the localization method through the selection of  $S$ . For example, assumptions about spatial smoothness, region of interest and spatial priors from an fMRI study can be embedded into the spatial bases.

In much the same way, matrix  $T$  implements the temporal smoothness property. It contains row-wise temporal bases, which force the estimated dipole activations to continue over the pre-defined temporal profiles. And again various prior knowledge about EEG temporal properties can be utilized through the selection of appropriate temporal bases. For example, wavelets or other common time-frequency bases can be used to isolate a particular frequency band or contrast other time-frequency characteristics.

Matrix  $\Theta$  contains new optimization variables. Element  $\Theta_{ij}$  holds the magnitude of an event in a cortical patch set by the  $i$  th column of  $S$  over the temporal profile set by the  $j$  th row of  $T$ . Hence the resulting solution  $D$  is composed of a linear superposition of individual event contributions. The number of cortical patches  $p$  is generally lower than the number of dipoles in a source model  $n$ , and the number of temporal bases  $t$  is lower than the number of samples  $k$ . Therefore, such representation of a solution can noticeably reduce the inverse problem complexity.

### 5.3.3 Source Localization for BCI

In general, BCIs provide a way to interact with software without physical movements. A limited number of software commands can be cast by interpreting the BCI user's brain activity. The majority of modern EEG-based BCI implementations rely on a particular machine learning algorithm, which is utilized to make this decision.

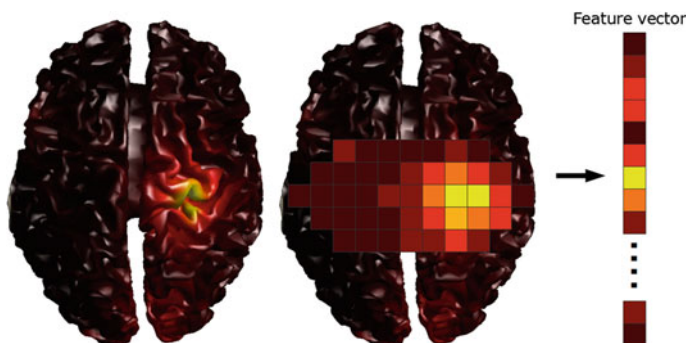


**Fig. 5.6** Schematic illustration of spatial feature extraction for BCI. Power topography used directly to form the feature vector

Within this paradigm the EEG signal is represented according to its characteristic traits on the feature extraction stage. Feature vectors, extracted from the data, are passed to a particular classification algorithm, which identifies the mental task being performed and makes a final interpretation decision. Examples of classifiers commonly used in BCI design are Linear Discriminant Analysis (LDA), Support Vector Machines (SVM), Artificial Neural Networks (ANN), and Hidden Markov Model (HMM) [20, 24].

As explained earlier in the chapter, source localization represents the EEG signal in terms of active sources located within a volume of the brain, hence, contrasting spatial features of the given data segment. The values of dipole moments from  $D$  can be used directly to form the feature vectors as shown in Fig. 5.6. This approach to feature extraction is applicable, when the spatial representation of the EEG signal provides sufficient information about the particular mental task being performed. Certain types of neurophysiological effects used in BCI design, such as SSVEP or P300, cannot be identified solely by locations of electrical activity.

Physiological studies show, that the execution of motor activity, or physical motion creates recognizable patterns in the mu-band (8–13 Hz) and sometimes beta-band (15–30 Hz) of EEG signals (as shown in Figs. 5.7 and 5.8) [28]. Apart from the motor activity itself, imagination of motion or Motor Imagery (MI) also creates similar detectable responses but of lower intensity. Since MI can be performed without actual movement, it can be used as a control signal for a BCI system [29]. A functional MRI study described in [22] shows that neural activations accompanying motion and motor imagery originate in the areas of motor cortex corresponding to the muscles involved. There is a large inter-subject variability of cortical locations representing the same types of movement, as well as significant level of overlapping between these areas. But the main conclusion of that research is that localization of activity during MI execution is highly informative for MI task detection. This validates the usage of source reconstruction methods for feature extraction in MI-based BCIs.

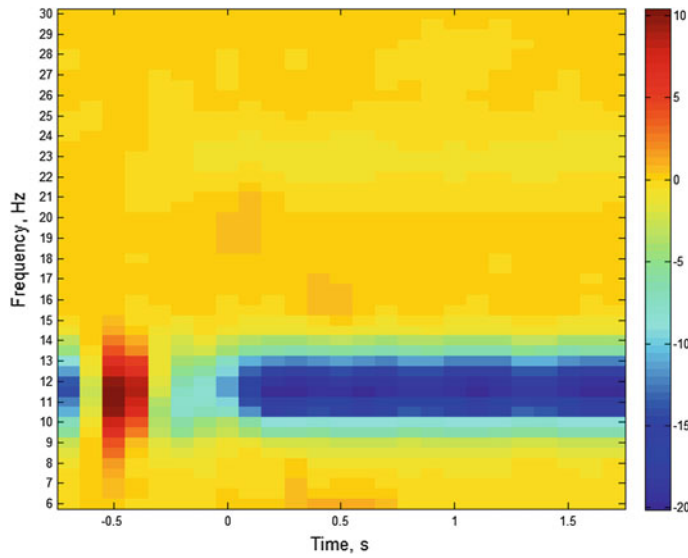


**Fig. 5.7** Time-frequency map of C3-channel of EEG recording during the execution of right-hand MI task. Magnitudes of average band power are represented by *color* with respect to baseline, estimated during idle period (-1 to 0 s). Time point 0 corresponds to the beginning of MI execution, after which ERD in the upper  $\mu$ -band can be observed

The EEG data used to obtain Figs. 5.7 and 5.8 is taken from BCI competition IV, dataset 2a. It contains 22-channel EEG recordings of 4 MI tasks performed by multiple subjects. Open-source FieldTrip framework for MEG/EEG data analysis was used in order to obtain and visualize these time-frequency maps.

Dimensionality of the feature vector is tightly connected with the size of the available training set. In order to create an accurate decision boundary the size of the training set has to be 5–10 times the size of the feature vector. This effect is often referred to as the curse of dimensionality [3]. Due to this constraint, in applications where training data is difficult to acquire, the size of the feature vector has to be significantly limited.

As shown earlier, brain imaging methods must rely on a certain head model, which can be generated analytically or from anatomical MR images. Such individual MR scans can often be unavailable, however, it is possible to use standard MR models, such as ICBM 152 atlas provided by Montreal Neurological Institute. This atlas is represented in a form of MR image, non-linearly averaged over 152 subjects. Although individual MR scans can provide more accurate information about the subject's head anatomy, and hence improve source localization precision, it is often impossible to use it in practical BCI implementations, since BCI would have to be configured individually for each subject. On the other hand standard MR atlases are publicly available and can be easily converted into head models to be used in BCIs feature extraction, hence they can be used as a compromise between localization accuracy and BCI complexity.

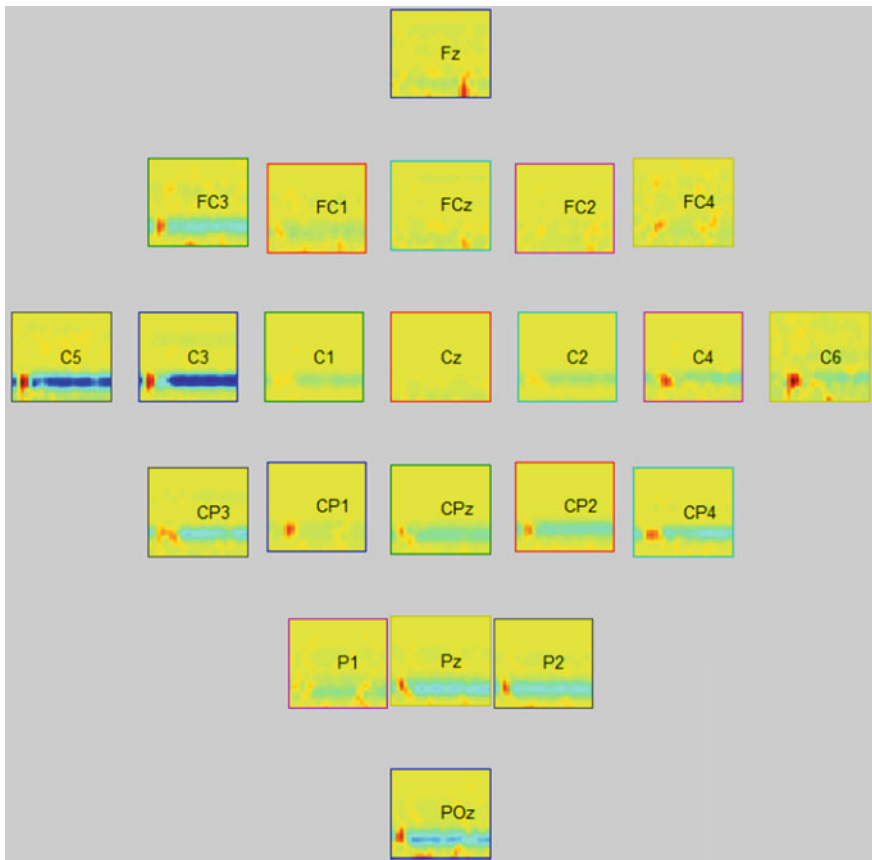


**Fig. 5.8** Time-frequency maps similar to Fig. 5.7 plotted for all electrodes for the given EEG sensor configuration during right-hand MI task. Contralateral ERD can be observed in the area around the C3 sensor, which fits into the expectations from [28]

## 5.4 Sparse Brain Imaging

### 5.4.1 Introduction to Sparse Brain Imaging

Earlier we have characterized the distributed inverse problem as underdetermined, having multiple numerically feasible solutions for given input data. Various implicit or explicit constraints should be applied to a solution space in order to regularize the localization method and obtain a unique solution, which can be used to form the feature vectors. Besides fore-mentioned anatomical constraints, sparse brain imaging methods rely on the fundamental assumption that, within a short period of time, very few cortical areas are electrically active. This assumption was repeatedly validated by various fMRI studies, e.g., in [22]. Therefore, sparse imaging methods

search for a solution with minimal energy localized over few dipoles with non-zero magnitude values.

Sparse source localization approaches generally minimize the cost function  $C(D)$ , which fits into the general formulation of Tikhonov regularization. It can be formally stated as:

$$C(D) = \|M - LD\| + \lambda \cdot f(D). \quad (5.24)$$

In Eq. (5.24) the term  $\|M - LD\|$  stands for the requirement of error minimization, whereas  $f(D)$  is the regularization term and  $\lambda$  is the regularization parameter set beforehand. A single unique solution can be obtained by minimization of  $C(D)$ , if the cost function has a global minimum.

One of the advantages of sparse localization methods is that instead of directly minimizing the cost function defined (5.24), the inverse problem can be solved by means of Linear Programming (LP). The nature of LP solutions guarantees the uniqueness of the estimated matrix  $D$ , corresponding to the global optimum of the LP problem. Alternatively, if it is required to handle non-linear inequality/equality constraints, the inverse problem can be solved by Second Order Cone Programming (SOCP). Common examples of open-source software tools used to solve LP and SOCP problems are SeDuMi and SDPT3, which are available in CVX package for Matlab [9, 10].

### 5.4.2 Approaches to Sparse Source Localization

The earliest adopted approach to brain imaging based on energy minimization is Minimum Norm Estimate (MNE) [13], which explains the given EEG measurement by minimizing the Euclidian norm ( $l_2$ -norm) of a solution. The norm of matrix  $D$  represents the global magnitude of a solution. Hence, the method's cost function takes the following form:

$$C(D) = \|M - LD\|_2 + \lambda \cdot \|D\|_2. \quad (5.25)$$

In terms of convex optimization, the problem can be formulated as follows:

$$\begin{aligned} & \underset{D}{\text{minimize}} && \|D\|_2 \\ & \text{subject to} && \|M - LD\|_2 \leq \beta, \end{aligned} \quad (5.26)$$

where  $\beta$  is the pre-defined allowable degree of error. This problem formulation is valid for a Single Measurement Vector (SMV) case, where  $M$  contains a single column vector of measurements and  $D$  is a single solution vector. Application of  $l_2$ -norm in the regularization term represents the Gaussian spatial prior of current field [7]. Due to the nature of the  $l_2$ -norm operator, MNE produces blurry solutions with low localization accuracy for both spherical and realistic head models [26]. Since

the sources are defined to be equal, MNE localization methods tend to favor weak and surface dipoles in the solution. In order to deal with this effect it is possible to use a weight matrix  $W$  to rebalance the source model. This approach is often referred to as the Weighted Minimum Norm Estimate (WMNE) and the problem (5.26) can be refined as follows:

$$\begin{aligned} & \underset{D}{\text{minimize}} && \|WD\|_2 \\ & \text{subject to} && \|M - LD\|_2 \leq \beta. \end{aligned} \quad (5.27)$$

The spatial weight matrix  $W$  can be interpreted as a spatial filter, thus the WMNE problem fits into the general model for spatio-temporal regularization in (5.23). Spatial weights can be generated from the lead field matrix, for example, by finding column-wise  $l_2$ -norms of  $L$ . Other popular strategies for spatial weight selection and their comparison can be found in [11].

In order to obtain a more concentrated sparse inverse solution, it is required to minimize the sum of absolute source magnitude values, i.e. by minimizing the  $l_1$ -norm of  $D$ . In this case the optimization problem takes the following form:

$$\begin{aligned} & \underset{D}{\text{minimize}} && \|D\|_1 \\ & \text{subject to} && \|M - LD\|_2 \leq \beta. \end{aligned} \quad (5.28)$$

Minimization of the  $l_1$ -norm of  $D$  applies the sparsity constraint with exponential current fields, which results in solutions with energy concentrated over a few sources. However, in high-resolution source models with a large number of dipoles it is often necessary to take into account the local propagation effects and constrain the local smoothness, as shown in Sect. 3.2. Sparse source localization methods originating from MNE are often called  $l_p$  Generalized Minimum Norm Estimates (GMNE), according to the type of regularization applied to method, such as the  $l_1$ -norm GMNE.

Examples of GMNE methods described earlier are generally applied to source models with constant orientation parameter  $\mathbf{e}$  for each dipole. The Sparse Source Imaging (SSI) method, presented in [7] performs a two-step GMNE procedure to find the inverse solution, by first estimating source orientations and then finding optimal magnitude values for these sources.

If  $M$  holds EEG data recorded over multiple time samples, it is required to solve a Multiple Measurement Vector (MMV) problem by analyzing the whole given block of data. GMNE imaging methods applied separately to individual columns of  $M$  often lead to the unrealistic solutions with source sparsity profile varying rapidly over time samples. It is necessary to avoid such solutions, if the neural activity is expected to vary slowly with respect to the sampling frequency.

Following the recommendations from [5, 14] it is possible to solve the MMV inverse problem by minimizing the sum of row-wise  $l_2$ -norms of  $D$ , e.g., for  $l_1$ -norm GMNE:

$$\begin{aligned} & \underset{D}{\text{minimize}} && |\langle D \rangle|_1 \\ & \text{subject to} && \|M - LD\|_2 \leq \beta, \end{aligned} \quad (5.29)$$

where  $|\langle D \rangle|_1 = \|\hat{l}_2(D)\|_1$  and  $\hat{l}_2(\cdot)$  denotes the operator returning a column vector of row-wise  $l_2$ -norms.

Minimization of the solution's energy has been proven to be a powerful approach to inverse problem solving, since the sparsity constraint is validated by the nature of EEG. In practice, imaging methods have various disadvantages, such as susceptibility to noise or low resolution, which often limits their application to a particular experimental paradigm or type of neural activity being observed on EEG. Hence, it is necessary to choose a certain localization method according to the application and experimental settings. Besides that, many disadvantages of localization methods can be alleviated by applying appropriate signal preprocessing techniques, such as application of region of interest, frequency filtering or ICA.

### 5.4.3 Examples of Sparse Source Localization

Performance of sparse localization methods can be demonstrated on a basic simulated example. Let us assume a single dipole  $\mathbf{d}$  with fixed location and orientation along the  $z$ -axis. For the current example, the head geometry was generated from the symmetric ICBM 152 head atlas by applying the BEM head model generation method, provided in FieldTrip framework. A relatively simple 22-channel EEG electrode layout was used, which corresponds to practical and mobile EEG systems used in BCI design. The source model is comprised of 1,443 dipoles located in a regular grid within a 1.5 cm thin cortical layer. The number of sources used in the current simulation is relatively small, which is typical for BCI applications with strict computational complexity limitations. The BEM head model as well as spatial properties of the given dipole and EEG configuration are shown in Fig. 5.9. After all the required parameters have been set, it is possible to solve the forward problem for the current configuration and thus obtain a lead field matrix  $L$ .

Let us assume that the given dipole represents a localized 12 Hz oscillatory activity, which corresponds to the upper  $\mu$ -band of EEG signal. The matrix  $D$  thus contains zero values for all dipole moments except for  $z$ -component of dipole  $\mathbf{d}$ , which is given by  $d_z(t) = 0.5\sin(2\pi f_d t) + 0.5$ , where the dipole oscillation rate  $f_d = 12$  Hz and  $t$  corresponds to a 250 Hz sampling frequency.

Having the dipole moments  $D$  and forward problem solution  $L$  set, it is possible then to obtain a measurement matrix  $M$ , which simulates a block of 22-channel EEG data recorded over 750 sampling points, corresponding to 3 s for a chosen sampling frequency. It can be done in a straight-forward manner by inserting  $D$  and  $L$  into Eq. (5.19). A noise matrix  $\varepsilon$  was then added to the measurement matrix, in order to simulate a more realistic noisy EEG signal.

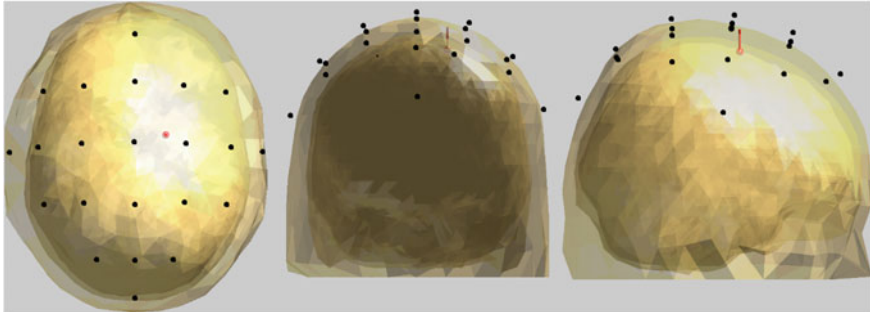


**Fig. 5.9** BEM head model, EEG sensor configuration and dipole location used in simulation. *Left to right:* X–Y view, X–Z view, Y–Z view. EEG electrode locations are represented by *black dots* on the skin surface

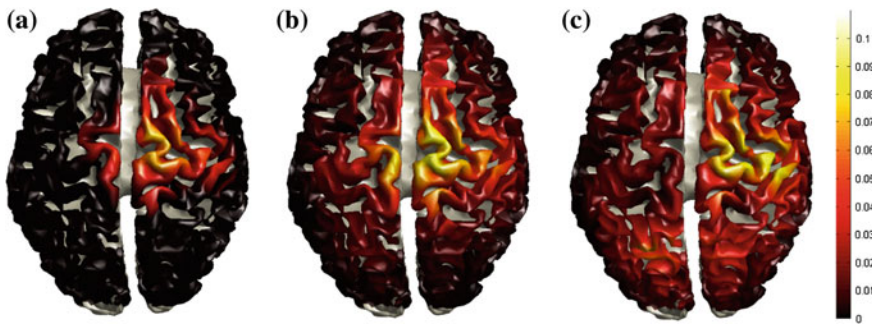


**Fig. 5.10**  $l_2$  GMNE localization results of a single time sample of the simulated EEG signal with various levels of noise. The used time sample of  $M$  corresponds to the maximum magnitude of **d**. Figures contain power topographies for three noise conditions estimated for the same regularization parameter  $\lambda$  and plotted on the same scale. **a** Noiseless case. **b**  $\frac{\|e\|_2}{\|M\|_2} = 0.3$ . **c**  $\frac{\|e\|_2}{\|M\|_2} = 0.7$

Localization results for different levels of noise were obtained as shown in Fig. 5.10 by applying the standard  $l_2$ -norm GMNE method to individual columns of  $M$ , corresponding to different sampling points.

After performing source localization, the newly obtained matrix  $\hat{D}$  contains dipole magnitude progressions over time. It is possible then to highlight certain temporal and frequency properties of the signal of interest in source space instead of EEG electrode space. For example, one can apply a band-pass filter to the signal from each dipole and obtain average band power for all locations in the source model, as shown in Fig. 5.11.

Since only a single dipole is simulated to be active over the observation time, it is expected that source reconstruction would produce much more focused results rather than the images presented in Fig. 5.11. However, localization results for all noise conditions are obtained with the same value of regularization parameter  $\lambda$  (see

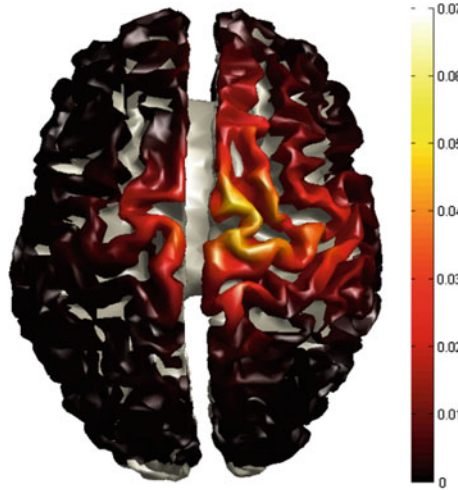


**Fig. 5.11** Topography of average 11–13 Hz band power of a noisy simulated EEG signal ( $\frac{\|\epsilon\|_2}{\|M\|_2} = 0.7$ ). Each row of  $\hat{D}$  can be treated as a separate channel containing dipole moment progressions over time. It is then possible to perform FFT over rows of  $\hat{D}$  and obtain the average of 11–13 Hz components for each source over 3 s of observation. Hence, this figure contains single scalar values of average band power obtained for every dipole visualized over the simulated brain surface

Eq. (5.25)). When setting the value of  $\lambda$ , it is necessary to take into account the trade-off between the solution sparsity and performance in the presence of noise. The lower value of  $\lambda$  sets a lower penalty for blurry solutions, where energy is spread over larger areas. However, such unfocused solutions can partially compensate for noise and produce more anatomically feasible images. Interpreting the results in Fig. 5.10, it is possible to say that source localization algorithms always produce a certain degree of error, which needs to be alleviated either on the forward/inverse problem stages by setting particular constraints to the solution, or by applying appropriate post-processing methods to extract the location of signal of interest from the estimated topographies. One straight-forward way to improve the localization accuracy is to increase a number of dipoles in the source model. However, increase of the spatial resolution increases the dimensionality of optimization variable  $\hat{D}$  and thus makes the inverse problem more computationally complex.

Source localization methods based on minimization of  $l_1$ -norm are capable of producing more sparse and focused solutions to the inverse problem when compared to  $l_2$  GMNEs. However, they behave quite differently in the presence of noise. Let us apply  $l_1$  GMNE with problem formulation described in (5.28) to the same simulated example as shown above. Localization results for the three different levels of noise are illustrated on the Fig. 5.12. In the noiseless case (Fig. 5.12a)  $l_1$  GMNE produces accurate sparse solution with a cluster of active dipoles at the

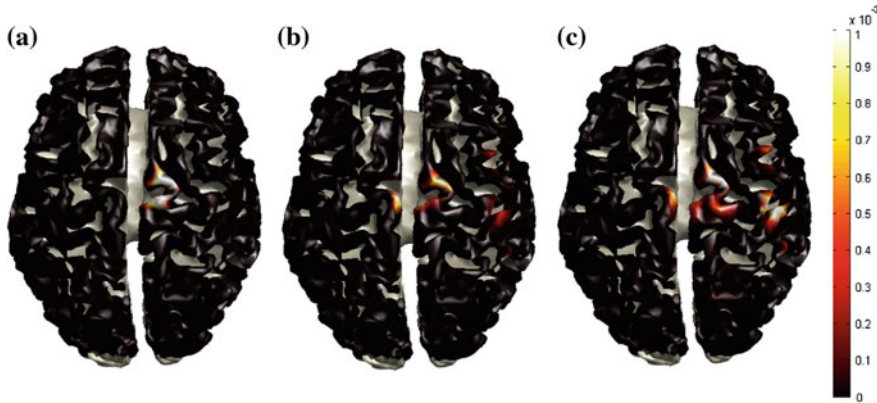


**Fig. 5.12**  $l_1$  GMNE localization results of a single time sample of the simulated EEG signal with various levels of noise. The used time sample of  $M$  corresponds to the maximum magnitude of **d**. Figure contain power topographies for three noise conditions estimated for the same regularization parameter  $\lambda$  and plotted on the same scale. **a** Noiseless case. **b**  $\frac{\|\varepsilon\|_2}{\|M\|_2} = 0.3$ . **c**  $\frac{\|\varepsilon\|_2}{\|M\|_2} = 0.7$

expected location, which is more preferable than  $l_2$ -norm minimization results from the Fig. 5.10a. However, in the presence of noise  $l_1$  GMNE tends to produce solutions with several disconnected active sources, as shown on Fig. 5.12b, c, which can lead to the ambiguity in results interpretation. This negative effect can be alleviated by introduction of additional constraints to the solution space validated by the parameters of neurological event to be localized.

## 5.5 Chapter Summary

The overall BCI performance is primarily defined by the accuracy of a chosen classifier. Linear classifiers such as LDA or SVM have been shown to be efficient in modern BCI implementations [20]. An interpretation decision is made by the classification algorithm with respect to a decision boundary, obtained from the available training data. This decision boundary separates trials corresponding to different types of mental tasks used as BCI control signals. In order to obtain a clear boundary and thus maximize the classification accuracy, both training data and BCI control signals have to be represented as feature vectors in a way to contrast characteristic features of a given type of EEG data. In the context of BCI design, such a signal representation is referred to as feature extraction.

In practical BCI implementations, a particular type of feature extraction can be defined according to the neurophysiological event being used as a control signal. If the control signal for different classes of data originates from different cortical locations, it is appropriate then to represent EEG data according to its spatial features. For example, this approach can be used in MI-based BCIs, where the BCI

command is defined by the type of imaginary movement being performed by the user. Imagination of movement is accompanied by ERD/ERS localized in the area of motor cortex corresponding to the muscles involved. Execution of different types of MI tasks results in different cortical power topographies, which can be contrasted and separated by the classifier.

EEG signal can be characterized by excellent temporal resolution and poor spatial resolution, due to low SNR, volume conduction effects and large correlation between EEG electrodes. Because of these effects, straight-forward extraction of spatial features from data in EEG space is impractical and cannot result in sufficient classification accuracy. However, it is possible to use prior knowledge about human neurophysiology, anatomy and EEG physics to extrapolate the given EEG data onto a source space of higher dimensionality. Various source localization methods can be utilized to perform such EEG data representation and form feature vectors from the estimated new data set with an improved spatial resolution.

Source localization methods rely on multiple assumptions and conditions used in both the forward and inverse problem solving process. At first, a certain type of head geometry, source model and EEG sensor configuration must be used relating the activation of each individual source to the skin surface potential and thus solve the forward problem. The lead field matrix or gain matrix, which is obtained as a solution of the forward problem, can then be used to relate the surface potentials in the given EEG recording to source magnitudes and hence solve the inverse problem.

The EEG inverse problem is an example of an ill-posed problem. Since the number of sources is usually significantly larger than the number of EEG electrodes, it is necessary to use multiple assumptions and signal properties in order to limit the solution space and obtain a unique solution. Various numerical approaches originating from different disciplines and scientific areas have been applied to the inverse problem, resulting in source localization methods varying in localization accuracy and complexity.

Solution sparsity is used as a fundamental constraint in a family of sparse source localization methods. Minimization of a solution's energy results in images with densely localized active cortical areas. However, localization accuracy of sparse imaging methods is significantly impaired for EEG signals with low SNR. In order to deal with the negative effects of noise, it is necessary to apply appropriate signal preprocessing techniques to EEG data before source reconstruction. In addition to its low computational complexity, the advantage of sparse source localization methods is that the inverse problem can usually be expressed in terms of a linear optimization problem. This gives the flexibility to set multiple anatomically validated constraints to the problem and hence produce more realistic images. Further improvement of sparse imaging approaches is possible through more accurate utilization of EEG signal properties and anatomical priors in both forward and inverse problem solving stage. This prior knowledge represented in a combination of solution constraints can provide better localization precision leading to improved classification accuracy and as a result better BCI reliability and performance.

## References

1. Azar, A., Balas, V., Olariu, T.: Classification of EEG-Based Brain-Computer Interfaces. Advanced Intelligent Computational Technologies and Decision Support Systems, Volume 486 of Studies in Computational Intelligence, pp. 97–106. Springer, New York (2014). doi:[10.1007/978-3-319-00467-9\\_9](https://doi.org/10.1007/978-3-319-00467-9_9)
2. Baillet, S., Mosher, J., Leahy, R.: Electromagnetic brain mapping. *IEEE Signal Process. Mag.* **18**(6), 14–30 (2001)
3. Bishop, C.M.: Pattern Recognition and Machine Learning, Volume 4 of Information Science and Statistics. Springer, Heidelberg (2006)
4. Bolstad, A., Van Veen, B., Nowak, R.: Space-time event sparse penalization for magneto-/ electroencephalography. *NeuroImage* **46**(4), 1066–1081 (2009)
5. Cotter, S., Rao, B., Engan, K.E.K., Kreutz-Delgado, K.: Sparse solutions to linear inverse problems with multiple measurement vectors. *IEEE Trans. Signal Process.* **53**(7), 2477–2488 (2005)
6. de Munck, J.C., Peters, M.J.: A fast method to compute the potential in the multisphere model. *IEEE Trans. Biomed. Eng.* **40**(11), 1166–1174 (1993)
7. Ding, L., He, B.: Sparse source imaging in electroencephalography with accurate field modeling. *Hum. Brain Mapp.* **29**(9), 1053–1067 (2008)
8. Finke, S., Gulrajani, R.M., Gotman, J.: Conventional and reciprocal approaches to the inverse dipole localization problem of electroencephalography. *IEEE Trans. Biomed. Eng.* **50**(6), 657–666 (2003)
9. Grant, M., Boyd, S.: Graph implementations for nonsmooth convex programs. In: Blondel, V., Boyd, S., Kimura, H. (eds.) Recent Advances in Learning and Control, Lecture Notes in Control and Information Sciences, pp. 95–110. Springer, New York (2008)
10. Grant, M., Boyd, S.: CVX: Matlab software for disciplined convex programming, version 2.1 (2014)
11. Grech, R., Cassar, T., Muscat, J., Camilleri, K.P., Fabri, S.G., Zervakis, M., Xanthopoulos, P., Sakkalis, V., Vanrumste, B.: Review on solving the inverse problem in EEG source analysis. *J. Neuroeng. Rehabil.* **5**(25), 1–33 (2008)
12. Hallez, H., Vanrumste, B., Grech, R., Muscat, J., De Clercq, W., Vergult, A., D'Asseler, Y., Camilleri, K.P., Fabri, S.G., Van Huffel, S., Lemahieu, I.: Review on solving the forward problem in EEG source analysis. *J. Neuroeng. Rehabil.* **4**(46), 1–29 (2007)
13. Hämäläinen, M.S., Ilmoniemi, R.J.: Interpreting magnetic fields of the brain: minimum norm estimates. *Med. Biol. Eng. Comput.* **32**(1), 35–42 (1994)
14. Hawes, M., Liu, W.: Robust sparse antenna array design via compressive sensing. In: Proceedings of 18th International Conference on Digital Signal Processing, Fira, pp. 1–5, 1–3 July 2013. doi:[10.1109/ICDSP.2013.6622797](https://doi.org/10.1109/ICDSP.2013.6622797)
15. He, B., Musha, T., Okamoto, Y., Homma, S., Nakajima, Y., Sato, T.: Electric dipole tracing in the brain by means of the boundary element method and its accuracy. *IEEE Trans. Biomed. Eng.* **34**(6), 406–414 (1987)
16. Johnson, C.R.: Computational and numerical methods for bioelectric field problems. *Crit. Rev. Biomed. Eng.* **25**(1), 1–81 (1997)
17. Lemieux, L., McBride, A., Hand, J.W.: Calculation of electrical potentials on the surface of a realistic head model by finite differences. *Phys. Med. Biol.* **41**(7), 1079–1091 (1996)
18. Limpiti, T., Van Veen, B.D., Wakai, R.T.: Cortical patch basis model for spatially extended neural activity. *IEEE Trans. Biomed. Eng.* **53**(9), 1740–1754 (2006)
19. Liu, H., Schimpf, P.H., Dong, G., Gao, X., Yang, F., Gao, S.: Standardized shrinking LORETA-FOCUSS (SSLOFO): a new algorithm for spatio-temporal EEG source reconstruction. *IEEE Trans. Biomed. Eng.* **52**(10), 1681–1691 (2005)
20. Lotte, F., Congedo, M., Léuyer, A., Lamarche, F., Arnaldi, B.: A review of classification algorithms for EEG-based brain-computer interfaces. *J. Neural Eng.* **4**(2), R1–R13 (2007)

21. Mason, S.G., Bashashati, A., Fatourechi, M., Navarro, K.F., Birch, G.E.: A comprehensive survey of brain interface technology designs. *Ann. Biomed. Eng.* **35**(2), 137–169 (2007)
22. Meier, J.D., Aflalo, T.N., Kastner, S., Graziano, M.S.A.: Complex organization of human primary motor cortex: a high-resolution fMRI study. *J. Neurophysiol.* **100**(4), 1800–1812 (2008)
23. Mosher, J.C., Lewis, P.S., Leahy, R.M.: Multiple dipole modeling and localization from spatio-temporal MEG data. *IEEE Trans. Biomed. Eng.* **39**(6), 541–557 (1992)
24. Nicolas-Alonso, L.F., Gomez-Gil, J.: Brain Computer interfaces, a review. *Sensors* **12**(2), 1211–1279 (2012)
25. Olejniczak, P.: Neurophysiologic basis of EEG. *J. Clin. Neurophysiol.* **23**(3), 186–189 (2006)
26. Pascual-marqui, R.D.: Review of methods for solving the EEG inverse problem. *Int. J. Bioelectromag.* **1**(1), 75–86 (1999)
27. Pascual-Marqui, R.D., Michel, C.M., Lehmann, D.: Low resolution electromagnetic tomography: a new method for localizing electrical activity in the brain. *Int. J. Psychophysiol.* **18**(1), 49–65 (1994)
28. Pfurtscheller, G., Brunner, C., Schlogl, A., Lopes da Silva, F.H.: Mu rhythm (de) synchronization and EEG single-trial classification of different motor imagery tasks. *NeuroImage* **31**(1), 153–159 (2006)
29. Pfurtscheller, G., Neuper, C.: Motor imagery and direct brain-computer communication. *Proc. IEEE* **89**(7), 1123–1134 (2001)
30. Salu, Y., Cohen, L.G., Rose, D., Sato, S., Kufta, C., Hallett, M.: An improved method for localizing electric brain dipoles. *IEEE Trans. Biomed. Eng.* **37**(7), 699–705 (1990)
31. Sanei, S., Chambers, J.: *EEG Signal Processing*, vol. 1. Wiley-Blackwell, New York (2007)
32. Schmidt, R.: Multiple emitter location and signal parameter estimation. *IEEE Trans. Antennas Propag.* **34**(3), 276–280 (1986)
33. Van Veen, B.D., van Drongelen, W., Yuchtman, M., Suzuki, A.: Localization of brain electrical activity via linearly constrained minimum variance spatial filtering. *IEEE Trans. Biomed. Eng.* **44**(9), 867–880 (1997)
34. Vanrumste, B., Van Hoey, G., Van de Walle, R., Van Hese, P., D'Have, M., Boon, P., Lemahieu, I.: The realistic versus the spherical head model in EEG dipole source analysis in the presence of noise. In: Proceedings of the 23rd Annual International Conference of the IEEE, Istanbul, vol. 1, pp. 994–997, 25–28 October 2001. doi:[10.1109/IEMBS.2001.1019121](https://doi.org/10.1109/IEMBS.2001.1019121)
35. Wolters, C.H., Kuhn, M., Anwander, A., Reitzinger, S.: A parallel algebraic multigrid solver for finite element method based source localization in the human brain. *Comput. Vis. Sci.* **5**(3), 165–177 (2002)
36. Zhang, Z.: A fast method to compute surface potentials generated by dipoles within multilayer anisotropic spheres. *Phys. Med. Biol.* **40**(3), 335–349 (1995)

# **Chapter 6**

## **Hippocampal Theta-Based Brain Computer Interface**

**L.C. Hoffmann, J.J. Cicchese and S.D. Berry**

**Abstract** Theta rhythm is a 3–12 Hz oscillatory potential observed in the hippocampus during cognitive processes ranging from spatial navigation to learning. The 3–7 Hz range occurs during immobility and depends upon the integrity of cholinergic forebrain systems. The amount of pre-training theta in the rabbit strongly predicts the acquisition rate of classical eyeblink conditioning and impairment of this system substantially slows the rate of learning. Recent experiments utilized a brain-computer interface that makes eyeblink training trials contingent upon the explicit presence or absence of hippocampal theta. Power spectral ratios based on continuous sampling of hippocampal local field potentials were used to ensure that each trial was triggered during the appropriate theta state. One group received training during high theta and the other during very low theta. The results have been consistent and substantial—theta-contingent training produces a two- to four-fold increase in learning speed, accompanied by striking differences in hippocampal, prefrontal and cerebellar electrophysiological patterns. Unlike many interfaces that serve as sensory or motor prostheses, our system appears to engage cognitive resources that accelerate the rate of associative learning. One mechanism for this improvement might be better coordination of the phase relationships in the essential circuitry that includes cerebellum, hippocampus and medial prefrontal cortex, as well as brainstem nuclei necessary for the sensory and motor events during each trial. This chapter reviews such findings and proposes experiments that use this cognitive BCI to clarify the essential roles and coordination of structures in the distributed system that underlies eyeblink conditioning.

---

L.C. Hoffmann (✉) · J.J. Cicchese · S.D. Berry  
Miami University, Oxford, OH, USA  
e-mail: hoffmannlc@austin.utexas.edu

J.J. Cicchese  
e-mail: cicchejj@miamioh.edu

S.D. Berry  
e-mail: berrysd@miamioh.edu

L.C. Hoffmann  
University of Texas at Austin, Austin, TX, USA

**Keywords** Hippocampus • Theta • Power spectra • Eyelid classical conditioning • Rabbit

### List of Abbreviations

BCI	Brain-computer interface
CR	Conditioned response
CS	Conditioned stimulus
HVI	Hemispheric lobule VI
I/E	Inhibitory/excitatory
IPN	Interpositus nucleus
ISI	Inter-stimulus interval
ITI	Inter-trial interval
LFP	Local field potential
LTD	Long-term depression
LTP	Long-term potentiation
T+	Theta-triggered
T-	Non-theta-triggered
UR	Unconditioned response
US	Unconditioned stimulus

## 6.1 Introduction

The findings of a unique line of experiments using a custom-designed brain–computer interface (BCI) have established that hippocampal theta reflects a brain state conducive to rapid acquisition of the stimulus contingency underlying eyeblink conditioning, requiring significantly fewer trials to reach asymptotic criteria of behavioral performance. These behavioral enhancements are consistently accompanied by significantly larger local field potential (LFP) and unit responses in hippocampus, qualitative differences in prefrontal cortex firing patterns, and significant rhythmicity in cerebellar LFPs. As suggested in several theoretical models [17, 19, 47, 49], theta oscillations may provide a basis for wide-ranging coordination of distributed brain systems, with cellular responses (including plasticity) that resonate to inputs related to theta phase. Our data and methods suggest that such theta-based temporal coordination throughout the eyeblink system can be a powerful tool in controlling and analyzing neural mechanisms that underlie the behavioral benefits. Here we review our BCI technology, model system and empirical findings along with the important implications of each to the study of oscillations in neurological systems and to the neurobiological foundations of learning and memory.

LFPs are the low frequency components of the recorded neural activity, which biologically range from delta to high gamma frequency (0.01–200 Hz). It is thought

that LFPs mostly reflect the sum of large numbers of postsynaptic discharges. The overall recorded signal thus represents the potential caused by the sum of all local currents on the surface of the electrode. LFPs are, therefore, thought to represent synaptic input as well as local processing. The LFP can be independent of the individual spiking outputs measured at a particular location [75]. However, there is a well-established systematic relationship between LFPs and units, in that most units in the brain have a preferential phase at which they are most likely to fire. A number of studies have demonstrated the phase coding of activity via LFPs. One of the most well-established examples of this temporal coding is, the firing of hippocampal place cells, which collectively represent a cognitive map of an animal's environment. Place cells show a systematic phase relationship to theta in the LFP [90]. These authors reported that hippocampal place cells encode an animal's location within the place field of a cell through the relation of its firing to the phase of theta frequency LFPs in the area. They report on the phenomenon of phase precession in which the place cell unit activity is modulated at a higher frequency than the frequency of the theta LFP—this results in a phase shift in the unit activity (relative to the LFP) from late to progressively earlier phases as the animal moves through the place field. This phenomenon provides a phase code for location, that is independent of the unit activity rate code (which also codes for location), and can be modulated by other external factors.

Hasselmo [47, 49] has also reported extensively on a unit-phase relation phenomenon in the context of encoding and retrieval processes in the hippocampus. In this case, theta is able to provide itself as a mechanism for temporal control over long-term potentiation (LTP) induction and by inference then, also, the storage and retrieval of info from hippocampus based on the phase relationship of incoming unit activity. Specifically, the peak of CA1 theta (or trough of fissure theta) corresponds to the period during which encoding of new information in the form of unit activity entering the hippocampus from entorhinal cortex takes place. The trough of CA1 theta (or peak of fissure theta) corresponds to the period during which retrieval of information from the hippocampus to entorhinal cortex occurs (corresponds with higher pyramidal cell firing activity). These phases allow for their corresponding function (encoding or retrieval) to occur based largely on the fact that the each is related to a shift on the continuum of stability and malleability of the network. Such empirically supported models have proved LFPs to be important to normal processing functions as opposed to the once held prejudice of LFPs as epiphenomena.

The definitive function of neurobiological oscillations is not completely established and continues to develop. As a whole these oscillatory rhythms are thought to act as timing signals in the brain. The cycle length of a given oscillatory frequency represents a repetitive temporal window in which information encoding and information transfer can take place. Furthermore, organizing and synchronizing activity within and among different brain regions is an important function served by oscillations that allows for very dynamic and transient forms of functional connectivity in the brain. By synchronizing and desynchronizing their activity in relation to each other, brain structures are able to functionally select which inputs arrive and are sent during a time window of maximal effect, and thereby cause a

change in the desired direction in the activity of the receiving group of neurons [40]. This can occur regardless of direct physical connections between regions of interest.

Motor coordination, perception through feature binding, memory and other cognitive functions, and even consciousness are thought to involve neurobiological oscillations and synchronization of neural networks [6, 19, 48, 107, 128]. Disruptions to these normal oscillatory patterns can consequently have devastating effects on these processes [104, 124]. Understanding the roles of oscillations, such as theta, and the processes by which they operate may inform our understanding of cognitive dysfunctions and provide innovative treatment options. Our interface allows us to examine not only normative or optimal function, but also the behavior of neural systems under uncoordinated or dysfunctional conditions. Here we present our systematic approach to the study of oscillatory potentials and their role in learning. Coverage begins with an introduction to the history, advantages and relevant circuitry of our model system, rabbit eyeblink classical conditioning. The development of this cognitive-enhancement BCI with its array of applications within this model system then follows. Such work includes our findings hippocampal theta modulation of prefrontal cortex and cerebellar electrophysiological responses as well as unique age-related learning enhancements. The chapter concludes with discussion of our theta-contingent BCI in the context of relevant research and progress in the field. Our innovative and unique approach has been highly productive over the last few years and takes our research in promising future directions for the neurobiology of cognitive processes.

## 6.2 Related Work

### 6.2.1 Model System: Rabbit Eyeblink Conditioning

Eyeblink classical conditioning has had a long history as a model paradigm for assessing the functions of systems involved in learning and memory, simplified by a highly controlled environment. Evolving from the pioneering ideas of learning theorists such as Pavlov and Estes, the fundamentals of this task involve repeatedly pairing a relatively neutral conditioned stimulus (CS), commonly a tone or light, with a reinforcing unconditioned stimulus (US), such as a corneal airpuff or mild periorbital shock that produces a reflexive, or unconditioned, response (UR). Such repeated CS-US pairings over a number of training trials eventually promotes acquisition of adaptively timed conditioned responses (CRs) that are indicative of learning. The adaptive nature of this behavioral CR is such that the eyelid closes in response to the tone CS and is precisely timed to peak prior to US onset in order to avoid the mildly aversive airpuff or shock stimulus [78, 92, 100]. The discrete and controlled nature of the conditioned and unconditioned stimuli and easily measured behavioral responses underlie the success of eyeblink conditioning as a tractable

model for studying neural mechanisms of learning. This paradigm has also proved well-suited for neurobiological analyses because the use of appropriate unpaired (CS alone) control procedures aid in distinguishing between areas of the brain that are responding to the sensory stimuli or the motor response and those that are selectively activated under conditions of CS-US paired learning.

Dating back to 1899, the first published report by Zwaardemaker and Lans used eyeblink conditioning as a means for studying simple forms of learning in humans. In the early 1960s, Gormezano and colleagues adapted eyeblink conditioning to rabbits, leading to its extensive use for over five decades to study associative learning and sensory-motor processes (for review, see [44]). Rabbits provided an ideal animal to use in conditioning studies because they allow for precise measures of neural processes and invasive treatments to analyze functional mechanisms. Also, rabbits are known to adapt quickly to restraint allowing for accurate measures of behavioral and neural responses with little or no inter-trial movement.

A number of variations of this task have been developed since its inception including delay, trace, discrimination/reversal and backward conditioning among others. Delay and trace eyeblink conditioning (Fig. 6.1) represent the most common forms and are importantly distinguished both by the duration of the inter-stimulus interval (ISI) between CS onset and US onset as well as the neural substrates required in each case [109]. In the simplest form of the task, delay eyeblink conditioning, the consistently preceding CS overlaps and co-terminates with the US leading to ISIs that range between 200 and 700 m in rabbits and a learning framework based on contiguity of stimuli. In contrast, trace eyeblink conditioning

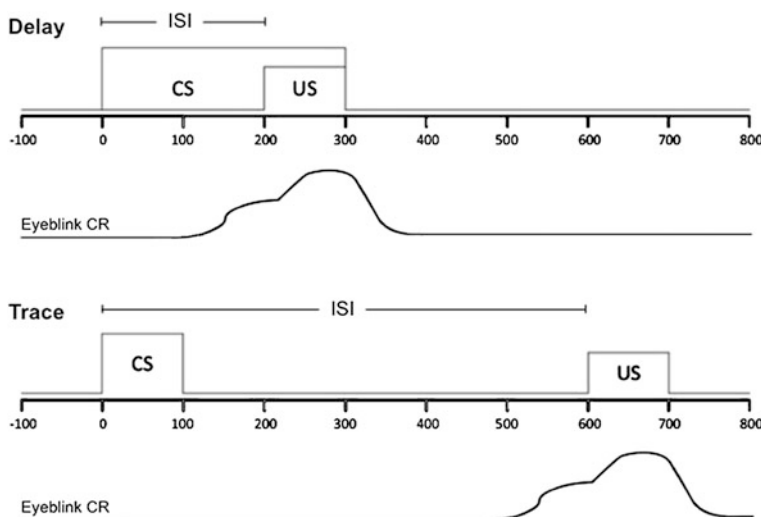


**Fig. 6.1** Delay and trace eyeblink conditioning stimuli with commonly used temporal parameters. Time = 0 ms indicates trial onset. Behavioral learning is measured by the number of CRs emitted by the subject. Adaptive eyeblink closures begin prior to US onset and extend into the US period in order to avoid the aversive stimulus

involves a CS that ends prior to delivery of the US. ISIs generally range from 600–1,000 ms and require a higher form of contingency learning by the subjects. This imposes additional demands on the subject as the CS and US do not co-occur and information about the CS must therefore be retained or “remembered” by the involved neural circuitry over a period of time between the two stimuli.

Due largely to Richard F. Thompson’s systems mapping approach, a convergence of lesion, pharmacological inactivation and neural recording studies has demonstrated that acquisition and retention of all forms of eyeblink conditioning rely on a highly localized brainstem-cerebellar circuit (for review, see [25, 117]). Specifically, it has been shown that lesions of the cerebellum that include the interpositus nucleus (IPN) ipsilateral to the trained eye prevent learning the CR [81]. Furthermore, lesions of this region after training abolish the already acquired CR [28]. The cerebellum has been suggested as the location of long-term storage of the memory trace since lesions and inactivations of the IPN carried out as late as 30 days after learning still abolish the CR [25]. Along with the deep nuclear region, cerebellar cortical areas (including anterior lobe) and dorsal accessory region of inferior olive are also among the essential structures for even the simplest forms of eyeblink conditioning [15, 42, 82, 91, 92, 134, 135]. As learning occurs, cells of the interpositus nucleus are known to increasingly inhibit the inferior olive. Due to its temporal properties, this inhibition serves as an important feedback signal back to cerebellar cortical Purkinje cells indicating prediction error and controlling learning [121]. It is suggested that cerebellar cortex Purkinje cell activity during the CS serves to disinhibit IPN cells, making it possible to elicit a behavioral response and to signal the induction of a long-term potentiation (LTP)-like phenomenon at CS-activated synapses in the IPN [77, 107].

Related to the behavioral CR, an increase in multiple unit activity, representing the number of action potentials of a large group of neurons, is seen in the cerebellum [24, 83]. Depending on the formation of this cerebellar neural model of the CR [28, 103], similar neural models of the CR emerge also in other brain structures, for example in the hippocampus [7]. Thus, both the behavioral and neural CRs seem to depend on an intact cerebellum. The hippocampus and prefrontal cortex are considered non-essential for delay eyeblink conditioning as learning is not prevented by forebrain lesions [68, 79, 85, 93, 99, 114, 120]. However, these regions are thought to play modulatory roles in that they can accelerate or delay behavioral acquisition [10, 97, 112].

Trace eyeblink conditioning appears to require the same brainstem-cerebellar circuit for acquisition and retention as delay eyeblink conditioning [119, 131] but, when the stimulus-free trace period is long enough (500-ms for rabbits) the hippocampus [87, 114, 127] and other forebrain areas such as the medial prefrontal cortex are required as well [68].

Lesion studies in human populations are consistent with what is known about the involved eyeblink circuitry and its basic organization in the rabbit brain [117]. Several studies have found that individuals with cerebellar damage show impaired

eyeblink conditioning largely in the absence of motor deficits that would been expected to interfere with performance of the unconditioned eyeblink responses [35, 113, 122, 132]. Research has also demonstrated in medial temporal lobectomy patients that subjects are able to learn simple delay eyeblink but are impaired with conditioning paradigms that are more complex, such as trace eyeblink [29, 33, 34, 41, 84]. Prefrontal roles observed in animals models have also been generally extended to humans [13, 101].

As a result of extensive research mapping the critical neural substrates, this paradigm is perhaps the most well-understood and extensively used neurobiological model for mammalian associative sensorimotor learning. Such work in animal models of conditioning have demonstrated close behavioral parallels with human eyeblink conditioning, lending support to the hypothesis that the learning shares common neurobiological substrates in humans and other mammals. These factors place rabbit eyeblink conditioning in an ideal position for use as a model system to study the roles of less understood phenomena (such as neurobiological oscillations) with a high level of validity and applicability to human populations.

### ***6.2.2 Theta-Triggering Interface Development and Initial Applications***

Neurobiological oscillations are widely known to act as timing signals in the brain, biasing input selection, facilitating synaptic plasticity, and coordinating activity within and across different regions [17, 21, 47, 73, 74, 107, 128]. Hippocampal cholinergic theta oscillations, which are low frequency, sinusoidal waves ranging from 3 to 7 Hz, serve as an index of hippocampal functional state and are within the bandwidth of oscillations that have been proposed to synchronize large areas or across long distances [17, 21, 45]. The natural ebb and flow of theta is a common feature across species, presumably allowing for its well-documented role in transient and state-specific timing functions [18, 45, 67, 72]. Normally, rabbits show episodes of theta that last for a few seconds, interspersed with irregular activity composed of several frequencies above and below the theta bandwidth. Delta (0.5–2.5 Hz), alpha (8–12 Hz), gamma (40–150 Hz) and ripple (150–200 Hz) have also been reported to occur in the awake animal. Cholinergic theta in the hippocampus relies on the integrity of inputs from medial septal nucleus and the lateral limb of the diagonal band of Broca, as lesions or pharmacological disruptions with anti-cholinergic drugs have been shown to significantly reduce the amount of theta or severely disrupt the regularity and amplitude of these waves [5, 10, 111, 118]; for review see [12].

In 1978, Berry and Thompson [9] unexpectedly discovered that amount of spontaneous hippocampal theta present prior to delay eyeblink conditioning was correlated with a faster learning rate in rabbits. Using 2-min pre-training LFP recordings from hippocampal CA1 region of rabbits prior to delay eyeblink

conditioning, Berry and Thompson applied a zero-crossing analysis to the waveforms and found that the amount of time characterized by a high proportion of 2–8 Hz compared to 8–22 Hz activity correlated negatively with the number of trials required to reach behavioral learning criterion. Thus, more theta yields faster learning (fewer trials). In addition to the correlation between the pre-training theta levels and learning rate, this study also demonstrated a significant correlation between the change in the amount of hippocampal theta activity across training and learning rate, fast learners moving towards a less synchronized state and slow learners towards a more synchronized theta state [11] resulting in more similar amounts of theta activity in all subjects after conditioning. These findings stressed the value of using extracellular LFPs as an index of neural processes, specifically hippocampal state, conducive to synaptic modification for learning. More recently, these original results have been replicated [88] and extended to human preparations [22, 23].

It has since been well documented that treatments disrupting hippocampal theta impair the acquisition of eyeblink conditioning [10, 38, 63, 97, 111, 114, 115]. A number of studies have also demonstrated the benefit of theta to learning and memory by artificially eliciting or enhancing theta to accelerate behavioral learning [36, 53, 65, 71, 123, 129]. One drawback to such lesion and drug studies is that they produce unnatural brain states, due to their permanent modification of the systems involved in theta and their inability to specifically coordinate theta with individual conditioning trials [112]. In a conditioning session, rabbit hippocampal theta typically occurs in epochs varying from two cycles to several seconds in duration, interrupted by periods of non-theta (either large irregular activity or sharp waves). This natural ebb and flow may be an important aspect of theta in cognitive processes [17]. Long-lasting or permanent treatments such as drugs or lesions prevent this natural fluctuation and may induce LFPs that look like theta but interact differently with the endogenous neural substrates. For example, electrical stimulation of medial septum (producing theta field potentials in hippocampus) has been shown to produce aberrant, “non-physiological” activity patterns in theta-related cells in the hippocampus [98]. One solution to this important problem of maximizing theta would be to let natural variation occur but restrict trials to make sure they coincide with endogenous hippocampal theta, as pursued in studies from our lab.

In our attempt to discern the significance of naturally occurring theta within conditioning sessions, we developed a BCI to limit eyeblink training to two naturally occurring extremes of hippocampal theta such that each of two groups can be trained in either the explicit presence (T+) or absence (T-) of on-going theta [102]. Our unique methods included chronic implantation of monopolar stainless steel electrodes with a frontal skull screw as a reference/ground. Electrodes were located in specific cell layers of hippocampus by recording of electrophysiological patterns during the lowering of electrodes in animals under general anesthesia. Custom bioamplifiers provide a gain of 3,500–8,000 for bandwidths of 0–25 Hz for LFPs and 500–5,000 for unit action potentials. During training, commercial software (LabView) samples LFP data at 100 Hz in the 0–25 Hz bandwidth. Fast Fourier-based power spectral analyses calculate a ratio of theta (3.5–8.5 Hz) to nontheta

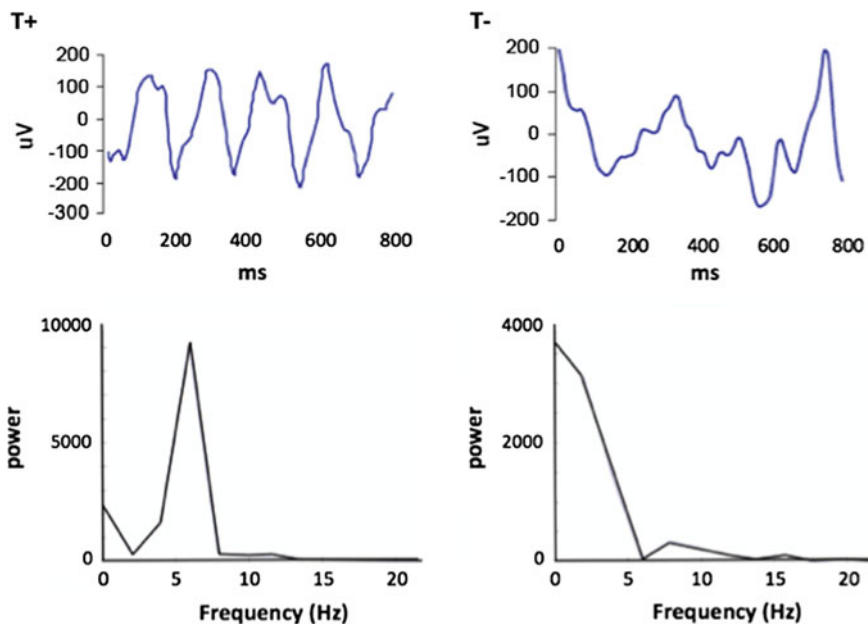


**Fig. 6.2** Examples of hippocampal slow-wave activity that triggered trials in the T+ and T- groups. Notice that slow-wave activity during T+ trials (top left) showed a predominance of activity in the theta band. Conversely, hippocampal activity during T- trials (top right) showed a mixture of frequencies higher and lower than the theta band. Below are representative spectrograms illustrating distributions of frequencies within a 0–22 Hz bandwidth that may trigger a trial in T+ (bottom left) or T- (bottom right). Note that T+ spectrograms have high theta and low delta and alpha, while T-, in this case is characterized by low theta and high delta

(0.5–3.5 Hz plus 8.5–12 Hz) during a 640 ms sample of spontaneous LFP data. This ratio was updated every 160 m with a partially overlapping sample (deleting the first 160 m of the prior sample and adding the most recent 160 m). If the ratio was 1.0 or greater for 3 successive samples (total of 960 ms), a training trial was initiated in the theta positive group (T+). If the ratio was below 0.3 for 3 successive samples, then a trial was initiated for the theta negative (T-) group. Thus, the behavioral training groups had trials under opposite extremes of theta in the spontaneous, pre-trial theta LFP (Fig. 6.2).

Unlike the pre-session baseline assessed in the 1978 study by Berry and Thompson [9], these methods created an on-line amplitude measure to restrict trial presentation dependent on frequency components of the hippocampus extracellular potential. Furthermore, it permitted assessment with trial-by-trial ‘resolution’ of how neurobiological oscillations (theta) influence learning rate. This technology served to hold hippocampal theta constant during training trials in the manner of a brain state “clamp” (analogous to the voltage clamp in basic neurophysiology) that can either maximize or minimize the impact of naturally occurring theta states. Rather than forcefully holding this parameter constant, our approach allows natural

fluctuations while ensuring that training trials and neural recordings are clearly in one theta state for each treatment group.

Using this technology, the initial study by Seager et al. found that delay eyeblink trial presentations during naturally occurring theta led to significant increases in learning rate relative non-theta conditions. Specifically, those animals receiving trials in the explicit presence of theta ( $T+$ ) reduced the number of trials required to reach asymptotic criterion (8 consecutive CRs out of 9 trials) by nearly half of what was required by animals receiving trials in the explicit absence ( $T-$ ) of theta (Fig. 6.3). These results were further interpreted in the context of yoked control groups, in which the inter-trial intervals (ITIs) were matched to  $T+$  or  $T-$  subjects but theta was not specifically controlled. This was important because the number of trials per session and the inter-trial interval are known to affect learning rate [14, 64, 94, 96, 116]. These groups also allowed for some inferences to be made regarding the direction of the behavioral effect, namely that  $T-$  animals performed significantly worse than animals in which theta was unregulated, while  $T+$  animals were not significantly different than either group of yoked controls. This study (and the original theta-learning findings in 1978) related hippocampal function to the rate of delay conditioning, and led to the important conclusion that appropriate activity in the hippocampus, while not being essential for learning, still modulates the neural processes important to conditioning. This is in line with the conclusions of aforementioned pharmacological manipulations supporting the idea that a dysfunctional hippocampus is more detrimental to learning than complete hippocampal removal [1, 4, 10, 97, 111, 118]. Since the hippocampus becomes part of the essential

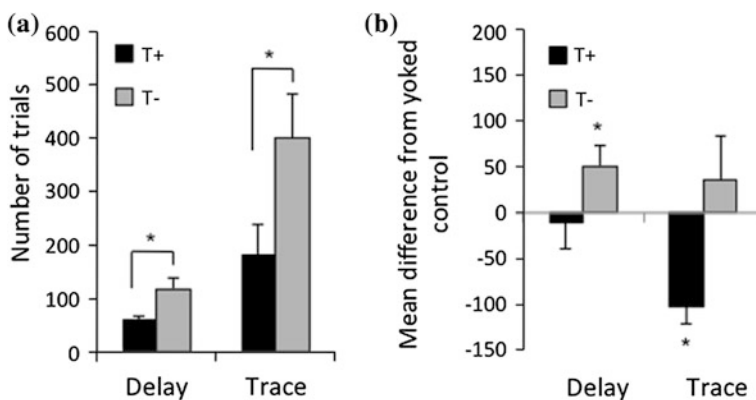


**Fig. 6.3** **a** Average trials to reach asymptotic responding (8/9 CRs) during delay and trace conditioning. **b** Average difference from yoked controls in number of trials to reach asymptote. Hippocampal non-theta contingent trial presentation leads to significant delays in trials to asymptotic responding in delay eyeblink. In contrast, theta-contingent trial presentation significantly accelerates learning in trace eyeblink conditioning. Yoked controls indicate that behavioral effects of theta triggering during delay conditioning are due to detriments in the  $T-$  condition, while effects during trace conditioning are due to  $T+$  enhancements. Asterisks indicate significance at  $\alpha = 0.05$

eyeblink circuitry only when the paradigm is altered so that there is no overlap between CS and US (trace conditioning), subsequent studies used the trace paradigm to examine the role of theta in hippocampus-dependent behavioral learning.

The first study to employ theta-contingent conditioning during trace eyeblink confirmed the originally observed behavioral benefit of pretrial theta-triggering in that T+ animals required significantly fewer trials to reach behavioral criterion than T- animals (Fig. 6.3) [46]. In addition, yoked behavioral controls revealed that the T+ animals learned significantly faster than their uncontrolled-theta counterparts. T- animals learned only marginally slower than their yoked controls. That is, theta-contingent trial presentation not only had a behaviorally beneficial impact, but also had a detrimental impact when theta was low or absent in the hippocampus. Importantly, the effect of theta on hippocampal unit conditioned responses during the tone and trace interval revealed major differences. On day 1, the unit responses in T+ and T- groups were the same, but on days 2 and 3, qualitative differences emerged. Specifically, in both CS and trace intervals the excitatory response increased in T+, whereas units in the T- group were actively inhibited below baseline (pre-CS) activity levels. It is well known that the cell populations in hippocampal area CA1 are dominated by pyramidal (output) neurons that outnumber interneurons by 10:1. This strongly suggests that the output of the hippocampus had failed to display increased excitability to conditioning stimuli when theta was not present and may explain the slower development of CRs in animals lacking theta. This is functionally important from a neurobiological standpoint because our finding requires active inhibitory processes, rather than simply a failure to increase firing rates. Additionally, persistent firing through the trace might be important for the documented role of forebrain structures in bridging the temporal gap between CS and US in early phases of trace eyeblink learning [60, 61, 62, 106, 114, 120, 126].

The modulation of electrophysiological responses in hippocampus during theta-contingent trace conditioning was further demonstrated in subsequent studies showing that hippocampal LFPs and multiple unit excitatory responses displayed much more rhythmicity in the theta band in the T+ group compared to T- [31, 50]. Among such findings, it was discovered that the phase of hippocampal theta rhythm ‘resets’ following evoked potentials to the conditioning stimuli [31], similar to what has been found during working memory tasks in rats [43, 80]. This reset correlates with optimal conditions in LFPs for a learning-related phenomenon known as long-term potentiation and may provide a mechanism for optimally timed neural responses within the hippocampus and extra-hippocampal structures. Darling et al. also examined hippocampal multiple unit responding during the trace period. Similar to Griffin et al. [46], unit responses in the T+ condition showed significantly enhanced excitation during the second half of the trace period (Fig. 6.4); however, unlike the Griffin et al. study, this enhancement was seen on day 1 of training, before consistent CR performance had emerged. This enhancement was present through the early (day of 5th CR occurrence) and late (day of 8/9 CRs) learning phases. Additionally, autocorrelations revealed that T+ units fired at ~6.25 Hz rhythm on the day of 5th CR, but T- units fired at no noticeable periodicity. The enhanced excitation and rhythmic firing at theta frequency in T+ animals over

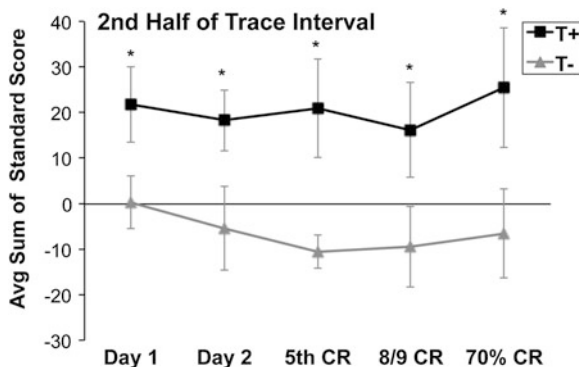


**Fig. 6.4** Hippocampal multiple unit responses during T+ and T- triggered trace eyeblink conditioning show significant differences in average sum of unit standard scores during the second half of the trace interval. Beginning on day 1 of training, standard scores are significantly higher in T+ than in T- responses ( $p < 0.05$ ). This significant difference continues from early learning (day 1, day 2 and day of 5th CR) through late learning criteria (day of 8/9 CRs and 70 % CRs)

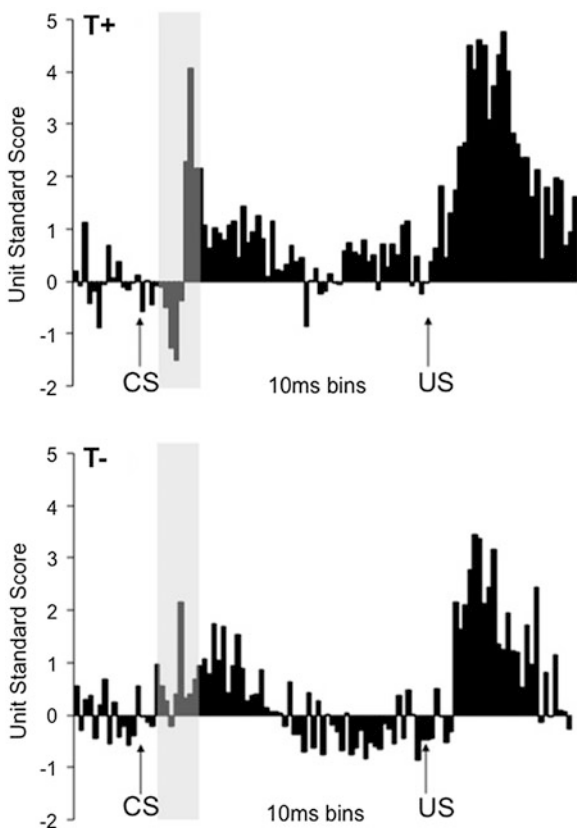
T- supports the notion of increased hippocampal plasticity early in training due to pre-trial theta state.

### 6.2.3 Extra-Hippocampal Modulation Using Our BCI

Recent theories and models of hippocampus have added increased emphasis to the possible coordinating role of oscillatory field potentials, such as theta, during learning and other cognitive processes. Because modulatory structures, such as the hippocampus, become necessary during trace eyeblink conditioning, it is important to explore the learning-related electrophysiology of extra-hippocampal structures that are also necessary for the task. Following this simplified logic, our laboratory has recently extended our studies of hippocampal theta-triggering to structures outside the hippocampus, specifically two areas known to play key roles in trace eyeblink conditioning: the cerebellum and the prefrontal cortex/caudal region of anterior cingulate cortex.

In the first of these experiments, we assessed the role of hippocampal pretrial theta state on neural response patterns in the prefrontal cortex/caudal anterior cingulate cortex. Using the theta-triggering paradigm during trace eyeblink conditioning, recordings revealed a hippocampal-dependent enhancement of multiple unit firing in prefrontal cortex [31]. In a previous study by Weible et al. [125], cell populations in the prefrontal cortex/caudal anterior cingulate had been found to display an inhibitory/excitatory (I/E) sequence following tone onset followed by neural excitation continuing through the trace and US periods. A different population of cells lacked the I/E sequence, gave little to no response during the trace interval and responded significantly less to the US. The authors interpreted the I/E

**Fig. 6.5** Average standard scores for medial prefrontal cortex multiple unit responses during hippocampal theta-contingent trace eyblink conditioning. As illustrated in the gray highlighted bar following CS onset, T+ animals (top) had a significantly higher CS-evoked I/E difference scores compared to T- animals (bottom;  $p < 0.05$ ). T+ prefrontal units also showed significantly greater excitation during the trace ( $p < 0.05$ ) and US periods ( $p < 0.05$ ) relative to the T- units



sequence as a signal-to-noise enhancement that increased the salience of the tone. The trace/US excitation was greatest in cells with large I/E sequences and the US excitation was greatest in cells that also exhibited larger CS excitation. Darling et al. [31] not only replicated the findings of two distinct populations of cells based on I/E responses but demonstrated that these response profiles were specific to hippocampal theta state. Specifically, our study discovered that the I/E sequence in prefrontal cortex was exclusive to the T+ condition and that there was greater trace/US excitation in animals with hippocampal theta (Fig. 6.5). Interestingly, the other Weible et al. mPFC response profile was seen in our T- group, thus likely occurring during hippocampal non-theta.

A possible interpretation of this finding was that the two response profiles or cell populations reported for prefrontal cortex were modulated by the presence or absence of theta in the hippocampus. An interesting finding, within which the interpretation of these results may be contextualized, was that prefrontal LFPs did not oscillate at theta frequency while hippocampal LFPs did. Given this detail, the unit response findings suggested that differences in pretrial theta state might be encoded or otherwise reflected in the response patterns of hippocampal output

neurons that project to target structures during a hippocampus-dependent task. Thus, even if the theta LFP itself may remain effectively within the hippocampus, information about theta state and phase could be transmitted to target structures such as lateral septum, prefrontal cortex, entorhinal cortex, brainstem, and cerebellum.

The findings of the prefrontal response modulation study suggested that hippocampal theta may enhance neural firing in distant areas that can facilitate the development and maintenance of CRs. If true of prefrontal cortex, it is likely that such enhancements would be found in other extra-hippocampal structures more intimately involved in eyeblink conditioning, such as the circuit closest to the motor output in cerebellum. To examine whether and how hippocampal theta oscillations modulated extra-hippocampal activity in the cerebellum, Hoffmann and Berry [50] recorded LFPs in hippocampal CA1, cerebellar interpositus nucleus (IPN) and cerebellar cortical lobule HVI in rabbits during hippocampal theta-contingent trace eyeblink conditioning. The resulting data demonstrated that hippocampal theta state could be used to synchronize hippocampal and cerebellar LFPs into a rhythmic theta oscillation that accompanies a striking cognitive benefit over non-theta conditioning. This effect reached four-fold increases for T+ relative to T- conditioning groups in early learning phases when animals were just beginning to emit CRs. The substantial increase in acquisition rate in the T+ condition was accompanied by a number of functionally relevant electrophysiological response profiles including: (1) Amplitude modulation of cerebellar evoked responses to conditioning stimuli; (2) Cerebellar theta oscillations that were time-locked to the sensory stimuli, i.e. strong rhythmic theta occurred immediately after CS onset in both cerebellar regions, continuing throughout the trace and US periods; (3) Precise (180 degree) phase synchronization of hippocampus and cerebellar IPN and HVI LFPs at 6–7 Hz theta frequency; (4) Precise (0 degree) phase synchronization at theta frequency between cerebellar nuclear (IPN) and cortical (HVI) LFPs. These findings were exclusive to the T+ triggered condition (Fig. 6.6).

Prior to this experiment, inactivation studies had suggested that the hippocampus and cerebellum interact in important ways during the task but it was unclear how this was accomplished since no direct pathways exist between the two structures. Our theta-contingent training technology allowed hippocampal theta to be used as a quasi-independent variable to further address this question. The resultant findings of T+ rhythmic coordination of hippocampal and cerebellar LFPs suggested hippocampal theta as a means for establishing a flexible long-distance functional connection between these two structures and as a means for regulating the functional properties of the anatomically distributed system for trace eyeblink conditioning. The precise phase locking over the substantial distance between hippocampus and cerebellum would be surprising if one region were directly driving the other and, instead, suggests a common pacemaker for both structures. If so, it is likely not a unitary pacemaker, as we have observed theta presence in either hippocampus or cerebellum while it is not present in the other. Regardless of the source(s) of this hippocampal–cerebellar synchrony, it can be concluded that a brain state indexed by hippocampal theta (and here exploited by our brain–computer interface) is reliable in predicting rhythmic versus non-rhythmic modes of information processing in the cerebellum.

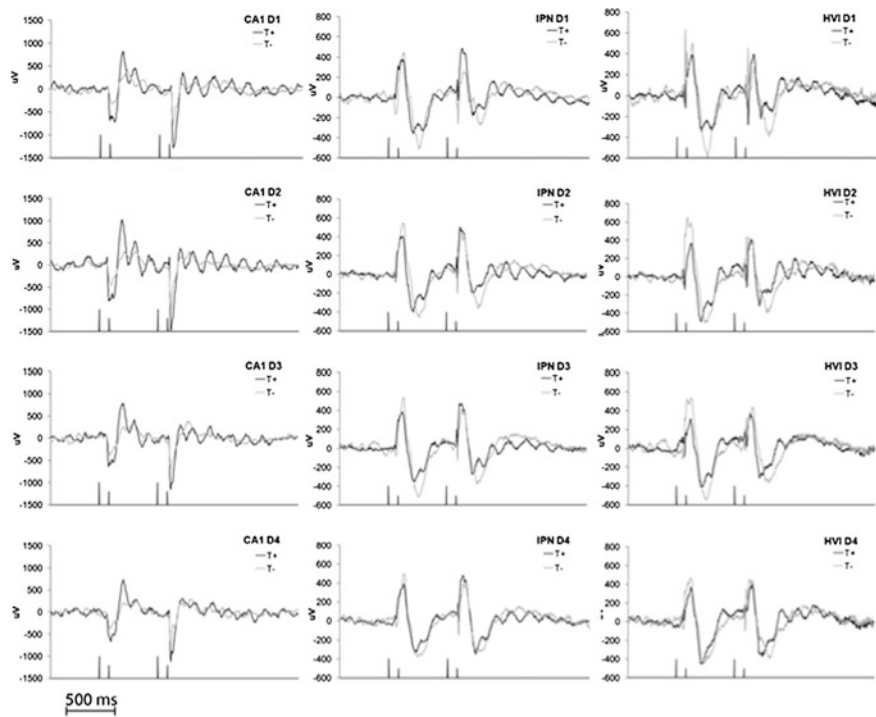


**Fig. 6.6** Average LFPs across the first four days of theta-contingent trace eyeblink conditioning. T+ LFPs display consistent short latency onset of robust and rhythmic theta oscillations that are precisely time-locked to the CS and US occurrences. T- LFPs are notably less organized at theta frequency across trials and days for hippocampus and cerebellum

Taken as a whole, our extra-hippocampal findings suggest that theta may serve to enhance learning through organizing the precise timing needed for learning both within and between structures essential to trace eyeblink conditioning.

#### 6.2.4 Amelioration of Age-Related Learning Deficits

Asaka et al. [4] replicated the beneficial behavioral effects of theta-contingent training and extended this interface-mediated enhancement to include trace eyeblink conditioning in aging rabbits. Young (~5 months) and older (~28 months) rabbits were trained during theta (T+) or as yoked controls with identical ITIs irrespective of hippocampal theta state. Both young and old animals' early learning rates (end of learning phase 1, which is commonly represented by the number of trials to reach 10th CRs) were facilitated by theta. Interestingly, the benefit of theta persisted in older rabbits throughout training, while asymptotic performance was not enhanced by theta in young animals (Fig. 6.7). This suggests that the aging

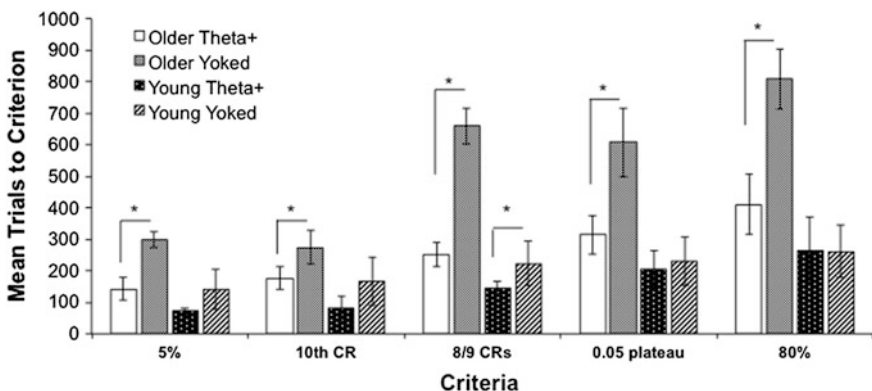


**Fig. 6.7** Average number of training trials required by each group to attain classic behavioral learning criteria and those criteria defined by the state-space model. Older T+ animals reached all learning criteria significantly faster than their yoked controls, while young T+ animals were not significantly different from their yoked counterparts on any criteria except 8/9 CRs. When behavioral criteria were clustered according to early and later learning phases (5 % and 10th CR versus 8/9 CRs, 0.05 plateau and 80 %), there was a highly significant interaction of age, treatment, and phase,  $p < 0.05$ . Post hoc comparisons substantiated a significant benefit of theta triggering in the early phase for both young and older groups ( $p < 0.05$  for each). In contrast, the later learning phase showed no theta-triggering benefit in young animals ( $p > 0.05$ ), but a continuing benefit in the older group ( $p < 0.05$ )

deficit in eyeblink conditioning may include theta-related performance impairments as well as a delay in acquiring the initial association between CS and US. In addition, we compared traditional early and asymptotic learning criteria to learning trajectories characterized by a state-of-the-art state-space learning model developed by Emery Brown's lab at MIT [110]. Using a Bernoulli probability model to describe our observed binary-valued behavioral responses (CR or UR) and a Gaussian state equation (random walk model) that served to describe the unobservable learning state process, this state-space model defines learning curves for individual animals as the probability of a correct response as a function of the learning state process. Briefly, a 5 % baseline criterion, which estimated the end of learning phase 1, and a 0.05 plateau criterion estimating the onset of asymptotic responding were identified for each animal. The baseline criterion was defined as the training trial on which the ideal observer was 95 % certain that the animal would emit CRs at a rate above chance (5 %) for the rest of the experiment. The 0.05 plateau criterion was defined as the point, after passing the 5 % criterion, at which the change in the probability of a correct response was less than 5 % for 10 consecutive trials. Using these criteria, the model was able to identify for each animal the precise "learning trial"—the first trial on which CR performance will be, with reasonable certainty, better than chance for the rest of training. Their indices replicated the substantial behavioral effects of theta-contingent training and provided theoretical and mathematical support for the use of such traditional learning criteria as trial of 10th CR, trials to 8/9 CRs, or 80 % CRs.

It should be emphasized that older animals given trials when exhibiting theta learned as rapidly as young yoked controls, thus ameliorating age-related learning impairment without pharmacological intervention to, for example, enhance cholinergic function. While theta depends on cholinergic activity, this study suggests that even an aging, cholinergically-impaired brain may exhibit useful indices (e.g. theta) of relatively normal system function during which learning may be unimpaired.

### 6.2.5 Current Directions

Darling [32] implemented the use of tetrode technology into our BCI studies in order to extend our theta-modulated electrophysiological findings to hippocampal responses at the single unit level. The procedure utilized specially manufactured micro-drive assemblies consisting of six micro-drives. Each micro-drive, containing one tetrode, could be independently lowered. Specialized signal processing software compared the extracted data streams from each wire of the tetrode to separate the waveforms into single neuron responses [57]. The sorted neurons were then classified as pyramidal cells or interneurons based on their firing properties, including waveform duration and spike rate [39]. Excitatory pyramidal cell responses were mostly related to associative training, being most prevalent in T+ paired animals; pyramidal cells in the T- groups demonstrated suppression below baseline during trials. The response of interneurons to the conditioning stimuli were generally most dependent on hippocampal state, showing excitatory responses in T+ groups and suppression in T- for both trained and unpaired groups. As a whole, the population of interneurons showed a double dissociation in that those that had excitatory responses to the conditioning stimuli were more prevalent in T+ animals while those that showed suppression were more common in T- animals.

This work has recently been extended to characterize the response profiles of individual sub-classes of interneurons recorded within hippocampal region CA1 [26]. Using a classification system developed by Klausberger and Somogyi [66] that defines interneuron classes based on systematic firing probabilities relative to on-going theta and non-theta ( $\sim 100\text{--}200$  Hz ripple) activity, this study identified responses of interneuron sub-types under theta and non-theta contingent trace eyeblink conditioning. Our findings are consistent with a model [30] in which the patterns of interneuron firing that are consistent with rapid acquisition tend to occur during theta, whereas firing patterns favorable to memory retrieval appear to disrupt early stages of learning in our T- group. We are now characterizing the response profiles of several classes of GABA interneurons under theta and non-theta conditions to assess the predictions of this model for hippocampal information processing during eyeblink conditioning.

In an important extension of our research, a recent study by Hoffmann and Berry [51, 52] has also investigated the role of cerebellar theta during trace eyeblink conditioning, using our interface to trigger training trials based on pretrial theta versus non-theta within the cerebellum. Chronic LFP recordings in hippocampal

CA1, cerebellar interpositus nucleus and cortical lobule HVI were used to assess the neural and behavioral impact of theta-based oscillatory dynamics in hippocampus and cerebellum during cerebellar theta-contingent trace eyeblink conditioning. We also directly compared them to those previously reported for hippocampal theta-contingent trace conditioning. Training trials were administered by our BCI either in the explicit presence or absence of pretrial cerebellar theta or hippocampal theta. This study showed that there were clear distinctions, depending on the stage of learning, between hippocampal and cerebellar theta triggering, which strongly suggests different processing functions of these two essential structures. Cerebellar non-theta induced slow learning may be relevant to our understanding of cognitive disorders and learning disabilities, often thought to result from impaired coordination of distributed brain systems.

### 6.3 Discussion

As discussed above, a major strength of this interface is that it allows the natural ebb and flow of theta in the awake, behaving rabbit. Studies that use drugs or lesions to control theta typically report unrelieved bouts of either theta or non-theta, rarely modeling the natural ebb and flow in the intact animal. Thus, our interface technology comes much closer to the natural brain state that accompanies hippocampal theta. By waiting for the naturally occurring theta activity, we created a trial-by-trial control of theta to produce a “brain state-clamp” that showed substantial state-dependent variations of learning rates during delay and trace eyeblink conditioning (for review, see [8]).

As detailed below, we are pursuing a basic understanding of how theta can optimize plasticity in the hippocampus and cerebellum, how it can select or enable qualitatively different processing patterns in prefrontal cortex and how beneficial coordination of the entire eyeblink conditioning distributed system can occur under theta conditions. One additional perspective that we have not emphasized is the use of non-theta conditions as models for brain dysfunction. While the specific details of neurological disorders differ markedly from syndrome to syndrome, our interface allows us to examine cognitive and behavioral processes under suboptimal conditions or outright dysfunction. Again, this can be produced in the absence of drugs or brain lesions that produce chronic and irreversible conditions and undesirable side effects. This can be especially useful in modeling neurological disorders that alternate with periods of remission or relatively normal function. One especially clear example of this would be the fact that, during delay eyeblink, the T- condition produces the major behavioral impact relative to yoked controls. On the other hand, in trace conditioning, the major behavioral benefit appears to occur in the T+ group, with T- being similar to the yoked controls. Since these tasks differ in their dependence upon hippocampal integrity (trace eyeblink requires the hippocampus and prefrontal cortex), our interface can be used to explore both improvement and impairment of cognitive processes in an undamaged and undrugged brain.

In the following sections, we discuss our findings as they fit into the larger perspective of neural plasticity mechanisms and into the mapping of essential and modulatory circuitry for the eyeblink learning model.

### 6.3.1 Models of Learning: Theta and Plasticity

The working hypothesis for our theta-triggering experiments is that this “state clamp” technique engages theta to coordinate trials with the timing of neural networks between the hippocampus and related structures that are important for acquiring the association between conditioning stimuli. This notion is very similar to parts of the model proposed by Hasselmo et al. [49], in which cue-related signals arriving in hippocampus (especially CA3) from association cortex, that occur in precise temporal relationship to peaks and troughs of theta, are thereby selected for strengthening or weakening (plasticity) or readout from memory (stability), respectively. This general idea of the role of theta is becoming more widely accepted as new data and models are generated [17, 20, 56, 73, 130]. In one empirical demonstration supporting this prominent model, Hyman et al. [54] found LTP induction was greatest during hippocampal theta peaks in contrast with long-term depression (LTD) induction being greatest during theta troughs. Furthermore, Hasselmo and colleagues have shown decreased stimulus-evoked potentials when stimuli are delivered at the peak of hippocampal fissure theta. They have interpreted such results as ideal phases of hippocampal theta for encoding and retrieval, respectively [133]. It is necessary to point out that hippocampal theta’s phase is dependent upon electrode placement since the potential recorded at the soma/basal dendrites of dorsal hippocampal CA1 pyramidal neurons is antiphasic with more ventral apical dendrite sites toward the hippocampal fissure [17]. The large majority of theta research in rats targets fissure theta due to the abundance of spatial sensory afferents from entorhinal cortex.

The encoding and retrieval phases are conducive to their separate functions due to differences in input strengths to CA1 from the entorhinal cortex and CA3. In the encoding phase, CA3 provides weak input to the general population of CA1 pyramidal cells, while entorhinal cortex provides strong input to select CA1 pyramids. Cells receiving entorhinal input show LTP at the CA3 to CA1 synapse. This strengthening is important for the retrieval phase where entorhinal cortex input is weak, but CA3 input is strong, allowing for CA1 cells that were previously strengthened to fire [49]. This model has been extended to incorporate functional roles for multiple sub-classes of hippocampal interneurons [30, 69].

Within this framework we can identify a potential mechanism for the behavioral benefits seen with theta-contingent training. As previously discussed, a phase reset in the hippocampal theta rhythm is seen following presentation of the CS [31]. The reset is more coherent in the T+ condition, allowing for the US to arrive consistently at the peak of pyramidal cell layer hippocampal theta (corresponding to a trough of fissure theta in Cutsuridis’ model). In terms of the model, the US is

arriving when the hippocampus is in the encoding phase of theta, allowing the CS-US association to develop. Similarly, because the phase reset ensures that the encoding phase of theta is present when the US arrives, it facilitates the retrieval phase  $\sim 200$  m preceding the airpuff when adaptive CRs should occur. Our hippocampal multiple-unit findings also fit into this context, in that the enhanced excitation seen late in the trace period likely reflects firing of pyramidal cells [31, 46]. This would indicate that there is increased output from CA1 to the entorhinal cortex during the retrieval phase of theta, as would be expected by the model. Importantly, in addition to using the theta model of plasticity to interpret our findings, theta-contingent training can be used to provide behavioral support for the model. Darling's (2011) findings have shown that behaviorally relevant phenomena coincide with the model's proposed phases of encoding (US arrival) and retrieval (time of adaptive CRs) during T+, but not T-, conditioning. This demonstration, along with the learning benefits seen in T+ animals, provides support for a possible behavioral role of these trial phases in an established model of associative learning.

### ***6.3.2 Theta-Modulated Interactions in the Eyeblink Circuitry***

Much attention has focused on the coordination of neural activity between the medial prefrontal cortex and the hippocampus during learning and memory tasks [37, 47, 126] for review). Although there are no direct projections between the medial prefrontal cortex and the hippocampus in the rabbit, there are numerous ipsilateral and contralateral connections between sub-regions and reciprocal thalamic projections [3, 16]. Some studies evidence the modulatory influence of prefrontal regions on hippocampal activity. For instance, Kyd and Bilkey [70] showed that lesions modified the response properties of rat hippocampal place cells during spatial navigation. Furthermore, hippocampal learning-related unit activity and hippocampal theta oscillations are known to modulate prefrontal activity [31, 55, 58, 86, 105]. Hyman et al. [47] have demonstrated that single unit activity in medial prefrontal cortex entrains to hippocampal theta during foraging and may reflect goal directed behavior. Siapas et al. [105] have found that the firing of medial prefrontal cortex single unit activity displayed phase locking to hippocampal theta, with prefrontal neurons firing at a preferred phase of hippocampal theta even in the absence of local cortical theta oscillations. This latter finding suggested that the timing of prefrontal unit activity with respect to hippocampal theta oscillations might be important for coordinating the plastic changes that underlie learning and memory formation within the hippocampus and the prefrontal cortex. This coordination between the prefrontal and the hippocampus, along with other cortical and subcortical structures, could facilitate conditioning by affecting levels of excitation and unit activation in the essential circuitry during eyeblink conditioning. One such scenario involves the role of prefrontal transmission of learning-related activity to the cerebellar eyeblink circuitry. Persistent prefrontal CS-related input is transmitted to cerebellum via pontine nucleus mossy and parallel fibers during trace

eyeblink learning so that CS information can overlap with temporally-separated US information. This prefrontal/pontine-mediated CS-US convergence is critical for trace eyeblink [60, 61, 62, 106]. Our 2011 report of differences in medial prefrontal I/E sequence during CS-elicited excitation supports the role of the prefrontal cortex in increasing the salience of the tone by increasing the signal-to-noise ratio [125] based on hippocampal theta-triggering condition. Because the T+ animals had a significantly higher I/E difference score, it is strongly suggested that hippocampal theta state provides a mechanism by which medial prefrontal neurons might enhance this phenomenon. This amplified CS input to cerebellum may underlie or facilitate the learning benefits of theta triggering by strengthening the subsequent CS-US association within the essential motor circuitry. The negative I/E difference score for T- animals late in training indicates an opposite effect, and suggests an inverse or reduction of the signal-to-noise ratio seen in T+ animals. This could hinder the T- group's ability to develop a strong CS-US association and delay the development of optimally timed behavioral responses.

In addition to this possible pathway by which our hippocampal theta-contingent training enhancements may exert their effects on eyeblink circuitry, transient functional connections between forebrain and cerebellum appear to be modulated by theta-triggering. An important indicator of the coordination among structures in the eyeblink system is the zero-lag cross-correlations observed between hippocampus and cerebellum at ~6–7 Hz. If one structure were driving the other's activity, we would predict a temporal lag between their responses that should correspond to the conduction velocity of the interconnecting pathways. The fact that there is no such lag suggests a common influence to both structures that is paced at theta frequency. The origins and pacemakers of theta within the hippocampus are well documented, however, ambiguity is introduced when theta coordination between hippocampus and cerebellum becomes essential because it is not well established which extra-cerebellar inputs and internal mechanisms might mediate such a relationship. It is clear that theta is a strong organizing principle in the cerebellum itself. Golgi and granule cells of the cerebellar cortex have been widely reported to have intrinsic resonant properties at theta frequency. However, currently there are still a number of input structures that could serve as candidates for any potential pacing or entrainment function during hippocampo-cerebellar synchronization, specifically. Some of the most likely candidates, based on anatomical connectivity and relevance to theta pacing include pontine nuclei as a component of the reticular activating system and the supramammillary and medial mammillary nuclei of the hypothalamus. Though the inferior olive is likely involved as a theta-supporting input structure for cerebellum [76], the lack of a clear pathway from inferior olive to the telencephalon makes it a less than likely candidate for bidirectional forebrain-cerebellum synchronization.

To further investigate hippocampal-cerebellar coordination, we have recently started collecting single-unit data in IPN during hippocampal theta-triggered conditioning. Since IPN cell firing is essential to performance of the conditioned behavioral response, it is important to understand how our theta-triggering affects these cells. Preliminary analyses have shown important differences between theta

conditions and across days of training. Specifically, IPN cells in the T+ condition show greater responses in the trace period on early trials with no CR than T- animals. This suggests that hippocampal theta enhances IPN unit responses before learning is established—perhaps accounting for more rapid cerebellar plasticity. Additionally, T- cells on the fourth day of training have greater excitation in the trace period than on the first day. Since the behavior of the T- group is improving by this day of training, it is not surprising that the T- suppression of IPN responding is beginning to disappear.

### ***6.3.3 Future Directions and Applications***

Our interface has revealed many theta-related effects in LFPs, multiple-units, and single-units in area CA1 of the hippocampus. However, there are other important subfields of the hippocampus that must be studied at the single-unit level to fully understand the role of theta in learning. Areas CA1, CA3, and the Dentate Gyrus form the trisynaptic loop of the hippocampus. Although the anatomical connectivity of these different subfields has been thoroughly documented, the learning-related functional differences between these subfields are not yet clear. Current work in our lab has begun recording from CA3 during eyeblink training contingent on theta-triggering in CA1. While data collection is ongoing, preliminary data have shown differences in pyramidal cell firing between areas CA1 and CA3, with CA3 cells showing increased firing rates in the T- condition compared to the T+ condition [27]. This is the opposite pattern shown by Darling [32] in CA1 pyramidal cells and could be related to differences in connectivity between the two areas. CA3 pyramidal cells have a higher number of recurrent collaterals than are seen in CA1. These collaterals would allow for excitation to spread through CA3, and in turn lead to imprecise signals being sent to CA1.

A group in Finland has supported a number of our findings using retrospective correlation analyses showing hippocampal theta related to rapid eyeblink conditioning both before and during training. They also reported enhanced hippocampus-cerebellum coordination under conditions of strong hippocampal theta. More recently, Nokia et al. [89] showed effects of hippocampal sharp wave ripple-contingent trace eyeblink during acquisition and extinction. These researchers reported that triggering on naturally-occurring ripple activity significantly increased acquisition rates but impaired extinction rates. However, the effects of triggering on hippocampal ripple may in fact be an indirect confirmation of our theta findings. This alternative interpretation centers around the fact that their methods produced a 200 m time lag between the pretrial ripple event that triggered a given training trial and initiation of the actual trial itself (conditioned stimulus onset). Given the very brief nature of ripple events (approximately 50 m; [2, 108], it is unclear what exact brain state was present at trial (CS) onset and whether it was consistent across all training trials. Fluctuation between theta and sharp wave ripple states characterizes the LFPs during awake immobility in the rabbit eyeblink preparation.

The increasing probability of theta epochs in rabbit hippocampal LFPs when a ripple event has ended raises the possibility that their trials could have been associated with sufficiently high values of hippocampal theta to benefit learning in one of the groups. In fact, Fig. 6.4c in their paper shows rapidly rising (>99th percentile) theta phase locking values just before CS onset in the fast learning ripple group. Thus, the period immediately before their trials replicated a major feature of our theta-triggering conditions and the within-trial stimulus evoked LFP events also matched our findings of increased theta after CS onset, during the trace interval and after the unconditioned stimulus. Unfortunately, the authors did not test for pre-CS group differences in the theta measures, despite a well-established literature that would suggest it as an important alternative to be ruled out before reaching strong conclusions about the role of hippocampal ripple oscillations. For comparison of the two studies, it is important to note that, given that our criterion theta sample lasts for 960 m, our trials would not have had ripple events 200 m before the CS onset as theirs did. Thus, even such brief periods of pretrial theta as theirs may be sufficient for rapid learning.

Generalizing across species, studies have shown theta oscillations to be implicated in human cognitive processing, with beneficial effects in acquisition, retrieval, verbal working memory tasks and spatial navigation [22, 23, 59, 72, 95]. If tasks could be acquired and performed during periods of maximal theta, cognitive processes might be enhanced. This raises the possibility that our methods might be used to ameliorate human cognitive deficits, such as age-related memory impairment, which we have already demonstrated using eyeblink conditioning in animals [4]. Our interface provides a useful means of observing and manipulating clearly different functional brain states, without lesions or drugs, that could be adapted in the future to other species, brain structures, or oscillatory frequencies. It will be necessary for human research to find noninvasive measures that reliably indicate the presence or absence of theta activity deep in the medial temporal lobe. Many of the findings in humans are from neurology patient populations with underlying pathology that justifies juxtadural or depth recordings. If we can develop reliable markers in the noninvasive scalp-recorded EEG signal, then studies in healthy volunteers would greatly accelerate our understanding. There are studies of human and animal cortical theta, but in the mouse, rat and rabbit, cortical theta does not accompany hippocampal theta or is, quite likely, volume conducted from the hippocampus into the closely overlying cortex. Basic studies must be performed to resolve these technical issues before advancing our understanding of theta in humans and as a remedy for neurological disorders.

## 6.4 Conclusion

In this chapter, we have summarized our recent findings of a substantial behavioral improvement of eyeblink conditioning contingent upon the presence of theta oscillations in hippocampus and cerebellum. A brain computer interface based on

continuous power spectral analysis of theta and non-theta frequency oscillatory potentials was used to ensure the occurrence of theta at the beginning of each trial, while allowing the natural fluctuations to occur in the inter-trial interval. We have argued that this is a more typical brain state for the rabbit than would occur after drugs or lesions that completely prevent or produce theta for long periods of time. Our results have demonstrated that theta is related to distinct patterns of unit and LFP response in the hippocampus, prefrontal cortex and cerebellum, thus characterizing relatively optimal or suboptimal information processing in a number of brain structures thought to be essential for eyeblink conditioning in mammals, including humans. Future studies are planned in which the optimal conditions can be evaluated in additional structures and non-optimal conditions can be used to model impairments of learning and memory that might occur in a variety of psychiatric or developmental disorders.

## References

1. Allen, M.T., Padilla, Y., Gluck, M.A.: Ibotenic acid lesions of the medial septum retard delay eyeblink conditioning in rabbits (*Oryctolagus cuniculus*). *Behav. Neurosci.* **116**(4), 733–738 (2002)
2. Andersen, P., Morris, R., Amaral, D., Bliss, T., O’Keefe, J.: *The Hippocampus Book*. Oxford University Press, New York (2007)
3. Arikuni, T., Ban, T.: Subcortical afferents to the prefrontal cortex in rabbits. *Exp. Brain Res.* **32**(1), 69–75 (1978)
4. Asaka, Y., Mauldin, K.N., Griffin, A.L., Seager, M.A., Shurell, E., Berry, S.D.: Nonpharmacological amelioration of age-related learning deficits: the impact of hippocampal theta-triggered training. *Proc. Natl. Acad. Sci. USA* **102**(37), 13284–13288 (2005)
5. Asaka, Y., Griffin, A.L., Berry, S.D.: Reversible septal inactivation disrupts hippocampal slow-wave and unit activity and impairs trace conditioning in rabbits (*Oryctolagus cuniculus*). *Behav. Neurosci.* **116**, 434–442 (2002)
6. Azar, A.T., Balas, V.E., Olariu, T.: Classification Of EEG-based brain-computer interfaces, advanced intelligent computational technologies and decision support systems. *Stud Comput Intell* **486**, 97–106 (2014)
7. Berger, T.W., Alger, B., Thompson, R.F.: Neuronal substrate of classical conditioning in the hippocampus. *Science* **192**(4238), 483–485 (1976)
8. Berry, S.D., Hoffmann, L.C.: Hippocampal theta-dependent eyeblink classical conditioning: coordination of a distributed learning system. *Neurobiol Learn Mem* **95**(2), 185–189 (2011)
9. Berry, S.D., Thompson, R.F.: Prediction of learning rate from the hippocampal electroencephalogram. *Science* **200**(4347), 1298–1300 (1978)
10. Berry, S.D., Thompson, R.F.: Medial septal lesions retard classical conditioning of the nictitating membrane response in rabbits. *Science* **205**(4402), 209–211 (1979)
11. Berry, S.D.: Septo-hippocampal activity and learning rate. In: Woody, C.D. (ed.) *Conditioning: Representation of Involved Neural Function*, pp. 417–431. Plenum Press, New York (1982)
12. Bland, B., Oddie, S.D.: Theta band oscillation and synchrony in the hippocampal formation and associated structures: the case for its role in sensorimotor integration. *Behav. Brain Res.* **127**(1–2), 119–136 (2001)

13. Blaxton, T.A., Zeffiro, T.A., Gabrieli, J.D.E., Bookheimer, S.Y., Carrillo, M.C., Theodore, W.H., Disterhoft, J.F.: Functional mapping of human learning: A positron emission tomography activation study of eyeblink conditioning. *J. Neurosci.* **16**(12), 4032–4040 (1996)
14. Brelsford, J., Theios, J.: Single session conditioning of the nictitating membrane in the rabbit: effect of intertrial interval. *Psychon Sci* **2**, 81–82 (1965)
15. Brodal, A.: *Neurological Anatomy*. Oxford University Press, New York (1981)
16. Buchanan, S.L., Thompson, R.H., Maxwell, B.L., Powell, D.A.: Efferent connections of the medial prefrontal cortex in the rabbit. *Exp. Brain Res.* **100**(3), 469–483 (1994)
17. Buzsáki, G.: Theta oscillations in the hippocampus. *Neuron* **33**(3), 325–340 (2002)
18. Buzsáki, G.: Neuroscience. Similar is different in hippocampal networks. *Science* **309**(5734), 568–569 (2005)
19. Buzsáki, G.: *Rhythms of the Brain*. Oxford University Press Inc, New York (2006)
20. Buzsáki, G., Draguhn, A.: Neuronal oscillations in cortical networks. *Science* **304**(5679), 1926–1929 (2004)
21. Canolty, R.T., Edwards, E., Dalal, S.S., Soltani, M., Nagarajan, S.S., Kirsch, H.E., Knight, R.T.: High gamma power is phase-locked to theta oscillations in human neocortex. *Science* **313**(5793), 1626–1628 (2006)
22. Caplan, J.B., Madsen, J.R., Raghavachari, S., Kahana, M.J.: Distinct patterns of brain oscillations underlie two basic parameters of human maze learning. *J. Neurophysiol.* **86**(1), 368–380 (2001)
23. Caplan, J.B., Madsen, J.R., Schulze-Bonhage, A., Aschenbrenner-Scheibe, R., Newman, E.L., Kahana, M.J.: Human theta oscillations related to sensorimotor integration and spatial learning. *J. Neurosci.* **23**(11), 4726–4736 (2003)
24. Choi, J.S., Moore, J.W.: Cerebellar neuronal activity expresses the complex topography of conditioned eyeblink responses. *Behav. Neurosci.* **117**(6), 1211–1219 (2003)
25. Christian, K.M., Thompson, R.F.: Neural substrates of eyeblink conditioning: Acquisition and retention. *Learn. Mem.* **10**(6), 427–455 (2003)
26. Cicchese, J. J. (2013). Identified interneurons of dorsal hippocampal area CA1 show different theta-contingent response profiles during classical eyeblink conditioning. Master's thesis. [http://rave.ohiolink.edu/etdc/view?acc\\_num=miami1367583089](http://rave.ohiolink.edu/etdc/view?acc_num=miami1367583089)
27. Cicchese, J.J., Berry, S.D.: Comparison of identified neural response profiles in CA1 and CA3 during theta-contingent eyeblink conditioning. Unpublished poster presentation at: The Annual Meeting of the Society for Neuroscience, 13–17 Oct 2012, New Orleans, LA (2012)
28. Clark, R.E., McCormick, D.A., Lavond, D.G., Thompson, R.F.: Effects of lesions of cerebellar nuclei on conditioned behavioral and hippocampal neuronal responses. *Brain Res.* **291**(1), 125–136 (1984)
29. Clark, R.E., Squire, L.R.: Classical conditioning and brain systems: The role of awareness. *Science* **280**(5360), 77–81 (1998)
30. Cutsuridis, V., Cobb, S., Graham, B.P.: Encoding and retrieval in a model of the hippocampal CA1 microcircuit. *Hippocampus* **20**(3), 423–446 (2010)
31. Darling, R.D., Takatsuki, K., Griffin, A.L., Berry, S.D.: Eyeblink conditioning contingent on hippocampal theta enhances hippocampal and medial prefrontal responses. *J. Neurophysiol.* **105**(5), 2213–2224 (2011)
32. Darling, R.D.: Single cell analysis of hippocampal neural ensembles during theta-triggered eyeblink classical conditioning in the rabbit. Unpublished doctoral dissertation. [http://rave.ohiolink.edu/etdc/view?acc\\_num=miami1225460517](http://rave.ohiolink.edu/etdc/view?acc_num=miami1225460517) (2008)
33. Daum, I., Channon, S., Canavan, A.G.: Classical conditioning in patients with severe memory problems. *J. Neurol. Neurosurg. Psychiatry* **52**(1), 47–51 (1989)
34. Daum, I., Channon, S., Polkey, C.E., Gray, J.A.: Classical conditioning after temporal lobe lesions in man: Impairment in conditional discrimination. *Behav. Neurosci.* **105**(3), 396–408 (1991)
35. Daum, I., Schugens, M.M., Ackermann, H., Lutzenberger, W., Dichgans, J., Birbaumer, N.: Classical conditioning after cerebellar lesions in humans. *Behav. Neurosci.* **107**(5), 748–756 (1993)

36. Deupree, D., Coppock, W., Willer, H.: Pretraining septal driving of hippocampal rhythmic slow activity facilitates acquisition of visual discrimination. *J. Comp. Physiol. Psychol.* **96**(4), 557–562 (1982)
37. Eichenbaum, H.: Hippocampus: mapping or memory? *Curr. Biol.* **10**(21), 785–797 (2000)
38. Fontan-Lozano, A., Troncoso, J., Munera, A., Carrion, A., Delgado-Garcia, J.: Cholinergic septo-hippocampal innervation is required for trace eyeblink classical conditioning. *Learn. Mem.* **12**(6), 557–563 (2005)
39. Fox, S., Ranck, J.: Electrophysiological characteristics of hippocampal complex-spike cells and theta cells. *Exp. Brain Res.* **41**(3–4), 399–410 (1981)
40. Fries, P.: A mechanism for cognitive dynamics: Neuronal communication through neuronal coherence. *Trends Cogn. Sci.* **9**(10), 474–480 (2005)
41. Gabrieli, J., McGlinchey-Berroth, R., Carrillo, M., Gluck, M., Cermak, L., Disterhoft, J.F.: Intact delay-eyeblink classical conditioning in amnesia. *Behav. Neurosci.* **109**(5), 819–827 (1995)
42. Garcia, K.S., Steele, P.M., Mauk, M.D.: Cerebellar cortex lesions prevent acquisition of conditioned eyelid responses. *J. Neurosci.* **19**(24), 10940–10947 (1996)
43. Givens, B.: Stimulus-evoked resetting of the dentate theta rhythm: relation to working memory. *NeuroReport* **8**(1), 159–163 (1996)
44. Gormezano, I.: Investigations of defense and reward conditioning in the rabbit. In: Black, A. H., Prokasy, W.F. (eds.) *Classical Conditioning II: Current Research and Theory*, pp. 151–181. Appleton Century Crofts, NY (1972)
45. Green, J.D., Arduini, A.A.: Hippocampal electrical activity in arousal. *J. Neurophysiol.* **17**(6), 533–557 (1954)
46. Griffin, A.L., Asaka, Y., Darling, R.D., Berry, S.D.: Theta-contingent trial presentation accelerates learning rate and enhances hippocampal plasticity during trace eyeblink conditioning. *Behav. Neurosci.* **118**(2), 403–411 (2004)
47. Hasselmo, M.E.: What is the function of hippocampal theta rhythm? Linking behavioral data to phasic properties of field potential and unit recording data. *Hippocampus* **15**(7), 936–949 (2005)
48. Hasselmo, M.E.: Neuronal rebound spiking, resonance frequency and theta cycle skipping may contribute to grid cell firing in medial entorhinal cortex. *Philos. Trans. R. Soc. Lond. B Biol. Sci.* **369**(1635), 20120523 (2014)
49. Hasselmo, M.E., Bodeldon, C., Wyble, B.P.: A proposed function for hippocampal theta rhythm: Separate phases of encoding and retrieval enhance reversal of prior learning. *Neural Comput.* **14**(4), 793–817 (2002)
50. Hoffmann, L.C., Berry, S.D.: Cerebellar theta oscillations are synchronized by hippocampal theta-contingent trace conditioning. *Proc. Natl. Acad. Sci. USA* **106**(50), 21371–21376 (2009)
51. Hoffmann, L.C.: Interactions between hippocampal and cerebellar theta oscillations during cerebellar theta-contingent trace eyeblink classical conditioning acquisition and extinction in the rabbit. Unpublished doctoral dissertation, Miami University (2013)
52. Hoffmann, L.C., Berry, S.D.: Differential role of network oscillations during acquisition and extinction of cerebellar theta-contingent trace eyeblink classical conditioning. Unpublished poster presentation at: The Annual Meeting of the Society for Neuroscience, 9–13 Nov 2013, San Diego, CA (2013)
53. Huerta, P.T., Lisman, J.E.: Heightened synaptic plasticity of hippocampal CA1 neurons during a cholinergically induced rhythmic state. *Nature* **364**(6439), 723–725 (1993)
54. Hyman, J.M., Wyble, B.P., Goyal, V., Rossi, C.A., Hasselmo, M.E.: Stimulation in hippocampal region CA1 in behaving rats yield long-term potentiation when delivered to the peak of theta and long-term depression when delivered to the trough. *J. Neurosci.* **23**(37), 11725–11731 (2003)
55. Hyman, J.M., Zilli, E.A., Paley, A.M., Hasselmo, M.E.: Medial prefrontal cortex cells show dynamic modulation with the hippocampal theta rhythm dependent on behavior. *Hippocampus* **15**(6), 739–749 (2005)

56. Jensen, O.: Information transfer between rhythmically coupled networks: Reading the hippocampal phase code. *Neural Comput.* **13**(12), 2743–2761 (2001)
57. Jog, M.S., Connolly, C.I., Kubota, Y., Iyengar, D.R., Garrido, L., Harlan, R., Graybiel, A.M.: Tetrode technology: advances in implantable hardware, neuroimaging, and data analysis techniques. *J. Neurosci. Methods* **117**, 141–152 (2002)
58. Jones, M.W., Wilson, M.A.: Phase precession of medial prefrontal cortical activity relative to the hippocampal theta rhythm. *Hippocampus* **15**(7), 867–873 (2005)
59. Kahana, M.J., Sekuler, R., Caplan, J.B., Kirschen, M., Madsen, J.R.: Human theta oscillations exhibit task dependence during virtual maze navigation. *Nature* **399**(6738), 781–784 (1999)
60. Kalmbach, B.E., Davis, T., Ohyama, T., Riusech, F., Nores, W.L., Mauk, M.D.: Cerebellar cortex contributions to the expression and timing of conditioned eyelid responses. *J. Neurophysiol.* **103**(4), 2039–2049 (2010)
61. Kalmbach, B.E., Ohyama, T., Kredier, J.C., Riusech, F., Mauk, M.D.: Interactions between prefrontal cortex and cerebellum revealed by trace eyelid conditioning. *Learn. Mem.* **16**(1), 86–95 (2009)
62. Kalmbach, B.E., Voicu, H., Ohyama, T., Mauk, M.D.: A subtraction mechanism of temporal coding in cerebellar cortex. *J. Neurosci.* **31**(6), 2025–2034 (2011)
63. Kaneko, T., Thompson, R.F.: Disruption of trace conditioning of the nictitating membrane response in rabbits by central cholinergic blockade. *Psychopharmacol.* **131**(2), 161–166 (1997)
64. Kehoe, E., Gormezano, I.: Effects of trials per session on conditioning of the rabbit's nictitating membrane response. *Bull. Psychon. Soc.* **2**, 434–436 (1974)
65. Kirov, R., Weiss, C., Siebner, H., Born, J., Marshall, L.: Slow oscillation electrical brain stimulation during waking promotes EEG theta activity and memory encoding. *Proc. Natl. Acad. Sci. USA* **106**(36), 15460–15465 (2009)
66. Klausberger, T., Somogyi, P.: Neuronal diversity and temporal dynamics: The unity of hippocampal circuit operations. *Science* **321**(5885), 53–57 (2008)
67. Kramis, R., Vanderwolf, C.H., Bland, B.H.: Two types of hippocampal rhythmical slow activity in both the rabbit and the rat: relations to behavior and effects of atropine, diethyl ether, urethane, and pentobarbital. *Exp. Neurol.* **49**, 58–85 (1975)
68. Kronforst-Collins, M.A., Disterhoft, J.F.: Lesions of the caudal area of rabbit medial prefrontal cortex impair trace eyeblink conditioning. *Neurobiol. Learn. Mem.* **69**(2), 147–162 (1998)
69. Kunec, S., Hasselmo, M.E., Kopell, N.: Encoding and retrieval in the CA3 region of the hippocampus: A model of theta-phase separation. *J. Neurophys.* **94**(1), 70–82 (2005)
70. Kyd, R., Bilkey, D.: Prefrontal cortex lesions modify the spatial properties of hippocampal place cells. *Cereb. Cortex* **13**(5), 444–451 (2003)
71. Landfield, P., Lynch, G.: Impaired monosynaptic potentiation in *in vitro* hippocampal slices from aged, memory-deficient rats. *J. Gerontol.* **32**(5), 523–533 (1977)
72. Lega, B., Jacobs, J., Kahana, M.: Human hippocampal theta oscillations and the formation of episodic memories. *Hippocampus* **22**(4), 748–761 (2012)
73. Lisman, J.: The theta/gamma discrete phase code occurring during the hippocampal phase precession may be a more general brain coding scheme. *Hippocampus* **15**(7), 913–922 (2005)
74. Llinas, R.: Inferior olive oscillation as the temporal basis for motricity and oscillatory reset as the basis for motor error correction. *Neuroscience* **162**(3), 797–804 (2009)
75. Logothetis, N.: The underpinnings of the BOLD functional magnetic resonance imaging signal. *J. Neurosci.* **23**(10), 3963–3971 (2003)
76. Marshall, S., Lang, E.: Inferior olive oscillations gate transmission of motor cortical activity to the cerebellum. *J. Neurosci.* **24**(50), 11356–11367 (2004)
77. Mauk, M.D., Garcia, K.S., Medina, J.F., Steele, P.M.: Does cerebellar LTD mediate motor learning? Toward a resolution without a smoking gun. *Neuron* **20**(3), 359–362 (1998)

78. Mauk, M.D., Ruiz, B.P.: Learning-dependent timing of Pavlovian eyelid responses: Differential conditioning using multiple interstimulus intervals. *Behav. Neurosci.* **106**(4), 666–681 (1992)
79. Mauk, M.D., Thompson, R.F.: Retention of classically conditioned eyelid responses following acute decerebration. *Brain Res.* **403**(1), 89–95 (1987)
80. McCartney, H., Johnson, A.D., Weil, Z.M., Givens, B.: Theta reset produces optimal conditions for long-term potentiation. *Hippocampus* **14**(6), 684–687 (2004)
81. McCormick, D.A., Clark, G.A., Lavond, D.G., Thompson, R.F.: Initial localization of the memory trace for a basic form of learning. *Proc. Natl. Acad. Sci. USA* **79**(8), 2731–2735 (1982)
82. McCormick, D.A., Steinmetz, J.E., Thompson, R.F.: Lesions of the inferior olfactory complex cause extinction of the classically conditioned eyeblink response. *Brain Res.* **359**(1–2), 120–130 (1985)
83. McCormick, D.A., Thompson, R.F.: Cerebellum: essential involvement in the classically conditioned eyelid response. *Science* **223**(4633), 296–299 (1984)
84. McGlinchey-Berroth, R., Carrillo, M.C., Gabrieli, J.D., Brawn, C.M., Disterhoft, J.F.: Impaired trace eyeblink conditioning in bilateral, medial-temporal lobe amnesia. *Behav. Neurosci.* **111**(5), 873–882 (1997)
85. McLaughlin, J., Skaggs, H., Churchwell, J., Powell, D.A.: Medial prefrontal cortex and Pavlovian conditioning: trace versus delay conditioning. *Behav. Neurosci.* **116**, 37–47 (2002). doi:[10.1037/0735-7044.116.1.37](https://doi.org/10.1037/0735-7044.116.1.37)
86. Mehta, M., Lee, A., Wilson, M.: Role of experience and oscillations in transforming a rate code into a temporal code. *Nature* **417**(6890), 741–746 (2002)
87. Moyer, J., Deyo, R., Disterhoft, J.F.: Hippocampectomy disrupts trace eye-blink conditioning in rabbits. *Behav. Neurosci.* **104**(2), 243–252 (1990)
88. Nokia, M., Penttonen, M., Korhonen, T., Wikgren, J.: Hippocampal theta (3–8 Hz) activity during classical eyeblink conditioning in rabbits. *Neurobiol. Learn. Mem.* **90**(1), 62–70 (2008)
89. Nokia, M., Penttonen, M., Wikgren, J.: Hippocampal ripple-contingent training accelerates trace eyeblink conditioning and retards extinction in rabbits. *J. Neurosci.* **30**(34), 11486–11492 (2010)
90. O'Keefe, J., Recce, M.: Phase relationship between hippocampal place units and the EEG theta rhythm. *Hippocampus* **3**(3), 317–330 (1993)
91. Perrett, S.P., Mauk, M.D.: Extinction of conditioned eyelid responses requires the anterior lobe of cerebellar cortex. *J. Neurosci.* **15**(3), 2074–2080 (1995)
92. Perrett, S.P., Ruiz, B.P., Mauk, M.D.: Cerebellar cortex lesions disrupt learning-dependent timing of conditioned eyelid responses. *J. Neurosci.* **13**(4), 1708–1718 (1993)
93. Powell, D.A., Skaggs, H., Churchwell, J., McLaughlin, J.: Posttraining lesions of the medial prefrontal cortex impair performance of Pavlovian eyeblink conditioning but have no effect on concomitant heart rate changes in rabbits (*Oryctolagus cuniculus*). *Behav. Neurosci.* **115**, 1029–1038 (2001)
94. Prokasy, W.F., Grant, D.A., Myers, N.A.: Eyelid conditioning as a function of unconditioned stimulus intensity and intertrial interval. *J. Exp. Psychol.* **55**(3), 242–246 (1958)
95. Raghavachari, S., Kahana, M.J., Rizzuto, D.S., Caplan, J.B., Kirschen, M.P., Bourgeois, B., Madsen, J.R., Lisman, J.E.: Gating of human theta oscillations by a working memory task. *J. Neurosci.* **21**, 3175–3183 (2001)
96. Salafia, W., Mis, F., Terry, W., Bartosiak, R., Daston, A.: Conditioning of the nictitating membrane response of the rabbit (*Oryctolagus cuniculus*) as a function of length and degree of variation of intertrial interval. *Anim. Learn. Behav.* **1**, 109–115 (1973)
97. Salvatierra, A.T., Berry, S.D.: Scopolamine disruption of septo-hippocampal activity and classical conditioning. *Behav. Neurosci.* **103**(4), 715–721 (1989)
98. Scarlett, D., Dypvik, A., Bland, B.: Comparison of spontaneous and septally driven hippocampal theta field and theta-related cellular activity. *Hippocampus* **14**(1), 99–106 (2004)

99. Schmaltz, L.W., Theios, J.: Acquisition and extinction of a classically conditioned response in hippocampectomized rabbits (*Oryctolagus cuniculus*). *J. compar. physiol. psychol.* **79**(2), 328–333 (1972)
100. Schneiderman, N., Gormezano, I.: Conditioning of the nictitating membrane of the rabbit as a function of CS-US interval. *J. Compar. Physiol. Psych.* **57**, 1881–1895 (1964)
101. Schreurs, B., McIntosh, A., Bahro, M., Herscovitch, P., Sunderland, T., Molchan, S.: Lateralization and behavioral correlation of changes in regional cerebral blood flow with classical conditioning of the human eyeblink response. *J. Neurophysiol.* **77**(4), 2153–2163 (1997)
102. Seager, M.A., Johnson, L.D., Chabot, E.S., Asaka, Y., Berry, S.D.: Oscillatory brain states and learning: impact of hippocampal theta-contingent training. *Proc. Natl. Acad. Sci. USA* **99**(3), 1616–1620 (2002)
103. Sears, L.L., Steinmetz, J.E.: Acquisition of classically conditioned-related activity in the hippocampus is affected by lesions of the cerebellar interpositus nucleus. *Behav. Neurosci.* **104**(5), 681–692 (1990)
104. Shusterman, V., Troy, W.: From baseline to epileptiform activity: a path to synchronized rhythmicity in large-scale neural networks. *Phys. Rev. E. Stat. Nonlin. Soft Matter Phys.* **77**(6), 061911
105. Siapas, A., Lubenov, E., Wilson, M.A.: Prefrontal phase locking to hippocampal theta oscillations. *Neuron* **46**(1), 141–151 (2005)
106. Siegel, J.J., Kalsbach, B., Chitwood, R.A., Mauk, M.D.: Persistent activity in a cortical-to-subcortical circuit: Bridging the temporal gap in trace eyelid conditioning. *J. Neurophysiol.* **107**(1), 50–64 (2012)
107. Singer, W.: Neuronal synchrony: a versatile code for the definition of relations? *Neuron* **24**(1), 49–65 (1999)
108. Skaggs, W.E., McNaughton, B.L., Permenter, M., Archibeque, M., Vogt, J., Amaral, D.G., Barnes, C.A.: EEG sharp waves and sparse ensemble unit activity in the macaque hippocampus. *J. Neurophysiol.* **98**(2), 898–910 (2007)
109. Smith, M., Coleman, S., Gormezano, I.: Classical conditioning of the rabbit's nictitating membrane response at backward, simultaneous, and forward CS-US intervals. *J. Comp. Physiol. Psychol.* **69**(2), 226–231 (1969)
110. Smith, A., Frank, L., Wirth, S., Yanike, M., Hu, D., Kubota, Y., Brown, E.: Dynamic analysis of learning in behavioral experiments. *J. Neurosci.* **24**(2), 447–461 (2004)
111. Solomon, P.R., Gottfried, K.E.: The septohippocampal cholinergic system and classical conditioning of the rabbit's nictitating membrane response. *J. Comp. Physiol. Psychol.* **95**(2), 322–330 (1981)
112. Solomon, P.R., Solomon, S.D., Vander Schaaf, E., Perry, H.E.: Altered activity in the hippocampus is more detrimental to classical conditioning than removing the structure. *Science* **220**(4594), 329–331 (1983)
113. Solomon, P.R., Stowe, G.T., Pendlebury, W.W.: Disrupted eyelid conditioning in a patient with damage to cerebellar afferents. *Behav. Neurosci.* **103**(4), 898–902 (1989)
114. Solomon, P.R., Vander Schaaf, E.R., Thompson, R.F., Weisz, D.J.: Hippocampus and trace conditioning of the rabbit's classically conditioned nictitating membrane response. *Behav. Neurosci.* **100**(5), 729–744 (1986)
115. Solomon, P.R., Groccia-Ellison, M.E., Flynn, D., Mirak, J., Edwards, K.R., Dunehew, A., Stanton, M.E.: Disruption of human eyeblink conditioning after central cholinergic blockade with scopolamine. *Behav. Neurosci.* **107**, 271–279 (1993)
116. Spence, K.W., Norris, E.B.: Eyelid conditioning as a function of the inter-trial interval. *J. Exp. Psychol.* **40**(6), 716–720 (1950)
117. Steinmetz, J.E., Woodruff-Pak, D.S. (eds.): *Eyeblink Classical Conditioning*, vol. 2. Animal Models, Kluwer, Boston (2000)
118. Stewart, M., Fox, S.: Do septal neurons pace the hippocampal theta rhythm? *Trends in Neurosci.* **13**(5), 163–168 (1990)

119. Takehara, K., Kawahara, S., Kirino, Y.: Time-dependent reorganization of the brain components underlying memory retention in trace eyeblink conditioning. *J. Neurosci.* **23**(30), 9897–9905 (2003)
120. Takehara-Nishiochi, K., McNaughton, B.L.: Spontaneous changes of neocortical code for associative memory during consolidation. *Science* **322**(5903), 960–963 (2008)
121. Thompson, R.F., Gluck, M.A.: Brain substrates of basic associative learning and memory. In: Lister, R.G., Weingartner, H.J. (eds.) *Perspectives on Cognitive Neuroscience*, pp. 25–45. Oxford University Press, New York (1991)
122. Topka, H., Valls Sole, J., Massaquoi, S., Hallett, M.: Deficit in classical conditioning in patients with cerebellar degeneration. *Brain* **116**(4), 961–969 (1993)
123. Tsanov, M., Manahan-Vaughan, D. (2009). Long-term plasticity is proportional to theta-activity. *PLoS One* **4**(6). doi:[10.1371/journal.pone.0005850](https://doi.org/10.1371/journal.pone.0005850)
124. Ulhaas, P.J., Singer, W.: Abnormal neural oscillations and synchrony in schizophrenia. *Nat. Rev. Neurosci.* **11**(2), 100–113 (2010)
125. Weible, A.P., Weiss, C., Disterhoft, J.F.: Activity of single neurons in caudal anterior cingulate cortex during trace eyeblink conditioning in the rabbit. *J. Neurophysiol.* **90**(2), 599–612 (2003)
126. Weiss, C., Disterhoft, J.F.: Exploring prefrontal cortical memory mechanisms with eyeblink conditioning. *Behav. Neurosci.* **125**(3), 318–326 (2011)
127. Weiss, C., Knuttilen, M., Power, J., Patel, R., O'Connor, M., Disterhoft, J.F.: Trace eyeblink conditioning in the freely moving rat: Optimizing the conditioning parameters. *Behav. Neurosci.* **113**(5), 1100–1105 (1999)
128. Welsh, J.P., Lang, E.J., Sugihara, I., Llinas, R.R.: Dynamic organization of motor control within the olivocerebellar system. *Nature* **374**(65241), 453–457 (1995)
129. Wetzel, W., Ott, T., Matthies, H.: Hippocampal rhythmic slow activity (“theta”) and behavior elicited by medial septal stimulation in rats. *Behav. Biol.* **19**(4), 534–542 (1977)
130. Williams, J.M., Givens, B.: Stimulation-induced reset of hippocampal theta in the freely performing rat. *Hippocampus* **13**(1), 109–116 (2003)
131. Woodruff-Pak, D.S., Lavond, D.G., Thompson, R.F.: Trace conditioning: Abolished by cerebellar nuclear lesions but not lateral cerebellar cortex aspirations. *Brain Res.* **348**(2), 249–260 (1985)
132. Woodruff-Pak, D.S., Papka, M., Ivry, R.B.: Cerebellar involvement in eyeblink classical conditioning in humans. *Neuropsychol.* **10**(4), 443–458 (1996)
133. Wyble, B.P., Linster, C., Hasselmo, M.E.: Size of CA1-evoked synaptic potentials is related to theta rhythm phase in rat hippocampus. *J. Neurophys.* **83**(4), 2138–2144 (2000)
134. Yeo, C.H., Hardiman, M.J., Glickstein, M.: Discrete lesions of the cerebellar cortex abolish the classically conditioned nictitating membrane response of the rabbit. *Behav. Brain Res.* **13**(3), 261–266 (1984)
135. Yeo, C.H., Hardiman, M.J., Glickstein, M.: Classical conditioning of the nictitating membrane response of the rabbit. Lesions of the cerebellar nuclei. *Exp. Brain Res.* **60**(1), 87–98 (1985)

# **Chapter 7**

## **Advanced fMRI and the Brain Computer Interface**

**Martyn Paley, Shwan Kaka, Heather Hilliard, Aleksandr Zaytsev,  
Adriana Bucur, Steven Reynolds, Wei Liu, Elizabeth Milne  
and Greg Cook**

**Abstract** Electrical signals generated by the brain which give rise to the EEG signal on the scalp create a magnetic field at the neuronal source of around 1 nano-Tesla (nT). Several authors have shown that changes in magnetic field of this order can be directly detected electromagnetically through MR signal modulation by high sensitivity MRI systems. An interesting fact is that this direct electromagnetic effect is independent of the strength of the magnetic field which is used for detection. Instead it is the stability of the system which controls the ability to detect such weak electromagnetic fields. This opens up the possibility of using low cost, open, low field strength MRI systems for dfMRI brain computer interfaces. Some authors have proposed the use of SQUID detection of fMRI at ultra-low field. Instead, we propose

---

M. Paley (✉) · S. Kaka · H. Hilliard · A. Bucur · S. Reynolds  
Academic Radiology, University of Sheffield, Sheffield, UK  
e-mail: m.n.paley@sheffield.ac.uk

S. Kaka  
e-mail: skkaka1@sheffield.ac.uk

H. Hilliard  
e-mail: heather.a.hilliard@doctors.org.uk

A. Bucur  
e-mail: a.bucur@sheffield.ac.uk

S. Reynolds  
e-mail: steven.reynolds@sheffield.ac.uk

A. Zaytsev · W. Liu · G. Cook  
Electronics and Electrical Engineering, University of Sheffield, Sheffield, UK  
e-mail: adzaytsev1@sheffield.ac.uk

W. Liu  
e-mail: w.liu@sheffield.ac.uk

G. Cook  
e-mail: g.cook@sheffield.ac.uk

E. Milne  
Psychology, University of Sheffield, Sheffield, UK  
e-mail: e.milne@sheffield.ac.uk

use of an intermediate, low cost, open MRI system used in conjunction with advance sensitivity enhancement methods such as cryogenic radiofrequency array coils together with polarization enhancement through the nuclear Overhauser effect (producing enhancements of  $\sim 10x$ ) and dynamic nuclear polarization (producing enhancements of  $\sim 10,000x$ ). Whilst this development is still in its infancy, much of the underlying technology required has already been proven and our future challenge is to integrate these sub-systems into a functional dfMRI based BCI device.

**Keywords** fMRI · dfMRI · BOLD · BCI · Dedicated MRI systems · GRACE · DNP · Overhauser enhanced MRI

## 7.1 Introduction

A Brain Computer Interface (BCI) needs to be fast, non-invasive and provide highly localized information on the source of function within the brain to allow rapid identification and selection of imagined responses. Until recently functional MRI could provide both non-invasive and highly localized source information on function within the brain but has been relatively slow compared to other methods such as EEG [3] and MEG (Hamalainen et al. [20] due to its reliance on convolution of the fast neuronal signals with the blood's slow hemodynamic response function (HRF  $\sim 6\text{--}10$  s). If it was possible to retain the advantages of fMRI and increase the temporal resolution, in a low cost, compact, open access MRI system then it may in fact be possible to consider MRI to be a competing technology for development of a BCI. This chapter aims to introduce and discuss a number of advanced MR methods and new technologies which may be useful for developing novel brain computer interfaces in future. Although functional MRI is traditionally performed at high magnetic field strength, new functional methods are being developed which are independent of field strength and which rely much more on the temporal stability of the system opening up the possibility of low cost, low field devices for use with a BCI.

The Blood Oxygenation Level Dependent (BOLD) response increases approximately linearly with magnetic field strength (Ogawa et al. [37]) and whole body magnets of 3, 7, 9.4 T and even 10.5 T are now being used for functional MRI research and in some cases for clinical practice. However, the slow HRF means that the real time response of the BOLD effect limits its use in a BCI which ideally require multiple updates each second to provide a smooth response. If functional MRI was capable of picking up the effects of neuronal and axonal firing directly then the temporal resolution could be increased to be similar to EEG and MEG, limited only by the data acquisition window and sequence repeat time. In principle, the direct effect is also more highly localized than the BOLD effect as it is not dependent on blood flow within the arteries, capillaries and veins which supply the firing axons with oxygen but measures the group of active neurons firing directly.

There are many opportunities for radical MRI designs at lower field strength, where the high magnet coil hoop stresses and requirement for cryogenic cooling required by high field superconducting magnets are relaxed. Resistive or permanent magnets can be used which have much lower power requirements and are much easier to construct and maintain as well as having much lower capital and running costs, potentially opening up the field of fMRI BCI. New methods are being developed to increase the sensitivity of low field MRI systems such as cryogenically-cooled radiofrequency coils which use simple liquid Nitrogen based cryostats and enhanced polarization methods such as Overhauser MRI or dissolution dynamic nuclear polarization enhancement which provide dramatic increases in sensitivity for low field MRI, making field strength a much less relevant factor. Rapid new MR acquisition strategies such as phase encode under-sampling and advanced image processing algorithms are opening up the ability of fMRI to automatically provide real time functional responses.

The chapter begins with a comparison of the established but slow BOLD fMRI method with the emerging direct, fast electromagnetic detection technique, dfMRI, in terms of spatial and temporal resolution in Sects. 7.2.1 and 7.2.2 respectively. Section 7.2.3 compares functional data acquired with both slow and fast methods using visual functional stimulation in human volunteers as an illustration of the potential of the fast method. Section 7.2.4 describes a novel method of measuring weak currents with MRI known as GRACE which has a very high frequency bandwidth for detecting fluctuating magnetic fields which could provide MRI with very high resolution, artifact free images but with the same frequency response as EEG or MEG. Section 7.2.5 illustrates functional MRI results obtained using a transcutaneous electrical nerve stimulation (TENS) device to stimulate the median nerve showing weak responses from the nerve at the stimulation frequency.

Section 7.3 moves on to look at new MRI technology which could be used for brain computer interfaces as well as methods to improve the inherent sensitivity for low field functional studies. Section 7.3.1 describes a dedicated, niche MRI system which has already been used extensively to image adult extremities and the whole body of neonates and which also has some limited access to image the cortex of the adult human brain. Developments of such systems with slightly larger magnet apertures may well prove useful in developing functional MRI for a BCI in future. Section 7.3.2 describes the development of cryogenic coils which can improve the sensitivity of such systems by factors of three to four. Section 7.3.3 discusses the emerging method of *in vivo* Overhauser MRI (OMRI) which can increase the sensitivity of MRI in real time by around 10 times and Sect. 7.3.4 describes another low cost, low field MRI system based on a resistive magnet. In Sect. 7.3.5 the revolutionary method of *in vivo* dissolution DNP is described which can increase sensitivity for <sup>13</sup>C nuclei by over 10,000 times, albeit for a limited acquisition window of a few 100 s which could provide the additional sensitivity required to make dfMRI much more reliable. <sup>13</sup>C nuclei have wide spectral dispersion and thus there is potential to make spectroscopic measurements even with a relatively low field MRI scanner.

Section 7.4.1 describes a proposal for a low cost MRI system for use in a BCI system based on integrating the technologies described in previous sections. Section 7.4.2 suggests how such a low cost, but high technology MRI system could be integrated with a practical BCI system in future. The chapter finishes with Sect. 7.5 which provides a Discussion and Conclusion reviewing progress towards production of an MRI based Brain Computer Interface.

## 7.2 BOLD Versus Direct Electromagnetic Detection fMRI

Blood oxygenation level dependent (BOLD) functional magnetic resonance imaging (fMRI) has revolutionized our ability to evaluate how the brain works in response to external stimuli and to resting states in almost real time. However, there are fundamental limits to both the spatial and temporal resolution of BOLD due to its reliance on the slow hemodynamic response function (6–12 s) and on a spatially distributed network of veins, arteries and capillaries which make it non-ideal for a Brain Computer Interface [21, 32, 37, 42]. Magnetoencephalography (MEG) has shown that it is possible to directly detect very weak magnetic fields associated with neuronal firing in real time [20] although accurate source localization remains a difficult problem for MEG. Electroencephalography (EEG) and optical imaging have also been used to measure neuronal firing with high temporal but poor spatial resolution [3, 5, 18, 31].

Applied Potential Tomography was developed in Sheffield in the early 1980s and used externally applied voltages to spatially measure current flow inside the human body [4]. Externally applied currents were also later used with magnetic resonance imaging for measurements within the human body. However, these measurements required rotation of the sample relative to  $B_0$  which complicated the process considerably [22, 45]. Rotating frame excitation was later proposed to avoid actual physical rotation of the sample [46]. In addition to these externally applied current methods, there has been increasing interest in detecting intrinsic weak magnetic field changes within the body in an attempt to use MRI for directly mapping neuronal activity. These studies have focused on investigating temporal modulation of the magnetic field by weak fluctuating current sources such as those generated by neurons and axons. Phantom studies have shown that such very weak magnetic fields ( $\sim 10^{-10}$  T) can actually be detected by MRI using either magnitude or phase reconstructed MR images [7, 8, 16, 24, 26, 48, 52].

In vivo studies of direct neuronal detection have investigated a range of stimulation paradigms and different cerebral sub-systems. However, the research field is still very much in an experimental phase and detection remains at the limit of sensitivity of current MRI systems. If this effect could be detected reliably it would be an excellent candidate for use in a Brain Computer Interface. Our recent work has focused on study of this alternative method of direct intrinsic electromagnetic detection fMRI (dfMRI) *in vivo* in assemblies of human neurons and axons [10–13, 39]. This method has an instantaneous response to neuronal firing events limited

temporally only by the data acquisition process itself and potentially has very high spatial resolution limited only by MR system sensitivity to the weak electromagnetic emissions of the nervous system.

### 7.2.1 Spatial Resolution of **BOLD Versus dfMRI**

MEG measures weak magnetic signals produced by neuronal populations using Superconducting Quantum Interference Devices (SQUIDs). EEG in comparison measures electric potentials on the scalp with electrodes connected to a sensitive voltmeter. Both techniques have high temporal resolution in the millisecond range but can only provide low resolution images through a complex inverse solution method. Spontaneous and evoked magnetic fields measured on the scalp, 2–4 cm from the current source are of the order of  $10^{-12}$ – $10^{-13}$  T as measured by MEG (Hamalainen et al. [20]). Modelling these fields as a current dipole and using the inverse square law implies magnetic fields of the order of  $10^{-9}$  T for spontaneous activity (e.g. alpha waves) and  $10^{-10}$  T for evoked activity (e.g. response to a strobe flash) at the location of a 2 mm sized current source within the brain. MRI is sensitive to the magnetic field changes directly located at the current source and so in principle should experience direct signal modulation from these much larger internal fields. This opens up the real possibility that MRI, given sufficient sensitivity to these weak magnetic field changes, can have both the high temporal resolution associated with MEG and EEG but also retain its own inherently high spatial resolution. In theory, this effect must work. However, the challenge is making an MRI system sensitive and stable enough to measure this weak modulation effect. This chapter outlines our progress towards achieving this exciting goal.

Although the image acquisition sequence (usually Echo Planar Imaging—EPI) specifies the nominal voxel resolution of a functional MR image, the spatial resolution of the BOLD effect is actually determined by the extent of the underlying vasculature including arteries, capillaries and draining veins which supply oxygenated blood to the brain. The supply of blood and oxygenation in these vessels change during task activation as oxyhaemoglobin is converted to deoxyhaemoglobin. Thus the resolution of the BOLD effect within the brain may be variable. To improve localization of the effect, steps are often taken to try and remove signal arising from the larger draining veins. Higher static magnetic field strengths help reduce signal from the draining veins due to a shorter blood relaxation rate  $R2^*$  but it is also possible to use a spin echo sequence at lower field strengths which helps localize the signal to the capillary bed close to where the active neurons are firing.

The direct electromagnetic effect dfMRI on the other hand does not rely at all on the brain vasculature (except to keep the neurons oxygenated) but is defined solely by the number and location of the actively firing neurons and axons. Thus the spatial resolution of the dfMRI experiment is in principle much higher than for BOLD.

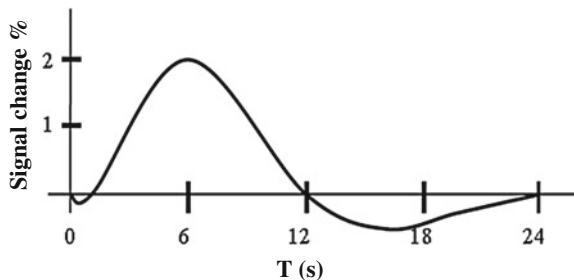


**Fig. 7.1** A schematic diagram of typical changes in the fMRI BOLD signal due to the adult human Hemodynamic Response Function (HRF) after a single event task activation. Neuronal activity is convolved with this function

### 7.2.2 Temporal Resolution of BOLD Versus dfMRI

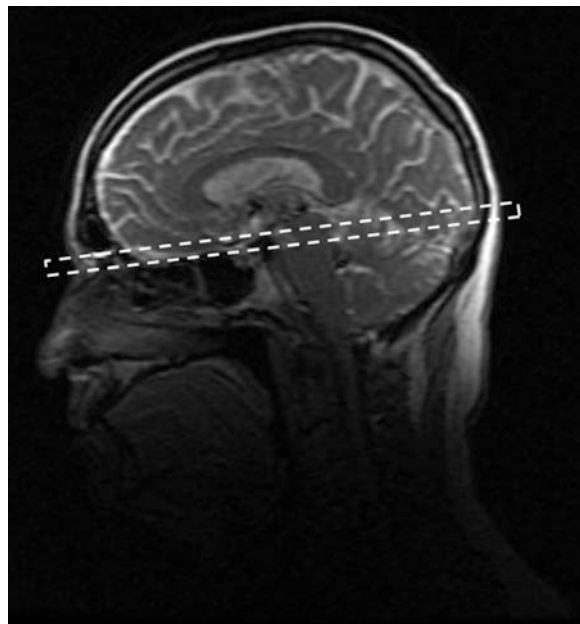
In terms of temporal resolution, the hemodynamic response lags behind the actual neuronal firing with a delay to maximum response of 6–12 s causing a consequent delay in the fMRI BOLD response as shown in Fig. 7.1. This hemodynamic response function (HRF) filter effectively defines the ultimate temporal resolution of BOLD fMRI and although a number of sophisticated paradigms have been used in an attempt to overcome this issue it remains a major problem.

The direct electromagnetic effect is limited by the temporal resolution of the MR image acquisition sequence rather than the individual neuronal firing events. All the field modulating events which occur after RF excitation integrated until the end of MR data acquisition will contribute to the phase modulation of the signal. However, it is possible to arrange for this temporal resolution to be in the millisecond range given sufficient detection sensitivity, thus improving dramatically on what can be achieved using BOLD.

### 7.2.3 Fast EPI fMRI Acquisition Method for dfMRI

The EPI sequence samples all the phase encoding required to produce an image within a single Free Induction Decay (FID) signal acquisition. EPI is usually acquired with a long repeat time 1–2 s for BOLD experiments but can be used with a much shorter repeat time (<100 ms) to look for higher frequency modulations, albeit with reduced signal to noise ratio. After initial experiments using test objects modulated by small coils with calibrated currents established that very weak magnetic fields (<1 nT) could be measured using fast echo planar imaging, it was decided to investigate whether the effect could be detected in adult human volunteers. The human optic nerve contains over a million nerve fibres which can be

**Fig. 7.2** Location of the single oblique slice used for rapid dfMRI of the human visual system passing through the optic nerves at the front and the visual cortex in the occipital lobe at the rear of the brain



induced to fire synchronously through a variety of stimulation paradigms. The optic nerve is also conveniently perpendicular to the main magnetic field meaning that the neuronal fields generated are in the correct direction to modulate the  $B_0$  field when the optic nerve fires.

In vivo experiments were performed at 1.5 T on healthy adult human subjects using single frequency stimulation either by a set of LED goggles or by a strobe. A single acquisition slice was planned through the optic nerves and visual cortex as shown in Fig. 7.2. Visual stimulation was applied asynchronously with the dfMRI acquisition as shown in Fig. 7.3.

An 8 channel head array coil was used for acquisition. Fat saturation was applied to remove signal from retro-orbital fat. A foam head mould and Velcro strap were used to minimize any head motion during imaging. Subjects were asked not to move their eyes or blink during the relatively short time course of imaging (79 s). Subjects were dark adapted for 15 min before the visual stimulus experiments started. All studies were performed in accordance with the local ethical guidelines for MR and with informed written consent. Figures 7.4 and 7.5 show typical experimental results.

Figure 7.5 shows a comparison of the BOLD response with dfMRI. Such direct responses, due to the direct electromagnetic effect, may be useful for developing a BCI in future [13, 38, 39].

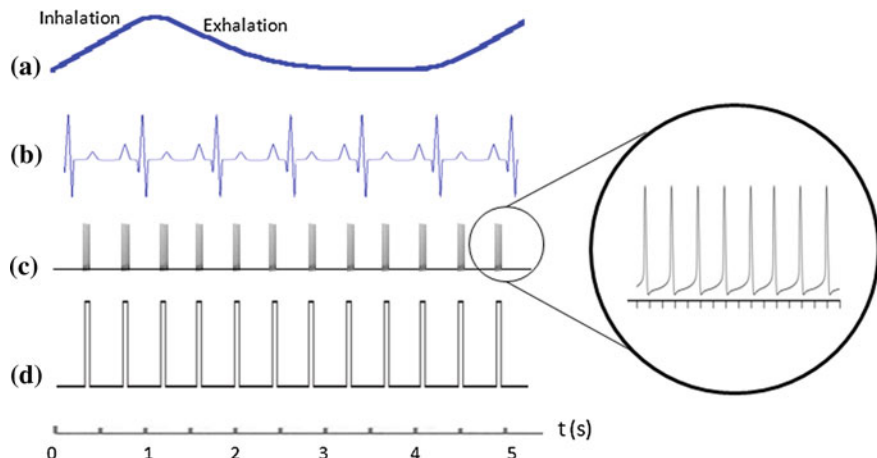


**Fig. 7.3** Schematic diagram showing typical relationship of breathing (a), cardiac pulsation (b), an action potential burst excited by the external stimulus (c) and data acquisition of the dfMRI acquisition time series (d)

#### 7.2.4 GRACE Method for High Spatial and Temporal Resolution dfMRI

The frequency response of a functional MRI scan is limited by the repeat time between successive image acquisitions. Typical BOLD fMRI scans which use Echo Planar Imaging use long repeat times of a second or more, thus limiting the stimulation frequency bandwidth which can be measured without aliasing to less than 0.5 Hz. A novel method has been developed which allows a very short repeat times to be used in the range of a few milliseconds enabling the bandwidth for MRI functional studies to be increased to a few hundred Hertz while retaining good geometric fidelity, unlike the conventionally used Echo Planar Imaging.

The Ghost Reconstructed Alternating Current Estimation (GRACE) [52] estimates alternating currents using ghost images created when the magnetic field from a fluctuating current periodically modulates the phase of the MR signal between successive phase encode views in a conventional 2D Fourier encoded sequence. GRACE has been tested on phantoms using both sinusoidal and square wave current waveforms and has been shown to detect fluctuating magnetic fields as low as  $10^{-10}$  T using sequential averaging.

Given a repetitive stimulus at frequency  $f$ , weak electrical signals in the optic nerve should modulate the local magnetic field and produce a weak displaced ghost image corresponding to the harmonics of the phase modulated MR signal spectrum, separated from the actual optic nerve by the distance

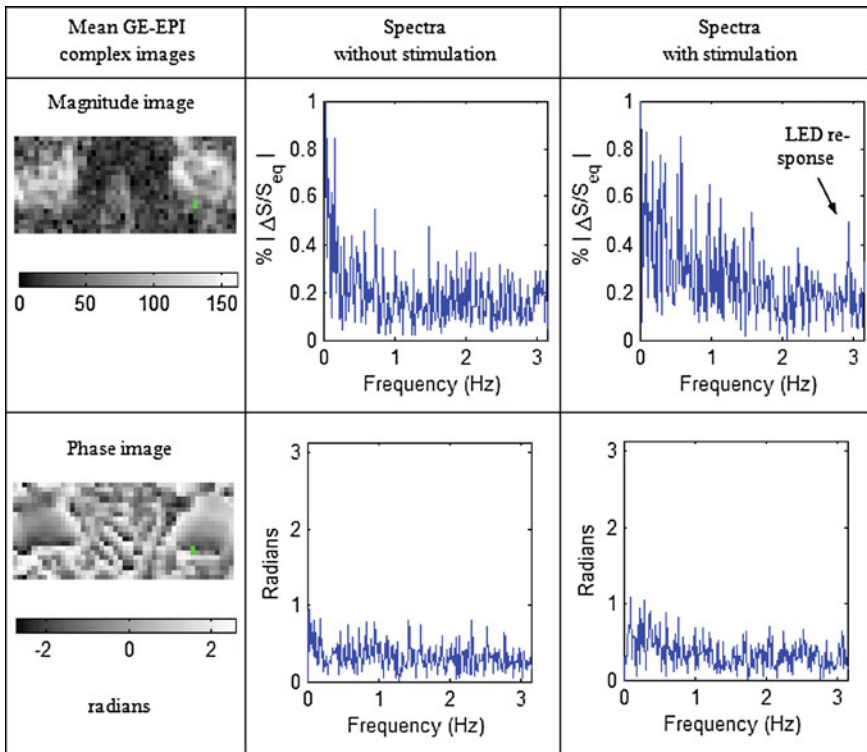


**Fig. 7.4** dfMRI spectral responses from visual LED stimulation were obtained from the ROI illustrated (*left*—green pixels) in the optic nerve by taking the Fourier transform of a time series of 500 EPI images acquired at 1.5 T with a very short TR = 88 ms. The spectral response of the optic nerve is shown without (*middle*) and with (*right*) visual stimulation by a sinusoidally modulated red light emitting diode at 3 Hz. A weak response of approximately 0.2 % signal modulation at the LED frequency of 3 Hz is seen in the magnitude spectrum but not the phase spectrum

$$\Delta S_n = n \times f \times \text{TR} \times \text{FOV} \times \text{NEX} \quad (7.1)$$

where  $n$  is the order of the ghost, TR is the acquisition repeat time, FOV is the Field of View and NEX is the number of excitations (averages).

A direct modulation response from the axons in the optic nerve should produce weak ghost image harmonics displaced to the left or right of the optic nerves in the noise around the head. The intensity of the ghosts depends critically on the PM modulation index generated by the axons and hence the resulting magnetic field. Figure 7.6 shows the results of a phantom experiment to demonstrate the generation of the GRACE ghost harmonics [52].

The GRACE method has been used in human volunteers to assess whether modulation of the axonal field from the optic nerve can be detected. In the example shown in Fig. 7.7, some motion of the eyeball can be seen but there is no obvious

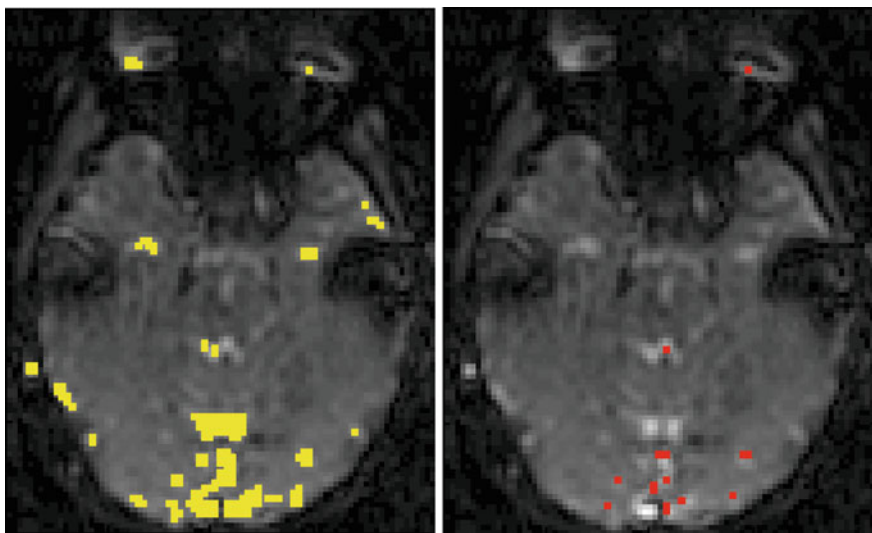


**Fig. 7.5** Comparison at 3 T of a BOLD and dfMRI analysis from a series of EPI images acquired using a flashing checkerboard stimulus presented to the visual field using an MR compatible display mounted on the head coil at 1.75 Hz with 5 blocks (OFF-ON-OFF-ON-OFF) of 30 s each. Analysis was performed using Statistical Mapping (GLM) with a Z-score of  $> 2.5$  showing correlations either at the block frequency (0.033 Hz) for BOLD (left—yellow pixels) or at the direct stimulus frequency (1.75 Hz) for the direct effect (right—red pixels) in the visual cortex and in the retina. The direct effect response appears to be more spatially localized than BOLD [13]

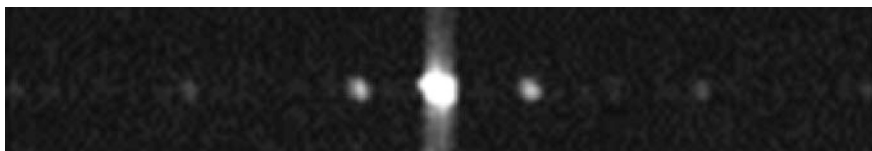
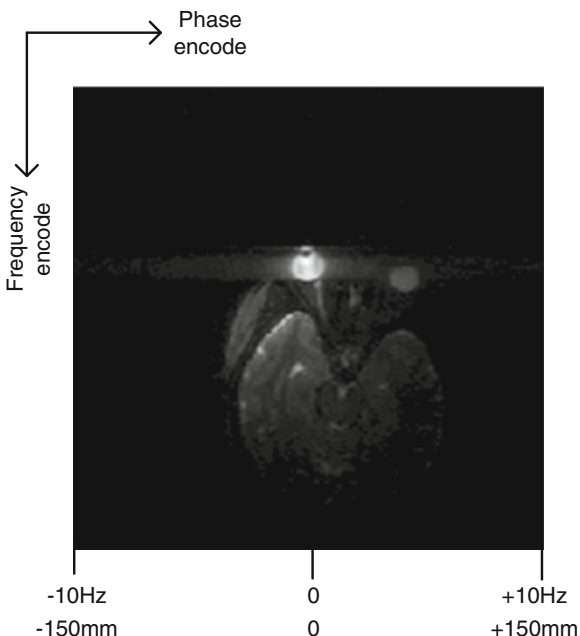


**Fig. 7.6** Experimental image of an oil capsule (centre of image) simulating an axial section of an optic nerve located adjacent to a straight wire driven with square wave modulation at frequency = 0.9 Hz and current  $I = 4.6$  mA and using a GRACE spin echo acquisition with TR = 100 ms, TE = 15 ms, FOV = 35 cm and NEX = 1. The ghost images are displaced from the actual object and the displacement distance allows the frequency of the modulation to be calculated, whilst the intensities of the different harmonic ghosts allows the amplitude and shape of the modulating waveform to be recreated

ghost from the optic nerve with strobe illumination at 4.5 Hz despite a measured signal to noise ratio of over 400:1. Experiments with strobe flash illumination in ten volunteers using a 3 T scanner showed possible weak ghost responses in only two cases [39]. This type of experiment may be easier to perform at lower magnetic field strength where there are fewer artifacts due to motion and physiological noise and where there are lower susceptibility artifacts.

**Fig. 7.7** A 25 frame sequentially averaged GRACE experiment using a surface coil and T2 weighted gradient echo sequence providing strong positive signal from the optic nerve in the axial plane. The horizontal scale is also calibrated in terms of where a GRACE ghost of a specific frequency would occur. The expected location of the ghost is at 4.5 Hz



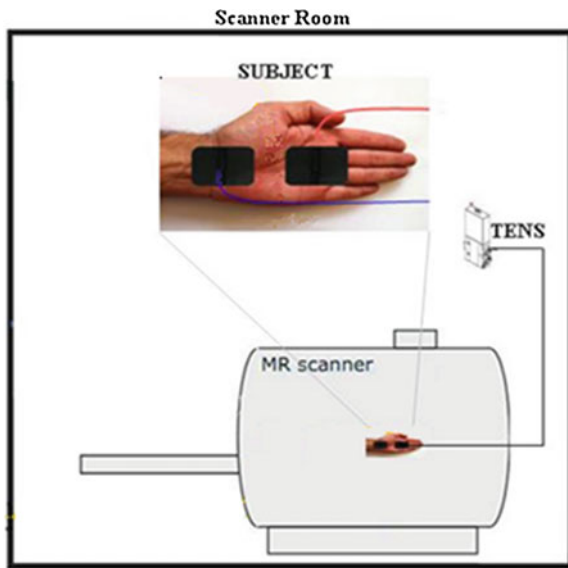
### 7.2.5 TENS Stimulation of the Median Nerve for dfMRI

Another method which can be used to try and detect direct neuronal firing using MRI is to induce peripheral nerve firing using applied electrical stimulation. Transcutaneous electrical nerve stimulation (TENS) uses pulsed voltages up to 40 V and currents up to 80 mA to induce nerve firing at a desired frequency (typically in the range 2.5–5 Hz for these experiments). Different pulse widths can also be used (typically 260  $\mu$ s for these experiments).

To stimulate the median nerve in the arm, the TENS device electrodes are positioned on the palm of the hand approximately 3 cm apart as shown in Fig. 7.8. The electrodes are connected to the TENS via a twisted pair cable to avoid the possibility of induced eddy currents from the MRI gradients and to locate the TENS device a suitable distance from the magnet to prevent the device being pulled into the magnet. The stimulus amplitude is adjusted until the subject reports feeling a mild shock but without any muscle twitch. fMRI is very sensitive to any subject movement which is minimized by firmly packing the wrist inside the closely fitting eight channel wrist array coil used for the median nerve experiments.

A series of 500 dynamic Echo Planar images are acquired with the TENS device firing simultaneously with a very short repeat time of 88 ms [23]. In addition image series are acquired without stimulation as a control. The much higher repeat time used for dfMRI, while producing lower SNR due to T1 saturation, allowed frequencies up to 6 Hz to be measured without aliasing compared to just 0.25 Hz in

**Fig. 7.8** Diagram showing location of the electrodes on the palm and positioning of the TENS device outside the magnet



conventional BOLD experiments. Images are analyzed by taking the Fourier transform of the time series from regions of interest located on the median nerve and in normal tissue for comparison. Spectral peaks at the stimulation frequency with a SNR  $> 3:1$  are accepted as responses if there are no equivalent responses in normal tissue or in the median nerve in control time series (Fig. 7.9).

Figure 7.10 shows the location of the axial slice and a high resolution image used to locate the position of the median nerve. Figure 7.11 (left) shows the location of two regions of interest (ROIs) on one frame of the acquired time series during TENS stimulation. Results similar to those shown in Fig. 7.11 (right) were observed in 18 out of 20 experiments using a stimulation frequency of 2.5 Hz and 17 of 20 experiments using a stimulation frequency of 3.5 Hz in a study performed on six

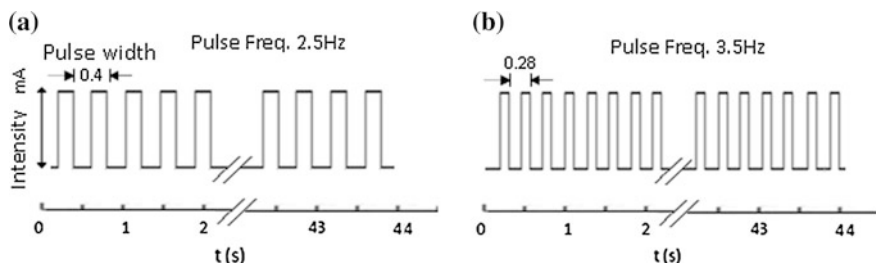


**Fig. 7.9** Stimulation paradigm for 2.5 Hz and 3.5 Hz TENS. The TENS stimulation was applied asynchronously with the dfMRI acquisition

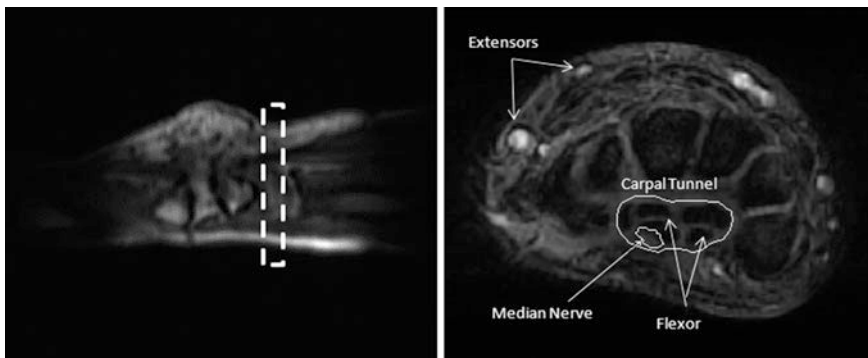


**Fig. 7.10** Localizer image showing a slice through the wrist selected for dfMRI acquisition (*left*). High resolution slice from a full 3D acquisition showing the location of the median nerve within carpal tunnel (*right*)

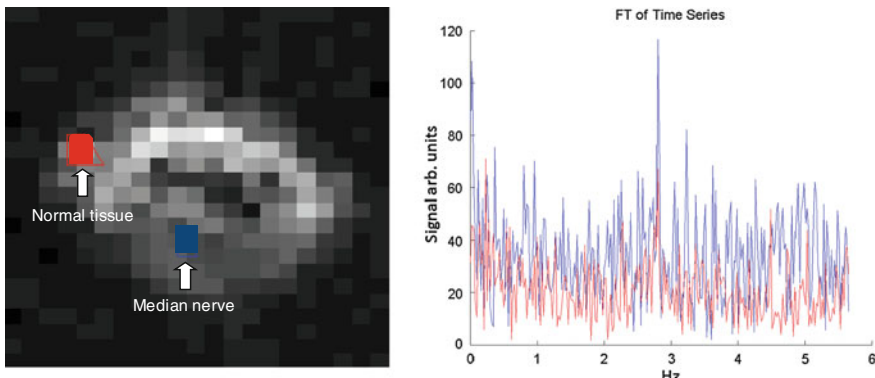


**Fig. 7.11** Echo Planar dfMRI image of the wrist: one image from a time series of 500 acquired during TENS stimulation at 2.8 Hz (*left*). Frequency response from median nerve (*blue trace*) and ‘normal tissue’ (*red trace*), showing a possible response from the median nerve at the applied TENS frequency of 2.8 Hz but no response from the normal tissue. Also, no response was seen from the median nerve in control experiments without stimulation applied

healthy volunteers suggesting that it may be feasible to directly detect TENS stimulated firing of the median nerve using dfMRI. However, the signal to noise ratio for detected responses in these experiments is very poor at  $\sim 3:1$  so the reliability may be insufficient for use in a control interface application without further advances in sensitivity. In addition, although the overall acquisition times are relatively short in duration ( $\sim 45$  s), the Fourier responses are effectively averaged over many electrical pulses (typically 100–150 pulses depending on frequency) [23].

## 7.3 Novel Low Field MRI Technology for dfMRI

This section looks at the potential of novel compact MRI system technology for use in Brain Computer Interfaces including cryogenic radiofrequency coils and the potential of hyperpolarization to revolutionise the sensitivity of dfMRI using low field MRI scanners. Direct electromagnetic effect functional MRI is fundamentally limited by the MRI system sensitivity for detection of weak magnetic fields from axons and neurons. Typically MR samples are only polarised to a few parts per million using a magnetic field. It is possible to externally boost this polarisation by a number of advanced techniques so that it approaches almost 100 % yielding a massive increase in the available signal. The MR polarization effects described here actually operate very effectively when imaging at low magnetic field strengths and could possibly be used to improve the sensitivity for dfMRI. Biologically compatible free radicals boost MRI sensitivity through a number of mechanisms. Overhauser MRI produces MR signal enhancement in real time through microwave irradiation of free radicals in the sample of interest which transfer their high polarisation to surrounding nuclei of interest. Dissolution DNP, on the other hand, produces a highly polarized sample using an external polarizer at very low temperatures with microwave irradiation of a free radical over a duration of many seconds (typically 1 h). Following rapid dissolution using a high pressure and temperature solvent, the enhanced polarisation solution is injected into a subject and acts as a metabolizing contrast agent. To enhance dfMRI the agents would need to enter or be in close proximity to the active axons or neurons which represents a developmental challenge to be overcome.

### 7.3.1 Compact Low Field MRI Systems for dfMRI Research

Most MRI systems involved in fMRI research have typically operated at magnetic field strengths of 1.5 T or higher and have a traditional cylindrical enclosed bore. This is because the BOLD effect relies on the susceptibility difference between oxygenated and non-oxygenated blood which produces a larger effect on the R<sub>2\*</sub> relaxation rate at higher field strength. In comparison, the direct electromagnetic effect is a fixed size modulation, independent of field strength and so can potentially be investigated using much lower magnet field strengths and hence cheaper MR systems.

The advantages of using lower fields for dfMRI research are:

- Physiological artifacts on the MRI signal from e.g. cardiac pulsation and respiration are much lower at lower field strength. This is primarily because the radiofrequency coils interact more weakly with the body at lower frequencies due to less inductive coupling.
- Acoustic noise is much lower if auditory stimulation paradigms are required

- Specific absorption rate, a measure of the biological heating effect of applied radiofrequency fields, is much lower, even at the electron spin resonance frequency, so enhancement methods such as Overhauser MRI (OMRI) can potentially be used where high electron spin polarization is transferred to the nuclear spins.
- System spectrometer stability is easier to control at lower frequency.
- Missile projectile effects are minimized and support equipment containing ferromagnetic materials can be brought closer to the magnet.
- It is possible to design more compact, open magnets at lower field strengths due to the lower stresses on components and no necessary requirement for use of a bulky cryostat.

A number of dedicated MRI systems aimed at scanning a specific part of rather than the whole body have begun to gain popularity. In the rest of this chapter, the design aspects of low cost MRI systems which could be useful for dfMRI research towards a brain computer interface are described.

Figure 7.13 illustrates the capability of the compact MRI system, shown in Fig. 7.12, to visualize the adult human brain for dfMRI research at low field. Some geometrical distortion of the image is observed at the top and bottom of the head as the uniform field of view of the system is a 160 mm sphere whereas the adult head is typically 220 mm (back to front)  $\times$  160 mm (side to side).

Only the top of the brain can be visualized with the current system due to the shoulders blocking further entry to the centre of the magnet. However, it can be used to scan the whole brains and bodies of neonates or small children [51]. The brain structures including gyral folds can be clearly observed and this type of image could also be used for attempting to detect dfMRI at low field using the GRACE method discussed above [52], together with a suitable brain stimulation paradigm e.g. TENS electrical stimulation of the median nerve to excite the motor-sensory strip. A new magnet design with a slightly increased gap and improved uniform field fitting inside the existing covers is currently under development and will allow the entire adult brain to be investigated in future.

### **7.3.2 Cryogenic Coils for Improved Sensitivity of Low Field MRI**

The performance of an MRI system depends critically on the sensitivity of its radiofrequency receiver coils. In turn, the performance of a radiofrequency coil depends on its Q factor where:

$$Q = \omega / \delta\omega \quad (7.2)$$

$\omega$  is the Larmor (operating) frequency of the coil and  $\delta\omega$  is the 3 db bandwidth of the coil.

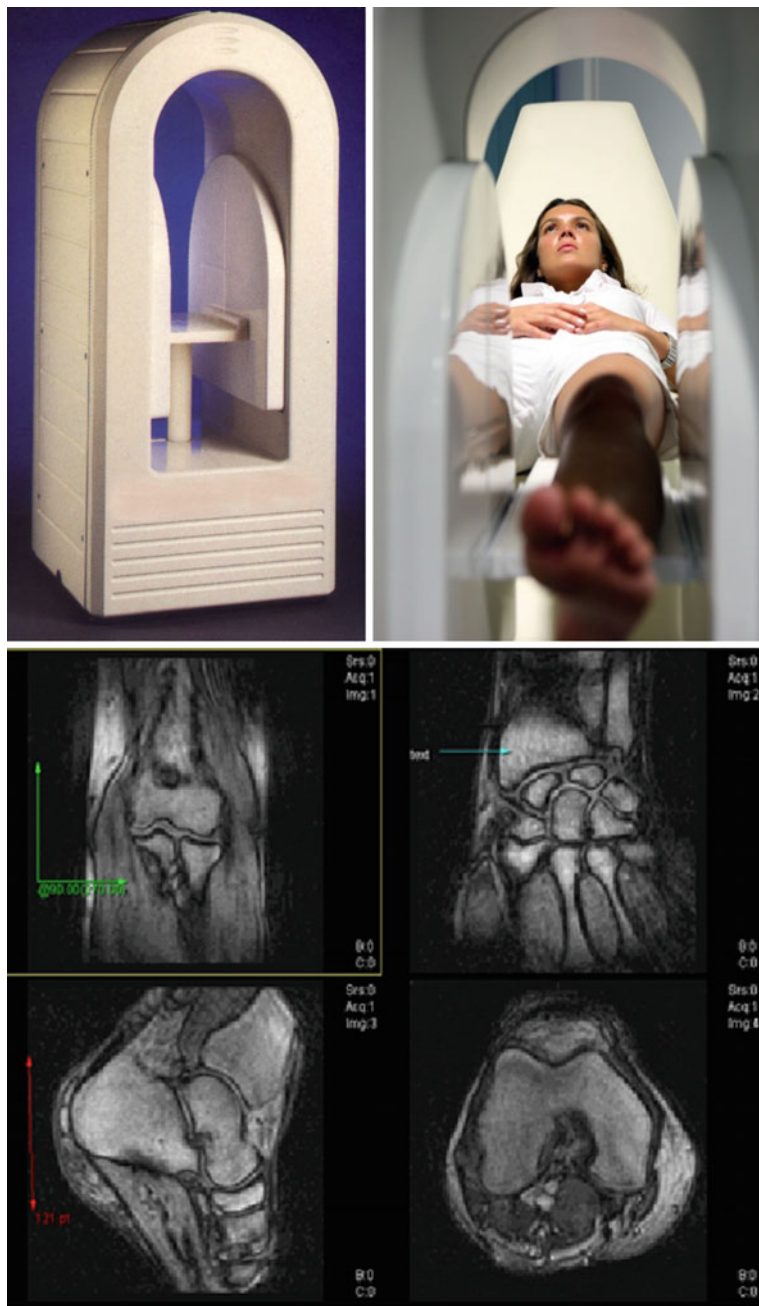
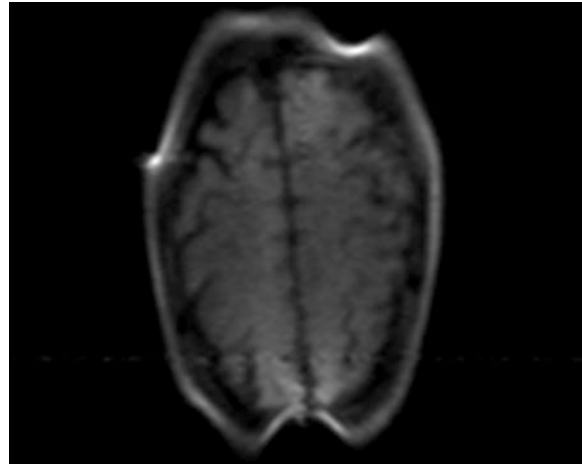


**Fig. 7.12** Low cost, compact 0.2 T Niche MRI system using a Neodymium Boron Iron magnet designed for imaging neonates and extremities. However, the system can also be used for imaging the top section of the adult cerebral cortex for dfMRI research at low field as shown in Fig. 7.13. The MR images above show an elbow, a wrist, an ankle and a knee in various acquisition planes demonstrating good spatial resolution (< 1 mm in plane) and high tissue contrast. The dimensions of the system are 530 (W) × 530 (D) × 1,100 (H) mm and the system only weighs 500 kg. The imaging volume is a 160 mm sphere and the magnet aperture measure 750 × 200 mm

**Fig. 7.13** Adult brain T1 weighted image in the axial plane (TR = 300 ms, TE = 20 ms, FOV = 256 mm, SLT = 5 mm, NEX = 2) acquired on the low field 0.2 T Niche dedicated MRI system



The Q factor is determined largely by the resistance of the coil so by manufacturing the coil using a high temperature superconducting material, which is superconducting at liquid Nitrogen temperatures, the Q can be increased dramatically providing significantly higher image signal to noise ratio.

Use of the superconducting surface receiver coil as seen in Fig. 7.14 was shown to improve the signal to noise ratio by a factor of up to four in direct comparison with an equivalent room temperature copper coil [9]. A typical image through the hand is shown in Fig. 7.15 illustrating very high signal to noise ratio. This is equivalent to increasing the field strength of the 0.2 T Niche MRI system as shown



**Fig. 7.14** Cryogenic superconducting radiofrequency coil designed to operate at 7.2 MHz and 77 K for use on the low field Niche MRI system. The outer diameter of the spiral coil is 100 mm and there are ten turns of superconducting material deposited on a sapphire base



**Fig. 7.15** Axial spin echo T1 weighted image acquired through the hand with the cryogenic superconducting coil above cooled to 77 K with liquid Nitrogen in a dedicated vacuum dewar on the 0.2 T Niche MRI system. This type of image could potentially be used with the GRACE method for detection of median nerve stimulation at low field. Note the much improved SNR and geometrical fidelity compared with the EPI image of the wrist acquired at the much higher field strength of 1.5 T shown in Fig. 7.12

in Fig. 7.12 up to 0.8 T in terms of MRI sensitivity. Arrays of such cryogenic coils could dramatically increase MRI sensitivity for dfMRI research of the brain at low field in a very compact unit which could be useful in future as a brain computer interface.

### 7.3.3 Overhauser Enhanced MRI

Dynamic Nuclear Polarization (DNP) in liquid state is a double magnetic resonance technique, which combines the high sensitivity of nuclear magnetic resonance (NMR) of water protons with the high specificity of free radicals EPR [19, 27, 33]. It is also called Proton-Electron Double Magnetic Resonance Imaging (PEDRI) [34] or Overhauser enhanced magnetic resonance imaging (OMRI) [6, 28, 41, 49], and is based on the Overhauser effect where the electron spin resonance (ESR) of the free radical is irradiated during the acquisition of an MR image [49]. It creates images of the free radical distribution in an object. The transfer of polarization from unpaired electron spins to the coupled proton spins results in the enhancement of the NMR signal in regions of the sample containing the free radical. This leads to the possibility of NMR imaging at very low magnetic fields [14, 15, 53, 29].

Nitroxyl radicals belong to the six-membered piperidine (TEMPO) or the five-membered pyrrolidine (PROXYL) class [35]. They are stable organic free radicals,

are less toxic and serve as in vitro and in vivo antioxidants. Their paramagnetic nature, with a single unpaired electron, means they can be used as imaging probes for in vivo ESR spectroscopy or imaging. Carbamoyl-PROXYL has been widely used as a spin probe for in vivo ESR imaging and reactive oxygen species (ROS) monitoring as well as a contrast agent for Overhauser imaging. It has also been used to evaluate in vivo free radical reactions and the redox status in living animals. To achieve maximum possible Overhauser enhancement, it is necessary to irradiate the ESR transition of the nitroxyl agent for at least  $3T_1$ . Benial et al. reported an optimum ESR irradiation time,  $T_{ESR}$  of 600 ms, a compromise between the signal enhancement and RF heating [6]. They also found that the enhancement factor reached a plateau for  $^{14}\text{N}$  and  $^{15}\text{N}$ -labeled carbamoyl-PROXYL at a concentration of 2.5–3.0 mM, and then started to decline above 3 mM. Detailed theories of PEDRI or OMRI can be found in the literature [14, 28, 53, 29] The enhancement factor,  $E$ , of the NMR signal of the  $^1\text{H}$  nuclei ( $I = \frac{1}{2}$ ) of water molecules with couplings to an unpaired electron spin  $S = \frac{1}{2}$  of a dissolved free radical, is given by:

$$E = \langle I_z \rangle / I_O = 1 - \rho fs |\gamma_s/\gamma_I| \quad (7.3)$$

where  $\langle I_z \rangle$  denotes the expectation value of the DNP,  $I_O$  is its thermal equilibrium value,  $\rho$  is the coupling parameter ( $-1 \leq \rho \leq 1/2$ ),  $f$  is the leakage factor ( $0 \leq f \leq 1$ ),  $s$  is the saturation parameter ( $0 \leq s \leq 1$ ),  $\gamma_s$  and  $\gamma_I$  are electron and proton gyromagnetic ratios respectively, and the absolute value of their ratio is 658. The coupling parameter  $\rho$  depends on the nature of the interaction between the contrast agent and the protons, the leakage factor  $f$  accounts for the fraction of nuclear relaxation caused by the presence of the paramagnetic contrast agent, the saturation parameter  $s$  is the amount of saturation of the EPR resonance. In an ideal situation, the maximum possible enhancement is  $-\gamma_s/2\gamma_I$ . A negative enhancement means a phase change of  $180^\circ$  in the NMR signal.

### 7.3.4 An Ultra-low Field Overhauser Enhanced dfMRI System

The use of DNP at very low magnetic field [35] offers some interesting advantages including very low magnet cost and high contrast in biological tissue [40]. DNP enhanced imaging experiments have been performed using a home-built low field MR system which operates at 8.2 mT, as shown in Fig. 7.16a [29]. The system was designed to produce a uniform field within a few parts per million (ppm) over a uniform sphere of about 100 mm. The magnet was supplied with 16 Amps from a DC power supply (Agilent 6673A, U.S.) and simply was air cooled. A split solenoid transmit-receive coil (30 mm diameter, 65 mm length, 11 mm gap in the middle) was used for NMR imaging, and was tuned to 348 kHz which is the frequency for  $^1\text{H}$  NMR at 8.2 mT. Another RF loop coil (30 mm diameter) was placed at the centre of the split solenoid to produce the corresponding irradiation at

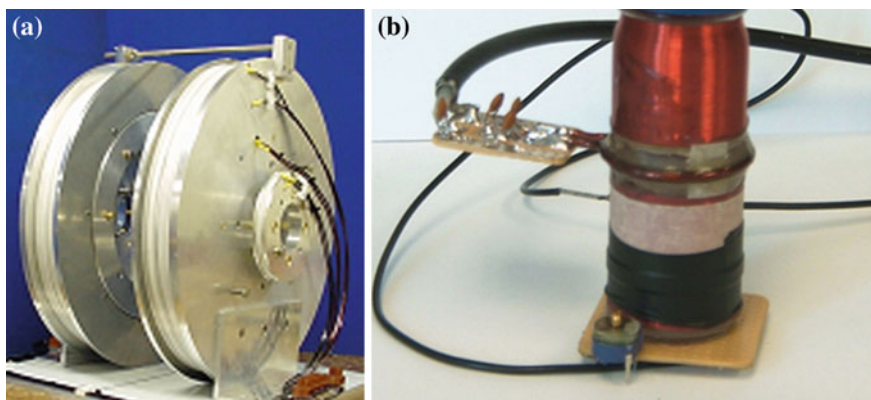


**Fig. 7.16** **a** Low field, inexpensive 8.2 mT MRI magnet useful for dfMRI research **b** DNP coil consisting of a solenoid coil for MR imaging and a loop coil (*centre*) for the EPR irradiation

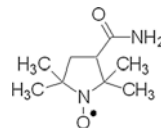


**Fig. 7.17** Chemical structure of 3-Carbamoyl-Proxyl (3-Carbamoyl-2,2,5,5-tetramethyl-1-pyrrolidineoxy)

the electron spin resonance frequency of 239 MHz (Fig. 7.16b). The ESR transmit coil was driven by a 50 W Power Amplifier (LZY-1 Mini-Circuit Europe, U.K.).

3-Carbamoyl-Proxyl (3-Carbamoyl-2,2,5,5-tetramethyl-1-pyrrolidineoxy) (Sigma Co., St. Louis, MO, USA) was used as the spin probe. Figure 7.17 shows the chemical structure. C-PROXYL was prepared in distilled water at a concentration of 3 mM, which has been reported to give optimum DNP enhancement [49]. The phantom was a cylindrical vial (28 mm diameter, 70 mm length) filled with ~40 ml 3-Carbamoyl-Proxyl solution. All experiments were performed at room temperature.

MR images acquired with a gradient echo sequence with an ESR pre-pulse of 600 ms as shown in Fig. 7.18.

Figure 7.19 shows images of the cylindrical phantom with and without the ESR irradiation present. It can be seen that the signal intensity close to the ESR surface coil dramatically increases when the electrons are excited producing dynamic nuclear polarization of the adjacent proton spins in water. Figure 7.20 shows vertical line profiles through the phantom illustrating clearly the massive signal increase due to the Overhauser effect.

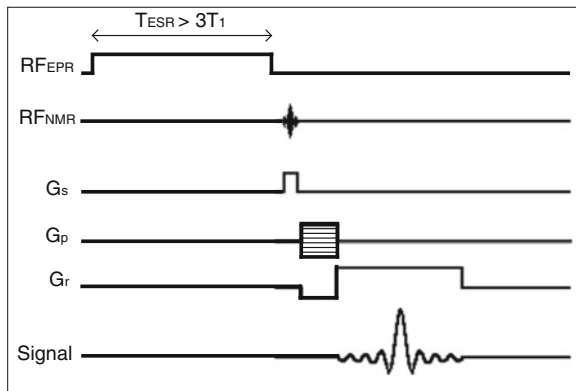


**Fig. 7.18** Sequence diagram for DNP imaging with a standard Gradient Echo (GE) sequence at an NMR frequency preceded by ESR saturation pulse at the electron spin resonance frequency (239 MHz) to produce Overhauser enhancement.  $T_{ESR} > 3T_1$

The potential of Overhauser enhanced MRI is thus to improve the sensitivity for detection of direct electromagnetic effects by factors of an order of magnitude. Whether interactions between electrons and ions may make O-MRI even more sensitive for detection of ionic currents is not yet known. However, O-MRI is subject to limitation by thermal SAR deposition of the high ESR frequency within the human body. This is why O-MRI works better at low magnetic field strengths where the ESR frequencies are much lower. However, the initial application of O-MRI to dfMRI is most likely to be for experiments in animals.

### 7.3.5 Dissolution Dynamic Nuclear Polarization Enhanced dfMRI

Dynamic Nuclear Polarization (DNP) is ideally performed at very low temperatures,  $\sim 1$  K. The magnetic resonance signal is enhanced above the room temperature thermal equilibrium value by up to four orders of magnitude by combining microwave irradiation of free radicals within the sample with the low temperature [1]. The free radicals are polarized to almost 100 % and then transfer this polarization to  $^{13}\text{C}$  nuclei in their vicinity. The sample is then rapidly dissolved back into the liquid phase using a high pressure and temperature solvent. The polarization is retained for a period of 1–2 min and is rapidly injected into a subject. Using  $^{13}\text{C}$  labelled metabolites, both the spectral and temporal resolution is dramatically increased compared to  $^1\text{H}$  MRS [30] allowing real time observation of metabolism in vivo [50, 54]. Hyperpolarized magnetization decays back to thermal polarization levels with the  $T_1$  rate. The  $T_1$  relaxation times for  $^{13}\text{C}$  can be in the range of seconds to minutes, depending on the local molecular environment and the signal fully decays within a time of  $\sim 5x$  the  $T_1$  value. Commercial polarizer systems are

**Fig. 7.19** Shows images of the uniform cylindrical phantom before (*top*) and after (*bottom*) the ESR irradiation at 239 MHz is switched on. The MR signal in the region of the ESR coil is enhanced by a factor of over 10 x which suppresses the signal from the rest of the phantom as seen in the *top* image

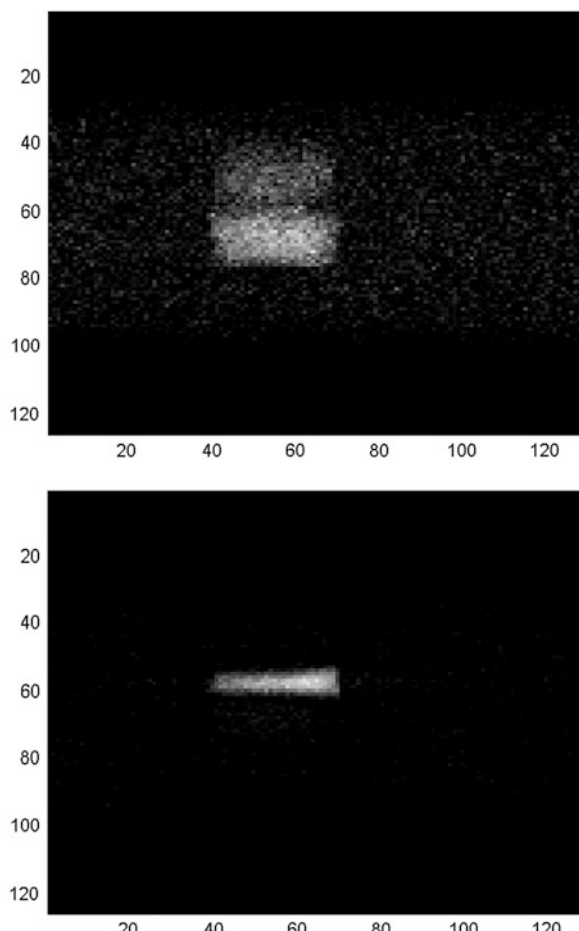


**Fig. 7.20** Shows a profile through the uniform cylindrical phantom before and after the ESR irradiation is switched on. After the ESR is switched on the MR signal in the region of the ESR coil is enhanced by a factor of over 10x

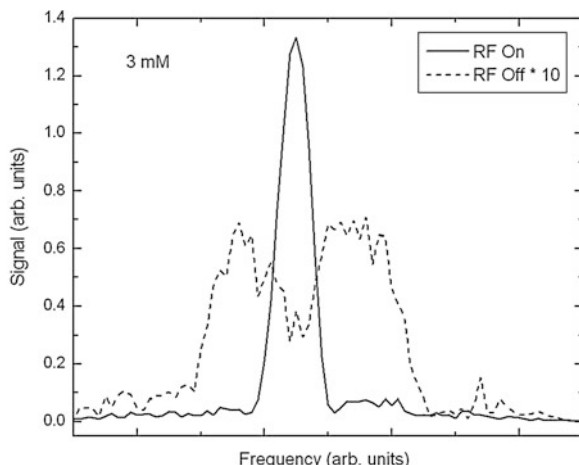




**Fig. 7.21** HyperSense dissolution DNP system operates at 1 K and a microwave frequency of 93.5 GHz to polarize a solution of trityl free radical together with a biological substrate which can be metabolized e.g. pyruvate. The DNP system enhances sensitivity for  $^{13}\text{C}$  nuclei by more than 10,000x. It may be possible in future to develop suitable contrast agents to enhance low field dfMRI using this technology. DNP works equally as well for low field strength MRI as the polarization generated does not depend on the field strength of the MR system used for imaging

available such as the Hypersense (Oxford Instruments, Oxford, UK) as shown in Fig. 7.21.

Automated injectors and sophisticated kinetic analysis help make this process quantitative [1, 25, 43, 44]. For hyperpolarized  $^{13}\text{C}_1$ -pyruvate, the signal lasts for a few minutes and thus must be quickly administered to a subject and  $^{13}\text{C}$  spectra rapidly acquired. The time series of acquired spectra or images are analyzed to produce intensity versus time plots which can be fitted to an appropriate kinetic model as shown in Fig. 7.22.

The sensitivity of the experiment is several orders of magnitude higher than obtained from normal, thermally polarized MR. This method may also be of use for enhancing dfMRI experiments at low field in future if suitable substrates can be developed. The wide spectral range of  $^{13}\text{C}$  nuclei mean that even at relatively low field, different compounds can be resolved spectrally. Sterile polarisers for human use are already available and are being used in clinical trials of prostate cancer [2].

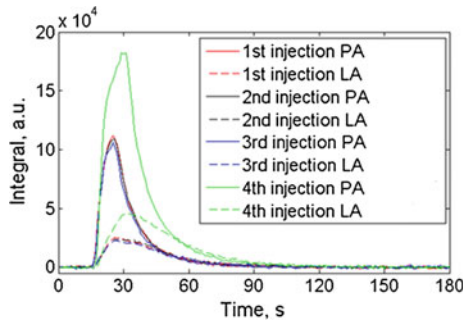


**Fig. 7.22** Shows a set of dissolution DNP experiments performed in a rat brain with and without the use of a flow diverter (4th injection—green trace) to minimise the effects of dead space within the injection cannula. Signal localisation was performed using a 20 mm  $^{13}\text{C}/^1\text{H}$  surface coil positioned over the animal head, with 8 mm slice selection in a coronal plane containing the brain.  $^{13}\text{C}$  spectroscopic data was acquired using a Gaussian pulse ( $20^\circ$  flip angle,  $\text{TR} = 1$  s) in a Bruker 7 T MRI system. Spectroscopic data containing the PA and lactate (LA) signals were processed in Matlab using customized software. A clear increase in the signal can be seen with use of the diverter which reduces partial volume effects for the injected metabolite. To be able to detect these signals from  $^{13}\text{C}$  nuclei in an active metabolite represents an increase in MR sensitivity of approximately 10,000x. Such an extreme increase in sensitivity may enable dfMRI experiments to be performed in future with appropriate metabolic agents targeted at neuronal and axonal events

## 7.4 A dfMRI Brain Computer Interface Proposal

The final section proposes a possible solution for a dfMRI Brain computer Interface and discusses the advanced MR technology which will need to be developed to achieve this exciting goal.

### 7.4.1 Advanced Open dfMRI System Design

It should be possible to combine the various elements of MR technology in terms of hardware, acquisition sequences and software described above into a cost effective low field research system for an MR based brain computer interface.

A 0.2 T permanent magnet with a  $350 \times 800$  mm aperture would be used with a close fitting co-planar Gradient and Transmit-Receive RF coil array. Cryogenic cooling of the RF coil arrays could be used to increase sensitivity. Feedback loops would be implemented to maintain very high magnet, gradient and RF stability, which is the real key to being able to detect dfMRI. Addition of a DNP system with a suitable hyperpolarized substrate could potentially bring the sensitivity of dfMRI to a practical level for use with BCI. Adoption of the GRACE ghost acquisition and analysis method would allow very high frequencies to be measured without the significant artifacts associated with EPI. This proposed new low field fMRI BCI system is illustrated in Fig. 7.23.

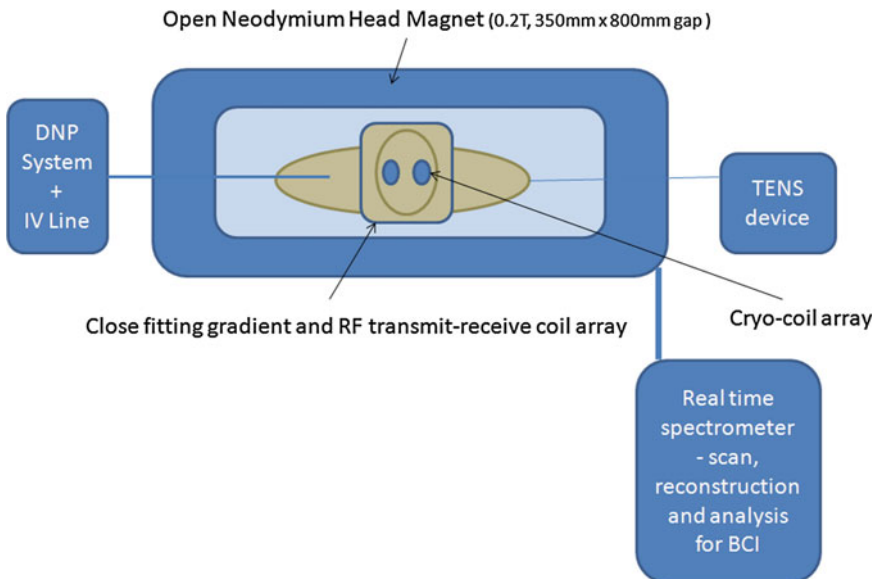


**Fig. 7.23** Shows a schematic diagram of a possible MR based Brain computer Interface based on a low field dfMRI design

#### 7.4.2 The dfMRI BCI

This chapter has concentrated on recent technology advances which could lead to the possibility of a cost-effective MRI based BCI system in future. A complete dfMRI BCI system would, as well as the acquisition equipment already described, require a sophisticated software package to rapidly analyze in real-time the acquired MR images for ghosts or spectral components corresponding to motor, visual, tactile, olfactory or auditory stimulation or perhaps more importantly, the associated mental imagery and compare them with previous images or training sets. This data would then be used to classify a brain computer response and output the appropriate control commands to the desired hardware interface as illustrated schematically in Fig. 7.24.

A dfMRI system could be enhanced by multi-modal operation in combination with both EEG and optical spectroscopy. EEG is easier to combine with MRI at lower field strengths due to less artifacts being generated by the MRI system on the EEG traces and optical spectroscopy is inherently MR compatible [3, 17, 36]. MRI can also be used to provide spatial boundary conditions for EEG and MEG reconstructions providing improved source localization. New hybrid MR-PET systems are also being discussed in terms of functional imaging which may eventually be useful for BCI developments, albeit most likely as research options only due to the high costs involved [47].

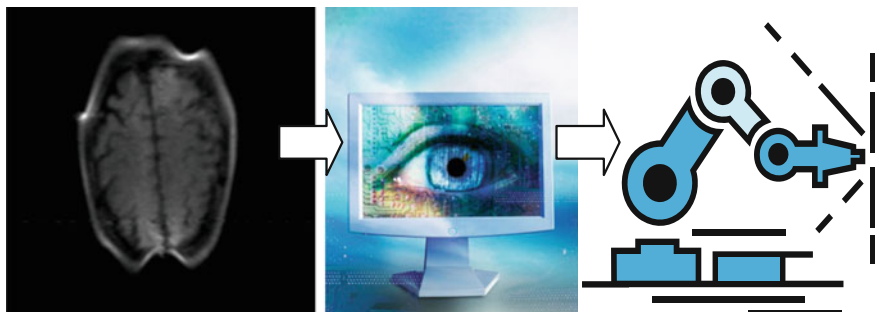


**Fig. 7.24** Overview of a dfMRI based BCI system

## 7.5 Discussion and Conclusions

Direct electromagnetic detection fMRI, although not yet fully established as a reliable clinical method, has great potential. The ability to detect neuronal responses with a temporal resolution of tens of milliseconds using MRI combined with sub millimeter spatial resolution has already been demonstrated in experimental settings and advances in detection sensitivity as provided by cryogenic radiofrequency coils and polarization enhanced contrast mechanisms are predicted to increase the reliability of this detection process in future.

The key to improvements in reliability of detection of the direct MRI effect is development of ultra-high stability spectrometer systems. This places a premium on engineering of the amplifier and coil systems which transmit, receive and spatially encode the MR signal as well as improvements in the inherent stability of the basic magnetic field. Low field, low cost magnets for BCI systems will require improved feedback systems to counteract the effects of temperature and mechanical vibrations; problems which are not really encountered with expensive, high field, cryogenic magnets. Digital control systems and radiofrequency synthesizers are already low cost but highly stable and of sufficient quality to provide the high temporal stability required.

New MRI acquisition strategies which radically under-sample the spatial information required to create an MR image are also increasing the ability of fMRI to measure real time responses and when linked with high speed parallel hardware based image processors, enable real time analysis of function in a reduced digital format that is potentially usable for a BCI robotic control system. The major advantage of MRI over other non-invasive methods currently is the accurate 3D spatial localization of the functional source which is likely to be a key factor in creating rich Brain Computer Interfaces. In fact the precise 3D capability of fMRI is probably the major reason for focusing effort on this modality. The ability of MRI to measure responses in peripheral nerves may also mean it could play a role in creating robotic limb interfaces in future.

In addition, MRI is compatible with other low cost functional methods such as EEG or ultrasound and combined systems which take advantage of each modality may play an important role. For example, MRI can be used to provide well defined boundary conditions to more accurately identify EEG dipole sources (see Chap. 4).

In conclusion, the new MR sensitivity enhancement methods discussed here could revolutionize the ability of dfMRI to measure brain function with unprecedented spatial and temporal resolution using compact, low cost, low field MRI systems. Such novel, personal MRI systems may eventually play a significant role in enabling sophisticated Brain Computer Interfaces with both high temporal and 3D spatial resolution.

## References

1. Ardenkjaer-Larsen, J.H., Fridlund, B., Gram, A., Hansson, G., Hansson, L., Lerche, M.H., Servin, R., Thaning, M., Golman, K.: Increase in signal-to-noise ratio of > 10,000 times in liquid-state NMR. *Proc. Natl. Acad. Sci. U. S. A.* **100**(1), 10158–10163 (2005)
2. Ardenkjaer-Larsen, J.H., Leach, A.M., Clarke, N., Urbahn, J., Anderson, D., Skloss, T.W.: Dynamic nuclear polarization polarizer for sterile use intent. *NMR Biomed.* **24**(1), 927–932 (2011)
3. Azar, A.T., Balas, V.E., Olariu, T.: Classification of EEG-based brain-computer interfaces. *Advanc. Intell. Comput. Technol. Decis. Support Syst. Comput. Intell.* **486**(2014), 97–106 (2014)
4. Barber, D.C., Brown, B.H.: Imaging spatial distributions of resistivity using applied potential tomography. *Electronics Lett.* **19**(22), 933–935 (1983)
5. Bechtereva, N.P., Abdullaev, Y.G.: Depth electrodes in clinical neurophysiology: neuronal activity and human cognitive function. *Int. J. Psychophysiol.* **37**(1), 11–29 (2000)
6. Benial, A.M.F., Ichikawa, K., Murugesan, R., Yamada, K., Utsumi, H.: Dynamic nuclear polarization properties of nitroxyl radicals used in Overhauser-enhanced MRI for simultaneous molecular imaging. *J. Magn. Reson.* **182**(1), 273–282 (2006)
7. Bodurka, J., Bandettini, P.A.: Toward direct mapping of neuronal activity: MRI detection of ultraweak, transient magnetic field changes. *Magn. Reson. Med.* **47**(6), 1052–1058 (2002)
8. Bodurka, J., Jesmanowicz, A., Hyde, J.S., Xu, H., Estkowski, L., Li, S.J.: Current induced magnetic resonance phase imaging. *J. Magn. Reson.* **137**(1), 265–271 (1999)
9. Cheong, H.S., Wild, J., Alford, N., Valkov, I., Randell, C., Paley, M.: A high temperature superconducting imaging coil for low-field MRI. *Concept Magn. Reson. B* **37B**(2), 56–64 (2010)
10. Chow, L.S., Cook, G.G., Whitby, E., Paley, M.N.: Investigating direct detection of axon firing in the adult human optic nerve using MRI. *Neuroimage* **30**(3), 835–846 (2006)
11. Chow, L.S., Cook, G.G., Whitby, E., Paley, M.N.: Investigation of MR signal modulation due to magnetic fields from neuronal currents in the adult human optic nerve and visual cortex. *Magn. Reson. Imag.* **24**(6), 681–691 (2006)
12. Chow, L.S., Cook, G.G., Whitby, E., Paley, M.N.: Investigation of axonal magnetic fields in the human corpus callosum using visual stimulation based on MR signal modulation. *J. Magn. Reson. Imag.* **26**(2), 265–273 (2007)
13. Chow, L.S., Dagens, A., Fu, Y., Cook, G.G., Paley, M.N.: Comparison of BOLD and direct-MR neuronal detection (DND) in the human visual cortex at 3T. *Magn. Reson. Med.* **60**(5), 1147–1154 (2008)
14. de Sousa, P.L., de Souza, R.E., Engelsberg, M., Colnago, L.A.: Mobility and free radical concentration effects in proton-electron double-resonance imaging. *J. Magn. Reson.* **135**(1), 118–125 (1998)

15. Dwek, R.A., Richards, R.E., Taylor, D.: Nuclear electron double resonance in liquids. *Annu. Rev. NMR Spectrosc.* **2**(1), 293–344 (1969)
16. Eyuboglu, B.M., Reddy, R., Leigh, J.S.: Imaging electrical current density using nuclear magnetic resonance. *Elektrik* **6**(1), 201–214 (1998)
17. Fazli, S., Mehnert, J., Steinbrink, J., Curio, G., Villringer, A., Müller, K.-R., Blankertz, N.: Enhanced performance by a hybrid NIRS-EEG brain computer interface. *NeuroImage* **59**(1), 519–529 (2012)
18. Gratton, G., Fabiani, M.: Fast optical signals: principles, methods and experimental results. In: Frostig, R.D. (ed.) *In vivo optical imaging of brain function*. CRC Press, Boca Raton (2002)
19. Guiberteau, T., Grucker, D.: Dynamic nuclear polarization at very low magnetic fields. *Phys. Med. Biol.* **43**(1), 1887–1892 (1998)
20. Hamalainen, M., Hari, R., Ilmoniemi, R.J., Knuutila, J., Lounasmaa, O.V.: Magnetoencephalography—theory, instrumentation, and applications to noninvasive studies of the working human brain. *Rev. Mod. Phys.* **65**(1), 413–497 (1993)
21. Hennig, J., Speck, O., Koch, M.A., Weiller, C.: Functional magnetic resonance imaging: a review of methodological aspects and clinical applications. *J. Magn. Reson. Imag.* **18**(1), 1–15 (2003)
22. Joy, M., Scott, G., Henkelman, M.: In vivo detection of applied electric currents by magnetic resonance imaging. *Magn. Reson. Imag.* **7**(1), 89–94 (1989)
23. Kaka, S., Paley, M.: Investigating possible fMRI responses in the median nerve during wrist stimulation by Transcutaneous Electrical Nerve Stimulation (TENS). In: *Proceedings of the ISMRM and ESMRMB Joint Annual Scientific Meeting*, p. 1,783. Milan, May 2014
24. Kamei, H.I.K., Yshikawa, K., Ueno, S.: Neuronal current distribution imaging using magnetic resonance. *IEEE Trans. Magn.* **35**(1), 4109–4111 (1999)
25. Kazan, S.M., Reynolds, S., Kennerley, A., Wholey, E., Bluff, J.E., Berwick, J., Cunningham, V.J., Paley, M.N., Tozer, G.M.: Kinetic modeling of hyperpolarized <sup>13</sup>C pyruvate metabolism in tumors using a measured arterial input function. *Magn. Reson. Med.* **70**(4), 943–953 (2013)
26. Konn, D., Gowland, P., Bowtell, R.: Towards the direct detection of neuronal activity in the brain: simulating and measuring the magnetic field from an extended current dipole in a homogeneous conducting sphere. In: *Proceedings of the 10<sup>th</sup> Annual Meeting of ISMRM*, p. 1,326, Hawaii (2002)
27. Krishna, M.C., Devasahayam, N., Cook, J.A., Subramanian, S., Kuppusamy, P., Mitchell, J. B.: Electron paramagnetic resonance for small animal imaging applications. *ILAR J.* **42**(1), 209–218 (2001)
28. Krishna, M.C., English, S., Yamada, K., Yoo, J., Murugesan, R., Devasahayam, N., Cook, J. A., Golman, K., Ardenkjaer-Larsen, J.H., Subramanian, S., Mitchell, J.B.: Overhauser enhanced magnetic resonance imaging for tumor oximetry: coregistration of tumor anatomy and tissue oxygen concentration. *PNAS* **99**(4), 523–529 (2002)
29. Krjukov, E., Fichele, S., Wild, J.M., Paley, M.N.J.: Design and evaluation of a low field system for hyperpolarized <sup>3</sup>-He gas imaging of neonatal lungs. *Conc. Magn. Reson. Part B* **31B**, 209–217 (2007)
30. Kurhanewicz, J., Vigneron, D.B., Brindle, K., Chekmenev, E.Y., Comment, A., Cunningham, C.H., Deberardinis, R.J., Green, G.G., Leach, M.O., Rajan, S.S., Rizi, R.R., Ross, B.D., Warren, W.S., Malloy, C.R.: Analysis of cancer metabolism by imaging hyperpolarized nuclei: prospects for translation to clinical research. *Neoplasia* **13**(2), 81–97 (2011)
31. Liu, A.K., Dale, A.M., Belliveau, J.W.: Monte Carlo simulation studies of EEG and MEG localization accuracy. *Hum. Brain Mapp.* **16**(1), 47–62 (2002)
32. Logothethis, N.K., Pauls, J., Augath, M., Trinath, T., Oeltermann, A.: Neurophysiological investigation of the basis of the fMRI signal. *Nature* **412**(6183), 150–157 (2001)
33. Lurie, D.J., Bussell, D.M., Bell, L.H., Mallard, J.R.: Proton-electron double magnetic resonance imaging of free radical solutions. *J. Magn. Reson.* **76**(1), 366–370 (1988)
34. Lurie, D.J., Foster, M.A., Yeung, D., Hutchison, J.M.S.: Design, construction and use of a large-sample field-cycled PEDRI imager. *Phys. Med. Biol.* **43**(1), 1877–1886 (1998)

35. Matsumoto, S., Yamada, K., Hirata, H., Yasukawa, K., Hyodo, F., Ichikawa, K., Utsumi, H.: Advantageous application of a surface coil to EPR irradiation in Overhauser-enhanced MRI. *Magn. Reson. Med.* **57**(4), 806–811 (2007)
36. Mullinger, K., Richard, Bowtell R.: Combining EEG and fMRI. Magnetic resonance neuroimaging methods in molecular biology **711**(1), 303–326 (2011)
37. Ogawa, S., Lee, T.M., Kay, A.R., Tank, D.W.: Brain magnetic resonance imaging with contrast dependent on blood oxygenation. *Proc. Natl. Acad. Sci. U.S.A.* **87**(1), 9868–9872 (1990)
38. Paley, M.N.J., Kryukov, E., Lamperth, M., Young, I.R.: An independent multichannel imaging research system for ultrashort echo time imaging on clinical MR systems. *Concepts Magn. Reson. Part B (Magn. Reson. Eng.)* **35B**(2), 80–88 (2009)
39. Paley, M.N.J., Chow, L.S., Whitby, E.H., Cook, G.G.: Modelling of axonal fields in the optic nerve for direct MR detection studies. *Image Vision Comput.* **27**(4), 331–341 (2009)
40. Planinsic, G., Guiberteau, T., Grucker, D.: Dynamic nuclear polarization imaging at very low magnetic fields. *J. Magn. Reson.* **B110**, 205–209 (1996)
41. Puwanich, P., Lurie, D.J., Foster, M.A.: Rapid imaging of free radicals in vivo using field cycled PEDRI. *Phys. Med. Biol.* **44**(1), 2867–2877 (1999)
42. Raichle, M.E.: Bold insights. *Nature* **412**(1), 128–130 (2001)
43. Reynolds, S., Bucur, A., Port, M., Alizadeh, T., Kazan, S.M., Tozer, G.M., Paley, M.N.: A system for accurate and automated injection of hyperpolarized substrate with minimal dead time and scalable volumes over a large range. *J. Magn. Reson.* **239C**, 1–8 (2013)
44. Reynolds, S., Kazan, S.M., Bluff, J.E., Port, M., Wholey, E., Tozer, G.M., Paley, M.N.J.: Fully MR compatible syringe pump for the controllable injection of hyperpolarized substrate in animals. *Appl. Magn. Reson.* **43**(1), 263–273 (2012)
45. Scott, G.C., Joy, M.L.G., Armstrong, R.L., Henkelman, R.M.: Sensitivity of magnetic resonance current density imaging. *JMR* **97**(1), 235–254 (1992)
46. Scott, G.C., Joy, M.L.G., Armstrong, R.L., Henkelman, R.M.: Rotating frame current density imaging. *Magn. Reson. Med.* **33**(3), 355–369 (1995)
47. Shah, N.J., Oros-Peusquens, A.-M., Arrubla, J., Zhang, K., Warbrick, T., Mauler, J., Vahedipour, K., Romanzetti, S., Felder, J., Celik, A., Rota-Kops, E., Iida, H., Langen, K.-J., Herzog, H., Neuner, I.: Advances in multimodal neuroimaging: Hybrid MR-PET and MR-PET-EEG at 3 T and 9.4 T. *J. Magn. Reson.* **229**(1), 101–115 (2013)
48. Singh, M.: Sensitivity of MR phase shift to detect evoked neuromagnetic fields inside the head. *IEEE Trans. Nucl. Sci.* **41**(1), 349–351 (1994)
49. Utsumi, H., Yamada, K., Ichikawa, K., Sakai, K., Kinoshita, Y., Matsumoto, S., Nagai, M.: Simultaneous molecular imaging of redox reactions monitored by Overhauser-enhanced MRI with 14 N- and 15 N-labeled nitroxyl radicals. *PNAS* **103**(5), 1463–1468 (2006)
50. Witney, T.H., Kettunen, M.I., Hu, D.E., Gallagher, F.A., Bohndiek, S.E., Napolitano, R., Brindle, K.M.: Detecting treatment response in a model of human breast adenocarcinoma using hyperpolarized [1-13C]pyruvate and [1,4-13C2] fumarate. *Br. J. Cancer* **103**(1), 1400–1406 (2010)
51. Whitby, E.H., Griffiths, P.D., Rutter, S., Smith, M.F., Sprigg, A., Ohadike, P., Paley, M.N.J.: Frequency and natural history of subdural haemorrhages in babies and relation to obstetric factors. *Lancet* **363**(9412), 846–851 (2004)
52. Yang, H., Cook, G.G., Paley, M.N.: Mapping of periodic waveforms using the ghost reconstructed alternating current estimation (GRACE) magnetic resonance imaging technique. *Magn. Reson. Med.* **50**(3), 633–637 (2003)
53. Youngdee, W., Planinsic, G., Lurie, D.J.: Optimization of field-cycled PEDRI for in-vivo imaging of free radicals. *Physics in Med. Bio.* **46**(1), 2531–2544 (2001)
54. Zierhut, M.L., Yen, Y.F., Chen, A.P., Bok, R., Albers, M.J., Zhang, V., Tropp, J., Park, I., Vigneron, D.B., Kurhanewicz, J., Hurd, R.E., Nelson, S.J.: Kinetic modeling of hyperpolarized 13C1-pyruvate metabolism in normal rats and TRAMP mice. *J. Magn. Reson.* **202**(1), 85–92 (2010)

## **Chapter 8**

# **Detection of Human Emotions Using Features Based on the Multiwavelet Transform of EEG Signals**

**Varun Bajaj and Ram Bilas Pachori**

**Abstract** Emotion classification based on electroencephalogram (EEG) signals is a relatively new area of research in the development of brain computer interface (BCI) system with challenging issues like induction of the emotional states and the extraction of the features in order to obtain optimum classification of human emotions. The emotion classification system based on BCI can be useful in many areas like as entertainment, education, and health care. This chapter presents a new method for human emotion classification using multiwavelet transform of EEG signals. The EEG signal contains useful information related to the different emotional states, which helps us to understand the psychology and neurology of the human brain. The features namely, ratio of the norms based measure, Shannon entropy measure, and normalized Renyi entropy measure are computed from the sub-signals generated by multiwavelet decomposition of EEG signals. These features have been used as an input to multiclass least squares support vector machine (MC-LS-SVM) together with the radial basis function (RBF), Mexican hat wavelet, and Morlet wavelet kernel functions for classification of human emotions from EEG signals. The classification performance of the proposed method for classification of emotions using EEG signals determined by computing the classification accuracy, ten-fold cross-validation, and confusion matrix. The proposed method has provided classification accuracy of 84.79 % for classification of human emotions namely happy, neutral, sadness, and fear from EEG signals with Morlet wavelet kernel function of MC-LS-SVM. The audio-video stimulus has been used for inducing the emotions in EEG signals. The experimental results are presented to show the effectiveness of the proposed method for classification of human emotions from EEG signals.

---

V. Bajaj (✉) · R.B. Pachori

Discipline of Electrical Engineering, Indian Institute of Technology Indore,  
Indore 452017, India  
e-mail: varun@iiti.ac.in

R.B. Pachori  
e-mail: pachori@iiti.ac.in

V. Bajaj  
Discipline of Electronics and Communication Engineering, PDPM Indian Institute  
of Information Technology, Design and Manufacturing Jabalpur, Jabalpur 482005, India

**Keywords** EEG signal • Multiwavelet transform (MWT) • Classification of emotions • Multiclass least squares support vector machine (MC-LS-SVM) • Brain computer interface (BCI)

## 8.1 Introduction

Brain computer interface (BCI) facilitates a connection between the human brain and external device like computer. The BCI system can be used for assisting the physically disabled and impaired people [1, 2]. The BCI system requires analysis, monitoring, measurement, and evaluation of electrical activity of the brain which is extracted by either a set of electrodes over the scalp or electrodes implanted inside the brain. The BCI system can be used for analysis and classification of EEG signals corresponding to different emotions.

Emotion is one of the main factors that affect activities of our day to day life. The applications of emotion classification may include medical areas like as neurology and psychology. The diagnosis of neurological disorders has been suggested based on automatic emotion recognition system using various signals like electromyogram (EMG), electrocardiogram (ECG) and facial images [3, 4]. Emotions expressed via speech and facial expressions are commonly used techniques for classification of human emotions [5, 6]. However, the speech and facial expressions may lead to false emotion. Therefore, it motivates the use of physiological signals like EEG signal for analysis and classification of human emotions. The EEG signals can play an important role in detecting the emotional states for developing the BCI based analysis and classification of emotions.

It should be noted that the EEG signal indicates the electrical potential differences corresponding to different emotions generated by human brain. The research areas like psychology, neurophysiology and BCI are focusing on the important indication of emotions using EEG signals. Different emotional states can be affected by conditions like age, gender, background, and ethnicity. Moreover, various people have lot of personal emotional experiences to the same stimulus. In [7, 8], it has been provided the significant differences in emotional states which are generated for autonomic nervous system. But automated classification was not carried out. Most of the emotions exist for very small interval of time in the range of few micro to milli seconds [9]. Generally emotions are developed at the deeper part of the human brain called limbic system, which initiates emotional interpretation of the EEG signals from the autonomic nervous system. These incoming signals propagates to hypothalamus to trigger the corresponding perceptive physiological effects like increase in heart rate, R-to-R interval and blood volume pulse. These processed signals travels to the amygdala, which is important part of human brain for learning connections to stimuli by comparing them to past experiences. Some of the results on emotion recognition research have shown that, the amygdala and corticothalamic connections mainly participate in emotion recognition process.

In addition, prefrontal cortex, cerebral cortex and occipital lobe areas also have significant role in provoking emotions such as happy, fear, and sad [10]. Regions of human brain which contribute for emotions are as follows: (a) sadness (left temporal areas), (b) sadness, happiness and disgust (right prefrontal cortex area), (c) anger (right frontal cortex activation) (d) fear (bilateral temporal activation), (e) sadness and happiness (contribute most of the brain areas) and (f) all emotions also share the areas (prefrontal cortex, cingulated gyrus, and temporal cortex).

Although most of the activation for emotions emerge in right hemisphere corresponding to different time-segments of EEG signals. The left hemisphere also plays a significant role in activation of emotions. Apparently, brain might be partly or entirely engaged to emotional processing during emotions like sadness, anger, happiness, disgust and fear. Thus, the results support the hypothesis that there are no exclusive emotion centers in the brain. But the results indicate that the several brain areas are activated during emotion processing in a well-defined and specific dynamic process. It has been noticed that left and right hemispheres of the brain together experience different classes of emotions [11]. The left hemisphere is responsible for approach. On the other hand, the right hemisphere is responsible for withdrawal. In [12], it has been explained that the left frontal region is an important center for self-regulation, motivation and planning. The damage of left frontal region can cause to apathetic behavior in combination with a loss of interest and pleasure in objects. The right anterior region contributes to high activation of right frontal and anterior temporal regions during arousal emotional states like fear and disgust. In [11], it has been noticed that there is less alpha power in right frontal regions for disgust than that for happiness while happiness caused less alpha power in the left frontal region than that of disgust. In addition, the analysis of EEG signals have been carried out for brain asymmetries during reward and punishment. It has been found that punishment has association with less alpha power in right mid and lateral frontal regions of the brain and reward has been associated with less alpha power in the left mid and lateral frontal regions [13]. In an experiment, it has been shown that alpha power over the left hemisphere increases in happy conditions in comparison to negative emotional conditions. During the study, the three emotions fear, happiness and sadness have been induced by using visual and auditory stimuli [10]. There are two to twenty basic or prototype emotions as defined by many researchers. Most of the theories suggests that each emotion reflects an particular motivational tendency and behavior. Emotions represent particular forms of action and physiological patterns [14]. The physiological patterns have been applied for classification of emotions into three types: (1) distress (2) interest and (3) pleasure [15]. The basic emotions as defined in [16] are as follows: anger, fear, sadness, disgust, surprise, curiosity, acceptance, and joy.

Most of the methods developed in the literature for neuropsychological studies have reported the correlations between EEG signals and emotional states. These methods have been based on time-domain analysis and frequency-domain analysis. In the time-domain analysis, event-related potentials (ERPs) components have reflected emotional states [17]. The ERP components of short to middle latencies have been shown to have correlation with valence [18, 19], whereas with the ERP

components of middle to long latencies have been shown to have correlation with arousal [20, 21]. The computation of ERPs requires averaging EEG signals over multiple trials, rendering ERP features inappropriate for online processing. However, recent development in single-trial ERP computation methods have resulted in a increased possibility to use ERP features for online emotional state estimation [22–24]. In the frequency-domain, the spectral power of different frequency bands corresponds to different emotional states. The frequency bands have been used for analysis of emotions (happy, sad, angry, fear) or neutral. It has been noted that stimulus can modulate the power synchronization with in frequency bands [25, 26]. In [27], it has been proved that the frontal alpha asymmetry reflects the approach/ avoidance aspects of emotion. The gamma band power has been related to some emotions like happiness and sadness [28, 29]. The theta power of ERS has been related to transitions in the emotional state [30–32]. In [33], the EEG signals have been decomposed into frequency bands and then principal component analysis (PCA) has been employed for reduction of features. These features have been used as input to the binary classifier for classification of emotions based in the bi-dimensional valence-arousal approach. In [34], the EEG signals have been used for recognition of human emotions with the help of humanoid robots. The aim of this experiment was to provide the ability for robots to detect emotion and react to it in the same way as occurring in a human to human interaction. The discrete wavelet transform (DWT) based features namely, energy, recoursing energy efficiency (REE) and root mean square (RMS) have been used for classification of four emotions (happy, disgust, surprise and fear) with Fuzzy C-Means (FCM) clustering [35].

In [36], the participants have been asked to remember past emotional events and the method has been used SVM classifier to obtained the classification accuracy of 79 % using EEG signals for three classes and 76 % using EEG signals for two classes. In another study [37], the wavelet coefficient and chaotic parameters like fractal dimension, correlation dimension and wavelet entropy have been used to extract features from EEG and psychophysiological signals. The selected features combined with linear discriminate analysis (LDA) and SVM, obtained classification accuracy 80.1 and 84.9 % for two classes of emotional stress using LDA and SVM respectively. In [38], the combination of music and story has been used as stimuli to introduce a user independent system. The classification accuracy as obtained with this method was 78.4 and 61.8 % for three and four classes respectively. In [39], film clips have been used to stimulate participants with five different emotions joy, anger, sadness, fear, and relax. The statistical features extracted from EEG have been used as input for SVM classifier as result 41.7 % of the patterns that have been correctly recognized.

In [40], a BCI system for the recognition of human emotions have been used with 64 channels EEG recording system. A Laplace filter has been applied for pre-processing of EEG signals. The wavelets transform algorithm has been used for features extraction from EEG signals and two different classifier namely the k nearest neighbors and linear discriminant have been used for classification of discrete emotions such as happiness, surprise, fear, disgust and neutral. The efficiency

of the asymmetry index (ASI) based emotional filters has been justified through an extensive classification process involving higher-order crossings and cross-correlation as feature-vector extraction techniques and a support vector machine classifier for six different classification scenarios in the valence/arousal space. This study has resulted in mean classification rates from 64.17 up to 82.91 % in a user-independent base, revealing the potential of establishing such a filtering for reliable EEG-based emotion recognition systems [41]. Electric potential associated with brain activities that has been measured thought EEG signals have a potential source for emotion detection. The power of EEG signal in the specific bandwidth or brain wave has been used for analysis for positive or negative expression particularly the change of power in alpha and beta wave [42]. In [43], different stimuli like sounds, images, and combination of both have been used to distinguish between three emotion classes (neutral, happy, unhappy). In [44], calm and excited emotions have been evoked using images, the best classification accuracy that has been archived 72 %. In [45], authors has compared three feature extraction methods based on fractal dimension of EEG signals including Higuchi, Minkowski Bouligand, and Fractional Brownian motion using kNN and SVM classifiers on four classes of emotions. The principal component analysis (PCA) has been used to correlate EEG features with complex music appreciation which has been used as input to the SVM classifier to classify EEG dynamics in four subjectively-reported emotional states [46]. In [47], a system has been proposed for estimating the feelings of joy, anger, sorrow and relaxation by using neural network, which has obtained classification accuracy of 54.5 % for joy, 67.7 % for anger, 59 % for sorrow and 62.9 % for relaxation. In [34], a system has been implemented based on EEG signals to enable a robot to recognize human emotions. Emotions have been evoked by images and classified in three different emotions, namely: pleasant, unpleasant and neutral.

The emotions have been elicited by stimulating participants with a Pong game and anagram puzzles. The four machine learning methods K-nearest neighbor, regression tree (RT), Bayesian network and SVM have been for emotion classification, the best average accuracy has been obtained with SVM 85.51 % [48]. In [49], the dynamic difficulty adjustment (DDA) mechanism has been developed for adjustment of game difficulty in real time based on anxiety measures. This demonstrates the interest of using affective computing for the purpose of game adaptation. In [50], the authors have proposed technique to continuously assess the emotional state of a player using fuzzy logic. The obtained results have shown that the emotional states have evolved according to the events of the game, but no exact measure of performance have been reported. This tool could be used to include the player's experience in the design of innovative video games. In [51], three emotional states namely boredom, anxiety, engagement have been detected from peripheral signals by using SVM classifier. The emotions have been elicited by using a Tetris game.

The features extracted form the mutual information and magnitude squared coherence estimation of EEG signals have been used as features for k-nearest neighbors (kNN) and SVM classifiers for classification of emotions. The performance of the EEG-based emotion recognition system has been then evaluated using

five-fold cross-validation [52]. In [53], features that have been extracted by independent component analysis (ICA) and the K-means algorithm have been used to distinguish emotions in EEG. [54] have investigated the use of the naive Bayes classifier, SVM, and ANN to detect different emotions in EEG. The EEG signals have been recorded from 10 participants by using the international affective picture system (IAPS) database. The frequency band power has been measured along with the cross-correlation between EEG band powers, the peak frequencies in the alpha band, and the Hjorth parameters [55].

The different emotional states using EEG signals have been measured by the Kolmogorov entropy and the principal Lyapunov exponent [56]. Non-linear dynamic complexity has been used to measure the complexity of the EEG signals during meditation [30]. The fractal dimension, the energy of the different frequency-bands, and the Lyapunov exponent have been used as features for the classification of human emotions [57]. The correlation dimension measures the complexity of EEG signals, which also has been used for analysis of human emotions [58]. The statistical and energy features obtained by using discrete wavelet transform (DWT) of EEG signal have been used for human emotion classification [59]. Wireless concept based detection of state of valence using EEG signals has been proposed in [60]. The higher order spectra (HOS) together with genetic algorithm have been used for classification of two emotional stress states with an average accuracy of 82 % [61].

The event related potential and event related oscillation based features have been proposed as input feature set for emotion classification [62]. The obtained classification accuracies are 79.5 and 81.3 % for Mahalanobis distance based classifier (MD) and support vector machine (SVM) respectively. The time-frequency domain based features have been suggested as input feature set to SVM classifier for classification of three emotional states [63]. The obtained average classification accuracy in this work is 63 % [63]. The methodology based on surface Laplacian (SL) filtering, wavelet transforms (WT) and linear classifier has been developed for classification of emotions using EEG signals [64]. The classification accuracies reported in this study are 83.04 and 79.17 % for kNN and linear discriminant analysis (LDA) respectively. The short-time Fourier transform (STFT) based features have been suggested as an input for SVM classifier for classification of emotions [65, 66]. The obtained classification accuracy in this work is 82.29 % for classification of four emotions using SVM classifier. The features obtained using higher order crossing have been used for classification of emotions using EEG signals [67]. The classification accuracy achieved with this methodology for six emotions is 83.33 %. Time and frequency domain based features have been suggested for classification of emotions from EEG signals [68]. The proposed methodology in this work has provided classification accuracy of 66.5 % considering four emotions [68]. The spectrogram, Zhao-Atlas-Marks and Hilbert-Huang spectrum based features have been used for classification of arousal and neutral with classification accuracy of 86.52 % [69].

The classification of emotions is probabilistic. The previous research on human emotion has dealt with classification using probability theory to estimate the human

emotional state by checking the presence or absence of a certain emotion [70, 71]. The techniques based on probability theory are still insufficient to handle all the facets of uncertainty in human emotion classification [72]. The fuzzy set theory can provide a systematic approach to process uncertain information, just as humans are able to interpret imprecise and inadequate information. In order to incorporate human expertise, the fuzzy C-means clustering (FCM) has been used to cluster each component to get different emotional descriptors [73]. These descriptors have been combined together to form the fuzzy-GIST in order to generate the emotional feature space for human emotion recognition [74]. The fuzzy sets have attracted interest in information technology, production techniques, decision making, pattern recognition, diagnostics, data analysis, etc. [75–77]. The neuro-fuzzy systems are fuzzy systems, which use ANN theory in order to determine their properties like fuzzy sets and fuzzy rules by processing data samples. Neuro-fuzzy systems employs fuzzy logic and artificial neural networks (ANNs) by utilizing the mathematical properties of ANNs in tuning rule-based fuzzy systems that represent the way humans process information. The adaptive neuro-fuzzy inference system (ANFIS) has shown to be significant in modeling of nonlinear functions. The ANFIS learns features in the data set and adjusts the system parameters based up on a given error criterion [78, 79]. The application of ANFIS in biomedical engineering have been reported to be significant for classification [80, 81]; Übeyli and Güler [82, 83] and data analysis [84]. The most prominent classification methods are support vector machine (SVM) [85], fuzzy k-means [86], and fuzzy c-means [87]. These classifier have been resulted in moderate classification accuracy for up to three [88], four [89], and five [39] distinct emotions. Other researchers have made efforts to study the operator engagement, fatigue, and workload by using EEG signals with respect to complexity of a task [90–94].

The emotion classification methods have been developed based on different feature extraction techniques from EEG signals. Many EEG signal analysis methods have employed preprocesses for reducing the artifacts. The recorded EEG signals in response to stimuli pass through the preprocessing step in which noise reduction algorithms and spatio-temporal filtering methods are applied to improve the signal-to-noise ratio (SNR). Then, the feature extraction step determines specific band powers, ERPs, and phase coupling indices that have correlation with the aimed emotional states. Commonly, this feature selection process is being optimized in order to achieve maximum emotion classification accuracy. The classification steps compute the most probable emotional states from the selected EEG features. The number of classes depend on the definition of the emotional state space like the continuous state of arousal and valence, or the discrete states.

In this chapter, we present an emotion classification system based on multi-wavelet transform (MWT) of EEG signals. The EEG signals have been acquired using audio-video stimulus. The MWT decomposes the EEG signals into a set of sub-signals. The features: ratio of the norms based measure, Shannon entropy measure, and normalized Renyi entropy measure have been computed from the sub-signals of the EEG signals. The extracted features have been used as an input to the multiclass least squares support vector machine (MC-LS-SVM) for emotion

classification from EEG signals. This chapter is organized as follows: Sect. 8.2 presents the experimental setup, pre-processing, the MWT, features extraction and MC-LS-SVM classifier. The experimental results and discussion for the emotion classification using EEG signals based on the proposed methodology have been provided in Sect. 8.3. Finally, Sect. 8.4 concludes the chapter.

## 8.2 Methodology

### 8.2.1 Experimental Setup

The EEG signals have been acquired from 8 healthy subjects (4 males and 4 females) during audio-video stimulus. The subjects were having age between 20–35 years. The subjects were undergraduate students or employees from Indian Institute of Technology Indore, India. A 16-channel EEG module (BIOPAC system, Inc.) with 10-20 electrode system was used for recording of EEG signals. The sampling frequency of EEG signals was 1,000 Hz. The bipolar montage has been used during recording of the EEG signals. The prefrontal cortex plays significant role in impulse control and in many other emotions [95, 96]. Therefore, the electrode positions Fp1/Fp2 and F3/F4 have been used to record the EEG signals. The right (A2) and left (A1) earlobes have been used for ground and reference electrodes respectively.

Generally, the number of basic emotions can be up to 15 [97]. The eight basic emotions such as anger, fear, sadness, disgust, surprise, curiosity, acceptance, and joy have been described in [16]. The emotions can be represented based on their valence (positive and negative) and arousal (calm and excited) with two dimensional scale [98]. The different ways of inducing emotions are: visual includes images and pictures [41], recalling of past emotional events [44], audio may be songs and sounds [99], audio-video includes film clips and video clips [100, 101]. In this work, we have studied four basic emotional states based on 2-D valence-arousal emotion model [102], which includes happy, neutral, sadness, and fear. In this study, the EEG signals have been obtained from eight subjects with 5 trials each using 3 audio-video stimulus. Figure 8.1 shows EEG data recording and main

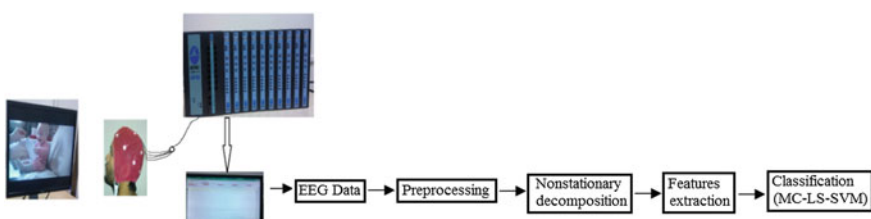


**Fig. 8.1** EEG data recording and main parts of the proposed methodology for emotion classification

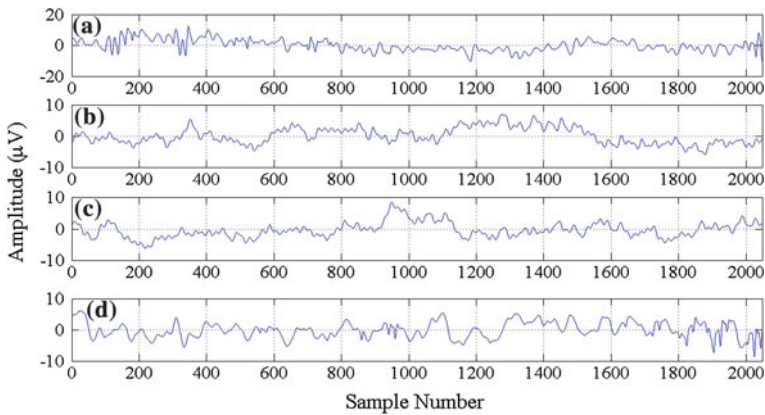
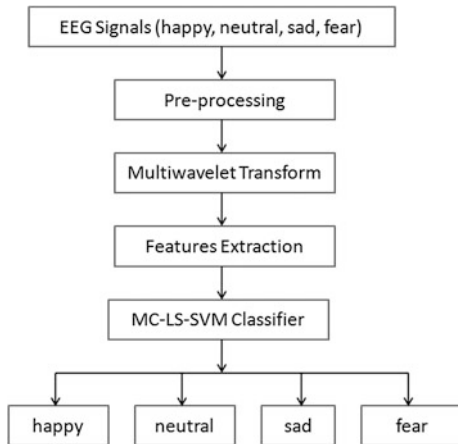


**Fig. 8.2** The EEG signals of different emotional states: **a** happy, **b** neutral, **c** sad, and **d** fear

**Fig. 8.3** The block diagram of proposed methodology for emotion classification from EEG signals



parts of the proposed methodology for emotion classification. The EEG signals for four emotional states: happy, neutral, sad and fear have been shown in Fig. 8.2. The subsections of the proposed method for emotion classification from EEG signals are shown in Fig. 8.3. The subsections include pre-processing, multiwavelet transform, feature extraction, and MC-LS-SVM classifier. The details of each subsection are explained as follows:

### 8.2.2 Pre-processing

The recorded EEG signals are contaminated with noise like power line, external interferences and other artifacts. The 8th order, band pass, Butterworth filter with a

bandwidth of 0.5–100 Hz has been used for removing noise. The 50 Hz notch filter has been applied to remove the noise due to power-line interference. The MWT requires pre-processing which includes generation of vectored input stream and pre-filtering. There are many ways to obtain the vectored input stream [103]. In this work, the vectored input stream has been obtained using repeated row pre-processing scheme. The matrix-valued multiwavelet filter bank also requires multiple streams of input as decided by multiplicity.

### 8.2.3 Multiwavelet Transform

The scalar wavelets which are obtained by mother wavelets by varying one scaling function have been widely used in non-stationary signal processing. The scalar wavelet have led to the notion of multiwavelets, which is a more recent generalization having more numbers of distinct scaling functions. It offers many theoretical and experimental advantages. For example, multiwavelets have been constructed to simultaneously possess symmetry, orthogonality, and compact support [104–108]. The multiwavelets have some unique characteristics that cannot be obtained with scalar wavelets. Multiwavelets can simultaneously provide perfect reconstruction while preserving length (orthogonality), good performance at the boundaries (via linear-phase symmetry), and a high order of approximation (vanishing moments). These features of multiwavelets cause to better performance of multiwavelets over scalar wavelets in image processing applications. Particular applications, where multiwavelets have been found to offer superior performance over single wavelets, include signal/image classification [107, 108], compression [104], and denoising [106]. The wavelet transform based features have been used for epileptic EEG signal classification and recognition [109, 110]. The multiwavelets attracted because of their significant characteristics, which consist of more than one scaling and wavelet functions. Multiwavelets simultaneously possess orthogonality, short support, symmetry, and a high order of approximation through vanishing moments, that all of them are important for signal processing application [103]. The performance of multiwavelet have shown superior as compare to scalars wavelets in image classification, denoising [106] and image compression [104]. In [111], it has been shown that the multiwavelet transform has an efficient signal processing technique for the feature extraction from EEG signals in comparison with scalar wavelet. It motivates us to use multiwavelet transform of EEG signals for classification of human emotions.

The standard multi-resolution analysis (MRA) for scalar wavelet uses one scaling function  $\phi(t)$  and one wavelet  $\psi(t)$ . The integer translates and the dilates of the scaling function are represented as  $\phi(t - k)$  and  $\phi(2^j t - k)$  respectively. The multiwavelet is the extension of scalar wavelet where multiple scaling functions and associated multiple wavelets are used. In case of multiwavelet, a basis for the subspace  $V_o$  is generated by translation of  $r$  scaling functions denoted by

$\phi_1(t - k), \phi_2(t - k), \dots, \phi_r(t - k)$ . The multiwavelet can be considered as vector-valued wavelets which satisfy the condition of two-scale relationship with involvement of matrices rather than scalars. The vector-valued scaling function  $\Phi(t) = [\phi_1(t), \phi_2(t), \dots, \phi_r(t)]^T$ , where  $T$  represents the transpose and the associated r-wavelets  $\Psi(t) = [\psi_1(t), \psi_2(t), \dots, \psi_r(t)]^T$  satisfies the following matrix dilation and matrix wavelet equations [103]:

$$\Phi(t) = \sum_k G[k] \Phi(2t - k) \quad (8.1)$$

$$\Psi(t) = \sum_k H[k] \Phi(2t - k) \quad (8.2)$$

where, the coefficients  $G[k]$  and  $H[k]$  are matrices. The matrices  $G[k]$  and  $H[k]$  are low-pass filter and high-pass filters for multiwavelet filter bank respectively. The multiplicity  $r$  is generally 2 for most of the multiwavelets [103]. The multiwavelet can simultaneously exhibit symmetry, orthogonality, and short support, which is not possible using scalar wavelet [103, 112]. In this study, we consider multiple scaling functions and multiwavelets which are developed by Geronimo, Hardin and Massopust (GHM) [113–115]. They are shown in Fig. 8.4. The GHM dilation and translation equations for this system have following four coefficients:

$$G_0 = \begin{bmatrix} \frac{3}{5} & \frac{4\sqrt{2}}{5} \\ \frac{-1}{10\sqrt{2}} & \frac{-3}{10} \end{bmatrix}, G_1 = \begin{bmatrix} \frac{3}{5} & 0 \\ \frac{9}{10\sqrt{2}} & 1 \end{bmatrix}, G_2 = \begin{bmatrix} 0 & 0 \\ \frac{9}{10\sqrt{2}} & \frac{-3}{10} \end{bmatrix}, G_3 = \begin{bmatrix} 0 & 0 \\ \frac{-1}{10\sqrt{2}} & 0 \end{bmatrix}; \quad (8.3)$$

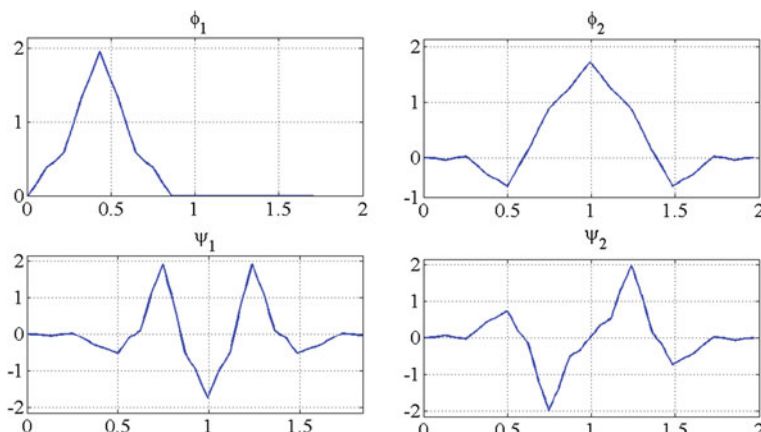


**Fig. 8.4** The GHM pair of scaling functions and wavelet functions

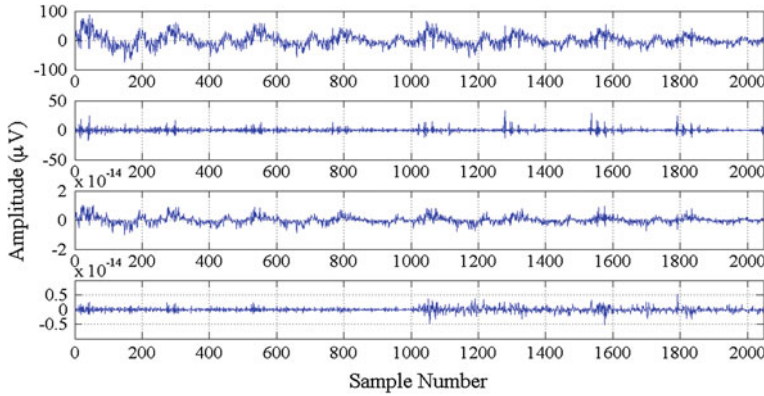


**Fig. 8.5** The third level sub-band signals obtained by multiwavelet decomposition of EEG signal corresponding to happy emotion as shown in Fig. 8.2a

$$H_0 = \begin{bmatrix} \frac{-1}{10\sqrt{2}} & \frac{-3}{10} \\ \frac{1}{10} & \frac{3\sqrt{2}}{10} \end{bmatrix}, H_1 = \begin{bmatrix} \frac{9}{10\sqrt{2}} & -1 \\ \frac{-9}{10} & 0 \end{bmatrix}, H_2 = \begin{bmatrix} \frac{9}{10\sqrt{2}} & \frac{-3}{10} \\ \frac{9}{10} & \frac{-3\sqrt{2}}{10} \end{bmatrix}, H_3 = \begin{bmatrix} \frac{-1}{10\sqrt{2}} & 0 \\ -1 & 0 \end{bmatrix}. \quad (8.4)$$

The GHM multiwavelet has several remarkable properties. The GHM scaling functions have short support of [0, 1] and [0, 2]. The scaling functions are symmetric and the system exhibit second order of approximation. Moreover, multiwavelet form symmetric/antisymmetric pair. Translates of scaling functions and wavelets satisfy orthogonality, which is not possible in case of scalar wavelet. Figures 8.5, 8.6, 8.7 and 8.8 show the third level sub-band signals as obtained by multiwavelet decomposition of EEG signal shown in Fig. 8.2a–d respectively.

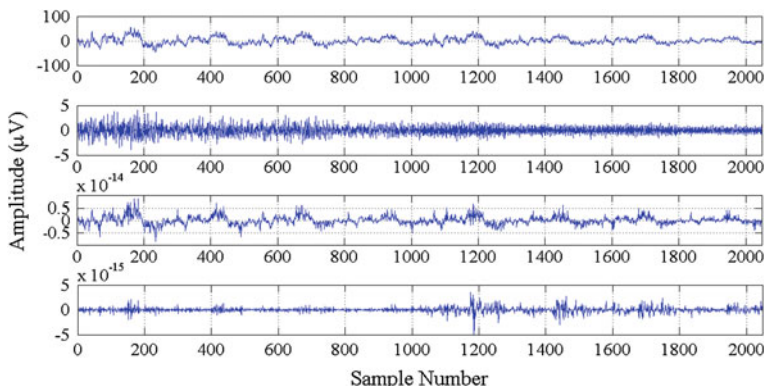


**Fig. 8.6** The third level sub-band signals obtained by multiwavelet decomposition of EEG signal corresponding to neutral emotion as shown in Fig. 8.2b

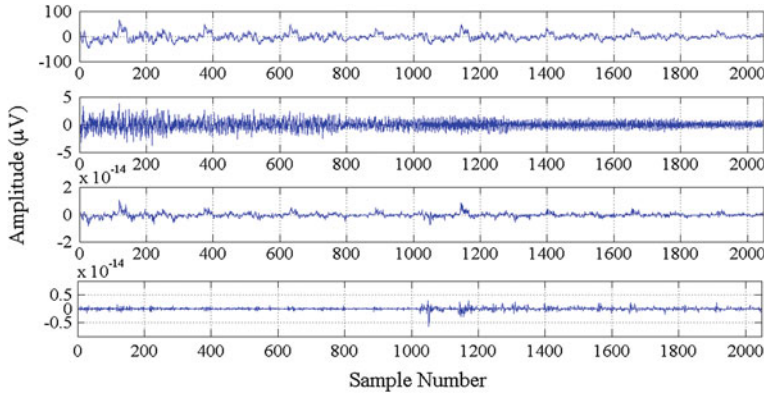


**Fig. 8.7** The third level sub-band signals obtained by multiwavelet decomposition of EEG signal corresponding to sad emotion as shown in Fig. 8.2c

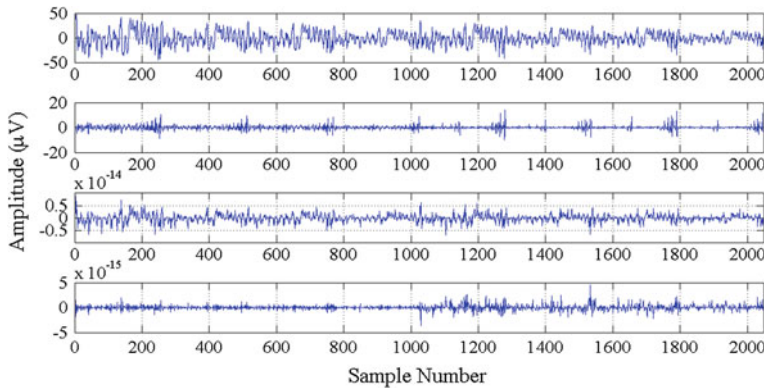


**Fig. 8.8** The third level sub-band signals obtained by multiwavelet decomposition of EEG signal corresponding to fear emotion as shown in Fig. 8.2d

### 8.2.4 Features Extraction

Many entropy based methods have been proposed for EEG signal analysis. Different approaches for computing entropy in physiological systems have been developed in the literature. In [116], the researchers have suggested that a measure of the entropy which is the rate of information of a chaotic system would be a useful parameter for characterizing such a system. In [117], the authors have developed a method to calculate the Kolmogorov-Smirnov (K-S) entropy of a time series. The modified version of Eckmann and Ruelle (E-R) entropy in [118], has been proposed by modifying the distance metric proposed in [119]. The authors have suggested a modification of E-R entropy by introducing statistical entropy named approximate

entropy (ApEn) [120]. However, it has been demonstrated that the method to compute ApEn introduces a bias, as the ApEn algorithm counts each sequence as matching itself [121]. In order to reduce this bias, the proposed modified version of the ApEn algorithm known as sample entropy (SampEn). The sample entropy measures the irregularity of the time series. In [122], the authors have compared approximation entropy and sample entropy method for neurophysiological signals. They have addressed issues related to the choice of the input parameters and have shown that the sample entropy approach has produced more consistent results. They have also shown that the sample entropy is less sensitive to the length of the data. Recently, the sample entropy has been used as a feature for the classification of different classes of EEG signals [123].

The features namely, the ratio of norms based measure, Shannon entropy measure and normalized Renyi entropy measure have been measured from sub-signals obtained from the multiwavelet decomposition of EEG signals. These features are briefly described as follows:

*Ratio of Norms Based Measure* Ratio of norms based measure is defined as the ratio of the fourth power norm and the square of second power norm [124]. It is expressed as:

$$E_{RN} = \frac{\sum_{n=1}^N |x[n]|^4}{\left[ \sum_{n=1}^N |x[n]|^2 \right]^2} \quad (8.5)$$

where,  $x[n]$  is signal under study.

*Shannon Entropy Measure* The Shannon entropy is a measure of uncertainty of the signal [125]. It can be defined as:

$$E_{SE} = - \sum_{k=1}^L p_k \log[p_k] \quad (8.6)$$

*Normalized Renyi Entropy Measure* The Renyi entropy measure can be normalized either with respect to signal energy or distribution volume [126]. In this study, the normalized Renyi entropy  $E_{NE}$  which is normalized with respect to signal energy has been used. The  $E_{NE}$  can be expressed as follows:

$$E_{NE} = \frac{1}{1-\alpha} \log \left[ \frac{\sum_{k=1}^L p_k^\alpha}{\sum_{k=1}^L |p_k|} \right] \quad (8.7)$$

where,  $\alpha$  is the order of Renyi entropy, which has been taken as 3 being the smallest integer value.

### 8.2.5 Multiclass Least-Squares Support Vector Machine

Multiclass support vector machine (SVM) classifiers have become popular in recent years in the fields of classification, regression analysis, and novelty detection [127]. Multiclass least squares support vector machine (MC-LS-SVM) algorithms have shown very promising results as EEG signal classifiers [128].

The effectiveness of the proposed features in emotion classification from EEG signals is evaluated using a MC-LS-SVM. The least squares support vector machines are a group of supervised learning methods that can be applied for classification of data [129–132]. For multiclass classification problem, we have considered the training data  $\{x_i, y_i^k\}_{i=1, k=1}^{i=P, k=m}$ , where  $y_i^k$  denotes the output of the  $k$ th output unit for pattern  $i$ . The  $P$  denotes the number of training dataset. The derivation of the MC-LS-SVM is based upon the following formulation [127, 133]:

$$\text{Minimize } J_{LS}^{(m)}(w_k, b_k, e_{i,k}) = \frac{1}{2} \sum_{k=1}^m w_k^T w_k + \frac{\gamma}{2} \sum_{i=1}^P \sum_{k=1}^m e_{i,k}^2 \quad (8.8)$$

with the following equality constraints:

$$\left\{ \begin{array}{l} y_1^1 [w_1^T g_1(x_i) + b_1] = 1 - e_{i,1}, \quad i = 1, 2, \dots, P \\ y_2^2 [w_2^T g_2(x_i) + b_2] = 1 - e_{i,2}, \quad i = 1, 2, \dots, P \\ \vdots \\ y_m^m [w_m^T g_m(x_i) + b_m] = 1 - e_{i,m}, \quad i = 1, 2, \dots, P \end{array} \right. \quad (8.9)$$

where,  $w_k$  and  $\gamma$  are the weight vector of  $k$ th classification error and the regularization factor respectively. The  $e_{i,m}$  and  $b_k$  denotes the classification error and the bias respectively. The  $g_k(\cdot)$  is a nonlinear function that maps the input space into a higher dimensional space. The Lagrangian multipliers  $\alpha_{i,k}$  can be defined for [128] as:

$$L^{(m)}(w_k, b_k, e_{i,k}; \alpha_{i,k}) = J_{LS}^{(m)} - \sum_{i,k} \alpha_{i,k} \left\{ y_i^{(k)} [w_k^T g_k(x_i) + b_k] - 1 + e_{i,k} \right\} \quad (8.10)$$

which provides the following conditions for optimality:

$$\left\{ \begin{array}{l} \frac{\partial L}{\partial w_k} = 0, \rightarrow w_k = \sum_{i=1}^P \alpha_{i,k} y_i^{(k)} g_k(x_i) \\ \frac{\partial L}{\partial b_k} = 0, \rightarrow \sum_{i=1}^P \alpha_{i,k} y_i^{(k)} = 0 \\ \frac{\partial L}{\partial e_{i,k}} = 0, \rightarrow \alpha_{i,k} = \gamma e_{i,k} \\ \frac{\partial L}{\partial \alpha_{i,k}} = 0, \rightarrow y_i^{(k)} [w_k^T g_k(x_i) + b_k] = 1 - e_{i,k} \end{array} \right. \quad (8.11)$$

where,  $i = 1, 2, \dots, P$  and  $k = 1, 2, \dots, m$ . Elimination of  $w_i$  and  $e_{k,i}$  provides the linear system as:

$$\begin{bmatrix} 0 & Y_M^T \\ Y_M & \Omega_M \end{bmatrix} \begin{bmatrix} b_M \\ \alpha_M \end{bmatrix} = \begin{bmatrix} 0 \\ \bar{1} \end{bmatrix}$$

with the following matrices:

$$Y_M = \text{blockdiag} \left\{ \begin{bmatrix} y_1^{(1)} \\ \cdot \\ \cdot \\ \cdot \\ y_P^{(1)} \end{bmatrix}, \dots, \begin{bmatrix} y_1^{(m)} \\ \cdot \\ \cdot \\ \cdot \\ y_P^{(m)} \end{bmatrix} \right\}$$

$$\Omega_M = \text{blockdiag} \{ \Omega_1, \dots, \Omega_m \} \quad \Omega_i^k = y_i^k y^k g_k^T(x) g_k(x_i) + \gamma^{-1} I$$

$$\bar{1} = [1, \dots, 1] \quad b_M = [b_1, \dots, b_m]$$

$$\alpha_{i,k} = [\alpha_{1,1}, \dots, \alpha_{P,1}; \dots; \alpha_{1,m}, \dots, \alpha_{P,m}]$$

where,  $K_k(x, x_i) = g_k^T(x) g_k(x_i)$  is kernel function, which satisfy Mercer condition [127]. The decision function of multiclass least square support vector machines (MC-LS-SVM) is defined as [134]:

$$f(x) = \text{sign} \left[ \sum_{i=1}^P \alpha_{ik} y_i^{(k)} K_k(x, x_i) + b_k \right] \quad (8.12)$$

The radial basis function (RBF) kernel for MC-LS-SVM can be defined as [45]:

$$K_k(x, x_i) = \exp \left[ \frac{-||x - x_i||^2}{2\sigma_k^2} \right] \quad (8.13)$$

where,  $\sigma_k$  controls the width of RBF function.

The multidimensional wavelet kernel function for MC-LS-SVM can be given as [134, 135]:

$$K_k(x, x_i) = \prod_{l=1}^d \psi \left( \frac{x^l - x_i^l}{a_k} \right) \quad (8.14)$$

The kernel function of Mexican hat wavelet for MC-LS-WSVM can be defined as [128]:

$$K_k(x, x_i) = \prod_{l=1}^d \left[ 1 - \frac{(x^l - x_i^l)^2}{a_k^2} \right] \exp \left[ -\frac{\|x^l - x_i^l\|^2}{2a_k^2} \right] \quad (15)$$

Similarly, the kernel function of Morlet mother wavelet for MC-LS-WSVM can be defined as [128]:

$$K_k(x, x_i) = \prod_{l=1}^d \cos \left[ \omega_0 \frac{(x^l - x_i^l)}{a_k} \right] \exp \left[ -\frac{\|x^l - x_i^l\|^2}{2a_k^2} \right] \quad (8.16)$$

where,  $x_i^l$  is the  $l$ th component of  $i$ th training data.

### 8.3 Results and Discussion

In the proposed method, the emotions measured by EEG signals more advantageous because it is difficult to influence electrical brain activity intentionally. The EEG signals are acquire using audio-video stimulus because it is more effective for evoking the emotion. The EEG signals are firstly pre-processed with repeated-row method to form an input signal vector, then the input signal vector is decomposed into sub-signals through GHM multiwavelet with 3-level decomposition. Multiwavelets offer simultaneously orthogonality, symmetry, and compact support and therefore outperform the scalar wavelets. The features namely, ratio of the norms based measure, Shannon entropy measure, and normalized Renyi entropy measure have been extracted from sub-signals as obtained by GHM multiwavelet decomposition of EEG signals. To the knowledge of the authors, there is no other work in the literature related to emotion classification using features based on multiwavelet transform of EEG signals. Emotion classification is multiclass classification problem. Recently it has been shown that wavelet based kernel is better as compared to RBF kernel of MC-LS-SVM classifier for multiclass classification problem. Therefore, it motivates to use these kernels with MC-LS-SVM classifier for emotion classification. These features have been used as an input to MC-LS-SVM classifier with the RBF kernel, Mexican hat and Morlet wavelet kernel for classification of emotions from EEG signals.

The classification performance of the MC-LS-SVM classifier for emotion classification can be determined by computing the classification accuracy, ten-fold cross-validation, and confusion matrix. The classification accuracy (Acc) can be defined as the ratio of the number of events correctly detected to the total number of events.

$$\text{Acc} = \frac{\text{number of correctly detected events}}{\text{total number of events}} \times 100 \quad (8.17)$$

**Table 8.1** The classification accuracy (%) with different kernels of the MC-LS-SVM classifier for emotion classification from EEG signals using GHM multiwavelet

Multiwavelet	Kernel Function (Parameters)	Happy (%)	Neutral (%)	Sad (%)	Fear (%)	Total Accuracy
GHM	RBF( $\sigma_k = 20$ )	87.50	78.33	82.50	75.00	80.83
	Mexican hat ( $a_k = 20$ )	85.33	83.33	74.16	73.33	79.04
	Morlet ( $\omega_0 = 0.5, a_k = 20$ )	89.17	81.67	85.00	83.33	84.79

In ten-fold cross-validation, a dataset  $Y$  is randomly divided into 10 disjoint subsets  $Y_1, Y_2, \dots, Y_{10}$  of nearly uniform size of each class. Then, the method is repeated 10 times and at every time, the test set is formed from one of the 10 subsets and remaining 9 subsets are used to form a training set. Then the average error across all 10 trials is computed in order to obtain the final classification accuracy. A confusion matrix contains information about the actual and predicted classifications performed by a classification method. Confusion matrix provides the common misclassifications in the classification of emotions from EEG signals.

Table 8.1 shows the classification accuracy (%) for RBF kernel, Mexican hat and Morlet wavelet kernel functions of the MC-LS-SVM classifier for emotion classification with GHM multiwavelet. The classification accuracy for happy 89.17 %, neutral 81.67 %, sad 85.00 %, and fear 83.33 % are obtained by proposed method. It has been observed that classification accuracy of happy class is greater compared to other class and neutral emotion have lesser classification accuracy may be due to influenced by the other class of emotion. The classification accuracy for classification of emotions from EEG signals obtained by proposed method is 84.79 % with Morlet wavelet kernel function of MC-LS-SVM classifier. Table 8.2 shows the confusion matrix for classification of emotions from EEG signals with Morlet wavelet kernel function. It has been observed that highest misclassification between sad and neutral emotion. Other observation happy and fear or happy and sad have same misclassification. Table 8.3 presents a comparison with the proposed method and other existing methods in the literature for emotion classification. It is clear from Table 8.3 that the proposed method has provided better classification

**Table 8.2** The confusion matrix of Morlet wavelet kernel function of the MC-LS-SVM classifier for classification of emotion from EEG signals

	Happy	Neutral	Sad	Fear
Happy	89.17	5.83	1.67	1.67
Neutral	4.17	81.67	7.50	6.67
Sad	3.33	7.50	85.00	8.33
Fear	3.33	5.00	5.83	83.33
Accuracy (%)	89.17	81.67	85.00	83.33

**Table 8.3** A comparison of classification accuracy of the different emotion classification methods

Authors	Stimulus	Classes	Feature extraction methods	Classifier	Accuracy (%)
Lin et al. [65]	Music	4	STFT	kNN, LDA	82.29
Wang et al. [68]	Video	4	Minimum redundancy maximum relevance	SVM	66.5
Proposed method	Audio-video	4	Multiwavelet transform	MC-LS-SVM	84.79

performance as compared to existing methods. It may be the effect of combination of proposed features extracted from MWT and MC-LS-SVM.

## 8.4 Conclusion

This chapter explores the capability of proposed features derived from MWT for classification of emotions from EEG signals. The EEG signals are firstly decomposed into several sub-signals through 3-level MWT with repeated-row preprocessing. The multiwavelet transform, the repeated-row preprocessing of the scalar input produces the oversampling of the EEG signal, which makes the extracted features more discriminative. In addition, the multiwavelet decomposition contains two or more scaling and wavelet functions, the low-pass and high-pass filters are matrices instead of scalars. The features namely, ratio of the norms based measure, Shannon entropy measure, and normalized Renyi entropy measure are extracted from the sub-signals obtained by multiwavelet decomposition of EEG signals. These features are then used as input for MC-LS-SVM classifier for automatic classification of emotions. The experimental results have indicated that Morlet wavelet kernel function of MC-LS-SVM classifier has provided classification accuracy of 84.79 % for classification of emotions from EEG signals.

The EEG signal processing based methodology for emotion classification may be improved further. The developed method in this chapter only captures the static properties in the EEG signal in response to emotional stimuli. The methodologies can be developed to include the temporal dynamics of emotional information processing in the human cognitive system. It is expected that this way of processing may estimate the emotional state more accurately. It would of interest to develop new nonstationary signal decomposition based methodology and machine learning algorithms for improving the classification accuracy in human emotion classification from EEG signals. In this study, the selection of parameters of kernel functions used in LS-SVM and kernel function has been done on the basis of the trial and error. In future, the research can be done for automatic selection of kernel functions and kernel parameters for automatic classification of human emotions from EEG signals.

**Acknowledgements** Financial support obtained from the Department of Science and Technology (DST) India, Fast track project titled “Analysis and Classification of EEG Signals based on Nonlinear and Non-stationary Signal Models”, project number SR/FTP/ETA-90/2010 is greatly acknowledged.

## References

1. Azar, A.T., Balas, V.E., Olariu, T.: Classification of EEG-based brain-computer interfaces. *Adv. Intell. Comput. Technol. Decis. Support Syst. Stud. Comput. Intell.* **486**(2014), 97–106 (2014). doi:[10.1007/978-3-319-00467-9\\_9](https://doi.org/10.1007/978-3-319-00467-9_9)
2. Murugappan, M., Rizon, M., Nagarajan, R., Yaacob, S.: Inferring of human emotional states using multichannel EEG. *Eur. J. Sci. Res.* **48**(2), 281–299 (2010)
3. Smith, M.J.L., Montague, B., Perrett, D.I., Gill, M., Gallagher, L.: Detecting subtle facial emotion recognition deficits in high functioning autism using dynamic stimuli of varying intensities. *Neuropsychologia* **48**(9), 2777–2781 (2010)
4. Vera-Munoz, C., Pastor-Sanz, L., Fico, G., Arredondo, M.T., Benuzzi, F., Blanco, A.: A wearable EMG monitoring system for emotions assessment. *Probing Experience Philips Res.* **8**, 139–148 (2008)
5. Essa, I.A., Pentland, A.P.: Coding analysis interpretation and recognition of facial expressions. *IEEE Trans. Pattern Anal. Mach. Intell.* **19**(7), 757–763 (1997)
6. Nwe, T.L., Foo, S.W., Silva, L.D.: Speech emotion recognition using hidden Markov models. *Speech Commun.* **41**(4), 603–623 (2003)
7. Ekman, P., Levenson, R.W., Freisen, W.V.: Autonomic nervous system activity distinguishes among emotions. *Science* **221**(4616), 1208–1210 (1983)
8. Winton, W.M., Putnam, L., Krauss, R.: Facial and autonomic manifestations of the dimensional structure of emotion. *J. Exp. Soc. Psychol.* **20**(3), 195–216 (1984)
9. Sander, D., Grandjean, D., Scherer, K.R.: A systems approach to appraisal mechanisms in emotion. *Neural Netw.* **18**(4), 317–352 (2005)
10. Baumgartner, T., Esslen, M., Jancke, L.: From emotion perception to emotion experience: emotions evoked by pictures and classical music. *Int. J. Psychophysiol.* **60**(1), 34–43 (2006)
11. Davidson, R.J.: Anterior cerebral asymmetry and the nature of emotion. *Brain Cogn.* **20**(1), 125–151 (1992)
12. Petrides, M., Milner, B.: Deficits on subject-ordered tasks after frontal- and temporal-lobe lesions in man. *Neuropsychologia* **20**(3), 249–262 (1982)
13. Sobotka, S.S., Davidson, R.J., Senulis, J.A.: Anterior brain electrical asymmetries in response to reward and punishment. *Electroencephalogr. Clin. Neurophysiol.* **83**(4), 236–247 (1997)
14. Garcia O., Favela J., Machorro R.: Emotional awareness in collaborative systems. In: *IEEE Proceedings on String Processing and Information Retrieval Symposium*, pp. 296–303. Cancun, 22–24 Sep 1999. doi: [10.1109/SPIRE.1999.796607](https://doi.org/10.1109/SPIRE.1999.796607)
15. Picard, R.W.: Toward machines with emotional intelligence. In: Matthews, G., Zeidner, M., Roberts, R.D. (eds.) *The Science of Emotional Intelligence: Knowns and Unknowns*. Oxford University Press, Oxford (2007)
16. Plutchik, R., Kellerman, H.: Emotion theory research and experience. New York Academic Press, New York (1980)
17. Olofsson, J.K., Nordin, S., Sequeira, H., Polich, J.: Affective picture processing: an integrative review of ERP findings. *Biol. Psychol.* **77**(3), 247–265 (2008)
18. Codispoti, M., Ferrari, V., Bradley, M.M.: Repetition and event-related potentials: distinguishing early and late processes in affective picture perception. *J. Cogn. Neurosci.* **19**(4), 577–586 (2007)

19. Olofsson, J.K., Polich, J.: Affective visual event-related potentials: arousal, repetition, and time-on-task. *Biol. Psychol.* **75**(1), 101–108 (2007)
20. Bernat, E., Bunce, S., Shevrin, H.: Event-related brain potentials differentiate positive and negative mood adjectives during both supraliminal and subliminal visual processing. *Int. J. Psychophysiol.* **42**(1), 11–34 (2001)
21. Cuthbert, B.N., Schu, H.T., Bradley, M.M., Birbaumer, N., Lang, P.J.: Brain potentials in affective picture processing: covariation with autonomic arousal and affective report. *Biol. Psychol.* **52**(2), 95–111 (2000)
22. Blankertz, B., Lemm, S., Treder, M., Haufe, S., Muller, K.R.: Single-trial analysis and classification of ERP components-a tutorial. *NeuroImage* **56**(2), 814–825 (2011)
23. Jarchi, D., Sanei, S., Principe, J.C., Makkiabadi, B.: A new spatiotemporal filtering method for single-trial estimation of correlated ERP subcomponents. *IEEE Trans. Biomed. Eng.* **58**(1), 132–143 (2011)
24. Vanderperren, K., Mijovic, B., Novitskiy, N., Vanrumste, B., Stiers, P., Van den Bergh, B.R., Lagae, L., Sunaert, S., Wagemans, J., Van Huffel, S., De Vos, M.: Single trial ERP reading based on parallel factor analysis. *Psychophysiology* **50**(1), 97–110 (2013)
25. Balconi, M., Lucchiari, C.: EEG correlates (event-related desynchronization) of emotional face elaboration: a temporal analysis. *Neurosci. Lett.* **392**(1–2), 118–123 (2006)
26. Balconi, M., Mazza, G.: Brain oscillations and BIS/BAS (behavioral inhibition/activation system) effects on processing masked emotional cues ERS/ERD and coherence measures of alpha band. *Int. J. Psychophysiol.* **74**(2), 158–165 (2009)
27. Gotlib, I.H., Ranganath, C., Rosenfeld, J.P.: Frontal EEG alpha asymmetry, depression, and cognitive functioning. *Cogn. Emot.* **12**(3), 449–478 (1998)
28. Keil, A., Muller, M.M., Gruber, T., Wienbruch, C., Stolarova, M., Elbert, T.: Effects of emotional arousal in the cerebral hemispheres: a study of oscillatory brain activity and event related potentials. *Clin. Neurophysiol.* **112**(11), 2057–2068 (2001)
29. Muller, M.M., Keil, A., Gruber, T., Elbert, T.: Processing of affective pictures modulates right-hemispheric gamma band EEG activity. *Clin. Neurophysiol.* **110**(11), 1913–1920 (1999)
30. Aftanas, L.I., Golocheikine, S.A.: Non-linear dynamic complexity of the human EEG during meditation. *Neurosci. Lett.* **330**(2), 143–146 (2002)
31. Aftanas, L.I., Reva, N.V., Varlamov, A.A., Pavlov, S.V., Makhnev, V.P.: Analysis of evoked EEG synchronization and desynchronization in conditions of emotional activation in humans: temporal and topographic characteristics. *Neurosci. Behav. Physiol.* **34**(8), 859–867 (2004)
32. Aftanas, L.I., Varlamov, A.A., Pavlov, S.V., Makhnev, V.P., Reva, N.V.: Affective picture processing: event-related synchronization within individually defined human theta band is modulated by valence dimension. *Neurosci. Lett.* **303**(2), 115–118 (2001)
33. Bos D.O.: EEG-based emotion recognition. The Influence of Visual and Auditory Stimuli, 1–17 (2006)
34. Schaaff, K., Schultz, T.: Towards an EEG-based emotion recognizer for humanoid robots. In: The 18th IEEE International Symposium on Robot and Human Interactive Communication, pp. 792–796. Toyama, 27 Sept.-2 Oct. 2009. doi: [10.1109/ROMAN.2009.5326306](https://doi.org/10.1109/ROMAN.2009.5326306)
35. Murugappan, M., Rizon, M., Nagarajan, R., Yaacob, S., Hazry, D., Zunaidi, I.: Time-frequency analysis of EEG signals for human emotion detection. In: 4th Kuala Lumpur International Conference on Biomedical Engineering, pp. 262–265. Kuala Lumpur, Malaysia, 25–28 June 2008. doi: [10.1007/978-3-540-69139-6-68](https://doi.org/10.1007/978-3-540-69139-6-68)
36. Chanel G., Ansari-Asl K., Pun T.: Valence-arousal evaluation using physiological signals in an emotion recall paradigm. In: IEEE International Conference on Systems, Man and Cybernetics Montreal Que, pp. 2662–2667, 7–10 Oct. 2007. doi: [10.1109/ICSMC.2007.4413638](https://doi.org/10.1109/ICSMC.2007.4413638)
37. Hosseini, S.A., Khalilzadeh, M.A., Changiz, S.: Emotional stress recognition system for affective computing based on bio-signals. *J. Biol. Syst.* **18**(1), 101–114 (2010)

38. Kim, K.H., Bang, S.W., Kim, S.R.: Emotion recognition system using short-term monitoring of physiological signals. *Med. Biol. Eng. Comput.* **42**(3), 419–427 (2004)
39. Takahashi, K.: Remarks on emotion recognition from bio-potential signals. In: 2nd International Conference on Autonomous Robots and Agents, pp. 186–191. Palmerston North, New Zealand, 13–15 Dec. 2004
40. Murugaan, M., Nagarajan, R., Yaacob, S.: Appraising human emotions using time frequency analysis based EEG alpha band features. In: Invative Techlogies in Intelligent Systems and Industrial Applications, pp. 70–75. Monash, 25–26 July 2009. doi: [10.1109/CITISIA.2009.5224237](https://doi.org/10.1109/CITISIA.2009.5224237)
41. Petrantonakis, P.C., Hadjileontiadis, L.J.: Adaptive emotional information retrieval from EEG signals in the time-frequency domain. *IEEE Trans. Signal Process.* **60**(5), 2604–2616 (2012)
42. Knyazev, G.G.: Motivation, emotion, and their inhibitory control mirrored in brain oscillations. *Neurosci. Biobehav. Rev.* **31**(3), 377–395 (2007)
43. Choppin A.: EEG-based human interface for disabled individuals: emotion expression with neural networks. Master thesis, Information processing, Tokyo Institute of Technology, Yokohama, Japan (2000)
44. Chanel G., Kronegg J., Grandjean D., Pun T.: Emotion assessment arousal evaluation using EEG's and peripheral physiological signals. In: Gunsel, B., Tekalp, AM., Jain, AK., Sankur, B. (eds.) *Multimedia Content Representation Classification and Security Springer Lectures Notes in Computer Sciences 4105*, pp. 530–537 (2006). doi: [10.1007/11848035-70](https://doi.org/10.1007/11848035-70)
45. Khosrowabadi, R., Rahman, A.W.A.: Classification of EEG correlates on emotion using features from Gaussian mixtures of EEG spectrogram. In: International Conference on Information and Communication Technology for the Muslim World, pp. E102–E107. Jakarta, 13–14 Dec. 2010. doi: [10.1109/ICT4M.2010.5971942](https://doi.org/10.1109/ICT4M.2010.5971942)
46. Lin, Y.P., Jung, T.P., Chen, J.H.: EEG dynamics during music appreciation. In: 31st Annual International Conference of the IEEE EMBS, pp. 5316–5319. Minneapolis, MN, USA, 3–6 Sept. 2009. doi: [10.1109/EMBS.2009.5333524](https://doi.org/10.1109/EMBS.2009.5333524)
47. Ishino, K., Hagiwara, M.: A feeling estimation system using a simple electroencephalograph. In: IEEE International Conference on Systems, Man and Cybernetics, pp. 4204–4209, 5–8 Oct. 2003. doi: [10.1109/ICSMC.2003.1245645](https://doi.org/10.1109/ICSMC.2003.1245645)
48. Rani, P., Liu, C., Sarkar, N., Vanman, E.: An empirical study of machine learning techniques for affect recognition in human-robot interaction. *Pattern Anal. Appl.* **9**(1), 58–69 (2006)
49. Liu, C., Agrawal, P., Sarkar, N., Chen, S.: Dynamic difficulty adjustment in computer games through real-time anxiety-based affective feedback. *Int. J. Hum. Compu. Interac.* **25**(6), 506–529 (2009)
50. Mandryk, R.L., Atkins, M.S.: A fuzzy physiological approach for continuously modeling emotion during interaction with play technologies. *Int. J. Hum Comput Stud.* **65**(4), 329–347 (2007)
51. Chanel G., Rebetez C., Bétrancourt M., Pun T.: Boredom, engagement and anxiety as indicators for adaptation to difficulty in games. In: Proceedings of the 12th International Conference on Entertainment Media Ubiquitous Era (MindTrek '08), pp. 13–17 (2008). doi: [10.1145/1457199.1457203](https://doi.org/10.1145/1457199.1457203)
52. Khosrowabadi, R., Heijnen, M., Wahab, A., Quek, H.C.: The dynamic emotion recognition system based on functional connectivity of brain regions. In: IEEE Intelligent Vehicles Symposium, pp. 377–381. San Diego, 21–24 June 2010. doi: [10.1109/IVS.2010.5548102](https://doi.org/10.1109/IVS.2010.5548102)
53. Petersen, M., Stahlhut, C., Stopczynski, A., Larsen, J., Hansen, L.: Smartphones get emotional: mind reading images and reconstructing the neural sources. *Affective Computing and Intelligent Interaction*, volume 6975 of *Lecture Notes in Computer Science*, pp. 578–587. Springer, Berlin (2011). doi: [10.1007/978-3-642-24571-8-72](https://doi.org/10.1007/978-3-642-24571-8-72)
54. Horlings, R., Datcu, D., Rothkrantz, L.J.M.: Emotion recognition using brain activity. In: Proceedings of the 9th International Conference on Computer Systems and Technologies and Workshop for PhD Students in Computing, pp. 1–6 (2008). doi: [10.1145/1500879.1500888](https://doi.org/10.1145/1500879.1500888)

55. Hjorth, B.: EEG analysis based on time domain properties. *Electroencephalogr. Clin. Neurophysiol.* **29**(3), 306–310 (1970)
56. Aftanas, L.I., Lotova, N.V., Koshkarov, V.I., Pokrovskaja, V.L., Popov, S.A., Makhnev, V. P.: Non-linear analysis of emotion EEG: calculation of Kolmogorov entropy and the principal Lyapunov exponent. *Neurosci. Lett.* **226**(1), 13–16 (1997)
57. Boostani, R., Moradi, M.H.: A new approach in the BCI research based on fractal dimension as feature and Adaboost as classifier. *J. Neural Eng.* **1**(4), 212–217 (2004)
58. Hoseingholizade, S., Golpaygani, M.R.H., Monfared, A.S.: Studying emotion through nonlinear processing of EEG. In: *Procedia-Social and Behavioral Sciences*, The 4th International Conference of Cognitive Science, vol 32, pp. 163–169 (2012)
59. Murugappan, M., Ramachandran, N., Sazali, Y.: Classification of human emotion from EEG using discrete wavelet transform. *J. Biomed. Sci. Eng.* **3**(4), 390–396 (2010)
60. Brown L., Grundlehner B., Penders J.: Towards wireless emotional valence detection from EEG. In: 2011 Annual International Conference of the IEEE Engineering in Medicine and Biology Society pp. 2188–2191. Boston, MA, 30 Aug.–3 Sept. 2011. doi: [10.1109/IEMBS.2011.6090412](https://doi.org/10.1109/IEMBS.2011.6090412)
61. Hosseini, S.A., Khalilzadeh, M.A., Naghibi-Sistani, M.B., Niazmand, V.: Higher order spectra analysis of EEG signals in emotional stress states. In: 2010 Proceedings of the 2nd International Conference on Information Technology and Computer Science, pp. 60–63. Kiev (2010b), 24–25 July 2010. doi: [10.1109/ITCS.2010.21](https://doi.org/10.1109/ITCS.2010.21)
62. Frantzidis, C.A., Bratsas, C., Papadelis, C.L., Konstantinidis, E., Pappas, C., Bamidis, P.D.: Toward emotion aware computing an integrated approach using multichannel neurophysiological recordings and affective visual stimuli. *IEEE Trans. Inf. Technol. Biomed.* **14**(3), 589–597 (2010)
63. Chanel, G., Kierkels, J.J.M., Soleymani, M., Pun, T.: Short-term emotion assessment in a recall paradigm. *Int. J. Hum Comput Stud.* **67**(8), 607–627 (2009)
64. Murugappan, M., Nagarajan, R., Yaacob, S.: Combining spatial filtering and wavelet transform for classifying human emotions using EEG signals. *J. Med. Biol. Eng.* **31**(1), 45–51 (2010)
65. Lin, Y.P., Wang, C.H., Jung, T.P., Wu, T.L., Jeng, S.K., Duann, J.R., Chen, J.H.: EEG-based emotion recognition in music listening. *IEEE Trans. Biomed. Eng.* **57**(7), 1798–1806 (2010)
66. Lin, Y.P., Wang, C.H., Wu, T.L., Jeng, S.K., Chen, J.H.: Multilayer perceptron for EEG signal classification during listening to emotional music. In: IEEE Region 10 Conference on TENCON 2007, pp. 1–3. Taipei, 30 Oct.–2 Nov. 2007. doi: [10.1109/TENCON.2007.4428831](https://doi.org/10.1109/TENCON.2007.4428831)
67. Petrantonakis, P.C., Hadjileontiadis, L.J.: Emotion recognition from EEG using higher order crossings. *IEEE Trans. Inf Technol. Biomed.* **14**(2), 186–197 (2010)
68. Wang, X.W., Nie, D., Lu, B.L.: EEG-based emotion recognition using frequency domain features and support vector machines. In: *Neural Information Processing of Lecture Notes in Computer Science*, vol. 7062, pp. 734–743. China, 13–17 Nov. 2011
69. Hadjidimitriou, S.K., Hadjileontiadis, L.J.: Toward an EEG-based recognition of music liking using time-frequency analysis. *IEEE Trans. Biomed. Eng.* **59**(12), 3498–3510 (2012)
70. Ball G., Breese J.: Modeling the emotional state of computer users. In: *Workshop on Attitude, Personality and Emotions in User-Adapted Interaction*, Banff, Canada (1999)
71. Hudlicka, E.: Increasing SIA architecture realism by modeling and adapting to affect and personality. In: *Socially Intelligent Agents Multiagent Systems, Artificial Societies, and Simulated Organizations*, vol 3, pp. 53–60 (2002). doi: [10.1007/0-306-47373-9\\_6](https://doi.org/10.1007/0-306-47373-9_6)
72. Dubois, D., Prade, H.: Possibility theory, probability theory and multiple-valued logics: a clarification. *Ann. Math. Artif. Intell.* **32**(1–4), 35–66 (2001)
73. Jang, J.S.R., Sun, C.T., Mizutani, E.: *Neuro-Fuzzy and Soft Computing: A Computational Approach to Learning and Machine Intelligence*. Prentice Hall Inc, Saddle River (1997)
74. Zhang, Q., Lee, M.: Fuzzy-gist for emotion recognition in natural scene images. In: IEEE 8th International Conference on Development and Learning, pp. 1–7. Shanghai, 5–7 June 2009. doi: [10.1109/DEVLRN.2009.5175518](https://doi.org/10.1109/DEVLRN.2009.5175518)

75. Dubois, D., Prade, H.: An introduction to fuzzy systems. *Clin. Chim. Acta* **270**(1), 3–29 (1998)
76. Kuncheva, L.I., Steimann, F.: Fuzzy diagnosis. *Artif. Intell. Med.* **16**, 121–128 (1999)
77. Nauck, D., Kruse, R.: Obtaining interpretable fuzzy classification rules from medical data. *Artif. Intell. Med.* **16**(2), 149–169 (1999)
78. Jang, J.S.R.: Self-learning fuzzy controllers based on temporal backpropagation. *IEEE Trans. Neural Networks* **3**(5), 714–723 (1992)
79. Jang, J.S.R.: ANFIS adaptive-network-based fuzzy inference system. *IEEE Trans. Syst. Man Cybern.* **23**(3), 665–685 (1993)
80. Belal, S.Y., Taktak, A.F.G., Nevill, A.J., Spencer, S.A., Roden, D., Bevan, S.: Automatic detection of distorted plethysmogram pulses in neonates and paediatric patients using an adaptive-network-based fuzzy inference system. *Artif. Intell. Med.* **24**(2), 149–165 (2002)
81. Usher, J., Campbell, D., Vohra, J., Cameron, J.: A fuzzy logic-controlled classifier for use in implantable cardioverter defibrillators. *Pacing Clin. Electrophysiol.* **22**(1), 183–186 (1999)
82. Übeyli, E.D., Güler, I.: Automatic detection of erythema-to-squamous diseases using adaptive neuro-fuzzy inference systems. *Comput. Biol. Med.* **35**(5), 421–433 (2005)
83. Übeyli, E.D., Güler, I.: Adaptive neuro-fuzzy inference systems for analysis of internal carotid arterial Doppler signals. *Comput. Biol. Med.* **35**(8), 608–702 (2005)
84. Virant-Klun, I., Virant, J.: Fuzzy logic alternative for analysis in the biomedical sciences. *Int. J. Comput. Biomed. Res.* **32**(4), 305–321 (1999)
85. Cristianini N., Taylor J.S.: An introduction to support vector machines and other kernel-based learning methods. Cambridge UK Cambridge University Press, Cambridge (2000)
86. Yang, Y.H., Liu, C.C., Chen, H.H.: Music emotion classification: a fuzzy approach. In: Proceedings of ACM Multimedia, pp. 81–84. Santa Barbara, CA, 23–27 Oct. 2006. doi: [10.1145/1180639.1180665](https://doi.org/10.1145/1180639.1180665)
87. Srinivasa, K.G., Venugopal, K.R., Patnaik, L.M.: Feature extraction using fuzzy C-means clustering for data mining systems. *Int. J. Comput. Sci. Netw. Secur.* **6**(3A), 230–236 (2006)
88. Murugappan, M., Rizon, M., Nagarajan, R., Yaacob, S., Zunaidi, I., Hazry, D.: EEG feature extraction for classifying emotions using FCM and FKM. *Int. J. Comput. Commun.* **1**(2), 21–25 (2007)
89. Murugappan, M., Rizon, M., Nagarajan, R., Yaacob, S., Zunaidi, I., Hazry, D.: Lifting scheme for human emotion recognition using EEG. In: International Symposium on Information Technology, pp. 1–7. Kuala Lumpur, Malaysia, 26–28 Aug. 2008. doi: [10.1109/ITSIM.2008.4631646](https://doi.org/10.1109/ITSIM.2008.4631646)
90. Berka, C., Levendowski, D.J., Cvetinovic, M.M., Petrovic, M.M., Davis, G., Lumicao, M.N., Zivkovic, V.T., Popovic, M.V., Olmstead, R.: Real-time analysis of EEG indexes of alertness, cognition, and memory acquired with a wireless EEG headset. *Int. J. Hum. Comput. Interact.* **17**(2), 151–170 (2004)
91. Besserve, M., Philippe, M., Florence, G., Laurent, F., Garnero, L., Martinerie, J.: Prediction of performance level during a cognitive task from ongoing EEG oscillatory activities. *Clin. Neurophysiol.* **119**(4), 897–908 (2008)
92. Freeman, F.G., Mikulka, P.J., Scerbo, M.W., Scott, L.: An evaluation of an adaptive automation system using a cognitive vigilance task. *Biol. Psychol.* **67**(3), 283–297 (2004)
93. Pope, A.T., Bogart, E.H., Bartolome, D.S.: Biocybernetic system evaluates indexes of operator engagement in automated task. *Biol. Psychol.* **40**(1–2), 187–195 (1995)
94. Wilson, G.F., Russell, C.A.: Real-time assessment of mental workload using psychophysiological measures and artificial neural networks. *Hum. Factors* **45**(4), 635–643 (2003)
95. Davidson, R.J., Jackson, D.C., Kalin, N.H.: Emotion plasticity context and regulation perspectives from affective neuroscience. *Psychol. Bull.* **126**(6), 890–909 (2000)
96. Niedermeyer, E., Silva, F.L.: *Electroencephalography basic principles clinical applications and related fields*. Baltimore MD Williams and Wilkins, New York (1993)
97. Ekman P.: Basic emotions. In: Dalgleish, T., Power, M. (eds.) *Handbook of Cognition and Emotion* Sussex. UK John Wiley & Sons Ltd, New York (1999)

98. Lang, P.J.: The emotion probe studies of motivation and attention. *Am. Psychol.* **50**(5), 372–385 (1995)
99. Kim, J., Andre, E.: Emotion recognition based on physiological changes in music listening. *IEEE Trans. Pattern Anal. Mach. Intell.* **30**(12), 2067–2083 (2008)
100. Koelstra, S., Muhl, C., Soleymani, M., Lee, J.S., Yazdani, A., Ebrahimi, T., Pun, T., Nijholt, A., Patras, I.: DEAP: a database for emotion analysis using physiological signals. *IEEE Trans. Affect. Comput.* **3**(1), 18–31 (2012)
101. Murugappan, M., Juhari, M.R.B.M., Nagarajan, R., Yaacob, S.: An investigation on visual and audiovisual stimulus based emotion recognition using EEG. *Int. J. Med. Eng. Inform.* **1**(3), 342–356 (2009)
102. Cowie R., Douglas-Cowie E., Savvidou S., McMahon E., Sawey M., Schroder M.: ‘Feeltrace’ an instrument for recording perceived emotion in real time. In: Proceedings of ISCA Workshop Speech and Emotion, pp. 19–24. Newcastle, UK (2000)
103. Strela, V., Heller, P.N., Strang, G., Topiwala, P., Heil, C.: The application of multiwavelet filter banks to image processing. *IEEE Trans. Image Process.* **8**(4), 548–563 (1999)
104. Cotronei, M., Lazzaro, D., Montefusco, L.B., Puccio, L.: Image compression through embedded multiwavelet transform coding. *IEEE Trans. Image Process.* **9**(2), 184–189 (2000)
105. Cotronei, M., Montefusco, L.B., Puccio, L.: Multiwavelet analysis and signal processing. *IEEE Trans. Circ. Syst. II* **45**(8), 970–987 (1998)
106. Hsung, T.S., Lun, D.P.K., Ho, K.C.: Optimizing the multiwavelet shrinkage denoising. *IEEE Trans. Signal Process.* **53**(1), 240–251 (2005)
107. Khouzani, K.J., Zadeh, H.S.: Multiwavelet grading of pathological images of prostate. *IEEE Trans. Biomed. Eng.* **50**(6), 697–704 (2003)
108. Wang, J.W.: Multiwavelet packet transforms with application to texture segmentation. *Electron. Lett.* **38**, 1021–1023 (2002)
109. Jahankhani, P., Kodogiannis, V., Revett, K.: EEG signal classification using wavelet feature extraction and neural networks. In: IEEE John Vincent Atanasoff 2006 International Symposium on Modern Computing, pp. 52–57. Sofia, 3–6 Oct. 2006. doi: [10.1109/JVAC.2006.17](https://doi.org/10.1109/JVAC.2006.17)
110. Kalayci, T., Ozdamar, O.: Wavelet preprocessing for automated neural network detection of EEG spikes. *IEEE Eng. Med. Biol. Mag.* **14**(2), 160–166 (1995)
111. Guo, L., Rivero, D., Pazos, A.: Epileptic seizure detection using multiwavelet transform based approximate entropy and artificial neural networks. *J. Neurosci. Methods* **193**(1), 156–163 (2010)
112. Plonka, G., Strela, V.: From wavelets to multiwavelet. In: Dahlen, M., Lyche, T., Schumaker, LL. (eds.) *Mathematical Methods for Curves and Surfaces II*. Vanderbilt University Press, Nashville, pp. 375–399 (1998)
113. Geronimo, J.S., Hardin, D.P., Massopust, P.R.: Fractal functions and wavelet expansions based on several scaling functions. *J. Approximation Theor.* **78**(3), 373–401 (1994)
114. Qumar, J., Pachori, R.B.: A novel technique for merging of multisensor and defocussed images using multiwavelets. In: IEEE Region 10 (TENCON 2005), pp. 1733–1738. Melbourne, 21–24 Nov. 2005. doi: [10.1109/TENCON.2005.300836](https://doi.org/10.1109/TENCON.2005.300836)
115. Xiaodong, W., Yanyang, Z., Zhengjia, H.: Multiwavelet denoising with improved neighboring coefficients for application on rolling bearing fault diagnosis. *Mech. Syst. Signal Process.* **25**(1), 285–304 (2011)
116. Shaw, R.: Strange attractors chaotic behavior and information flow. *Naturforsch* **36A**, 80–112 (1981)
117. Grassberger, P., Procaccia, I.: Estimation of the kolmogorov entropy from a chaotic signal. *Phys. Rev. A* **28**(4), 2591–2593 (1983)
118. Eckmann, J.P., Ruelle, D.: Ergodic theory of chaos and strange attractors. *Rev. Mod. Phys.* **57**(3), 617–656 (1985)
119. Takens, F.: Invariants related to dimension and entropy. In: Proceedings of 13th Coloquio Brasileiro de Matematica, Rio de Janeiro, Brazil (1983)

120. Pincus, S.M.: Approximate entropy as a measure of system complexity. *Proc. Natl. Acad. Sci.* **88**(6), 2297–2301 (1991)
121. Richman, J.S., Moorman, J.R.: Physiological time-series analysis using approximate entropy and sample entropy. *Am. J. Physiol. Heart Circ. Physiol.* **278**(6), H2039–H2049 (2000)
122. Chen X., Solomon I.C., Chon K.H.: Comparison of the use of approximate entropy and sample entropy applications to neural respiratory signal. In: Proceedings of the IEEE Engineering in Medicine and Biology 27th Annual Conference, pp. 4212–4215. Shanghai China (2005), 17–18 Jan. 2006. doi: [10.1109/IEMBS.2005.1615393](https://doi.org/10.1109/IEMBS.2005.1615393)
123. Song, Y., Lio, P.: A new approach for epileptic seizure detection sample entropy based extraction and extreme learning machine. *J. Biomed. Sci. Eng.* **3**(6), 556–567 (2010)
124. Jones, D., Parks, T.W.: A high resolution data-adaptive time-frequency representation. *IEEE Trans. Acoust. Speech Sign. Process.* **38**(12), 2127–2135 (1990)
125. Shannon, C.E.: A mathematical theory of communication. *Bell Syst. Tech. J.* **27**, 379–423 (1948)
126. Renyi, A.: On measures of entropy and information. *Proc. Fourth Berkeley Symp. Math. Stat. Probab.* **1**, 547–561 (1961)
127. Sengur, A.: Multiclass least-squares support vector machines for analog modulation classification. *Expert Syst. Appl.* **36**(3), 6681–6685 (2009)
128. Bajaj, V., Pachori, R.B.: Automatic classification of sleep stages based on the time-frequency image of EEG signals. *Comput. Methods Programs Biomed.* **112**(3), 320–328 (2013)
129. Bajaj, V., Pachori, R.B.: Classification of seizure and nonseizure EEG signals using empirical mode decomposition. *IEEE Trans. Inf Technol. Biomed.* **16**(6), 1135–1142 (2012)
130. Bajaj V., Pachori R.B.: EEG signal classification using empirical mode decomposition and support vector machine. In: International Conference on Soft Computing for Problem Solving, AISC 131, pp. 623–635. Roorkee, India, (2012b), 20–22 December 2011. doi: [10.1007/978-81-322-0491-6-57](https://doi.org/10.1007/978-81-322-0491-6-57)
131. Suykens, J.A.K., Vandewalle, J.: Least squares support vector machine classifiers. *Neural Process. Lett.* **9**(3), 293–300 (1999)
132. Vapnik, V.: The nature of statistical learning theory. Springer, New York (1995)
133. Suykens, J.A.K., Vandewalle, J.: Multiclass least squares support vector machines. In: International Joint Conference on Neural Networks, pp. 900–903. Washington, DC, Jul 1999. doi: [10.1109/IJCNN.1999.831072](https://doi.org/10.1109/IJCNN.1999.831072)
134. Xing, Y., Wu, X., Xu, Z.: Multiclass least square wavelet support vector machines. In: IEEE International Conference on Networking Sensing and Control, pp. 498–502. Sanya, 6–8 April 2008. doi: [10.1109/ICNSC.2008.4525268](https://doi.org/10.1109/ICNSC.2008.4525268)
135. Zavar, M., Rahati, S., Akbarzabeh, M.R., Ghasemifard, H.: Evolutionary model selection in a wavelet-based support vector machine for automated seizure detection. *Expert Syst. Appl.* **38**(9), 10751–10758 (2011)

## **Chapter 9**

# **A Configurable, Inexpensive, Portable, Multi-channel, Multi-frequency, Multi-chromatic RGB LED System for SSVEP Stimulation**

**Surej Mouli, Ramaswamy Palaniappan and Ian P. Sillitoe**

**Abstract** Steady state visual evoked potential (SSVEP) is extensively used in the research of brain-computer interface (BCI) and require a controllable and configurable light source. SSVEP requires appropriate control of visual stimulus parameters, such as flicker frequency, light intensity, multi-frequency light source and multi-spectral compositions. Light emitting diodes (LEDs) are extensively used as a light source as they are energy efficient, low power, multi-chromatic, have higher contrast, and support wider frequency ranges. Here, we present the design of a compact versatile visual stimulus which is capable of producing simultaneous multiple frequency RGB LED flicker suitable for a wide range of SSVEP paradigms. The hardware is based upon the open source Arduino platform and supports on-the-fly reprogramming with easily configurable user interface via USB. The design provides fourteen independent high output channels with customisable output voltages. The flicker frequencies can be easily customised within the frequency range of 5–50 Hz, using a look-up table. The LED flickers are generated with single RGB LEDs which generate the required colour or frequency combinations for combined multi-frequency flicker with variable duty cycle to generate SSVEP. Electroencephalogram (EEG) signals have been successfully recorded from five subjects using the stimulator for different frequencies, colours, duty cycle, intensity and multiple frequency RGB source, thereby demonstrating the high usability, adaptability and flexibility of the stimulator. Finally we discuss the possible improvements to the stimulator which could provide real time user feedback to reduce visual fatigue and so increase the level of user comfort.

---

S. Mouli · I.P. Sillitoe

School of Engineering, University of Wolverhampton, Telford, UK  
e-mail: surej.m@wlv.ac.uk

I.P. Sillitoe

e-mail: i.sillitoe@wlv.ac.uk

R. Palaniappan (✉)

School of Computing, University of Kent, Medway, UK  
e-mail: r.palani@kent.ac.uk

**Keywords** Brain-computer interface · Electroencephalogram · LED · Steady-state visual evoked potential

## 9.1 Introduction

Human machine systems refer to the combination of human and machines to accomplish certain tasks through communication between human and machines. This can be considered as an interaction of two systems which communicate with each other in order to fulfil a task. The means of communication include movements, dialogues or by means of non-muscular actions. Human computer interaction (HCI) is a process of inputting the information and getting the desired output through external devices. Many types of HCI exist, some use direct interaction without any detailed processing of the data, whereas other systems use complex algorithms to extract the required output for performing the tasks. Other than data interaction, figures, images, colours and sound are also used in HCI for performing tasks. HCI make use of different muscular movement or signals from human body so as to communicate with the external world using interfacing technology. This has become an active research area in the recent years [1]. Modern HCI systems also use more intelligent interactive systems such as *learn and process* where the computer analyses the data and interprets it intelligently to avoid mistakes and improve accuracy [2]. The data analysis methods used in HCI are closely coupled to the purpose of the system and the computer usually analyses the data it receives in response to an action performed by human.

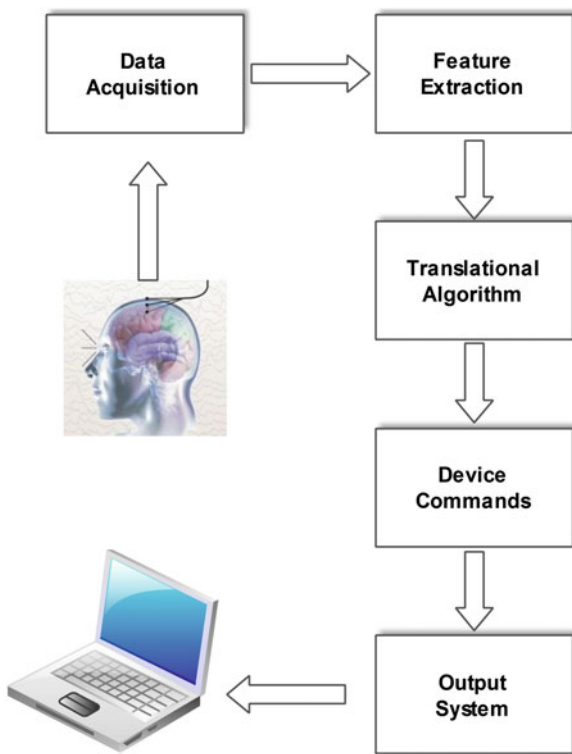
One innovative and widely researched area of HCI is Brain-computer Interface (BCI). BCI is a type of non-muscular communication system that conveys the changes in brain wave activity directly to an external device in order to perform some desired task [3]. Figure 9.1 shows the basic BCI interface for data acquisition and processing. The system acquires the signal from the brain using electrode fitted on the scalp, the extremely low potential signals are digitised and processed in a hierarchy of stages to extract useful information for external interaction.

EEG contains detailed information on different states of brain and is useful in understanding the physiological condition of a person and is present in different parts of the brain. Electrodes are fitted on these specific areas to record EEG. This helps in analysing the EEG for specific disabilities or to evaluate the functional performance of any particular action.

Berger [4] identified that specific waves were present in EEG in the range of 8–12 Hz and named these as alpha waves. Later researchers identified many additional sub-bands in particular, delta (0–3.65 Hz), theta (3.65–7.25 Hz), alpha (7.25–14.5 Hz) and beta (14.5–29 Hz) [5]. The use of the sub-band structure aids the classification and analysis of EEG signals.

BCI can be categorised into two types namely invasive BCI and non-invasive BCI. Invasive BCI requires surgical procedures to implant electrode on the surface of the brain to directly read the activity but produces high quality signals for

**Fig. 9.1** Basic data flow scheme in BCI



experiments. Non-invasive BCI uses sensors which are mounted on a cap or a headband on the scalp. Often non-invasive BCI requires pre-preparation of the skin and/or the use of conductive gel, in order that the signal has a suitably high signal-to-noise ratio (SNR). The strength of EEG signal is also strongly affected by the gravity induced changes in cerebrospinal fluid (CSF) layer thickness [6]. The attenuation of the EEG signal is proportional to the thickness of CSF layer. This property has been used to identify certain neurodegenerative disease caused by thickening of the CSF layer.

Active research has been done in the area of dry electrodes to overcome the pre-preparation procedures and to make EEG data available for various automation and control systems [3, 7]. However, currently, the SNR of dry electrode signals is typically lower than that produced by conductive gel electrodes.

Hybrid BCI attempts to combine different modalities to improve the performance of the BCI system and to make it easier to apply to a wider range of applications [8–10]. Hybrid BCI systems attempt to combine one BCI with another BCI in order to improve the quality of signals or to counteract the weaknesses inherent in a single mode system. BCI based systems are evolving as an independent communication tool to circumvent the issues that disabled people face in their lives and assist in performing basic activities.

BCI is a very complex system that requires in-depth research to develop a real time communication and processing platform to be used in real life applications. People with severe disabilities such as amyotrophic lateral sclerosis, spinal cord injury, accidental limb loss or any other restrictions in movement could be supported by BCI [11–15]. Studies show that patients with access to BCI technology recover more quickly from serious communication disabilities [16].

Research shows promising signs in using BCI to prevent and delay the onset of dementia, Alzheimer's and Parkinson's diseases in elderly people [17, 18]. BCI could also be considered as an alternative communication medium for disabled people to operate devices such as computers, assistive chairs or to communicate with the external world [15]. Since BCI is translating user's volitional intents to command an external interface, no muscular action is required by the user and this could be used by any paralysed individual [19]. These concepts could also be used to support handicapped people as their sensory motor and cortices remains intact even with loss or absence of a particular physical limb. The spatiotemporal activation produced by moving an absent limb is similar to one compared with a healthy individual [20]. Algorithms and techniques to decipher these patterns and translating them to device control would help numerous disabled people to easily cope with life. Non-invasive BCI has become an increasingly active research area in the recent years for practical applications using EEG. EEG based BCI paradigms can be used as a non-muscular control for communication since they use the electrical activity of the human brain to interact with the external environment [14, 15, 21].

In the past 20 years, BCI research has led to many innovations encouraged by new understandings of brain signals [21]. The majority of BCI data analysis requires off-line data processing, where the data is recorded from the participating subject and analysed at a later stage. Real-time data processing methods require more sophisticated hardware and more importantly, ease of use. Prolonged real-time use would require comfortable dry electrodes and wireless connectivity to a portable recording system.

Different paradigms such as slow cortical potential (SCP), P300, and visual evoked potential (VEP) are being used in EEG research [11, 13, 17]. SCP signals are recorded from the scalp and reflect the changes of activity level of cortical tissues [22]. SCP is correlated with cognitive and motor performance. Negative SCP shift exhibits increased cortical excitability and positive SCP shifts reveal the cortical inhibition. VEP based paradigms have been explored widely by researchers to support or control external devices using visual stimulus [15, 23–30]. VEP based BCI technology can be further divided into those based on transient and steady state responses. A transient VEP with varying amplitudes of negative and positive peaks is generated when visual stimulus flickers at a lower rate and it requires complex detection procedures when compared to the steady state responses [31]. P300 is one such transient VEP and depends on endogenous cognitive process and is one of the most used control signals for VEP based BCI. P300 is usually a large and positive deflection in the EEG and requires a defined number of repetitive stimulations. P300 is well known for use in the alphanumeric speller design [32]. This works in synchronous mode and is based on continuous attention of user towards the stimulus.

Steady state VEP (SSVEP), is a repetitive sinusoidal like waveform with its frequency synchronised with the frequency of the visual stimulus and it is generated in the visual cortex [33, 34]. SSVEP can be modulated by the attention of participating subject towards the stimulus and it is possible to ascertain the focus of a subject's attention when presented with multiple target stimuli with specific flicker rates. The SSVEP has attracted enormous attention due to its phase locked characteristics and better SNR, reduced training time and ability to achieve higher information transfer rate (ITR) in BCI systems [35]. Research studies have shown that the amplitude of the response in the specific stimulus frequency varies with the different subjects, colour, intensity and the type of stimulus [25, 28, 29, 36, 37]. Often SSVEP signals are corrupted with other noise such as background EEG, artifacts and external noise such as power-line interference and specific signal processing techniques will need to be employed to reduce these undesired effects.

Even though SSVEP responses are sufficiently high for practical purposes, it is not always comfortable for subjects for longer periods of time especially when the stimulus is presented using LEDs. Amplitude-frequency characteristics of SSVEP in humans have larger amplitudes from the alpha to low beta ranges and reach its maximum amplitude at approximately 13 Hz, flickers with frequencies higher than 31 Hz produces poor SSVEP response and weaker SNR [38]. Studies show low frequencies give higher responses as compared to high frequency stimuli, though the latter are more comfortable with subjects. Investigations done on overt and covert attention shows that SSVEP is more reliable with overt attention and covert attention amplitudes are far smaller than overt mode [39].

The remainder of the chapter is organised as follows. Section 9.2 summarises the related work using various visual stimulator's for generating SSVEP. Section 9.3 refers to the procedure, related hardware and software used in this experiment in developing the visual stimulus. Following Sect. 9.4 explains the results from different frequencies and EEG peaks. Next Sect. 9.5 summarises the complete experiment including the issues faced and is followed by Sect. 9.6 detailing the future possibilities and directions.

## 9.2 Related Work

SSVEP was first investigated for BCI by Middendorf et al. [40] and in their experiment, each presented target was flashed at a specific frequency. A subject's gaze was determined by using spectral measures of the recorded EEG signal. The maximal amplitude in the frequency domain was at the frequency component identical to the flicker rate of the target that had the subject's attention. This method has become the paradigm of choice by many subsequent BCI researchers using SSVEP. The SSVEP properties allow target stimuli to be independently tagged by flicker rate and make it an ideal paradigm for a BCI. Further, SSVEP based BCI has the most important advantage of not requiring prior training, whilst offering high information transfer rate, and has been found to be suitable for numerous BCI

applications such as keypad entry [41], device control [42], and assistive control [15]. The selection of frequencies in SSVEP allows artifact reduction such as blinks and background EEG and therefore SSVEP based BCI systems are more robust than other systems such as transient VEP (that uses P300 potentials below 8 Hz) and imaginary movement based BCI systems (that use mu and beta rhythms). Recent researches in signal processing techniques have opened more doors towards developing intelligent real time algorithms for extraction and processing of EEG data that is suitable for SSVEP [17].

As mentioned, flashing stimuli of different patterns and sources has been used in the past to evoke brain potentials [8, 43, 44]. Recent research studies have shown that the amplitude of the response in the specific stimulus frequency varies with the different subject, colour, intensity and the type of stimulus [6, 29, 39]. A survey on popular devices used for creating visual stimulus such as cathode-ray-tubes (CRT), liquid crystal display (LCD), thin film transistor (TFT) display and light emitting diode (LED) based sources, identifies LED based visual stimulus as having higher bit rates when compared to other forms [45]. CRT and LCD based stimuli have comparatively low resolution, lower refresh rates and generate electromagnetic interference (EMI) emissions [46], which would add additional noise to the recorded EEG.

Visual fatigue is another major issue in SSVEP based BCI and users may suffer from visual fatigue when staring at a visual stimulus flickering for longer periods of time. Researchers have conducted studies on the effect of visual stimulus on subject's comfort and identified higher frequencies are more comfortable for the subjects and thereby reduce visual fatigue [37, 47–49].

Research based on customisation of stimulation for enhancing performance in SSVEP based BCI by Lopez et al. [28], shows SNR of the signal is significantly dependant on the combination of frequencies in visual stimulus. The study recommends the selection of appropriate stimulus configuration to avoid degradation in ITR. This study also highlights that it is possible to use this technique with subjects who are unable to control their gaze.

Investigation on high speed SSVEP based BCI for various frequency pairs and inter-source distances were performed by Resalat et al. [35], where the study showed the response to the stimulus could be small and that the inter-source distance of 14 cm was optimal. The research used a high speed Max one classifier for seven different frequency pairs and five different inter source distances. The study identified the best frequency pair which gave the highest classification accuracy was 10 and 15 Hz, and that a sweep length of 0.5 s provided the highest ITR.

The form of the visual stimulus presented to the user has a direct impact on the efficiency of SSVEP generated [36]. Most available LCD/CRT screens are based on 60–120 Hz refresh rates and can therefore only display only a limited number of individual flickering stimuli. Multiple flickering blocks which flicker at different frequencies may cause difficulties for the user when focusing on single stimulus, since the target stimuli are spatially separated on the same screen and the user's attention is distracted. This has the effect of reducing the SSVEP response significantly in covert BCI systems [50].

Research on dual frequency stimulation for SSVEP to increase the number of visual stimuli has been carried out by Hwang et al. [25]. The experiment was based on combining two different patterns of visual stimuli flickering at different frequencies in one single visual stimulus. This solves the issues with user attention shift which was confirmed with offline and online experiments.

A survey undertaken on stimulation methods [51] in SSVEP BCI compared various methods used for visual stimulus from traditional CRT based flickers to more controllable LED based stimulus. The study has considered user safety, bit rate and user comfort for the entire visual stimulus. Screen based stimulus are limited by the screen refresh rates and it is difficult to generate a precise flicker frequency for stimulus. However, LED based stimuli are driven by relatively simple hardware where the flicker frequency can always be confirmed with a digital oscilloscope. The study also found that SSVEP signals are affected by colour stimulus and signal strength varies with colour. The survey recommended the use of phase changes in the stimuli, so as to increase the number of visual stimulus. Overall, the study suggested LED based stimulus as compared to other conventional stimulus as LED based ones gave the highest bitrates. Improvement in the stimulus will also enhance the SSVEP SNR, and simplifies the signal processing and enables the use of more targets.

LEDs are more common, low cost, easily portable, have low power consumption and provide flexible means to customise a visual stimulus [52–54]. LED stimulus has the advantage of generating the required colour using RGB LEDs in the same source thus avoiding the issues in attention shifts [50]. The response in SSVEP amplitude for different colour stimulus could also be studied for different subjects for optimum performance [55]. The locations of the stimulus can be easily customised in comparison with the LCD based stimulus. The portability and lower power consumption of the hardware required for LED based stimulus is also an added advantage in mobile BCI applications. Most of the parameters in LED based stimulus, such as frequency, colour and intensity, can be programmatically controlled and this can be used to reduce the visual fatigue or improve the personal preference choice of the user.

LEDs are widely used in research for visual stimulation to increase the comfortability and reduce visual fatigue [56]. However, existing visual stimulators [52, 57, 58] based on LEDs have their limitations, as they are limited in their customisation capabilities, are not easy to program and often not possible to control LEDs individually. For a BCI researcher with a non-technical background, designing an easily controllable visual stimulator is technically challenging, since it requires an understanding of electronics and programming. In our design, we have reduced the complexity of controlling and simplified the customisation of the visual stimulator for the developer. The use of the open source electronics prototyping platform Arduino [59] simplifies the design and makes it more accessible for users with little or no prior electronics background.

The Arduino platform has been adapted by many researchers to implement either a practical or functional requirement of different designs. A recent study on LED stimulator to measure the murine pupillary light reflex in rodents demonstrates a simple application in light stimuli [58].

Arduino uses single board computing concept which is completely open source and reduces the programming complexity. It is adapted from open source project Wiring [60] and supports variety of sensors using built-in control ports. Arduino uses an intuitive programming method based on an open framework Processing [61], and is supported by an active user group which is constantly contributing for the development and research.

Arduino has development boards with different form factors namely Arduino Uno, Arduino Mega, Arduino Mini, Arduino Micro and so on [59]. In our design we have used Arduino Uno as shown in Fig. 9.2 since it's compatible with most of the off shelf expansion boards (Shields) and requires little or no prior knowledge in integrating electronic modules. The majority of these shields have the same printed circuit board (PCB) footprint so that it can be mounted directly over the main processor board. However, driving the RGB LED does require more current than the Arduino Uno controller board can deliver. To overcome this, we have used a constant current driving shield as shown in Fig. 9.3 which is a readily available

**Fig. 9.2** Arduino Uno

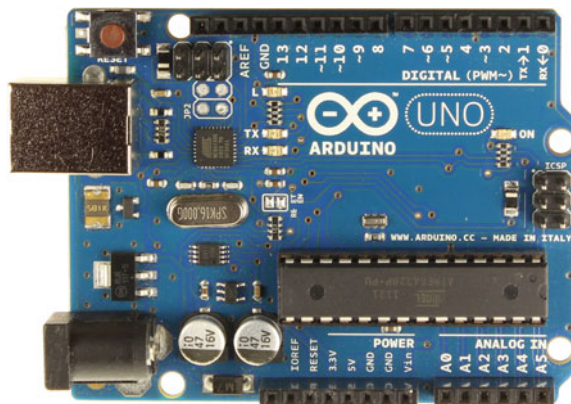


**Fig. 9.3** FET shield



pre-built plug-in module which sits over the main board [44]. This board is chosen since it fits easily on top of the Arduino Uno and also it has a wide operating voltage range from 2 to 24 V. This shield is completely independent from Arduino's operating voltage and is also capable of driving LEDs up to 3 W in constant current mode. The RGB LED can be connected securely with the screw connectors and does not require any soldering on board.

## 9.3 Materials and Methods

### 9.3.1 Design of Visual Stimulator

SSVEP visual stimulus requires light source flashing at different frequencies in the range of 6–50 Hz, in addition it is necessary to be able to precisely control the frequency and duty cycle of the flickers and control the flashing of a number of LEDs simultaneously. For the experimental setup, different colour classification would be required using primary colours Red, Green, and Blue from the same source to avoid attention shifts [50]. The platform is designed to fulfil these requirements using a wide range of high power RGB LEDs without the need to alter the hardware. The hardware platform is reusable, customisable and cheap to build with off shelf components costing less than 80. Figure 9.4 shows the basic blocks for the visual stimulus.

#### 9.3.1.1 Hardware Platform

The hardware platform for SSVEP visual stimulator consists of the core component Arduino Uno, adjustable power supply for driving the RGB LEDs and the high current output driver circuit. The system is powered by a 12 V DC power supply using rechargeable batteries, which makes it portable and avoids electromagnetic interference from the power lines. Programming the Arduino programming is performed using a USB interface connected to any PC with Arduino integrated development environment (IDE) loaded.

Arduino Uno has several ports which are grouped as inputs and outputs. Figure 9.5 shows the port layout on Arduino UNO. Arduino UNO has 14 digital

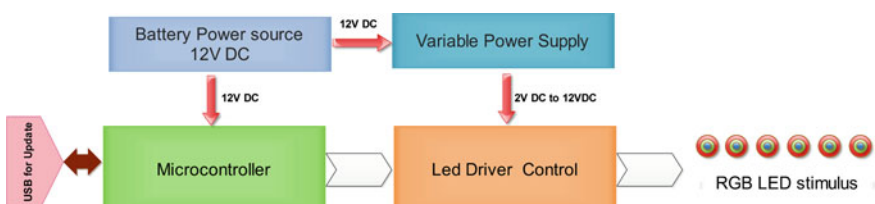


**Fig. 9.4** Visual stimulus control block

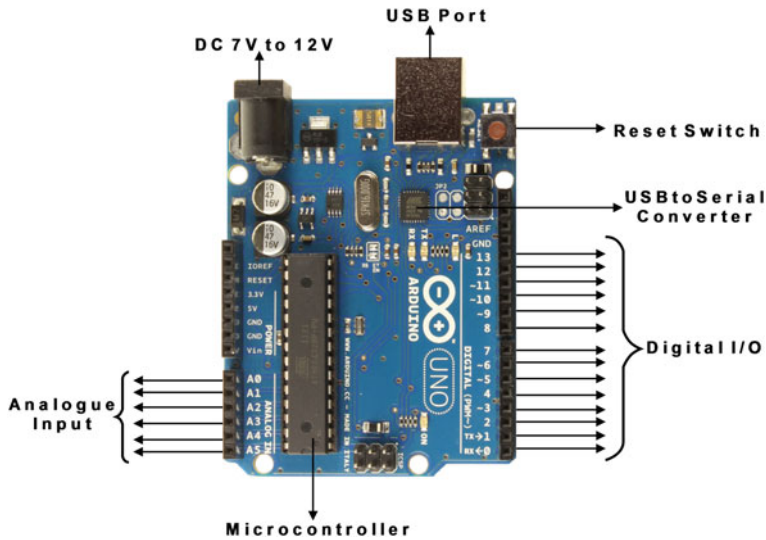


**Fig. 9.5** Arduino Uno basic connectivity layout

input/output (I/O) and six analogue input ports. In this prototype, we used twelve digital outputs to control either four RGB LEDs or 12 individual LEDs. Out of the 14 I/O lines, six of them can be used for pulse width modulation (PWM). PWM can be used to vary the intensity of individual colours or blending of different colours from one colour to another gradually.

For initial testing of Arduino Uno, LEDs can be connected with a  $330\ \Omega$  resistor in series directly to the output ports. Each I/O pin can deliver up to 40 mA which would be adequate if a single LED is used. Whereas high power RGB LED's current requirements varies from 300 to 1,500 mA depending on the brightness. The use of the Field-Effect-Transistor (FET) shield in this design has a current capacity of 8 A per channel and a wider operating voltage range of 2–24 V DC. This addresses almost all the custom requirement either in power handling capacity or different voltage requirements for making any experimental visual stimulus.

### 9.3.1.2 Microcontroller

The Arduino communicates with the host via the USB port. The initial setup requires installation of the Arduino USB drivers for the corresponding operating system in the host computer to create a virtual serial port. The Arduino communicates using serial protocol to the host using a USB to serial converter chip installed on board.

Programming the Arduino or writing sketches is via a customised IDE based on Processing [61]. The code written inside the user interface, which is fairly simple, is converted to C language and compiled before uploading to the microcontroller.

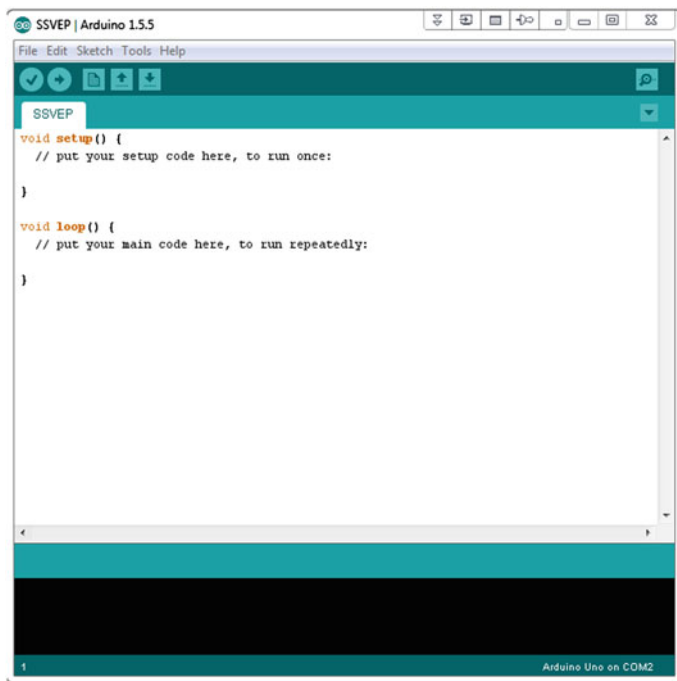


**Fig. 9.6** Arduino IDE

When uploading process is completed, Arduino can be disconnected from the host and Arduino is then functionally independent of the PC. Usually the programming cycle of an Arduino consists of four steps; (i) interfacing Arduino to the host computer via the USB port (ii) writing the program (sketch) for the desired task (iii) uploading the program to the board and waiting until the board resets (iv) disconnect and board is ready to execute the required task. The IDE is free and can be downloaded from Arduino website [59] and is as shown in Fig. 9.6.

Power consumption of Arduino mainly depends on the operating frequency of the microcontroller. Arduino Uno uses ATmega328 at a clock frequency of 16 MHz and draws a current of approximately 10 mA in active mode and 2.5 mA in idle mode. The functionalities in Arduino can be extended with shields (add on boards) that can be plugged directly on top of the main board. There are many such boards from official supporters as well as from the open source community. There is expansion shield for Bluetooth capability that can be used to connect with mobile devices in order to exchange data or control a device. Wired networking functionalities can be achieved with Ethernet shield and can be used to connect Arduino directly to a router to exchange data in a network. Biofeedback shield, *SHIELD-EKG-EMG* expands the Arduino capabilities to capture electrocardiography and electromyography signals. This shield opens new possibilities in monitoring heartbeat, gesture recognition and muscular activity. Touch screen capabilities can be added with *TouchShield Slide* for

a widescreen precise viewing, tactile sensing and adding direct interaction with Arduino. LED shields like *LoL Shield White* and *Neo Pixel Shield* could be utilised for creating experimental visual stimulus for SSVEP applications. The data logging shield which can be stacked over other data capturing shields previously mention can be used as a standalone platform for continuously recording the data on removable memory card for later analysis. The Lithium battery pack shield can be used to make Arduino portable and avoid an external power supply. Interconnection of wireless Arduino platforms can be developed using Zigbee shields to form a low level serial controlled mesh network to exchange data.

### 9.3.1.3 RGB LED

LEDs are the light source for the coming years and are being widely accepted due to its low power consumption, longer life and lower heat dissipation [62]. LED as shown in Fig. 9.7 comes in various shapes and colours and with or without in built constant current circuitry to maintain the correct luminance. These modules have different input voltage requirements that may vary from 3 to 12 V DC. The colour combined LED or RGB LED has red, green and blue LEDs embedded within a single die, each of which can be controlled individually. RGB LEDs can generate a range of colours by changing the controlling PWM signals to the individual LEDs. This chromatic control can be achieved with Arduino without involving any feedback sensors.

As mentioned earlier, LEDs can be classified in different groups. In this study, LED package based on surface mount device (SMD) technology is used, since they are available for higher power and have integral heat sinks as shown in Fig. 9.8. SMD LEDs can be easily mounted on any surface with removable glue, and their positions can be altered easily without the need of soldering. A RGB LED package has six terminals, two for each colour pair comprising of an anode and a cathode.

**Fig. 9.7** Various types of LEDs available for vision research



**Fig. 9.8** RGB LED mounted on heat dissipating plate



Anodes or cathodes can be grouped together to form a common anode configuration or common cathode configuration, respectively. In the prototype, we have used common anode configuration to match the design requirements of the LED driver FET shield.

RGB LEDs require more current than the conventional types. The current has to be maintained throughout the experiment to get the optimum results. The prototype used RGB LEDs with output power of 1 W for SSVEP EEG recording. A constant current source at 3 V was provided from a battery source using DC-DC converters with variable control, to allow customisation of output voltage for alternative RGB LEDs. The voltage range can be adjusted from 0.8 to 32 V DC depending on the input voltage. The controllable voltage source permits the use of a wide range of LEDs from different manufacturers to be tested and analysed with this prototype.

When LED is lit, the LED temperature rises with time until a balance state is reached and the brightness of LED decreases with any further rise in LED temperature [30]. This needs to be addressed when using the stimulator for prolonged periods of time. In our prototype, LED used has a built-in aluminium plate on which the LED is mounted and dissipates the heat.

#### 9.3.1.4 Software

The software for Arduino is fully open source and is downloadable from Arduino online. The IDE is supported for major operating systems, like Windows and Mac OSX with 32 bit support and Linux with both 32 and 64 bit support. For our design, we have used the Windows 7 platform for the IDE. The current stable IDE version at the time of writing this document is version 1.0.5 and there also exist a beta version 1.5.5 with the support for newer boards. The IDE is fully compatible with older version of boards as well.

The installation begins when the setup package is deployed and it installs all the required drivers and libraries for all Arduino platforms. The Arduino board can be

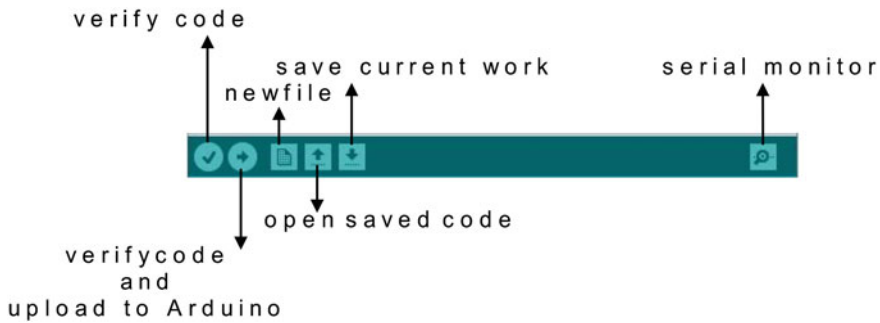


**Fig. 9.9** Arduino IDE menu descriptions

plugged in via the USB cable and the operating system will automatically identify the board and load the required drivers. The system also installs a virtual serial port to communicate with the Arduino and this port number can be identified from the device manager in the com port section for Windows. The Arduino board and the port should be selected as in Fig. 9.9 to ensure the proper operation. It also displays the available boards that are supported by the IDE.

The IDE has a clear and simple menu layout as shown in Fig. 9.10 for basic operations. The first menu icon checks code for errors in the code which will be highlighted for correction. The second menu icon does verify, compile and upload in one step. This can be used to change the numeric values for the flicker frequency and to update the code in Arduino easily. These menus are followed by control for creating, opening and saving the programs. There is also an advanced control for monitoring the serial communication to check the communication with Arduino and host computer.

The use of USB connection is recommended as it protects the platform from external power supply errors or mistakes that could damage the Arduino itself. A sample program to flicker a single LED at 7 Hz on port three is shown in Fig. 9.11. The initial procedure comprises of declaring the values for ports and primary data. In the sample code, LED1 is assigned to port number three in Arduino and the initial value is set as low for the off state. The interval time is set as 70 ms for 7 Hz. This is calculated with basic time and frequency relation  $F = 1/T$ . Here, the frequency is 7 Hz; time would be  $1/7$  which is 0.14285 s. For flickering requirements the LED has to be switched off for every half cycle, this requires the time to be divided by two ( $0.14285/2$ ). The new time value would be 0.07142 s, since the software uses milliseconds, it would be 71.4 ms. This theoretical value of 71.4 ms, actually generates a frequency of 6.92 Hz when measured at the LED, a small correction was required to get the precise value of 7 Hz flicker frequency at the LED. Error correction values may need to be changed according to the length of the cables used to connect the RGB LED module to the FET shield and in addition they may also vary different with power sources. Initially, it is always better to confirm the frequency of flicker using a digital frequency counter so it can be precisely measured.

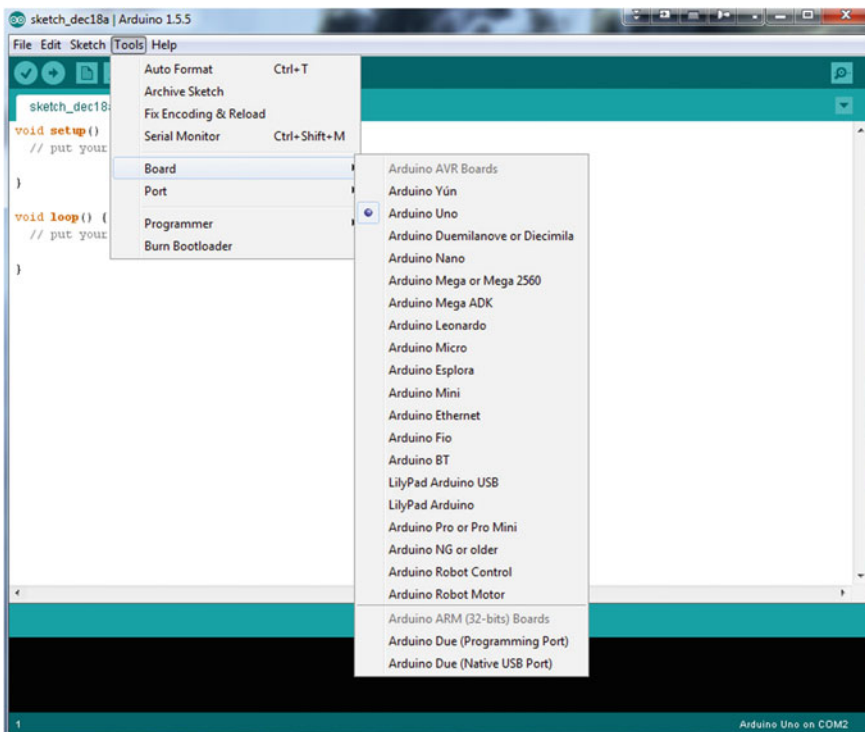
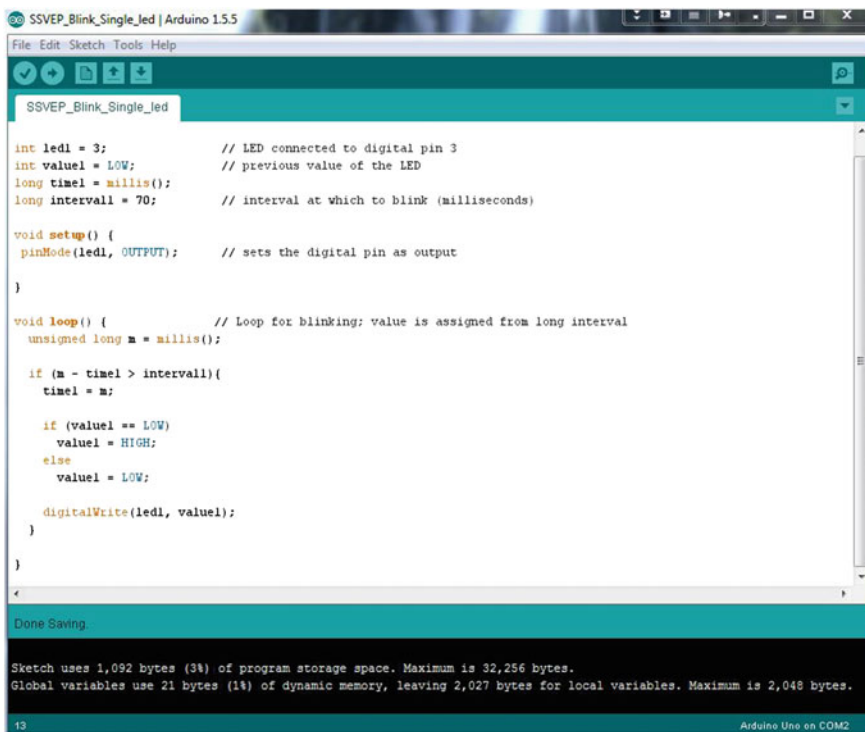


**Fig. 9.10** Arduino IDE menu descriptions

The code for single LED flicker has four declared values, LED port, LED state, time in milliseconds and time interval. Additional LED can be added by duplicating each part of the code and assigning the correct port numbers. The complete Arduino code can be downloaded from <http://ssvep.co.uk/files/multichannelflicker.zip>.

### 9.3.1.5 Look-up Table

Table 9.1 can be used to assign the frequencies of flicker values. Assigning the values as in the table to the time interval variable generates the desired flicker frequency. This makes it possible to generate dual frequency pairs which can have one common frequency. For example, if first RGB LED has green flashing at 7 Hz and red flashing at 10 Hz, the second RGB LED can also flash red at 7 Hz and blue at 15 Hz. Flashing frequency is completely independent of number of times the values are being used to generate the required flickers. The complete range of frequency and time interval values can be calculated with basic frequency and time relation as mentioned before. Appropriate error correction values must be applied to time interval to get the precise frequency for LED flickers.



The screenshot shows the Arduino IDE interface with the following details:

- Title Bar:** SSVEP\_Blink\_Single\_Led | Arduino 1.5.5
- Menu Bar:** File Edit Sketch Tools Help
- Sketch Area:**

```

int led1 = 3;           // LED connected to digital pin 3
int value1 = LOW;       // previous value of the LED
long timel = millis();  // time at which to blink (milliseconds)
long interval = 70;    // interval at which to blink (milliseconds)

void setup() {
  pinMode(led1, OUTPUT); // sets the digital pin as output
}

void loop() {           // Loop for blinking; value is assigned from long interval
  unsigned long m = millis();

  if (m - timel > interval){
    timel = m;

    if (value1 == LOW)
      value1 = HIGH;
    else
      value1 = LOW;

    digitalWrite(led1, value1);
  }
}

```
- Status Bar:** Done Saving.
- Bottom Status:** Sketch uses 1,092 bytes (3%) of program storage space. Maximum is 32,256 bytes.  
Global variables use 21 bytes (1%) of dynamic memory, leaving 2,027 bytes for local variables. Maximum is 2,048 bytes.
- Bottom Right:** Arduino Uno on COM2

**Fig. 9.11** Code to flicker a single LED at 7 Hz

**Table 9.1** Lookup table for time interval value to generate the desired frequency

Frequency (Hz)	Time interval (ms)
7	70
8	61
9	54
10	49
11	44
12	40
13	37
20	24
25	19
35	13

### 9.3.1.6 Prototype and Setup

The completed prototype is as shown in Fig. 9.12. It consists of the base computing platform Arduino Uno, FET driver shield, RGB LED's, voltage regulator and

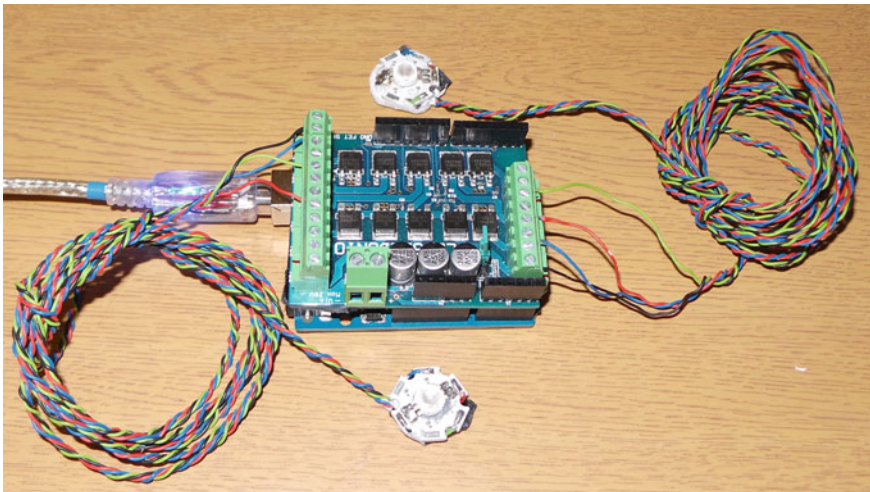


**Fig. 9.12** Prototype of SSVEP stimulator

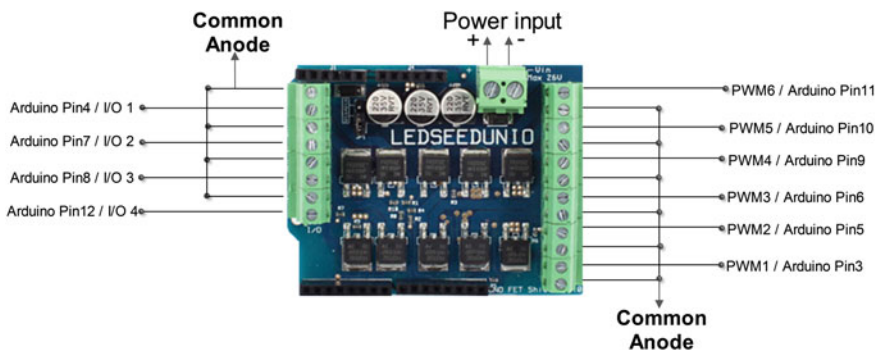


**Fig. 9.13** FET shield pin connection for RGB LED

battery. The FET board sits on the expansion pins mounted on the Arduino board and is plugged into the Arduino board by aligning the corresponding pins. Once the FET board has been mounted, the RGB LED wires need to be connected to the corresponding screw headers on the FET shield, as shown in Fig. 9.13, which shows the screw header mapping for Arduino board's output pins.

The pin PWM 1 to PWM 6 can be used as pulse width modulator outputs which could be used for controlling the intensity or blending of colours using three primary colours red, green and blue. These PWM outputs can also be used as normal outputs for controlling the flicker frequency. The signal on the lefthand connector can only work as normal input or output mode and do not have the ability for PWM.

The anodes of all the output ports are internally tied together to be used in common anode configuration mode of RGB LED. The power is connected to the

terminal marked power input. The terminal has positive (+) and negative (-) signs marked and care should be taken while connecting the leads as it will damage the shield if the polarities are reversed.

The RGB LEDs when assembled would have four connections one of which will be combined as the common anode and three others will be for red, green and blue. The common anode can be connected to any of the common anode screw header on the shield and other colours can be connected to other output terminals depending upon the required colour, frequency or multi-chromatic flicker. The power supply for the RGB LED based on the voltage requirement can be connected to the power screw header on FET shield.

Once the program has been successfully uploaded, the Arduino resets itself where upon it can be disconnected from the USB for standalone operation. The Arduino can be powered from a normal 9 V pp3 battery, using a pp3 to barrel adapter jack for standalone operation after programming. The LEDs connected to the output port will flicker according to the programmed values and can be customised using the values in the look-up table or using the frequency time conversion relations as explained previously.

### 9.3.1.7 EEG Recording Test

The EEG data recording system used for this study is g.Mobilab+ from g.tec (<http://www.gtec.at>). It is a portable biosignal acquisition and analysis system capable of recording multimodal signals on a standard PC or other mobile computing devices. This system can be used to investigate brain signals (EEG), heart signals (ECG) muscular activity, eye movements or other body signals. It has eight channels and a removable internal storage card where data can be stored and analysed later. The system can communicate to host via Bluetooth or using customised serial cable in case of Bluetooth connectivity issues. g.Mobilab+ is equipped with low noise biosignal amplifier and a 16-bit analogue to digital converter with 256 Hz sampling. An external switch signal can also be used to control the start and stop of signal capture. This device is battery powered in order to avoid any external interference from the mains.

The software for g.Mobilab+ is provided by the manufacturer with extensive documentation which covers various operating systems and details of libraries available for further development. The setup procedure also provides support for Bluetooth drivers which assigns a virtual serial port in the computer and communicates using serial protocol. Libraries are also provided for Matlab (Mathworks Inc) integration and data can be directly recorded using Matlab for real-time analysis and processing.

The main unit is interfaced via cable to an external high gain amplifier and analogue to digital converter for recording the EEG data. The EEG sensors are connected to this high gain amplifier which senses the EEG signal from the scalp, which is relatively very small and in the range of microvolts. The EEG sensors are fixed in specific locations on the EEG cap and conductive gel is applied on the

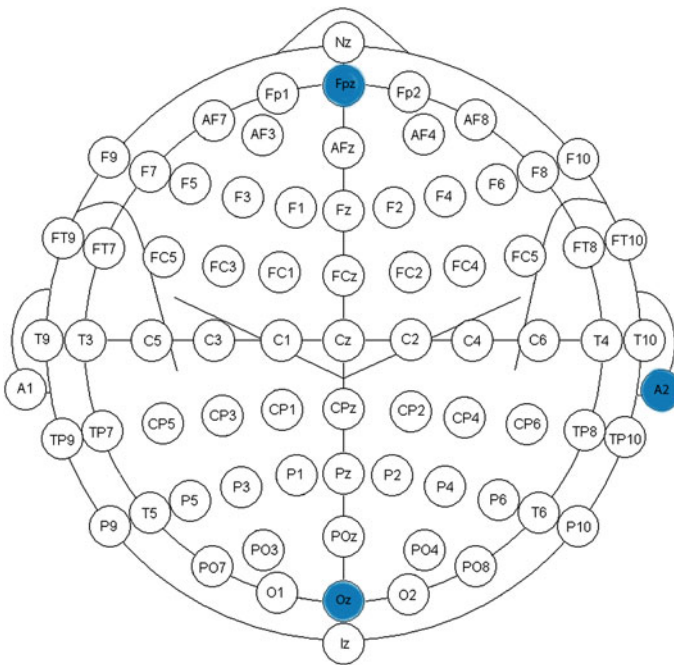


**Fig. 9.14** Electrode positions used for data collection

surface to improve the signal quality. The external unit has wired connectivity to the main unit. The experiment used minimum number of sensors and connections were made to GND, CH1 and CH2 of the amplifier unit. This device is also battery powered and support gel based electrodes. The initial test was run using the sample demo program to ensure the data is being sent to computer and validated with the test signal provided in the test program. Sample test runs at different frequencies have been performed to ensure the correct EEG recording before final test were executed. This also ensured the correct EEG connectivity between host computer and EEG capture unit.

For testing the proposed visual stimulus hardware, it was programmed for selected frequencies between 5 and 50 Hz and the output was connected to high power RGB LED via the shield. The visual stimulus hardware is capable of producing 14 different frequency flickers simultaneously for complex SSVEP applications.

The stimulus is activated and the data is recorded using the gtec EEG hardware. The subject was seated comfortably at a distance of 60 cm from the visual stimulus which was placed at eye level. The EEG cap fitted with gtec active electrodes at locations Oz and Fz (Fig. 9.14) and used with electrode conductive gel, producing single channel bipolar SSVEP data. The third electrode is fitted on right ear lobe of the subject and serves as ground connection. This setup does not require any skin preparation.

**Table 9.2** Parameters used for stimulus evaluation

Colour	Frequencies (Hz)	No of samples	Time (s)	Total time
Red	7, 8, 9, 10	$4 \times 5$	30	600
Blue	7, 8, 9, 10	$4 \times 5$	30	600
Green	7, 8, 9, 10	$4 \times 5$	30	600

For each trial, one of the RBG LED cathodes was connected to the microcontroller for the desired frequency and colour. The recording trials were for 30 s for each frequency or colour and the results transferred directly to Matlab for analysis. This process was repeated for all three colours (red, green and blue) and for frequencies 7, 8, 9 and 10 Hz as in Table 9.2. Each recording sample had duration of 30 s and was repeated 5 times for each frequency and colour. The subject was given a rest period of 1 min after each recording.

Each frequency and colour had five trials with the same subject. The performance for all the colours from the RGB LED was good and the heat dissipation on the LED was negligible even after prolonged usage. The SSVEP response was accurate for all the colours and frequency ranges throughout the experiment.

Visual stimulus was tested for simultaneous outputs with different frequencies using digital oscilloscope and had the accuracy of 0.1 Hz at all the programmed frequency ranges. The SSVEP results exhibited the exact flicker frequency of the stimulus. The SSVEP responses for different colours were also examined to check the functionality of the stimulus. In the colour combination test, two colours in RGB LED were flickered at two different frequencies and EEG was recorded, the power spectral density results exhibited two different peaks at the same frequencies of the flickering colours. Overall the stimulator could be used in various combinations for colour, frequency and simultaneous channels.

## 9.4 Results

### 9.4.1 Frequency Test

The system was integrated as described in the prototype section. Four RGB LED modules were connected to 12 data out connectors of the FET shield. The frequency was measured at the LED end to ensure the precise measurement of flicker frequency. EEG hardware g.Mobilab+ was connected to serial port of the computer using USB to serial converter which assigns a virtual communication port for data recording. The sensor cables were connected to GND, CH1 and CH2 of the EEG unit and the other end fixed to EEG cap using gel for data recording. Individual tests were conducted for a single frequency, dual frequency, single colour and multiple colours using single RGB LED with terminals activated according to the requirements.

### 9.4.2 Single Frequency

Single frequency test were conducted with RGB LED at all frequency ranges and programmed frequency values were confirmed against the generated value with the frequency counter in oscilloscope. The same frequency LED stimulus was used for SSVEP generation and EEG signals were recorded. The power spectral density values were computed and a visible peak was detected with the same frequency as the LED stimulus. The screen capture from the oscilloscope in Fig. 9.15 shows a flicker at 7 Hz which is the same as the programmed value in Arduino. Figure 9.16 shows the power spectral density of a SSVEP EEG with 7 Hz flicker and it clearly shows the peak at normalised value of 0.05469 which is equivalent to 7 Hz with sampling frequency of 250 Hz. Similarly all frequency ranges were compared with programmed values and generated values.

The SSVEP EEG was recorded and verified for the presence of the same frequency as that of the visual stimulus. For SSVEP trials, EEG was recorded for 30 s as shown in Fig. 9.17 for each colour and frequency. Five trials were recorded, which gave 150 segments, with each segment consisting of 1 s of SSVEP signal. Four healthy subjects (three females, one male) in the age group 2,545 years volunteered for this study and none of the subjects had any previous experience with BCI. All subjects had perfect or corrected vision. The same subjects participated in all tests using the same prototype hardware.

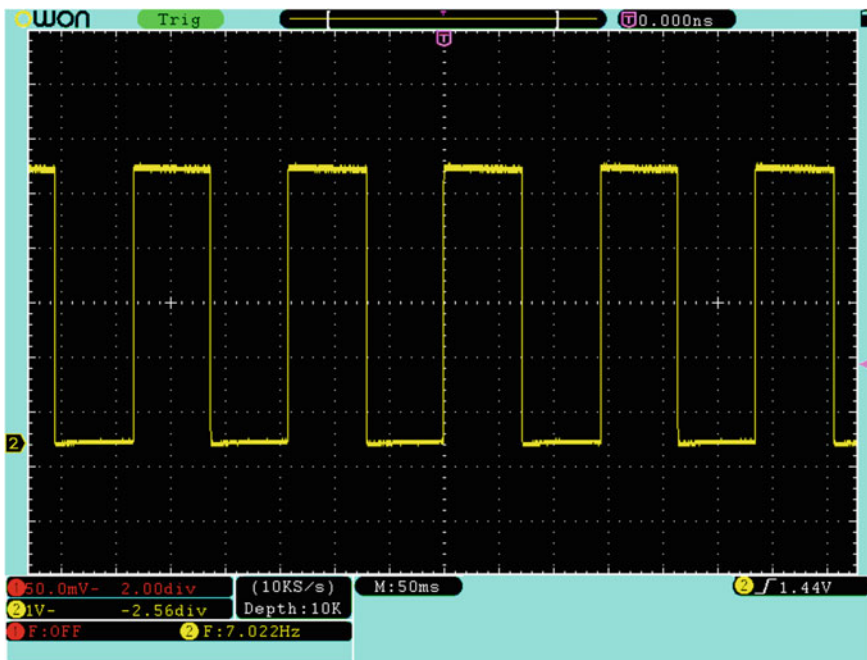


**Fig. 9.15** Flicker waveform at 7 Hz

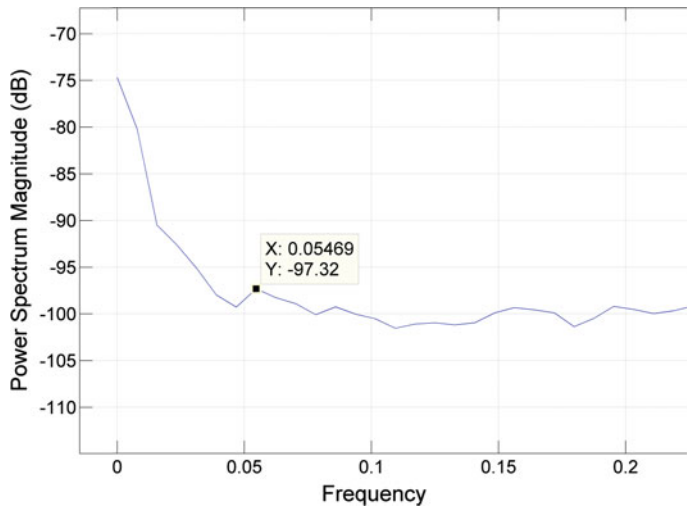
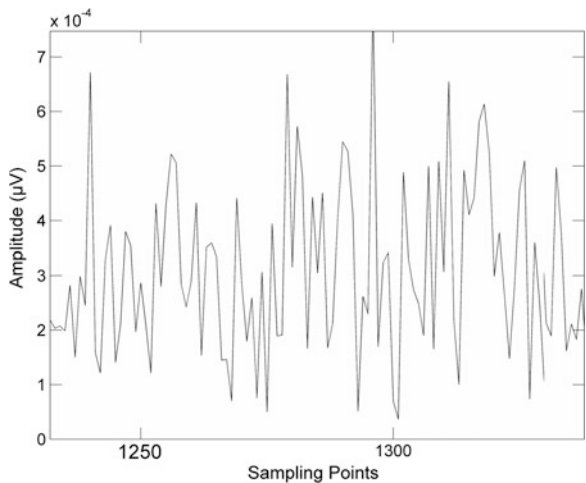


**Fig. 9.16** SSVEP EEG for 7 Hz stimulus

**Fig. 9.17** Sample EEG recorded to test the visual stimulus



Each 30 s of EEG recording was filtered with a forward-reverse Elliptic IIR bandpass filter and segmented into 1 s EEG segments and analysed with Fast Fourier Transform (FFT). Table 9.3 shows the filter parameters used. The maximum amplitudes of the FFT using the filtered SSVEP signal for all the 150 segments were computed and stored for further analysis. This process was repeated for all the frequencies and three colours generated by the visual stimulus.

All tests confirmed the Arduino platform can generate continuous and precise visual flickers to generate SSVEP in EEG.

**Table 9.3** Values of parameters used in data processing

Freq (Hz)	Order	Passbd (Hz)	Stopbd edge (Hz)	Max passbd ripp (dB)	Min stopbd attn (dB)
7	4	6–8	5,9	0.1	30
8	4	7–9	6,10	0.1	30
9	4	8–10	7,11	0.1	30
10	4	9–11	8,12	0.1	30

#### 9.4.3 Multiple Frequency

The frequency stability of multiple visual stimuli were tested by connecting two different frequency outputs at the same time to RGB LED and comparing the frequency at the LED with the programmed values. The programmed values and real flicker frequencies were exactly same and were stable throughout the test. Figure 9.18 shows the two frequency values of 9 and 11 Hz. The same RGB stimulus was used to generate SSVEP and EEG was recorded. The RGB LED had both colour terminals, red and green connected to the FET shield at same time with two different frequencies. This produces two colours flashing simultaneously with different frequencies creating two peaks in recorded EEG which had the same

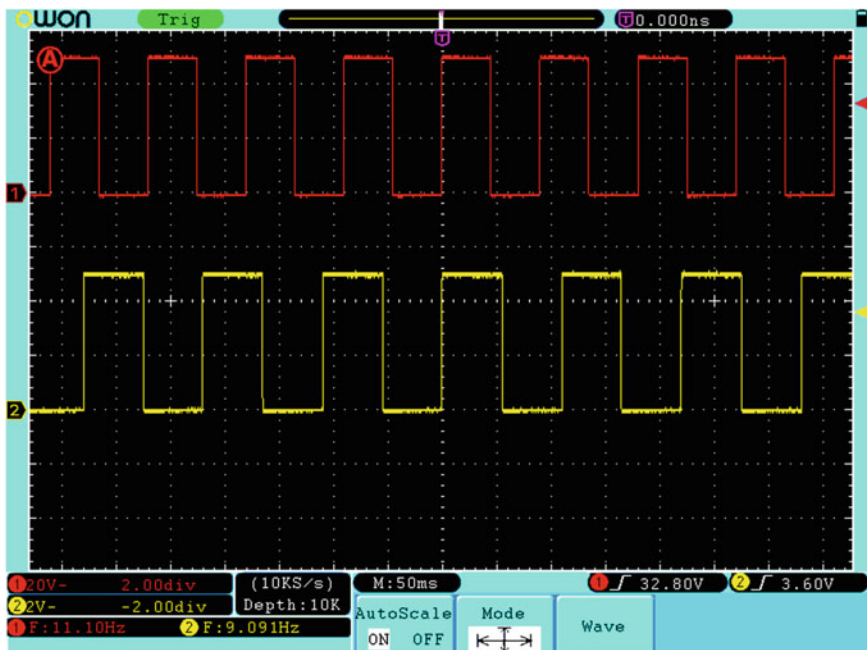


**Fig. 9.18** Two simultaneous frequencies used in RGB LED stimulus

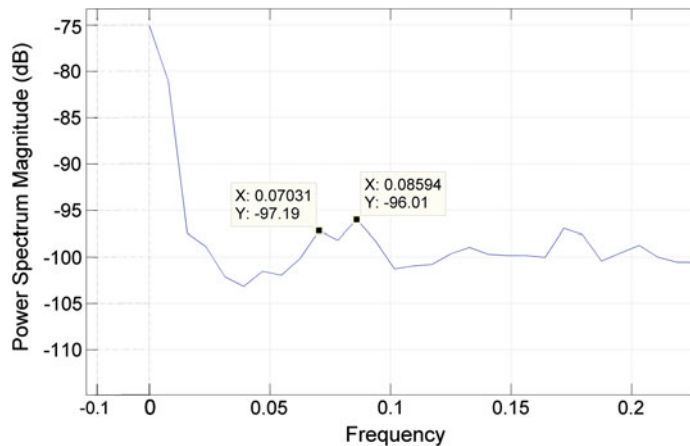


**Fig. 9.19** Visible peaks for two different frequencies in recorded EEG with SSVEP

frequency as the flicker. The power spectral density analysis shows the two frequency peaks of 9 and 11 Hz confirming the functionality of the stimulus as shown in Fig. 9.19. The two different flickers using different colours generated by the stimulus also identify the possibility of using a single source with different frequency flickers. The visible peaks in the EEG show both these frequencies. More RGB LEDs can be connected to the remaining digital outputs and can be programmed for more complex SSVEP analysis.

## 9.5 Discussion

The SSVEP visual stimulator met all the criteria for which it was designed. The system is easily configurable for any desired frequency with the look-up table and can be updated through USB. The system can be easily customised for different type of LEDs with varying operating voltages and power requirements. It can simultaneously provide fourteen different frequency outputs without reprogramming. With the availability of different shields, the base configuration can be expanded for data recording or interactions without complex hardware design and realised using off shelf components and ready to use libraries. The availability of stack on power shield makes the system very compact, portable and also reduces the induced power line noises for better quality output flickers. Multiple colours at different frequencies using RGB LEDs demonstrate the possibilities of this platform for EEG and vision research.

The gtec initial setup faced a few minor issues with connectivity via Bluetooth. The Bluetooth driver provided did not work as it should though the virtual port was created and the sample program provided by the manufacturer worked without any issues. The connectivity with the EEG hardware and Matlab was not stable and the

data could not be transferred. This was resolved using the default Bluetooth drivers provided in the operating system rather than the one recommended by the manufacturer.

The EEG experiments with the stimulus also showed that some frequencies did not evoke any changes in the EEG for certain subjects and this should be taken into account when investigating with such SSVEP systems. The subjects were able to choose the colour of the stimulus that they were comfortable and this reduced visual fatigue thereby allowing longer measurement periods.

## 9.6 Conclusion

The visual stimulator was tested successfully for colour, frequency, portability and design simplicity. The prototype platform is easy to build with off shelf components and economical for many different areas of vision research. Even though it is focused towards SSVEP research for BCI, it can also be used for investigating the influence of colours in EEG research. This prototype could address visual fatigue in SSVEP to a certain extent by giving choice of colours and frequency to subjects. Subjects participated in the study strongly preferred certain colours against others as they felt it was easy to focus on specific colours. Most users preferred green and blue as they felt these were less straining to the eyes. The amplitude of the detected peaks in the EEG was prominent when green stimulus was used and this area could be further explored. The subjects found that they could use green stimulus for longer periods as compared to red and blue over all frequency ranges. Another interesting finding is that the use of a simultaneous combination of two colours with different frequencies from a single source. In such a case, the EEG results showed two distinct peaks of these two different frequencies. Further work could be undertaken to investigate whether such an approach can allow BCI systems with shorter response times.

This study could be extended to investigate the effect of dry electrodes. The g. Mobilab+ supports the use of dry electrodes with a different pre-amplifier, and can be used for capturing EEG data for SSVEP analysis. Further work may include the study of light intensity and colour variation influences in SSVEP by using PWM techniques to reduce visual fatigue when using dry electrodes. Algorithms could be developed for analysing and processing the data to extract the required features. Different methods such as FFT, Canonical Correlation Analysis (CCA) and Empirical Mode Decomposition (EMD) could be employed to enhance data analysis for any required task. Since with dry electrodes the performance degrades as compared to wet electrodes, there would be a need for improving SNR and may require complex dynamic data processing algorithms.

Since this study used the minimum number of electrodes to collect the EEG data, it would require higher quality electrodes for reliability and good performance.

As such, future research could also explore the possibility for developing high quality dry electrodes that may enhance the reliability and quality of the recorded EEG signal.

The Arduino Uno platform could be replaced using other powerful variants from the Arduino family or other open source hardware with built-in digital signal processing capabilities. Hardware platform worth mentioning are Intel Galileo, Udoos and Raspberry Pi. These newer platforms are similarly supported by the open-source community and are equipped with numerous I/O ports and processing power. Using these platforms, further research could develop advanced signal processing algorithm for real-time feature extraction of EEG data to control external applications or devices accurately and efficiently with minimum number of electrodes in a single device. Such systems would be able to improve the accuracy and also minimise the computing time for data processing with reliable connectivity and mobility to perform real-time EEG tasks.

## References

1. Wu, Z., Kang, L., Shen, F., Fang, B.: The closed-loop human-computer interface: active information acquisition for vision-brain-hand to computer (VBH-C) interaction based on force tablet. In: Proceedings of First International Conference on Neural Interface and Control, China, 26–28 May 2005, pp. 1–5. doi:[10.1109/ICNIC.2005.1499828](https://doi.org/10.1109/ICNIC.2005.1499828) (2005)
2. Chao, G.: Human-computer interaction: process and principles of human-computer interface design. In: International Conference on Computer and Automation Engineering, ICCAE '09, 8–10 March 2009, Bangkok, pp. 230–233. doi:[10.1109/ICCAE.2009.23](https://doi.org/10.1109/ICCAE.2009.23) (2009)
3. Cincotti, F., Mattia, D., Aloise, F., Bufalari, S., Schalk, G., Oriolo, G., Cherubini, A., Marcianni, M.G., Babiloni, F.: Non-invasive braincomputer interface system: towards its application as assistive technology. *Brain Res. Bull.* **75**(6), 796–803 (2008)
4. Berger, H.: Über das Elektrenkephalogramm des Menschen. ISHN (1929)
5. Pal, P.R., Khobragade, P., Panda, R.: Expert system design for classification of brain waves and epileptic-seizure detection. In: Proceedings of IEEE Students' Technology Symposium (TechSym), Kharagpur, 14–16 Jan 2011, pp. 187–192. doi:[10.1109/TECHSYM.2011.5783822](https://doi.org/10.1109/TECHSYM.2011.5783822) (2011)
6. Rice, J.K., Rorden, C., Little, J.S., Parra, L.C.: Subject position affects EEG magnitudes. *NeuroImage* **64**, 476–484 (2013)
7. Chi, Y., Wang, Y.-T., Wang, Y., Maier, C., Jung, T.-P., Cauwenberghs, G.: Dry and noncontact EEG sensors for mobile brain-computer interfaces. *IEEE Trans. Neural Syst. Rehabil. Eng.* **20**(2), 228–235 (2012)
8. Allison, B., Brunner, C., Altstötter, C., Wagner, I., Grissmann, S., Neuper, C.: A hybrid ERD/SSVEP BCI for continuous simultaneous two dimensional cursor control. *J. Neurosci. Methods* **2**(209), 299–307 (2012)
9. Brunner, C., Allison, B.Z., Krusienski, D.J., Kaiser, V., Müller-Putz, G.R., Pfurtscheller, G., Neuper, C.: Improved signal processing approaches in an offline simulation of a hybrid braincomputer interface. *J. Neurosci. Methods* **188**(1), 165–173 (2010)
10. Fazli, S., Mehnert, J., Steinbrink, J., Curio, G., Villringer, A., Müller, K.-R., Blankertz, B.: Enhanced performance by a hybrid NIRSEEG brain computer interface. *NeuroImage* **59**(1), 519–529 (2012)

11. Birbaumer, N., Ghanayim, N., Hinterberger, T., Iversen, I., Kotchoubey, B., Kubler, A., Perelmouter, J., Taub, E., Flor, H.: A spelling device for the paralysed. *Nature* **398**(6725), 297–298 (1999)
12. De Massari, D., Matuz, T., Furdea, A., Ruf, C.A., Halder, S., Birbaumer, N.: Braincomputer interface and semantic classical conditioning of communication in paralysis. *Biol. Psychol.* **92**(2), 267–274 (2012)
13. Donchin, E., Spencer, K., Wijesinghe, R.: The mental prosthesis: assessing the speed of a P300-based brain-computer interface. *IEEE Trans. Rehabil. Eng.* **8**(2), 174–179 (2000)
14. Lled, L.D., Beda, A., Iez, E., Azorn, J.M.: Internet browsing application based on electrooculography for disabled people. *Expert Syst. Appl.* **40**(7), 2640–2648 (2013)
15. Muller-Putz, G.R., Pfurtscheller, G.: Control of an electrical prosthesis with an SSVEP-based BCI. *IEEE Trans. Biomed. Eng.* **55**(1), 361–364 (2008)
16. Brumberg, J.S., Nieto-Castanon, A., Kennedy, P.R., Guenther, F.H.: Brain-computer interfaces for speech communication. *Speech Commun.* **52**(4), 367–379 (2010)
17. Lee, T.-S., Juinn Goh, S., Quek, S.Y., Guan, C., Cheung, Y.B., Krishnan, K.R.: Efficacy and usability of a brain-computer interface system in improving cognition in the elderly. *Alzheimers Dementia* **9**(4), P296 (2013)
18. Liberati, G., Veit, R., Dalboni da Rocha, J., Kim, S., Lul, D., von Arnim, C., Raffone, A., Belardinelli, M.O., Birbaumer, N., Sitaram, R.: Combining classical conditioning and brain-state classification for the development of a brain-computer interface (BCI) for Alzheimer's patients. *Alzheimers Dementia* **8**(4), P515 (2012)
19. Pires, G., Nunes, U., Castelo-Branco, M.: Evaluation of brain-computer interfaces in accessing computer and other devices by people with severe motor impairments. *Procedia Comput. Sci.* **14**, 283–292 (2012)
20. Gunyesu, A., Akin, H.L.: An SSVEP based BCI to control a humanoid robot by using portable EEG device. In: Proceedings of 35th Annual International Conference of the IEEE Engineering in Medicine and Biology Society (EMBC), 3–7 July 2013, Osaka, pp. 6905–6908. doi:[10.1109/EMBC.2013.6611145](https://doi.org/10.1109/EMBC.2013.6611145) (2013)
21. Wolpaw, J.R., Birbaumer, N., McFarland, D.J., Pfurtscheller, G., Vaughan, T.M.: Brain-computer interfaces for communication and control. *Clin. Neurophysiol.* **113**(6), 767–791 (2002)
22. Ergenoglu, T., Demiralp, T., Beydagl, H., Karamsel, S., Devrim, M., Ermutlu, N.: Slow cortical potential shifts modulate P300 amplitude and topography in humans. *Neurosci. Lett.* **251**(1), 61–64 (1998)
23. Azar, A.T., Balas, V.E., Olariu, T.: Classification of EEG-based brain-computer interfaces. *Adv. Intell. Comput. Technol. Dec. Support Syst.* **486**, 97–106 (2014). doi:[10.1007/978-3-319-00467-9\\_9](https://doi.org/10.1007/978-3-319-00467-9_9)
24. Edlinger, G., Guger, C.: A hybrid brain-computer interface for improving the usability of a smart home control. In: Proceedings of International Conference on Complex Medical Engineering (CME), 1–4 July 2012, Kobe, pp. 182–185. doi:[10.1109/ICCME.2012.6275714](https://doi.org/10.1109/ICCME.2012.6275714) (2012)
25. Hwang, H.-J., Hwan Kim, D., Han, C.-H., Im, C.-H.: A new dual-frequency stimulation method to increase the number of visual stimuli for multi-class SSVEP-based braincomputer interface (BCI). *Brain Res.* **1515**, 66–77 (2013)
26. Hwang, H.-J., Lim, J.-H., Lee, J.-H., Im, C.-H.: Implementation of a mental spelling system based on steady-state visual evoked potential (SSVEP). In: Proceeding of International Winter Workshop on Brain-Computer Interface (BCI), 18–20 Feb 2013, Gangwo, pp. 81–83. doi:[10.1109/IWW-BCI.2013.6506638](https://doi.org/10.1109/IWW-BCI.2013.6506638) (2013)
27. Lopez-Gordo, M.A., Pelayo, F., Prieto, A.: A high performance SSVEP-BCI without gazing. In: Proceedings of International Joint Conference on Neural Networks (IJCNN), Barcelona, 18–23 July 2010, pp. 1–5. doi:[10.1109/IJCNN.2010.5596325](https://doi.org/10.1109/IJCNN.2010.5596325) (2010)
28. Lopez-Gordo, M.A., Prieto, A., Pelayo, F., Morillas, C.: Customized stimulation enhances performance of independent binary SSVEP-BCIs. *Clin. Neurophysiol.* **122**(1), 128–133 (2011)

29. Nishifuji, S., Kuroda, T., Tanaka, S.: EEG changes associated with mental focusing to flicker stimuli under eyes closed condition for SSVEP-based BCI. In: Proceedings of SICE Annual Conference (SICE), Akita, 20–23 Aug 2012, pp. 475–480. ISBN: 978-1-4673-2259-1 (2012)
30. Yueh-Ru, Y.: Implementation of a colorful RGB-LED light source with an 8-bit microcontroller. In: Proceedings of 5th IEEE Conference on Industrial Electronics and Applications (ICIEA), Taichung, 15–17 June 2010, pp. 1951–1956. doi:[10.1109/ICIEA.2010.5515525](https://doi.org/10.1109/ICIEA.2010.5515525) (2010)
31. Brikou, A., Tzelepi, A., Papathanasopoulos, P., Bezerianos, A.: Simultaneous estimation of the transient and steady-state VEP using the Prony method. In: Proceedings of the 16th Annual International Conference of the IEEE Engineering in Medicine and Biology Society, Engineering Advances: New Opportunities for Biomedical Engineers, 3–6 Nov 1994, Baltimore, Vol. 1, pp. 193–194. doi:[10.1109/EMBS.1994.411813](https://doi.org/10.1109/EMBS.1994.411813) (1994)
32. Krusinski, D.J., Sellers, E.W., McFarland, D.J., Vaughan, T.M., Wolpaw, J.R.: Toward enhanced P300 speller performance. *J. Neurosci. Methods* **167**(1), 15–21 (2008)
33. Herrmann, C.S.: Human EEG responses to 1–100 Hz flicker: resonance phenomena in visual cortex and their potential correlation to cognitive phenomena. *Exp. Brain Res.* **137**(3–4), 346–353 (2001)
34. Pastor, M.A., Artieda, J., Arbizu, J., Valencia, M., Masdeu, J.C.: Human cerebral activation during steady-state visual-evoked responses. *J. Neurosci.* **23**(37), 11621–11627 (2003)
35. Resalat, S.N., Saba, V., Afshideh, F., Heidarnejad, A.: High-speed SSVEP-based BCI: study of various frequency pairs and inter-sources distances. In: Proceedings of IEEE-EMBS International Conference on Biomedical and Health Informatics (BHI), Hong Kong, 5–7 Jan 2012, pp. 220–223. doi:[10.1109/BHI.2012.6211550](https://doi.org/10.1109/BHI.2012.6211550) (2012)
36. Cecotti, H., Rivet, B.: Effect of the visual signal structure on steady-state visual evoked potentials detection. In: Proceedings of IEEE International Conference on Acoustics, Speech and Signal Processing (ICASSP), 22–27 May 2011, Prague, pp. 657–660. doi:[10.1109/ICASSP.2011.5946489](https://doi.org/10.1109/ICASSP.2011.5946489) (2011)
37. Teng, C., Feng, W., Peng Un, M., Pui-In, M., Mang, I.V., Yong, H.: Flashing color on the performance of SSVEP-based brain-computer interfaces. In: Proceedings of Annual International Conference of the IEEE Engineering in Medicine and Biology Society (EMBC), San Diego, 28 Aug 2012–1 Sept 1 2012, pp. 1819–1822. doi:[10.1109/EMBC.2012.6346304](https://doi.org/10.1109/EMBC.2012.6346304) (2012)
38. Po-Lei, L., Chia-Lung, Y., Cheng, J.Y.S., Chia-Yen, Y., Gong-Yau, L.: An SSVEP-based BCI using high duty-cycle visual flicker. *IEEE Trans. Biomed. Eng.* **58**(12), 3350–3359 (2011)
39. Walter, S., Quigley, C., Andersen, S.K., Mueller, M.M.: Effects of overt and covert attention on the steady-state visual evoked potential. *Neurosci. Lett.* **519**(1), 37–41 (2012)
40. Middendorf, M., McMillan, G., Calhoun, G., Jones, K.S.: Brain-computer interfaces based on the steady-state visual-evoked response. *IEEE Trans. Rehabil. Eng.* **8**(2), 211–214 (2000)
41. Yijun, W., Ruiping, W., Xiaorong, G., Bo, H., Shangkai, G.: A practical VEP-based brain-computer interface. *IEEE Trans. Neural Syst. Rehabil. Eng.* **14**(2), 234–240 (2006)
42. Martinez, P., Bakardjian, H., Cichocki, A.: Fully online multicommand brain-computer interface with visual neurofeedback using SSVEP paradigm. *Comput. Intell. Neurosci.* **2007**, 1–13 (2007)
43. Bakardjian, H., Tanaka, T., Cichocki, A.: Optimization of SSVEP brain responses with application to eight-command brain-computer interface. *Neurosci. Lett.* **469**(1), 34–38 (2010)
44. Hwang, H.J., Lim, J.H., Jung, Y.J., Choi, H., Lee, S.W., Im, C.H.: Development of an SSVEP-based BCI spelling system adopting a QWERTY-style LED keyboard. *J. Neurosci. Methods* **208**(1), 59–65 (2012)
45. Zhu, D., Bieger, J., Garcia Molina, G., Aarts, R.M.: A survey of stimulation methods used in SSVEP-based BCIs. *Comput. Intell. Neurosci.* **2010**, 12 (2010)
46. Strasburger, H., Wstenberg, T., Jncke, L.: Calibrated LCD/TFT stimulus presentation for visual psychophysics in fMRI. *J. Neurosci. Methods* **121**(1), 103–110 (2002)
47. Mun, S., Park, M.-C., Park, S., Whang, M.: SSVEP and ERP measurement of cognitive fatigue caused by stereoscopic 3D. *Neurosci. Lett.* **525**(2), 89–94 (2012)

48. Punsawad, Y., Wongsawat, Y.: Motion visual stimulus for SSVEP-based BCI system. In: Proceedings of Annual International Conference of the IEEE Engineering in Medicine and Biology Society (EMBC), San Diego, 28 Aug 2012–1 Sept 2012, pp. 3837–3840. doi:[10.1109/EMBC.2012.6346804](https://doi.org/10.1109/EMBC.2012.6346804) (2012)
49. Volosyak, I., Valbuena, D., Luth, T., Malechka, T., Graser, A.: BCI demographics II: how many (and what kinds of) people can use a high-frequency SSVEP BCI? *IEEE Trans. Neural Syst. Rehabil. Eng.* **19**(3), 232–239 (2011)
50. Zhang, D., Gao, X., Gao, S., Engel, A., Maye, A.: An independent brain-computer interface based on covert shifts of non-spatial visual attention. In: Proceedings of Annual International Conference of the IEEE Engineering in Medicine and Biology Society, Minneapolis, 3–6 Sept 2009, pp. 539–542. doi:[10.1109/IEMBS.2009.5333740](https://doi.org/10.1109/IEMBS.2009.5333740) (2009)
51. Zhu, D., Molina, G., Mihajlovic, V., Aarts, R.: Phase synchrony analysis for SSVEP-based BCIs. In: Proceedings of 2nd International Conference on Computer Engineering and Technology (ICCET), Chengdu, 16–18 April 2010, Vol. 2, pp. 329–333. doi:[10.1109/ICCET.2010.5485465](https://doi.org/10.1109/ICCET.2010.5485465) (2010)
52. Da Silva Pinto, M.A., de Souza, J.K.S., Baron, J., Tierra-Criollo, C.J.: A low-cost, portable, micro-controlled device for multi-channel LED visual stimulation. *J. Neurosci. Methods* **197**(1), 82–91 (2011)
53. Demontis, G.C., Sbrana, A., Gargini, C., Cervetto, L.: A simple and inexpensive light source for research in visual neuroscience. *J. Neurosci. Methods* **146**(1), 13–21 (2005)
54. Rogers, B., Shih, Y.-Y.I., Garza, B.D.L., Harrison, J.M., Roby, J., Duong, T.Q.: A low cost color visual stimulator for fMRI. *J. Neurosci. Methods* **204**(2), 379–382 (2012)
55. Mouli, S., Palaniappan, R., Sillitoe, I.P., Gan, J.Q.: Performance analysis of multi-frequency SSVEP-BCI using clear and frosted colour LED stimuli. In: Proceedings of IEEE 13th International Conference on Bioinformatics and Bioengineering (BIBE), Chania, 10–13 Nov 2013, pp. 1–4. doi:[10.1109/BIBE.2013.6701552](https://doi.org/10.1109/BIBE.2013.6701552) (2013)
56. Cao, F., Li, D., He, X., Gao, Y., Cheng, M., Zou, N.: Effects of flicker on vision in LED light source dimming control process. In: Proceedings of IET International Conference on Communication Technology and Application (ICCTA), 14–16 Oct. 2011, Beijing, pp. 255–258. doi:[10.1051/ita:2007005](https://doi.org/10.1051/ita:2007005) (2011)
57. Prueckl, R., Guger, C.: Controlling a robot with a brain-computer interface based on steady state visual evoked potentials. In: Proceedings of International Joint Conference on Neural Networks (IJCNN), Barcelona, 18–23 July 2010, pp 1–5. doi:[10.1109/IJCNN.2010.5596688](https://doi.org/10.1109/IJCNN.2010.5596688) (2010)
58. Teikari, P., Najjar, R.P., Malkki, H., Knoblauch, K., Dumortier, D., Gronfier, C., Cooper, H. M.: An inexpensive Arduino-based LED stimulator system for vision research. *J. Neurosci. Methods* **211**(2), 227–236 (2012)
59. Arduino: <http://www.arduino.cc> (2005). Accessed 1 March 2014
60. Wiring: <http://wiring.org.co> (2003). Accessed 1 March 2014
61. Processing: <http://www.processing.org> (2003). Accessed 1 March 2014
62. Guoqiao, T.: Modelling of LED light source reliability. In: Proceedings of 20th IEEE International Symposium on the Physical and Failure Analysis of Integrated Circuits (IPFA), 15–19 July 2013, Suzhou, pp. 255–258. doi:[10.1109/IPFA.2013.6599163](https://doi.org/10.1109/IPFA.2013.6599163) (2013)

## **Part III**

# **Views on Applications**

# **Chapter 10**

## **EEG Based Brain Computer Interface for Speech Communication: Principles and Applications**

**Kusuma Mohanchandra, Snehanshu Saha and G.M. Lingaraju**

**Abstract** EEG based brain computer interface has emerged as a hot spot in the study of neuroscience, machine learning and rehabilitation in the recent years. A BCI provides a platform for direct communication between a human brain and a computer without the normal neurophysiology pathways. The electrical signals in the brain, because of their fast response to cognitive processes are most suitable as non-motor controlled mediation between the human and a computer. It can serve as a communication and control channel for different applications. Though the primary goal is to restore communication in severely paralyzed population, the BCI for speech communication fetches recognition in a variety of non-medical fields, the silent speech communication, cognitive biometrics and synthetic telepathy to name a few. A survey of diverse applications and principles of the BCI technology used for speech communication is discussed in this chapter. An ample evidence of speech communication used by “locked-in” patients is specified. Through the aid of assistive computer technology, they were able to pen their memoir. The current state-of-the-art techniques and control signals used for speech communication is described in brief. Possible future research directions are discussed. A comparison of indirect and direct methods of BCI speech production is shown. The direct method involves capturing the brain signals of the intended speech or speech imagery, processes the signals to predict the speech and synthesizes the speech

---

**K. Mohanchandra (✉)**

Department of Computer Science & Engineering, Medical Imaging Research Centre,  
Dayananda Sagar College of Engineering, Bangalore 560 078, India  
e-mail: kusumalak@gmail.com

**S. Saha**

Department of Computer Science & Engineering and CBIMMC, PESIT South,  
Bangalore 560 100, India  
e-mail: snehanshusaha@pes.edu

**G.M. Lingaraju**

Department of Information Science & Engineering, M. S. Ramaiah Institute of Technology,  
Bangalore 560 054, India  
e-mail: gmlraju@gmail.com

production in real-time. There is enough evidence that the direct speech prediction from the neurological signals is a promising technology with fruitful results and challenging issues.

**Keywords** Brain computer interface • Locked-in syndrome • Electroencephalography • Silent communication • Imagined speech

## 10.1 Introduction

Humans use computers through interfaces such as keyboard, mouse, touch screen, digital camera or a data glove (Fig. 10.1). These interfaces have one thing in common: they need physical movement of the user. This physical movement may not be possible in the physically “locked-in” [76] patients. A Brain Computer Interface (BCI) is a device in which a person uses his brain to control the machine to be used. The machine can be a computer, wheelchair, robot, an assistive or an alternative communication device. BCI is a promising technology that provides a direct communication between the brain and a computer for conveying messages to the external world from one’s thoughts, without using any of the appendages. It provides an individual a non-muscular [87] way to communicate and control his surroundings. Each time we do a task or think of performing one, our brain generates distinct signals. These signals corresponding to the activity have a pattern. Exploring and identifying this pattern are challenging and form the crux of any BCI task. A BCI picks the signals from the brain of an user in the form of Electroencephalography (EEG). Feature extraction and classification leads to these signals being translated into meaningful commands to drive the device. Due to its tremendous potential the BCI attracts huge investments and research activities from around the world to facilitate and accelerate development. BCI has a wide range of applications across a variety of fields, both medical and non-medical. At the outset, we review the principles and practical applications of BCI related to speech communication, including “locked-in” patients, synthetic telepathy, cognitive biometrics and silent speech communication.

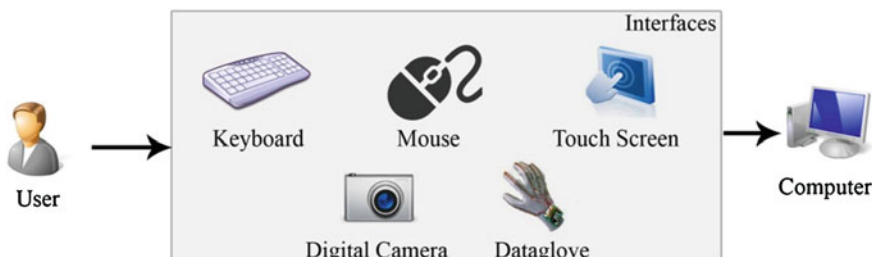


**Fig. 10.1** Conventional human computer interfaces

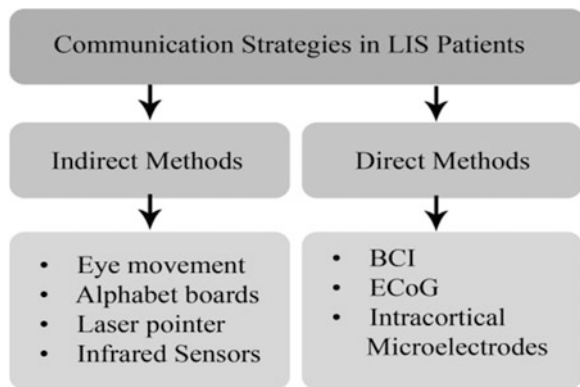
Thousands of severely disabled people are unable to communicate due to paralysis, locked-in syndrome (LIS) or other neurological disorders. Reinstating communication with these patients is a major challenge. The BCI is used by people deprived of expressing through speech. LIS is a condition in which the patient is awake and conscious, but “locked-in” an immobile body. The voluntary motor paralysis prevents the subject from communicating by the way of words or body movements. The subject wishes to speak or move as he is able to perceive his environment, but is unable to communicate due to “locked-in” state. The inability to communicate with others is distressing. The recent advances in computer based communication technology and BCI have enabled these people to communicate and control their surroundings and access the internet. This has improved the quality of life of the patients and helped them live with dignity.

Several BCI techniques evolved over the past decade restoring communication to persons with severe paralysis. These assistive devices range from a simple binary (yes/no) communication device, the speller device, a virtual keyboard to imagined speech communication to name a few. Birbaumer et al. [5] and Perelmuter et al. [64] have developed a speller device for a “locked-in” person to compose letters. Binary tree structured decision of the BCI is used, dividing the alphabet into successive halves until the desired letter is selected. A similar kind of speller is portrayed by Wolpaw et al. [86] where the alphabets iteratively divide into fourths instead of halves. Donchin et al. [20] has developed a method based on the P300 component of event-related potentials. The rows and columns of a two dimensional alphabet grid are illuminated in a sequence, and allow the user to select the desired letter. A 2-D cursor navigation to select letters from a WiViK virtual keyboard for “locked-in” subjects is suggested by Kennedy et al. [38].

At its most basic level, communication for “locked-in” patients involves a simple yes-no scheme [24] based on eye movements. One eye blink means “yes” and two blinks mean “no”; others may look up for “yes” and look down for “no”. For more detailed communication, alphabet boards may be used. The letters on the alphabet board may be arranged in the order frequently used, or in the form of blocks or a grid. An assistant goes through the letters one by one until the patient blinks to choose a letter. A laser pointer controlled by head movement can be used for faster communication. Special infrared sensors that react to eye movement can also be employed. The patient can move the cursor or select a letter by staring at it and then snap on it by blinking. This technology serves as a rehabilitation measure for patients suffering from classical and incomplete LIS as it is proven to control the residual movements. But the indirect communication systems have few major disadvantages. Though these systems are precise, the letter choice rate is as slow as one word/min, thereby limiting the user’s fluency. Moreover, these indirect methods fail to improve the patient’s behavioral abnormalities and do not address improving their psychological condition [74]. These methods fail to improve the constraints related to speech communication capabilities as well.

In an effort to handle the aforementioned problems and make BCI speech production more natural and fluent, direct methods are being developed. Figure 10.2 summarizes the direct and indirect methods of speech. The direct method involves

**Fig. 10.2** Communication strategies in LIS patients



capturing the brain signals of the intended speech, treat the signals to predict the speech and synthesize the speech production in real-time. The direct method of speech communication in BCI has extensive claims both in medical and universal applications. In this perspective, Suppes et al. [78, 79] used EEG and MEG signals to characterize speech imagery of words and sentences. DaSalla et al. [17] has developed a BCI for vowel speech imagery using EEG. Brumberg et al. [11, 12, 15] and Guenther et al. [27, 28] have developed speech BCI using EEG and ECoG. The decoded signals from the imagined speech are used to drive a speech synthesizer. Leuthardt et al. [48–50] have shown that ECoG is associated with different overt and imagined phoneme articulations. This enables invasive monitoring of human patients to control one-dimensional computer cursors rapidly and accurately. Extensive study is being borne out in this topic by numerous research groups.

## 10.2 Evidences of Speech Communication in Locked-in Patients

In this chapter, we introduce a few examples of LIS affected patients and their achievements inspite of severe impairment. Stephen Hawking, one of the most brilliant theoretical physicists in history and the author of “A Brief history of Time”, has a motor neuron disorder since his adult lifetime. Hawking communicates by selecting words from a series of menus along the screen, by urging a switch in his hand or operated by head or eye motion. The chosen words are stored and staged to a speech synthesizer, thus enabling him to communicate up to 15 words a minute [77]. He has written books and lots of scientific documents and delivered many scientific and popular talks by using this device. A victim of LIS, Jean-Dominique Bauby, penned a book, titled—“The Diving Bell and the Butterfly” (An award-winning movie of the same name). Through the script he showed the world that a deficiency does not hold back from achieving [3]. Bauby communicated by blinking his left eyelid to choose letters from an alphabet board. He founded an

Association of Locked-In Syndrome (ALIS) with the intent to aid patients suffering from LIS and their families. The French-based ALIS registered 367 LIS affected patients [43] between 1997 and 2004. This database serves as the foundation for the research performed on the patient population. Julia Tavalaro, a wheelchair-bound quadriplegic, was in a vegetative state, and could just move her head and eyes, but her senses were intact [44]. Tavalaro trained her residual movements to use a computer and eventually penned her own memoirs “Look Up for Yes”. Philippe Vigand, another victim of LIS, cultivated an infrared camera which in turn enabled him to “speak” and “write” by blinking his eyes [25]. This magic camera helped Philippe write his memoir, entitled “Only the Eyes Say Yes”. He has written about the evolution of his sickness and demonstrated his willingness to face new challenges. Another poignant testimony of LIS comes from Judy Mozersky who lost the entire bodily motion except her eyes. Through the aid of assistive computer technology, she has been able to continue her studies at Cornell. Her memoir, “Locked-In: A Young Woman’s Battle with Stroke” [55] has been published by the National Stroke Association.

These people with courage and hope have rebuilt their lives despite their supposedly insurmountable conditions. This implies the need to key out and appreciate the views and feelings surging behind the quiet and stillness of those who are “locked-in”. It is documented that the inability to communicate is alarming and more devastating than the inability to move. As an outcome, rehabilitation strategies for patients with LIS have focused on finding ways to aid communication using various means available for a finicky patient. Clinicians believe that in the majority of cases, improved communication improves patient’s quality of life and allows them to be more involved with family and society. Austrian researchers have categorized LIS into 3 subtypes shown in Fig. 10.3 [4]. (a) Classical LIS, in which conscious patients are completely immobile except for eye movement and blinking. (b) Incomplete LIS, in which minimal residual movement is preserved in parts of

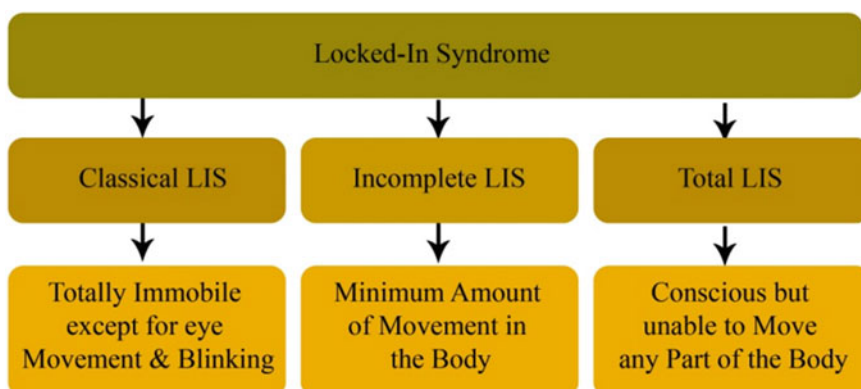


**Fig. 10.3** Classification of locked-in syndrome (LIS)

the body besides the eyes. (c) Total LIS, in which patients are conscious but unable to move any muscle. Rehabilitation can be made available for the classical LIS patients, a few of incomplete LIS patients, but not viable for total LIS patients.

### 10.3 Supplementary Target BCI Applications for Speech Communication

BCI for speech communication is prominently perceived as an alternative augmentative communication (AAC) device for severely disabled people. As illustrated in Fig. 10.4, it delivers its application in a variety of non-medical fields. Research on synthetic telepathy is being carried out by the U S Army, with the intention to allow its soldiers to communicate [19] just by thinking. In 2008, the U S Army awarded a \$4 million contract to a team of scientists from three American universities. They are University of California (led by Mike D'Zmura) at Irvine, Carnegie Mellon University, and University of Maryland. The aim is to build up a thought-helmet, a device that can read and broadcast the unspoken speech of soldiers. The goal was to enable silent communication among the soldiers. The thought-helmet extracts the brain signals of the soldier who hopes to communicate silently, interprets the signals to speech, and conveys those to a radio speaker or an earpiece worn by other soldiers. The developers [9, 11, 22] are working towards decoding the brain signals associated with speech. To begin with, a message is interpreted by a synthetic voice to be delivered in the soldier's own voice specifying his position and distance from the recipient. The team, directed by Schalk, is pursuing the invasive Electrocorticography (ECOG) approach. The second group, headed by Mike D'Zmura, is using EEG, a noninvasive brain-scanning technique better suited for an actual thought-helmet.

Silent speech communication is one of the most interesting future technologies which enable speech communication without using the sounds created during the vocalization process. The silent speech interface [18] allows people to communicate

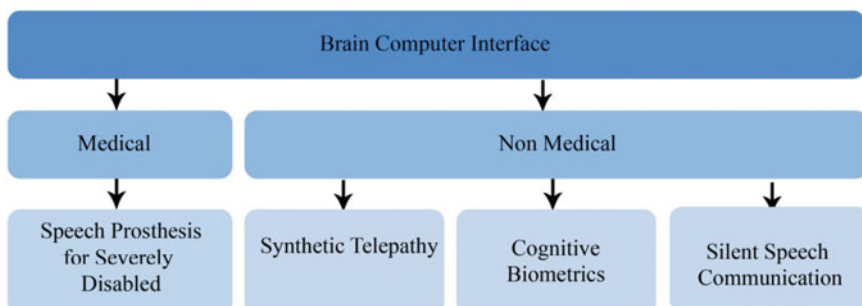


**Fig. 10.4** Applications of BCI in speech communication

with each other by using a whispering sound or even soundless speech. Furthermore, the voice-disabled individual can use his tongue and mouth movements. The process then allows the silent speech interface technology [14] to produce the voice on his behalf thereby facilitating communication with others. This technology is used by NASA astronauts who need to communicate, without the voices not being known due to surrounding noise. In preliminary experiments, NASA scientists found that small, button-sized sensors, fixed under the jawbone and on either side of the throat [56] could collect the signals. The signals are then sent to the processor and a computer program to translate them into words. These subvocal speech systems can be made use of in space suits, in noisy environment and airport towers to capture air-traffic controller [56] commands. The subvocal speech systems might be used by a person who has lost his voice permanently. A person using the subvocal speech system [21] thinks of phrases and talks to himself in silence. But the tongue and vocal cords do receive speech signals from the brain. These biological signals are tapped and fed to the speech system for further analysis. Chuck Jorgensen and his team [36, 37] are developing silent speech recognition at NASA's Ames Research Center. They developed special software trained to recognize six words and 10 digits repeated sub-vocally. The word recognition rate was 92 %. The speech system is trained to learn the words—"stop", "go", "left", "right", "alpha" and "omega", and the digits 0–9. With these sub-vocalized words, the software performed simple searches on the internet and controlled a web browser program.

The sub-vocalized or imagined speech can be used as a new feature for biometrics [72] as opposed to the traditional methods. This new class of biometrics based on cognitive aspects of human behavior, called cognitive biometric, is a novel approach to user authentication. The brain state of individuals used for the authentication mechanism increases the robustness and enable cross validation when used in combination with traditional biometric methods. The biometric approaches based on the biological features of humans [42, 52, 62, 63, 69–71] have distinct advantages over traditional methods. The cognitive biometric cannot be hacked, stolen or transferred from one person to another as they are unique for each person.

Speech communication has an extensive scope in various domains of applications. But the challenges in processing the EEG signals are significant. The EEG signals are extremely complex and prone to internal and external interference. Advancement in sensor technology, data acquisition techniques and robust signal processing algorithms may lead to efficient usage of speech communication in diverse applications and may overcome the challenges posed.

## 10.4 BCI Design Principles

BCI research is a comparatively young and multidisciplinary [53] field integrating researchers from engineering, neuroscience, psychology, physiology and other healthcare fields. BCIs use brain signals to control and communicate with the

computer or any external device. Hence the need to assess the brain signals and render the information into compliant electrical signals is important. There are several cases of existing BCI, classified based on the sensory systems and control signal systems.

### ***10.4.1 Types of BCI***

The neuroimaging techniques used in BCI can be broadly classified into invasive and non-invasive methods. Invasive BCIs involve implanting electrodes inside the brain and the non-invasive ones include haptic controllers and EEG scanners. The basic purpose of these devices is to comprehend the electrical signals in the brain and translate them as signals sensed by external devices. Invasive modalities need to implant microelectrode arrays inside the skull within the brain, which involves expert surgeons with high precision skills. The problem with this device is that a scar tissue forms over the device as a reaction to the extraneous matter. This reduces its efficacy and increases the health risk to the patient. Though, they possess the best signal to noise ratio the need to undergo complex surgical procedure causing a permanent hole in the skull is not worth taking the risk. Multiple degrees of freedom can be achieved only through invasive approaches. Partially invasive BCIs are implanted inside the skull, but over the brain. They spread out electrode arrays on the surface of the brain. Although the signal strength is less feeble, it eliminates the problem of scar tissue formation, e.g. ECoG or intracranial EEG (iEEG). Noninvasive BCI is the most used neuroimaging methods, dealing with general brain-waves that are dampened by passing through the skull, nonetheless receptive enough to extract the signals with specific information. The EEG is the most widely used non-invasive technique and most studied in recent times. Other non-invasive methods considered for capturing brain signals include magneto encephalography (MEG), functional magnetic resonance imaging (fMRI) and near infrared spectrum imaging (NIRS). The invasive and non-invasive methods are summarized in Table 10.1.

According to the nature of the input signals used, BCI systems can be classified as exogenous or endogenous. Exogenous BCI uses external stimulus such as sound or picture to elicit the brain activity, while the endogenous BCI is based on self-regulation [59] of brain rhythms and potentials without external stimuli. Table 10.2 summarizes the differences between exogenous and endogenous BCIs.

BCI systems are classified based on the input data processing techniques as synchronous or asynchronous. Synchronous BCIs [68] analyze brain signals during a pre-defined time window. The user is expected to send commands during this specific period and any signal outside this window is ignored. The asynchronous BCI analyzes the brain signals continuously irrespective of user command and therefore is more natural than synchronous BCI. Asynchronous BCIs are computationally heavier and complex. Table 10.3 summarizes the differences between the two.

**Table 10.1** Summary of neuroimaging techniques

Neuroimaging method	Modality	Activity measured	Advantages	Limitations
Invasive	ECoG	Electrical	Good spatial resolution, higher signal-to-noise ratio than EEG	Highly invasive, surgical incision into the skull needed to implant the electrodes
Noninvasive	EEG	Electrical	Noninvasive, ease of use, low cost and high temporal resolution	Low spatial resolution on the scalp, poor signal-to-noise ratio
	MEG	Magnetic fields associated with electrical activity	Higher spatiotemporal resolution than EEG	Too bulky and expensive modality, not practical for real-time analysis
	fMRI	Hemodynamic	High spatial resolution, low invasiveness, absence of radiation exposure, and relatively wide availability	Indirect markers of brain electrical activity, low temporal resolution of 1 or 2 s, physiological delay from 3 to 6 s, highly susceptible to head motion artifacts
	NIRS	Hemodynamic	Low cost, high portability, an acceptable temporal resolution in the order of 100 ms, might be a good alternative to EEG as conductive gel and electrodes are not used	The spatial resolution is low in the order of 1 cm; communication speeds in NIRS-based BCIs are limited due to inherent delays of the hemodynamic response

**Table 10.2** Main differences between exogenous and endogenous BCI

Approach	Brain signals	Advantages	Disadvantages
Exogenous BCI	Steady state visually evoked potential (SSVEP) and P300	Training can be set up with ease and speed. Least EEG channel required	Maintaining attention to external stimuli, may cause fatigue, irritability and tiredness to the user
Endogenous BCI	Slow cortical potentials (SCP) and sensorimotor rhythms	Free of any stimulation, can be operated at one's own will, useful for physically challenged people	Elaborate training, not every user is able to obtain control, Multichannel EEG recordings required for good performance, Lower data rate

**Table 10.3** Major differences between synchronous and asynchronous BCIs

Approach	Advantages	Disadvantages
Synchronous BCI	Design and performance evaluation are simpler, the user can blink and do other movements when brain signals are not analyzed and thus avoid generating artifacts	Not a natural interaction
Asynchronous BCI	Not required to wait for external cues, offers a more natural interaction	Design and performance evaluation are complex

### 10.4.2 EEG Based BCI

A common method for designing a BCI [61] is to use EEG signals extracted during mental tasks. The EEG is the most widely used neuroimaging methods, due to its high temporal resolution, comparative low cost, portability, and few risks to the users. The EEG records the brain's electrical activity along the scalp produced by the firing of neurons within the brain. However, the signals are of low resolution [59] as the signals travel through the scalp, skull, and many other layers. So the original signal strength in the electrodes becomes weaker, to the order of microvolts and turns out to be very sensitive to noise. Noise is a key factor [2] in EEG signals. It reduces the signal to noise ratio and decreases the ability to extract meaningful information from the recorded signals. The noise may be either due to other current fields in the brain or external noise sources. EEG signal is measured as the potential difference over time, between the active electrode and the reference electrode. The international 10–20 system accessed from Brain Master Technologies Inc. [10] is shown in Fig. 10.5. The multichannel EEG sets contain up to 128 or 256 active

**Fig. 10.5** A standard 10–20 international electrode placement system

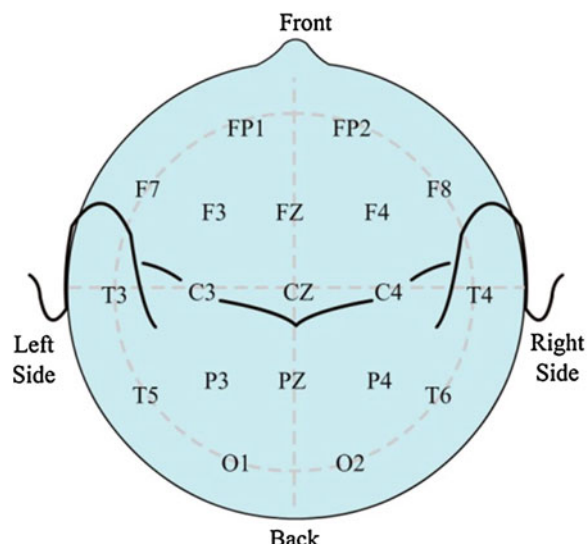


**Table 10.4** Frequency bands in the brain signal

EEG bands	Frequency (Hz)	Distribution	State of mind
Delta	0.5–4	Central cerebrum and parietal lobes	Deep sleep, non-REM sleep
Theta	4–8	Frontal, parietal and temporal lobes	Drowsiness, first stage of sleep
Alpha	8–13	Most prominent at occipital and parietal lobe	Relaxed wakefulness with eyes closed
Mu	8–12	Central electrodes, over motor and somatosensory cortex	Shows rest state motor neurons
Beta	13–30	Frontal and central regions	Highly alert and focused
Gamma	>30	Very localized	Higher mental activity, including perception and consciousness [30]

electrodes. These electrodes are made of silver chloride ( $\text{AgCl}$ ). A gel is used which creates a conductive path between the skin and the electrode for the flow of current. Electrodes that do not use gels, called ‘dry’ electrodes are made of materials such as titanium and stainless-steel.

EEG signals consist of a set of frequency bands. These frequency bands are identified as delta ( $\delta$ ), theta ( $\theta$ ), alpha ( $\alpha$ ), beta ( $\beta$ ), and gamma ( $\gamma$ ). Relevant characteristics of these bands are mentioned in Table 10.4.

The EEG can be modified [29] by motor imagery, successfully used by patients with severe motor impairments (e.g., late stage of amyotrophic lateral sclerosis) to aid them communicate with their environment. The need for brain signals with a higher resolution has restricted the recovery of motor disabilities, despite the exceptional convenience of EEG based BCI applications.

#### 10.4.3 Control Signals Used in BCI for Speech Communication

The physiological phenomena of the brain signals can be tapped, decoded and modulated, to control a BCI system. These signals are regarded as control signals in BCIs. The control signals employed in current BCI systems are classified as visual evoked potentials (VEP), slow cortical potentials (SCP), P300 evoked potentials, and sensorimotor rhythms (SMR). Wang et al. [83] has listed the signal controls with their main features (refer Table 10.5).

EEG records the electrical activity arising from the neurons residing in the cerebral cortex using the scalp electrodes. The brain electrical activity may be spontaneous or evoked due to specific external or internal stimulus/events. Responses to stimulus are termed as event-related potentials (ERP). Event-related potentials are time locked to physical stimuli and help capture neural activity related

**Table 10.5** Summary of control signals [83]

Signal	Physiological phenomena	Number of choices	Training	Information transfer rate (bits/min)
VEP	Brain signal modulations in the visual cortex	High	No	60–100
SCP	Slow voltages shift in the brain signals	Low (2 or 4, very difficult)	Yes	5–12
P300	Positive peaks due to infrequent stimulus	High	No	20–25
Sensorimotor rhythms	Modulations in the sensorimotor rhythms synchronized to motor activities	Low (2–5)	Yes	3–35

to sensory and cognitive processes. Event-related potentials can be elicited by a wide variety of sensory, cognitive or motor events. The EEG activity reflects the summed activity [65] of postsynaptic potentials. An electrical potential is produced when neurons, to the order of thousands or millions, fire in tandem. The ERPs are categorized as exogenous and endogenous. ERPs occurring within the first 100 ms after the onset of stimulus [31, 80] are termed sensory or exogenous as they depend on the physical parameters of the stimulus. Exogenous ERPs are obligatory responses to the presentation of physical stimulus like visual, audio or intensity. In contrast, ERPs generated with the latency in the range of 100 ms up to several seconds are termed cognitive or endogenous. The endogenous ERPs reveal the manner in which the subject evaluates the stimulus. They depend on behavioral and psychological processes of the event. The ERPs are characterized by their latency and amplitude, relative to stimulus onset. ERPs with a latency ranging from 500 ms to around 10 s are categorized as slow cortical potentials (SCP). The EEG signals are extremely complex and prone to noise. To separate the EEG signals from the background noise, the signals are time locked and averaged across many trials, thus improving the signal-to-noise ratio.

#### 10.4.3.1 Visually Evoked Potentials

The VEP is an evoked potential and elicited when users view a flickering stimulus of different frequencies in the range of 3.5–75 Hz. The brain generates electrical activity of the identical frequency or multiples of the frequency of the visual stimulus. Spectral analysis of EEG in visual areas i.e. occipital lobe shows the frequency components that can later be mapped to the device commands. These modulations are easy to detect since the amplitude of VEPs increases a great deal [82] as the stimulus is moved closer to the central visual field. This control signal needs very little training. However, the drawback of this control signal is that the user has to keep his eyes fixed at one point bereft of any random movement.

Lee et al. [45–47] exposed the subjects (participants of the experiment) with a  $5 \times 5$  matrix that contained flashing stimuli of digits, characters, and symbols displayed on the LCD screen. The cells of the matrix flicker in a random sequence. Participants have to gaze at the cell containing the digit or character they want to select. The potential at the occipital cortex are measured, and the matrix cell which elicited large signal amplitude is considered as the target cell the participant wanted to select. Successful communication with a high information transfer rate is achieved as a consequence. The evoked potential serves as an efficient and reliable tool for disabled people to communicate with external environments. BCI based on VEP entails that the user should be able to control the gaze direction precisely.

#### 10.4.3.2 Slow Cortical Potentials

Slow cortical potentials [34] are potential shifts of the cerebral cortex, in the frequency range below 1–2 Hz and may persist over several seconds. One of the first communication devices in BCI, the Thought Translation Device (TTD) developed by Birbaumer and his colleagues [5–7, 32, 33] uses SCPs to control the movement of an object on a computer screen. The TTD supports completely paralyzed patients with basic communication ability. The patients are trained to self-regulate SCPs voluntarily to navigate a binary-tree spelling device. In each selection, the choice is between selecting or not selecting a set of one or more letters [87] until a single letter is chosen. A backup or erase option exists as well. Self-regulation of SCPs is critical as the rate of information provided by SCP based BCI are sensibly low. For instance Lutzenberger et al. [51] and Rockstroh et al. [73], trained patients to self-regulate their SCP by providing feedback and positive reinforcement of correct responses. Continuous practice and extensive training are required to use SCP based BCI.

#### 10.4.3.3 The P300 Event-Related Potential

A P300 wave is an endogenous event related potential component [35] created due to infrequent auditory, visual, or somatosensory stimuli. The signal is characterized by an increase in time series amplitude approximately 300 ms after the stimulus onset. Increase in signal amplitude is more prominent at the parietal and occipital electrodes, although observed at several other locations on the scalp. P300 was suggested by Farwell and Donchin [20, 23, 75] for operating a letter speller BCI but of late investigated by another research group [26, 40, 60]. It is seen in response to the oddball paradigm, that the target stimulus with rare and irregular occurrences is presented within a series of the standard stimulus. For example, if a subject is viewing a random series of names, in every 3 s occasionally if one of these is the subject's name, a P300 wave is generated. The P300 wave is produced in response to this rarely presented, recognized, meaningful stimulus. The P300 is larger for less probable events [20].

The speller device consists of a matrix of letters, numbers and symbols. The rows and columns of the matrix are highlighted in sequence. To select a letter, the user has to focus attention on the cell containing the target letter. When a row or column has the chosen letter, a P300 component of the ERP is elicited. The BCI detects the character by determining the row and column, which produced a P300 response and the corresponding character, is printed on the screen. The use of P300 based BCIs does not need user initial training. Nevertheless, the performance may be reduced because the user gets used to the infrequent stimulus [16] and so the P300 amplitude is decreased. A common form of P300 based spelling BCI uses a  $6 \times 6$  matrix that has 26 letters of the alphabet and numbers 0–9. In every trial, each row and column are illuminated once for a period of 100–175 ms, totaling 12 events, two containing the target item and ten containing non-target items characterizing an oddball paradigm. The presentation sequence is repeated several times per selection and the signals are averaged to improve the P300 signal to noise ratio for reliable detection.

#### 10.4.3.4 Sensorimotor Rhythms

Sensorimotor rhythms comprise  $\mu$  (8–12 Hz) and  $\beta$  (18–25 Hz) rhythms, localized in the primary sensory or motor cortical areas. A decrease in  $\mu$  and  $\beta$  rhythms is associated with movement or preparation of movement labeled as event-related desynchronization (ERD). An increase of  $\mu$  and  $\beta$  rhythms is associated with relaxation labeled event-related synchronization (ERS) [39]. These rhythms also occur with motor imagery, i.e. imagining the movement and also with cognitive tasks.

This technique developed by Wolpaw et al. [85], is used to control one and two dimensional cursor movements on a computer screen [41, 81, 88]. People have learned to control  $\mu$  and  $\beta$  amplitudes in the absence of movement or sensation, including those with LIS. Increased  $\mu$  rhythm amplitude [54] moves the cursor towards the top target and decreased  $\mu$  rhythm amplitude does so towards the bottom target. Pfurtscheller and colleagues at the Graz University [57, 58, 66, 67] have developed a BCI for two-state classification using the mental imagery strategy. Different motor imagery such as, imagination of left-hand, right-hand, or foot movement is used to elicit the brain activity in the sensorimotor areas in response to a visual cue.

#### 10.4.3.5 Intracranial Method—ECoG

As mentioned in earlier sections, speech communication for severely paralyzed people can be achieved using EEG or ECoG. The ECoG method requires implantation of microelectrodes into the outer layers of the human cortex. Kennedy et al. [38] has described an invasive method to drive a BCI, where an “Amyotrophic lateral sclerosis” (ALS) affected patient learned to control the cursor to produce

synthetic speech and type. Brumberg and colleagues have developed a BCI to control an artificial speech synthesizer by an individual with “locked-in” syndrome during imagined speech [12, 27, 28]. The neural signal recorded from an implanted electrode in the speech motor cortex of a human volunteer is used to drive an artificial speech synthesizer. Leuthardt et al. [48–50] demonstrated that ECoG activity recorded from the surface of the brain enables users to control a one-dimensional computer cursor rapidly and accurately. The ECoG signals associated with different types of motor and speech imagery are identified and used to control two dimensional joystick movements.

Though, speech prosthesis for paralyzed individuals can be achieved using cortical surface electrodes (e.g. ECoG) or intra-cortical microelectrodes, the EEG is the most preferred technology [84] because of its excellent temporal resolution, non-invasive characteristics, portability and reasonably low price. However, due to volume conduction through the scalp, skull, and other layers of the brain, the spatial resolution of EEG signals diminish and needs to be improved.

Though EEG is endowed with high temporal resolution, its poor spatial resolution makes it almost essential to be trained extensively by the users. However, ECoG has significant clinical risks limiting its usage.

## 10.5 Challenges and Future Research Directions for Speech Communication BCI

Several crucial issues need to be handled to facilitate expanded use of BCI technology in speech communication... Most of the existing techniques use fMRI for processing of languages and speech areas of the brain as it has a good spatial resolution. But fMRI has limited temporal resolution. The high temporal resolution of EEG and ECoG has the potential to demonstrate the functional relation between the language and speech areas of the brain. Neuroscience research [8] has shown that imagined speech activate the frontal cortex as well as Broca’s and Wernicke’s areas. The change in neural activity in the language areas of the brain needs to be understood clearly. The EEG signals are usually recorded in high-dimensional space and the size of data makes it computationally intensive on the classifier. To address this issue, competitive dimension reduction techniques [1] and spatial filters are to be identified. An important attribute of spatial filtering [2] is to reduce the number of channels on the scalp and at the same time retain all the information needed for the classification. The electrodes that do not contribute to the activity may be discarded thereby reducing the number of electrodes considerably.

Another key issue is whether it is practically useful to the actual target population. The patient population in need of BCI has severe neurological diseases [13] causing extensive changes in EEG patterns and the power spectrum. Due to their continuous degenerative state, a decrease in spectral power is possible, which induces classification errors.

To achieve success rates and stability in BCI, the evoked potentials from event related potentials are considered (e.g. P300, VEP). However, it may not be possible to provide external stimulus in every possible situation. For the patient population, the sensory perception is often impaired or degrades continuously, evading any external stimulus. Therefore, the need to self-regulate the brain signals is critical. For other applications such as silent speech communication and cognitive biometrics, the usage is outside the lab environment, rendering the supply of external stimulus infeasible. Therefore, the necessity to self-regulate the endogenous signals (e.g. SCP) is required. However, this implies extensive training for the user, in order to produce the same signals every time.

A combination of advances in sensor technology, data acquisition systems, standard methods and metrics for evaluation and reliable algorithms can propel the use of BCI for speech communication to diverse directions.

## 10.6 Conclusion

The research and development in BCI for speech communication have attracted great attention and investigation from many research groups across varied realms of interest. Though the primary goal of BCI technology is to restore communication in severely paralyzed population, the speech communication has expanded its application in silent speech communication, synthetic telepathy and cognitive biometrics.

The most common BCI applications use EEG for recording the neural activity. The EEG based speller devices are either controlled by evoked potential (VEP, P300, SMR) or by self-regulation of SCP and motor imagery for selection of letters from a visual display or a binary speller device. The EEG study confirms that it is feasible to use non-invasive neurophysiology method to control the spelling device. Though these indirect methods empower speech communication, they are not at rates, fast enough for conversational or near conversational speech. The slow speech production may cause the disabled users to withdraw from social interactions in frustration. To overcome the drawbacks of EEG based speller devices, the intracranial electrodes (ECoG) are used for signal acquisition. The ECoG boasts of an improved signal to noise ratio (SNR). The risk of neurosurgery, the cost involved and ethical issues make invasive methods impractical except for users who are severely disabled.

In recent times, researchers are investigating the feasibility of performing direct speech production from different neurological signals for more natural and fluent speech production. The direct method involves capturing the brain signals of the intended speech or speech imagery, process the signals to predict the speech and synthesize the speech output in real-time. The direct method of speech communication in BCI has an extensive scope of medical and general applications. Extensive work is being carried out in this field by several research groups. To promote the feasibility of BCI for speech imagery, we must take into account the psychological

factors and the advances in EEG pattern recognition techniques. With the advancement in technology, faster and more accurate communication may be achieved with EEG based BCI systems for direct speech production.

## References

1. Azar, A.T., Balas, V.E., Olariu, T.: Classification of EEG-based brain–computer interfaces. Springer International Publishing in Advanced Intelligent Computational Technologies and Decision Support Systems, pp. 97–106. Springer International Publishing, Switzerland (2014)
2. Bashashati, A., Fatourechi, M., Ward, R.K., Birch, G.E.: A survey of signal processing algorithms in brain–computer interfaces based on electrical brain signals. *J. Neural Eng.* **4**(2), R32 (2007)
3. Bauby, J.D.: The diving bell and the butterfly: a memoir of life in death. Translated from the French by Jeremy Leggatt. Alfred A. Knopf, Inc, New York (1997)
4. Bauer, G., Gerstenbrand, F., Rumpl, E.: Varieties of the locked-in syndrome. *J. Neurol.* **221**(2), 77–91 (1979)
5. Birbaumer, N., Kübler, A., Ghanayim, N., Hinterberger, T., Perelmouter, J., Kaiser, J., Flor, H.: The thought translation device (TTD) for completely paralyzed patients. *IEEE Trans. Rehabil. Eng.* **8**(2), 191 (2000)
6. Birbaumer, N., Hinterberger, T., Kubler, A., Neumann, N.: The thought-translation device (TTD): neurobehavioral mechanisms and clinical outcome. *IEEE Trans. Neural Syst. Rehabil. Eng.* **11**(2), 120–123 (2003)
7. Birbaumer, N., Cohen, L.G.: Brain–computer interfaces: communication and restoration of movement in paralysis. *J. Physiol.* **579**(3), 621–636 (2007)
8. Blank, S.C., Scott, S.K., Murphy, K., Warburton, E., Wise, R.J.: Speech production: Wernicke Broca and beyond. *Brain* **125**(8), 1829–1838 (2002)
9. Bogue, R.: Brain-computer interfaces: control by thought. *Ind. Robot. Int. J.* **37**(2), 126–132 (2010)
10. Brain Master Technologies Inc. (n.d). The international 10–20 system (electronic print). <http://www.brainmaster.com/generalinfo/electrodeuse/eegbands/1020/1020.html>. Accessed 10 Nov 2013
11. Brigham, K., Kumar, B.V.: Imagined speech classification with EEG signals for silent communication: a preliminary investigation into synthetic telepathy. In: The 4th International IEEE Conference on Bioinformatics and Biomedical Engineering (iCBBE), pp. 1–4. Chengdu, China, 18–20 June 2010
12. Brumberg, J.S., Kennedy, P.R., Guenther, F.H.: Artificial speech synthesizer control by brain-computer interface. In: Proceedings of the 10th Annual Conference of the International Speech Communication Association (INTERSPEECH 2009), pp. 636–639. International Speech Communication Association, Brighton, U.K., 6–10 Sept 2009
13. Brumberg, J.S., Guenther, F.H.: Development of speech prostheses: current status and recent advances. *Expert Rev. Med. Devices* **7**(5), 667–679 (2010)
14. Brumberg, J.S., Nieto-Castanon, A., Kennedy, P.R., Guenther, F.H.: Brain–computer interfaces for speech communication. *Speech Commun.* **52**(4), 367–379 (2010)
15. Brumberg, J.S., Wright, E.J., Andreasen, D.S., Guenther, F.H., Kennedy, P.R.: Classification of intended phoneme production from chronic intracortical microelectrode recordings in speech-motor cortex. *Fronti. Neurosci.* **5**(65), 1–14 (2011)
16. Cipresso, P., Carelli, L., Solca, F., Meazzi, D., Meriggi, P., Poletti, B., Riva, G.: The use of P300-based BCIs in amyotrophic lateral sclerosis: from augmentative and alternative communication to cognitive assessment. *Brain Behav.* **2**(4), 479–498 (2012)

17. DaSalla, C.S., Kambara, H., Sato, M., Koike, Y.: Single-trial classification of vowel speech imagery using common spatial patterns. *Neural Netw.* **22**(9), 1334–1339 (2009)
18. Denby, B., Schultz, T., Honda, K., Hueber, T., Gilbert, J.M., Brumberg, J.S.: Silent speech interfaces. *Speech Commun.* **52**(4), 270–287 (2010)
19. Discover magazine: The army's bold plan to turn soldiers into telepaths. <http://discovermagazine.com/2011/apr/15-armys-bold-plan-turn-soldiers-into-telepaths#.UZe6-9isOSo>. Accessed 10 Nov 2013
20. Donchin, E., Spencer, K.M., Wijesinghe, R.: The mental prosthesis: assessing the speed of a P300-based brain-computer interface. *IEEE Trans. Rehabil. Eng.* **8**(2), 174–179 (2000)
21. D'Zmura, M., Deng, S., Lappas, T., Thorpe, S., Srinivasan, R.: Toward EEG sensing of imagined speech. In: Jacko J.A. (ed.) *Human-Computer Interaction New Trends, Part I, HCII 2009, LNCS 5610*, pp. 40–48. Springer, Berlin (2009)
22. D'Zmura, M.: MURI: synthetic telepathy. MURI: Imagined Speech & Intended Direction. <http://cnslab.ss.uci.edu/muri/research.html>. Accessed 10 Nov 2013
23. Farwell, L.A., Donchin, E.: Talking off the top of your head: toward a mental prosthesis utilizing event-related brain potentials. *Electroencephalogr. Clin. Neurophysiol.* **70**(6), 510–523 (1988)
24. Foster, J.B.: Locked-in syndrome: advances in communication spur rehabilitation. *Psychiatr. Times (issue of Appl. Neurol.)* **3**(1) (2007 January). [http://www.jordanafoster.com/article.asp?a=neuro/20070101\\_Locked-in\\_Syndrome](http://www.jordanafoster.com/article.asp?a=neuro/20070101_Locked-in_Syndrome). Accessed 10 Nov 2013
25. Gosseries, O., Bruno, M.A., Vanhaudenhuyse, A., Laureys, S., Schnakers, C.: Consciousness in the locked-in syndrome. The neurology of consciousness: Cognitive neuroscience and neuropathology, 191–203. Academic Press, Oxford (2009)
26. Guan C, Thulasidas M, Wu J (2004) High performance P300 speller for brain-computer interface. In: The 2004 IEEE International Workshop on Biomedical Circuits and Systems, 1–3 Dec 2004, Singapore, pp. S3–S5. doi:[10.1109/BIOCAS.2004.1454079](https://doi.org/10.1109/BIOCAS.2004.1454079)
27. Guenther, F.H., Brumberg, J.S., Wright, E.J., Nieto-Castanon, A., Tourville, J.A., Panko, M., Kennedy, P.R.: A wireless brain-machine interface for real-time speech synthesis. *PLoS one* **4**(12), e8218 (2009)
28. Guenther, F.H., Brumberg, J.S.: Brain-machine interfaces for real-time speech synthesis. In: The 2011 Annual International Conference of the IEEE on Engineering in Medicine and Biology Society, EMBC, 30 Aug–03 Sep 2011, Boston, MA, USA, pp. 5360–5363, 2011 August
29. Guger, C., Schlogl, A., Neuper, C., Walterspacher, D., Stein, T., Pfurtscheller, G.: Rapid prototyping of an EEG-based brain-computer interface (BCI). *IEEE Trans. Neural Syst. Rehabil. Eng.* **9**(1), 49–58 (2001)
30. Herrmann, C.S., Demiralp, T.: Human EEG gamma oscillations in neuropsychiatric disorders. *Clin. Neurophysiol.* **116**(12), 2719–2733 (2005)
31. Hinojosa, J.A., Martin-Lloeches, M., Rubia, F.J.: Event-related potentials and semantics: an overview and an integrative proposal. *Brain Lang* **78**(1), 128–139 (2001)
32. Hinterberger, T., Kübler, A., Kaiser, J., Neumann, N., Birbaumer, N.: A brain–computer interface (BCI) for the locked-in: comparison of different EEG classifications for the thought translation device. *Clin. Neurophysiol.* **114**(3), 416–425 (2003)
33. Hinterberger, T., Mellinger, J., Birbaumer, N.: The thought translation device: structure of a multimodal brain-computer communication system. In: The 2003 First International IEEE EMBS Conference on Neural Engineering, 20–22 March 2003, Capri Island, Italy, pp. 603–606 (2003). doi:[10.1109/CNE.2003.1196293](https://doi.org/10.1109/CNE.2003.1196293)
34. Hinterberger, T., Houtkooper, J.M., Kotchoubey, B.: Effects of feedback control on slow cortical potentials and random events. In: The 2004 Parapsychological Association Convention, 05–08 August 2004, Vienna, pp. 39–50 (2004)
35. Johnson, R.: On the neural generators of the P300 component of the event-related potential. *Psychophysiology* **30**(1), 90–97 (1993)

36. Jorgensen, C., Lee, D.D., Agabont, S.: Sub auditory speech recognition based on EMG signals. In: The IEEE International Joint Conference on Neural Networks, 20–24 July 2003, Portland, OR, vol. 4, pp. 3128–3133 (2003). doi:[10.1109/IJCNN.2003.1223240](https://doi.org/10.1109/IJCNN.2003.1223240)
37. Jorgensen, C., Binsted, K.: Web browser control using EMG based sub vocal speech recognition. In: The IEEE 38th Annual Hawaii International Conference on System Sciences, HICSS'05, 3–4 January 2005, Hilton Waikoloa Village, Island of Hawaii (Big Island), vol. 09, pp. 294c–294c (2005). doi:[10.1109/HICSS.2005.683](https://doi.org/10.1109/HICSS.2005.683)
38. Kennedy, P.R., Bakay, R.A., Moore, M.M., Adams, K., Goldwaith, J.: Direct control of a computer from the human central nervous system. *IEEE Trans. Rehabil. Eng.* **8**(2), 198–202 (2000)
39. Krepki, R., Blankertz, B., Curio, G., Müller, K.R.: The Berlin Brain-Computer Interface (BBCI)—towards a new communication channel for online control in gaming applications. *Multimed. Tools Appl.* **33**(1), 73–90 (2007)
40. Krusinski, D.J., Sellers, E.W., McFarland, D.J., Vaughan, T.M., Wolpaw, J.R.: Toward enhanced P300 speller performance. *J. Neurosci. Methods* **167**(1), 15–21 (2008)
41. Kübler, A., Nijboer, F., Mellinger, J., Vaughan, T.M., Pawelzik, H., Schalk, G., Wolpaw, J.R.: Patients with ALS can use sensorimotor rhythms to operate a brain-computer interface. *Neurology* **64**(10), 1775–1777 (2005)
42. Kusuma, M., Lingaraju, G.M., Prashanth, K., Vinay, K.: Using brain waves as new biometric feature for authenticating a computer user in real-time. *Int. J. Biometrics Bioinf.* **7**(1), 49 (2013)
43. Laureys, S., Pellas, F., Van Eeckhout, P., Ghorbel, S., Schnakers, C., Perrin, F., Goldman, S.: The locked-in syndrome: what is it like to be conscious but paralyzed and voiceless?. *Prog. Brain Res.* **150**, 495–611 (2005)
44. Laureys, S., Celesia, G., Cohadon, G., Lavrijsen, F., León-Carrión, J., Sannita, W.G., Dolce, G.: Unresponsive wakefulness syndrome: a new name for the vegetative state or apallic syndrome. *BMC Med.* **8**(1), 68 (2010)
45. Lee, PLWuCH, Hsieh, J.C., Wu, Y.T.: Visual evoked potential actuated brain computer interface: a brain-actuated cursor system. *Electron. Lett.* **41**(15), 832–834 (2005)
46. Lee, P.L., Hsieh, J.C., Wu, C.H., Shyu, K.K., Wu, Y.T.: Brain computer interface using flash onset and offset visual evoked potentials. *Clin. Neurophysiol.* **119**(3), 605–616 (2008)
47. Lee, P.L., Sie, J.J., Liu, Y.J., Wu, C.H., Lee, M.H., Shus, C.H., Shyu, K.K.: An SSVEP-actuated brain computer interface using phase-tagged flickering sequences: a cursor system. *Ann. Biomed. Eng.* **38**(7), 2383–2397 (2010)
48. Leuthardt, E.C., Schalk, G., Wolpaw, J.R., Ojemann, J.G., Moran, D.W.: A brain–computer interface using electrocorticographic signals in humans. *J. Neural Eng.* **1**(2), 63 (2004)
49. Leuthardt, E.C., Miller, K.J., Schalk, G., Rao, R.P., Ojemann, J.G.: Electrocorticography-based brain computer interface—the Seattle experience. *IEEE Trans. Neural Syst. Rehabil. Eng.* **14**(2), 194–198 (2006)
50. Leuthardt, E.C., Gaona, C., Sharma, M., Szrama, N., Roland, J., Freudenberg, Z., Schalk, G.: Using the electrocorticographic speech network to control a brain–computer interface in humans. *J. Neural Eng.* **8**(3), 036004 (2011)
51. Lutzenberger, W., Elbert, T., Rockstroh, B., Birbaumer, N.: Biofeedback produced slow brain potentials and task performance. *Biol. Psychol.* **14**(1), 99–111 (1982)
52. Marcel, S., Millán, J.D.R.: Person authentication using brainwaves (EEG) and maximum a posteriori model adaptation. *IEEE Trans. Pattern Anal. Mach. Intell.* **29**(4), 743–752 (2007)
53. Mason, S.G., Birch, G.E.: A general framework for brain-computer interface design. *IEEE Trans. Neural Syst. Rehabil. Eng.* **11**(1), 70–85 (2003)
54. McFarland, D.J., Miner, L.A., Vaughan, T.M., Wolpaw, J.R.: Mu and beta rhythm topographies during motor imagery and actual movements. *Brain Topogr.* **12**(3), 177–186 (2000)
55. Mozersky, J.: Locked in: a young woman's battle with stroke. Golden Dog Press, Canada, Dundurn (2000)

56. NASA.: NASA develops system to computerize silent ‘subvocal speech’ (March 17 2004). [http://www.nasa.gov/home/hqnews/2004/mar/HQ\\_04093\\_subvocal\\_speech.html](http://www.nasa.gov/home/hqnews/2004/mar/HQ_04093_subvocal_speech.html). Accessed 10 Nov 2013
57. Neuper, C., Wörz, M., Pfurtscheller, G.: ERD/ERS patterns reflecting sensorimotor activation and deactivation. *Prog. Brain Res.* **159**, 211–222 (2006)
58. Neuper, C., Scherer, R., Wriessnegger, S., Pfurtscheller, G.: Motor imagery and action observation: modulation of sensorimotor brain rhythms during mental control of a brain–computer interface. *Clin. Neurophysiol.* **120**(2), 239–247 (2009)
59. Nicolas-Alonso, L.F., Gomez-Gil, J.: Brain computer interfaces—a review. *Sensors* **12**(2), 1211–1279 (2012)
60. Nijboer, F., Sellers, E.W., Mellinger, J., Jordan, M.A., Matuz, T., Furdea, A., Kübler, A.: A P300-based brain–computer interface for people with amyotrophic lateral sclerosis. *Clin. Neurophysiol.* **119**(8), 1909–1916 (2008)
61. Palaniappan, R.: Utilizing gamma band to improve mental task based brain-computer interface design. *IEEE Trans. Neural Syst. Rehabil. Eng.* **14**(3), 299–303 (2006)
62. Palaniappan, R., Mandic, D.P.: EEG based biometric framework for automatic identity verification. *J. VLSI Signal Process. Syst. Signal Image Video Technol.* **49**(2), 243–250 (2007)
63. Palaniappan, R.: Two-stage biometric authentication method using thought activity brain waves. *Int. J. Neural Syst.* **18**(01), 59–66 (2008)
64. Perelmouter, J., Birbaumer, N.: A binary spelling interface with random errors. *IEEE Trans. Rehabil. Eng.* **8**(2), 227–232 (2000)
65. Peterson, N.N., Schroeder, C.E., Arezzo, J.C.: Neural generators of early cortical somatosensory evoked potentials in the awake monkey. *Electroencephalogr. Clin. Neurophysiol./Evoked Potentials Sect.* **96**(3), 248–260 (1995)
66. Pfurtscheller, G., Neuper, C., Flotzinger, D., Pregenzer, M.: EEG-based discrimination between imagination of right and left hand movement. *Electroencephalogr. Clin. Neurophysiol.* **103**(6), 642–651 (1997)
67. Pfurtscheller, G., Neuper, C.: Motor imagery and direct brain-computer communication. *Proc. IEEE* **89**(7), 1123–1134 (2001). doi:[10.1109/5.939829](https://doi.org/10.1109/5.939829)
68. Pfurtscheller, G., Neuper, C., Müller, G.R., Obermaier, B., Krausz, G., Schlögl, A., Schrank, C.: Graz-BCI: state of the art and clinical applications. *IEEE Trans. Neural Syst. Rehabil. Eng. (a publication of the IEEE Eng. Med. Biol. Soc.)* **11**(2), 177–180 (2003)
69. Poulos, M., Rangoussi, M., Alexandris, N., Evangelou, A.: Person identification from the EEG using nonlinear signal classification. *Methods Inf. Med.* **41**(1), 64–75 (2002)
70. Ravi, K.V.R., Palaniappan, R.: Recognising individuals using their brain patterns. In: The IEEE Third International Conference on Information Technology and Applications (ICITA), 4–7 July 2005, Sydney, NSW, vol. 2, pp. 520–523 (2005). doi:[10.1109/ICITA.2005.282](https://doi.org/10.1109/ICITA.2005.282)
71. Ravi, K.V.R., Palaniappan, R.: Leave-one-out authentication of persons using 40 Hz EEG oscillations. In: The IEEE International Conference on Computer as a Tool (EUCON), 21–24 November 2005, Belgrade, Serbia and Montenegro, vol. 2, pp. 1386–1389 (2005)
72. Revett, K., Deravi, F., Sirlantzis, K.: Biosignals for user authentication-towards cognitive biometrics?. In: The IEEE International Conference on Emerging Security Technologies (EST), 6–8 September 2010, Canterbury, United Kingdom, pp. 71–76 (2010)
73. Rockstroh, B., Elbert, T., Lutzenberger, W., Birbaumer, N.: The effects of slow cortical potentials on response speed. *Psychophysiology* **19**(2), 211–217 (1982)
74. Schlosser, R.: Roles of speech output in augmentative and alternative communication: narrative review. *Augment. Altern. Commun.* **19**(1), 5–27 (2003)
75. Sellers, E.W., Donchin, E.: A P300-based brain–computer interface: initial tests by ALS patients. *Clin. Neurophysiol.* **117**(3), 538–548 (2006)
76. Smith, E., Delargy, M.: Locked-in syndrome. *Br. Med. J.* **330**(7488), 406 (2005)
77. Stephen, H.: Read a preview from my brief history (n d). <http://www.hawking.org.uk>. Accessed 10 Nov 2013

78. Suppes, P., Lu, Z.L., Han, B.: Brain wave recognition of words. *Proc. Natl. Acad. Sci. U S A* **94**(26), 14965–14969 (1997)
79. Suppes, P., Han, B.: Brain-wave representation of words by superposition of a few sine waves. *Proc. Natl. Acad. Sci.* **97**(15), 8738–8743 (2000)
80. Sur, S., Sinha, V.K.: Event-related potential: an overview. *Ind. Psychiatr. J.* **18**(1), 70–73 (2009). doi:[10.4103/0972-6748.57865](https://doi.org/10.4103/0972-6748.57865)
81. Vaughan, T.M., McFarland, D.J., Schalk, G., Sarnacki, W.A., Krusienski, D.J., Sellers, E.W., Wolpaw, J.R.: The Wadsworth BCI research and development program: at home with BCI. *IEEE Trans. Neural Syst. Rehabil. Eng.* **14**(2), 229–233 (2006)
82. Wang, Y., Gao, X., Hong, B., Gao, S.: Practical designs of brain–computer interfaces based on the modulation of EEG rhythms. In: Graimann, Bernhard, Pfurtscheller, Gert, Allison, Brendan (eds.) *Brain-Computer Interfaces*, pp. 137–154. Springer, Berlin (2010)
83. Wang, J., Xu, G., Xie, J., Zhang, F., Li, L., Han, C., Sun, J.: Some highlights on EEG-based brain computer interface. *Sciencepaper Online* (2012). [http://www.paper.edu.cn/en\\_releasepaper/content/4488562](http://www.paper.edu.cn/en_releasepaper/content/4488562). Accessed 10 Nov 2013
84. Wester, M., Schultz, T.: Unspoken speech-speech recognition based on electroencephalography. Master's thesis, Universität Karlsruhe (TH), Karlsruhe, Germany (2006)
85. Wolpaw, J.R., McFarland, D.J., Neat, G.W., Forneris, C.A.: An EEG-based brain-computer interface for cursor control. *Electroencephalogr. Clin. Neurophysiol.* **78**(3), 252–259 (1991)
86. Wolpaw, J.R., McFarland, D.J., Vaughan, T.M.: Brain-computer interface research at the Wadsworth Center. *IEEE Trans. Rehabil. Eng.* **8**(2), 222–226 (2000)
87. Wolpaw, J.R., Birbaumer, N., McFarland, D.J., Pfurtscheller, G., Vaughan, T.M.: Brain–computer interfaces for communication and control. *Clin. Neurophysiol.* **113**(6), 767–791 (2002)
88. Wolpaw, J.R., McFarland, D.J.: Control of a two-dimensional movement signal by a noninvasive brain-computer interface in humans. *Proc. Natl. Acad. Sci. U S A* **101**(51), 17849–17854 (2004)

# **Chapter 11**

## **Web-Based Intelligent EEG Signal Authentication and Tamper Detection System for Secure Telemonitoring**

**Aniruddha Mukherjee, Goutami Dey, Monalisa Dey  
and Nilanjan Dey**

**Abstract** In recent times, the augmented influence of globalization in the medical domain is quite noticeable and is very much evident from the modern medical approaches. Exchanging medical information using communication technologies to provide health care services for mutual availability of therapeutic case studies amongst various geographically distant diagnostic centers or hospitals is a very common practice now a days. However, during the exchange of medical data which is of critical importance, unauthorized entities may interfere. These entities may also modify the data which is unacceptable. In this chapter, we propose a novel approach to design a robust online biomedical content authentication and tamper detection system, where a watermark is embedded on the biomedical information to be sent, to protect its integrity and safety. In the current work, the medical data exchanged is an Electroencephalogram Signal (EEG signal), and the watermark that is embedded is the logo of the hospital or Electronic Patient Record (EPR). The proposed process is accomplished by coloring the EEG signal data in the file which can be sent to the authorized user by sending the data file or URL. The receiver decodes the received file and extracts the embedded watermark. The similarity between the original and received watermark claims that the medical data has not been tampered. And thus, this proposed intelligent web based system of binary image watermarking into the EEG data, along with the high level of robustness, imperceptibility and payload that it provides, proposed system can serve as an accurate authentication and tamper detection system.

---

A. Mukherjee · G. Dey · M. Dey (✉)  
JIS College of Engineering, Kalyani, India  
e-mail: monalisa.dey.21@gmail.com

A. Mukherjee  
e-mail: aniruddha.mukherjee1@gmail.com

G. Dey  
e-mail: goutamidey783@gmail.com

N. Dey  
Bengal College of Engineering and Technology, Durgapur, India  
e-mail: neelanjan.dey@gmail.com

**Keywords** Authentication · Tamper detection · Watermarking · Electronic patient record · EEG signal

## 11.1 Introduction

Watermarking is a technology of impressing any form (image or text) onto paper which provides evidence of its authenticity. However in the recent years with the growth of internet, digital media is replacing analog media very fast. Digital media is basically the digital representation of audio, video, text etc. Thus digital watermarking [3] is an extension of the traditional watermarking concept in the current digitized world. It is a process of embedding information (watermark) into 1D or 2D signal, image, video or text as evidence of its ownership as well as to maintain the security and concealment. Unlike the traditional printed watermarks, digital watermarks are designed to be invisible or inaudible. As the digital watermark does not modify the size of the carrier signal, the copy of the digital data generated after embedding a watermark is same as the original. Thus, it not only protects the quality of the host signal but also the integrity and security of the embedded data. Tampering of vulnerable data (image or signal) is the intentional or unintentional manipulation of the data or corrupting the data by executing malicious code in order to make it irretrievable and destructing or transforming the critical information it contains. Digital watermarking is also effective in detecting data tampering and corruption of data (image/signal) and hence is successful in maintaining the authenticity and safety of the image/signal.

Watermarking can be of several types depending on the type of carrier data, viz. image watermarking, video watermarking, audio watermarking and text watermarking.

The three main elements for the watermarking process are the watermark, the encoder which embeds the information to be hidden then verifying the watermarked content received using File Checksum Integrity Verifier (FCIV) and the decoder or the extractor which extracts the hidden information. Commonly embedding is done on digital document (text, audio, video and image) using encoder and authenticating them by incorporating watermark [19] in order to track the credibility of the digital data. After the watermarked data is received by the authorized receiver, the received information is verified using checksum to check if the extracted information is authenticated then the embedded watermark is extracted from watermarked content.

The advancement of technology has influenced the health care industry exponentially. Sophisticated medical technologies are constantly being developed leading to more accurate diagnostic results. Currently sharing of medical data is being done with the help of internet by health care professionals. The biomedical images or signals can be readily transferred or received via computer networks. These images and signals can then be easily transmitted, received, processed and

used by health care centers for mutual study. The conventional diagnosis methods are now getting replaced by the e-diagnosis system where the recipient and the provider of health care do not have to be present in the same physical location.

In the current scenario, biomedical information (images or signals) are exchanged between geographically dissimilar diagnostic centers for mutual study of the biomedical data in order to provide more accurate diagnostic results and appropriate treatments. During the transit of such vulnerable and exposed critical data, unauthorized entities may interfere and transform these images or signals intentionally or unintentionally. This may lead to the loss of decisive data and inaccurate diagnosis, so high confidentiality and authenticity is required to exchange biomedical information through an unsecured open network between various diagnostic centers. A solution to this is watermarking a medical image or signal [4], which will ensure authenticity and integrity of the biomedical information. In the medical field, since the medical images are very crucial in making critical judgments, any distortion of these data or change of quality may lead to erroneous diagnosis results. Thus, before watermarking medical data, several constraints should be taken care of to ensure the data is not hampered in any way. However, little amount of distortion can be overlooked for high level copyright protection and authentication.

The watermarking process of the biomedical images [30, 31] and signal includes embedding and extracting the watermark given that the embedded watermark is imperceptible, that is it should not be visible to the naked human eyes. An effective digital watermark must possess some properties namely, robustness [29], easily recoverable and imperceptible. And in this system, before extraction of the embedded watermark, the checksum verification helps in tracking whether the watermarked EEG signal is tampered or modified outside the system. For checksum verification, File Checksum Integrity Verifier (FCIV) can be calculated using:

1. Message Digests (MD5)
2. SHA-1/SHA-256/SHA-512 cryptographic hash values.
3. The requirements for using the MD5 or SHA-1/SHA-256/SHA-512 cryptographic hash values are:
  4. The claimed identity of the sender can be verified by the receiver.
  5. The content transmitted by the sender cannot be later repudiated by the sender.
  6. The receiver has not possibly concocted the message himself.

FCIV verifies whether the tampering has occurred in the received watermarked EEG signal and which helps the health care provider to track whether the information retrieved is authentic. If the EEG signal is tampered then the health care providers avoid making diagnosis based on that EEG signal and if the EEG signal is not tampered health care providers can continue with the detection of the disease or the diagnosis.

This current study is on medical information exchange between various different diagnostic centers located anywhere across the world for mutual study and to improve the diagnosis result, with high level of authentication and credibility of the medical contents which contains crucial information. In this study the biomedical

medical content is the EEG signal and the watermark (the hidden information) is a binary image containing authenticity and credible information about the health care center which ensures the receiver (physician or health care provider) that the EEG signal information has probity. The watermark is embedded in the EEG signal and this watermarked EEG signal is transferred from one health care organization to other ensuring authenticity and safety of the content it is transferring.

The rest of the paper is described as follows: the study starts briefly by presenting the review works on watermarking of biomedical data in Sect. 11.2. It is followed by a succinct overview of the Electroencephalographic signal in Sect. 11.3. Sections 11.4 and 11.5 provides a detailed and lucid description of the proposed algorithm used for tamper detection and authentication of biomedical information. Section 11.6 provides a comprehensive discussion of the results obtained. In Sect. 11.7, we conclude the paper and discuss directions for future research.

## 11.2 Related Work

A fair amount of study has been done in the field of watermarking of biomedical images and signals, in order to maintain authentication and safety. In this literature review various biomedical images and signals watermarking schemes are reported.

Podilchuk et al. [24] presented a general framework for watermark embedding and extraction along with a review of some of the watermarking algorithms for different media types described in the literature. Lim et al. [19] reported a web based image authentication using invisible fragile watermark. Coatrieux et al. [4] reported the relevance of watermarking in medical imaging. Wakatani [30] presented digital watermarking for ROI medical images by using compressed signature image. Tang et al. [29] proposed a digital image watermarking scheme that combines image feature extraction and image normalization which survived geometric distortion and signal processing attacks. Jiu-ming et al. [16] introduced the wavelet transform and its technical application in digital watermarking in speech signals. The signals of non-encrypted speech before or encrypted speech after were also played and compared by them in their work. Engin et al. [10] proposed a wavelet transformation based watermarking technique for ECG (Electrocardiogram). Nambakhsh et al. [22] presented a novel blind watermarking technique with secret key by embedding ECG signals in medical images. The embedding was using the embedded zero-tree wavelet (EZW) algorithm. Their method was able to utilize about 15 % of the host image for embedding the watermark. Giakoumaki et al. [12] proposed multiple image watermarking applied to health information management. In 2006, Kallel et al. [17] proposed a secure fragile watermarking algorithm for medical image authentication in the DCT Domain. Raul et al. [26] presented data hiding scheme for medical images. Wu et al. [31] reported tamper detection and recovery for medical images using near lossless information hiding technique. Fotopoulos et al. [11] presented medical image authentication and self-correction through an adaptive reversible watermarking technique. Ma et al. [20] reported a

review on the current segmentation algorithms for medical images. Kimoto [18] proposed an advanced method for watermarking digital signals in bit-plane structure. Golpira et al. [13] presented reversible blind watermarking for medical images based on wavelet histogram shifting. Memon et al. [21] proposed multiple watermarking of medical images for content authentication and recovery. Oueslati et al. [23] presented an approach for maximizing the strength of a watermark using the concept of fuzzy logic. Saraswathi [27] discussed a method to perform speech authentication using watermarking technique. The watermark was embedded in the low intensity points detected in the speech signal. Rather sending the speech signal the extracted features were sent to the receiver for authentication. The proposal was of a blind watermarking technique in which the host signal was not required for watermark extraction. Authentication was done by detecting the errors in the signal based on their extracted features. Poonkuntran et al. [25] proposed a messy watermarking technique for the authentication of any medical image. Aggarwal et al. [1] presented role of segmentation in medical imaging with comparative study. Chang-hui et al. [3] published their work which dealt with the digital watermarking technology on three different processing stages for enhancing the robustness of digital watermarking based on the argument of invisibility. The first stage was pre-processing the watermark signal. The second stage was watermark embedding strength degree. And the third stage was the watermark embedding and extraction. The embedding and extraction of the watermark signal was done through the trained neural network. Ibaida et al. [15] proposed a technique of watermarking the ECG signals with patient biomedical information in order to confirm patient/ECG linkage integrity. After performing several tests they found out that a marginal amount of signal distortion will not affect the overall quality of the ECG signal. He et al. [14] proposed a self-synchronized watermark technology to protect the electrocardiogram (ECG) signal. Their study confirmed that the use of wavelet-based quantization watermarking on ECG signal is adequate for patient protection. Soliman et al. [28] proposed a secure and adaptive medical image authentication scheme using swarm intelligence. Dey et al. [5] proposed a DWT-DCT-SVD based blind watermarking technique of gray image in electrooculogram signal. Dey et al. [6] proposed a Lifting Wavelet Transformation based technique of binary watermark embedding within the Photoplethysmographic (PPG) signal as well as the process of extracting watermark from the PPG signal. Dey et al. [5] proposed a DWT-DCT-SVD based intravascular ultrasound video watermarking technique. Dey et al. [7] analyzed the photoplethysmographic signals which were modified by a reversible watermarking technique using prediction-error in wireless telecardiology. Dey et al. [8], [9] proposed an edge based blind watermarking technique of medical images without devalorizing diagnostic parameters. In their work, the watermark was added in the boundaries between the Region of Interests and the Region of Non-Interest in the medical image.

### 11.3 Electroencephalographic Signal (EEG)

Our brain is composed of billions of neurons which talk (exchange information) to each other using electrical signals. This results in the generation of a huge amount electrical activity in the brain. EEG (electroencephalogram) is a tool which tracks this electrical activity of the brain over a short period of time. It measures and records the brain wave pattern and detects the brain activity involved in the various types of cognitive functions. The term “electro” denotes the electrical signals that are exchanged between the billions of nerve cells present in the brain, for communicating with each other, “encephalo” means head and “gram” is the printed record that is obtained after performing EEG.

EEG tests are done by placing electrodes on the scalp. Electrodes are nothing but electrical conductors and hence are used to detect electricity. The test is carried on for about 30–40 min. During this time, no electricity is put into or taken out of the patient. The electrical impulses along the brain are then observed while the patient is sleeping or awake or when the patient is asked to take deep breaths etc. Next the detected electrical impulses sent to a machine called an electroencephalograph, which records the signals for further studies [2].

EEG records patterns of electrical activities in the brain as waveforms of varying amplitude and frequency measured in voltage. The basic brain waves that are recorded and used for are the among alpha, beta, theta, and delta rhythms.

- Alpha waves generally occur in the state of relaxation, when your eyes are closed but you are aware of the surroundings. These waves emit at a frequency of 8–12 cycles per second.
- Beta waves are emitted occur at a frequency of 13–30 cycles per second. They occur when we are alert, agitated or anxious, and are also linked with the usage of sedatives or tranquilizer.
- Theta waves most commonly occur during a near sleep state when the individual is extremely drowsy. These waves are emitted at a frequency of 4–7 cycles per second.
- Delta waves emit at a frequency of 0.1–4 cycles per second. They generally occur in the state of deep sleep.

One of the most common diagnostic applications of EEG is to monitor epileptic disorders. However, it may happen that a patient having a tendency of seizures may have a normal EEG at a particular time. In such cases, EEG is either repeated more than once, or is done for a longer period. It is also used to diagnose other medical conditions like tumors, brain diseases, head injuries, hemorrhage etc. EEG results are studied to detect sleep disorders like insomnia, track the brain activities of an individual in a coma, monitor the brain during any brain surgery etc. It also forms as a surety test for brain death.

## 11.4 Proposed Method

Ideally a secured sharing of information between the health care centers requires some basic security services like privacy, authentication, integrity and nonrepudiation. In this study, basic objective is to detect tampering and ensure authentication of the biomedical information. There might be several types of attacks which compromise with the security of information, the attacks such as:

1. Interruption during the transfer of information, transformation.
2. Alteration attacks in which attacker can interfere and can send a altered information which causes tampering of the information.
3. Bugging, attackers can listen to the information and use the information in their own interest.
4. Imitating.

In the proposed study, the watermark (logo of a hospital, health care center or patient's historical data) is considered as a chunk and is taken as a byte array. Values in the byte array can vary from  $-128$  to  $127$  ( $-2^7$  to  $(2^7 - 1)$ ). The number is represented as a signed binary number by reserving 8 bits for magnitude and appending one more bit for sign representation. So total there will be 9 bits which will represent the signed binary number. Byte is an 8 bit integer data type and here 9 bits are used to represent each signed number, so by widening casting or automatic casting in Java (implementation of the proposed study is done using Java), the byte data type is widened to int data type implicitly. Hence the conversion from byte array to int array is done automatically.

For example, the given Fig. 11.1 is a byte array,

Conventionally, representing a signed numbers can be done using any one of the three possible ways which include:

1. Signed magnitude representation.
2. Signed 1's complement representation.
3. Signed 2's complement representation

Example: representation of  $-9$  with 8 bits

1. Using signed magnitude representation (Fig. 11.2)
2. Using signed 1's complement representation (Fig. 11.3)
3. Using signed 2's complement representation (Fig. 11.4)

Conventionally the most significant bit position is reserved for sign bit and remaining bits are used to show the magnitude. And when the binary number is positive, the sign bit is '0' and when the number is negative the sign bit is '1'.

120	50	30	-110	.....	-60	80
-----	----	----	------	-------	-----	----

**Fig. 11.1** Byte array

1	0	0	0	1	0	0	1
---	---	---	---	---	---	---	---

**Fig. 11.2** Representation of  $-9$  using signed magnitude

1	1	1	1	0	1	1	0
---	---	---	---	---	---	---	---

**Fig. 11.3** Representation of  $-9$  using signed 1's complement

1	1	1	1	0	1	1	1
---	---	---	---	---	---	---	---

**Fig. 11.4** Representation of  $-9$  using signed 2's complement

1	0	1	1	1	1	0	0	0
---	---	---	---	---	---	---	---	---

**Fig. 11.5** 9 bit binary equivalent of 120

The representation of signed number using signed magnitude representation and 1's complement representation cannot be done in this study as it takes into account  $+0$  and  $-0$  whereas in 2's complement representation it includes only one type of zero that is  $+0$ . Still in this study signed number's representation is not done in any of these three ways.

In this study, the signed numbers in the int array whose range varies from  $-128$  to  $127$  is represented using a different technique in which all of the 8 bits are used to represent the magnitude of the number simply by finding its binary equivalent. And appending one more bit that is the 9th bit in the MSB place in order to represent the sign. For negative value the MSB is 0 and for positive value the MSB is 1, so total 9 bits are required to represent the signed value.

For example, binary equivalent of 120 is shown in Fig. 11.5.

Main reason of representing the signed values in this way instead of representing by 2's complement is because representing the numbers in 2's complement manner would increase the complexity as it would include

1. First checking the MSB of the 8 bit binary representation if it is 1 or 0. If it is 1 then the value is negative otherwise if the MSB is 0 then the value is positive.
2. If the MSB is 1 then 2's complementing the binary number to find the magnitude of the binary number keeping in mind that the number is negative.

So in order to remove this complexity and ambiguity, representation is done with 9 bits. And moreover as the color model used in this study is RGB color model so in order to divide R (red), G (green) and B (blue) in equal number of bits it was

R	0	0	1
G	1	1	1
B	0	0	0

**Fig. 11.6** 3 bits binary representation of R, G and B**Fig. 11.7** Example decimal equivalent of red (R), green (G) and blue (B)

necessary to represent the values in the byte array using 9 bits, so that R, G and B can be represented using 3 bits each.

The value (only magnitude) in each cell has to be converted into 8 bits binary equivalent and the sign of each value is represented by the 9th bit which is appended in the most significant bit (MSB) position. Then the 9 bits are equally divided into 3 parts R which represents red, G which represents green and B which represents blue i.e. 3 bits for R, 3 bits for G and 3 bits for B. 3 bit binary representation of R, G and B is shown in Fig. 11.6.

Hiding of image (watermark) can be done in two possible ways:

1. Text color
2. Text background color

In this study we have colored the text. Amount of colors red (R), green (G) and blue (B) depends on the values stored in the int array which in turn depends on the watermark (binary image or logo) which is to be embedded in the EEG signal data. By the combination of amount of three colors red (R), green (G) and blue (B), the resultant color will be colored in each EEG signal values (Fig. 11.7). Hence this colored EEG signal data is what is called as watermarked EEG signal.

EEG signal data are colored with different colors i.e. watermark is embedded in the signal data. And this watermarked EEG signal is transferred from one health care center to the other through unsecured open network which may cause tampering of EEG signal due to the transformation and forgery attacks by the attackers or corrupting the data by executing malicious code which may make the data irretrievable and may cause the loss of decisive data. As a result there will be loss of decisive EEG signal data. After reaching the receiver (health care center), the watermarked EEG signal is verified using FCIV (File Checksum Integrity Verifier) which checks whether the watermarked EEG signal is tampered or corrupted. Depending on the verification, the embedded watermark is extracted, then the

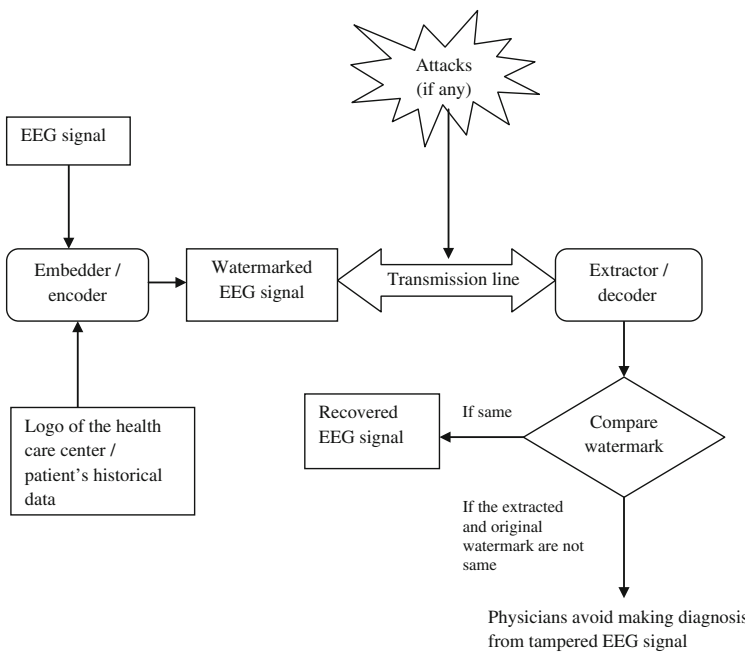


**Fig. 11.8** The process of embedding and extracting the watermark to and from the EEG signal

physicians make decisions based on the EEG signal retrieved. If the FCIV shows the file is tampered then physician does not do the diagnosis and further treatments based on the tampered EEG signal as it may lead to erroneous diagnosis and may cause fatal. The entire process is shown in Fig. 11.8.

## 11.5 Explanation of the Proposed Method

Figure 11.9 depicts an example of transfer of EEG signals between physicians, diagnostic centers and a hospital to improve the diagnostic results which helps in proper and accurate treatment of the patient. Logo or the image which is to be watermarked is taken as a byte array in which each value stored in the byte array is converted to 9 bits binary equivalent due to which conversion from byte array to int array takes place implicitly, and then these 9 bits in turn is divided into three colors R, G and B.

The colour model used in this study is RGB i.e. combining red, green and blue colour, whose amounts depends on the decimal equivalent of the 3 bits retrieved from R array, G array and B array, the resultant of these three colours are then coloured in each of the EEG signal value. For example, if decimal equivalent of R, G and B is 0 for three of them then it gives black colour (shown in Fig. 11.7).

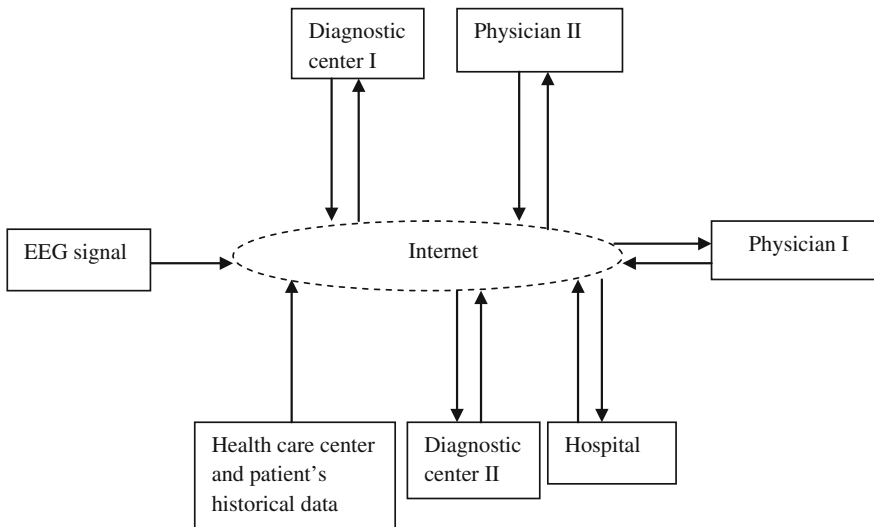


**Fig. 11.9** Transfer of medical image between physicians, diagnostic centers and hospital for second opinion

In our study if the 9 bit binary is 100110011 then R = 100, G = 110 and B = 011 and possible no. of colour codes from binary values are {111,110,100,011, 001,010,101,000} which is equal to 8. So maximum possible combination (in RGB) = R{Colour codes } × G{Colour codes } × B{Colour codes } =  $2^9 = 512$ . The EEG signal data can be coloured by 512 different colours. And the range of R, G, and B itself is 0–255 and the combination of Red, Green and Blue values from 0 to 255 gives a total of more than 16 million different colours ( $256 \times 256 \times 256$ ) and most modern monitors are capable of displaying at least 16,384 different colors.

Similarly with different combinations of red, green and blue, distinct colours will be formed which will be then coloured in each EEG data. As a result all the data of the EEG signal will get coloured hence the watermark is embedded in the EEG signal data. Watermarked signal after reaching the authorized user, the watermark is extracted from the watermarked EEG signal after checksum verification. If the extracted watermark is similar to the original watermark then the physician will start the diagnosis process using the recovered EEG signal acquainted of the fact that the EEG signal is not tampered and is credible and believable. If the extracted watermark is different from the original watermark then the physician will avoid making any diagnosis or further treatments based on that EEG signal data retrieved as the file is tampered or corrupted by the attackers and the decisive information in the signal retrieved is already lost. In this way this scheme is helping to detect the tampering of EEG signal.

## 11.6 Results and Discussion

In the following section, Figs. 11.10, 11.11, 11.12, 11.13, 11.14, 11.15, 11.16, 11.17, 11.18, 11.19 depicts the entire proposed approach.

The Fig. 11.10 depicts the Home Screen where the sender can input the EEG signal data file by selecting “As a file” the sender can input the data as a file. While

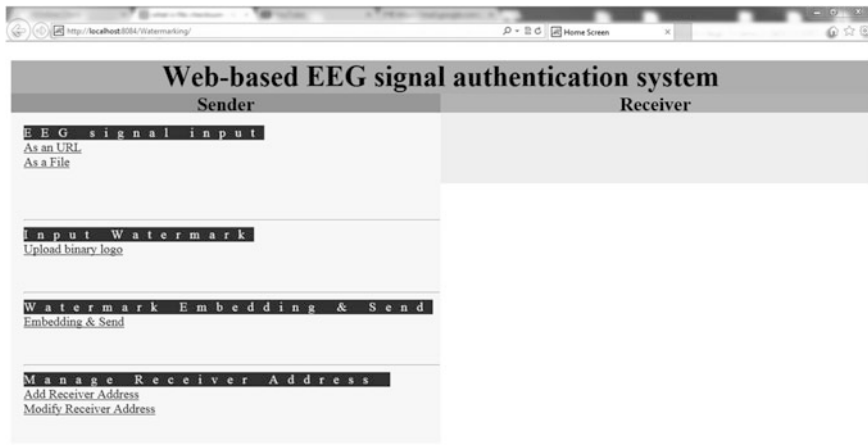


**Fig. 11.10** Home screen

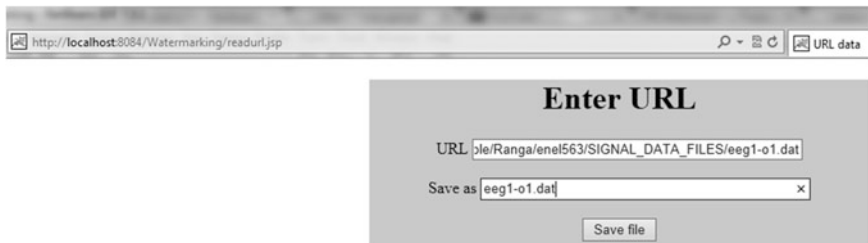


**Fig. 11.11** Input data (as an URL)



**Fig. 11.12** Input binary logo as a watermark

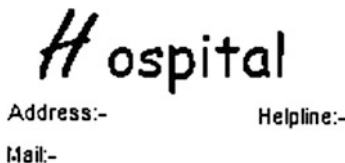


**Fig. 11.13** Logo of the hospital (Watermark)

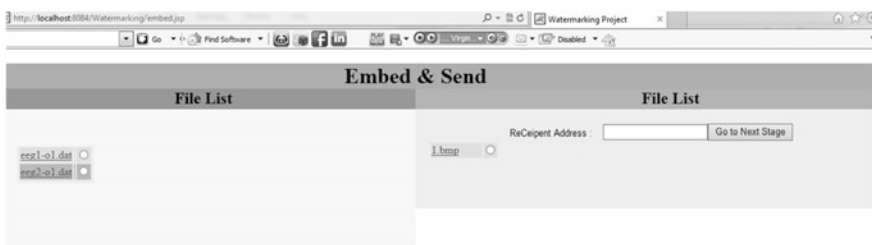


**Fig. 11.14** Watermark Embedding and send into the recipient end

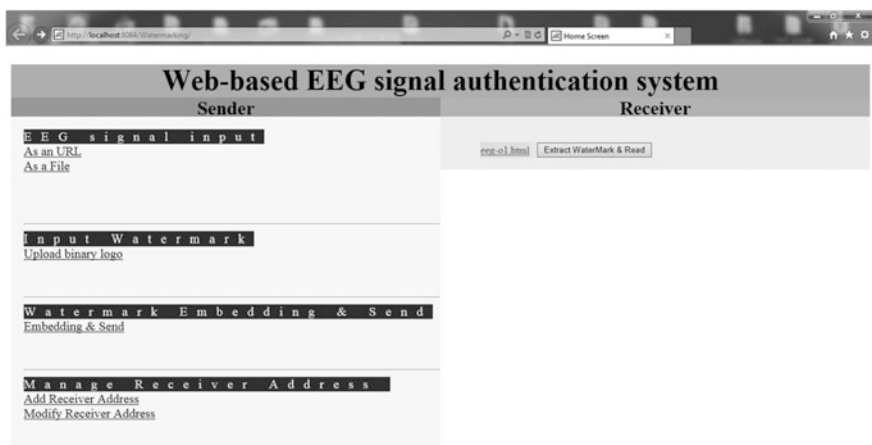


**Fig. 11.15** Received watermarked EEG signal

uploading the file, the file can be browsed from the computer and the data file can be chosen for uploading. The file is uploaded. Sender can input the EEG signal data by adding the URL by selecting “As an URL” directly.

Sender can input the watermark that is binary logo of the health care center or diagnostic center by selecting “Upload Binary logo”. Then the receiver’s address is added by selecting “Add Receiver Address”. The sender can also modify the receiver’s address by selecting “Modify Receiver Address”. Then after inputting the

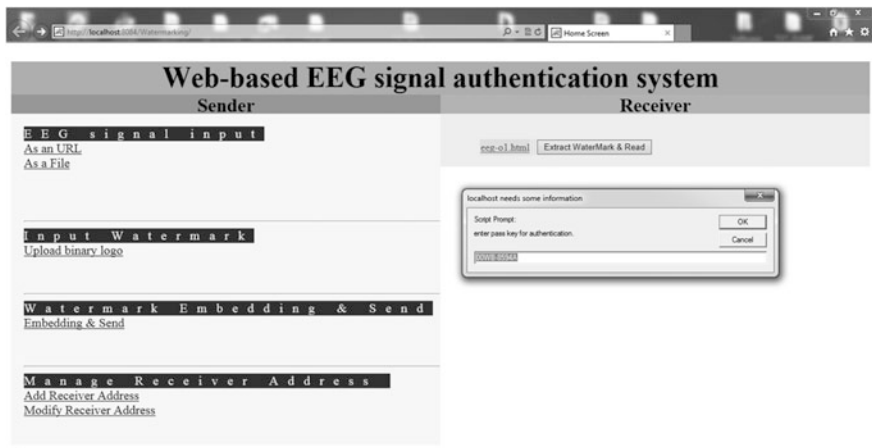


**Fig. 11.16** Extracting EEG signal

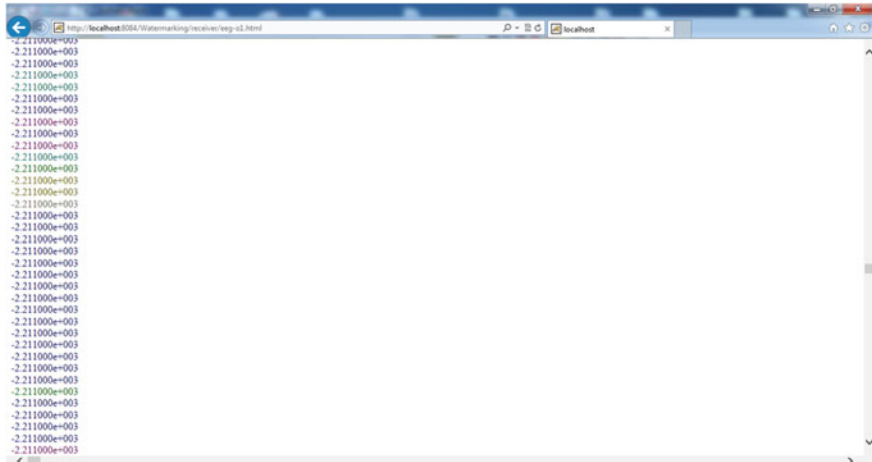


**Fig. 11.17** Watermark embedded EEG signal

EEG signal data, watermark and the receiver's address, the watermark will get embedded and sent when the sender selects “Embedding and Send”. So the watermarked EEG signal data file is sent to other health care center or diagnostic center for improved diagnosis and mutual study of the EEG signal which in turn will lead to better treatment.

Figure 11.11 depicts how the sender can input the URL instead of data file. This URL constitutes a reference to the EEG signal data which is to be watermarked.

**Fig. 11.18** Modified source file

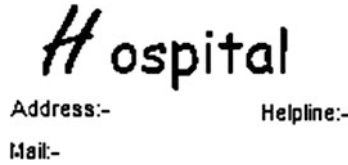


**Fig. 11.19** Logo of the hospital extracted

Figure 11.12 shows the how the sender can upload the binary logo by browsing the files in the computer selecting “Browse...” and selecting the required file. Then selecting “Upload”. The watermark is uploaded.

Figure 11.13 depicts how a typical watermark will look like. This watermark is embedded in the EEG signal data and as a result of embedding, watermarked EEG signal data will have each data coloured with different colours.

Figure 11.14 shows how the watermark is embedded in the EEG signal data. And then the EEG signal data is sent to the recipient's end.

Figure 11.15 depicts the received watermarked signal at recipient's end. Then the checksum verification of the received watermarked EEG signal is done using FCIV to track whether the received EEG signal is tampered or corrupted.

Figure 11.16 depicts extraction of the EEG signal. Depending on the result of FCIV which will check if the file is tampered or not. If the file is not tampered then the EEG signal is extracted for diagnosis.

Figure 11.17 show how the watermarked EEG signal look like. Each data in the EEG signal is coloured using RGB colour model.

Figure 11.18 shows the modified source file

Figure 11.19 shows the watermark extracted at the receiver's end. This watermark is the binary logo of the hospital or diagnostic center or any other health care center which ensures the receiver that the EEG signal received is reliable and can be used for diagnosis.

In this current study, the image is taken as a chunk and is considered as a byte array then for representing each value in each cell of the byte array, 9 bits are required so the conversion from byte array to int array takes place implicitly in java by implicit casting then 9 bits are divided equally into R (red), G (green) and B (blue) each of which contains 3 bits. Depending upon the decimal equivalent of red, green and blue colour, the resultant colour is then coloured in EEG data. Similarly all the data in the EEG signal is coloured hence watermark is embedded in the EEG signal data. Now after reaching the authorized user, the FCIV checks whether the EEG signal is tampered or corrupted then depending on the verification, watermark is then extracted. And the diagnosis is done after identifying whether there is any tamper in the EEG signal or not and whether the EEG signal is authenticated and credible. Thus this approach ensures authenticity, credibility of the image or signal and confidentiality of the biomedical image or signal.

The current proposed system deals with EEG signals, in future it can be further extended to be more generalised for other signals like Electrocardiography (ECG), Electromyography (EMG), Magneto-encephalography (MEG), Electronystagmography (ENG), etc. The size of the image or the logo(watermark) is a constraint as if the size of the image is large then the size of the byte array will be large as a result there will be more number of colours than the number of data in the EEG signal data. So this will lead to incomplete watermarking. In this current study, testing is done with only binary watermark (which is black and white watermark), so the implementation can be done in future using coloured watermark.

## 11.7 Conclusion

Various schemes for watermarking biomedical images or signals have been already proposed. The current proposed system is a fragile watermarking system in which the host data (biomedical image or signal) can be modified by the attackers. It will ensure authenticity. When the watermarked EEG signal manipulates it will lead to the distortion which will be tracked by the File Checksum Integrity Verifier (FCIV) which in turn will help the authorized user (which can be a health care organisation or a physician) to detect whether the EEG signal is tampered or not. Depending on the verification if the extracted watermark and the original watermark are different then the EEG signals are considered to be tampered, whereas if the extracted watermark and the original watermark are same then the EEG signal is not tampered or corrupted and hence health care providers can continue with the diagnosis based on the EEG signal which is recovered. So it not only serves for high level authentication system but also for tamper detection.

## References

1. Aggarwal, P., Vig, R., Bhadoria, S., Dethé, C.G.: Role of segmentation in medical imaging: a comparative study. *Int. J. Comput. Appl.* **29**(1), 54–61 (2011)
2. Azar, A.T., Balas, V.E., Olariu, T.: Classification of EEG-based brain-computer interfaces. In: Advanced Intelligent Computational Technologies and Decision Support Systems, Studies in Computational Intelligence, vol. 486, pp. 97–106. Springer, Switzerland (2014)
3. Chang-Hui, Y., Wan-Li, F., Hong, Z.: The digital watermarking technology based on neural networks. In: IEEE 2nd International Conference on Computing, Control and Industrial Engineering (CCIE), vol. 1, pp. 5–8. IEEE (2011, Aug)
4. Coatrieux, G., Maitre, H., Sankur, B., Rolland, Y., Collorec, R.: Relevance of watermarking in medical imaging. In: IEEE EMBS International Conference on Information Technology Applications in Biomedicine, pp. 250–255. IEEE (2000)
5. Dey, N., Biswas, D., Roy, A.B., Das, A., Chaudhuri, S.S.: DWT-DCT-SVD based blind watermarking technique of gray image in electrooculogram signal. In: 12th International Conference on Intelligent Systems Design and Applications (ISDA), pp. 680–685. IEEE (2012, Nov)
6. Dey, N., Biswas, S., Das, P., Das, A., Chaudhuri, S.S.: Lifting wavelet transformation based blind watermarking technique of photoplethysmographic signals in wireless telecardiology. In: World Congress on Information and Communication Technologies (WICT), pp. 230–235. IEEE (2012, Oct)
7. Dey, N., Biswas, S., Roy, A.B., Das, A., Chowdhuri, S.S.: Analysis of photoplethysmographic signals modified by reversible watermarking technique using prediction-error in wireless telecardiology. In: 47th Annual National Convention of the Computer Society of India organized by The Kolkata Chapter (2013)
8. Dey, N., Das, P., Roy, A.B., Das, A., Chaudhuri, S.S.: DWT-DCT-SVD based intravascular ultrasound video watermarking. In: World Congress on Information and Communication Technologies (WICT), pp. 224–229. IEEE (2012, Oct)
9. Dey, N., Maji, P., Das, P., Biswas, S., Das, A., Chaudhuri, S.S.: An edge based blind watermarking technique of medical images without devalorizing diagnostic parameters. In: International Conference on Advances in Technology and Engineering (ICATE), pp. 1–5. IEEE (2013, Jan)
10. Engin, M., Çidam, O., Engin, E.Z.: Wavelet transformation based watermarking technique for human electrocardiogram (ECG). *J. Med. Syst.* **29**(6), 589–594 (2005)
11. Fotopoulos, V., Stavrinou, M.L., Skodras, A.N.: Medical image authentication and self-correction through an adaptive reversible watermarking technique. In: 8th International Conference on BioInformatics and BioEngineering, (BIBE), pp. 1–5. IEEE (2008, Oct)
12. Giakoumaki, A., Pavlopoulos, S., Koutsouris, D.: Multiple image watermarking applied to health information management. *IEEE Trans. Inf. Technol. Biomed.* **10**(4), pp. 722–732 (2006)
13. Golpira, H., Danyali, H.: Reversible blind watermarking for medical images based on wavelet histogram shifting. In: IEEE International Symposium on Signal Processing and Information Technology (ISSPIT), pp. 31–36. IEEE (2009, Dec)
14. He, X., Tseng, K.K., Huang, H.N., Chen, S.T., Tu, S.Y., Zeng, F., Pan, J.S.: Wavelet-based quantization watermarking for ECG signals. In: International Conference on Computing, Measurement, Control and Sensor Network (CMCSN), pp. 233–236. IEEE (2012, July)
15. Ibaida, A., Khalil, I., van Schyndel, R.: A low complexity high capacity ECG signal watermark for wearable sensor-net health monitoring system. In: Computing in Cardiology, pp. 393–396. IEEE (2011, Sept)
16. Jiu-ming, L.V., Jing-Qing, L., Xue-hua, Y.: Digital watermark technique based on speech signal. In: 3rd International Conference on Computational Electromagnetics and Its Applications, (ICCEA), pp. 541–544. IEEE (2004, Nov)

17. Kallel, I.F., Kallel, M., Bouhlel, M.S.: A secure fragile watermarking algorithm for medical image authentication in the DCT domain. In: Information and Communication Technologies, (ICTTA), vol. 1, pp. 2024–2029. IEEE (2006, April)
18. Kimoto, T.: An advanced method for watermarking digital signals in bit-plane structure. In International Conference on Communications (ICC), pp. 1–5. IEEE (2009, June)
19. Lim, Y., Xu, C., Feng, D.D.: Web based image authentication using invisible fragile watermark. In: Proceedings of the Pan-Sydney area workshop on Visual information processing, vol. 11, pp. 31–34 (2001, May)
20. Ma, Z., Tavares, J.M.R., Jorge, R.N., Mascarenhas, T.: A review of algorithms for medical image segmentation and their applications to the female pelvic cavity. *Comput. Methods Biomed. Biomed. Eng.* **13**(2), 235–246 (2010)
21. Memon, N.A., Gilani, S.A.M., Qayoom, S.: Multiple watermarking of medical images for content authentication and recovery. In: 13th International Multitopic Conference (INMIC), pp. 1–6. IEEE (2009, Dec)
22. Nambakhsh, M.S., Ahmadian, A., Ghavami, M., Dilmaghani, R.S., Karimi-Fard, S.: A novel blind watermarking of ECG signals on medical images using EZW algorithm. In: 28th Annual International Conference Engineering in Medicine and Biology Society (EMBS), pp. 3274–3277. IEEE (2006, August)
23. Oueslati, S., Cherif, A., Solaiman, B.: Maximizing strength of digital watermarks using fuzzy logic. *Signal Image Process. Int. J. (SIPIJ)* **1**(2), 112–124 (2010)
24. Podilchuk, C.I., et al.: Digital watermarking: algorithms and applications. *Signal Process. Magazine, IEEE* **18**(4), 33–46 (2001)
25. Poonkuntran, S., Rajesh, R.S.: A messy watermarking for medical image authentication. In: International Conference on Communications and Signal Processing (ICCP), pp. 418–422. IEEE (2011, Feb)
26. Raul, R.C., Claudia, F.U., Trinidad-Bias, G.D.J.: Data hiding scheme for medical images. In: 17th International Conference on Electronics, Communications and Computers, (CONIELECOMP), pp. 32–32. IEEE (2007, Feb)
27. Saraswathi, S.: Speech authentication based on audio watermarking. *Int. J. Inf. Technol.* **16**(1), 34–43 (2010)
28. Soliman, M. M., Hassanien, A.E., Ghali, N.I., Onsi, H.M.: An adaptive watermarking approach for medical imaging using swarm intelligent. *Int. J. Smart Home* **6**(1), 37–50 (2012)
29. Tang, C.W., Hang, H.M.: A feature-based robust digital image watermarking scheme. *IEEE Trans. Signal Process.* **51**(4), 950–959 (2003)
30. Wakatani, A.: Digital watermarking for ROI medical images by using compressed signature image. In: Proceedings of the 35th Annual Hawaii International Conference on System Sciences, (HICSS), 2002, pp. 2043–2048. IEEE (2002)
31. Wu, J.H., Chang, R.F., Chen, C.J., Wang, C.L., Kuo, T.H., Moon, W.K., Chen, D.R.: Tamper detection and recovery for medical images using near-lossless information hiding technique. *J. Digital Imag.* **21**(1), 59–76 (2008)

# **Chapter 12**

## **Competing and Collaborating Brains: Multi-brain Computer Interfacing**

**Anton Nijholt**

**Abstract** In this chapter we survey the possibilities of brain-computer interface applications that assume two or more users, where at least one of the users' brain activity is used as input to the application. Such 'applications' were already explored by artists who introduced artistic EEG applications in the early 'seventies' of the previous century. These early explorations were not yet supported by advanced signal process methods, simply because there was no computing support possible, and interest in artistic applications faded until it reappeared in more recent years. Research in neuroscience, signal processing, machine learning and applications in medical, assistive BCIs prevailed. It was supported by computer science that provided real-time and off-line processing to analyze and store large amounts of streaming or collected data. With the possibility to access cheap shared and distributed storage and processing power, as it became available in the last decade of the previous century and the first decade of this century, different kinds of BCI applications, following a general interest in digital games, interactive entertainment and social media, became visible. These are domains where experience, fun and emotions are more important than efficiency, robustness and control. BCI provides user and application with a new modality that can be manipulated and interpreted, in addition to other input modalities. This has been explored, but mostly from the point of view of a single user interacting with an application. In this chapter we look at BCI applications where more than one user is involved. Games are among the possible applications and there are already simple games where gamers compete or collaborate using brain signal information from one or more players. We consider extensions of current applications by looking at different types of multi-user games, including massively multi-player online role-playing games. We mention research—distinguishing between active and passive BCI—on multi-participant BCI in non-game contexts that provides us with information about the possibilities of collaborative and competitive multi-brain games and that allows us to develop a vision on such games. The results of the literature study are collected in a table

---

A. Nijholt (✉)

Human Media Interaction, University of Twente, PO Box 217, 7500 AE Enschede,  
The Netherlands

e-mail: a.nijholt@utwente.nl

where we distinguish between the various forms of interaction between players (participants) in collaborative and competitive games and team activities.

**Keywords** Brain-computer interfaces · EEG · Multi-brain games · Multi-player games · Social games · Collaborative decision making · Videogames

## 12.1 Introduction

Pervasive and ubiquitous computing requires multi-user interfaces for environments and devices that offer professional, recreational and social applications. These interfaces are also multimodal, and mouse, keyboard or joystick are joined by more natural input modalities including touch and gestures. Moreover, rather than providing these environments and devices with explicit input, their sensors also know how to monitor us and support us in our activities in pro-active ways. Multi-user applications, where sensor-equipped environments monitor users in order to support them in their activities or to provide useful information for the owners of the environments are being introduced. Obvious examples are home environments, office and meeting environments, but also multitouch tables and distributed game and entertainment environments that have multiple users. We may think of children using tangibles playing together in a sensor-equipped room or public space, but also of physically co-located players competing or collaborating in a videogame, or multi-user online games with physically distributed players. Apart from traditional input devices, there can be simultaneous input from multiple users using gestures, facial expressions, bodily movements and various kinds of natural or user-manipulated physiological input, including input provided by brain signals.

In previous years we have seen a growing interest in brain-computer interfacing (BCI) in the human-computer interaction (HCI) community. Before that, BCI was researched with the aim to help disabled persons and provide them, among other things, with a hands-free ‘communication channel’ to type messages, to control prostheses, or to navigate a wheelchair [2]. Our research, instead, has focused on BCI for ‘healthy’ users, in particular on its use for games [26, 30]. There are good reasons to do so. In games and entertainment applications we are not limited by thoughts and concerns that relate to patients and disabled persons. We can use our fantasy and can allow situations and events in non-real-life situations, happening in virtual worlds and videogames. We can allow cooperation and competition with multiple and distributed users and we can allow interaction modalities and effects that are unusual but nevertheless can be believable, given the context of the game. Gamers don’t behave as disabled people in need of support. They have different motivations and expectations. That introduces problems and new challenges. Game designers have to design for challenges or otherwise to make use of the existing challenges in a meaningful manner, rather than to avoid them.

In 2012 a roadmap for BCI research was published (eds Allison et al. [1]). The roadmap was initiated by the FP7 research program of the European Union. The roadmap stayed close to traditional BCI research. It hardly took into account new research opportunities coming from embedding BCI research in HCI research, in particular multimodal interaction [10, 27] and artificial intelligence research. The problems (or challenges) that were identified in the roadmap (reliability, proficiency, bandwidth, convenience, support, training, utility, image, standards and infrastructure) do also rise when we look at BCI for games, entertainment and artistic applications. However, they can be dealt with in a different way. A game is about challenges and an interactive art installation may be provocative and surprising rather than that it acts according to our expectations; it may allow teasing, frustrating [34] and deceiving. Hence, rather than being effective in a traditional sense, such applications are about manipulating experiences (van de Laar [17], and satisfying psychological needs (for example, showing competence in dealing with challenges and socializing) [11], and not necessarily about efficiency and convenience. Hence, such applications require knowledge about the affective state of the user [24]. Efforts to develop a new, more long-term, roadmap for BCI research are reported in [4].

A bottleneck that prevents wide-spread use of BCI is the set-up encumbrance. A standard configuration requires an EEG cap with several electrodes, it has to be positioned on the head of the user, gel is required between scalp and electrodes to get good signals, and only after ten or more minutes of preparation time the user is physically connected to the BCI device. Presently so-called ‘dry’ electrodes that don’t require conductive gel and wireless connections have been introduced, reducing set-up time. Attractive headsets are now becoming available from BCI game companies. A second bottleneck is reliability. People can be trained to use a BCI, but not everybody can perform in a satisfactory way. BCI signals are subject-dependent and even for one subject there is variability depending on mood, emotions and fatigue. For certain applications repeated trials are needed in order to be able to make a decision about a mental state or to be able to map detected brain activity to appropriate control or communication commands. However, also for this bottleneck there are positive research developments such as progress in signal analysis, artifact removal methods, and machine learning. Moreover, for some applications, as we will discuss in this chapter, rather than recognizing brain activity of one user and deciding how to use it, we can have recognition of brain activity of many collaborating users involved in the same task. Maybe this multi-brain computer interfacing can lead to more reliable decisions and certainly it can lead to new and interesting applications of BCI.

Both for traditional BCI and multi-brain BCI it is useful to distinguish between active and passive BCI. Active BCI requires real-time or near real-time BCI. There is voluntary control of brain activity, meant to control an application. In a passive BCI situation the brain activity of a user is monitored. The user is not necessarily aware of this monitoring and does not attempt to steer it. This information can be used to adapt the environment, but not necessarily in real-time.

### ***12.1.1 Organization of this Chapter***

Taking into account these observations, in this chapter we discuss and survey current applications and ideas on multi-brain-computer interfaces, with the aim of using these ideas in future multi-brain BCI games and other future applications. We start in Sect. 12.2 by looking at early multi-brain applications, in particular ‘applications’ and ideas pursued by artists. They were among the first designers of BCI real-time interaction technology and their applications required the measurement of brain activity of interacting participants or the collecting of brain activity of audience members in order to have the (multimedia) environment and audience members react and interact. Other non-artistic applications involving EEG recordings of several users at the same time followed for example to measure audience appreciation of events or products or to measure and analyze involvement and performance in collective tasks, either for real-time or off-line purposes. Section 12.3 is about two important characteristics of games: competition and collaboration. We look at existing multi-brain BCI applications with these two characteristics in mind. Section 12.4 provides an inventory of multi-brain BCI games from the point of view of numbers of participating collaborating and competing (teams) of gamers. In Sect. 12.5 we present a table in which we summarize characteristics of existing multi-brain applications with the observations of Sect. 12.4 (competition and collaboration) and 12.5 (users and teams) in mind. Finally, in Sects. 12.6 and 12.7, we have a discussion, have some observations on future applications and present some conclusions.

## **12.2 Brain Activity Measurements from Multiple Brains**

Clearly, gamers use their brains to compete and to collaborate, hence, whenever more than one player is involved in a game we can talk about multi-brain games. But, of course, without explicit measuring of their brain activity it is better to speak of multi-user or multi-party games. Before looking more closely to what we call multi-brain games it is useful to have some remarks about multi-brain BCI applications in general. That is, applications where BCI is used in the context of information extracted from multiple brains. In Sect. 12.2.1 we review early artistic multi-brain BCI applications. Section 12.2.2 has some observations on useful, useful rather than playful, multi-brain BCI applications. Both sections introduce ideas and developments that help to introduce multi-brain BCI games in forthcoming sections of this chapter.

### ***12.2.1 Early Multi-brain BCI Applications***

Interestingly, artistic BCI applications date older than assistive BCIs. Consciously producing alpha states and monitoring them by EEGs was first described in

Kamiya's influential paper in *Psychology Today* [15]. Five years later Jacques Vidal, in another seminal paper, introducing the concept of 'brain-computer interfacing', asked how to put brain signals to work "... *in man-computer communication or for the purpose of controlling such external apparatus as prosthetic devices or spaceships ...*" [41]. Kamiya's references to Zen and LSD may have sparked interest, but even before these publications we saw composers and musicians such as Alvin Lucier, Pierre Henry, Richard Teitelbaum, John Cage, and David Rosenboom show interest, experiment, compose and perform using brain signals. In the early seventies of the previous century Nina Sobell designed a brainwave drawing game where participants had to synchronize their alpha activity in a Lissajous visualization of their joint brain activity [36].

Many of these early artistic experiments are described in "Biofeedback and the Arts" (ed Rosenboom [35]). In a 1972 TV show David Rosenboom performed with John Lennon and Yoko Ono in a brainwave controlled interactive music performance. Sonification, visualization and modifying otherwise produced multimedia received attention. But there were other applications. One of them, 'Alpha Garden', designed by Jacqueline Humbert in 1973, had two persons control the flow of water through a garden hose and sprinkler system by synchronizing their alpha activity. Another one, also designed by Humbert in 1974, was 'Brainwave Etch-a-Sketch'. Here, two participants had to control their alpha waves, where one participant could move a dot on an oscilloscope along the x-axis, and the other participant could move the dot along the y-axis. In this way they could cooperate to produce a drawing on the screen. In another performance experiment ('Music from Brains in Fours') Rosenboom had brain activity of four musicians integrated with information about body temperature and galvanic skin response in order to provide input to a performance.

In these applications we see audio or visual representation of brain activity and the control of these representations. But also the voluntary or involuntary control or modification by brain activity of multimedia not directly produced from brain activity. And we see applications where synchrony between the brain activities of users guides such applications. It should be noted that in these early applications of multi-brain activity the possibility to analyze brain signals or to (machine) learn from previous interactions was extremely poor. That changed in later years.

Employing computers for artistic BCI applications required cooperation between artists and researchers in computer science, human-computer interaction, neuroscience and brain-computer interfacing. In the period 1975–2000 there are few interesting artistic applications of BCI, let alone multi-brain applications. In this period each of these areas had its own problems and challenges and they mainly focused on more efficient problem solving, rather than on providing users with artistic, emotional or entertaining experiences. This has changed considerably in our 21st Century. Interest in efficient problem solving, efficient searching, efficient access to information and access to (mediated) communication is of course still there. But now we can conclude that this technology is already available, not only to support our home and professional activities, but also our activities related to sports, learning, entertainment, and arts. That is, applications that become possible

through advanced and efficient computer processing, but where this efficiency is used to offer the user the possibility to have fun, become entertained or relaxed, rehabilitate, or learn.

### ***12.2.2 Current Multi-brain BCI Research and Applications***

There are various kinds of applications where it is useful to know how people experience a certain event or product. We can have questionnaires, we can look at facial expressions and we can measure (neuro-) physiological characteristics of the potential users. The latter may yield information that is more reliable than that can be obtained by asking or observing participants in an experiment. For example, brain activity from multiple persons can be measured and analyzed for neuromarketing purposes. This can be done on an individual basis and there is no need to use the results of the analysis in real-time, that is, no feedback to the user is necessary in real-time. In neurocinematics [13] similarities in spatiotemporal responses across movie viewers are studied. Here, future applications may require real-time processing of such brain activity in order to have collective or individual decisions about the continuation of a movie while watching.

But, if we remain more closely to current BCI research activity, there is certainly more research in which multi-brain activity is investigated and where the immediate goal is not yet real-time applications, but where real-time applications, also in the context of games, can be foreseen or appear already in prototype applications. However, mostly, at this moment in this research no active BCI control by users is present. There is, for example, measuring and analyzing of brain activity of persons engaged in the same task. It is investigated how this engagement shows in their brain activity. But there can be an added aim to learn from this in order to support and improve this joint activity. This can then be done off-line, taking care of better conditions for future joint activity. And one step further, doing this analysis and interpreting the information in real-time, that is, when the joint activity takes place, and then using this information to support and guide the users in their activity.

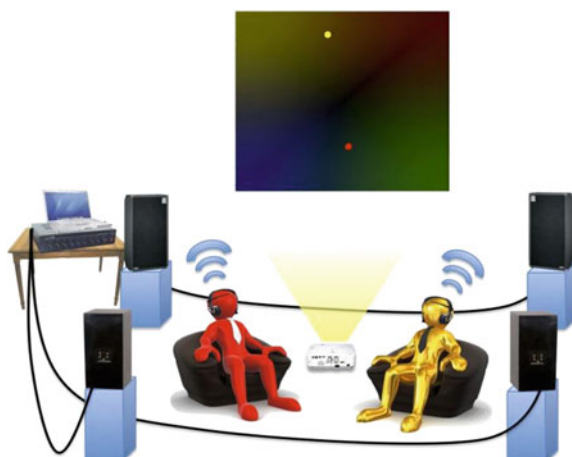
Whenever there is joint activity, the assumption is that there is some activity synchrony visible in the brain activity of the participants. Clearly, a conversation is a joint activity and coordination and nonverbal synchrony, including mimicking, is a well-known phenomenon. As reported in [37], there is also a spatiotemporal coupling of the speaker's and the listener's brain activity. In that particular research fMRI is used to record brain activity, hence, rather far away from the multi-brain game applications we have in mind. Nevertheless, the results support our idea that brain activity from different persons can be measured, analyzed and integrated in order to be used as a source of information to guide behavior and to control or adapt an environment in which the persons perform their activity. As is the case in other research on speaker-listener synchrony, the tighter the coupling between activities, the more successful is the joint task. This neural coupling between two interacting subjects is studied at many places, both with fMRI and EEG, for example at New

York University, in cooperation with the artist Marina Abramovic [5] and at the German Max Planck Institute (Müller and Lindenberger [25]. As a possible application of such research, can we off-line improve the conditions that lead to more synchrony in an interaction? How do we model a social robot or an embodied agent (avatar) such that its awareness of this synchrony can be used to have real-time adaptation of behavior?

There are already many examples of artistic applications where at least one of the cooperating participants contributes by giving the system access to his or her brain signals. In the previous section we looked at some of these early (multi-brain) research and artistic activities. Nowadays, more than 40 years later, we have cheap and commercially available headsets. Moreover, we have the possibility to embed (multi-brain) BCI in multimedia environments that offer audio, visualizations, haptics, and animations without extreme efforts or costs. Also, there is growing interest in computer generated entertainment, meaning the BCI and human-computer interaction researchers turn to artistic and entertainment applications and artists find it more easy to use this available technology to express their ideas. We mention a few examples.

In [23] ‘Let me Listen to your Brain’ is introduced. It is a project on collaborative music composition where EEG is used to get information about the affective state of one of the collaborators. Musical phrase selection while composing music, but now with possibly two users that control different aspect of a composition using their brain signals is discussed in [6]. In [21] we have four musicians (a violinist, a flautist, a cellist, and a ‘brainist’), where during the performance the brainist delivers drone sounds by re-experiencing emotions (classified by EEG) that has been associated with the sounds during a training session. In [19] the MoodMixer system is introduced. Here we have two participants, each wearing an EEG headset with which relaxation and sustained attention is measured. This information is used to position each of them on a two-dimensional audiovisual musical interface, the x-axis for relaxation, the y-axis for attention (see also Fig. 12.1). Changes in the

**Fig. 12.1** MoodMixer  
(Image courtesy Grace Leslie  
and Tim Mullen, University  
of California, San Diego)



cognitive states of the participants lead to changes in the audiovisual landscape. Participants can try to learn to control these cognitive states and then define little games and they can cooperate to achieve certain effects or composition lines. Sound samples and visual flashes can also be triggered by eye blinks. In principle, more participants, also wearing EEG headsets, can be added to the system.

More players that actively contribute to a music performance through their brain control are present in the Multimodal Brain Orchestra (MBO) presented in [18]. This orchestra has four performers and a conductor. Two of the four performers can use P300 to trigger emotionally classified discrete sound events. Two other performers use SSVEP to modulate articulation and accentuation of an earlier recorded MIDI sequence. The conductor uses a WII-mote as a baton and can decide when the sound events have to be triggered and he can decide about tempo modulations. Hence, evoked brain activity from different performers is directed by the conductor. There is feedback from the music and visualization.

Using knowledge about a collective mental state of an audience may lead to audience participation in entertainment and artistic events. As an example we mention DECONcert, performed in 2003 at the University of Toronto, where 48 people's EEG signals were used to affect a computationally controlled soundscape [22]. Hence, we can think of BCI as an audience participation technology. Other performance arts events in which multi-brain BCI was used are also reported in this paper, including a communal bathing experience in which water waves, sound waves and brain waves were integrated (Fig. 12.2).

Another performance arts example is [8]. Off-the-shelf BCI headsets for mobile users are used to measure audience response to live events and performances. This information can be used to adapt performances to changes in response. This can be

**Fig. 12.2** Water waves, sound waves, and brain waves  
(Reprinted from [22])



done autonomously, but such information can also be provided to, for example, a DJ or VJ who then adapts his or her performance to the audience response [9].

We can focus a little more on multi-party or team activity. What kind of brain activity can we detect and integrate when we have a team of ‘players’ (not necessarily players in a game, but, more generally, persons involved in a joint activity). Can we get information about progress (successful collaboration) and use this information to improve conditions for such team activity? And, as a next step, based on real-time analysis and integration, being able to support and improve the joint activity? For example, during a meeting, can we decide and make group members aware that there is a convergence or divergence of opinions? In a multi-user game with participating teams, and when obtained real-time, such information can certainly help to win the game. Clearly, game, entertainment and artistic environments can be designed in such a way that each kind of combination of one and more persons, individual and joint voluntary control of brain activity and other, not consciously produced brain activity, can be used to play a role during game play.

Chris Berka and her colleagues [38] have a research program that aims at studying team cognition using BCI. They use wireless EEG headsets to measure attention, engagement and mental workload of the members of a team that has to play a serious game: a submarine piloting and navigation simulation. The aim is to achieve measures of the quality of the team performance and use these measures to adapt and rearrange tasks and responsibilities for more optimal team performance. At this moment this adaptation and rearrangement is not done in real-time. In a multi-user entertainment game such information can also be used to remove team members or to rearrange tasks among team members for a next game session. But obviously, real-time adaptation would be much more useful.

In this example (Stevens [38], team members do not manipulate their brain activity. Brain activity is monitored; hence we have a passive multi-brain BCI application. Rather than monitoring one individual engaged in a task, a group of collaborating persons (the team) is monitored with the aim to achieve and maintain ‘neurophysiologic synchrony’ (a positive team rhythm). While in this case the team effort concerns a serious game (a simulation of a critical real-world situation), the application could as well be a multiplayer entertainment game with competing teams and where optimal team performance is a goal as well. Being able to improve, in real time, decision processes by measuring and aggregating activity of all the brains of people involved in the decision making, as can be the case in multi-user games that allow the forming of teams, makes it also possible to issue commands to a game as the result of volatile team brain activity. We will return to this in later sections of this chapter.

## 12.3 Competition and Collaboration Using BCI

Competition and collaboration are important characteristics of games. For that reason we now look at research in which BCI is studied from a competition and collaboration point of view. Other characteristics of games and how they relate to

BCI can be found in [11]. A viewpoint in the examples that we discuss in this section is that at least two players are involved. And that at least one of them has his or her brain activity measured and it plays a role in the game. This can be to control the game (active BCI) or to adapt the game (scenario, levels, and environment) to the user. In the latter case the user does not consider these game changes as unnatural and is not necessarily aware (and hence does not try to influence it) that game changes are caused by his or her brain activity.

As a side note, notice that we consider these issues in the context of *human-computer* interaction. Hence, one of the partners involved in a game may as well be an artificial agent (physically or virtually embodied agent, e.g., a social robot or a virtual receptionist) or the environment or a device that acts and is supposed to interact in a humanlike way. As an example we can mention the study of [40] where a humanlike robot teacher has access to the brain activity (attention/level of engagement) of a student and adapts his behavior to this activity by raising his voice or have more expressive gestures. In a competitive game environment knowledge about brain activity of a human opponent may give an unfair advantage to such an artificial agent. But that is also the case in a competitive game where a human player has access to the (interpretation of) brain signals of a competitor without having his own brain activity being exposed.

Obviously, when more than one person is involved in a BCI game, the social setting will have impact. Are players co-located or distributed? Is there an audience? What does the audience see and is there interaction between audience and players? In [29] the aim of the research was to investigate the use of BCI in a social setting (a small group of friends or relatives) and in particular the presence and the role of bodily actions of one of the group members playing a simple commercial BCI game while others are watching. In this game the BCI control is obtained from brain activity related to relaxation and concentration. Players used bodily actions (gestures, gaze, and facial expressions) to achieve a desired mental state. But they also used bodily actions to indicate their thoughts to the spectators in the group.

Interactions between co-located BCI gamers have been studied in [12]. We designed a game for research purposes: Mind the Sheep! (MTS!). It can be implemented as a single-player game, a cooperative multi-player game and, although we didn't experiment with that, a competitive multiplayer game. Moreover, it allows both BCI and non-BCI play for players. In our study we introduced a two-player cooperative version of this game to study social interaction between players. Both co-located players wear an EEG cap. The game visualization consists of a 2D map that contains simple representations of a meadow, a sheep pen, dogs and sheep. Players select and move dogs around to herd and eventually fence the sheep in. A dog can be selected with BCI (SSVEP evocation). The players can cooperate through gestures (see Fig. 12.3) and speech to develop and execute a joint strategy. But of course, they see also at the screens what actions the other player takes. There is no integration of brain signals. If one player stops, the other can continue but may take more time to finish the task.

It is more usual to have two-player games where the players compete, each player volitionally using his or her brain activity to compete. This competition point of view,

**Fig. 12.3** Two gamers cooperating while playing Mind the Sheep!



where only BCI as input modality to a game is used, can be illustrated with two more examples from earlier research. Consider a BCI version of the well-known Pong game, a virtual tennis game that can be played by two gamers that control their bats (up and down) to hit a tennis ball back to their opponent. Motor imagery (imagine hand movements) has been used to implement a BCI version of this game [16]. That is, individual motor imagery controls the bats, but there is no processing that looks at—or compares—the brain activities of the individual players.

This is different in what was probably the first competitive BCI game, Brainball (Hjelm et al. [14]). In this game we have two players competing. They are expected to compete by relaxing and their performance is measured by EEG. The player who is the best in relaxing wins. The game is made more interesting by visualization of the players' performances that control a ball moving on a table between the two players, seated at opposite ends of the table. This visualisation has impact on their performance and makes the game also attractive for an audience that can decide to support or disturb relaxation of a player. Clearly we need real-time BCI measurement and control of this rolling ball. Brain activity of the players is compared and the difference determines the direction of the ball (moving into the direction of the player who is less relaxed). Hence, this is a different kind of competition, from the point of view of processing brain activity, than in the BrainPong example.

There are of course more examples where players manipulate their brain activity in order to play a particular BCI game. Our interest is in games where players have to compete or collaborate to play a certain game using brain activity. For example, in a two-player game players have to relax to issue a command, for example, to fire a gun at their opponent in a 'Mexican Stand-off'. But certainly, being able to look at and experience the performance of their opponent, a gamer can try to increase his or her performance by comparing it with the performance of the opponent. Depending on the visualization or other information communicated to the gamers, such a stand-off game can be compared with a relaxation-based BrainPong game.

Very interesting and certainly a nice example of a multi-brain game is "BrainArena" [3]. It very much illustrates, in a simple setting, some of the ideas

mentioned above. It is a simple football game with a ball and goalposts displayed on a screen in front of the two players. There exist two versions of the game, a collaborative and a competitive one. The players wear EEG caps and use motor imagery (imaging left or right hand movement) to get the ball rolling in the direction of the goalposts. In the competitive version their actions are opposed and the player with the best performance wins, in the collaborative version the brain activities are merged and players steer the ball in the desired direction. Hence, in the competitive version it can be seen as a motor imagery version of the earlier mentioned BrainBall game. It can also be compared with a motor imagery version of BrainPong, but in that case each player has its own object (a bat) to control, while in BrainArena they compete to control an object (the ball).

Less obvious is a cooperative two-player game where one player's brain activity is used to support the second gamer in his or her task. This second gamer does not necessarily use BCI. In [32] the authors look at games where players have different roles. One player is physically active while a second player uses his or her mastery of brain activity to provide favorable conditions for the performance of the first player. As mentioned in that paper, new games can be designed where a player's (traditional) game controller input can be modulated by collaborating BCI input, or where game activity is modulated by joint authority over game control input. Clearly, this includes a situation where brain activity of both players is measured and used in the collaborative control of a game. But it also allows games where there is competitive control over a game object. The authors introduce a Multi-User Video Environment (MUVE) that has been designed with both cooperation and competition in mind. Brain activity of one or more players can be used to disturb the physical control input of an opponent or opponents (or the other way around) and competition can be based on BCI input only. In Fig. 12.4 this work is illustrated with a FPS (First Person Shooter) game, where one player is using a Wii Zapper and brain activity of the second gamer controls the steadiness of the crosshairs.

**Fig. 12.4** Brain support from one player for the player using the Wii Zapper in a FPS (Image courtesy Chad Stevens, NASA Langley Research Center)



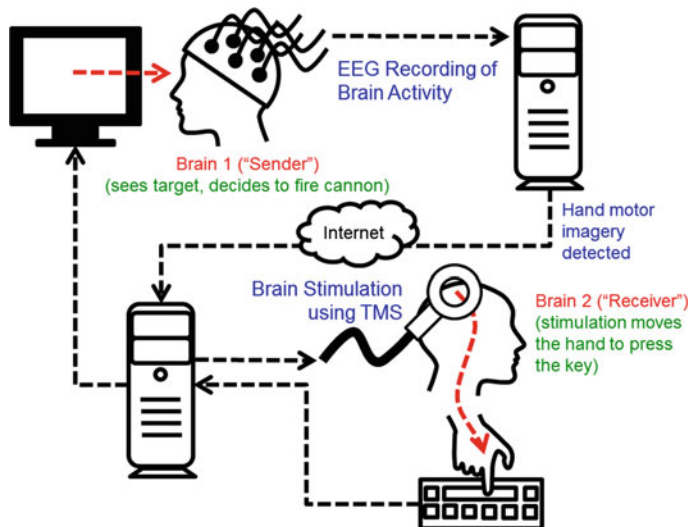


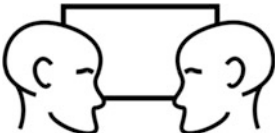
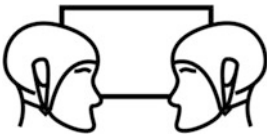
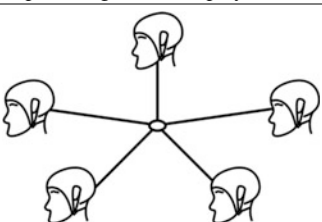
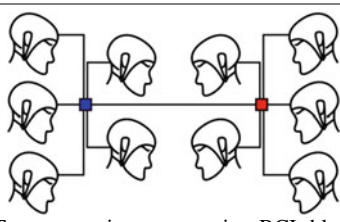
**Fig. 12.5** Brain-to-brain communication for games (Image courtesy of R. P. N. Rao and A. Stocco, University of Washington)

Maybe even more interesting is a situation where we translate EEG recordings of brain signals from one gamer to a brain stimulating pulse for a collaborating (or maybe even a competing) gamer. A pilot study on this brain-to-brain communication is presented in [33]. In this study one gamer (“the Sender”) uses motor imagery (right hand movement) when a canon has to be fired to destroy a rocket. However, this action is delegated to a second gamer (“the Receiver”). The brain signals of the sender are detected and when recognized as motor imagery, over the internet transmitted and translated to a transcranial magnetic stimulation (TMS) pulse to the left motor brain region of the Receiver. This causes an up-down movement if the hand of the Receiver which results in pressing the “fire” key on the keyboard. In Fig. 12.5 we have illustrated the Sender-Receiver communication.

EEG monitoring of brain activity in order to make decisions about brain stimulation is of course not new. In fact, commercial hardware is entering the market where wireless recording and stimulation are integrated in the same headset. This offers the possibility that multiple players have access to each other’s brains, not only to detect and interpret brain activity, but also to stimulate brain regions in order to get certain tasks done or to prevent certain tasks to be done.

In Table 12.1 we have collected the various ways gamers can use BCI. Clearly, brain stimulation as discussed above can be an added parameter to these possibilities. In Sect. 12.5 (Table 12.2) we have more examples of BCI game and team activity situations that are illustrated by one or more of the figures in Table 12.1.

**Table 12.1** Various ways of competing and collaborating with and without BCI caps

	
Two (or more) players collaborating in a cooperative game. No BCI input	Two (or more) players, collaborating in a cooperative game. One player uses BCI
	
Two (or more) players, collaborating in a cooperative game. Both players use BCI	Two (or more) players, competing in a competitive game. No BCI input
	
Two (or more) players, competing in a competitive game. One player uses BCI	Two (or more) players, competing in a competitive game. Both players use BCI
	
Online collaboration using BCI	Two competing teams using BCI: blue team (left) versus red team (right)

## 12.4 More About Multi-brain Games

We now have seen various possibilities for BCI input to games where players compete or collaborate. Usually this concerns two players, but suggestions that involve generalizations to more players are sometimes given. Moreover, the social setting of a game and associated social interactions emerged as an interesting research issue.

Interestingly, in what appears to be the oldest BCI game (BrainBall), there is a volitional contest by both players to control the same object in the game. In the other examples players use their brain activity to perform their own task in a collaborative or competitive game (MTS!, BrainPong), or they try to influence (in a collaborative or in a competitive way) the performance of the other player (MUVE). More subtleties in these distinctions can be introduced, e.g. by looking at dimensions such as social interaction and audience involvement and the role of passive

**Table 12.2** A survey of multi-brain games and multi-brain team activities

Game or application	Description	Competition and cooperation
BrainBall (Hjelm et al. [14]). Two players, sitting at opposite ends of a table. On the table is a steel ball that can roll along a magnetic strip on the table	The ball rolls away from the player who is most relaxed. Or, the other way around, to the player who is most stressed. The brain activity of the two players is also visualized on a screen. Often there is a noisy audience	In the competitive mode players compete in relaxation. A player loses when the ball reaches his table edge. In the cooperative mode the players keep the ball in the center or keep it moving from one edge to the other
BrainPong [16]. Two players. Pong is a virtual tennis game where key-board keys (up/down) are used to move a bat. A simple 2D virtual environment, displaying the bats of the two players and the ball moving between them is required	A player has to move a bat upwards or downwards in order to return a ball hit by his opponent. This has been done using different BCI paradigms: measurement of stress and relaxation, motor imagery, evoked potentials and ERP's	The game is competitive and turn-taking. No fusion or comparison of brain activity. Players can anticipate actions and make decisions based on this anticipation. The game has been played in noisy environments
BCI Connect Four [20]. In the traditional ‘Connect Four’ game two players take turns in choosing columns in a 6 (rows) to 7 (columns) matrix where to drop coins. The players’ aims are to get 4 own coins connected, before the other does	The ‘odd-ball’ paradigm using visual flashing of the columns is used to have gamers choose a particular column in the matrix. Nine EEG sensors are used in the centroparietal and occipital regions	This is a competitive game. During a turn an opponent can also try to interfere with the brain activity of the other player by trying to disrupt a choice. There is simultaneous use of BCI and fusion (comparison) of brain activity to decide a winner
BrainArena [3]. Two goals are displayed on a screen; a ball is displayed between them. Players have to steer the ball to one of the goals	Motor imagery (movement of the hands) has to be used to steer the ball in a goal. Eight EEG channels located around the right and left motor cortices. Obviously, such a game can be played in a solo, collaborative and competitive mode	In the collaborative mode the players want to score in the same goal; their brain activity is summed. In the competitive mode players have to score in the opposite goals, hence, the strength of their brain activity is compared to determine the winner
MUVE (Multi-User Virtual Environment, introduced in [32]), allows the implementation of multi-user games where physiological information is used to modulate a player’s physical activity	MUVE has been shown to provide a gamer’s physiological information (including EEG information) to a first person shooter game in order to increase crosshairs steadiness of a Wii Zapper	Relaxing or concentrating can support a main player’s performance (cooperative mode) or decrease his performance (competitive mode)
Space Navigation [31]. Users are asked to navigate a spacecraft (in a simulator) and pass a planet as close as possible	Spaceship control is done using a ring around the spaceship. 8 Positions are distinguished, representing directions in which to steer. Circles in turn flash allowing a P300 target choice	Two players cooperate in joint pointer control. Early fusion (averaging of the ERP input) and late fusion (averaging the individual pointer movement decisions) are considered

(continued)

**Table 12.2** (continued)

Game or application	Description	Competition and cooperation
MTS! [12] is a video game that allows two co-located players—using multi-modal input—to command dogs to certain positions on a virtual meadow in order to herd sheep inside a fence	SSVEP is used to choose one of the dogs that has to chase the moving sheep. There is a trade-off between being certain that SSVEP is successful and being able to start chasing the sheep	Depending on the version gamers can collaborate using various combinations of input modalities, including BCI. There is no fusion of their modalities, but they see each other's actions
Assess the quality of the performance of a submarine piloting and navigation team. Rearrange team or tasks when necessary [38]	EEG monitoring of engagement, workload and alertness using 9-channel wireless headsets	Team members can have different tasks. Speech interaction between team members
Online collaboration in a perceptual decision task [7]	On-line collaboration of a group of 20 subjects to distinguish, using ERPs, car and face images	No interaction between subjects. Fusion is done at a decision level using voting procedures
Collaboration in a movement planning task [42]. Decide about movement and plan a visually guided right-hand reaching task	Group of 20 subjects. Three different methods for fusing EEG information: ERP averaging, feature concatenating, and voting	No interaction between subjects. In this case the voting method (fusion on decision level) turned out to be optimal
Online collaborative decision making in a visual target decision task (Yuan et al. [44])	Groups of 6 participants. Decide between face images (Go tasks) and car images (NoGo tasks). Single-trial EEG-based decision making by averaging ERPs	No interaction between subjects. Experiments suggest that collaborative BCI can accelerate reliable decision making in real time
MultiMind [39]. Aggregate biometric information from a number of individuals for joint decision making for (potential) security-related applications	Two subjects wearing Emotiv Epoc headsets. They watch a sequence of slides with humorous content and their emotional response is fused to obtain a collected assessment of the presented information	No interaction between subjects. Although the approach is called multibrain signal fusion, it seems that fuzzy logic is used to fuse information about the subjects' facial expressions collected by the headsets

BCI in these games. And, of course, we need to look at the consequences of having more than (just) two players involved in multi-party and multi-brain games.

When looking at a possible definition of multibrain computer interfacing it now should be clear that it is unwise to be restrictive. Clearly, two or more persons need to be involved. Brain activities of two or more persons have to be integrated in the application. But, not necessarily at the same time and not necessarily in a synchronous way. In traditional multimodal interaction research we have one person interacting with an application using different modalities. The modalities can complement each other and fusion of the different modalities helps to solve

ambiguities and can lead to more robustness. Usually three levels of fusion are distinguished, the data level, the feature level and the decision level. Fusion is meant to make the interaction effort stronger, to make clearer what is intended by an individual user.

We can also speak of fusion at different levels in the case of a cooperative game. For example brain activity of two or more players can be combined to have them make a particular decision in a game or to have them lift a spaceship in a virtual game environment, a task that would have been much more difficult if only brain activity of one player could be used. This is not some peculiar property of the brain activity modality. Lifting hand and arm gestures, facial expressions, or gaze behavior of two or more gamers could be implemented to have the same result. Or, any combination of different modalities that are used by different persons in a joint effort.

In the case of brain activity, comparable brain activity seems to be the most obvious first choice for data level fusion. But that may change in the future when we learn more about dependencies between different BCI paradigms. In a cooperative game situation fusion at the level of decision making can mean making a joint decision or doing a joint activity, but it can also mean a division of labor where players take responsibility for subtasks that help in reaching their joint goal.

Also in a competitive game where two or more persons are involved we can talk about fusion of information coming from different modalities and coming from different participants. Again, for the sake of discussion, let us focus on the brain activity modality. When we have competing players, rather than ‘adding’ information, on whatever level, we let the system (interface, game) compare (‘subtract’) information and make decisions that benefit the ‘winner’ or ‘winners’ who have outperformed with their joint brain activity the losers. Deciding when and how a team of BCI gamers has outperformed another team for deciding about or doing a particular activity can again be done at the data, feature and decision level. However, it should be mentioned that at each level different information is available to guide decisions. As an example, at the decision level we can use common sense and domain knowledge and we know about methods from artificial intelligence research that help us to represent and to reason about such knowledge. At every level of fusion, methods are available that take into account level context.

All these observations make it more difficult to get closer to a definition of multibrain games. Or, less difficult, to a decision that we should accept that there cannot be one definition and that multibrain games are just games in which measured brain activity of two (or more) gamers can be used to control commands or will be used to adapt a game to its users. Fusion of modalities of one user is an issue, but also fusion of modality information coming from different users (competing or collaborating) is an issue. There is another issue, when we talk about fusion, who is taking care of it? In traditional human-computer interaction a multi-sensor system provides input to computing power and intelligence that makes decisions. In games, but not only in games, human decision making can also be used to decide about how to integrate and fuse information, including brain activity

information, coming from different modality sources and from different users and made available to a human decision maker or (game) team leader. In fact, in the Multimodal Brain Orchestra (see Sect. 12.2.2) it is the human conductor that makes decisions about the fusion of the classification results obtained from the EEGs (SSVEP and P300). In this example there is, if we understand it well, no ‘adding up’ or otherwise processing of joint activity at the level of brain signals or features extracted from brain signals.

Having now discussed the different ways brain activity from two or more sources can be integrated (without claiming completeness), we now look at research that has been done in the past and that supports our ideas about having multibrain BCI games in the near future by demonstrating that brain activity of multiple persons can be used in applications. Some examples, not really aimed at collective decision making or performing an action through collective brain activity were already mentioned in Sect. 12.2. We already mentioned team cognition [38] and audience response and participation using BCI [8, 22].

Game applications of this audience response can be thought of, but even more interesting is being able to improve, in real time, decision processes by measuring and aggregating activity of all the brains of people involved in the decision making process, as might be the case in multi-user games that allow the forming of teams. Teams allow some kind of ‘collective wisdom’ to make decisions. Real-time decision making by a team of users rather than an individual user has been investigated in [7]. In this research twenty users had to make perceptual decisions, that is, deciding when confronted with a series of pictures whether a particular picture was a face or a car. Prediction of a decision based on aggregated (ERP) brain activity turned out to be possible and, compared with an individual user, both the decision accuracy and decision speed could be improved. Collaborative classification of visual targets, but now using visually evoked potentials (VEPs) was also investigated in [43]. Clearly, applying such research results in a multi-player game context can make those games more interesting to play.

Collaborative brain-computer interfaces have also been studied by Wang and colleagues [42]. It is investigated how EEG data from twenty users can be used to predict and decide about the planning of movements. Clearly, as they mention, this is the kind of information that can be used in a multi-player game that allows the forming of teams and can have team performance included in the game, rather than just have input from individual players only.

## 12.5 Distinguishing Multi-brain Games

In Table 12.2 we have collected the characteristics of many of the games and systems we discussed above. Some systems not discussed above are also included in the table [20, 31, 39, 44].

## 12.6 Discussion

We discussed the use of BCI as an input modality in a multiparty context and the various ways brain activity can be integrated in game contexts. We focused on integrating brain activity from multiple persons. It is clear that many problems related to BCI in general have to be attacked. It can also be concluded, as we did in [26], that it nevertheless is possible to design multiparty games in which multi-brain activity is included, and that it can be done in such a way that it introduces interesting challenges to the gamers (and the designers), rather than assuming that no efficient or robust use can be made of this technology. In the context of games, entertainment and artistic applications robustness and efficiency are not the right keywords.

We discussed multi-brain applications from the viewpoints of competition and collaboration. There is a growing number of BCI games where indeed we have competing and collaborating gamers. The games are simple and although they are fun to play, until now this is only done in research environments. Moreover, in these cases BCI is not integrated in a game context where other modalities play an important role, except for the MTS! game, but in that case the BCIs of the gamers are not integrated, and the Wii Zapper game, but there only BCI is used for one of the gamers. But we certainly can expect that in future research more complex multi-brain games will appear. And adding brain stimulation to the many situations we already distinguished will increase the possibilities to introduce challenging multi-brain games enormously.

Also the research and applications that tell us about the fusion of brain activity of more than two persons, and even from tenths of persons to make group decisions or adapt the game, a performance or an environment to group preferences or changes in cognitive state or emotions give us a view of the future where we can have multi-brain applications in a MMORPG (Massively Multiplayer Online Role-Playing Game). Many of these games assume gamers to form teams that can compete or collaborate. Team decisions or team leader's decisions in a MMORPG can be based on collective thoughts of a team or a sub team. Obviously, synchrony of thoughts is a problem here. However, natural game events can trigger joint and synchronized event related brain activity among team members. The potential role of 3rd party team communication software such as TeamSpeak should be considered. And again, perfectness would be unnatural. A 'synchronized kill' in the "Ghost Recon, Future Soldier" game does not have to be perfect. Joint brain and synchronized brain activity can be triggered because of various artificial stimuli that are designed in the game. There can be natural moments to take an explicit vote on how to continue or make an otherwise important decision. But fast decision making based on merging of brain activities of a large team, accepting that not yet everyone in the team is ready for it or agrees with the majority, is also natural.

However, such observations should not be confined to a video game situation with multiple users only. For every video game situation we can find a serious game situation where trainees have to learn to make decisions and the serious game

environment should have models that allow predicting, anticipating and processing different ways of EEG information coming from multiple sources. Serious game environments train for real applications.

There are lots of context issues that we are aware of or that we are made aware of when we participate in more traditional interfaces that allow collaborative or—less common—competitive activities. So we should look at what it means, in a brain-computer interface situation, what impact it has when we are aware of others' actions and intentions, how we perceive this awareness, what kind of feedback do we get on our contribution to a collaborative or competitive activity and what kind of control do we feel about our possibility to contribute [45].

## 12.7 Conclusions

In this chapter we surveyed the state-of-the-art of research in applications where the applications require input from multiple persons and where at least for one person input from a BCI is obtained. One may think of applications where users compete or collaborate, but also applications where input collected from different individuals is processed and made visible or audible in art performances.

This view on the use of BCI raises interesting questions. It is only recently that in BCI research interest emerged in looking at integrating or making use of different BCI paradigms in one application for one individual user. The example individual user used to be a disabled person not being able to communicate or control by using his or her muscles. However, users without such disabilities can move around freely, can gesture, can speak and have meaningful facial expressions. These display information—intended or unconsciously—that can be interpreted and that complement information obtained from the interpretation of brain signals, or the other way around, knowing about an interpretation of brain signals can support other communication modalities. There needs to be a fusion of information at the level of signals (when possible), features or decisions. Clearly, this requires quite a different research approach than is usual in traditional BCI research that is focused on signals coming from a particular region of the brain and that preferably should not be disturbed by any other brain activity at all.

In this chapter we looked at the situation where the information that is obtained in the human-computer interface and that is communicated to the application did come from different persons. The application can have input from users looking at one particular modality only—for example, for all users there is integration of their brain signals—or different users provide information to the application that is coming from different interaction modalities—for example, the physiological information from one user is used to modulate the BCI command signals from a second user. Clearly, giving all possible input modalities, combinations of input modalities, and voluntarily expression and involuntarily releasing of information through these modalities, it should be clear that more insight need to be acquired about this fusion of information, whether it is on the signal level (source signals

associated with different activity modalities), feature level, or decision level. In addition, from the point of view of applications, we need to experiment with applications where this fusion is guided by characteristics of the users, the context and the kinds of applications.

**Acknowledgements** A preliminary version of this chapter appeared in the LNCS proceedings of the 2013 HCII conference [28]. I'm grateful to Nelson Nijholt for providing information about multi-player games and taking care of some illustrations. This research has been supported by the European Community's 7th Framework Programme (FP7/2007–2013) under grant agreement Nr. 609593: The Future of Brain/Neuronal Computer Interaction: Horizon 2020 (BNCI Horizon 2020).

## References

1. Allison, B.Z., Dunne, S., Leeb, R., del Millan, J.R., Nijholt, A.: Future BNCI: a roadmap for future directions in brain/neuronal computer interaction research. In: DG Information Society and Media (Directorate “ICT Addressing Societal Challenges”, Unit “ICT for Inclusion”) Under the Seventh Framework Programme [FP7/2007-2013] of the European Union. [http://bnci-horizon-2020.eu/images/bncih2020/FBNCI\\_Roadmap.pdf](http://bnci-horizon-2020.eu/images/bncih2020/FBNCI_Roadmap.pdf). Accessed 5 June 2014
2. Azar, A.T., Balas, V.E., Olariu, T.: Classification of EEG-based brain-computer interfaces. In: Iantovics, B., Kountchev, R. (eds.) Advanced Intelligent Computational Technologies and Decision Support Systems, Studies in Computational Intelligence, vol. 486, pp. 97–106. Springer, Heidelberg (2014). doi: [10.1007/978-3-319-00467-9\\_9](https://doi.org/10.1007/978-3-319-00467-9_9)
3. Bonnet, L., Lotte, F., Lécuyer, A.: Two brains, one game: design and evaluation of a multi-user BCI video game based on motor imagery. IEEE Trans. Comput. Intell. AI Games **5**(2), 185–198 (2013)
4. Brunner, C., Blankertz, B., Cincotti, F., Kübler, A., Mattia, D., Miralles, F., Nijholt, A., Otal, B., Salomon, P., Müller-Putz, G.R.: BNCI Horizon 2020—Towards a Roadmap for Brain/Neural Computer Interaction. In: Stephanidis, C., Antona, M. (eds.) Universal Access in Human-Computer Interaction (UAHCI 2014), 8th International Conference, Heraklion, Crete, Greece, June 2014. Lecture notes in computer science, vol. 8513, pp. 475–486. Springer, Heidelberg (2014)
5. Dikker, S.: Neuroscience experiment I: measuring the magic of mutual gaze. (Real-time interactive neuroimaging art installation). In: Collaboration with Marina Abramovic, Matthias Oostrik, and Representatives of the Art and Science: Insights into Consciousness Workshops, The Watermill Center, New York. <http://www.youtube.com/watch?v=Ut9oPo8sLJw>. Accessed 5 June 2014
6. Eaton, J., Miranda, E.R.: Real-time notation using brainwave control. In: Bresin, R. (ed.) Proceedings of the 2013 Sound and Music Computing Conference, pp. 130–135. Stockholm, Sweden (2013)
7. Eckstein, M.P., Das, K., Pham, B.T., Peterson, M.F., Abbey, C.K., Sy, J.L., Giesbrecht, B.: Neural decoding of collective wisdom with multi-brain computing. NeuroImage **59**(1), 94–108 (2011)
8. Fan, Y.-Y., Myles Sciotto, F.: BioSync: an informed participatory interface for audience dynamics and audiovisual content co-creation using mobile PPG and EEG. In: Proceedings 13th International Conference on New Interfaces for Musical Expression (NIME), pp 248–251. KAIST, Daejeon, Korea, May 2013
9. Gates, C., Subramanian, S., Gutwin, C.: Djs' perspectives on interaction and awareness in nightclubs. In: Carroll, J.M., Coughlin, J. (eds.) Proceedings of the 6th Conference on Designing Interactive Systems, ACM, pp. 70–79, June 2006

10. Gürkök, H., Nijholt, A.: Brain-computer interfaces for multimodal interaction: a survey and principles. *Human Comput. Interact.* **28**(5), 292–307 (2012)
11. Gürkök, H., Nijholt, A., Poel, M.: Brain-computer interface games: towards a framework. In: Herrlich, M., Malaka, R., Masuch, M. (eds.) *Proceedings 11th International Conference on Entertainment Computing (ICEC 2012)*, Lecture Notes in Computer Science, vol. 7522, pp. 144–157. Springer, Heidelberg (2012)
12. Gürkök, H., Nijholt, A., Poel, M., Obbink, M.: Evaluating a multi-player brain-computer interface game: challenge versus co-experience. *Entertainment Comput.* **4**(3), 195–203 (2013)
13. Hasson, U., Landesman, O., Knappmeyer, B., Vallines, I., Rubin, N., Heeger, D.J.: Neurocinematics: the neuroscience of film. *Projections* **2**(1), 1–26 (2008)
14. Hjelm, S.I., Browall, C.: Brainball: using brain activity for cool competition. In: *Proceedings of the First Nordic Conference on Computer-Human Interaction (NordiCHI 2000)*, Stockholm, Sweden (2000)
15. Kamiya, J.: Conscious control of brain waves. *Psychol. Today* **1**(11), 56–60 (1968)
16. Krepki, R., Blankertz, B., Curio, G., Müller, K.R.: The Berlin brain-computer interface (BBCI)—towards a new communication channel for online control in gaming applications. *Multimed Tools Appl.* **33**(1), 73–90 (2007)
17. van de Laar, B., Gürkök, H., Plass-Oude Bos, D., Nijboer, F., Nijholt, A.: User experience evaluation of brain-computer interfaces. In: Allison, B.Z., et al. (eds.) *Towards Practical Brain-Computer Interfaces: Bridging the Gap from Research to Real-World Applications*, pp. 223–237. Springer, Heidelberg (2012)
18. Le Groux, S., Manzolli, J., Verschure, P.F.M.J., Sanchez, M., Luvizotto, A., Mura, A., Valjamäe, A., Guger, C., Prueckl, R., Bernardet, U.: Disembodied and collaborative musical interaction in the multimodal brain orchestra. In: *Conference on New Interfaces for Musical Expression (NIME 2010)*, pp. 309–314 (2010)
19. Leslie, G., Mullen, T.: MoodMixer: EEG-based collaborative sonification. In: Jensenius A.R., Tveit, A., Godøy, R.I., Overholt, D. (eds.) In: *Proceedings 11th International Conference on New Interfaces for Musical Expression (NIME)*, pp. 296–299. Oslo, Norway (2011)
20. Maby, E., Perrin, M., Bertrand, O., Sanchez, G., Mattout, J.: BCI could make old two-player games even more fun: a proof of concept with “Connect Four”. *Adv. Human Comput. Interact.* **2012**(124728), 8 (2012)
21. Makeig, S., Leslie, G., Mullen, T., Sarma, D., Bigdely-Shamlo, N., Kothe, C.: First demonstration of a musical emotion BCI. In: D’Mello, S., Graesser, A., Schuller, B., Martin, J.-C. (eds.) *Proceedings of the 4th international conference on Affective computing and intelligent interaction (ACII’11), Part II*. Lecture notes in computer science, vol. 6975, pp. 487–496. Springer, Heidelberg (2011)
22. Mann, S., Fung, J., Garten, A.: DECONcert: making waves with water, EEG, and music. In: Kronland-Martinet, R., Ystad, S., Jensen, K. (eds.) *Computer Music Modeling and Retrieval, 4th International Symposium, CMMR 2007*. Lecture notes in computer science, vol. 4969, pp. 487–505. Springer, Heidelberg (2008)
23. Mealla, S., Väljamäe, A., Bosi, M., Jordà, S.: Let me listen to your brain: physiology-based interaction in collaborative music composition. In: *CHI 2011 Workshop paper*, pp 1–4 (2011)
24. Mühl, C., Chanel, G., Allison, B., Nijholt, A.: A survey of affective brain computer interfaces: principles, state-of-the-art, and challenges. *Brain Comput. Interfaces* **1**(2), 66–84 (2014)
25. Müller, J.V.: Lindenberger U (2012) Intra- and interbrain synchronization and network properties when playing guitar in duets. *Front Hum Neurosci.* **6**(3), 12 (2012)
26. Nijholt, A., Oude Bos, D., Reuderink, B.: Turning shortcomings into challenges: brain-computer interfaces for games. *Entertainment Comput.* **1**(2), 85–94 (2009)
27. Nijholt, A., Allison, B.Z., Jacob, R.K.: Brain-computer interaction: can multimodality help? In: *13th International Conference on Multimodal Interaction*, Alicante, Spain, pp. 35–39. ACM, NY, USA, Nov 2011
28. Nijholt, A., Gürkök, H.: Multi-brain games: cooperation and competition. In: Stephanidis, C., Antona, M. (eds.) *Proceedings Universal Access in Human-Computer Interaction. Design*

- Methods, Tools, and Interaction Techniques for Inclusion. Lecture notes in computer science, vol. 8009, pp. 652–661. Springer, Heidelberg (2013)
29. O'Hara, K., Sellen, A., Harper, R.: Embodiment in brain-computer interaction. In: Proceedings of the SIGCHI Conference on Human Factors in Computing Systems (CHI'11), pp. 353–362. ACM, NY, USA
30. Plass-Oude Bos, D., Reuderink, B., van de Laar, B., Gürkök, H., Mühl, C., Poel, M., Nijholt, A., Heylen, D.: Brain-computer interfacing and games. In: Tan, D., Nijholt, A. (eds.) Brain-Computer Interfaces: Applying Our Minds to Human-Computer Interaction, pp. 149–178. Springer, London (2010)
31. Poli, R., Cinel, C., Matran-Fernandez, A., Sepulveda, F., Stoica, A.: Towards cooperative brain-computer interfaces for space navigation. In: Proceedings of the 2013 International Conference On Intelligent User Interfaces (IUI '13), pp. 149–159. ACM, New York, NY, USA (2013)
32. Pope, A.T., Stevens, C.L.: Interpersonal biocybernetics: connecting through social psychophysiology. Proceedings of the 14th ACM International Conference on Multimodal Interaction (ICMI '12), pp. 561–566. Santa Monica, CA, USA, ACM, NY, USA (2012)
33. Rao, R.P.N., Stocco, A.: Direct brain-to-brain communication in humans: A pilot study. <http://homes.cs.washington.edu/~rao/brain2brain/experiment.html>. Accessed 5 June 2014
34. Reuderink, B., Poel, M., Nijholt, A.: The impact of loss of control on movement BCIs. IEEE Trans. Neural Syst. Rehabil. Eng. **19**(6), 628–637 (2011)
35. Rosenboom, R. (ed.): Biofeedback and the arts: results of early experiments. Aesthetic Research Centre of Canada, Vancouver (1976)
36. Sobell, N.: Streaming the brain. IEEE Multimedia **9**(3), 4–8 (2002)
37. Stephens, G.J., Silbert, L.J., Hasson, U.: Speaker-listener neural coupling underlies successful communication. Proc. Natl. Acad. Sci. U.S.A. **107**(32), 14425–14430 (2010)
38. Stevens, R., Galloway, T., Berka, C., Behneman, A.: A neurophysiologic approach for studying team cognition. In: Proceedings Interservice/Industry Training, Simulation, and Education Conference (IITSEC), pp 1–8 (2010)
39. Stoica, A.: MultiMind: multibrain signal fusion to exceed the power of a single brain. In: Proceedings 2012 Third International Conference on Emerging Security Technologies, PP. 94–98. IEEE Computer Society, Lisbon, Portugal (2012)
40. Szafir, D., Mutlu, B.: Pay attention! Designing adaptive agents that monitor and improve user engagement. Proceedings of the SIGCHI Conference on Human Factors in Computing Systems (CHI'12), Austin, TX, USA, May 2012, pp. 11–20. ACM, New York, USA (2012)
41. Vidal, J.J.: Toward direct brain-computer communication. Ann. Rev. Biophys. Bioeng. **2**, 157–180 (1973). doi:[10.1146/annurev.bb.02.060173.001105](https://doi.org/10.1146/annurev.bb.02.060173.001105)
42. Wang, Y., Jung, T.P.: A collaborative brain-computer interface for improving human performance. PLoS ONE. [www.plosone.org](http://www.plosone.org) **6**(5), e20422:1–11 (2011)
43. Yuan, P., Wang, Y., Gao, X., Jung, T.-P., Gao, S.: A collaborative brain-computer interface for accelerating human decision making. In: Stephanidis, C., Antona, M. (eds.) Proceedings Universal Access in Human-Computer Interaction: Design Methods, Tools, and Interaction Techniques for eInclusion. Lecture notes in computer science, vol 8009, PP. 672–681. Springer, Heidelberg (2012)
44. Yuan, P., Wang, Y., Gao, X., Jung, T.-P., Gao, S.: A collaborative brain-computer interface for accelerating human decision making. In: Stephanidis, C., Antona, M. (eds.) Proceedings Universal Access in Human-Computer Interaction: Design Methods, Tools, and Interaction Techniques for eInclusion. Lecture notes in computer science, vol. 8009, PP. 672–681. Springer, Heidelberg (2013)
45. Yuill, N., Rogers, Y. Mechanisms for collaboration: a design and evaluation framework. ACM Trans. Comput. Human Interact. **19**(1), Article 1 (2012)

# **Chapter 13**

## **Mood Recognition System Using EEG Signal of Song Induced Activities**

**Rakesh Deore and Suresh Mehrotra**

**Abstract** Music is referred to as language of emotions. Music induces emotion in the brain. These emotions are subject not only types of music, but also the sensitivity of the person subjected to music. Dissimilar cases of songs as relax, patriotism, happiness, romantic or sadness will induce different types of brain activities generating different EEG signals. EEG signal is applied to measure electrical activity of the brain. These EEG signal contain precious information of the different moods of subject. In this work, we proposed a mood recognition system using EEG signal of Song Induced activity. The main purpose is to analyze alpha rhythm of EEG signal related to the left hemisphere, and right hemisphere regions of the brain. We have selected 10 male subjects in the age group of 20–25. The electrodes placed on the scalp of the subject as per the International 10–20 standard. Each test was conducted for 25 min, with eye closed and each subject was asked to concentrate on the given tasks. In this study, we have created EEG dataset containing data of five mental tasks of ten different subjects. We determine the alpha rhythms in the left hemisphere are more predominant over the right hemisphere for emotions. Thus we conclude that the left region of the brain gives more response to the emotions rather than the right region. Here we reduce the EEG database from brain region to left hemisphere. Further we reduce it to single electrode as F7 which reside in left region. The database generated in our study may be used to interface the brain with computer to mood recognition system. This will have wide varieties of applications in the future. For example, the entertainment industries may use it for composition of songs as per their effect on the brain. This study also shows that alpha power frequency carries useful information related to mood recognition. These features are separated using Linear Discriminate Analysis.

**Keywords** Human Computer Interaction • Electroencephalography • Brain Computer Interaction • Alpha Power • Music • Linear Discriminate Analysis

---

R. Deore (✉)

Department of Computer Science, P.R. Ghogrey Science College, Dhule, India  
e-mail: rakeshsdeore@gmail.com

S. Mehrotra

Department of Computer Science, Babasaheb Ambedkar University, Aurangabad, India  
e-mail: sureshmehrotra16@gmail.com

### 13.1 Introduction

The Human Computer Interaction (HCI) is media of communication between the individual user and the computer [39]. There is currently no agreement upon definition of range of topics which forms the area of HCI. Based on the definition given by the ACM special Interest group on Computer Human curriculum development it states that, Human Computer Interaction is a discipline concerned with the design evaluation and implementation of interactive computing systems for human use in a social context and with study of major phenomenon surrounding them [13, 40]. The main objective of HCI is to invent new interfaces of computer and make it more usable in daily life. For the last few years, it inspired new solutions primarily for the benefits of user as a human being. One motivation for doing research on HCI is to influence the design of future systems. This study can have its most significant effect on future design. It reveals the aspects of human tasks and activities most in need and discovers efficient ways to provide it. Such research can be vital to synthesis and invention of computer use. HCI provides the methodology and process for creating interface, methods for implementing interfaces. It minimizes the barrier of communication between user and Machine. It develops new interfaces and interaction techniques. Researchers in HCI are developing new design methodologies and experimenting with new hardware devices. Brain Computer Interfacing (BCI) is one of the important area under HCI. It is challenging area of research in which communication to computer system can be performed through thought process. In a 1875, Richard Caton was the first person who discovers the presence of electrical currents in the brain. He studied action potentials from the exposed brains of rabbits and monkeys [41]. In 1924, a German neuropsychiatric Hans Berger used his ordinary radio equipment to amplify the brains electrical activity measured on the human scalp. This was the first Electroencephalogram (EEG) recording of humans. He showed that weak electric currents generated in the brain can be recorded without opening the skull, and depicted graphically on a strip of paper [37]. The action that he observed changes according to the functional status of the brain, such as during sleep, anesthesia, lack of oxygen and in particular neural diseases such as in epilepsy. He was correct in his assertion that brain activity changes in a consistent and recognizable way when the general situation of the subject changes, as from relaxation to alertness [9]. Berger was the first to use the word electroencephalogram to describe the brain electric potentials in humans [5]. He laid the foundations for many of the present applications for EEG. He was the father of EEG. Now a day Electroencephalogram (EEG) is the electrical activity of an alternating type. Brain structures generated EEG. Metal electrodes and conductive media records the EEG signal [32]. EEG measured directly from the cortical surface using electrodes is the electrocardiogram (ECOG) while when using a depth probe is electro gram [6]. BCI technology provides a direct interface between a brain and a computer. In the first international BCI workshop held in June 1999 in Rensselaerville, New York involving 22 research groups, a formal definition of the term BCI was set forward [43].

A brain-computer interface is a communication system that does not depend on the brains normal output pathways of peripheral nerves and muscles.

In basic terms, a BCI involves monitoring brain activity (via a brain imaging technology) and detecting characteristic brain pattern alterations that the user controls in order to communicate (via digital signal processing algorithms) with the outside world [35, 43]. In a BCI, messages and commands expressed not by muscle contractions as with conventional communication means, but rather by electrophysiological signals generated within the brain [2, 9]. Communication through thought process needs to understand brain functioning. It also involves through understanding of electrical signals generated in brain due to thought process. The brain may externally access through monitoring it via electroencephalogram (EEG) signals. The important task is to understand the thought process through EEG signals. If one can correlate thought process through EEG signals, it is possible to monitor thought process through electroencephalogram (EEG) signals. Extensive research has been carried out in the domain taking different types of controlled thought process. Number of different researchers built the mood recognition system using visual stimuli such as facial expression [3, 7, 11] and video clips [22, 25, 31]. Music induces emotion in mind [10]. These emotions are dependent not only types of music, but also sensitivity of the person subjected to music. Different types of songs like patriotism, happiness, romantic or sadness will induce different types of brain activities generating different EEG signals. Features from these EEG signals may be extracted to identify different types of music. Thus music is powerful generator of emotions which activates the different brain regions. Based on this basic principle, it is possible to design a system which offers mood recognition system.

The remainder of the chapter is organized as follows: Sect. 13.2 describes literature survey. Section 13.3 explains the basic components of BCI system. Materials and Methods are given in Sect. 13.4. Section 13.5 describe the EEG data analysis. In this section we process EEG data of different brain regions. Section 13.6 discussed the conclusion of work.

## 13.2 Literature Survey

Number of different researchers work to associate music and EEG signals to develop mood recognition system. Ito et al. [18] proposed the EEG analysis method by using the Fractal Analysis (FA) and the Neural Network (NN). They were used FA to extract the characteristics data of the EEG. These EEG data characteristics were estimated using NN. The classification of the EEG pattern were done by computer simulations. The EEG pattern was classified under four conditions, which were listening to Rock music, Schmaltzy Japanese ballad music, Healing music, and Classical music [18]. Huisheng et al. [17] processed the EEG signal and found the location in brain when a person was enjoying different rhythm music. They acquired the EEG signal with Phoenix Digital EEG system having 128 channels.

These signals were compared with the ones before the subjects enjoying the music. They found Significant differences between these signals [17]. Karthick et al. [21] were classified the effect of two types of music on the electroencephalogram (EEG) activity. They were examined, under Indian Carnatic classical and rock music. They studied about 300 s of EEG data. The analyse EEG data using the detrended fluctuation analysis (DFA) algorithm, and multiscale entropy (MSE) method. They found that both methods showed significant difference in the electroencephalogram of with and without music. They state that MSE method showed higher values of entropy for both types of music, indicating that the complexity of the electroencephalogram increased with the brain processes music [21]. Ito et al. [19] proposed a method for detecting the mood using music. They analyzed EEG frequencies containing significant and immaterial information components. These frequency combinations were thought to express personal features of EEG activity. In the proposed method, they calculated the spectrum of these frequency combinations rates that did not include the noise frequency components. It was evaluated whether the music had matched the user's mood through a simple threshold processing. They were used a genetic algorithm (GA) [19]. Yuan-Pin et al. [44] investigated an approach to recognize the emotion responses during multimedia presentation using the electroencephalogram (EEG) signals. The association between EEG signals and music-induced emotion responses was investigated in three factors, including: (1) the types of features, (2) the temporal resolutions of features, and (3) the components of EEG. The results showed that the spectrum power asymmetry index of EEG signal was a sensitive marker to reflect the brain activation related to emotion responses, especially for the low frequency bands of delta, theta and alpha components. Besides, the maximum classification accuracy was obtained around success rate of 92.73 % by using support vector machine (SVM) based on 60 features derived from all EEG components with the feature temporal resolution of one second. As such, it was able to provide key clues to develop EEG-inspired multimedia applications, in which multimedia contents could be offered interactively [44]. Vijayalakshmi et al. [42] explained the acute central system effects of relaxation techniques. They conducted a study of the EEG patterns of 10 subjects who were given an audio stimulus of Alpha music. The EEG was acquired using BI-OPAC Student Lab with suitably placed silver/silver chloride electrodes to study the effects of Alpha music on Alpha and Beta rhythms of the subjects. Research showed Alpha waves were predominantly observed in healthy relaxed individuals. Since anxiety and stress were major emotional contents of human beings, the goal of this experiment was to assess the means of relaxation and concentration using Alpha music, which influenced the alpha and beta rhythms significantly. For each subject, three EEG recordings were taken. One before the alpha music stimulus, one after 6 min of Alpha music and the last towards the end of alpha music. There was an increase in the maximum amplitudes of Alpha waves either after 6 min or after 12 min of alpha music. However, the maximum amplitude of beta waves showed a decline of up to 40. Yun-Pin et al. [45] performed the EEG based experiments to study the ongoing brain activity between emotional states and brain activity. This study was applied to machine-learning algorithms to categorize EEG dynamics

according to subject self-reported emotional states during music listening. A framework was proposed to optimize EEG-based emotion recognition by systematically (1) seeking emotion-specific EEG features and (2) exploring the efficacy of the classifiers. Support vector machine was employed to classify four emotional states (joy, anger, sadness, and pleasure) and obtained an averaged classification accuracy of 82.29. As one can see from the extensive work done in classification of the EEG signals as per mood induced by some external effect. There was no work done earlier related to effect of Indian music in inducing different types of music. One of the objectives in our work was to understand EEG signals induced by different types of music in different subjects. It involves (a) designing experiments to acquired EEG signals, (b) extracting features from these acquired signals and (c) classifications of the features as per mood induced by songs.

### 13.3 Experimental Setup

For the study, 10 subjects were selected. They were explained the purpose of the experiments. Songs selected were categorized in four groups as per their popular classification. These songs are listed in Table 13.1. All subjects were familiar with these songs and were agreed with classification of the songs. Brain signals measured from 19 electrodes mounted on the scalp. To exclude the possibility of influence from non central nervous system activity, EMG recorded additionally. Those channels used to remove noise from EEG signal.

#### 13.3.1 EEG Equipments

The primary EEG recording system consists of electrodes with conductive media, amplifiers with filters, an analog-to-digital (A/D) converter and a recording device to store the data. In conjunction with the electrode gel electrodes sense the signal from the scalp surface. Amplifiers bring the Micro volt and Nano volt signals in a range where they can be digitized accurately. The A/D converter changes signals from analog to digital form. That can be ultimately stored or viewed on a computer. An electrode is an electrical conductor used to make contact with a nonmetallic part of a circuit [20].

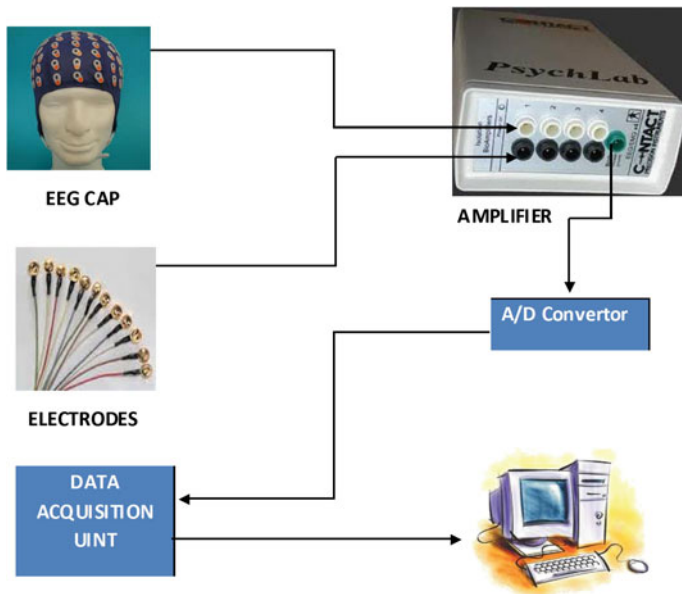
In the case of EEG, electrodes provide the interface between the skin and the recording apparatus. It transforms the ionic current on the skin to the electrical current in the electrode. Conductive electrolyte media ensure a good electrical contact by lowering the contact impedance at the electrode interface [36]. In the scalp recorded EEG, the neuronal electrical activity recorded non-invasively using small metal plate electrodes. Recordings can be made using either reference electrodes or bipolar linkages. The number of the electrodes used may vary from one study to another study. The voltages, of the order of Micro volts (V), must be carefully recorded to avoid interference and digitized so that it can be stored and

**Table 13.1** Mental tasks with their description

Sr. no	Mental task	Description
1	Relax	Subject was asked to lie on bed without any activity
2	Happy	Subject listen to the happy mood song such as 1. Koyal Boli Duniya Doli Singer:-Lata Mangeshkar and Rafi 2. Meri Zindagi Mein Aaye Ho Singer:-Sonu Nigam and Sunidi Chavhan
3	Sad	Subject listen to the sad mood song such as 1. Tanhaai, tanhaai Singer:-Sonu Nigam 2. Khone Dil Se Wo Mehndi Ratachne Lage Singer:-Poonam Kumar
4	Romantic	Subject listen to the romantic mood song such as 1. Rim Jhim Ke Geet Sawan Singer:-Lata Mangeshkar and Rafi 2. Ajnabii Mujhko Itna Bataa Singer:-Lata Mangeshkar
5	National	Subject listen to the patriotic mood song such as 1. Mere Desh Kee Dharatee, Sonaa Ugale Singer:-Mehendra Kapoor, 2. Yahan Yahan Saara Jahan Dekh Liya Singer:-A.R. Rehman

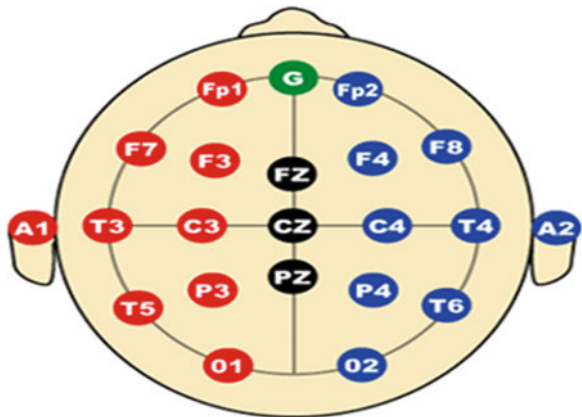
viewed on a computer. The amplitude of the recorded potential depends on the intensity of the electrical source, on its distance from the recording electrodes, its spatial orientation, and on the electrical properties of the structures between the source and the recording electrode. The EEG acquisition system is as depicted in Fig. 13.1. The greatest contributions to the scalp recorded signals result from potential changes which (a) occur near the recording electrodes, (b) produced by cortical dipole layers orientated towards the recording electrode at a 90° angle to the scalp surface, (c) generated in a large area of tissue, and (d) rise and fall at rapid speed [6] (Fig. 13.2).

Figure 13.3 shows the 10/20 system. This system is an internationally recognized method for electrode placement. It describes the location of scalp electrodes. The system based on the relationship between the locations of an electrode and the underlying area of the cerebral cortex. The Number 10 and 20 refers to the fact that the distances between adjacent electrodes are either 10. It allows measurement of potential changes over time in a primary electrical circuit conducting between signal (active) electrode and reference electrode. An extra third electrode called as the ground electrode required for getting a differential voltage. An amplifier records this voltage. It subtracts the active and reference channels from it. The placement of the ground electrode plays a significant role in the measurement. Typically the forehead



**Fig. 13.1** EEG acquisition system

**Fig. 13.2** An international 10–20 system of electrode placement



(FPz), ear lobe, wrist or leg is the preferred ground location. The EEG recordings can be divided into two primary categories: reference recordings and scalp-to-scalp bipolar linkages. In the reference recording, each electrode referred to either a distant reference electrode, one common electrode on each side of the head or to the combined activity of two or more electrodes. The reference electrode must be placed on the parts of the body where the electrical potential remains fairly constant. The most preferred reference linked ears as it is relative electrical inactivity, easy to use, and symmetry. The vertex (Cz) is also predominant due to its central location.

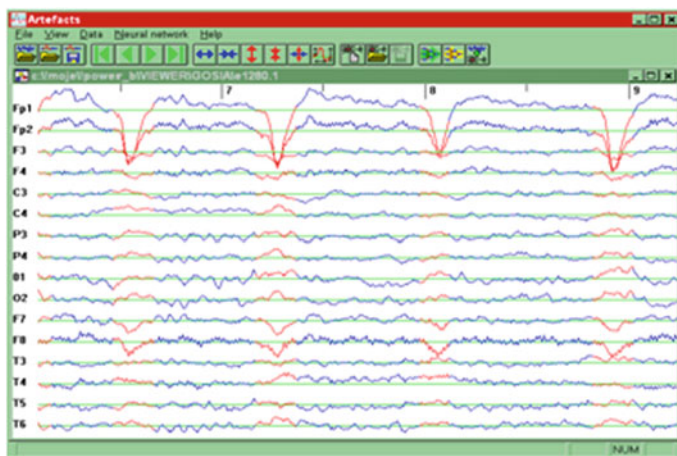


**Fig. 13.3** Sample EEG signal with artifacts

Reference-free methods represented as a common average reference, weighted average reference, and source derivation. These methods use the average or the weighted average of the activity at all electrodes as the reference. This can be carried out by means of a resistor network or digitally as part of the post - processing method. These do not suffer the same artifact problems associated with an actual physical reference. Bipolar recordings are differential measurements made between successive pairs of electrodes [16, 38]. Bipolar referencing is not commonly used due to placement issues and a lack of spatial resolution.

### 13.3.2 Artifacts

Artifacts are undesirable potentials of non-cerebral origin that contaminate the EEG signals [12]. As they can misinterpret as originating from the brain, there is a need to reduce or ideally remove them from the EEG recording to facilitate accurate interpretation. Typical EEG artifacts originate from two sources, technical and physiological [34].

Technical artifacts are mainly due to line interference, equipment malfunction or result from poor electrode contact. Incorrect gain, offset or filter settings for the amplifier will cause clipping, saturation or distortion of the recorded signals. Technical artifacts can be avoided through proper apparatus set-up, meticulous inspection of equipment and consistent monitoring. Physiological artifacts arise from a variety of bodily activities that are either due to movements, other bioelectrical potentials or skin resistance fluctuations. The predominant physiological artifacts include (1) Electro oculographic activity (EOG, eye) (2) Scalp recorded electromyography activity (3) Electrocardiographies activity (ECG, heart). These artifacts are always present to

some extent and are typically much more prominent on the scalp than the macroscopic cerebral potentials. This results an undesirable negative signal-to-noise ratio in the EEG. Physiological artifacts are often involuntary and hence cannot be controlled or turned off during acquisition. They pose a much greater challenge than technical artifacts to avoid or remove them. For the purposes of BCI system design, there exist various EEG signal properties that discriminate brain function. The next section focuses on one of the EEG signal category as a Rhythmic Brain activity.

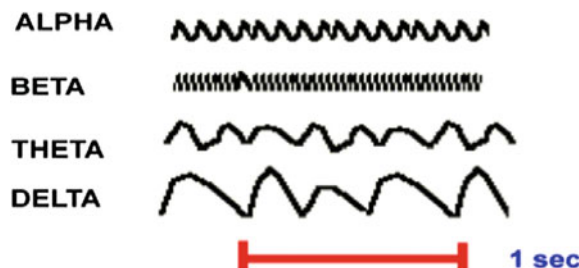
### 13.3.3 Rhythmic Brain Activity

Frequency is one of the most significant criteria for assessing abnormality in clinical EEG and for understanding functional behavior in cognitive research [34]. With billions of oscillating communities of neurons as its source, the human EEG potentials are manifested as periodic unpredictable oscillations with intermittent bursts of oscillations having spectral peaks in certain observed bands: 0.1–3.5 Hz (delta,  $\delta$ ), 4–7.5 Hz (theta,  $\theta$ ), 8–13 Hz (alpha,  $\alpha$ ), 14–30 Hz (beta,  $\beta$ ).

Figure 13.4 illustrates examples of these EEG rhythms. The band range limits associated with the brain rhythms, particularly beta can be subject to contradiction and are often further sub-divided into sub-bands that can further distinguish brain processes [23, 24].

- (a) Delta ( $\delta$ ) The frequency range of delta brain rhythm is in between 0.1 and 4. Its normal amplitude is <100 (V). This frequency is dominant in infants during deep stages of adult sleep and serious organic brain diseases. These frequency occurs after transaction of the upper brain stem separating the reticular activating system.
- (b) Theta ( $\theta$ ) The frequency range for theta is between 8 and 13. Its normal amplitude in 20–60 (V). They are Rare in EEG of awake adults. These frequencies are dominant during emotional stress in some adults.
- (c) Alpha ( $\alpha$ ) The frequency range of alpha is between 8 and 13. Its normal amplitude is in 20–60 (V). They are fully present when a subject is mentally inactive, alert, with eyes closed. Blocked or attenuated by deep sleep, attention. When a person is alert and their attention is directed to a specific activity, the alpha waves are replaced by waves of higher frequency and lower amplitude. Eye opening/closure offers the most effective manipulation.

**Fig. 13.4** Examples of an EEG rhythm



- (d) Beta ( $\beta$ ) The frequency range of beta is between 14 and 30. Its normal amplitude is less than 20 (V). Beta I waves have lower frequencies, which disappear during mental activity. Beta II waves have higher frequencies, appear during tension and intense mental activity.

### ***13.3.4 Application of EEG***

This section highlights the many clinical and cognitive research applications that have been established over the years for EEG. In his original papers, Hans Berger laid the foundations for most of today's clinical uses for EEG. The greatest advantage of EEG over other brain imaging technologies is speed and cost. Complex patterns of neural activity can be recorded with millisecond resolution.

According to Bickford [4] research and clinical applications of the EEG in humans and animals are to:

- Monitor alertness, coma and brain death.
- Locate areas of damage following head injury.
- Test afferent pathways (by evoked potentials).
- Monitor cognitive engagement (alpha rhythm).
- Produce biofeedback situations, alpha, etc.
- Control anesthesia depth (servo anesthesia).
- Investigate epilepsy and locate seizure origin.
- Test epilepsy drug effects.
- Assist in experimental cortical excision of epileptic focus.
- Monitor human and animal brain development.
- Test drugs for convulsive effects.
- Investigate sleep disorder and physiology.

Though the EEG has a reduced spatial resolution, it has an excellent temporal resolution of less than a millisecond [15]. It is also relatively inexpensive and simple to acquire. So it is the only practical non-invasive brain imaging modality for repeated real-time brain behavioral analysis. For this reason, the remainder of this thesis will focus on EEG as the input brain imaging modality for HCI design. The next section explains the anatomical and physiological structure of the brain.

### ***13.3.5 Human Brain***

This section explains the anatomical and physiological structure of the brain. It focuses on how the brain generates electrical activity that can be recorded on the scalp. In order to understand the generation of electrical current, we must first look at the fundamental of the brain cell, the neuron.

### 13.3.5.1 The Neuron

In the EEG, the potentials are due to the summation of the electrical potentials of many brain nerve cells, called neurons [15]. The human brain at birth consists of approximately 100-billion (10<sup>11</sup>) neurons at an average density of 104 neurons per cubic mm [36]. The number of neurons decreases with age [33]. Neurons share the same characteristics and have the same parts as other cells, but the electrochemical aspect lets them transmit electrical signals and pass messages to each other over long distances. Neurons have three basic parts. Its parts are illustrated in Fig. 13.5.

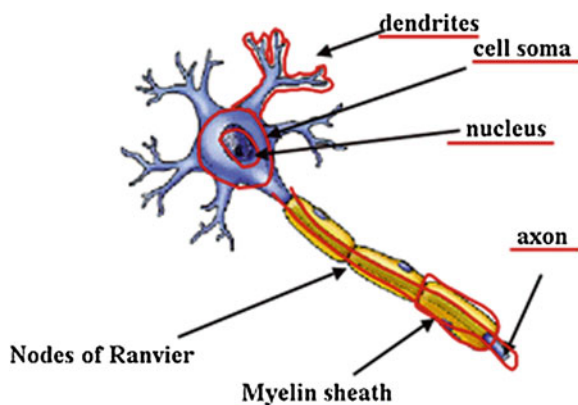
**Cell Body**—This central part has all of the necessary components of the cell, such as the nucleus (contains DNA), endoplasmic reticulum and ribosome (for building proteins) and mitochondria (for supplying energy). If the cell body dies, the neuron dies.

**Axon**—This long, cable-like projection of the cell carries the electrochemical message (action potential—AP) along the length of the cell.

**Dendrites**—These small, branch-like projections of the cell make connections to other cells and allow communication with other neurons. Dendrites can be located on one or both ends of the cell.

There exist different types of neurons that can have varying structures depending on their functionality. Sensory, motor and cortical pyramidal cell neurons are examples of such different types. The pyramidal neuron cell is the most prevalent neuron cell in the cerebral cortex, particularly in the cortical peaks and valleys (gyri and sulci respectively) that are parallel to the scalp. It is the key neuron structure responsible for the most electrical activity recordable by EEG. It has a long straight dendrite that extends up perpendicularly towards the surface of the brain. Hence most neurons in the cerebral cortex have parallel dendrites, which cause a summation of potentials in one direction. In inter-neuron communication system, electrical activity consists mostly of  $\text{Na}^+$ ,  $\text{K}^+$ ,  $\text{Ca}^{2+}$  and  $\text{Cl}^-$  ions that are pumped through channels in neuron membranes in the direction governed by the membrane potential [30]. When neurons activated by means of an electrochemical

**Fig. 13.5** General structure of neuron



concentration gradient, local current flows produced. The electrical activity of neurons can be divided into two subsets: action potentials (AP) and postsynaptic potentials (PSP). If the PSP reaches the threshold conduction level of the postsynaptic neuron, the neuron fires and an AP initiated. The electrical potentials generated by low frequency summed inhibitory and excitatory PSPs from pyramidal neuron cells. It creates electrical dipoles between the soma and apical dendrites. These PSPs summate in the cortex and extend to the scalp surface where they recorded as the EEG. Nerve cell APs have a much smaller potential field distribution and are much shorter in duration than PSPs. APs do not contribute significantly to either scalp or clinical intracranial EEG recordings. Only large populations of active neurons can generate electrical activity recordable on the scalp. Alison et al. [1] lists four prerequisites, which must be met for the activity of any network of neurons to be visible in an EEG recording:

- i. The neurons must generate most of their electrical signals along an axis oriented perpendicular to the scalp.
- ii. The neuronal dendrites must be aligned in parallel so that their field potentials summate to create a signal which detectable at a distance.
- iii. The neurons should fire in near synchrony.
- iv. The electrical activity produced by each neuron needs to have the same electrical sign. Thus a majority of neuronal communication remains invisible to EEG [1].

### **13.3.6 BCI Framework**

This section highlights and explains the functional components involved in an EEG-based BCI system. The basic components required for implementation are depicted in Fig. 13.6 and summarized as follows:

The data acquisition stage involves the recording of the raw EEG data from electrodes at specific locations on the scalp that form the input to the BCI system [8]. Choices such as the number, position and density of electrodes determine the input channels. The pre-processing stage of the acquisition process involves amplification, analog filtering and A/D conversion. The next stage is an optional information optimization stage that involves improving the signal-to-noise ratio (SNR) by removing artifacts and reducing information redundancy from the EEG channels.

Feature extraction is the most important stage to any BCI. It involves the development of command-dependent discriminatory features of the pre-processed EEG signals by employing DSP algorithms to identify with command-related activity. It is this stage that often characterizes the BCI design approach. If robust features that are resilient to artifacts and the volumetric smearing effect of the neuronal signals can be extracted, the need for the previous information optimization stage is reduced. It also reduces the challenge on the classifier to discriminate

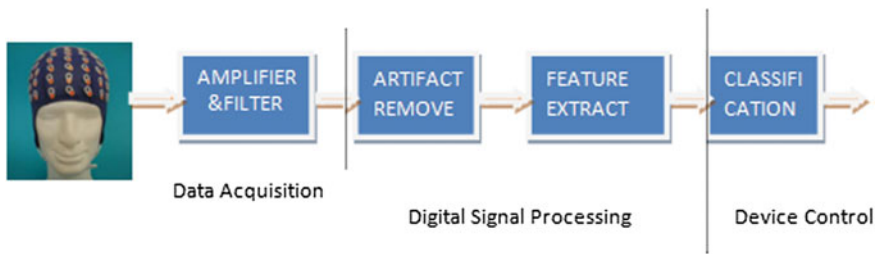


**Fig. 13.6** Functional components of EEG based BCI systems

between the features of different controls. It is important to note that the experimental paradigm is as crucial as the feature extraction methods for the consistent elicitation of physiological brain patterns.

The classification or feature translation stage involves the identification of the feature patterns to facilitate the categorization of the users commands [43]. It can be anything from a simple threshold or linear model to a complex nonlinear neural network based classifier that can be trained to categorize the features according to the control selection. Most classifiers are based on a probabilistic approach whereby the class of highest probability is chosen. A nothing class can be included to offer a no selection instead of a control.

The output of the classification stage is the controlling input of the device. The device control transforms the classification into a device action. The output of the classification stage may instruct the device that no appropriate control was classified and hence to perform no action. Mason [27] proposed a general framework for brain-computer design in the hope of standardizing terminology and functional models to facilitate the benchmarking of BCI systems. They proposed the generic functional model for a BCI system in Fig. 13.7. They stressed the importance of having such a model to compare the performance of BCI communication technologies within the research community [27].

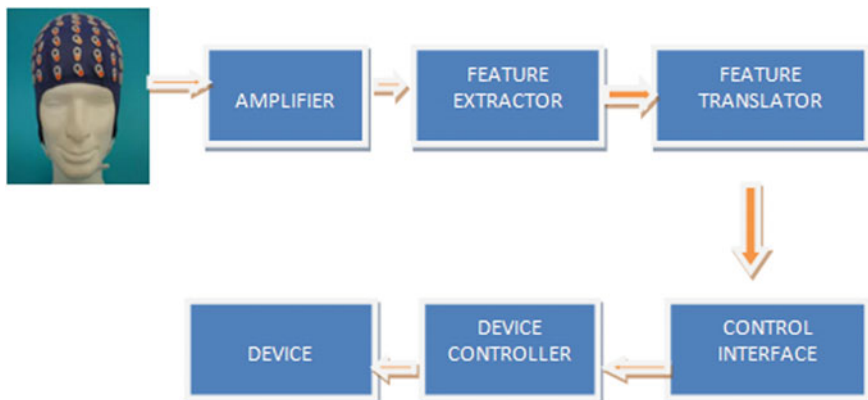


**Fig. 13.7** Proposed functional model of EEG based BCI systems

With the explanation of the various components of a BCI system listed above, the question still remains about how the BCI design process begins and how all these components interlink. The preliminary stage to any BCI requires an investigation into the paradigm and the brain activity which one hopes to generate to offer distinguishable controls [48]. This requires recording numerous sessions or trials of data to later examine for distinguishable features. The averaging of trials at the time or frequency domain is initially carried out in the hope of observing a general characteristic pattern. The greatest challenge is to see if this characteristic activity can be elicited on a single-trial basis or over a small segment of continuous EEG data. The feature extraction methods must be employed to represent EEG characteristics by a number of values that can distinguish the different brain activity and resulting controls on a single-trial or online basis. Thus a BCI system can be designed using this human-controlled EEG activity alteration to offer control.

### ***13.3.7 Categorization***

This section aims to highlight a number of ways to describe or characterize a BCI system while at the same time identifying and explaining the various options.

**Invasive or Non-invasive BCI:** Electric currents produced by synchronizing synaptic currents within the brain. It can be measured by (list by order of increasing invasiveness) scalp recorded EEG which uses epidural electrodes or intra cortical electrodes known as electrocorticography (ECoG). Scalp recorded EEG based BCIs are most common because they are non-invasive and cheap. Intra cortical electrodes achieve higher spatial resolution at the expense of spatial coverage and significant increase in cost and risk. Single neuron cortical activity has been successfully applied in BCI systems [14, 26]. Aside from the practical issues such as cost, invasiveness and comfort, the choice of invasive versus non-invasive recordings depends on the volume of cortical tissue producing useful information, the ability of the intra cortical electrode to locate the appropriate tissue masses, and on the ability of the scalp EEG to produce stable, robust, intentional signals that can be controlled by the user (Figs. 13.8 and 13.9).

**Online or Offline BCI:** The fundamental aspect to a BCI is that it can be implemented in real time to facilitate actual direct user control. Offline systems are for theoretical simulations of an actual BCI system to facilitate exploratory investigations of the BCI components. This makes it possible to examine, for example, different electrode positions, pre-processing and feature extraction methods, classifiers etc. Offline systems quote a predicted or simulated accuracy by employing unbiased methods for separating training and test data, for example cross-fold validation. The performance can be compared with a similarly implemented online BCI without feedback provided that all the recorded EEG Data is used, i.e. no EEG data are rejected containing EOG or EMG artifacts. As most training data during an offline investigation has rejected artifact corrupted trials, the performance could be very different to an actual online real-life implementation where Artifacts and EEG

**Fig. 13.8** *Invasive* electrode placement

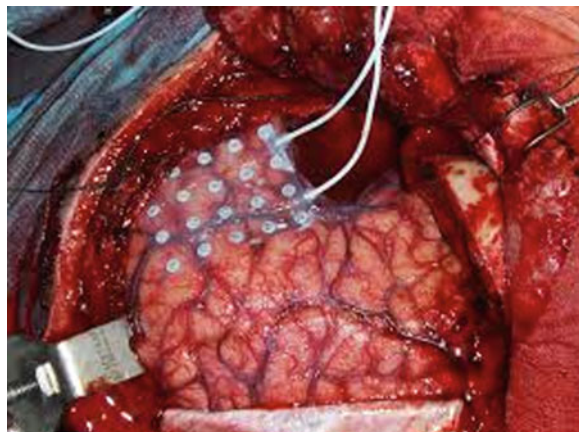
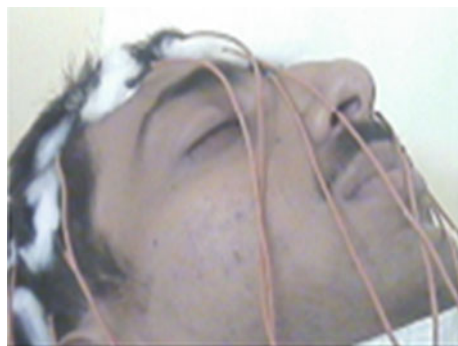


**Fig. 13.9** *NonInvasive* electrode placement



inter-trial variability could cause significant feature outliers that would result in poor control classifications. Online systems require the signal processing components of the BCI framework to be done in real-time. Real-time implemented systems make it possible to provide feedback to the user. As feedback is such an integral part of a BCI framework, particularly in the operant conditioning approach, online systems are the only true indicator of a BCI performance (Fig. 13.10).

**Universal or Individual:** Universal BCIs assume that by gathering EEG data from multiple users it is possible to find features and a classification function that will be valid in general for every user. In individual BCI design, the system is tailored to the individual and the fact that no two individuals are the same both physiologically and psychologically. Adaptive systems such as the Adaptive Brain Interface project [28, 29] boast the adaptability of the system to the user, time and psychological variations. A universal BCI design that is too general will have poor performance.

**Independent or Dependent:** Dependent BCIs rely on upon the ocular activity to generate a specific EEG pattern, i.e. a visual evoked potential (VEP) associated with the direction of visual attention [29]. If a person has the use of their eye muscles, there exist a number of eye-tracking or eye-blinking based methods of



**Fig. 13.10** Online BCI system

communication that offer better performance than BCI systems. Independent BCIs do not require any muscular intervention of any kind to generate the command-related EEG activity. This approach is more closely linked to the definition of a BCI system set out in [43].

**Paradigm:** BCI can be categorized according to what kind of imagery or mental tasks the users are required to perform in order to generate the command-related EEG activity. This choice is closely linked with the type of brain activity or neural mechanism that the BCI designer wishes to exploit. Motor imagery is one of the most common methods of EEG elicitation that has been used in many BCI. It is used to generate sensory motor activity. Mental tasks such as arithmetic or spatial relations have also been used. Visual related tasks have been heavily exploited in the area of P300 and VEP elucidation. BCIs based on the Operant Conditioning approach may leave the choice of imagery or mental strategy up to the user.

### 13.4 Materials and Methodology

Music induces emotion in mind. These emotions are dependent not only kinds of music, but also sensitivity of the person subjected to music. However, songs may be classified as per their overall effect on the mind. For this study, we used the

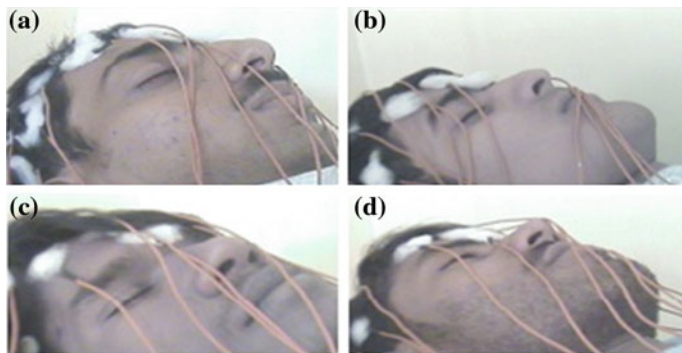


**Fig. 13.11** An example of acquisition of EEG signals

classification based on the basis of songs appeal with respect to patriotism, happiness, romantic or sadness. The Table 13.1 gives names of popular Indian songs as per their general classification as considered in the work. Understanding of induced brain signals due to hearing of music will be essential information for training computers to identify different types of music.

#### 13.4.1 Subject Selection

We have selected 10 male subjects in the age group of 20–25. The subjects were found to be healthy without any mental disorder. They did not have any communication problem. Also, they had healthy vision. All Subjects were instructed to sit comfortably on an armchair in front of the screen in the research lab.

The lab electromagnetically was shielded to minimize the effects of noise. Figure 13.11 shows an example of acquisition of EEG signal.

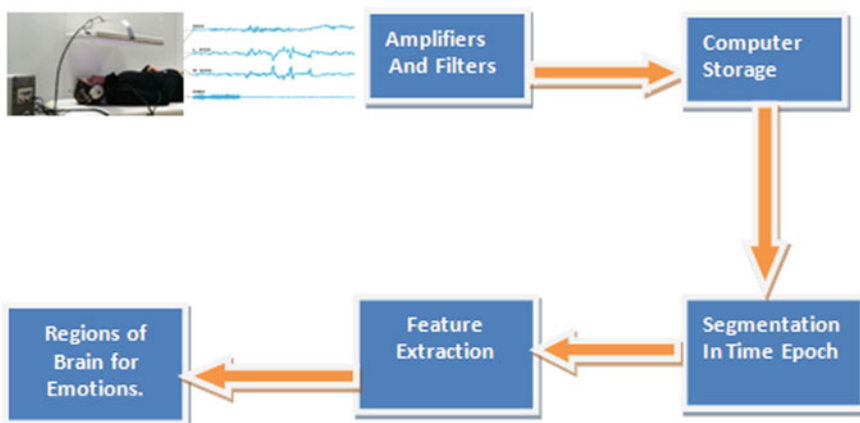


**Fig. 13.12** An overview of proposed offline BCI system for mood recognition

### **13.4.2 Procedure**

All subjects were educated about objective of the experiments. They were told that this experiment had been designed to be used for BCI as mood recognition system. In this study, we have created EEG dataset containing data of five mental tasks of ten different subjects. The electrodes placed on the scalp of the subject as per the International 10–20 standard. Each test was conducted for 25 min, with eye closed and each subject was asked to concentrate on these given tasks. For all modes, the subjects were asked to sit comfortably on a chair along with the headphones. They were told that it is important to change their mood according to song. Subject were carefully listen the different types of music in a quite room. Figure 13.12 shows the proposed model of BCI system for mood recognition.

### **13.4.3 Apparatus and Recording Procedure**

The EEG signals was captured by the commercial available EEG machine, i.e. RMS (Recorders and Medicare Systems) EEG-32 Super Space machine as shown in Fig. 13.13. Each acquisition experiment was recorded for 5 min with sampling rate of 250/s i.e. the sample time between two sample was 4 ms. The other parameters of the EEG machine were set as follows: low filter: 1 Hz, high filter: 70 Hz, sensitivity: 7 V, number of channels: 17, sweep speed: 30 mm/s and Montage: BP PARA (R). As mentioned above, the experiment was conducted on 10 subjects. The electrodes were placed on scalp of the subject as per the international 10–20 standard as given in Fig. 13.2. The data acquisition was done in each case for 5 min. The different parameters of the EEG machine were set as follows: low filter 1 Hz, High filter 70 Hz, sensitivity at 7 V, number of channel 19, sweep speed 30 mm/s, Montage set BPPARA (R) for all the experiments. The EEG signal has been processed by statistical analysis methods such as Principle Component Analysis (PCA) and Linear Discriminate Analysis (LDA).



**Fig. 13.13** Photograph of RMS-EEG-32 Super Spec machine

The Tables 13.2, 13.3, 13.4, 13.5 and 13.6 shows the values of delta ( $\delta$ ), Theta ( $\theta$ ), Alpha ( $\alpha$ ), and Beta ( $\beta$ ) frequency power band during relax, sad, happy, National and Romantic mode respectively. We are interested in different brain regions so the Electrodes are divided according to the brain region as left hemisphere, right hemisphere and center hemisphere. Here we firstly covert the time domain data into frequency domain using Fourier transform as shown in Fig. 13.14.

This frequency domain data is divided into four rhythms: 0.1–3.5 Hz (delta,  $\delta$ ), 4–7.5 Hz (theta,  $\theta$ ), 8–13 Hz (alpha,  $\alpha$ ), 14–30 Hz (beta,  $\beta$ ). Delta wave is associated with deep sleep. It is high amplitude and low frequency wave. Theta corresponds to sleep and Brain Injury. Alpha represents relaxation and alertness. If the alpha frequency is less then it indicated the more activity. It is inversely proportional to degree of alertness. Beta rhythm is more active during the problem solving task. In this study we are concentrating on alpha rhythms. For each rhythm we have calculated the mean frequency of window size equal to 5 as shown in Fig. 13.15.

**Table 13.2** Region wise EEG data of different electrodes in relax mode activity

Electrodes	Relax mode data			
<i>Left</i>	<i>Delta</i>	<i>Theta</i>	<i>Alpha</i>	<i>Beta</i>
FP1	35.61039	3.548158	4.646447	0.525526
F7	2.435526	1.356711	2.459605	0.320921
F3	1.823816	2.045526	2.873289	0.415395
T3	2.969079	1.761447	3.992763	0.478421
C3	2.035263	2.304605	4.400395	0.557632
T5	5.530789	3.101579	6.144342	1.140263
P3	4.788289	2.333026	8.504342	1.171842
O1	5.708026	1.996053	5.090263	0.764737
<i>Right</i>			4.763931	
FP2	29.77434	3.099605	4.6725	0.49
F4	3.448816	2.242368	4.026053	0.472368
F8	2.887632	1.617368	2.942763	0.308289
C4	2.086053	1.879605	3.442632	0.441447
T4	4.182763	2.040526	3.880132	0.433158
P4	5.035658	2.487368	7.784474	1.285395
T6	6.584474	2.996447	6.025921	1.030132
O2	7.614605	2.436053	6.310395	0.911842
<i>Center</i>			4.885609	
FZ	2.515789	2.175658	3.958684	0.424211
Cz	2.623026	2.334868	3.366053	0.460526
P2	4.233158	2.664868	8.147368	1.0475
			5.157368	

**Table 13.3** Region wise EEG data of different electrodes in sad mode activity

Electrodes	Sad mode data			
	<i>Delta</i>	<i>Theta</i>	<i>Alpha</i>	<i>Beta</i>
<i>Left</i>				
FP1	6.848816	2.374474	4.089342	0.470132
F7	2.885395	1.303289	2.219868	0.346316
F3	2.595658	1.481053	2.200263	0.452237
T3	1.996184	1.375921	3.843816	0.538553
C3	2.089737	1.427763	4.206711	0.577895
T5	13.93553	3.692105	4.339079	0.991316
P3	3.6525	1.763289	5.789737	1.073289
o1	8.462237	2.7225	3.890658	0.694211
<i>Right</i>			3.822434	
FP2	7.450921	2.843553	4.218816	0.466316
F4	3.712105	2.457237	3.121447	0.556053
F8	3.702105	1.635395	2.934868	0.349737
C4	1.319474	1.287763	4.211184	0.406711
T4	4.313158	1.749605	4.842368	0.469342
P4	3.222368	1.893026	6.302237	1.011711
T6	3.960658	2.219342	4.456974	0.832632
o2	3.171579	2.123947	4.419211	0.860263
<i>Center</i>			4.313388	
FZ	2.603947	2.181842	3.619342	0.499605
Cz	2.727632	1.904737	3.773289	0.543026
P2	2.792895	2.393158	7.901447	1.152632
			5.098026	

## 13.5 Data Analysis

Table 13.7 denotes the mean values of alpha rhythms in left, right and center regions of brain for different moods.

As we know that alpha rhythm is inversely proportional to the brain activity that is if alpha rhythm is more then it indicates the less activity in brain and if it is less then it indicates the more activity in brain. From table it is cleared that subject has performed more activity in the brain for Happy and National Song mode as compared to sad and Romantic Song mode. Also the alpha value of National Song mode is much lesser as compared to alpha value of other moods, so subjects generates more activity in the brain for National Mode. So we say that the subject is more

**Table 13.4** Region wise EEG data of different electrodes in Happy mode activity

Electrodes	Happy mode data			
	<i>Delta</i>	<i>Theta</i>	<i>Alpha</i>	<i>Beta</i>
<i>Left</i>				
FP1	9.942895	1.728026	2.978684	0.480658
F7	2.081711	0.717105	1.438289	0.255
F3	1.463026	1.026842	1.534737	0.337105
T3	1.769474	0.852368	2.636579	0.386711
C3	1.510921	1.089079	3.345132	0.484079
T5	6.889474	1.824474	3.475395	0.79
P3	2.834079	1.278816	5.437632	1.155789
o1	2.947632	1.389211	2.838684	0.710132
<i>Right</i>			2.960641	
FP2	10.22132	1.861184	3.273158	0.453289
F4	2.782368	1.491579	2.636711	0.485526
F8	4.684342	1.171711	2.186842	0.320263
C4	1.186184	0.913684	2.592105	0.383947
T4	3.015395	1.131053	3.053947	0.419211
P4	4.705	1.277632	4.578816	1.115132
T6	3.001711	1.667237	3.689737	0.784737
o2	3.151974	1.539342	3.039211	0.745526
<i>Center</i>			3.131316	
FZ	2.316842	1.655789	2.643289	0.396974
Cz	2.483289	1.541974	2.266711	0.400526
P2	2.152368	1.694474	5.421316	0.963158
			3.443772	

alert National Song Mode. From Fig. 13.16, it is cleared that the emotional intensity which is inversely proportional to alpha rhythm is more for National mode and decreased from National to Romantic, Romantic to Happy and Happy to Sad mode.

### 13.5.1 Region Wise Data Analysis

This section explains the EEG data analysis in left and right hemisphere.

Table 13.8 gives the distance matrix of mean values of alpha rhythms in right region of brain. From distance matrix it is cleared that sad song mode is closer to relax song mode and the distance between relax mode and national song mode, happy mode and romantic mode is more. Also distance between the sad mode and

**Table 13.5** Region wise EEG data of different electrodes in national mode activity

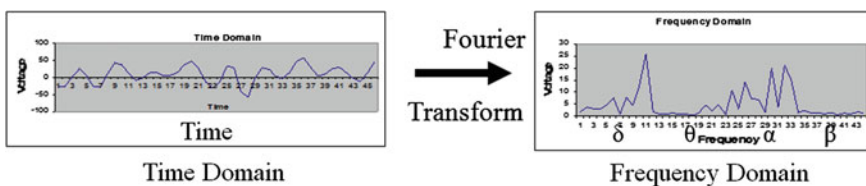
Electrodes	National mode data			
	<i>Delta</i>	<i>Theta</i>	<i>Alpha</i>	<i>Beta</i>
<i>Left</i>				
FP1	12.52684	2.065658	2.268158	0.526711
F7	1.836184	0.887368	1.290526	0.356447
F3	1.803553	1.229474	1.494342	0.418553
T3	2.331053	0.918158	2.456447	0.497237
C3	1.876447	1.110526	2.940395	0.582895
T5	4.679474	1.732368	4.071447	1.028026
P3	4.098684	1.463684	5.681184	1.210658
o1	4.008158	1.473158	2.356789	0.693289
<i>Right</i>			2.819911	
FP2	11.37	2.029342	2.578684	0.491974
F4	2.664868	1.701447	2.423158	0.472763
F8	2.156842	1.229211	1.752895	0.311184
C4	1.668553	1.213684	2.241053	0.441974
T4	3.044342	1.378816	2.455132	0.481447
P4	4.546579	1.64	4.098947	1.548684
T6	3.311974	1.712632	3.537368	1.001447
o2	5.170132	1.579605	3.556447	0.943289
<i>Center</i>			2.830461	
FZ	2.277105	1.811842	2.447632	0.425132
Cz	2.481842	1.651579	2.2875	0.403026
P2	2.704079	1.878026	4.415526	1.011579
			3.050219	

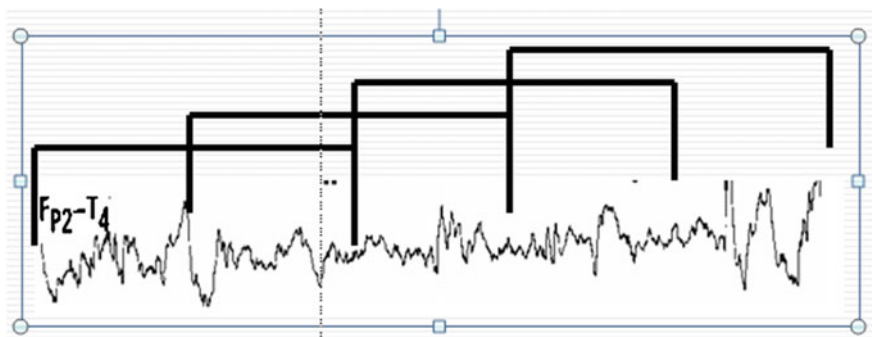
happy mode, romantic mode and National mode is more. Thus we say that the subject is more relaxed in sad song mode and more alert in national song mode (Table 13.9).

Table 13.8 gives the distance matrix of mean values of alpha rhythms in left region of brain. From distance matrix it is cleared that sad song mode is closer to relax song mode and the distance between relax mode and national song mode is more. Subject is more relaxed in sad song mode and more alert in national song mode. This shows that the EEG signal carries useful information related to different moods of a person. EEG signal contains large data. We can reduce this data by finding more active region for emotion. Again it is possible to reduce this data by finding electrode position which is more active. Now we analyse this data according to different electrode positions in different regions (Figs. 13.17, 13.18, 13.19, 13.20, 13.21, 13.22, 13.23, 13.24, 13.25, 13.26, 13.27, 13.28, 13.29, 13.30 and 13.31).

**Table 13.6** Region wise EEG data of different electrodes in romantic mode activity

Electrodes	Romantic mode data			
	<i>Delta</i>	<i>Theta</i>	<i>Alpha</i>	<i>Beta</i>
<i>Left</i>				
FP1	8.154079	2.411842	3.451316	0.488158
F7	1.790395	1.058816	1.497105	0.235263
F3	1.994474	1.343947	1.600132	0.335789
T3	1.843289	1.225658	2.692895	0.393816
C3	1.675526	1.233289	3.185263	0.456316
T5	5.898421	2.286447	3.748026	0.691974
P3	3.166447	1.546974	5.665658	1.174211
o1	3.888158	1.953947	3.414079	0.631842
<i>Right</i>			3.156809	
FP2	7.963026	2.540395	4.053816	0.492632
F4	4.284079	2.751579	3.083158	0.588421
F8	3.063553	1.547105	2.037632	0.330789
C4	1.890132	1.471447	2.849342	0.396184
T4	2.917763	1.671579	2.713026	0.417368
P4	3.508947	1.938289	4.976579	1.180658
T6	2.698289	2.411447	3.783684	0.756184
o2	3.148158	2.207763	3.809605	0.753289
<i>Center</i>			3.413355	
FZ	2.487237	2.125921	2.562763	0.425526
Cz	2.393553	1.772237	2.148289	0.361316
P2	2.333421	2.113816	5.897105	1.025658
			3.536053	

**Fig. 13.14** Time domain and frequency domain data



**Fig. 13.15** EEG data divided into window size of 5

**Table 13.7** Region wise mean EEG data of different electrodes in different mode activity for subject1

Modes	Left	Right	Center
Relax song mode	4.763931	4.885609	5.157368
Happy song mode	2.960641	3.131316	3.443772
Sad song mode	3.8222434	4.313388	5.098026
National song mode	2.819911	2.830461	3.05219
Romantic song mode	3.156809	3.413355	3.536053

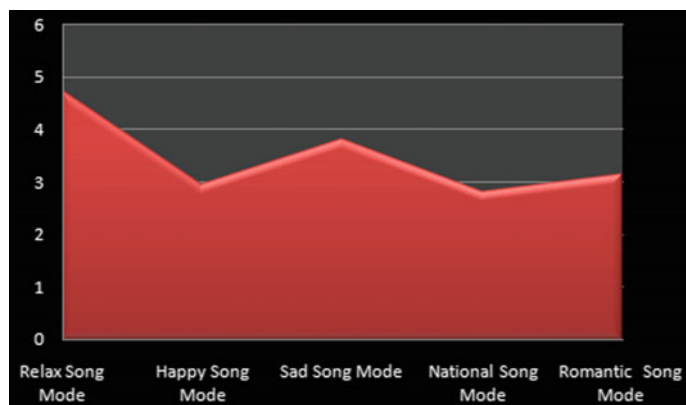


**Fig. 13.16** Alpha rhythms for all moods

**Table 13.8** Distance matrix of mean values of EEG data in right region

	Relax	Happy	Sad	National	Romantic
Relax	0	1.754293	0.572221	2.055148	1.472254
Happy	1.754293	0	1.182072	0.300855	0.282039
Sad	0.572221	1.182072	0	1.482927	0.900033
National	2.055148	0.300855	1.482927	0	0.582894
Romantic	1.472254	0.282039	0.900033	0.582894	0

**Table 13.9** Distance matrix of mean values of EEG data in left region

	Relax	Happy	Sad	National	Romantic
Relax	0	1.80329	0.941497	1.94402	1.607122
Happy	1.80329	0	0.861793	0.14073	0.196168
Sad	0.941497	0.861793	0	1.002523	0.665625
National	1.94402	0.14073	1.002523	0	0.336898
Romantic	1.607122	0.196168	0.665625	0.336898	0

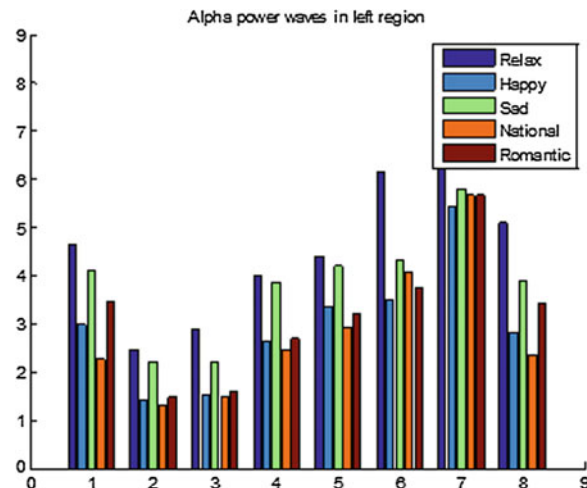
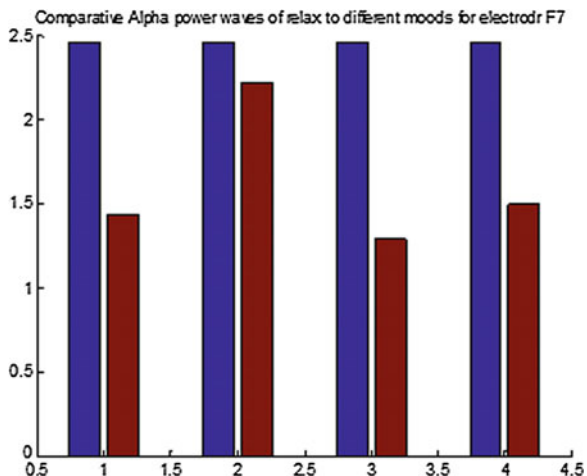
**Fig. 13.17** Alpha power waves in left region

Table 13.10 shows mean alpha frequency for all electrodes in different regions.

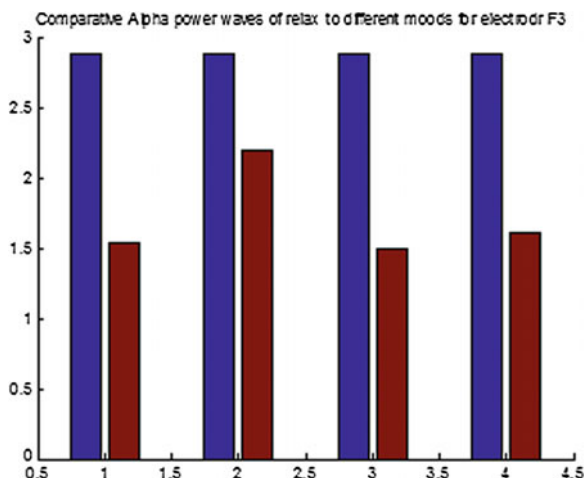
Figure 13.32 shows the graph of Mean alpha rhythms in different brain regions. From graph it is cleared that the emotions more active in left region as compared to right region of brain. From Table 13.10 the electrode F7 of left region of brain is more active as compared to other electrodes.

Table 13.11 shows the mean values of alpha power of different electrodes of all subjects in left hemisphere region. The table contains the mean values of alpha power of different relax mode, Happy Mode, Sad Mode, National Mode and

**Fig. 13.18** Comparative alpha power waves of relax to different moods for electrode F7



**Fig. 13.19** Comparative alpha power waves of relax to different moods for electrode F3



**Fig. 13.20** Comparative alpha power waves of relax to different moods for electrode T3

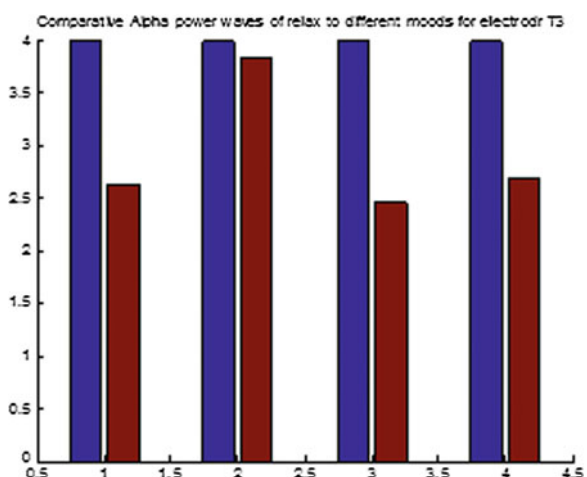


**Fig. 13.21** Comparative alpha power waves of relax to different moods for electrode C3

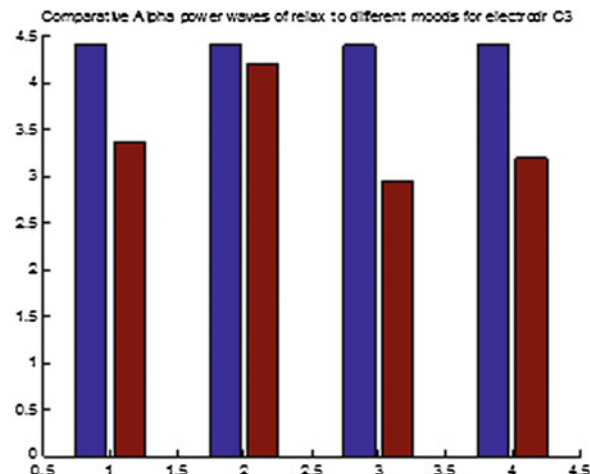


**Fig. 13.22** Comparative alpha power waves of relax to different moods for electrode T5

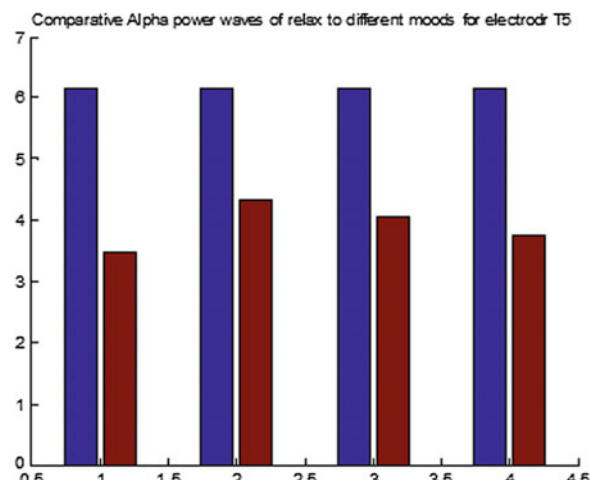


**Fig. 13.23** Alpha power waves in right region

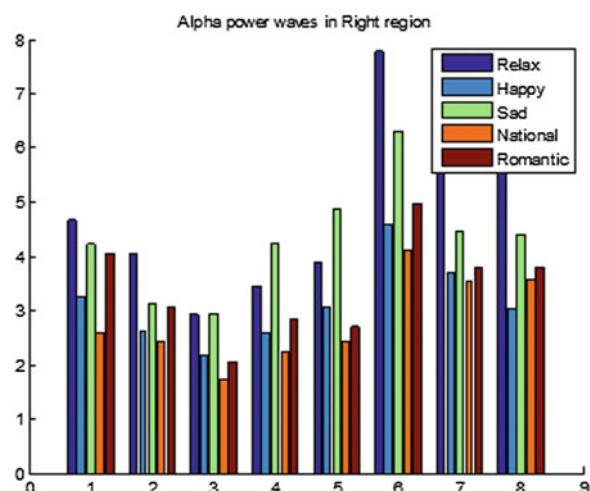


**Fig. 13.24** Comparative alpha power waves of relax to different moods for electrode F4

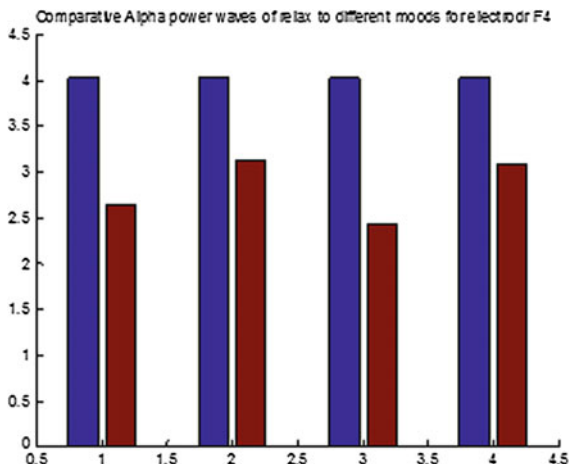


**Fig. 13.25** Comparative alpha power waves of relax to different moods for electrode F8

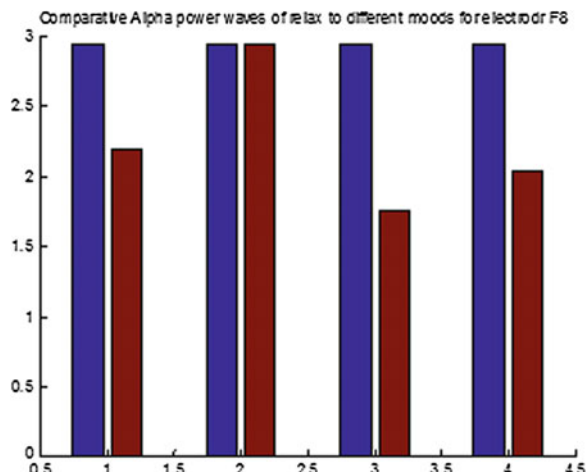


**Fig. 13.26** Comparative alpha power waves of relax to different moods for electrode c4

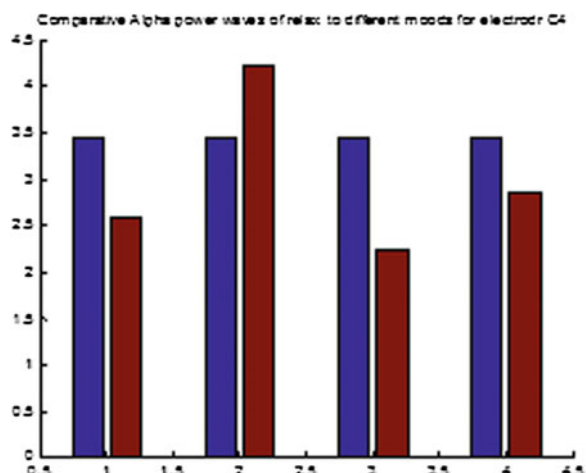


**Fig. 13.27** Comparative alpha power waves of relax to different moods for electrode T4

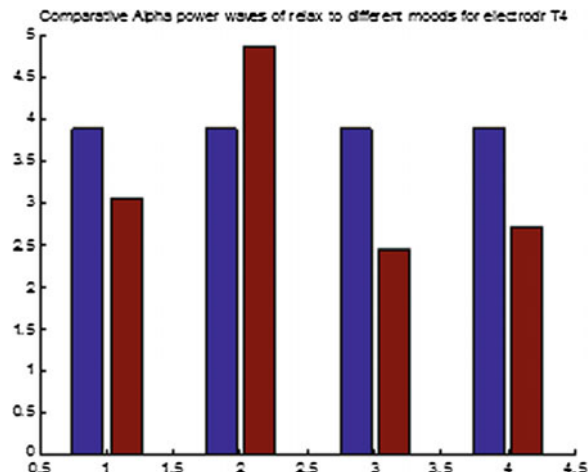


**Fig. 13.28** Comparative alpha power waves of relax to different moods for electrode T6

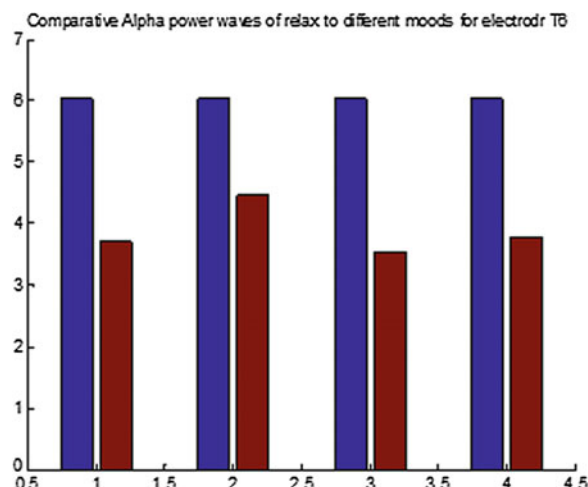


**Fig. 13.29** Alpha power waves in center region

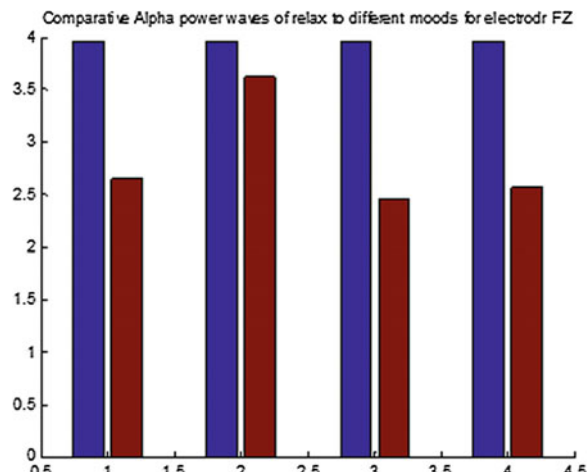


**Fig. 13.30** Comparative alpha power waves of relax to different moods for electrode Fz

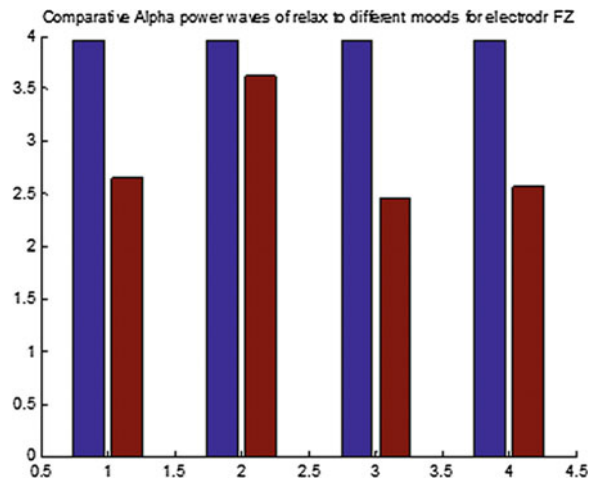
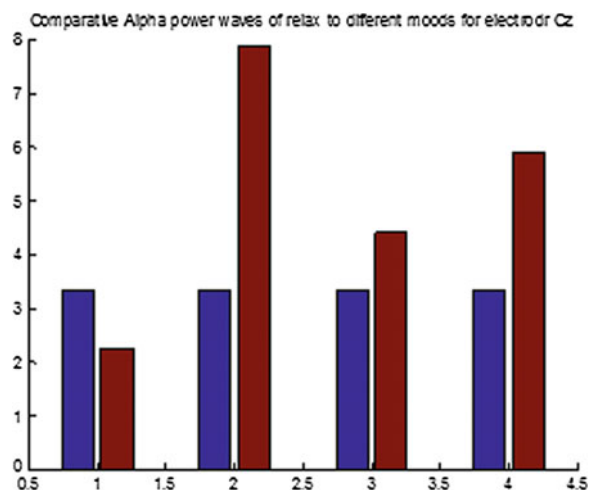


**Fig. 13.31** Comparative alpha power waves of relax to different moods for electrode cz

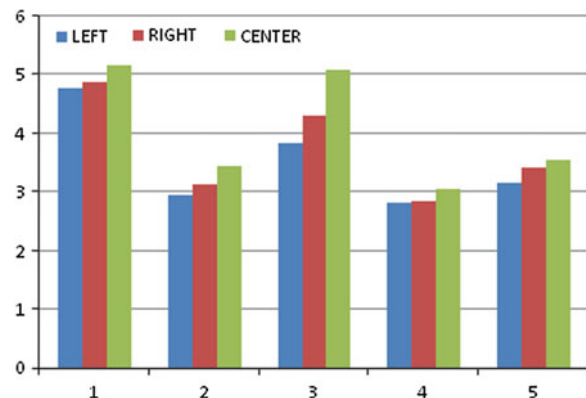


Romantic mode. We also calculate the average values for all subjects. From table it is clear that the alpha value for relax mode is more this means that less activity in brain for relax mode. It is also observed that we are less alert in sad mode as compared to Happy, National and Romantic mode. So it is possible to make clear distinction between the different activities in left hemisphere.

Table 13.12 shows the distance matrix for mean values of alpha power of different electrodes of all subjects in left hemisphere region. From distance matrix we observe that the value of sad mode is closer to relax mode that is less activity. It is also possible to distinguish the activity (sad, Happy) (Sad, National) and (Sad, Romantic) and the distance is  $>0.2$ . The values of Happy, National and Romantic are little close to each other. That is natural because the National Mode and

**Table 13.10** Mean alpha frequency for selected electrodes

Electrode	Relax	Happy	Sad	National	Romantic
F7	2.45961	1.43829	2.21987	1.29053	1.49711
F3	2.87329	1.53474	2.20026	1.49434	1.60013
T3	3.99276	2.63658	3.84382	2.45645	2.69289
C3	4.40039	1.53474	2.20026	1.49434	1.60013
T5	6.14434	3.47539	4.33908	4.07145	3.74803
F4	4.02605	2.63671	3.12145	2.42316	3.08316
F8	2.94276	2.18684	2.93487	1.75289	2.03763
C4	3.44263	2.592105	4.211184	2.241053	2.849342
T4	3.88013	3.05395	4.84237	2.45513	2.71303
T6	6.02592	3.68974	4.45697	3.53737	3.78368
Fz	3.95868	2.643289	3.619342	2.447632	2.562763
Cz	3.36605	2.26671	7.90145	4.41553	5.89711

**Fig. 13.32** Graph of mean alpha rhythms in different brain regions

Romantic mode always corresponds to Happy Mode. The person experiences the happy emotions in National and Romantic mode. Thus it is possible to distinguish all the activities.

Table 13.13 shows the mean values of alpha power of different electrodes of all subjects in right hemisphere region. The table contains the mean values of alpha power of different relax mode, Happy Mode, Sad Mode, National Mode and Romantic mode. We also calculate the average values for all subjects. From table it is clear that the alpha value for relax mode is more, this means that less activity in brain for relax mode. It is also observed that we are less alert in sad mode as compared to Happy, National and Romantic mode. So it is possible to make clear distinction between the different activities in right hemisphere.

**Table 13.11** Alpha power EEG data of all subjects in left hemisphere

Subject	Relax	Happy	Sad	National	Romantic
Subject1	4.763931	2.960641	3.822434	2.819911	3.156809
Subject2	12.34842	9.966793	10.53576	11.89535	9.743734
Subject3	1.816595	1.068355	1.499737	1.556776	2.154868
Subject4	15.18015	20.16189	19.44457	17.87863	20.13546
Subject5	7.822977	3.698947	4.228569	4.247039	2.867928
Subject6	0.419326	0.531201	0.616135	0.409704	0.544227
Subject7	4.300641	1.120938	2.64528	0.947023	1.488964
Subject8	1.689359	0.859984	0.713832	0.863931	0.739342
Subject9	2.255822	1.648109	2.036316	1.590066	1.84273
Subject10	2.995	0.990461	1.679556	0.905477	1.114153
Average	5.359222	4.300732	4.722219	4.311391	4.378822

**Table 13.12** Distance matrix of alpha power EEG data of all subject in left hemisphere

	Relax	Happy	Sad	National	Romantic
Relax	0	1.0584	0.6370	1.0478	0.9804
Happy	1.0584	0	0.4214	0.0106	0.0780
Sad	0.6370	0.4214	0	0.4108	0.3433
National	1.0478	0.0106	0.4108	0	0.06743
Romantic	0.9804	0.0780	0.3433	0.06743	0

**Table 13.13** Alpha power EEG data of all subjects in right hemisphere

Subject	Relax	Happy	Sad	National	Romantic
Subject1	4.8856	3.1313	4.3134	2.8305	3.4134
Subject2	18.96076	16.83107	17.21783	18.54388	17.68658
Subject3	1.472763	0.919523	1.237336	1.224112	1.719605
Subject4	17.19579	23.20265	20.06566	19.56446	22.33031
Subject5	5.509194	2.989638	3.007566	2.84051	2.278586
Subject6	0.445839	0.558536	0.636776	0.394474	0.605905
Subject7	6.919211	1.328635	3.149885	1.075395	1.689013
Subject8	7.912736	6.994478	7.089778	6.639047	7.103343
Subject9	3.766678	1.820313	3.890033	1.655428	2.436842
Subject10	5.839707	4.407395	5.489906	4.147237	4.770092
Average	7.290827	6.218354	6.609817	5.891504	6.403368

**Table 13.14** Distance matrix of alpha power EEG data of all subject in right hemisphere

	Relax	Happy	Sad	National	Romantic
Relax	0	1.072473	0.68101	1.399323	0.887459
Happy	1.072473	0	0.391463	0.32685	0.185014
Sad	0.68101	0.391463	0	0.718313	0.206449
National	1.399323	0.32685	0.718313	0	0.511864
Romantic	0.887459	0.185014	0.206449	0.511864	0

**Table 13.15** Comparative EEG data of all subjects in left and right hemisphere

Region	Relax	Happy	Sad	National	Romantic
Left	5.359222	4.300732	4.722219	4.311391	4.378822
Right	7.290827	6.218354	6.609817	5.891504	6.403368
%Dominance	24.84	44.58	39.97	36.65	46.24

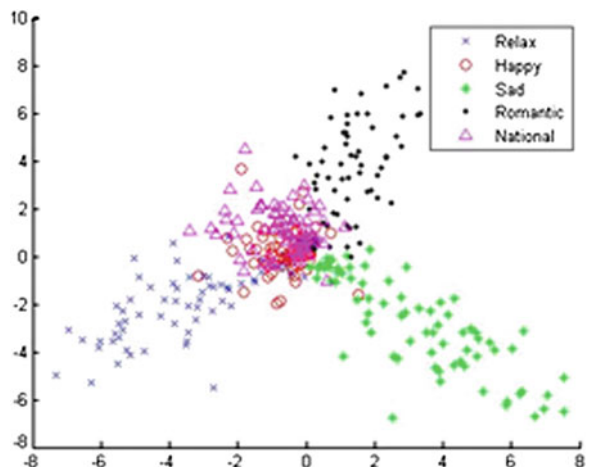
The Table 13.14 shows the distance matrix for mean values of alpha power of different electrodes of all subjects in left hemisphere region. From distance matrix we observe that the value of sad mode is closer to relax mode that is less activity. It is also possible to distinguish the activity (sad, Happy) (Sad, National) and (Sad, Romantic) and the distance is  $>0.2$ . Also it is possible to distinguish the between (Happy, National) (Happy, Romantic) and (National, Romantic mode) which is not possible in Left Hemisphere. This proves that the emotions are more separable in right hemisphere as compared to left hemisphere.

Table 13.15 shows the comparative EEG data of all subjects in left hemisphere and Right hemisphere. From the data it is cleared that the emotions are left dominant. The dominance is less for relax activity and it is maximum for romantic mode.

### 13.5.2 Linear Discriminate Analysis on Alpha Power Rhytm

Linear Discriminate Analysis is a well known scheme for feature extraction and dimension reduction. It has been widely used in many applications such as face recognition, image retrieval, microarray classification. LDA projects the data onto a lower dimensional vector space such that the ratio of the between class distance to the within class distance is maximized, thus achieves maximum discrimination (Figs. 13.33, 13.34, 13.35, 13.36, 13.37 and 13.38).

**Fig. 13.33** EEG signal classification using lda for subject1



**Fig. 13.34** EEG alpha power signal analysis using lda for subject1

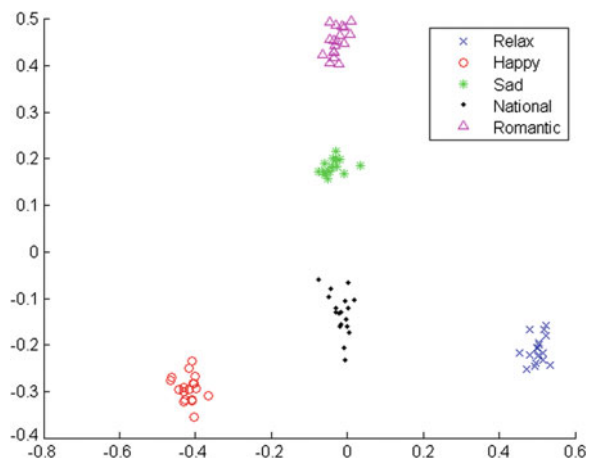


**Fig. 13.35** EEG signal classification using lda for subject2

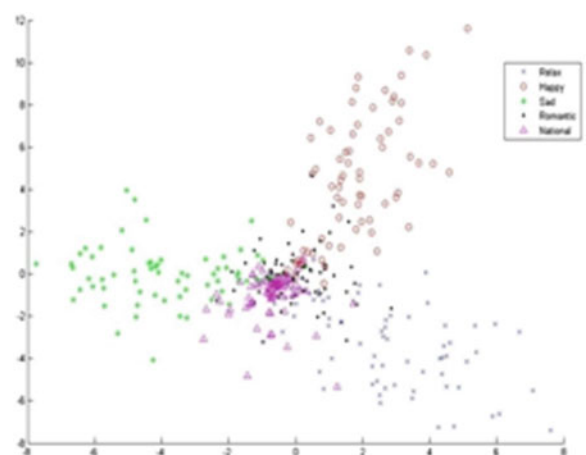


**Fig. 13.36** EEG alpha power signal analysis using lda for subject2

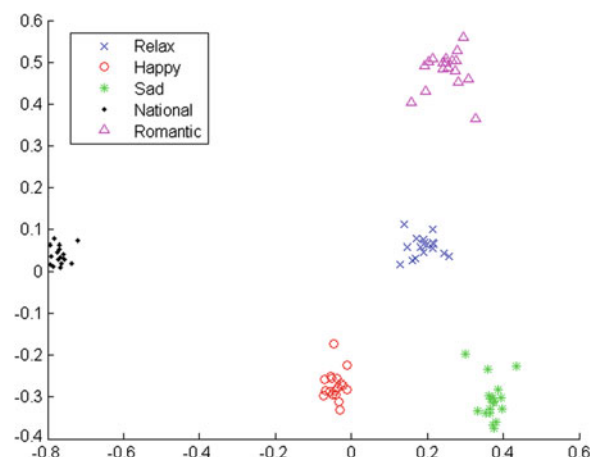


**Fig. 13.37** EEG signal classification using lda for subject1

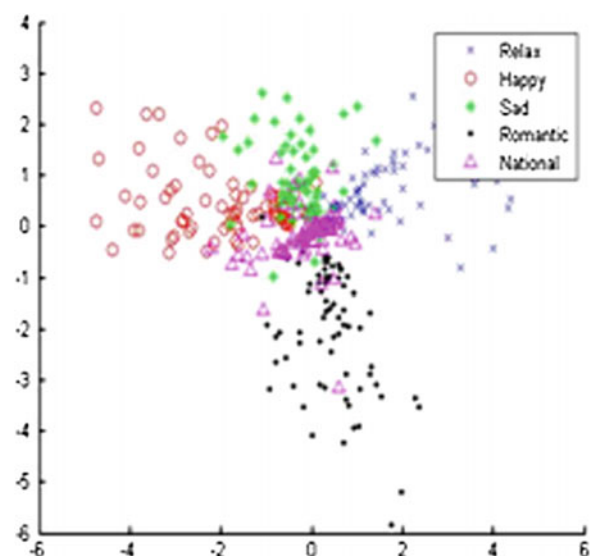
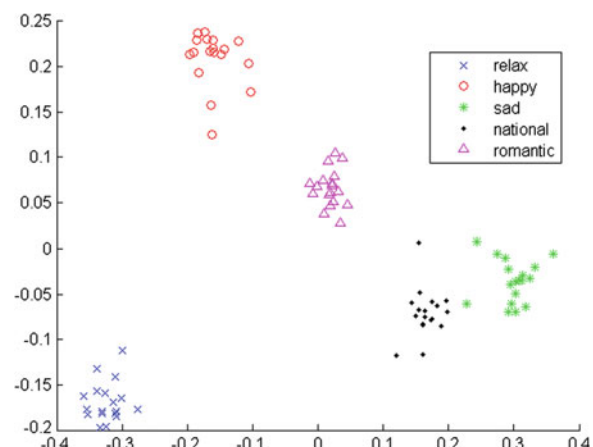


**Fig. 13.38** EEG alpha power signal analysis using lda for subject1



## 13.6 Conclusion

This study successfully achieves the goal to design a system which provides a data base which can be used for the design of mood recognition system. In this study we show that it is possible to recognize the different moods of person using EEG signal. One of the parameters may be used the alpha power. Larger values of alpha powers indicate activities related to moods induced by National, Happy, Romantic songs, whereas smaller values correspond to Sad mood. So it is possible to distinguish these different moods using alpha power values. Also we observe the different brain locations as Left Hemisphere and Right Hemisphere to recognize the significance according to different moods. We find the signals in the left hemisphere are more dominant over the right hemisphere for emotions. This means that the mood EEG signals are more powerful in left region as compared to right regions. Thus we conclude that the left region of brain gives more response to the emotions rather than right region. Here we reduce the EEG database from brain region to left hemisphere. Further we reduce it to single electrode as F7 which reside in left region. The data base generated in our study may be used to interface brain with computer for mood recognition system. This has wide varieties of applications in future. For example, the entertainment industries may use it for composition of songs as per their effect on brain. This research is useful as it concentrate on single electrode. We also developed linear discriminate analysis based system for classification emotions related to song induced activity.

## References

1. Alison, B.Z., Wolpow, E.W., Wolpow, J.R.: Brain computer system: progress and prospects. *Expert Rev. Med. Devices* **4**(4), 463–474 (2000)
2. Azar, A.T., Balas, V.E., Olariu, T.: Classification of EEG-based brain-computer interfaces. *Adv. Intell. Comput. Technol. Decision Support Syst. Stud. Comput. Intell.* **486**, 97–106 (2014)
3. Balconi, M., Lucchiari, C.: EEG correlates (event-related desynchronization) of emotional face elaboration: a temporal analysis. *Neurosci. Lett.* **392**(1–2), 118–123 (2006)
4. Bickford, R.D.: Electroencephalography. Adelman George Encycl. *Neurosci.* **244**, 371–373 (1987)
5. Bronzino, J.D.: Principles of Electroencephalography. The Biomedical Engineering Handbook. CRC Press, Boca Raton (2000)
6. Carlson, N.R.: Structure and Functions of the Nervous System. Foundations of Physiological Psychology. Allyn and Bacon, Boston (2002)
7. Chakraborty, Bhowmik, A., Das, S., Halder, A., Konar, A., Nagar, A.K.: Correlation between stimulated emotion extracted from EEG and its manifestation on facial expression. In: IEEE International Conference on IEEE Systems, Man and Cybernetics (SMC 2009), pp. 3132–3137 (2009)
8. Cincotti, F., Mattia, D., Aloise, F., Bufalari, S.: High-resolution EEG techniques for brain computer interface applications. *J. Neurosci. Methods* **167**(1), 31–42 (2008)
9. Collura, T.F.: History and evolution of electroencephalographic instruments and techniques. *Clin. Neurophysiol.* **10**(4), 476–504 (1993)

10. Esslen, M., Pascual-Marqui, R.D., Hell, D., Kochi, K., Lehmann, D.: Expression, perception, and induction of musical emotions: a review and a questionnaire study of everyday listening. *J. New Music Res.* **33**(4), 217–238 (2004)
11. Esslen, M., Pascual-Marqui, R.D., Hell, D., Kochi, K., Lehmann, D.: Brain areas and time course of emotional processing. *Neuroimage* **21**(4), 118–123 (2004)
12. Fatourechi, M., Bashashati, A., Ward, R.K., Birch, G.E.: EMG and EOG artifacts in brain computer interface systems: a survey. *Clin. Neurophysiol.* **118**(3), 480–494 (2007)
13. Gaines, B.R.: A conceptual framework for person-computer interaction in distributed systems. *IEEE Trans. Syst. Man Cybern.* **18**, 532–541 (1988)
14. Graimann, B., Huggins, J.E., Levine, S.P., Pfurtscheller, G.: Visualization of significant ERD/ERS patterns in multichannel EEG and ECOG data. *Clin. Neurophysiol.* **113**(1), 43–47 (2002)
15. Gratton, G., Fabiani, M.: Shedding light on brain function: the event-related optical signal. *Trends Congnitive Sci.* **5**(8), 363–375 (2001)
16. Hewson, D.J., Duchne, J., Hogrel, J.-Y.: Changes in impedance at the electro skin interface of surface EMG electrodes during long term EMG recordings. In: IEEE 23rd Annual Conference on IEEE/EMBS (2001)
17. Huisheng, L., Wang, M., Hongqiang, Y.: EEG model and location in brain when enjoying music. In: 27th Annual International Conference on IEEE Engineering in Medicine and Biology Society (IEEE-EMBS 2005), pp. 2695–2698 (2005)
18. Ito, S., Mitsukura, Y., Fukumi, M., Akamatsu, N.: Feature extraction of the EEG during listening to the music using the factor analysis and neural networks. In: Proceedings of the International Joint Conference on IEEE Neural Networks, pp. 2263–2267 (2003)
19. Ito, S. I., Mitsukura, Y., Fukumi, M., Jianting, C.: Detecting method of music to match the users mood in prefrontal cortex EEG activity using the GA. In: International Conference on IEEE Biomedical and Pharmaceutical Engineering (ICBPE 2006), pp. 1798–1806 (2007)
20. Jasper, H.H.: Report of the committee on methods of clinical examination in electronic photography: the ten-twenty electrode system of the international federation. *Electroencephalogr. Clin. Neurophysiol.* **10**(2), 371–375 (2006)
21. Karthick, N., Thajudin, A.V., Joseph, P.K.: Music and the EEG: a study using nonlinear methods. In: International Conference on IEEE Biomedical and Pharmaceutical Engineering (ICBPE 2006), pp. 424–427 (2005)
22. Khosrowabadi, R., Quek, H.C., Wahab, A., Ang, K.K.: EEG-based emotion recognition using self-organizing map for boundary detection. In: 20th International Conference on IEEE Pattern Recognition (ICPR), pp. 4242–4245 (2010)
23. Klimesch, W.: EEG alpha and theta oscillations reflect cognitive and memory performance: a review and analysis. *Brain Res. Rev.* **29**(2–3), 169–195 (2000)
24. Klimesch, W., Doppelmayr, M., Russegger, H., Pachinger, T., Schwaiger, J.: Induced alpha band power changes in the human EEG and attention. *Neurosci. Lett.* **244**(2), 73–76 (1998)
25. Kwon, M., Kang, J.-S., Lee, M.: Emotion classification in movie clips based on 3D fuzzy GIST and EEG signal analysis. In: 2013 International Winter Workshop on IEEE Brain-Computer Interface (BCI), pp. 67–68 (2013)
26. Levine, S.P.: A direct brain interface based on event-related potentials. *IEEE Trans. Rehabil. Eng.* **8**(2), 180–185 (2000)
27. Mason, S.G.: A general framework for brain-computer interface design. *IEEE Trans. Neural Syst. Rehabil. Eng.* **11**(1), 70–85 (2003)
28. Millan, J.R., Hauser, A., Renkens, F.: Adaptive brain interfaces—ABI: simple features, simple neural network, complex brain-actuated devices. In: IEEE Conference Proceeding, pp. 297–300 (2002)
29. Millan, J.R., Mourino, J.: Asynchronous bci and local neural classifiers: an overview of the adaptive brain interface project. *IEEE Trans. Rehabil. Eng.* **11**(2), 159–161 (2003)
30. Morrison, J.H., Patrick, R.H.: Life and death of neurons in the aging brain. *Science* **278**, 412–419 (1997)

31. Murugappan, M.: Human emotion classification using wavelet transform and KNN. In: 2011 International Conference on IEEE Pattern Analysis and Intelligent Robotics (ICPAIR), vol. 1, pp. 148–153 (2011)
32. Niedermeyer, E., Silva, L.D.: *Electroencephalography: Basic Principles, Clinical Applications and Related Fields*. Lippincott Williams and Wilkins, Baltimore (1999)
33. Nunez, P.L., Cutillo, B.A.: *Neocortical dynamics and human EEG rhythms*. Oxford University Press, Oxford (1995)
34. Picton, T., Bentin, S., Berg, P., Donchin, E., Hillyard, S.: Guidelines for using human event-related potentials to study cognition: recording standards and publication criteria, pp. 127–152. Cambridge University Press, Cambridge (2000)
35. Reza, F.-R.: P300-based speller brain-computer interface. In: Naik, G.R. (ed.) *Recent advances in biomedical engineering*, In Tech (2009). doi:[10.5772/7483](https://doi.org/10.5772/7483)
36. Sanei, S. Chambers, J.: *EEG Signal Processing*. Wiley, New York (2007)
37. Tepilan, M.: Fundamentals of EEG measurement. *Meas. Sci. Rev.* **2**(2), 1–11 (2002)
38. Teplan, M.: Fundamentals of EEG measurement. *Meas. Sci. Rev.* **2**(2), 1–11 (2002)
39. Tripathi, K.P.: A study of interactivity in human computer interaction. *Int. J. Comput. Appl.* **16**(6), 1–3 (2011). <http://www.ijcaonline.org/volume16/number6/pxc3872724.pdf>
40. Turban, E., Aronson, J.E.: *Decision Support Systems and Intelligent Systems*. Pearson Education, New Delhi (2003)
41. Vidal, J.J.: Real-time detection of brain events in EEG. In: *IEEE Proceedings of the IEEE*, pp. 633–641 (1977)
42. Vijayalakshmi, K., Sridhar, S., Khanwani, P.: Estimation of effects of alpha music on EEG components by time and frequency domain analysis. In: *Computer and Communication Engineering (ICCCE)*, pp. 1–5 (2010)
43. Wolpaw, J.R.: Brain-computer interface technology: a review of the first international meeting. *IEEE Trans. Rehabil. Eng.* **8**(2), 164–173 (2000) (see also *IEEE Trans. Neural Syst. Rehabil.*)
44. Yuan-Pin, L., Chi-Hong, W., Tien-Lin, W., Shyh-Kang, J., and Jyh-Horng, C. (2008). Support vector machine for EEG signal classification during listening to emotional music. In: *IEEE 10th Workshop on Multimedia Signal Processing*, pp. 127–130 (2008)
45. Yuan-Pin, L., Chi-Hong, W., Tzyy-Ping, J., Tien-Lin, W., Shyh-Kang, J., Jeng-Ren, D., Chen, J.-H.: EEG-based emotion recognition in music listening. In: *IEEE Transactions on Biomedical Engineering*, pp. 1–130 (2010)

# **Chapter 14**

## **Digit Recognition System Using EEG Signal**

**Rakesh Deore, Bharati Gawali and Suresh Mehrotra**

**Abstract** Based on Linear Discriminate analysis (LDA), Principle Component Analysis we explore the characteristics of multichannel Electroencephalogram (EEG), which is recorded from no of subjects recognizing different numbers displayed on the screen by a GUI software designed in Visual Basic 6. The scaling exponent of each digit is different especially at positions C3 and C4, and at positions O1 and O2. LDA exhibits its robustness against noises in our works. We could benefit more from the results of this paper in designing mental tasks and selecting brain areas in brain-computer interface (BCI) systems. The objective of this system is to report the work done related to sensitivity of EEG signals related to specific thought process. The thought process was chosen to be numbers (0–9). The main objective of this work is the analysis and classification of EEG signals among the men and machines and provide a secure communication interface. EEG recordings of six male right-handed subjects in the age group of (20–25) were taken. The subjects were normal without any mental disorder. They did not have any problem in communicating and had normal vision. All subjects have good knowledge of digits. A simple display system in visual basic is prepared for the project. This system generates random number with interval of 2 s. After every 2 s a random number is displayed on the screen. The recording was captured for 3 min. This process was repeated for five times. The EEG signal has been processed by statistical analysis methods such as LDA and PCA. It was found that the EEG signals are sensitive to thought process. So it is possible to recognize thought process through EEG signals. In our ten digit thought process, we get ten distinct clusters by analyzing EEG signals through statistical technique like LDA and PCA. The recognition rate of LDA is 70 %. The recognition rate of PCA is 37 %. So we

---

R. Deore (✉)

Department of Computer Science, P.R. Ghogrey Science College, Dhule, India  
e-mail: rakeshsdeore@gmail.com

B. Gawali · S. Mehrotra

Department of Computer Science, Babasaheb Ambedkar University, Aurangabad, India  
e-mail: bharti\_rokane@yahoo.co.in

S. Mehrotra

e-mail: sureshmehrotra16@gmail.com

establish that LDA is more powerful method as compared to PCA. We observe that the EEG signal is more dominant on right hemisphere as compared to left hemisphere. The data base created has potential to be used as a digital recognition system. It has tremendous applications in design of security system.

**Keywords** Linear discriminate analysis · Principle component analysis · Human computer interaction · Digit recognition

## 14.1 Introduction

Recently developments in computer and digital signal processing made it possible to associate electroencephalogram (EEG) signal for communication between human and computer. Information security has become a significant issue in recent years as new ways of information exchange arise due to rapid development of computing, information and internet technologies. The primary benefit of EEG-based Human Computer Interaction (HCI) systems is that no motor output (including speech) required [5, 6, 9–11, 13, 14, 18–20, 21–24, 26, 28–30, 32–34]. Some of the issues regarding the information security handled by taking advantage of HCI system. The proposed system tries to device a new secure method of communication between human and machine e.g. inputting security code. In this chapter, we have dealt problems related to brain activities induced by some external activities like digit recognition. It is shown that the EEG signals are sensitive to these external activities and it is possible to identify the external activities by analyzing the EEG signals [2]. These signals are qualitative in nature and very difficult to quantify them. The alpha power and beta power may be used to quantify these activities. It will be more specific if we can recognize thoughts process through EEG signals. These thought process will be more specific. The system will have tremendous applications like physically disabled peoples to communicate with computer through electroencephalogram (EEG) signal interface and using thought passwords security systems etc. The objective of the present chapter is report the work done related to sensitivity of EEG signals related to specific thought process. The thought process was chosen to be numbers (0–9). The main objective of this work is the analysis and classification of EEG signals among the men and machines and provide a secure communication interface. The electrical nature of the human nervous system has been recognized for more than a century. It is well known that the variation of the surface potential distribution on the scalp reflect functional activities emerging from the brain. This surface potential variation can be recorded by affixing an array of electrodes to the scalp and measuring the voltage between pairs of these electrodes, which are then filtered, amplified and recorded. The resulting data is called EEG (Electroencephalogram) signals. The EEG has small signal amplitude in range of microvolt. EEG can help diagnose conditions such as seizure disorders, strokes, brain tumors, head trauma, and other physiological problems. The pattern of EEG

activity changes with the level of a person's arousal. A relaxed person has many slow EEG waves whereas an excited person has many fast waves. A standardized system of electrode placement is the international 10–20 system. A common problem with EEG data is contamination from muscle activity on the scalp. It is desirable to remove such artifacts to get a better picture of the internal workings of the brain [16]. As the neurons in our brain communicate with each other by firing electrical impulses this creates an electrical field that travels through the cortex, the skull and the scalp. The fundamental assumption behind the EEG signal is that it reflects the dynamics of electrical activity in populations of neurons. The crucial property of such populations is that they can work in synchrony. The EEG is supposed to be generated by oscillations between the cortex and the thalamus. These oscillations seem to be generated by physical properties of a neuron and by functions of the ionic channels in the cell walls of the thalamic cell. The thalamus is a kind of relay station which passes all information. The potential fluctuation that is generated by sum of potentials in the cortex and thalamus is measured by calculating potential difference between the actual measuring electrode and the reference electrode. The signals picked by the electrodes may be combined to channels or a channel corresponds to a single electrode. The signal is then amplified and filtered from artifacts [31]. The research work provides an opportunity for people who are physically challenged to interact with system like any other human [25]. The role of signal processing is crucial in the development of real-time Brain Computer Interface. The several improvements have been made in this area but none of them have been successful enough to use them in a real system. The goal of creating more effective classification algorithms, have focused numerous investigation in the search of few techniques of feature extraction. In this chapter, we are going to address the problems which belong to the framework of HCI research. Here, we focused on the study of Electroencephalogram (EEG) signal and signal classification techniques through Linear Discriminate Analysis (LDA) and Principle Component Analysis (PCA). The EEG signal is a unique and valuable measure of the brains electrical function. The study of EEG signal helps to investigate neuropsychological process that could be utilized to implement a HCI system. LDA and PCA statistical methods isolate the discriminant component and dimension reduction of large data. The design and implementation of HCI system requires sound knowledge of data acquisition process, EEG waveform characteristics; signal processing methodologies for feature extraction and classification. The research objectives are summarized as follows

- Examine electroencephalography as a means of identifying mental activity such as Digit Recognition.
- Investigate the statistical methods for classification that will classify the EEG signals related to mental activity such as digit recognition.
- Develop experimental BCI systems for digit recognition.
- Identify the regions in the brain activated by different mental activities such as digit recognition.
- Detection of dominated brain regions for digit recognition activity.

The remainder of the chapter is organized as follows: Sect. 14.2 describes literature survey. Section 14.3 explains the experimental data acquisition. Experimental analysis is given in Sect. 14.4. Section 14.5 describe the feature extraction process in detail. In this section we process EEG data of different brain regions. Section 14.6 discussed the conclusion of work.

## 14.2 Literature Survey

The Electroencephalogram (EEG) is a unique and valuable measure of brains electrical function. Electrical Signals are produced by brain activity were first recorded from the cortical surface in animals by Ricard Carton (1875) and from human scalp by Beger [4]. EEG activities mainly used for clinical diagnosis and explores brain function. Now a day different researchers shows that brain activity might serve an entirely different purpose that they might provide the brain with another means of conveying messages and commands to external world. EEG is one such technique which measures the electric fields that are produced by the activity in the brain [1, 27]. EEG signals arise due to electrical potential produced by the brain. EEG spectrum contain characteristic waveforms which fall in 4 frequency bands viz alpha (8–13 Hz), beta (13–30 Hz), theta (4–8 Hz), delta (<than 4 Hz). Alpha waves are found in normal awake people, not engaged in intense mental activity, which disappear when a person is asleep. Beta waves with higher frequency are seen during intense mental activity and stress. Delta waves occur during deep sleep, during infancy and in serious organic brain diseases. Theta waves appear during emotional stress in adults in sleep, particularly during disappointment and frustration [15]. Literature review of similar work which focuses more on identification from EEG of healthy subjects rather than classification of pathological cases for diagnosis were made [3, 8, 17]. EEG is collected at the millisecond level, in contrast to the longer time intervals required for traditional measures such as mouse clicks or user responses. This permits effective monitoring of workload fluctuations in very rapid decision-making processes that are unobservable using traditional methods. As security issue is always challenging to the real world applications many biometric approaches, such as fingerprint, iris and retina, have been proposed to improve recognizing accuracy or practical facility in individual identification in security. However, there is little research on individual identification using EEG methodology mainly because of the complexity of EEG signal collection and analysis in practice [35]. In future we can work to extract individual specific information from a persons EEG and use this information to develop identification methods like EEG biometry.

## 14.3 Experimental Data Acquisition

We designed a fixed setup for a study with six subjects. They all have no or very little experience about BCI system. Brain signals measured from 19 electrodes mounted on the scalp. To exclude the possibility of influence from non central nervous system activity, EOG and EMG recorded additionally. Those channels used to remove noise from EEG signal.

### 14.3.1 Methodology

Subject Selection: EEG recordings of six male right-handed subjects in the age group of (20–25) were taken. The subjects were normal without any mental disorder. They did not have any problem in communicating and had normal vision. Subjects were made to sit comfortably on an arm chair facing the screen in electromagnetically shielded room. The subjects had given their written consent for recording EEG signals before participating. All subject have good knowledge of digits. Procedure: All subjects were instructed that this experiment has been designed to be used for HCI. They came to the laboratory and were instructed about the nature of task which was to be administered. The experiment was conducted in a quite room. The subject were briefed about the EEG procedure and Digit Project. A simple display system in visual basic is prepared for the project. This system generates random number with interval of 2 s. After every 2 s a new number is displayed on the screen. Subjects were told that it important to think number that is displayed on screen. Here we repeat this procedure for 3 min. Thus we get data of 90 digit in single trail. The complete procedure repeated for 3 times on the same subject. Finally we process 270 digit of data in three trails. Here we get EEG data of digits (0–9). In 270 readings the data of each digit is repeated random times. The data of first two trails is used for training and the data of last trail is used for testing. Demonstration of display system was shown to each subject before experiment start so that he was more familiar to the task and we will get proper signals (Figs. 14.1 and 14.2).

### 14.3.2 Apparatus and Recording Procedure

The EEG signals, for each mode, was captured by RMS (Recorders and Medicare Systems) EEG-32 Super Space machine shown in Fig. 14.3 for 3 min with sampling rate of 250/s. The other parameters of the EEG machine were set as follows: low filter: 1 Hz, high filter: 70 Hz, sensitivity: 7 V, number of channels: 17, sweep speed: 30 mm/s and Montage: BP PARA (R). As stated above, the experiment was conducted on six subjects. The electrodes were placed on scalp of subjects as per the international 10–20 standard as given in Fig. 14.4. The EEG signal has been processed by statistical analysis methods such as LDA and PCA.

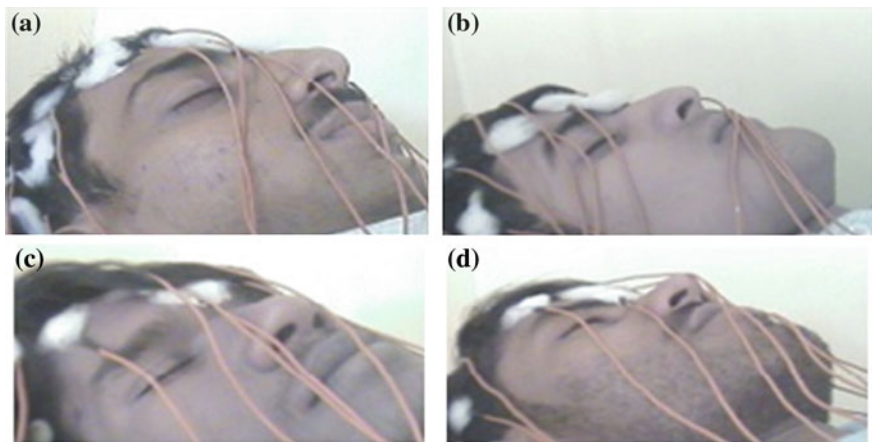


**Fig. 14.1** Acuisition of EEG signals from different subjects **a** Pukhraj Shrishrimal **b** Vishal Wagh **c** Vishal Waghmare **d** Amit Shelke



**Fig. 14.2** Snapshot of digit display system



**Fig. 14.3** Photograph of RMS-EEG -32 super spec machine

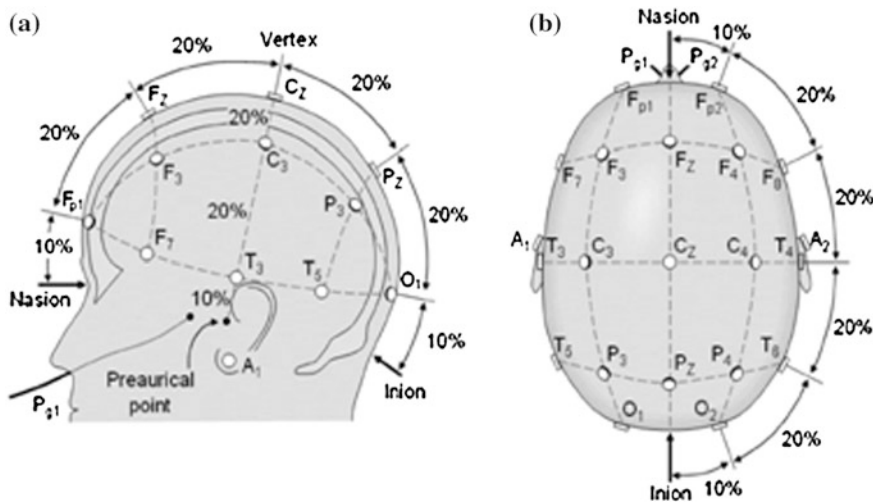


**Fig. 14.4** An international 10–20 system of electrode placement

## 14.4 Experimental Analysis

The EEG recordings were captured according to the time of numbers generated on the GUI. The readings were statistically analyzed. There are four frequency bands associated with the EEG signals. All four bands with their functionalities are listed in Table 14.1. The Delta frequency up to 4 HZ has been found dominant during some continuous attention tasks [7].

By observing the Table 14.1, we concentrated on the probability of signals of all 19 electrodes for recognizing the number. The Linear Discriminate analysis (LDA) and Principle Component Analysis techniques are used for data classification and dimensionality reduction. They easily handle the case where the Within-class frequencies are unequal and their performance has been examined on randomly generated test data. These methods maximize the ratio of between-class variance to the within-class variance in any particular data set thereby guaranteeing maximal separability. The use of LDA and PCA for data classification are applied for classification of all ten numbers in a hope of providing better classification.

### 14.4.1 Linear Discriminate Analysis

Linear Discriminate Analysis is a well known scheme for feature extraction and dimension reduction. It has been widely used in many applications such as face recognition, image retrieval, microarray classification. LDA projects the data onto a lower dimensional vector space such that the ratio of the between class distance to

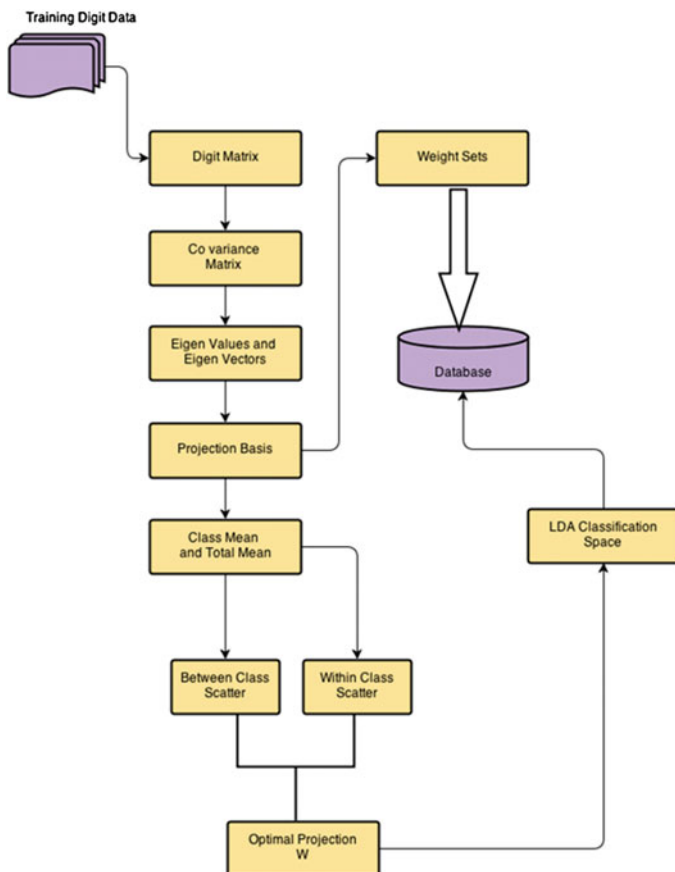


**Fig. 14.5** Flowchart for linear discriminant analysis

**Table 14.1** Frequency Rhythms associated with EEG signal

Name	Frequency	Location
Delta	Up to 4	Has been found dominant during some continuous attention task
Theta	4 to <8	Appears in drowsiness or arousal condition in children and adults
Alpha	8–13	Found to be prominent in relaxed reflecting condition
Beta	13–30	Has been found in alert working active, busy or anxious thinking, or active concentration

the within class distance is maximized, thus achieves maximum discrimination. LDA aims to find a vector space  $G$  spanned by  $g_i$  where  $G = [g_1, g_2, \dots, g_l]$  such that each  $a_i$  is projected onto  $G$  by  $(g_1^T \cdot a_i, \dots, g_l^T \cdot a_i)^T \in R^l$ . Assume that the original data in  $A$  is partitioned into  $k$  classes as  $A = \{a_1, a_2, \dots, a_k\}$  where  $a_i$  contains points from the  $i$ th class. LDA aims to find the optimal transformation  $G$  such that

the class structure of the original high dimensional space is preserved in the low dimensional space. In general if each class is tightly grouped, but well separated from the other classes, the quality of considered to be high. In discriminant analysis two scatter matrices, called as within class ( $S_w$ ) and between-class ( $S_b$ ) matrices, are used to quantify the quality of cluster. It is easy to verify that trace ( $S_w$ ) measures the closeness of the vectors within the classes, while trace ( $S_b$ ) measures the separation between classes. In the low dimensional space resulting from the linear transformation. Linear Discriminant Analysis is a simple probabilistic approach to classification in which each class is assumed to follow a normal distribution. LDA generated the cluster for different digits as shown in Fig. 14.6. From Fig. 14.6 it is clear that it is possible to distinguish the different digits (Fig. 14.6).

#### 14.4.2 Principle Component Analysis

Principal Component analysis is commonly used to project data samples to lower-dimensional subspace that maximizes the variance of projected data. Principal Component Analysis finds direction of most variance in the data by computing singular value decomposition on the mean centred data matrix [12]. PCA is usually applied to a collection of samples from all classes. PCA identifies the largest variations in the data via the principle components (PC) and represent the data in a

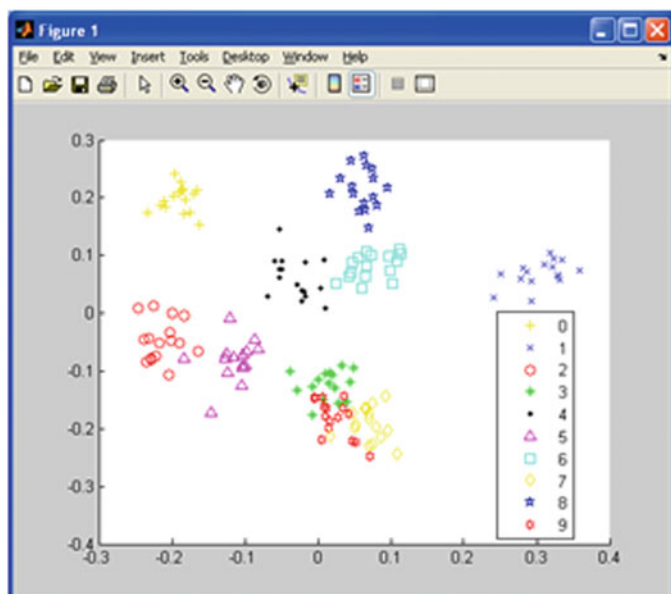


**Fig. 14.6** Graph showing the clusters of different classes using LDA

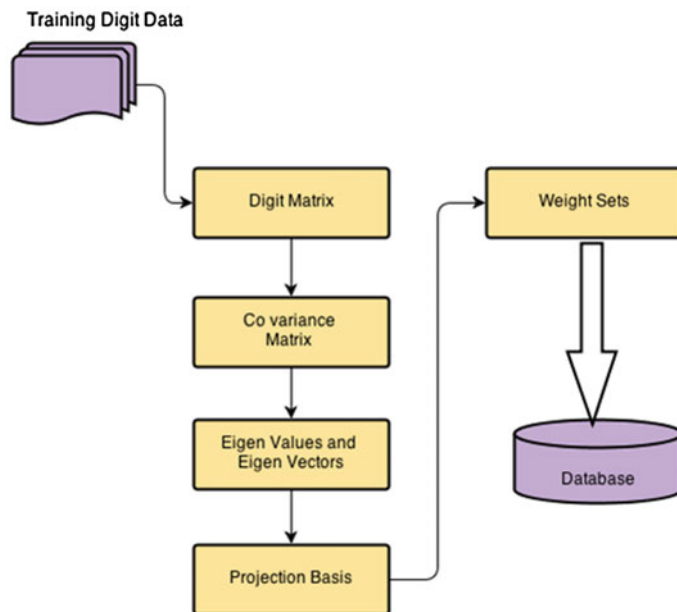
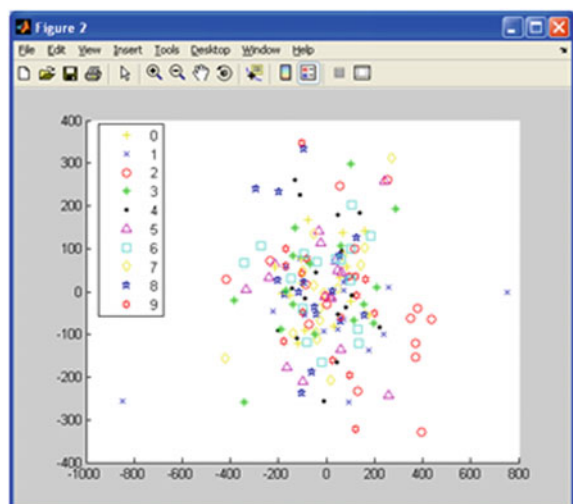


**Fig. 14.7** Flowchart for principle component analysis

coordinate system defined by the PCs. PCA generated the clusters for different digits in the following format. From the following figure we may say that there is no clear distinction between different digits (Figs. 14.7 and 14.8).

**Fig. 14.8** Graph showing the clusters of different classes using PCA



#### 14.4.3 Comparative Study of LDA and PCA

The graphs are shown in following Figs. 14.9, 14.10, 14.11, 14.12, 14.13, 14.14, 14.15, 14.16, 14.17 and 14.18 shows the sample EEG signal from digits 0–9. This signal carry data from all 19 electrodes. As EEG signal is divided into four frequencies. So the graph shows 76 different points (Figs. 14.19, 14.20 and 14.21).

Now lets visualise the training data and the testing data for the digit 0. From graph is shown in following Fig. 14.22 it is clear that the training data and testing data set exhibit the same behaviour. So it is possible to recognise digit 0 as 0. We similarly analyse the data for all other digits, we get the same behaviour. This shows that the EEG signal carry useful information related to all digits. This analysis gives the base to build the digit recognition system using EEG signal. Number generator software generates number at random. Table 14.2 shows the total

**Fig. 14.9** Sample EEG signal for digit 0 of training dataset

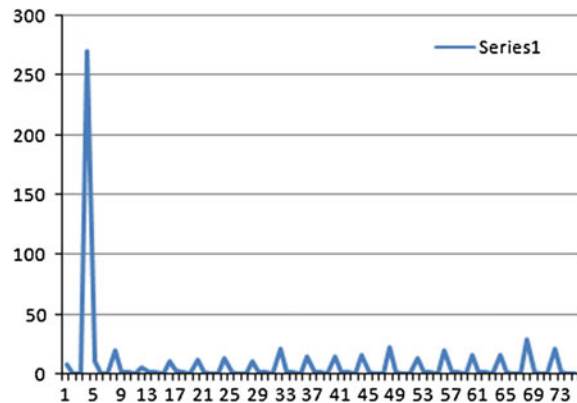


**Fig. 14.10** Sample EEG signal for digit 1 of training dataset

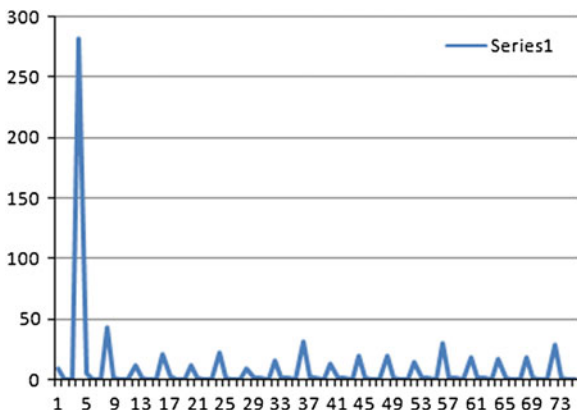


**Fig. 14.11** Sample EEG signal for digit 2 of training dataset

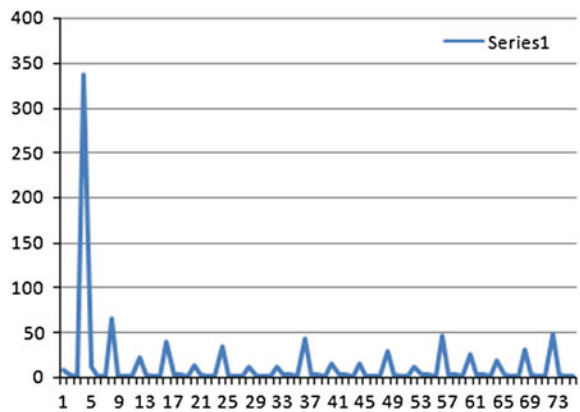


**Fig. 14.12** Sample EEG signal for digit 3 of training dataset

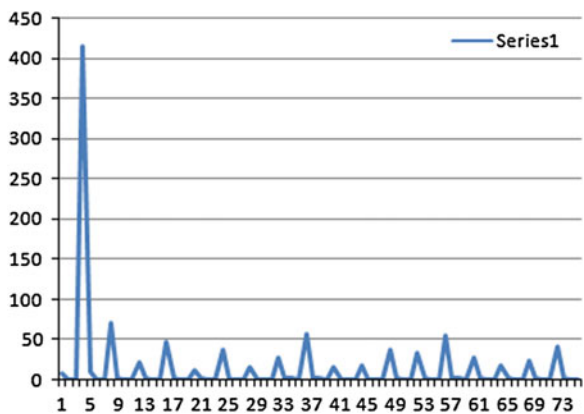


**Fig. 14.13** Sample EEG signal for digit 4 of training dataset

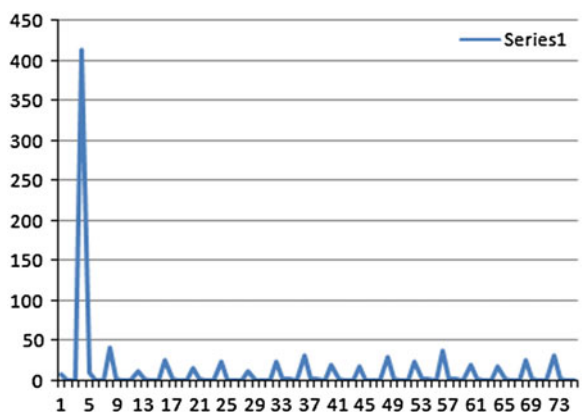


**Fig. 14.14** Sample EEG signal for digit 5 of training dataset

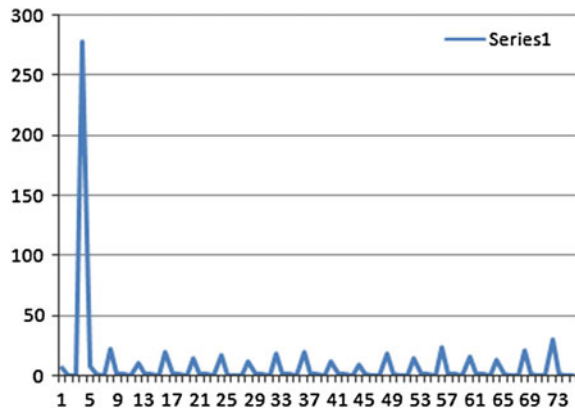


**Fig. 14.15** Sample EEG signal for digit 6 of training dataset

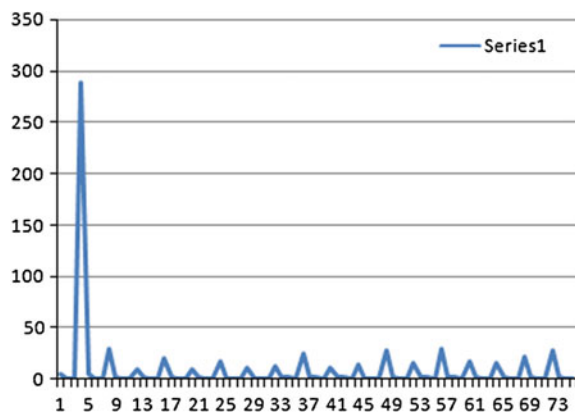


**Fig. 14.16** Sample EEG signal for digit 7 of training dataset

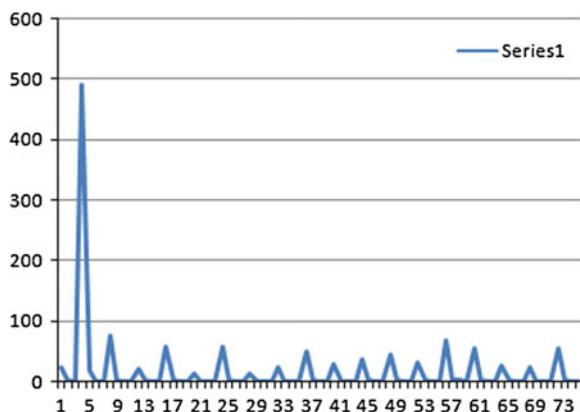


**Fig. 14.17** Sample EEG signal for digit 8 of training dataset

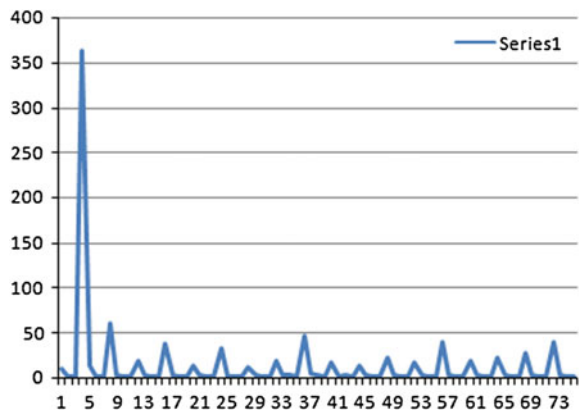


**Fig. 14.18** Sample EEG signal for digit 9 of training dataset

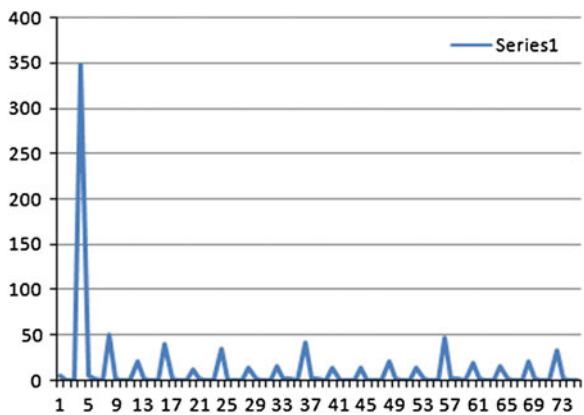


**Fig. 14.19** Sample EEG signal for digit 0 of training dataset1

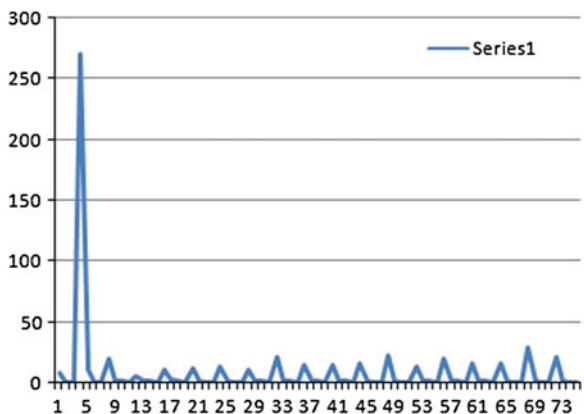


**Fig. 14.20** Sample EEG signal for digit 0 of training dataset2

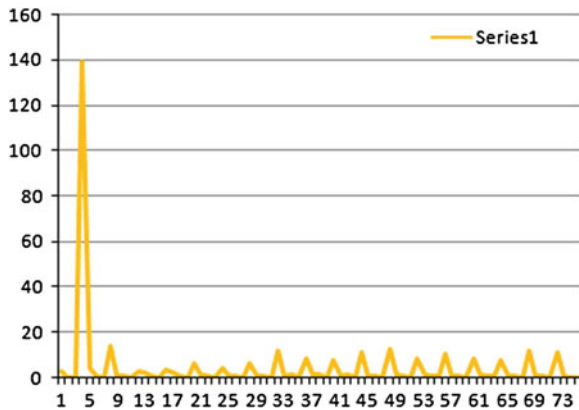
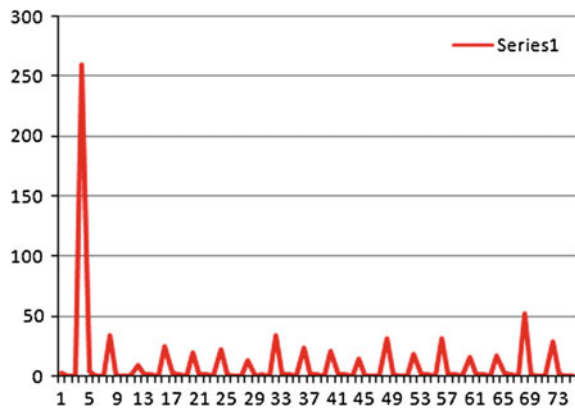


**Fig. 14.21** Sample EEG signal for digit 0 of testing dataset1



number of training and testing datasets for each digit. Numbers are generated at random, therefore the training and testing dataset of each digit vary.

Now We build the training data base using LDA and PCA. The Table 14.3 gives the recognition rate of LDA and PCA methods.

Table 14.3 shows that the recognition rate of LDA method is better than PCA. LDA exhibits 70.931 % recognition rate for digit recognition. PCA exhibits 37.557 % of recognition rate for digit recognition. Following figure shows the clusters of different digits using LDA and PCA (Figs. 14.23, 14.24, 14.25, 14.26, 14.27 and 14.28).

From the above discussion it is cleared that LDA is more applicable for EEG signal analysis. So we used LDA for our further research. Until now we processed the complete EEG data with all four frequency. We also check all probabilities of frequencies such as (alpha) (beta) (delta) (theta) (alpha beta) (alpha delta) (alpha theta) (alpha beta delta) (alpha delta theta) (beta delta theta). Their corresponding

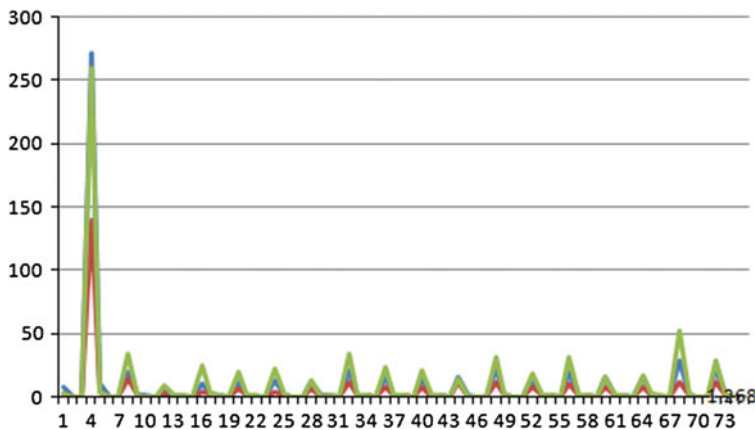


**Fig. 14.22** EEG signal of training and testing data for digit 0

**Table 14.2** Information of training and testing data

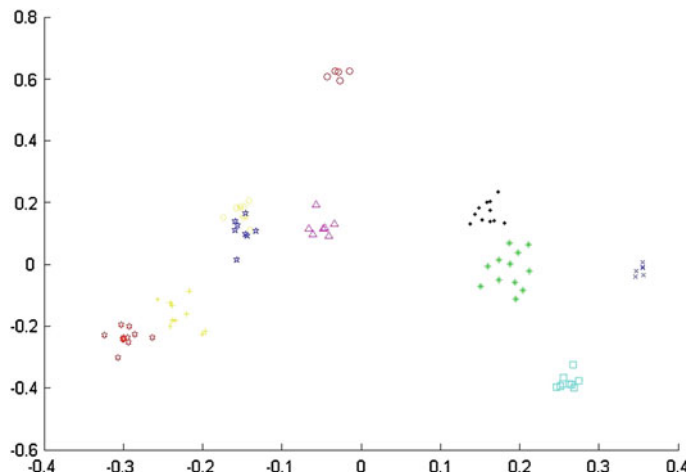
Digit data	Training data set	Testing data set
0	20	10
1	12	6
2	10	5
3	24	12
4	22	11
5	14	7
6	20	10
7	16	8
8	20	10
9	22	11
Total	180	90

graphs are as shown in following figures (Figs. 14.29, 14.30, 14.31, 14.32, 14.33, 14.34, 14.35, 14.36, 14.37, 14.38, 14.39 and 14.40).

Table 14.4 shows the average digit recognition rate using LDA. We are interested to see which frequency rhythm is more active during digit recognition activity. Digit recognition is a compounding of multiple bodily functions, then we didn't get proper clusters for individual frequencies. Then we tried multiple combinations of different frequencies. We establish that all frequencies take part in digit recognition activity.

**Table 14.3** Comparative recognition rate using LDA and PCA

Digit	Recognition rate using LDA	Recognition rate using PCA
0	59.32	23.21
1	82.23	61.23
2	59.54	21.78
3	89.25	45.23
4	62.23	45.12
5	38.23	9.5
6	84.56	40.17
7	97.27	53.23
8	73.23	45.89
9	63.45	30.21
Average	70.931	37.557

**Fig. 14.23** EEG signal classification using LDA for subject1

#### 14.4.4 Region Wise Data Analysis

The 10/20 system or International 10/20 system is an internationally recognized method for electrode placement. It describes the location of scalp electrodes. The system based on the relationship between the locations of an electrode and the underlying area of the cerebral cortex. The Number 10 and 20 refers to the fact that the distances between adjacent electrodes are either 10 or 20 % of total front, back or right, left distance of the skull. Each site has a letter to identify the lobe and a number to identify the hemisphere location [11]. The Brain is divided as Left

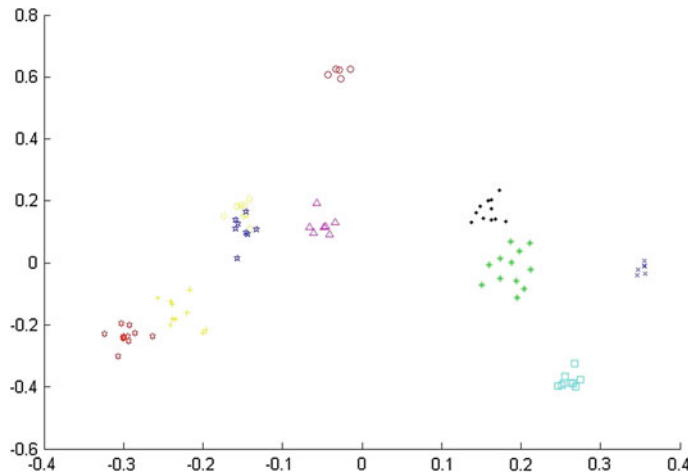


**Fig. 14.24** EEG signal classification using LDA for subject2

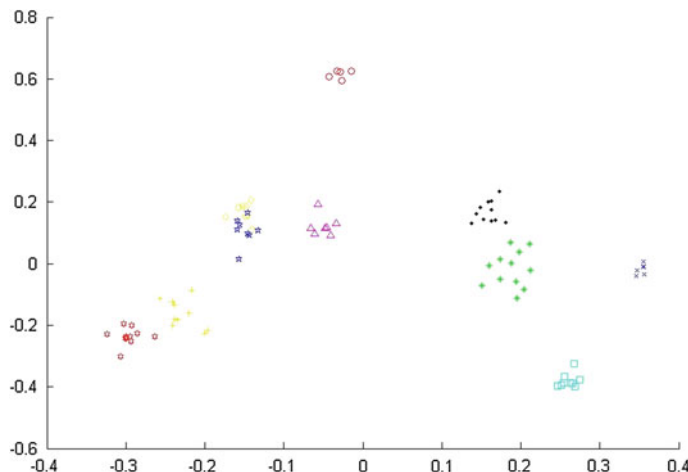


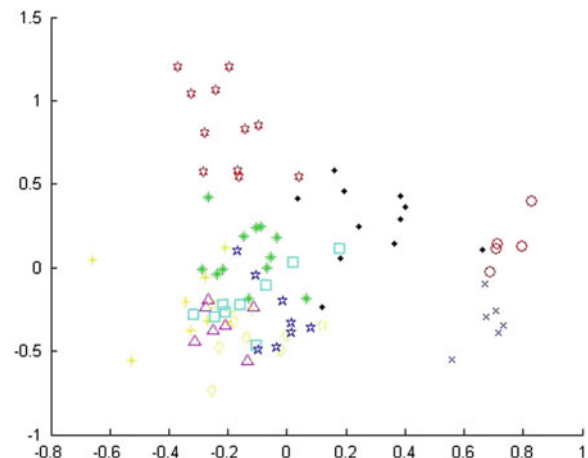
**Fig. 14.25** EEG signal classification using LDA for subject3

Hemisphere and Right Hemisphere. Even numbers (2, 4, 6, 8) refer to an electrode positions on the right hemisphere. Odd numbers (1, 3, 5, 7) refer to electrode positions on the left hemisphere. Table 14.5 gives electrodes with their lobes.

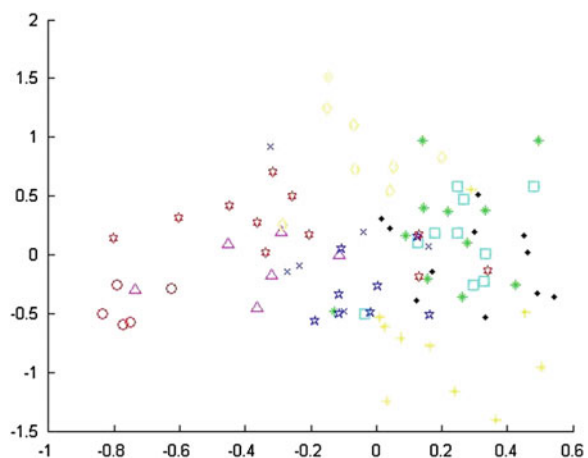
Since the architecture of the brain is non-uniform and the cortex is functionally organized, the EEG can vary depending on the location of the recording electrodes.

The Table 14.6 shows the values of different frequency power band during digit recognition. The Electrodes are divided according to the brain region as left hemisphere, right hemisphere and center hemisphere.

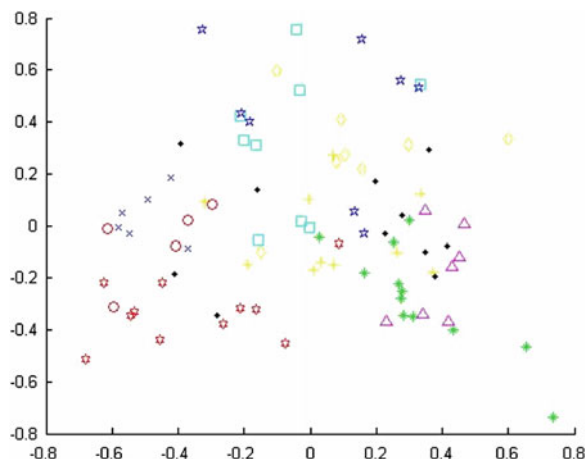
**Fig. 14.26** EEG signal classification using PCA for subject1



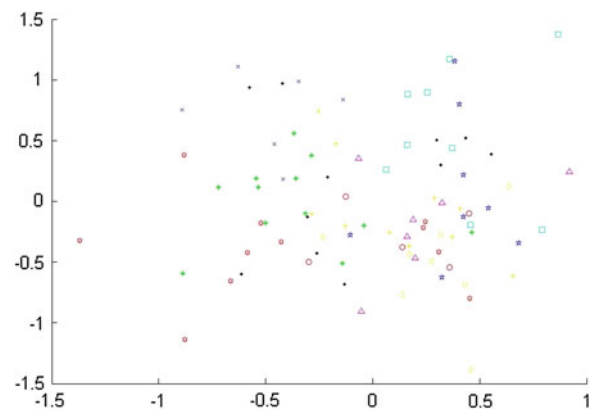
**Fig. 14.27** EEG signal classification using PCA for subject2



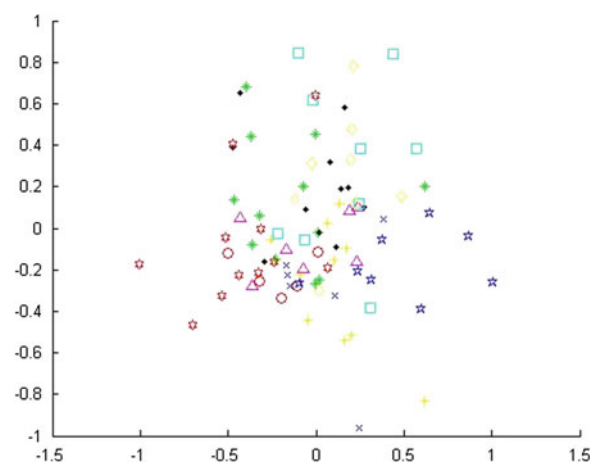
**Fig. 14.28** EEG signal classification using PCA for subject3



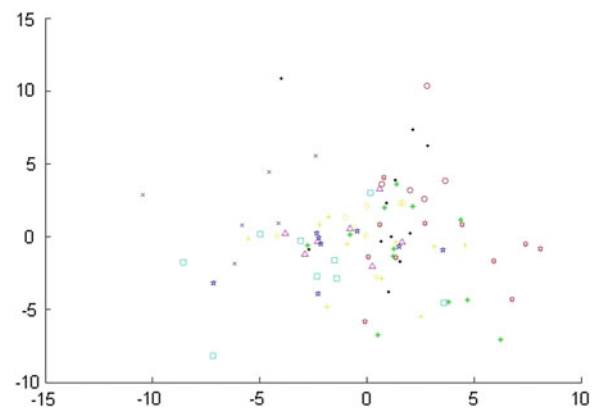
**Fig. 14.29** EEG alpha signal classification using LDA



**Fig. 14.30** EEG beta signal classification using LDA



**Fig. 14.31** EEG delta signal classification using LDA



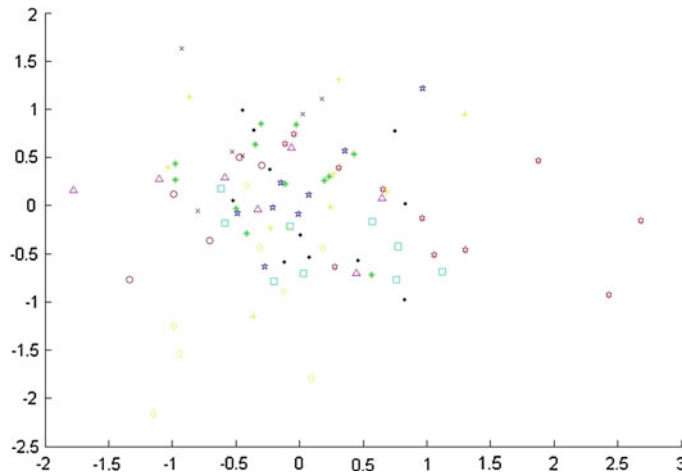
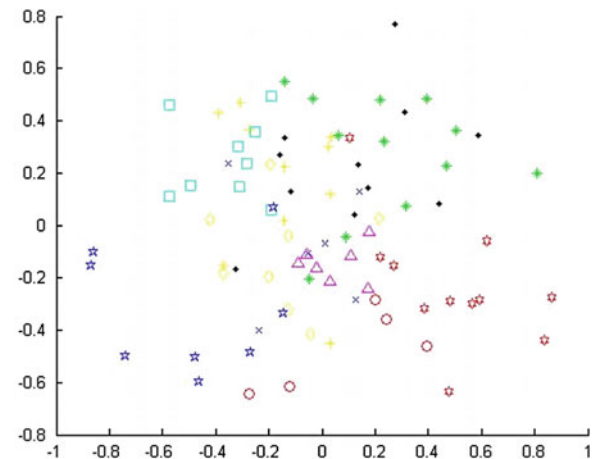


**Fig. 14.32** EEG theta signal classification using LDA

**Fig. 14.33** EEG alpha, beta signal classification using LDA



The Table 14.7 shows the summary of different frequency power band during digit recognition. In both regions each digit has different mean frequency. This implies that it is possible to distinguish the different digits using this EEG signal. The EEG signal frequency on the right region is smaller than the EEG frequency on left region.

The Tables 14.8 and 14.9 shows the distance matrices of EEG signal in left and right hemisphere. From both distance matrices it is vindicated that there is a significant conflict between each couple of digits.

**Fig. 14.34** EEG alpha delta signal classification using LDA

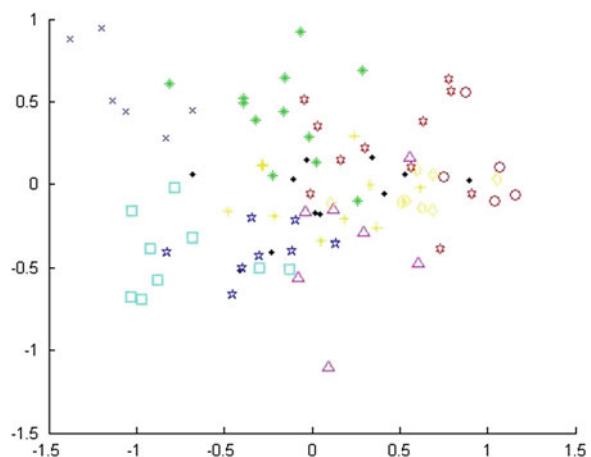


**Fig. 14.35** EEG alpha theta signal classification using LDA

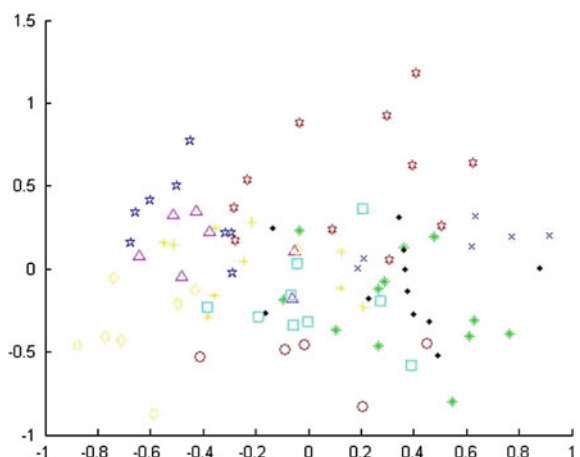


**Fig. 14.36** EEG beta theta signal classification using LDA

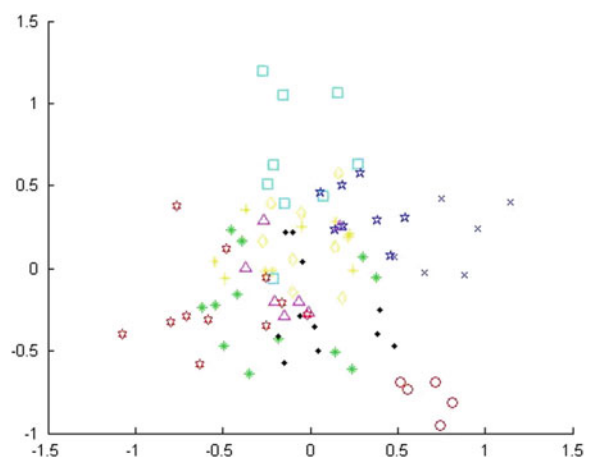


**Fig. 14.37** EEG beta theta signal classification using LDA

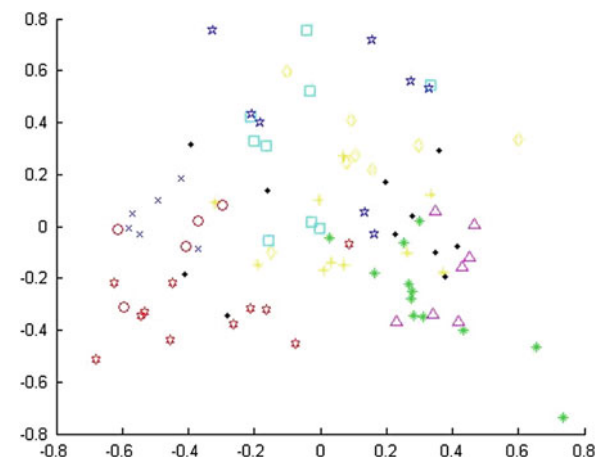


**Fig. 14.38** EEG alpha beta theta signal classification using LDA

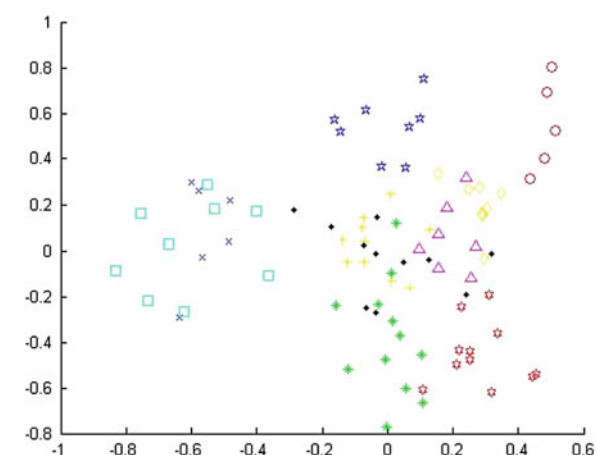


**Fig. 14.39** EEG alpha beta theta signal classification using LDA

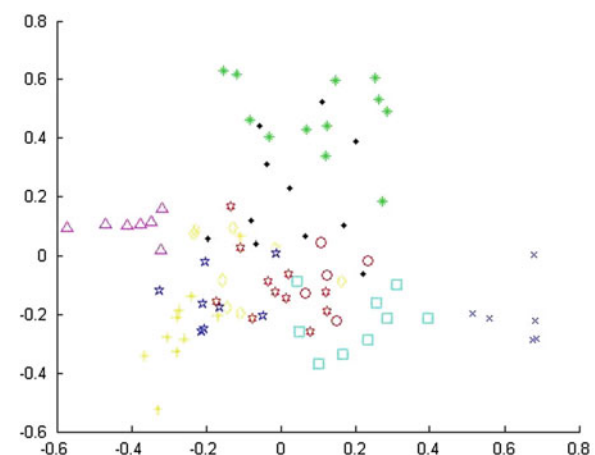


**Fig. 14.40** EEG beta delta theta signal classification using LDA

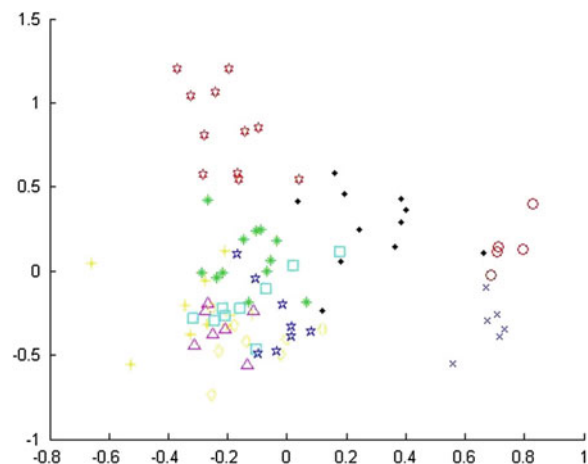


**Table 14.4** Comparison of recognition rate of different frequency probabilities using LDA

Average recognition rate using LDA (%)	Frequency probabilities
23	Alpha
28	Beta
39	Delta
34	Theta
41	Alpha beta
43	Alpha delta
41	Alpha theta
45	Beta delta
46	Beta theta
52	Delta theta
63	Alpha beta theta
57	Alpha delta theta
54	Beta delta theta
70	Alpha beta delta theta

**Table 14.5** Electrode with their lobes

Electrode	Lobe
F	Frontal
T	Temporal
C	Central
P	Parietal
O	Occipital

**Table 14.6** Mean EEG data in different regions of the brain

	Left	0	1	2	3	4	5	6	7	8	9
FP1	1.153	1.125889	1.181765	1.552	0.79	0.803333	0.819333	0.895933	0.982593	0.849	
F7	1.266	0.984	0.779333	1.01	1.158	1.187556	0.738756	0.764876	0.929488	0.909	
F3	1.267	1.040778	1.064531	1.124	1.208	0.836444	0.898644	1.015864	0.941586	1.041	
T3	0.877	0.637444	0.957494	0.658	0.878	0.792	0.6072	0.92172	0.905172	0.929	
C3	1.11	1.023333	0.957037	1.374	1.722	1.258	1.2598	1.31998	1.550998	1.712	
T5	0.921	0.807889	1.039765	0.738	1.091	0.880111	0.785011	0.697501	0.69175	0.875	
O1	0.589	0.697667	1.271963	0.536	0.875	0.835	0.7475	0.62175	0.695175	0.705	
Mean	1.026143	0.902429	1.035984	0.998857	1.103143	0.941778	0.836606	0.891089	0.95668	1.002857	
Right	0	1	2	3	4	5	6	7	8	9	
FP2	1.098	0.9900889	0.90121	0.263	0.941	0.910111	0.892011	0.854301	0.77243	0.865	
F4	0.913	0.834778	1.023864	0.771	0.773	0.832556	0.916256	1.097626	0.888763	1.024	
F8	0.672	0.464667	0.488296	0.431	0.418	0.419778	0.521978	0.486198	0.43762	0.473	
C4	1.511	1.061222	0.989025	0.606	1.723	1.337	1.0087	1.07387	1.622387	1.077	
T4	0.725	0.632778	0.712531	0.641	0.921	0.769	0.8369	0.64369	0.777369	0.577	
P3	1.582	1.745778	0.636198	1.675	1.476	1.402889	1.074289	1.158429	1.655843	1.965	
P4	1.133	0.600333	2.04337	1.11	0.997	0.866333	0.812633	0.849263	0.780926	0.759	
T6	0.829	0.814333	1.240481	0.797	0.943	0.658111	0.717811	0.643781	0.752378	0.866	
O2	0.728	0.805333	0.23837	0.774	0.791	0.649	0.7189	0.64289	0.590289	0.675	
Mean	1.025714	0.874921	0.906896	0.862	1.038429	0.87173	0.81303	0.785446	0.945259	0.913143	

**Table 14.7** Summary of mean EEG data in different regions of the brain

Digit	Left	Right
0	1.026143	1.025714
1	0.902429	0.874921
2	1.035984	0.906896
3	0.998857	0.862
4	1.103143	1.038429
5	0.941778	0.87173
6	0.836606	0.81303
7	0.891089	0.785446
8	0.95668	0.945259
9	1.002857	0.913143

Table 14.10 gives the mean values of all subjects 10 digit data in left hemisphere region of brain. The digit 3 having maximum EEG power where as digit 0 having minimum EEG power.

Table 14.11 gives the mean values of all subjects 10 digit data in right hemisphere region of brain. Here we get the same behavior i.e. digit 3 having maximum EEG power where as digit 0 having minimum EEG power. From Tables 14.10 and 14.11 we observe that the EEG signal values are more dominant on right hemisphere as compared to left hemisphere. The percentage of left dominance is listed in Table 14.12.

## 14.5 Feature Extraction

In this section we process the different level frequency data. In order to process frequency data we need to select time series data for interval of two second, convert it into different frequency level using FFT. The xls file for such data looks like as shown in following table (Table 14.13, Fig. 14.41).

In our experiment setup we store data of 90 digits with interval of 2 s for each digit. When data acquisition process completes we get 90 xls files which contains the eeg data of all 90 digits. Thus data stored is very large. In order to process this data we perform following steps

1. First store the EEG data into xls file, save the file with name which is easy to process and indicates the interval of data as shown in following Fig. 14.42. These files contains frequency domain data of different digits which are separated by time interval of 2 s.
2. Now we write the following code so that it is possible to gather the scattered data from different file into a single file.

**Table 14.8** Distance matrix of mean EEG data in left hemisphere

	0	1	2	3	4	5	6	7	8	9
0	0	0.123714	0.009841	0.027286	0.077	0.084365	0.189537	0.135054	0.069463	0.023286
1	0.123714	0	0.133556	0.096429	0.200714	0.039349	0.065822	0.011339	0.054252	0.100429
2	0.009841	0.133556	0	0.037127	0.067159	0.094206	0.199378	0.144895	0.079304	0.033127
3	0.027286	0.096429	0.037127	0	0.104286	0.057079	0.162251	0.107768	0.042177	0.004
4	0.077	0.200714	0.067159	0.104286	0	0.161365	0.2466537	0.212054	0.146463	0.100286
5	0.084365	0.039349	0.094206	0.057079	0.161365	0	0.105171	0.050689	0.014903	0.061079
6	0.189537	0.065822	0.199378	0.162251	0.266537	0.105171	0	0.054483	0.120074	0.166251
7	0.135054	0.011339	0.144895	0.107768	0.212054	0.050689	0.054483	0	0.065591	0.111768
8	0.069463	0.054252	0.079304	0.042177	0.146463	0.014903	0.120074	0.065591	0	0.046177
9	0.023286	0.100429	0.033127	0.004	0.100286	0.061079	0.166251	0.111768	0.046177	0

**Table 14.9** Distance matrix of mean EEG data in right hemisphere

	0	1	2	3	4	5	6	7	8	9
0	0	0.150794	0.118818	0.163714	0.012714	0.153984	0.212684	0.240268	0.080455	0.112571
1	0.150794	0	0.031975	0.012921	0.165508	0.00319	0.06189	0.089475	0.070338	0.038222
2	0.118818	0.031975	0	0.044896	0.131533	0.035166	0.093866	0.12145	0.038363	0.006247
3	0.163714	0.012921	0.044896	0	0.176429	0.00973	0.04897	0.076554	0.083259	0.051143
4	0.012714	0.163508	0.131533	0.176429	0	0.166698	0.225398	0.252983	0.09317	0.125286
5	0.153984	0.00319	0.035166	0.00973	0.166698	0	0.0587	0.086284	0.073529	0.041413
6	0.212684	0.06189	0.093866	0.04897	0.225398	0.0587	0	0.027584	0.132229	0.100113
7	0.240268	0.089475	0.12145	0.076554	0.252983	0.086284	0.027584	0	0.159813	0.127697
8	0.080455	0.070338	0.038363	0.083259	0.09317	0.073529	0.132229	0.159813	0	0.032116
9	0.112571	0.038222	0.006247	0.051143	0.125286	0.041413	0.100113	0.127697	0.032116	0

**Table 14.10** EEG power values in left hemisphere of brain

	0	1	2	3	4	5	6	7	8	9
Subject 1	1.0261	0.9024	1.0360	0.9989	1.1031	0.9418	0.8366	0.8911	0.9567	1.0029
Subject 2	1.0711	1.0779	1.0390	0.9723	1.0523	1.0407	1.0346	1.6559	1.0138	0.9673
Subject 3	1.0554	1.0419	1.0608	1.1416	0.9650	1.0055	0.9873	1.0975	1.1799	1.5090
Subject 4	1.5036	1.5286	1.3543	1.3497	1.3217	1.3756	1.4088	1.5036	1.4555	1.2551
Subject 5	1.3541	1.4317	1.4282	1.2687	1.4810	1.4937	1.3974	1.3012	1.2788	1.4683
Subject 6	4.6539	5.5040	5.8861	8.0934	4.9996	4.8135	6.3965	4.7318	7.0833	4.2311
Average	1.7774	1.9144	1.9674	2.3041	1.8205	1.7785	2.0102	1.8635	2.1613	1.7390

**Table 14.11** EEG power values in right hemisphere of brain

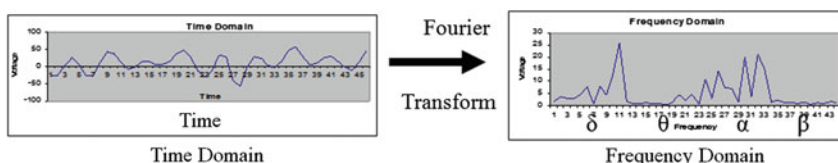
	0	1	2	3	4	5	6	7	8	9
Subject 1	1.0257	0.8749	0.9069	0.8620	1.0384	0.8717	0.8130	0.7854	0.9453	0.9131
Subject 2	0.9601	0.8114	0.8276	0.8320	0.8431	0.8826	0.8070	1.3117	0.9629	0.8246
Subject 3	0.7820	0.9148	0.9421	0.8826	0.7706	0.7809	0.7989	0.9461	0.8164	1.0874
Subject 4	1.2512	1.3153	1.2599	1.2907	1.3213	1.2990	1.2579	1.2530	1.2730	1.0867
Subject 5	1.1519	1.1572	1.1044	1.1137	1.1899	1.2018	1.1352	1.0597	1.0454	1.1470
Subject 6	2.5467	3.1508	3.3169	5.1240	3.5869	3.0108	3.4961	3.1298	4.8533	3.3229
Average	1.2863	1.3707	1.3930	1.6842	1.4584	1.3411	1.3847	1.4143	1.6494	1.3969

**Table 14.12** EEG power dominance

	0	1	2	3	4	5	6	7	8	9
L	1.7774	1.9144	1.9674	2.3041	1.8205	1.7785	2.0102	1.8635	2.1613	1.7390
R	1.2863	1.3707	1.3930	1.6842	1.4584	1.3411	1.3847	1.4143	1.6494	1.3969
D	27.63	28.40	29.19	26.90	19.89	24.59	31.11	24.10	23.68	19.67

**Table 14.13** EEG power sample data

Electrode	F-Range (Hz)	Abs power (V ** 2)	Rel power (%)	PPF (Hz)	MPF (Hz)
FP1-CAR	0.0–4.0	320.27	93	2	2
	4.0–8.0	23.06	6.7	4	4
	8.0–12.0	1.01	0.3	8.5	8.5
	12.0–16.0	0.2	0.1	12.5	13
FP2-CAR	0.0–4.0	477.89	94.4	2	2
	4.0–8.0	27.22	5.4	4	4.5
	8.0–12.0	0.7	0.1	8	8.5
	12.0–16.0	0.22	0	15.5	13
F7-CAR	0.0–4.0	6.97	76.9	1	1.5
	4.0–8.0	1.24	13.7	5.5	5.5
	8.0–12.0	0.39	4.3	8.5	8.5
	12.0–16.0	0.46	5.1	14.5	14.5
F3-CAR	0.0–4.0	5.42	56.8	1	1
	4.0–8.0	2.03	21.2	7	6
	8.0–12.0	1.26	13.2	11	10.5
	12.0–16.0	0.84	8.8	12.5	13
FZ-CAR	0.0–4.0	3.82	46	1.5	1
	4.0–8.0	2.78	33.5	7	5.5
	8.0–12.0	0.8	9.7	8.5	10
	12.0–16.0	0.9	10.8	12	13
F4-CAR	0.0–4.0	5.66	63.6	0	0.5
	4.0–8.0	2.01	22.5	6	6
	8.0–12.0	0.53	6	10.5	10.5
	12.0–16.0	0.7	7.9	12.5	13

**Fig. 14.41** Time domain and frequency domain data

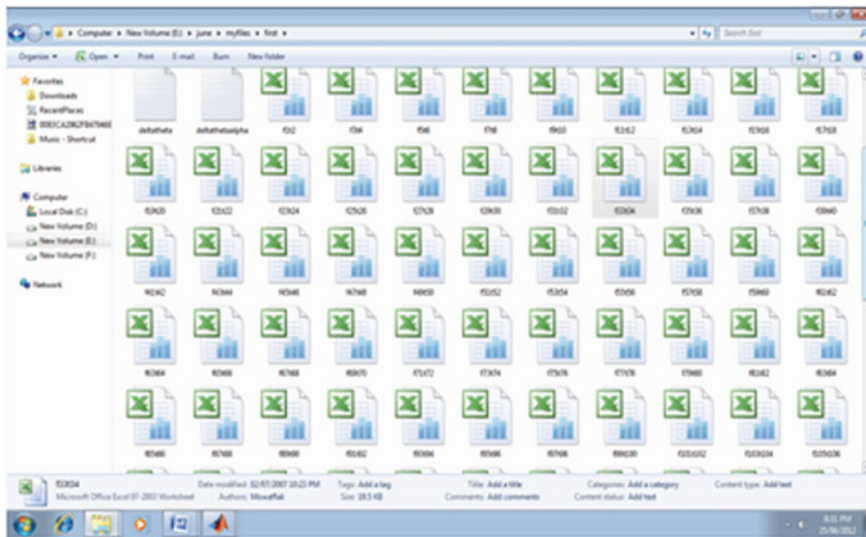


**Fig. 14.42** Figure showing the name scheme for xls file

```

filename = 'E:\june\myfiles\first\f'
wfilename = '\june\myfiles\first\first.xls'
j = 2
for i = 0 : 2 : 178
begin
filename1 = strcat(filename,int2str(i+1)',t',int2str(i+2)',.xls')
s = xlsread(filename1,'c3 : c96')
s = transpose(s)
range = strcat('a',int2str(j),':cp',int2str(j))
xlswrite(wfilename,s,range)
j = j + 1
end

```

3. Now data looks like.
4. Remove the artifacts from EEG data.
5. Apply LDA method to generate distinct classes and analyze this classes.
6. Following figure shows the classification between all ten numbers using LDA (Table 14.14, Fig. 14.43).
7. Data generated by LDA is as follows.

Table 14.15 shows the cluster information for digit zero. The cluster contains total ten points with center at  $(-0.0016, 0.1466)$  and radius  $= 0.01931$ . Out of the ten points only five points are inside the circle. So we say that the density of cluster is 50 %.

**Table 14.14** EEG data of different digits at different electrodes

Digit	FP1				FP2			
	Alpha	Theta	Delta	Beta	Alpha	Theta	Delta	Beta
0	6.6	3.88	1.57	0.64	20.71	5.8	2.19	1.33
1	307.08	7.89	1.18	0.45	378.32	9.06	0.73	0.36
1	1099.21	29.37	0.69	0.56	600.3	6.53	0.8	0.81
1	178.76	1.95	0.7	0.34	294.3	2.68	0.7	0.29
2	39.27	3.76	1.16	0.69	35.88	3.31	0.7	0.39
2	329.91	65.23	2.92	0.49	531.62	95.3	1.95	0.31
2	1796.51	1.9	1.27	0.47	942.38	2.52	1.13	0.32
3	84.96	4.36	0.43	0.35	113.62	4.62	0.42	0.12
4	21.87	1.36	0.38	0.25	19.68	4.52	0.2	0.25
4	276.9	5.78	0.26	0.4	435.76	9.89	0.74	0.27
5	8.34	0.93	0.63	0.24	12.91	1.69	1.06	0.4
5	127.71	2.73	0.88	0.15	266.54	3.79	0.52	0.32
5	473.01	8.41	1.36	0.43	758.05	8.26	1.01	0.22
6	1406.7	5.09	1.76	0.41	1471.16	7.8	2.02	0.31
6	35.01	1.83	0.72	0.21	71.91	2.02	0.41	0.12
6	50.83	5.9	1.02	0.47	89.54	9.02	0.82	0.62
7	320.27	23.06	1.01	0.2	477.89	27.22	0.7	0.22
7	117.25	3.07	0.51	0.28	192.26	3.79	0.57	0.16
7	283.35	23.11	1.02	0.17	451.97	33.8	1.17	0.52
8	375.29	7.24	1.45	0.19	563.83	10.78	0.53	0.42
9	61.88	1.12	0.87	0.26	118.35	1.11	1.43	0.14

Table 14.16 shows the cluster information for digit one. The cluster contains total six points with center at  $(0.107965628, 0.093447148)$  and radius = 0.238866421. Out of the six points five points are inside the circle. So we say that the density of cluster is 83 %. Table 14.17 shows the cluster information for digit two. The cluster contains total five points with center at  $(-0.064113698, 0.096575553)$  and radius = 0.065449459. Out of the five points three points are inside the circle. So we say that the density of cluster is 60 %.

Table 14.18 shows the cluster information for digit three. The cluster contains total eleven points with center at  $(0.032867432, -0.22817591)$  and radius = 0.288061438. Out of the eleven points ten points are inside the circle. So we say that the density of cluster is 91 %.

Table 14.19 shows the cluster information for digit four. The cluster contains total eleven points with center at  $(0.106169638, 0.034016434)$  and radius

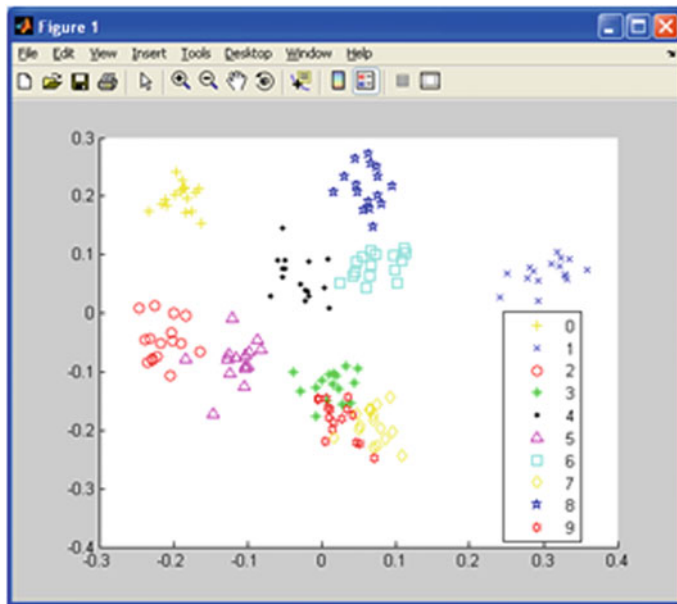


**Fig. 14.43** Graph showing the clusters of different classes using LDA

**Table 14.15** Cluster information for digit-0

X	Y	Distance from center of cluster
0.0093	0.1466	0.0017
0.0046	0.1903	0.0444
0.0026	0.1191	0.0269
-0.0159	0.1268	0.0192
0.0020	0.1437	0.0027
-0.0123	0.1181	0.0279
-0.0040	0.1754	0.0296
0.0083	0.1313	0.0147
-0.0087	0.1410	0.0052

= 0.109176504. Out of the eleven points seven points are inside the circle. So we say that the density of cluster is 64 %.

Table 14.20 shows the cluster information for digit five. The cluster contains total seven points with center at (0.10241185, 0.034016434) and radius = 0.103655998. Out of the seven points two points are inside the circle. So we say that the density of cluster is 40 %.

Table 14.21 shows the cluster information for digit six. The cluster contains total seven points with center at (-0.278322, 0.140508139) and radius = 0.279101655.

**Table 14.16** Cluster information for digit-1

X	Y	Distance from center of cluster
0.1056	0.0928	0.8920
0.1090	0.0988	0.1081
0.1026	0.1028	0.1084
0.1092	0.0946	0.1080
0.1107	0.0805	0.1087
0.1108	0.0912	0.1080

**Table 14.17** Cluster information for digit-2

X	Y	Distance from center of cluster
-0.0717	0.1189	2.0642
-0.0597	0.0793	0.0664
-0.0609	0.0886	0.0646
-0.0641	0.1005	0.0642
-0.0642	0.0957	0.0641

**Table 14.18** Cluster information for digit-3

X	Y	Distance from center of cluster
0.0330	-0.2168	2.9672
0.0258	-0.1912	0.0495
0.0347	-0.2304	0.0329
0.0353	-0.2425	0.0358
0.0305	-0.1763	0.0614
0.0384	-0.2199	0.0339
0.0301	-0.2959	0.0753
0.0339	-0.2577	0.0442
0.0086	-0.2293	0.0329
0.0461	-0.1991	0.0439
0.0324	-0.2192	0.0341

Out of the seven points six points are inside the circle. So we say that the density of cluster is 86 %.

Table 14.22 shows the cluster information for digit seven. The cluster contains total five points with center at (-0.006807753, 0.287239623) and radius = 0.157660533. Out of the five points six points are inside the circle. So we say that the density of cluster is 100 %.

**Table 14.19** Cluster information for digit-4

X	Y	Distance from center of cluster
0.1062	0.0086	0.1092
0.1065	0.0292	0.1063
0.0942	0.0332	0.1062
0.1074	0.0539	0.1080
0.0973	0.0516	0.1076
0.1034	0.0021	0.1109
0.1130	0.0682	0.1115
0.1047	0.0179	0.1074
0.1054	0.0380	0.1062
0.1039	0.0768	0.1145
0.1260	-0.0053	0.1132

**Table 14.20** Cluster information for digit-5

X	Y	Distance from center of cluster
0.0945	-0.3761	0.1024
0.1093	-0.4021	0.1057
0.0954	-0.3837	0.1027
0.1021	-0.3582	0.1039
0.1110	-0.3592	0.1038
0.1036	-0.3912	0.1035
0.1009	-0.3609	0.1035

**Table 14.21** Cluster information for digit-6

X	Y	Distance from center of cluster
-0.2701	-0.1206	0.2790
-0.2752	-0.1909	0.2828
-0.2725	-0.1219	0.2789
-0.2829	-0.1526	0.2786
-0.2803	-0.1493	0.2785
-0.2894	-0.1298	0.2785
-0.2806	-0.1372	0.2783

Table 14.23 shows the cluster information for digit eight. The cluster contains total eight points with center at (0.045618502, 0.013377525) and radius = 0.048312754. Out of the eight points six points are inside the circle. So we say that the density of cluster is 75 %.

Table 14.24 shows the cluster information for digit nine. The cluster contains total eleven points with center at (-0.035999385, 0.122955778) and radius =

**Table 14.22** Cluster information for digit-7

X	Y	Distance from center of cluster
-0.0062	0.2886	0.0069
0.0026	0.2885	0.0069
-0.0122	0.2819	0.0087
-0.0008	0.2775	0.0119
-0.0139	0.2444	0.0434

**Table 14.23** Cluster information for digit-8

X	Y	Distance from center of cluster
0.0606	-0.0017	0.0480
0.0392	0.0186	0.0459
0.0399	0.0189	0.0460
0.0498	0.0185	0.0459
0.0433	0.0454	0.0557
0.0405	-0.0133	0.0528
0.0465	0.0047	0.0464
0.0451	0.0159	0.0457

**Table 14.24** Cluster information for digit-9

X	Y	Distance from center of cluster
-0.0383	0.1054	0.0401
-0.0619	0.0842	0.0529
-0.0432	0.1419	0.0407
-0.0182	0.1393	0.0396
-0.0407	0.1491	0.0445
-0.0158	0.1231	0.0360
-0.0393	0.1237	0.0360
-0.0247	0.1364	0.0384
-0.0402	0.1208	0.0361
-0.0410	0.1524	0.0465
-0.0326	0.0763	0.0589

0.042695393. Out of the eleven points seven points are inside the circle. So we say that the density of cluster is 64 %. All data points in a single cluster are called as cluster feature (CF). Let CF is a data structure summarizing information about all points in the dataset.

$$CF = (n, LS)$$

where LS is linear sum of n data points.

$$ie \sum_{i=1}^n x_i \sum_{i=1}^n y_i$$

where n is the number of data points in data set. Mean of data set provides the center of  $(x_0, y_0)$  of the distribution. Then the distance of each point in a cluster from the center of cluster is given by Vidal [31].

$$Distance = \sqrt{(x_i - x_0)^2 + (y_i - y_0)^2}$$

The radius of cluster is calculated as

$$\frac{\sum_{i=1}^n \sqrt{(x_i - x_0)^2 + (y_i - y_0)^2}}{n}$$

So the resultant values of center and radius for different clusters is as follows.

From Table 14.25 we observe that the EEG signal for digits 0–9 is different. It is possible to separate the digits. Table 14.26 shows the radius of cluster for digit 0 having minimum value and the radius of cluster for digit 3 having maximum values. Also the digit 7 having maximum recognition rate of 100 % and digit 5 having minimum recognition rate of 40 %. From table it is clear that each digit is well separable. So it is possible to recognize the digit using EEG and LDA.

**Table 14.25** center and radius for different clusters

Digit	X	Y	Distance
0	-0.0016	0.145886	0.019312253
1	0.107965628	0.093447148	0.238866421
2	-0.064113698	0.096575553	0.065449459
3	0.032867432	-0.22817591	0.288061438
4	0.106169638	0.034016434	0.109176504
5	0.10241185	-0.375910337	0.103655998
6	-0.278322	-0.140508139	0.279101655
7	-0.006807753	0.287239623	0.157660533
8	0.045618502	0.013377525	0.048312754
9	-0.035999385	0.122955778	0.042695393

**Table 14.26** clusters information in terms of radius and density

Digit	Radius	Density (%)
0	0.019312253	50
1	0.238866421	83
2	0.065449459	60
3	0.288061438	91
4	0.109176504	64
5	0.103655998	40
6	0.279101655	86
7	0.157660533	100
8	0.048312754	75
9	0.042695393	64

## 14.6 Conclusion

Recording are sampled at 250 Hz for 90 s so length of data is very large. But it is transformed using Fourier transformation into frequency data. For each digit we get 19 scaling exponent responding each channel. The data is filtered by band pass filter. The effective component of EEG is usually supposed to be concentrated at 1–30 HZ and frequency of baseline excursion is comparatively lower (1 HZ) and the frequency of power interruption and EMG interruption is higher ( $\geq 50$  HZ). So we set the parameters as Low filter 1 Hz, High filter 70 Hz, Number of channels: 06, Sweep speed 30 mm/s and Montage: BP PARA (R). Considering the calculation results for the same digit, the results of one subject during each trail are comparatively consistent. Linear Discriminate Analysis and Principle Component analysis are well known scheme for feature extraction and dimension reduction. We have trail dataset having size of 180 and testing dataset having size of 90. The recognition rate of LDA is approximately 70 %. Similarly the recognition rate of PCA is 37 %. Thus LDA is more powerful than PCA for feature extraction. After we study the different probabilities of frequency. From the number of observations we conclude that all factors of EEG signal are important. So we get accurate recognition rate for all frequency components. The frequency is different for different digits. also there is well separation between the clusters of digits. Thus we proposed an effective method for extracting properties of EEG data. This study is used to effectively extract EEG features related to Digits. Here we also concentrated region wise study of EEG signal. From the data it is cleared that the EEG power of right hemisphere is more dominant than left hemisphere. In these studies we were concentrated on 19 electrodes. Our study is foundation for using Brain Computer Interface in security systems. It was found that the EEG signals are sensitive to thought process. So it is possible to recognize thought process through EEG signals. In our ten digit thought process, we successfully separates ten digits by analyzing

EEG signals through statistical technique like LDA. The data base created has potential to be used as a digital recognition system. It has tremendous applications in design of security system.

## References

1. Abdullah, M.K.: Analysis of eeg signal for practical biometric system. In: IEEE EMBS Conference on Biomedical Engineering and Sciences (IECBES), pp 303–306 (2010)
2. Azar, A.T., Balas, V.E., Olariu, T.: Classification of eeg-based brain-computer interfaces. *Adv. Intell. Comput. Technol. Decis. Support Syst. Stud. Comput. Intell.* **486**, 97–106 (2014)
3. Babilioni, F.: Linear classification of low-resolution eeg patterns produced by imagined hand movement. *Proc. IEEE* **8**(2), 186–188 (2000)
4. Berger, H.: Under das electrenkephalogramm desmenchen. *Arch. Psychiat Nervenk* **87**, 527–570 (1929)
5. Birbaumer, N., Roberts, L.E., Lutzenberger, W., Rockstroh, B., Elbert, T.: Area-specific self-regulation of slow cortical potentials on the sagittal midline and its effects on behavior. *Electroenceph. Clin. Neurophysiol.* **84**(4), 353–361 (1992)
6. Cincotti, F., Mattia, D., Aloise, F., Bufalari, S.: High-resolution eeg techniques for braincomputer interface applications. *J. Neurosci. Methods* **167**(1), 31–42 (2008)
7. Deore, R., Janvale, G., and Mehrotra, S.: Comparative study of algorithms for EEG signal related to song induced activity. In: International Conference on Science, Engineering and Spirituality (2010)
8. Deore, R.S., Gawali, B.W., and Mehrotra, S.C.: Extraction and detection of electroencephalogram (EEG) properties in number recognition system using linear discriminate analysis and EEG. *Int. J. Res. Rev. Sig. Acquisition Process.* **201**(5) (2012)
9. Donchin, E.: Event Related Potentials in Man, pp. 349–441. Academic, New York (1978)
10. Farwell, L., Donchin, E.: Taking off the top of your head: Toward a mental prosthesis utilizing event-related brain potentials. *Electroenceph. Clin. Neurophysiol.* **70**(6), 510–523 (1988)
11. Flotzinger, D., Pfurtscheller, G., Neuper, C., Berger, J., and Mohl, W.: Classification of nonaveraged EEG data by learning vector quantization and the influence of signal preprocessing. In: IEEE Engineering in Medicine and Biology Society. Proceedings of the 15th Annual International Conference of the IEEE, pp. 263–264 (1993)
12. Janvale, G.B., Gawali, B.W., Deore, R.S., Deshmukha, S., Marwale, A., Mehrotra, S.: Song induced mood recognition system using EEG signals. *J. Indian Acad. Neurosci.* **17**(2), 60–64 (2009)
13. Kalcher, J., Flotzinger, D., Neuper, C., Golly, S., Pfurtscheller, G.: Graz brain-computer interface II:Toward communication between humans and computers based on online classification of three different EEG patterns. *Med. Biol. Eng. Comput.* **34**(5), 382–388 (1996)
14. Keim, Z.A., Aunon, J.I.: Man-machine communications through brain-wave processing. *IEEE Eng. Med. Bio. Mag.* **9**, 55–57 (1990)
15. Klimesch, W.: EEG alpha and theta oscillations reflect cognitive and memory performance: a review and analysis. *Brain Res. Rev.* **29**(2–3), 169–195 (2000)
16. Klimesch, W., Doppelmayr, M., Russegger, H., Pachinger, T., Schwaiger, J.: Induced alpha band power changes in the human eeg and attention. *Neurosci. Lett.* **244**(2), 73–76 (1998)
17. Kostov, A.: Parallel man-machine training in development of eeg-based cursor control. *Proc. IEEE* **8**(2), 203–205 (2000)
18. Kotchoubey, B., Schleichert, H., Lutzenberger, W., Birbaumer, N.: A new method for self-regulation of slow cortical potentials in a timed paradigm. *Appl. Psychophysiol. Biofeedback* **22**(2), 77–93 (1997)

19. Pfurtscheller, G., Aranibar, A.: Evaluation of event-related desynchronization (ERD) preceding and following voluntary self-paced movement. *Electroencephal. Clin. Neurophysiol.* **46**(2), 138–146 (1979)
20. Pfurtscheller, G., Berghold, A.: Patterns of cortical activation during planning of voluntary movement. *Electroenceph. Clin. neurophysiol.* **72**(3), 250–258 (1989)
21. Pfurtscheller, G., Flotzinger, D., Mohl, W., Peltoranta, M.: Prediction of the side of hand movements from single-trial multi-channel EEG data using neural networks. *Electroenceph. Clin. Neurophysiol* **82**, 313–315 (1992)
22. Pfurtscheller, G., Kalcher, J., Neuper, C., Flotzinger, D., Pregenzer, M.: On-line EEG classification during externally-paced hand movements using a neural network-based classifier. *Electroenceph. Clin. Neurophysiol.* **99**, 416–425 (1996)
23. Pfurtscheller, G., Neuper, C., Schlogl, A., Lugger, K.: Separability of EEG signals recorded during right and left motor imagery using adaptive autoregressive parameters. *IEEE Trans. Rehabil. Eng.* **6**(3), 316–325 (1998)
24. Pfurtscheller, G., Pregenzer, M., Neuper, C.: Visualization of sensorimotor areas involved in preparation for hand movement based on classification of mu and central beta rhythms in single EEG trials in man. *Neurosci. Lett.* **181**(7), 43–46 (1994)
25. Pregenzer, M., Pfurtscheller, G., and Andrew, C.: Improvement of EEG classification with a subject-specific feature selection. In: ESANN (1995)
26. Pregenzer, M., Pfurtscheller, G., Flotzinger, D.: Automated feature selection with a distinction sensitive learning vector quantizer. *Electroenceph. Clin. Neurophysiol.* **11**, 19–29 (1996)
27. Rao, S., Abhang, P., Mehrotra, S.C.: Region wise emotion recognition using eeg brain signals. In: Proceeding of International Conference on Machine Intelligence Application to Power, Signal Processing, Communication and Control, pp. 123–127 (2010)
28. Sanei, S., Chambers, J.: EEG Signal Processing. Wiley, New York (2007)
29. Sutter, E.: The brain response interface: communication through visually induced electrical brain responses. *J. Microcomput. Appl.* **15**(1), 31–45 (1992)
30. Vidal, J.: Toward direct brain-computer communication. *Annu. Rev. Biophys. Bioeng.* **2**, 157–180 (1973)
31. Vidal, J.J.: Real time detection of brain events in EEG. In: IEEE Proceeding IEEE, pp. 633–664 (1977)
32. Wolpaw, J.R., Birbaumer, N., McFarland, D.J., Pfurtscheller, G., Vaughan, T.M.: Brain computer interfaces for communication and control. *Clin. Neurophys.* **113**(6), 767–791 (2002)
33. Wolpaw, J.R., McFarland, D.J.: Multichannel EEG-based braincomputer communication. *Electroenceph. Clin. Neurophysiol.* **90**(6), 444–449 (1994)
34. Wolpaw, J.R., McFarland, D.J., Neat, G.W., Forneris, C.: An EEGbased brain-computer interface for cursor control. *Electroenceph. Clin. Neurophysiol.* **78**(3), 252–259 (1991)
35. Zhao, Q., Peng, H., Hu, B., Liu, Q., Liu, L., Qi, Y., Li, L.: Improving individual identification in security check with an eeg. *Brain Inf.* **6334**, 145–155 (2010)